frontiers | Research Topics

Transcription regulation - Brain development and homeostasis - A finely tuned and orchestrated scenario in physiology and pathology, volume II

Edited by
Estela Maris Muñoz and Veronica Martinez Cerdeño

Published in
Frontiers in Molecular Neuroscience
Frontiers in Aging Neuroscience

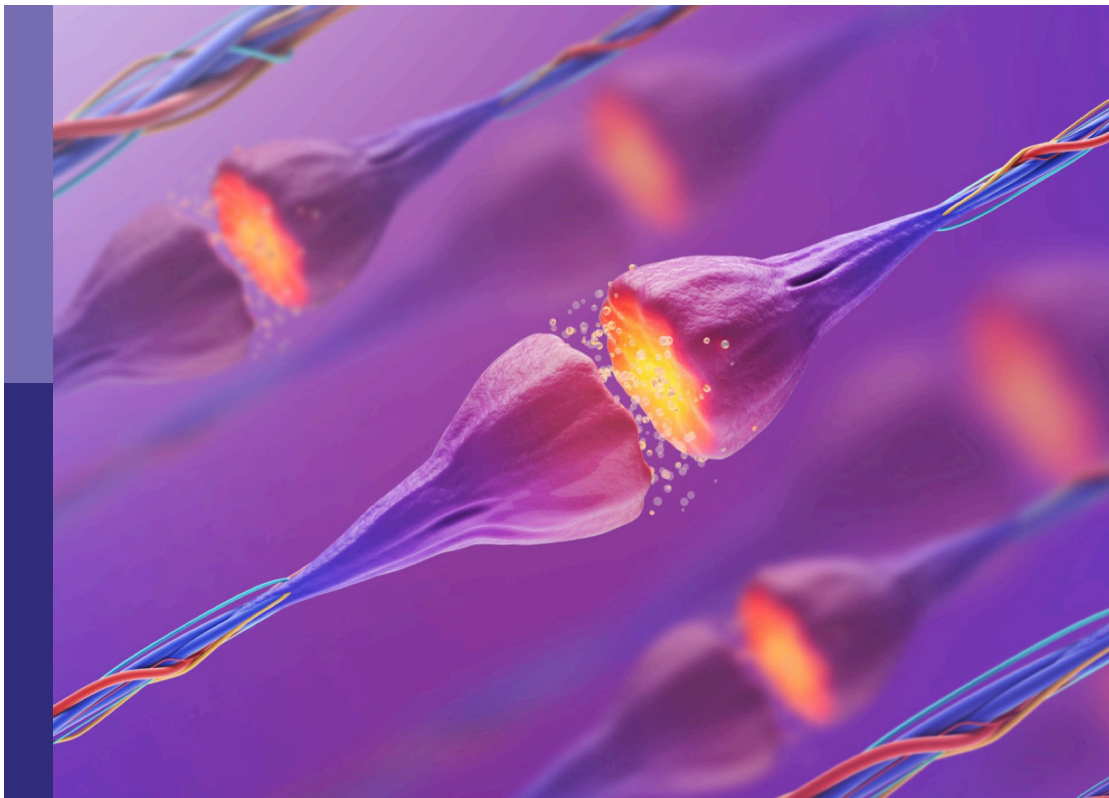

ISSN 1664-8714
ISBN 978-2-8325-3381-9
DOI 10.3389/978-2-8325-3381-9

About Frontiers

Frontiers is more than just an open access publisher of scholarly articles: it is a pioneering approach to the world of academia, radically improving the way scholarly research is managed. The grand vision of Frontiers is a world where all people have an equal opportunity to seek, share and generate knowledge. Frontiers provides immediate and permanent online open access to all its publications, but this alone is not enough to realize our grand goals.

Frontiers journal series

The Frontiers journal series is a multi-tier and interdisciplinary set of open-access, online journals, promising a paradigm shift from the current review, selection and dissemination processes in academic publishing. All Frontiers journals are driven by researchers for researchers; therefore, they constitute a service to the scholarly community. At the same time, the *Frontiers journal series* operates on a revolutionary invention, the tiered publishing system, initially addressing specific communities of scholars, and gradually climbing up to broader public understanding, thus serving the interests of the lay society, too.

Dedication to quality

Each Frontiers article is a landmark of the highest quality, thanks to genuinely collaborative interactions between authors and review editors, who include some of the world's best academicians. Research must be certified by peers before entering a stream of knowledge that may eventually reach the public - and shape society; therefore, Frontiers only applies the most rigorous and unbiased reviews. Frontiers revolutionizes research publishing by freely delivering the most outstanding research, evaluated with no bias from both the academic and social point of view. By applying the most advanced information technologies, Frontiers is catapulting scholarly publishing into a new generation.

What are Frontiers Research Topics?

Frontiers Research Topics are very popular trademarks of the *Frontiers journals series*: they are collections of at least ten articles, all centered on a particular subject. With their unique mix of varied contributions from Original Research to Review Articles, Frontiers Research Topics unify the most influential researchers, the latest key findings and historical advances in a hot research area.

Find out more on how to host your own Frontiers Research Topic or contribute to one as an author by contacting the Frontiers editorial office: frontiersin.org/about/contact

Transcription regulation - Brain development and homeostasis - A finely tuned and orchestrated scenario in physiology and pathology, volume II

Topic editors

Estela Maris Muñoz — CONICET Dr. Mario H. Burgos Institute of Histology and Embryology (IHEM), Argentina

Veronica Martinez Cerdeño — University of California, Davis, United States

Citation

Muñoz, E. M., Martinez Cerdeño, V., eds. (2023). *Transcription regulation - Brain development and homeostasis - A finely tuned and orchestrated scenario in physiology and pathology, volume II*. Lausanne: Frontiers Media SA.

doi: 10.3389/978-2-8325-3381-9

Table of contents

frontiers | Frontiers in Molecular Neuroscience

TYPE Editorial
PUBLISHED 05 September 2023
DOI 10.3389/fnmol.2023.1280573

OPEN ACCESS

EDITED AND REVIEWED BY
Clive R. Bramham,
University of Bergen, Norway

*CORRESPONDENCE
Estela M. Muñoz
✉ munoz.estela@fcm.uncu.edu.ar;
✉ emunoz@mendoza-conicet.gob.ar

RECEIVED 20 August 2023
ACCEPTED 25 August 2023
PUBLISHED 05 September 2023

CITATION
Muñoz EM and Martínez Cerdeño V (2023) Editorial: Transcription regulation — Brain development and homeostasis — A finely tuned and orchestrated scenario in physiology and pathology, volume II.
Front. Mol. Neurosci. 16:1280573.
doi: 10.3389/fnmol.2023.1280573

Editorial: Transcription regulation — Brain development and homeostasis — A finely tuned and orchestrated scenario in physiology and pathology, volume II

Estela M. Muñoz[1]* and Verónica Martínez Cerdeño[2]

[1]Institute of Histology and Embryology of Mendoza (IHEM), National University of Cuyo (UNCuyo), National Scientific and Technical Research Council (CONICET), Mendoza, Argentina, [2]Department of Pathology and Laboratory Medicine, Institute for Pediatric Regenerative Medicine, Shriners Hospitals for Children of Northern California, and MIND Institute at the UC Davis Medical Center, University of California Davis School of Medicine, Sacramento, CA, United States

KEYWORDS

transcription, transcription factors, brain, neurodevelopment, diseases

Editorial on the Research Topic
Transcription regulation—Brain development and homeostasis—A finely tuned and orchestrated scenario in physiology and pathology, volume II

The Research Topic (RT) discussed herein is the second volume of a Research Topic focused on transcription factors (TF) and transcription regulation in the healthy and diseased brain. The previously published first volume was compiled into a well-visited and well-read E-Book (with more than 61,000 total views and downloads, to date) (Muñoz et al., 2021, 2022). Encompassed in this second volume are eleven peer-reviewed manuscripts including five original articles, four reviews, one mini review, and one brief research report. Seventy-five authors took part in this initiative, from eleven countries: Argentina, Australia, Austria, Denmark, Germany, Italy, India, Spain, Sweden, United Kingdom, and United States.

Among the interesting contributions, Xia et al. summarize the current knowledge of transcription regulation of the respiratory neurons in the brainstem. These neurons are responsible for generating, monitoring, and adjusting breathing patterns in response to external and internal demands. Thus, these motor neurons represent key actors of breathing (or respiration), which is an elementary but complex and dynamic behavior. First, the authors present generalities of the transcriptional programs that drive the anterior-posterior and the dorsal-ventral patterning of the developing brainstem, emphasizing its neuronal diversity. Next, they discuss the transcriptional control that secures the specification of certain groups of neurons that form the central respiratory system in the hindbrain. This discussion includes the pontine groups, and the neurons of both the dorsal and the ventral medullary respiratory columns. Lastly, the authors consider disturbances of TF-coding genes (e.g., mutations in *PHOX2B* and *LBX1*) that cause congenital respiratory syndromes, as a possible path to further understand the genesis, specification, and function of respiratory neurons and the basis of breathing. The review is well-illustrated, and the readers can visit

the following references for further details (Alexander et al., 2009; Hernandez-Miranda and Birchmeier, 2015; Hernandez-Miranda et al., 2017, 2018; Isik and Hernandez-Miranda, 2022; Lowenstein et al., 2023).

The prefrontal cortex (PFC) is a large brain region that compromises a diversity of neuronal and non-neuronal cell types. The timely appearance and connectivity of these cells during development are crucial for normal PFC anatomy and functions (Cadwell et al., 2019). PFC is involved in fundamentally important brain processes, such as cognition and memory. In this RT, Singh and Tiwari focus their brief research report on the developing human PFC. The authors aimed to identify transient cell states that emerge during the cellular developmental trajectories of the major cortical cell types and their underlying gene regulatory circuitry, with respect to early (8–13 gestational weeks, GW), mid (16–19 GW), and late (23–26 GW) fetal stages. The authors reanalyzed two publicly available single-cell RNA sequencing (scRNA-seq) datasets (Zhong et al., 2018; Bhaduri et al., 2021), by using advanced computational approaches including CellRank for cellular trajectory reconstruction (Lange et al., 2022), the partition-based graph abstraction (PAGA) method for cell fate connectivity (Wolf et al., 2019), and the iQcell platform for gene regulatory network dissection (Heydari et al., 2022). The authors present and discuss cellular trajectories for neuronal and oligodendroglial lineages and key drivers of cell fate decisions, as well as novel TF regulatory networks [e.g., SOX8/SOX10-driven gene expression programs for the oligodendrocyte progenitor cell (OPC) lineage (Stolt et al., 2005; Garcia-Leon et al., 2018)]. They concluded that the precise characterization of the cellular and molecular heterogeneity of the developing and mature human cortex is essential to understanding brain functions and regulation, and to identifying the causes and potential interventions for neurodevelopmental and neurological disorders.

Cell state transitions and the underlying transcriptional regulatory mechanisms during the neural induction stage were studied *in vitro* by Gupta et al.. They performed a longitudinal analysis of the transcriptome of human induced pluripotent stem cells (hiPSC), as these cells were undergoing 8-day neural induction (Shi et al., 2012; Lee et al., 2020). The authors identified distinct functional modules by following the temporal dynamics of key TFs (e.g., OTX2, KEAP and NRF2), and subsequent changes in the expression profiles of their target genes. These modules are related to the transition whereby pluripotency is lost as distinct neural identity is gained, cell cycle progression, metabolic reprogramming, stress response, and genome integrity. Some of the modules may operate throughout the entire initiating process, but they may use different gene signatures. Finally, the authors focused their attention on the precociously expressed TF OTX2 (Rath et al., 2006; Acampora et al., 2013), for which they propose diverse mechanisms throughout the neural induction stage. This was validated by knocking down *OTX2* expression by CRISPRi prior to neural induction. The authors emphasize the widespread remodeling of the whole cell that takes place during the induction of one specific lineage.

The hiPSC model was also used by Schuster et al. to study GABAergic interneuron development and function in the Mowat-Wilson syndrome (MWS). This epileptic neurodevelopmental disorder is caused by heterozygous variants in the *ZEB2* gene, which encodes the TF ZEB2 (Mowat et al., 1998; Zweier et al., 2002). Inhibitory cortical and hippocampal GABAergic neurons require a functional ZEB2 for correct migration and differentiation, to maintain hence a balanced overall neuronal activity (Miquelajauregui et al., 2007; Van Den Berghe et al., 2013). In this original article, the authors confirm that ZEB2 haploinsufficiency alters the GABAergic fate trajectory and its function. They transcriptomically compared hiPSC lines derived from fibroblasts of two related MWS subjects carrying the heterozygous non-sense variant c.1027C>T (p.Arg343*) in exon 8, with those from two healthy donors. The authors used a 65-day protocol that started with neural induction and concluded with GABAergic differentiation (Schuster et al., 2019). Dysregulation of specific genes related to transcription control, cell fate decisions and patterning, and epilepsy, is presented and discussed. Mixed cell identities to the detriment of the GABAergic neuron type, impaired migration of neural stem cells (NSC), and altered electrophysiological properties of differentiated GABAergic interneurons, were found. This finding has led the authors to propose their data (and the *in vitro* MWS model) as a framework for further study to better understand the underlying cellular and molecular basis behind the neuropathogenesis and seizures in MWS, that could potentially lead to interventions of the disease.

Arcuschin et al. contributed to this Research Topic with a mini review that links mechanisms of robustness with neurodevelopment. The robustness of a biological system is defined as its ability to buffer internal and external perturbations, generated by genetic and epigenetic variations, molecular noises or environmental fluctuations, in favor of promoting a reliable output or a particular phenotype (Barkai and Shilo, 2007; Felix and Wagner, 2008). Neurodevelopment in multicellular organisms involves complex signaling interactions between participating cells, as they develop (Silbereis et al., 2016). Fluctuations in these signals may impact gene regulatory networks (GRN) that control cell type trajectories and patterning, as well as other aspects not discussed in this article. Therefore, robustness strategies are essential during normal neural development. First, the authors compare the concept of robustness with the lack of phenotype variability. Next, they present the developing nervous system, with its cellular heterogeneity, sequential cell type genesis (neurogenesis followed by gliogenesis), and broad spectrum of internal and external regulatory signals [e.g., gradients of morphogens such as Shh (Sagner and Briscoe, 2017)], as a model to study and define mechanisms of robustness. At the transcriptional level, the authors address the redundancy of TFs due to gene duplication [e.g., Gsx1 and Gsx2 (Chapman et al., 2018)], as well as the presence of multiple TF binding sites within a specific enhancer and multiple enhancers for the expression of a particular gene (e.g., *Shh*, *Krox20*, and *Pax3*), as mechanisms to buffer perturbations during neurodevelopment. In addition, they present miRNAs [e.g., miR-9a for the Senseless TF (Cassidy et al., 2013)], and the chromatin conformation and promoter architecture, as having roles that contribute to gene expression robustness. At a higher and more complex level (from cells to systems), the authors consider the robustness of interlocking GRNs, as well as the influence of cell-to-cell interactions. Finally, the authors discuss how alterations in

robustness mechanisms, or their surpassing by excessive disruptors, may lead to neurodevelopmental disorders including microcephaly, FXS (fragile X syndrome), and ASD (autism spectrum disorder).

The potential association of FXTAS with variations in the human *AQP4* gene was studied by Elias-Mas et al.. Aquaporin 4 (AQP4) is a highly expressed brain water channel that is essential for fluid homeostasis (Szczygielski et al., 2021). In fact, the dysfunction of AQP4 has been related to several degenerative conditions including Alzheimer's (AD) disease and Parkinson's (PD) disease (Mader and Brimberg, 2019). FXTAS (fragile X-associated tremor/ataxia syndrome) is also a neurogenerative disease with a late onset and impaired motor and cognitive functions. FXTAS is linked to *FMR1* gene premutations (55–200 CGGs) (Cabal-Herrera et al., 2020). Not all *FMR1* premutation carriers, however, present clinical symptoms. An investigative search to identify additional risk factors led the authors to conduct this study. Elias-Mas et al. compared the frequency of seven disease-related single nucleotide polymorphisms (SNP) across the *AQP4* gene in both FXTAS and non-FXTAS individuals, by genotyping 160 *FMR1* premutation Caucasian carriers (59% were clinically positive for FXTAS). No significant association with the risk of developing FXTAS was found for any of the analyzed SNPs neither for the major and minor allele haplotypes (HTMa and HTMi); conclusion that was maintained after correction by multiple tests. The authors discuss the limitations of their study regarding sample sizes and age differences between FXTAS and non-FXTAS groups. They also stated the need to further study AQPs and the glymphatic system, to either confirm or discard their involvement in FXTAS initiation and its progression.

Regarding genetic defects and developmental abnormalities, Bernardinelli et al. present two novel sequence variants of *POU3F4*: g.5284delA and g.6045T>A, which encode truncated protein products of the TF POU3F4, p.S74Afs*8 and p.C327*, respectively. These mutations were identified by genotyping two male Caucasian subjects, who had been diagnosed with typical hallmarks of POU3F4-related hearing loss [incomplete partition of the cochlea type 3 and enlarged vestibular aqueduct (Roesch et al., 2021)]. The authors studied the pathogenicity of these novel sequences in cell-based assays, by analyzing their subcellular distribution and transcriptional activity. Of these defective proteins, only p.C327* did successfully reach the cell nucleus, which was explained by the presence of two of the three nuclear localization signals (NLS) predicted in the wild type (WT) POU3F4. However, it was noted that the spatial pattern of the nuclear p.C327* was different than that of the WT POU3F4. In addition, both variants failed to properly activate the expression of a reporter gene and to enhance the transcription of POU3F4-driven genes, which were identified by RNA-seq under the influence of the WT TF. Among these genes, the authors selected *SLC6A20* for further analysis due to the essential function of SLC6A20 as an amino acid transporter, as well as the association that this class of transporters has with some pathologies, notably hearing loss and cognitive impairment (Swarna et al., 2004; Takanaga et al., 2005; Broer et al., 2008). However, a straightforward correlation between genotypes and phenotypes was not found in these individuals, suggesting that a higher level of complexity may be involved.

Kaltschmidt et al. address the human genetics of NF-kappa B signaling, as it applies to neurodegenerative diseases and malignant brain tumors. Although the NF-κB family of TFs has been extensively involved in inflammation and cancer, it is also well-accepted that it influences a broad range of cellular processes, including within the nervous system (Kaltschmidt and Kaltschmidt, 2009). NF-κB functions are executed via a selection of canonical, non-canonical and atypical pathways (Kaltschmidt et al., 2021), all of which are concisely presented in this article. Then, the authors discuss the synaptic location of NF-κB in certain brain regions (e.g., cerebellum, cortex, and hippocampus), and its retrograde transport from the synapsis to the cell nucleus. The authors suggest that these characteristics might make NF-κB a suitable messenger to communicate feedback for regulating gene expression, which could contribute to synaptic plasticity (Kandel, 2001). Additional related topics are introduced, including a comparison of constitutive vs. inducible NF-κB activities in glutamatergic neurons, and animal models to study the impact of altered NF-κB signaling in learning and memory, and in brain regeneration. In their discussion of the pathophysiology and genetics of both AD and PD, and how they are impacted by the TNFα/NF-κB pathway, the authors propose new target genes, as well as new theories and hypotheses (Snow and Albensi, 2016; Panicker et al., 2021; Bellenguez et al., 2022). Finally, the authors summarize current knowledge related to NF-κB signaling and glioblastoma multiforme (GBM), in terms of growth, invasiveness, and angiogenesis (Smith et al., 2008; Wang et al., 2021). The authors conclude that the recent genetic evidence around the NF-κB pathway may lead to new research and therapeutic approaches for treating neurodegenerative diseases and brain tumors.

Maurya et al. contributed to this RT with an extensive review about microglia, and their involvement in brain development, homeostasis, diseases, and therapeutics. The authors discuss the origin of these innate immune cells (Sierra et al., 2016), and the mechanisms of their interaction with both neurons and non-neuronal cells, including those mediated by exosomes (Muñoz, 2018, 2022; Kalluri and Lebleu, 2020; Guo et al., 2021; Hazrati et al., 2022). Key genes in microglia biology are discussed, as well as their regulation and dysregulation, especially related to several pathological conditions [e.g., AD, PD, multiple sclerosis (MS) and neurodevelopmental diseases]. Included among these genes, are those that encode the TFs PU.1, Sall1, and NF-κB (Smith et al., 2013; Frakes et al., 2014; Buttgereit et al., 2016; Cakir et al., 2022). Additionally, current knowledge and perspectives are discussed about the use of microglia as a target for the diagnosis, monitoring and treatment of diverse pathologies.

Circadian rhythms of physiological and behavioral processes are the result of a proper communication between cells and timing cues (*Zeitgebers*; e.g., environmental light). At the molecular level, the circadian intracellular machinery consists of interlocking transcriptional-translational feedback loops (TTFL) controlled by clock genes (CG), which encode activating and inhibitory TFs [e.g., Clock, Bmal1, Pers and Crys (Hastings et al., 2018)]. These TFs operate in a time-synchronized manner via binding to specific sequences [e.g., E-box (Muñoz et al., 2002, 2006; Muñoz and Baler, 2003)], present in the regulatory regions of their target genes. These genes are known as clock-controlled genes (CCG), and they are

involved in a broad range of cellular functions. In this Research Topic, Fagiani et al. review current knowledge related to the circadian molecular machinery within different brain regions and within different brain cell types, including neurons, astrocytes, and microglia (Hayashi et al., 2013; Brancaccio et al., 2017; Wang et al., 2020). The authors discuss the bidirectional interplay between the core circadian clock and various neurotransmitters [e.g., dopamine, serotonin, noradrenaline, glutamate, and GABA (Miyamoto et al., 2012; Korshunov et al., 2017; Maejima et al., 2021)], and its impact on neuronal activity and the daily timekeeping of brain functions. Discussion is included about circadian alterations in adverse contexts [e.g., AD and PD (Breen et al., 2014; Videnovic et al., 2014)]. Furthermore, they predict that a deeper understanding of the space/time/sex-dependent circadian control of brain physiology may lead to a better comprehension of circadian disruptions in the onset and progression of natural aging, as well as neurological and neurodegenerative diseases and their remedies.

Regulation (and dysregulation) by microRNAs represent a promising avenue in nervous system-related diseases, especially as biomarkers and as prognostic tools (Romano et al., 2017; Elshelmani et al., 2020, 2021). In their original article, Aggio-Bruce et al. reveal an early serum microRNA signature of retinal regression. The authors used samples from both a pre-clinical photo-oxidative damage (PD) mouse model (Natoli et al., 2016), and patients who were clinically diagnosed with either early age-related macular degeneration (AMD) (Wu et al., 2016) or late-stage AMD (Holz et al., 2017). Respective controls were used for each sample group. The expression of ∼800 miRNAs was measured using OpenArray™, and differential abundance from controls was determined using the HTqPCR R package followed by pathway analysis with the DAVID functional annotation tool. The results showed that the altered circulating microRNAs correlated well with human retina pathology. Overlapping animal and human data led the authors to define a preliminary microRNA panel with higher stringency. Some of these microRNAs (e.g., let-7i/g-5p, miR-26a-5p, miR-19a-3p and miR-574-3p) may represent good candidates for early diagnosis of AMD before vision is lost. The authors also discuss similarities and discrepancies between their data and those previously published (Szemraj et al., 2015; Ren et al., 2017).

Overall, the original research and review articles of this second volume illustrate the complexity behind a healthy and diseased nervous system, and how TFs and transcription regulation are essential in pacing its development and functions. We expect this Research Topic will encourage researchers to delve deeper into the role of TFs and transcription regulation in homeostatic and adverse conditions. There is potential here to uncover novel biomarkers that could lead to new prognostic tools and new therapeutic remedies.

Author contributions

EM: Writing—original draft, Writing—review and editing. VM: Writing—review and editing.

Funding

EM is a member of the CONICET scientific career at IHEM-UNCuyo-CONICET, Mendoza, Argentina. Supported by grants from ANPCyT (Argentina; PICT 2017-499; PICT 2021-314; http://www.agencia.mincyt.gob.ar), and CONICET (Argentina; PUE 2017; http://www.conicet.gov.ar). VM is Professor in the Department of Pathology and Laboratory Medicine, UC Davis School of Medicine, Sacramento, USA. Supported by grants from NIMH and NINDS (USA; RO1 MH094681; https://www.nimh.nih.gov; RO1 NS107131; https://www.ninds.nih.gov).

Acknowledgments

We thank Urs Albrecht (Université de Fribourg, Switzerland), Wolfgang Baehr (University of Utah, United States), Isabel Varela-Nieto (Spanish National Research Council-CSIC, Spain), Jun Yan (University of Queensland, Australia), and Yuchio Yanagawa (Gunma University, Japan), who edited five of the eleven articles included in this RT. We also thank Raymond D. Astrue for editing the Editorial.

Conflict of interest

The authors declare that the research was conducted in the absence of any commercial or financial relationships that could be construed as a potential conflict of interest.

The author(s) declared that they were an editorial board member of Frontiers, at the time of submission. This had no impact on the peer review process and the final decision.

Publisher's note

References

Acampora, D., Giovannantonio, D. i., and Simeone, L. G. (2013). Otx2 is an intrinsic determinant of the embryonic stem cell state and is required for transition to a stable epiblast stem cell condition. *Development* 140, 43–55. doi: 10.1242/dev.085290

Alexander, T., Nolte, C., and Krumlauf, R. (2009). Hox genes and segmentation of the hindbrain and axial skeleton. *Annu. Rev. Cell Dev. Biol.* 25, 431–56. doi: 10.1146/annurev.cellbio.042308.113423

Barkai, N., and Shilo, B. Z. (2007). Variability and robustness in biomolecular systems. *Mol. Cell* 28, 755–60. doi: 10.1016/j.molcel.2007.11.013

Bellenguez, C., Kucukali, F., Jansen, I. E., Kleineidam, L., Moreno-Grau, S., Amin, N., et al. (2022). New insights into the genetic etiology of Alzheimer's disease and related dementias. *Nat. Genet.* 54, 412–436. doi: 10.1038/s41588-022-01024-z

Bhaduri, A., Sandoval-Espinosa, C., Otero-Garcia, M., Oh, I., Yin, R., Eze, U. C., et al. (2021). An atlas of cortical arealization identifies dynamic molecular signatures. *Nature* 598, 200–204. doi: 10.1038/s41586-021-03910-8

Brancaccio, M., Patton, A. P., Chesham, J. E., Maywood, E. S., and Hastings, M. H. (2017). Astrocytes control circadian timekeeping in the suprachiasmatic nucleus via glutamatergic signaling. *Neuron* 93, 1420–1435. e5. doi: 10.1016/j.neuron.2017.02.030

Breen, D. P., Vuono, R., Nawarathna, U., Fisher, K., Shneerson, J. M., Reddy, A. B., et al. (2014). Sleep and circadian rhythm regulation in early Parkinson disease. *JAMA Neurol.* 71, 589–595. doi: 10.1001/jamaneurol.2014.65

Broer, S., Bailey, C. G., Kowalczuk, S., Ng, C., Vanslambrouck, J. M., Rodgers, H., et al. (2008). Iminoglycinuria and hyperglycinuria are discrete human phenotypes resulting from complex mutations in proline and glycine transporters. *J. Clin. Invest.* 118, 3881–92. doi: 10.1172/JCI36625

Buttgereit, A., Lelios, I., Yu, X., Vrohlings, M., Krakoski, N. R., Gautier, E. L., et al. (2016). Sall1 is a transcriptional regulator defining microglia identity and function. *Nat. Immunol.* 17, 1397–1406. doi: 10.1038/ni.3585

Cabal-Herrera, A. M., Tassanakijpanich, N., Salcedo-Arellano, M. J., and Hagerman, R. J. (2020). Fragile X-associated tremor/ataxia syndrome (FXTAS): pathophysiology and clinical implications. *Int. J. Mol. Sci.* 21, 91. doi: 10.3390/ijms21124391

Cadwell, C. R., Bhaduri, A., Mostajo-Radji, M. A., Keefe, M. G., and Nowakowski, T. J. (2019). Development and arealization of the cerebral cortex. *Neuron* 103, 980–1004. doi: 10.1016/j.neuron.2019.07.009

Cakir, B., Tanaka, Y., Kiral, F. R., Xiang, Y., Dagliyan, O., Wang, J., et al. (2022). Expression of the transcription factor PU.1 induces the generation of microglia-like cells in human cortical organoids. *Nat. Commun.* 13, 430. doi: 10.1038/s41467-022-28043-y

Cassidy, J. J., Jha, A. R., Posadas, D. M., Giri, R., Venken, K. J., Ji, J., et al. (2013). miR-9a minimizes the phenotypic impact of genomic diversity by buffering a transcription factor. *Cell* 155, 1556–67. doi: 10.1016/j.cell.2013.10.057

Chapman, H., Riesenberg, A., Ehrman, L. A., Kohli, V., Nardini, D., Nakafuku, M., et al. (2018). Gsx transcription factors control neuronal versus glial specification in ventricular zone progenitors of the mouse lateral ganglionic eminence. *Dev. Biol.* 442, 115–126. doi: 10.1016/j.ydbio.2018.07.005

Elshelmani, H., Wride, M. A., Saad, T., Rani, S., Kelly, D. J., Keegan, D., et al. (2020). Identification of novel serum microRNAs in age-related macular degeneration. *Transl. Vis. Sci. Technol.* 9, 28. doi: 10.1167/tvst.9.4.28

Elshelmani, H., Wride, M. A., Saad, T., Rani, S., Kelly, D. J., Keegan, D., et al. (2021). The role of deregulated microRNAs in age-related macular degeneration pathology. *Transl. Vis. Sci. Technol.* 10, 12. doi: 10.1167/tvst.10.2.12

Felix, M. A., and Wagner, A. (2008). Robustness and evolution: concepts, insights and challenges from a developmental model system. *Heredity* 100, 132–40. doi: 10.1038/sj.hdy.6800915

Frakes, A. E., Ferraiuolo, L., Haidet-Phillips, A. M., Schmelzer, L., Braun, L., Miranda, C. J., et al. (2014). Microglia induce motor neuron death via the classical NF-kappaB pathway in amyotrophic lateral sclerosis. *Neuron* 81, 1009–1023. doi: 10.1016/j.neuron.2014.01.013

Garcia-Leon, J. A., Kumar, M., Boon, R., Chau, D., One, J., Wolfs, E. W. S., et al. (2018). SOX10 single transcription factor-based fast and efficient generation of oligodendrocytes from human pluripotent stem cells. *Stem Cell Rep.* 10, 655–672. doi: 10.1016/j.stemcr.2017.12.014

Guo, M., Hao, Y., Feng, Y., Li, H., Mao, Y., Dong, Q., et al. (2021). Microglial exosomes in neurodegenerative disease. *Front. Mol. Neurosci.* 14, 630808. doi: 10.3389/fnmol.2021.630808

Hastings, M. H., Maywood, E. S., and Brancaccio, M. (2018). Generation of circadian rhythms in the suprachiasmatic nucleus. *Nat. Rev. Neurosci.* 19, 453–469. doi: 10.1038/s41583-018-0026-z

Hayashi, Y., Koyanagi, S., Kusunose, N., Okada, R., Wu, Z., Tozaki-Saitoh, H., et al. (2013). The intrinsic microglial molecular clock controls synaptic strength via the circadian expression of cathepsin S. *Sci. Rep.* 3, 2744. doi: 10.1038/srep02744

Hazrati, A., Soudi, S., Malekpour, K., Mahmoudi, M., Rahimi, A., Hashemi, S. M., et al. (2022). Immune cells-derived exosomes function as a double-edged sword: role in disease progression and their therapeutic applications. *Biomark Res.* 10, 30. doi: 10.1186/s40364-022-00374-4

Hernandez-Miranda, L. R., and Birchmeier, C. (2015). CO(2) in the spotlight. *Elife* 4, 86. doi: 10.7554/eLife.08086

Hernandez-Miranda, L. R., Ibrahim, D. M., Ruffault, P. L., Larrosa, M., Balueva, K., Muller, T., et al. (2018). Mutation in LBX1/Lbx1 precludes transcription factor cooperativity and causes congenital hypoventilation in humans and mice. *Proc. Natl. Acad. Sci. USA.* 115, 13021–13026. doi: 10.1073/pnas.1813520115

Hernandez-Miranda, L. R., Ruffault, P. L., Bouvier, J. C., Murray, A. J., Morin-Surun, M. P., Zampieri, N., et al. (2017). Genetic identification of a hindbrain nucleus essential for innate vocalization. *Proc. Natl. Acad. Sci. USA.* 114, 8095–8100. doi: 10.1073/pnas.1702893114

Heydari, T. M, A. L., Fisher, C. L., Aguilar-Hidalgo, D., Shukla, S., Yachie-Kinoshita, A., Hughes, M., et al. (2022). IQCELL: a platform for predicting the effect of gene perturbations on developmental trajectories using single-cell RNA-seq data. *PLoS Comput. Biol.* 18, e1009907. doi: 10.1371/journal.pcbi.1009907

Holz, F. G., Sadda, S. R., Staurenghi, G., Lindner, M., Bird, A. C., Blodi, B. A., et al. (2017). Imaging protocols in clinical studies in advanced age-related macular degeneration: recommendations from classification of atrophy consensus meetings. *Ophthalmology* 124, 464–478. doi: 10.1016/j.ophtha.2016.12.002

Isik, E. G., and Hernandez-Miranda, L. R. (2022). Early development of the breathing network. *Handb. Clin. Neurol.* 188, 125–149. doi: 10.1016/B978-0-323-91534-2.00002-3

Kalluri, R., and Lebleu, V. S. (2020). The biology, function, and biomedical applications of exosomes. *Science* 367, 6977. doi: 10.1126/science.aau6977

Kaltschmidt, B., and Kaltschmidt, C. (2009). NF-kappaB in the nervous system. *Cold Spring Harb. Perspect. Biol.* 1, a001271. doi: 10.1101/cshperspect.a001271

Kaltschmidt, C., Greiner, J. F. W., and Kaltschmidt, B. (2021). The transcription factor NF-kappaB in stem cells and development. *Cells* 10, 2024. doi: 10.3390/cells10082042

Kandel, E. R. (2001). The molecular biology of memory storage: a dialogue between genes and synapses. *Science* 294, 1030–8. doi: 10.1126/science.1067020

Korshunov, K. S., Blakemore, L. J., and Trombley, P. Q. (2017). Dopamine: A Modulator of Circadian Rhythms in the Central Nervous System. *Front. Cell. Neurosci.,* 11, 91. doi: 10.3389/fncel.2017.00091

Lange, M., Bergen, V., Klein, M., Setty, M., Reuter, B., Bakhti, M. Pe'er, D., et al. (2022). CellRank for directed single-cell fate mapping. *Nat. Methods* 19, 159–170. doi: 10.1038/s41592-021-01346-6

Lee, H., Nowosiad, P., Dutan Polit, L. M., Price, J., Srivastava, D. P., Thuret, S., et al. (2020). Apolipoprotein E expression pattern in human induced pluripotent stem cells during *in vitro* neural induction. *F1000Res* 9, 353. doi: 10.12688/f1000research.23580.1

Lowenstein, E. D., Cui, K., and Hernandez-Miranda, L. R. (2023). Regulation of early cerebellar development. *FEBS J.* 290, 2786–2804. doi: 10.1111/febs.16426

Mader, S., and Brimberg, L. (2019). Aquaporin-4 water channel in the brain and its implication for health and disease. *Cells* 8, 90. doi: 10.3390/cells8020090

Maejima, T., Tsuno, Y., Miyazaki, S., Tsuneoka, Y., Hasegawa, E., Islam, M. T., et al. (2021). GABA from vasopressin neurons regulates the time at which suprachiasmatic nucleus molecular clocks enable circadian behavior. *Proc. Natl. Acad. Sci. USA.* 3, 118. doi: 10.1073/pnas.2010168118

Miquelajauregui, A., Van De Putte, T., Polyakov, A., Nityanandam, A., Boppana, S., Seuntjens, E., et al. (2007). Smad-interacting protein-1 (Zfhx1b) acts upstream of Wnt signaling in the mouse hippocampus and controls its formation. *Proc. Natl. Acad. Sci. USA.* 104, 12919–24. doi: 10.1073/pnas.0609863104

Miyamoto, H., Nakamaru-Ogiso, E., Hamada, K., and Hensch, T. K. (2012). Serotonergic integration of circadian clock and ultradian sleep-wake cycles. *J. Neurosci.* 32, 14794–803. doi: 10.1523/JNEUROSCI.0793-12.2012

Mowat, D. R., Croaker, G. D., Cass, D. T., Kerr, B. A., Chaitow, J., Ades, L. C., et al. (1998). Hirschsprung disease, microcephaly, mental retardation, and characteristic facial features: delineation of a new syndrome and identification of a locus at chromosome 2q22-q23. *J. Med. Genet.* 35, 617–23. doi: 10.1136/jmg.35.8.617

Muñoz, E., and Baler, R. (2003). The circadian E-box: when perfect is not good enough. *Chronobiol. Int.* 20, 371–88. doi: 10.1081/CBI-120022525

Muñoz, E., Brewer, M., and Baler, R. (2002). Circadian transcription. Thinking outside the E-Box. *J. Biol. Chem.* 277, 36009–17. doi: 10.1074/jbc.M203909200

Muñoz, E., Brewer, M., and Baler, R. (2006). Modulation of BMAL/CLOCK/E-Box complex activity by a CT-rich cis-acting element. *Mol. Cell. Endocrinol.* 252, 74–81. doi: 10.1016/j.mce.2006.03.007

Muñoz, E. M. (2018). Microglia-precursor cell interactions in health and in pathology. *Biocell* 42, 41–45. doi: 10.32604/biocell.2018.07011

Muñoz, E. M. (2022). Microglia in circumventricular organs: the pineal gland example. *ASN Neuro.* 14, 17590914221135697. doi: 10.1177/17590914221135697

Muñoz, E. M., Martinez Cerdeño, V., De Souza, F. S. J., Rath, M. F. eds. (2022). Transcription regulation—Brain Development and Homeostasis—A finely tuned and orchestrated scenario in physiology and pathology. *Front. Media SA.* 4, 2. doi: 10.3389./978-2-88974-457-2

Muñoz, E. M., Souza, D. e., and Rath, F. S. J. M. F., and Martinez Cerdeño, V. (2021). Editorial: transcription regulation-brain development and homeostasis-a finely tuned and orchestrated scenario in physiology and pathology. *Front. Mol. Neurosci.* 14, 834607. doi: 10.3389/fnmol.2021.834607

Natoli, R., Jiao, H., Barnett, N. L., Fernando, N., Valter, K., Provis, J. M., et al. (2016). A model of progressive photo-oxidative degeneration and inflammation in the pigmented C57BL/6J mouse retina. *Exp. Eye Res.* 147, 114–127. doi: 10.1016/j.exer.2016.04.015

Panicker, N., Ge, P., Dawson, V. L., and Dawson, T. M. (2021). The cell biology of Parkinson's disease. *J. Cell Biol.* 220, 95. doi: 10.1083/jcb.202012095

Rath, M. F., Muñoz, E., Ganguly, S., Morin, F., Shi, Q., Klein, D. C., et al. (2006). Expression of the Otx2 homeobox gene in the developing mammalian brain:

embryonic and adult expression in the pineal gland. *J. Neurochem.* 97, 556–66. doi: 10.1111/j.1471-4159.2006.03773.x

Ren, C., Liu, Q., Wei, Q., Cai, W., He, M., Du, Y., et al. (2017). Circulating miRNAs as potential biomarkers of age-related macular degeneration. *Cell. Physiol. Biochem.* 41, 1413–1423. doi: 10.1159/000467941

Roesch, S., Rasp, G., Sarikas, A., and Dossena, S. (2021). Genetic determinants of non-syndromic enlarged vestibular aqueduct: a review. *Audiol. Res.* 11, 423–442. doi: 10.3390/audiolres11030040

Romano, G. L., Platania, C. B. M., Drago, F., Salomone, S., Ragusa, M., Barbagallo, C. A., et al. (2017). Retinal and circulating miRNAs in age-related macular degeneration: an *in vivo* animal and human study. *Front. Pharmacol.* 8, 168. doi: 10.3389/fphar.2017.00168

Sagner, A., and Briscoe, J. (2017). Morphogen interpretation: concentration, time, competence, and signaling dynamics. *Wiley Interdiscip. Rev. Dev. Biol.* 6, 271. doi: 10.1002/wdev.271

Schuster, J., Sobol, M., Fatima, A., Khalfallah, A., Laan, L., Anderlid, B. M., et al. (2019). Mowat-Wilson syndrome: generation of two human iPS cell lines (UUIGPi004A and UUIGPi005A) from siblings with a truncating ZEB2 gene variant. *Stem Cell Res.* 39, 101518. doi: 10.1016/j.scr.2019.101518

Shi, Y., Kirwan, P., and Livesey, F. J. (2012). Directed differentiation of human pluripotent stem cells to cerebral cortex neurons and neural networks. *Nat. Protoc.* 7, 1836–46. doi: 10.1038/nprot.2012.116

Sierra, A., Castro, De., Del Rio-Hortega, F., Rafael Iglesias-Rozas, J., Garrosa, J. M., and Kettenmann, H. (2016). The "Big-Bang" for modern glial biology: translation and comments on Pio del Rio-Hortega 1,919 series of papers on microglia. *Glia* 64, 1801–40. doi: 10.1002/glia.23046

Silbereis, J. C., Pochareddy, S., Zhu, Y., Li, M., and Sestan, N. (2016). The cellular and molecular landscapes of the developing human central nervous system. *Neuron* 89, 248–68. doi: 10.1016/j.neuron.2015.12.008

Smith, A. M., Gibbons, H. M., Oldfield, R. L., Bergin, P. M., Mee, E. W., Faull, R. L., et al. (2013). The transcription factor PU.1 is critical for viability and function of human brain microglia. *Glia* 61, 929–42. doi: 10.1002/glia.22486

Smith, D., Shimamura, T., Barbera, S., and Bejcek, B. E. (2008). NF-kappaB controls growth of glioblastomas/astrocytomas. *Mol. Cell. Biochem.* 307, 141–7. doi: 10.1007/s11010-007-9593-4

Snow, W. M., and Albensi, B. C. (2016). Neuronal gene targets of NF-kappaB and their dysregulation in Alzheimer's disease. *Front. Mol. Neurosci.* 9, 118. doi: 10.3389/fnmol.2016.00118

Stolt, C. C., Schmitt, S., Lommes, P., Sock, E., and Wegner, M. (2005). Impact of transcription factor Sox8 on oligodendrocyte specification in the mouse embryonic spinal cord. *Dev. Biol.* 281, 309–17. doi: 10.1016/j.ydbio.2005.03.010

Swarna, M., Jyothy, A., Usha Rani, P., and Reddy, P. P. (2004). Amino acid disorders in mental retardation: a two-decade study from Andhra Pradesh. *Biochem. Genet.* 42, 85–98. doi: 10.1023/B:BIGI.0000020464.05335.79

Szczygielski, J., Kopanska, M., Wysocka, A., and Oertel, J. (2021). Cerebral microcirculation, perivascular unit, and glymphatic system: role of aquaporin-4 as the gatekeeper for water homeostasis. *Front. Neurol.* 12, 767470. doi: 10.3389/fneur.2021.767470

Szemraj, M., Bielecka-Kowalska, A., Oszajca, K., Krajewska, M., Gos, R., Jurowski, P., et al. (2015). Serum microRNAs as potential biomarkers of AMD. *Med. Sci. Monit.* 21, 2734–42. doi: 10.12659/MSM.893697

Takanaga, H., Mackenzie, B., Suzuki, Y., and Hediger, M. A. (2005). Identification of mammalian proline transporter SIT1 (SLC6A20) with characteristics of classical system imino. *J. Biol. Chem.* 280, 8974–84. doi: 10.1074/jbc.M413027200

Van Den Berghe, V., Stappers, E., Vandesande, B., Dimidschstein, J., Kroes, R., Francis, A., et al. (2013). Directed migration of cortical interneurons depends on the cell-autonomous action of Sip1. *Neuron* 77, 70–82. doi: 10.1016/j.neuron.2012.11.009

Videnovic, A., Lazar, A. S., Barker, R. A., and Overeem, S. (2014). 'The clocks that time us'–circadian rhythms in neurodegenerative disorders. *Nat. Rev. Neurol.* 10, 683–93. doi: 10.1038/nrneurol.2014.206

Wang, X. L., Wolff, S. E. C., Korpel, N., Milanova, I., Sandu, C., Rensen, P. C. N., et al. (2020). Deficiency of the circadian clock Gene Bmal1 reduces microglial immunometabolism. *Front. Immunol.* 11, 586399. doi: 10.3389/fimmu.2020.586399

Wang, Y., Yi, K., Liu, X., Tan, Y., Jin, W., Li, Y., et al. (2021). HOTAIR up-regulation activates NF-kappaB to induce immunoescape in gliomas. *Front. Immunol.* 12, 785463. doi: 10.3389/fimmu.2021.785463

Wolf, F. A., Hamey, F. K., Plass, M., Solana, J., Dahlin, J. S., Gottgens, B., et al. (2019). PAGA: graph abstraction reconciles clustering with trajectory inference through a topology preserving map of single cells. *Genome Biol.* 20, 59. doi: 10.1186/s13059-019-1663-x

Wu, Z., Ayton, L. N., Luu, C. D., Baird, P. N., and Guymer, R. H. (2016). Reticular pseudodrusen in intermediate age-related macular degeneration: prevalence, detection, clinical, environmental, and genetic associations. *Invest. Ophthalmol. Vis. Sci.* 57, 1310–6. doi: 10.1167/iovs.15-18682

Zhong, S., Zhang, S., Fan, X., Wu, Q., Yan, L., Dong, J., et al. (2018). A single-cell RNA-seq survey of the developmental landscape of the human prefrontal cortex. *Nature* 555, 524–528. doi: 10.1038/nature25980

Zweier, C., Albrecht, B., Mitulla, B., Behrens, R., Beese, M., Gillessen-Kaesbach, G., et al. (2002). "Mowat-Wilson" syndrome with and without Hirschsprung disease is a distinct, recognizable multiple congenital anomalies-mental retardation syndrome caused by mutations in the zinc finger homeo box 1B gene. *Am. J. Med. Genet.* 108, 177–81. doi: 10.1002/ajmg.10226

frontiers | Frontiers in Molecular Neuroscience

REVIEW
published: 01 July 2022
doi: 10.3389/fnmol.2022.937174

The Circadian Molecular Machinery in CNS Cells: A Fine Tuner of Neuronal and Glial Activity With Space/Time Resolution

Francesca Fagiani[1†], Eva Baronchelli[2†], Anna Pittaluga[3,4], Edoardo Pedrini[1], Chiara Scacchi[2], Stefano Govoni[2] and Cristina Lanni[2,5]*

[1]*Institute of Experimental Neurology, IRCCS San Raffaele Hospital and Vita-Salute San Raffaele University, Milan, Italy,* [2]*Department of Drug Sciences, Pharmacology Section, University of Pavia, Pavia, Italy,* [3]*Department of Pharmacy (DiFar), School of Medical and Pharmaceutical Sciences, University of Genoa, Genoa, Italy,* [4]*Center of Excellence for Biomedical Research, 3Rs Center, University of Genoa, Genoa, Italy,* [5]*Centro 3R (Inter-University Center for the Promotion of the 3Rs Principles in Teaching and Research), Italy*

OPEN ACCESS

Edited by:
Urs Albrecht,
Université de Fribourg, Switzerland

Reviewed by:
Shimon Amir,
Concordia University, Canada
Tomaz Martini,
Swiss Federal Institute of Technology Lausanne, Switzerland

***Correspondence:**
Cristina Lanni
cristina.lanni@unipv.it

[†]These authors have contributed equally to this work

Specialty section:
This article was submitted to Molecular Signalling and Pathways, a section of the journal Frontiers in Molecular Neuroscience

Received: *05 May 2022*
Accepted: *07 June 2022*
Published: *01 July 2022*

Citation:
Fagiani F, Baronchelli E, Pittaluga A, Pedrini E, Scacchi C, Govoni S and Lanni C (2022) The Circadian Molecular Machinery in CNS Cells: A Fine Tuner of Neuronal and Glial Activity With Space/Time Resolution. Front. Mol. Neurosci. 15:937174. doi: 10.3389/fnmol.2022.937174

The circadian molecular machinery is a fine timekeeper with the capacity to harmonize physiological and behavioral processes with the external environment. This tight-knit regulation is coordinated by multiple cellular clocks across the body. In this review, we focus our attention on the molecular mechanisms regulated by the clock in different brain areas and within different cells of the central nervous system. Further, we discuss evidence regarding the role of circadian rhythms in the regulation of neuronal activity and neurotransmitter systems. Not only neurons, but also astrocytes and microglia actively participate in the maintenance of timekeeping within the brain, and the diffusion of circadian information among these cells is fine-tuned by neurotransmitters (e.g., dopamine, serotonin, and γ-aminobutyric acid), thus impacting on the core clock machinery. The bidirectional interplay between neurotransmitters and the circadian clockwork is fundamental in maintaining accuracy and precision in daily timekeeping throughout different brain areas. Deepening the knowledge of these correlations allows us to define the basis of drug interventions to restore circadian rhythms, as well as to predict the onset of drug treatment/side effects that might promote daily desynchronization. Furthermore, it may lead to a deeper understanding of the potential impacts of modulations in rhythmic activities on the pace of aging and provide an insight in to the pathogenesis of psychiatric diseases and neurodegenerative disorders.

Keywords: circadian rhythms, microglia, astrocyte, neurotransmitters, brain areas, neuron

INTRODUCTION

Circadian rhythms are the basis of daily life, enabling the adaptation and adjustment of physiological and behavioral processes—from the brain to the peripheral organs—with the external environment. The entrainment and synchronization of the endogenous circadian oscillator rely on external timing cues, also called *Zeitgebers*, which allow the internal molecular clockwork to align with the environment. Light represents the main external cue that, through the retinohypothalamic tract (RHT; Gooley et al., 2001; Chen et al., 2011), is transmitted to the hypothalamic

suprachiasmatic nucleus (SCN), the master circadian pacemaker (Stephan and Zucker, 1972; Ralph et al., 1990; Hastings et al., 2003). The SCN contains approximately 10,000 neurons, each of them displaying a cell-autonomous circadian clock that is able to coordinate all the other "slave" and peripheral oscillators located in nearly every mammalian organ. Noteworthy, the synchronization of peripheral clocks is not only hierarchically orchestrated by the hypothalamic circadian pacemaker through direct neuronal innervations but also through multiple soluble molecular signals, *i.e.*, daily rhythms of glucocorticoids (Dibner et al., 2010). At the molecular level, the internal cellular clockworks are known as autoregulatory transcriptional–translational feedback loops (TTFLs; as schematized in **Figure 1**). The circadian locomotor output cycles kaput (*Clock*) and the brain and muscle Arnt-like protein 1 (*Bmal1*) are central players in the regulation of this loop. As positive regulators of the circadian cycle, they interact together to form the Clock:Bmal1 heterodimer in the cytoplasm. The latter translocates into the nucleus where it binds the Enhancer Box (E-box) response elements on the promoters of *Period* (*Per1, Per2, Per3*) and *Cryptochrome* (*Cry1, Cry2*), the core clock components of the negative arm of the TTFL (Hastings et al., 2018; Cox and Takahashi, 2019). Upon translation and nuclear accumulation, Per and Cry proteins inhibit the transcriptional activity of Clock:Bmal1 heterodimer. During night-time hours, Per and Cry proteins are progressively phosphorylated by the casein kinase 1ε/δ (CK1ε/δ) and adenosine 3',5'-monophosphate (AMP) kinase (AMPK) respectively, ubiquitinated by their specific E3 ubiquitin ligase complexes, and finally degraded by the proteasome (Shirogane et al., 2005), thus turning off their inhibitory effect on Clock:Bmal1 and allowing for the onset of a new oscillatory cycle (Koike et al., 2012). In addition to the core loop, further regulators are represented by the nuclear receptors *Rev-erbα* (also known as *Nr1d1*), *Rev-erbβ* (also known as *Nr1d2*), and the retinoic acid orphan receptors *Rorα*, *Rorβ*, and *Rorγ* (*Rorα/β/γ*), which together form a second TTFL that steadies the robustness of the main TTFL, by regulating the rhythmic oscillation of *Bmal1* expression throughout the day. In particular, *Rorα/β/γ* positively regulate the transcription of *Bmal1* gene, whereas *Rev-erbα/β* act as transcriptional repressors of its expression, by both competing for binding to Retinoic acid receptor-related Orphan Receptor Element (RORE) sites present on *Bmal1* gene promoter (Preitner et al., 2002; Koike et al., 2012).

At the same time, also the intracellular calcium influx, membrane depolarization, and cAMP signaling, which all follow a daily rhythmical pattern, play a key role in the regulation of the biological transcriptional clock and in the establishment of the neuronal firing rhythms (Lundkvist et al., 2005; O'Neill et al., 2008). Indeed, through a cascade pathway these additional players are able to induce the phosphorylation of the calcium/cAMP response element binding protein (CREB) which, in turn, binds calcium/cAMP regulatory elements (CREs) sequences present on *Per1* and *Per2* gene promoters (Travnickova-Bendova et al., 2002; O'Neill et al., 2008), thus regulating their transcription and creating additional positive feedback loops involved in the generation of daily rhythm.

The pathways described above, however, are not the only mechanisms involved in the generation of rhythm. The TTFL, in fact, regulates the oscillations of approximately 20% of all the genome (Panda et al., 2002). Many other levels of regulation, such as post-transcriptional, translational, and post-translational modifications, play a critical role in coordinating rhythmicity. These modifications impact cellular localization, protein stability, and protein-protein interactions, and are essential for the modulation of multiple biological responses and for the establishment of a fine-tuning rhythmicity (Brenna and Albrecht, 2020). Besides, alterations or mutations of the kinases or on the target sequences responsible for these post-translation modifications can result in several diseases strictly linked to the circadian system, such as sleep disorders, neurodegenerative, and psychiatric diseases, and also cancer (Schwab et al., 2000; Xu et al., 2005; Fang et al., 2015; Brenna and Albrecht, 2020).

Since the circadian molecular machinery acts as a temporal variable, orchestrating a number of physiological functions and processes in the central nervous system (CNS), it is fundamental to acquire an understanding of the molecular mechanisms regulated by the clock in the different brain areas and within the different CNS cells. Therefore, in this review, we aim to critically discuss evidence regarding the role of circadian rhythms in the regulation of neuronal activity and neurotransmitter systems.

THE CIRCADIAN ELECTRICAL ACTIVITY

In the SCN, circadian timekeeping is a dynamic process characterized by reciprocal interactions between the molecular oscillations of the clock machinery and the electrical activity of neurons. TTFLs are able to orchestrate, in a circadian manner, the variations of Na^+ and K^+ currents (Flourakis et al., 2015), as well as the intracellular concentration of Ca^{2+} ($[Ca^{2+}]_i$; Brancaccio et al., 2013), responsible, in turn, for the regulation of neuronal activity. Remarkably, the $[Ca^{2+}]_i$, moving into cells through voltage-operated calcium channels activated by electrical firing (VOOC), NMDA-type glutamate receptors (NMDARs), or released by intracellular stores (Harvey et al., 2020), plays a pivotal role in the modulation of the biological clockwork (Brancaccio et al., 2013). Indeed, the electrical activation due to the peak of $[Ca^{2+}]_i$ triggered by a light signal has been found to induce the expression of *Per1* and *Per2* genes, thereby affecting the expression of the positive TTFL components (Brancaccio et al., 2013). Notably, at circadian time 6 (CT6) light signals induce Ca^{2+} influx and activate a phosphorylation cascade pathway involving the protein kinase A and G (PKA and PKG), the Ca^{2+}/calmodulin-dependent protein kinase (CaMK), the mitogen-activated protein kinases (MAPK) and the extracellular-signal-regulated kinases (ERK). This pathway leads to the phosphorylation of CREB, which, after being activated by the cAMP-regulated transcriptional co-activator 1 (CRTC1), heterodimerizes with the histone acetyltransferase CREB binding protein (CBP) and then, at CT9, binds the CRE sequences present on *Per* gene promoters (Gau et al., 2002; Parra-Damas et al., 2017), leading to the consequent transcription of *Per1 (*at

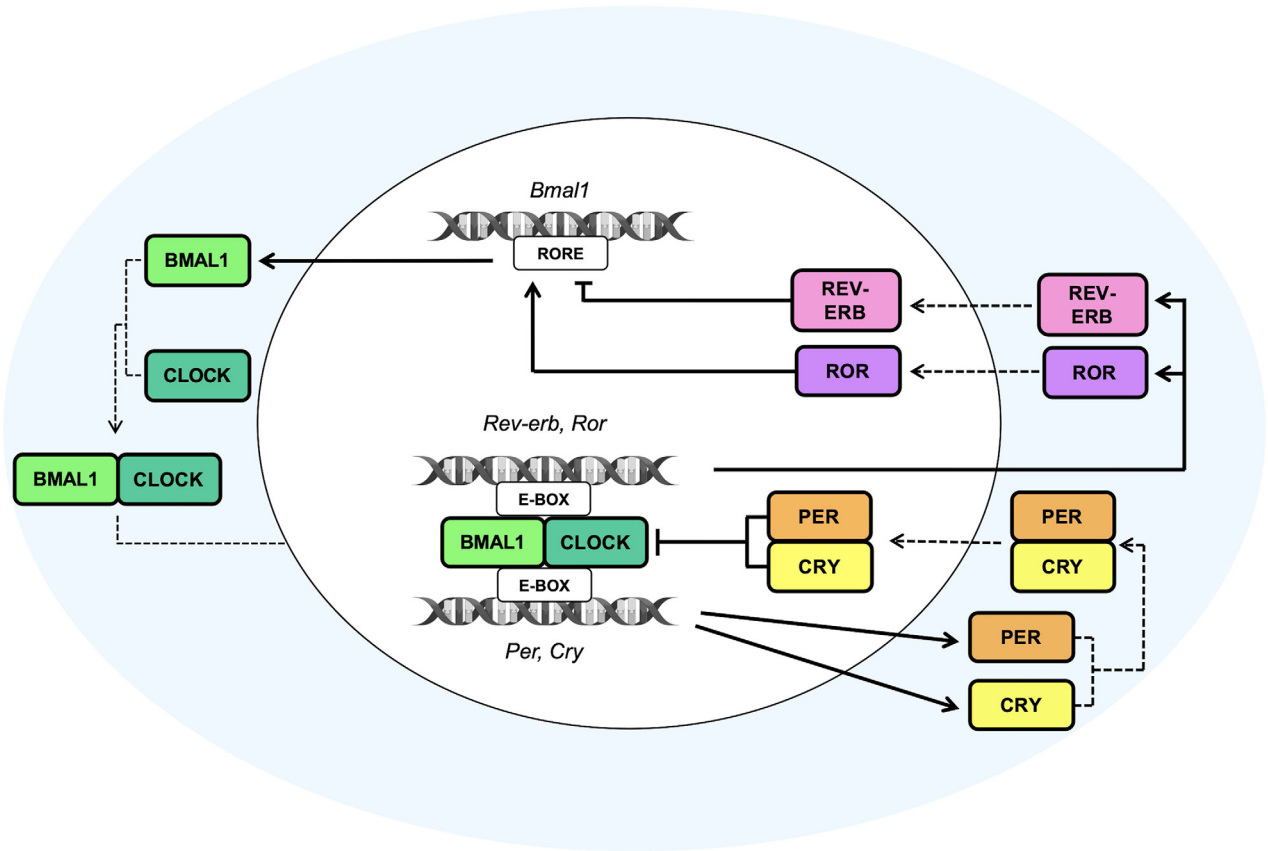

FIGURE 1 | The molecular clock machinery. Schematic view of the molecular transcriptional–translational feedback loops (TTFLs) that coordinate the multiple cellular clocks across the mammalian body. The heterodimeric complexes given by the brain and muscle Arnt-like protein 1 (*Bmal1*) and circadian locomotor output cycles kaput (*Clock*) bind the Enhancer Box response element (E-box) on Period (*Per*) and Cryptochrome (*Cry*) gene promoters to induce the daytime expression of Per and Cry proteins, which, in turn, inhibit the transcriptional activity of Clock:Bmal1 heterodimer. The subsequent nocturnal degradation of Per and Cry proteins suppresses their inhibitory effect on Clock:Bmal1 heterodimer and allows to start a new oscillatory cycle. An additional feedback loop, consisting of the nuclear receptors *Rev-erb* and the retinoic acid orphan receptors *Ror*, is involved in the establishment of the rhythmic expression of *Bmal1* throughout the day. *Ror* and *Rev-erb* are both transcribed by the binding of the heterodimer Clock and Bmal1 to the E-box sequences on their gene promoters. Particularly, *Ror* positively regulates the transcription of the *Bmal1* gene, whereas *Rev-erb* acts as a transcriptional repressor of its expression, by both competing for binding Retinoic acid receptor-related Orphan Receptor Element (RORE) sites present on the *Bmal1* gene promoter. The cooperation and synchronization of all of these loops, that are the basis of the molecular clock machinery, contribute to the generation of daily rhythm.

CT10) and *Per2* (at CT12; Brancaccio et al., 2013). Moreover, Brenna et al. recently demonstrated that Per2 supports the stimulus-dependent induction of the *Per1* gene by regulating the CREB/CRTC1/CBP complex. Accordingly, upon light or forskolin stimuli, Per2 acts as a co-factor of CREB promoting the formation of a transactivation complex on the CRE element of the *Per1* gene. In particular, Per2 has been shown to facilitate the interaction between CREB and its co-regulator CRTC1, thereby inducing complex formation (Brenna et al., 2021).

Furthermore, since the release of $[Ca^{2+}]_i$ follows a circadian pattern orchestrated by the TTFLs, the bidirectional interlink between the clockwork and the neural signaling creates a closed loop that drives the rest-activity cycle of the neuronal activity (Brancaccio et al., 2013; **Figure 2**). These findings demonstrate that TTFL is strongly sensitive to the electrical state, and that the coupling between the clock machinery and Ca^{2+} activity is fundamental for a proper generation of rhythm and for a robust timekeeping within the brain. Hence, the electrical activity seems to play a key role in re-setting the intracellular clock, contributing to the suppression of neuronal activity during the night, and to the induction of a subsequent electrical firing peak with the coming of the next circadian day.

THE CLOCK IN NEUROTRANSMISSION

Data concerning the synthesis and the uptake of neurotransmitters and their correlation with the expression/functions of circadian pacemakers support the role of certain transmitters (*e.g.*, dopamine -DA-, serotonin -5-HT-, and γ-aminobutyric acid -GABA-) as fine-tuners of daily rhythmicity (Terazono et al., 2003; Imbesi et al., 2009; Nakamaru-Ogiso et al., 2012; Barca-Mayo et al., 2017; Brancaccio et al., 2017; Maejima et al., 2021; Palm et al., 2021). Deepening the knowledge of these correlations may lay the foundation of drug interventions aimed

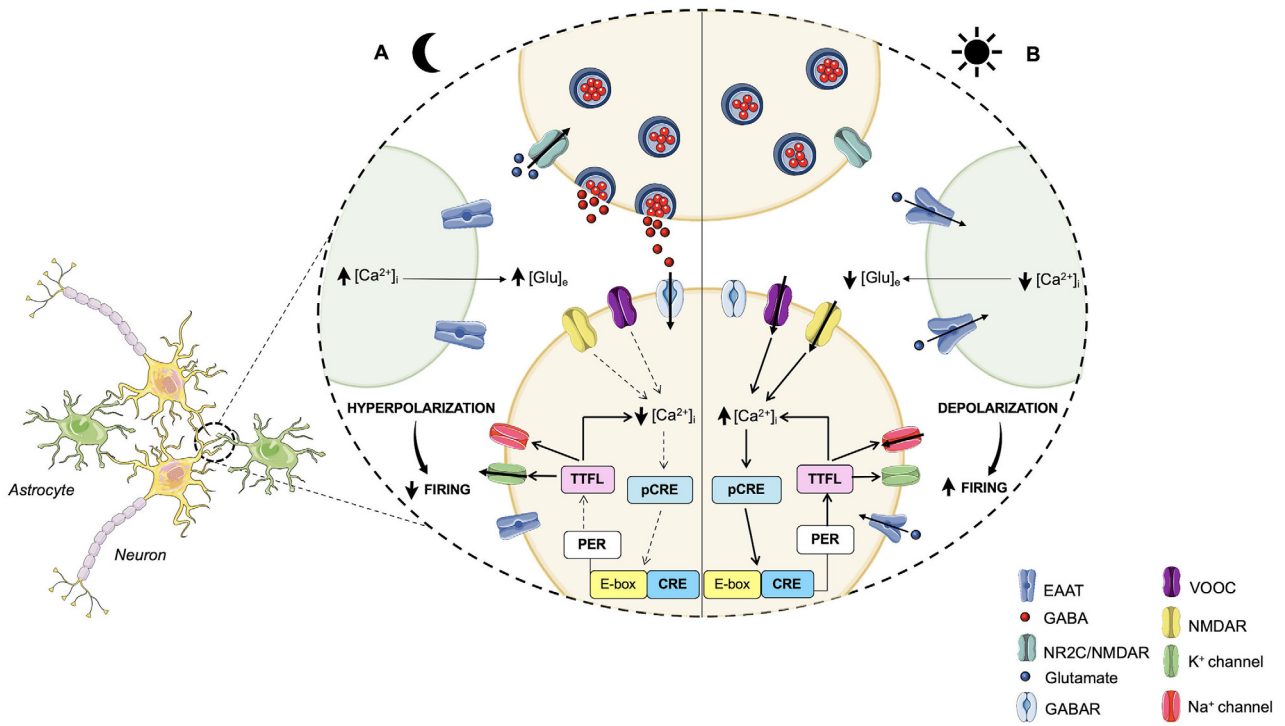

FIGURE 2 | Circadian molecular regulation of neuron-astrocyte crosstalk. The circadian timekeeper in the SCN is dictated by reciprocal interactions between the molecular oscillations of the clock machinery and the electrical activity of neurons, which lead to the establishment of a daily rhythm. **(A)** During the night, astrocytes are active and their $[Ca^{2+}]_i$ is high, leading to an increased release of extracellular Glu, which, in turn, through the NR2C/NMDA receptors, is able to induce the release of GABA from presynaptic neurons. GABA acts on the postsynaptic GABA receptors and exerts its inhibitory effect on neurons that during the night are less active. In fact, the neuronal $[Ca^{2+}]_i$ is low, and, as a result, the loop that impacts the TTFLs is blunted. However, the TTFL activates the K^+conductances, thus leading to a hyperpolarization of the cell membrane and to a dampened firing. **(B)** During the daytime, when astrocytes are quiescent with a low $[Ca^{2+}]_i$, Glu is re-uptaken by astrocytes and neurons and, consequently, its extracellular levels are decreased. On the other hand, neurons are active and neuronal $[Ca^{2+}]_i$, whose oscillations are controlled by the TTFL, is high. The neuronal electrical activity stimulates the activation of the Ca^{2+}/cAMP-responsive elements (CREs) on *Per* genes, thus promoting the transcription of *Per1* and *Per2* genes. Subsequently, the transcription of these TTFL components leads to a further rise in the $[Ca^{2+}]_i$ and to the activation of Na^+ currents that results in cell membrane depolarization and a heightened firing.

at restoring circadian rhythms, but also at predicting the onset of side effects related to drug treatment/abuse that might cause daily desynchronization. Besides the events discussed so far, other specific mechanisms dictating the strength and the specificity of chemical transmission would deserve attention due to their potential role in circadian rhythmicity. In relation to the latter, we will briefly discuss how the mode of synaptic communication, the co-localization of different neurotransmitters, and the intensity of the releasing stimulus (Albers et al., 2017) may be relevant to the rhythmicity of the neurotransmitter-clock protein crosstalk.

Regarding the synaptic communication, catecholaminergic and indolaminergic projections originate from a limited number of neurons in defined central areas, *i.e.*, the *locus coeruleus* (LC) for noradrenaline (NA), the *substantia nigra* (SN), and the ventral tegmental area (VTA) for DA or the *raphe nucleus* for 5-HT (Descarries and Mechawar, 2000; Vizi et al., 2004). Once released, the neurotransmitter diffuses through the biophase to reach receptors located postsynaptically, a process named "volume transmission" to assure the communication among sites within the same brain area or even in adjacent brain regions (Fuxe et al., 2012; Olivero et al., 2020). In this regard, DA, which controls the daily rhythmicity in mammals (Imbesi et al., 2009; Hood et al., 2010), is actively released from dopaminergic projections and reaches the postsynaptic structures by "volume transmission" (Descarries and Mechawar, 2000), which are located also in vicinal regions (*i.e.*, the striatum, the SCN). Here, the activation of dopaminergic receptors (*i.e.*, the D1 and D2 receptors) elicits functional responses, including the tuning of clock proteins, *i.e.*, the Per1 and 2 proteins (Imbesi et al., 2009; Hood et al., 2010). Therefore, DA diffusion allows the propagation of the dopaminergic input during the diurnal period, favoring a widespread circadian regulation of biological processes. However, the efficiency of the DA "volume transmission" strictly depends on the continuous replenishment of the presynaptic vesicle, that is ensured by the storage of the newly-synthetized transmitter or by the re-uptake of the released amine, which are both efficiently controlled by clock proteins (see Section "The Dopaminergic System"). Besides the SN and the VTA, dopaminergic cells also represent the largest percentage of

the resident cells in the retina. Here, the highest concentration of DA is reached during the day due to multiple excitatory signals, including light, and it is controlled by melatonin. DA diffuses by "volume transmission" also in the brain regions to enable the communication between the amacrine cells (that are dopaminergic in nature) and the horizontal and the bipolar cells, as well as the photoreceptor-containing processes (Witkovsky, 2004). The mechanism of "volume transmission" in the CNS dictates a virtuous "clock protein-transmitter loop" that favors the diurnal control of some circadian regulators. An interesting feature of the retinal amacrine cells (Hirasawa et al., 2009) and in general of the DA-positive neuronal processes in the SCN and striatum (Romei et al., 2016), is that these cells are also specialized for GABA. Dopaminergic cells cannot synthesize GABA, but can efficiently recapture this amino acid, mainly at nerve endings (Romei et al., 2016), where it is co-stored with DA. The uptake of GABA in dopaminergic terminals, which is an event that would occur preferentially when the $[GABA]_{out}$ exceeds the physiological level, triggers a concomitant release of the catecholamine. Since GABA acts preferentially as a nocturnal controller of circadian rhythms and has an opposite outcome with respect to DA in controlling the expression of the clock genes [*i.e.*, *Per2* (Ruan et al., 2008)], it is possible that the GABA-induced carrier-mediated release of DA may have a role in permitting the transition from the nocturnal to the diurnal phase of the daily circadian rhythmicity.

The SCN is composed of GABAergic neuronal subtypes and glial cells. As well as many neurons, a large part of the GABAergic SNC neurons also contains neuropeptides. Therefore, depending on the stimulus, these neurons preferentially release both GABA and neuropeptides. When the concomitant release of neuropeptides and GABA occurs, this may affect the GABA outcomes, causing an indirect impact on the daily timekeeping due to the modifications of the hierarchical organization of the neuronal control of the clock oscillation. Interestingly, the co-release of neuropeptides and GABA in the SCN and in some other hypothalamic regions has been recently related to the dyssynchronization of the clock circadian molecules, particularly *Clock* and *Period*, that occurs in stress conditions (Wong and Schumann, 2012).

In the mammalian brain, serotonin availability in the biophase varies following a circadian pattern from day to night. The serotonergic projections from the medial *raphe nucleus* converge in the SCN and in the retino-hypothalamic tract, where the indolaminergic signal is mainly mediated by presynaptic 5-HT1B receptors (Selim et al., 1993; Pickard et al., 1999; Smith et al., 2001). 5-HT1B receptors are also largely expressed in GABA terminals, particularly in the SCN neurons and in the RHT, where their activation inhibits the exocytosis of the inhibitory amino acid. 5HT modulates the effect of light on the clock at both early and late night (Morin, 1999) time points, with variable effects when applied at night. Furthermore, a recent study using a rat *in vivo* microdialysis revealed that diurnal changes in 5-hydroxyindole-acetic acid (5-HIAA) levels, the principal 5-HT metabolite, could be observed also in other brain regions that receive the serotonergic projections, in particular, in the prefrontal cortex (PFC), but not in the hippocampus; this metabolic activation might be related to enhanced neuronal activity of 5-HT (Daszuta and Barrit, 1982; Nakayama, 2002). The contribution of 5-HT to the expression and function of clock proteins might depend on the phase of the day and on brain areas but again largely involves the control of the GABAergic innervation.

Notably, based on evidence from the literature suggesting a functional crosstalk between neurotransmitter systems and the circadian clockwork, we will summarize evidence showing such bidirectional interplay (as schematized in **Table 1**). Accordingly, robustness and precision in daily timekeeping have been reported to rely on the punctual intercellular communication, mediated by neurotransmitters, among CNS cells (Herzog et al., 2004; Hastings et al., 2018).

The Dopaminergic System

Dopamine (DA) is produced in midbrain neurons of the *substantia nigra* (SN) and ventral tegmental area (VTA) and it is involved in the regulation of locomotion, sleep-wake cycle, learning, motivation, and reward. DA levels have been shown to display a circadian oscillation in several brain areas, such as the retina, midbrain, striatum, olfactory bulb, and hypothalamus (Korshunov et al., 2017).

In particular, the retina is the first region of CNS to deal with light information and it is responsible for its transmission to SCN through the retino-hypothalamic pathway (Gooley et al., 2001; Hattar et al., 2006; Prigge et al., 2016). Studies on mammalian retinas show that DA has the highest peak of synthesis during the daytime, whereas it is reduced during the nighttime. Doyle et al. (2002) found that in rats with normal and dystrophic retinas, DA content and turnover, as observed by measuring its two major metabolites 3,4-dihydroxyphenylacetic acid (DOPAC) and homovanillic acid (HVA), follow a daily rhythmicity with the peak during the light phase. Besides, they also reported that cones and rodes are not required for generating DA circadian rhythmicity, since the latter was maintained also in rats with dystrophic retinas (Doyle et al., 2002). Moreover, dopamine has been reported to stimulate the expression of the core clock component *Per1* in retinal neurons, especially through the activation of D1 and D2 receptors, whose specific role is currently a matter of debate. In intact m$Per2^{Luc}$ retinal explants, stimulation of D1 receptors resulted in *Per1* upregulation by activating the extracellular signal-regulated kinase (ERK)-mitogen-activated protein kinase (MAPK) pathway. Enhanced phosphorylation of the cAMP-responsive element-binding protein (CREB) has been found to promote the cAMP-response elements (CRE)-mediated transcription of *Per1* gene (Ruan et al., 2008). In line with such evidence, Yujnovsky et al. (2006) reported an increase in *Per1* transcription in mouse NG108–15 cells, induced by the activation of dopamine D2 receptor (D2R) by D2 agonists, such as quinpirole. Indeed, the stimulation of D2 receptors led to the activation of the MAPK transduction cascade, to an increase in CREB phosphorylation and the recruitment of the Clock:Bmal1 heterodimer, thus resulting in an enhanced *Per1* transcription. A marked reduction of the Clock:Bmal1 activation and, consequently, of *Per1* levels was also observed in the retina

TABLE 1 | The clock around neurotransmission.

Clock genes	Experimental model	Neurotransmitter players	Circadian interactions	References
RETINA				
Per1	*mPer2*^{Luc} mouse retinal explants	Retinal D1 receptors	Stimulation of D1 receptors results in the upregulation of the *Per1* gene *via* the activation of ERK-MAPK-CREB pathway.	Ruan et al. (2008)
Per1	*Mouse NG108-15 cells*	Retinal D2 receptors	Activation of D2 receptors leads to an increase in the transcription of the *Per1* gene *via* the activation of ERK-MAPK-CREB cascade.	Yujnovsky et al. (2006)
Per2	Cultured *mPer2*^{Luc} retinal explants	GABA-A and GABA-C receptors	The treatment with a GABA-A or GABA-C receptor agonist significantly suppresses *Per2* levels, probably acting on a posttranscriptional level, and partly by stimulating case in kinase.	Ruan et al. (2008)
Per1, Bmal1	Cultured *mPer2*^{Luc} retinal explants	GABAergic system	GABA co-administration is able to increase the mRNA levels of *Per1* and *Bmal1*.	Ruan et al. (2008)
CORTEX				
Per1	Mice	Noradrenergic system	Administration of NA highly induces *Per1* mRNA expression in the mice cerebral cortex during the light phase, probably through the activation of cAMP-PKA and MAPK-CREB pathways.	Burioka et al. (2008)
Npas2, Clock	Cortical astrocytes cultures from *Npas2* and *Clock* mutant mice	Glutamate transporter EAAT1	Mutation of *Npas2* and *Clock* results in a decrease in the mRNA levels of the glutamate transporter EAAT1.	Beaulé et al. (2009)
Bmal1, Cry1, Per2	Mouse cortical neurons	GABA-A receptors	The activation of GABA-A receptors is able to entrain rhythmic oscillations of *Bmal1*, *Cry1,* and *Per2* expression that, in turn, is completely suppressed inhibiting them.	Barca-Mayo et al. (2017)
Bmal1	*Bmal1*cKO mice	GABA transporters Gat1 and Gat3	The KO of *Bmal1* in astrocytes significantly decreases the expression of Gat1 and Gat3 in the cortex.	Barca-Mayo et al. (2017)
STRIATUM				
Per2	*Per2*^{Brdm1} mutant mice	MAO-A gene	*Per2* appears to induce the transcription of MAO-A gene, probably due to its action on the E-boxes of the MAO-A transcriptional promoter.	Hampp et al. (2008)
Per2	Male Wistar rats	D2 receptors	D2 antagonists decrease the rhythmical amplitude of *Per2* transcription, that is, in turn, restored by D2 agonists, thus indicating a key role of D2 receptors in the regulation of *Per2* gene expression, probably *via* the activation of ERK-MAPK-cAMP-CREB cascade.	Hood et al. (2010)
Per1, Bmal1, Clock, Npas2	Cultured mouse striatal neurons	D1 receptors	Treatments with D1 receptor agonists lead to an increase in mRNA levels of *Per1, Bmal1, Clock, and Npas2*.	Imbesi et al. (2009)

(Continued)

TABLE 1 | Continued

Clock genes	Experimental model	Neurotransmitter players	Circadian interactions	References
Per1, Clock	Cultured mouse striatal neurons	D2 and D3 receptors	Treatments with D2 and D3 receptor agonists repress the transcription of *Per1* and *Clock* genes.	Imbesi et al. (2009)
Rorα	Mouse	D3 receptors	*Rorα* upregulates D3 receptor transcription probably due to its binding to the DRD3 promoter.	Ikeda et al. (2013)
Rev-erbα	Mouse	D3 receptors	*Rev-erbα* periodically inhibits D3 receptor transcription probably due to its binding to the DRD3 promoter.	Ikeda et al. (2013)
Per2	G*Per2* mutant mice	D3 receptors	Deletion of *Per2* in glial cells shows an increase in D3 receptor mRNA levels.	Martini et al. (2021)
Per2	G*Per2* mutant mice	GABA transporter	Gat2 Deletion of *Per2* in glial cells increases the expression of *Gat2* in the NAc.	Martini et al. (2021)
VTA				
Rev-erbα	*Rev-erbα* knockout (RKO) mice Immortalized DAergic cell lines (CATH.a)	TH gene	Suppressive mechanism of *Rev-erbα* on the regulation of TH gene expression, by acting on RRE/NBRE1 elements located in TH promoters.	Chung et al. (2014)
Clock	*Clock*Δ*19* mutant mice	TH gene	*Clock* suppresses the expression of TH gene, through a possible interaction of *Clock* with the E-boxes sequences on TH gene promoter.	McClung et al. (2005)
Clock	*Clock*Δ*19* mutant mice	Dopamine neurons	Deletion of the *Clock* leads to an increase in the bursting and firing rate of VTA dopamine neurons, probably induced by the down-regulation of a voltage-gated potassium channel (*KcnQ2*).	McClung et al. (2005)
HYPOTHALAMUS				
Per2	G*Per2* mutant mice	GABA transporter Gat1	Deletion of *Per2* in glial cells significantly decreases the expression of *Gat1* in the hypothalamus.	Martini et al. (2021)
SCN				
Per2, Rev-erbα	Sudanian grass rats	5-HT 5-HT receptors	Treatments with a 5-HT agonist and selective 5-HT reuptake inhibitor increase *Per2* and *Rev-erbα* mRNA levels, enhancing light-induced phase delays at CT12.	Cuesta et al. (2008)
Per1, Rev-erbα, Rev-erbβ	Sudanian grass rats	5-HT 5-HT receptors	Treatments with a 5-HT agonist and selective 5-HT reuptake inhibitor increase *Per1*, *Rev-erbβ,* and *Rev-erbα* mRNA levels, reinforcing light-induced phase-advances at CT0.	Cuesta et al. (2008)
Rorβ	Sudanian grass rats	5-HT 5-HT receptors	Treatments with a 5-HT agonist and selective 5-HT reuptake inhibitor decrease *Rorβ* transcription.	Cuesta et al. (2008)
Per 2	$Per2^{Brdm1}$ mutant mice	Glutamate transporter EAAT1	Mutation of *Per2* leads to a reduction in the SCN expression of EAAT1, thus resulting in a hyper-glutamatergic state.	Spanagel et al. (2005)

(Continued)

TABLE 1 | Continued

Clock genes	Experimental model	Neurotransmitter players	Circadian interactions	References
Per2	Mouse SCN slices	Glutamate transporter EAAT3	Inhibition of EAAT3 transporter leads to an increase of the extracellular Glu levels, which consequently causes a dramatically reduction of the amplitude and robustness of *Per2* gene oscillations.	Brancaccio et al. (2017)
Per2	Mouse SCN slices	NR2C subunits of the NMDA receptors	NR2C inhibition abolishes circadian oscillations of intracellular Ca^{2+}, provokes nighttime depolarization of SCN dorsal neurons, and reduces the amplitude and lengthens the period of *Per2* oscillations.	Brancaccio et al. (2017)
Per2	Avp-Vgat$^{-/-}$ mice	Vesicular GABA transporter (Vgat)	The deletion of the vesicular GABA transporter (Vgat) in arginine vasopressin-producing (AVP) neurons, leads to a delay in the peak phase of *Per2* oscillations resulting in a lengthened activity time of mice circadian behavioral rhythms.	Maejima et al. (2021)
Bmal1	*Bmal1*cKO mice	GABA transporters Gat1 and Gat3	The deletion of astrocytic *Bmal1* leads to a noteworthy reduction of the expression of GABA transporters *Gat1* and *Gat3* in the SCN and in astrocytes.	Barca-Mayo et al. (2017)
PERIPHERAL SYSTEM				
Per1	Mice	Noradrenergic receptors	Activation of noradrenergic receptors by α/β-adrenoreceptor agonists increases m*Per1* expression in mice liver in a concentration-dependent manner.	Terazono et al. (2003)
Per1, Per2, Bmal1	SCN-lesioned arrhythmic mice	Noradrenergic system	Lesions of the SCN cause a loss of liver daily expression of m*Per1*, m*Per2*, and m*Bmal1* and of NA content.	Terazono et al. (2003)
Bmal1, Per1, Per3	Human dermal fibroblast	Noradrenergic system	The exposure to different NA concentrations was able to reduce the expression of *Bmal1* at ZT12 and *Per1* at ZT20, and to increase *Per3* mRNA levels at ZT4.	Palm et al. (2021)

of D2R-null mice, thus indicating the importance of D2 receptors in mediating retinal circadian expression (Yujnovsky et al., 2006).

Besides the retina, the circadian activity of the dopaminergic signaling system has also been reported in the midbrain and striatum, possibly transmitted through the neuronal projections from the SCN to these areas, such as *via* the orexinergic system (ORX) in the lateral hypothalamus (LH), the *lateral habenula* (LHb), the paraventricular thalamic nucleus (PVT), and the medial preoptic nucleus (MLPO; Abrahamson and Moore, 2001; Mendoza and Challet, 2014). These innervations from the SCN are able to regulate DA firing, expression, and metabolism. Notably, the LHb acts as an inhibitory pathway on the VTA. Accordingly, its activation has been found to decrease the firing of dopaminergic neurons (Bourdy and Barrot, 2012; Lecca et al., 2012). Furthermore, activation of the ORX system in the VTA has been shown to be implicated in the regulation of the plasticity of the dopaminergic system, as well as in locomotion, reward, motivation, and addiction (Borgland et al., 2006; Narita et al., 2006). Consequently, the rhythmical dopaminergic activity in the striatum relies on this SCN-VTA pathway. All these findings suggest that the intricate circuit of interconnections between SCN and the different brain areas plays a pivotal role in establishing the proper circadian rhythmicity of the dopamine system in the VTA and in the striatum.

DA signaling, synthesis, transport, and degradation are all under circadian regulation. Promoters of genes encoding for

tyrosine hydroxylase (TH, the rate-limiting enzyme of DA synthesis), dopamine transporter (DAT), and monoamine oxidase A (MAO-A, the key enzyme that regulates DA degradation) have been found to contain E-Box sequences and to display circadian rhythmicity in their expression (Yoon and Chikaraishi, 1994; Sleipness et al., 2007; Hampp et al., 2008). In this regard, Sleipness and coworkers (Sleipness et al., 2007) demonstrated that electrolytic lesions of the SCN in rats alter the day-night variations in the expression of the DA transporter and synthetase in the midbrain. Remarkably, many studies revealed that the firing of dopaminergic neurons and the expression of TH protein in the VTA change during the day, with a peak during the daytime (Webb et al., 2009). In particular, *Clock* and *Rev-Erbα* have been found to be implicated in the reduction of *TH* expression in the VTA (McClung et al., 2005; Chung et al., 2014). Notably, Chung et al. (2014) demonstrated, in *in vitro* and *in vivo* studies on wild-type and *Rev-erbα* knockout (RKO) mice, an increase in *TH* mRNA expression and DA extracellular content in RKO compared to WT mice. These findings indicate a loss of rhythmicity and a parallel hyper-activation of the dopaminergic system in RKO mice, suggesting that *Rev-erbα* may negatively regulate *TH* gene expression. In particular, *Rev-erbα* has been shown to control *TH* expression by acting on RRE/NBRE1 (NGFI-B response element) elements located in *TH* promoters through the recruitment of the histone deacetylase 3 (HDAC3) complexes. The latter negatively regulates permissive histone acetylation, resulting in the inhibition of the transcriptional activation of the *TH* gene promoter (Chung et al., 2014). Furthermore, McClung and coworkers revealed that *TH* expression in mice was downregulated by *Clock*. Indeed, *TH* mRNA expression and protein levels were strongly increased in the VTA of *Clock*Δ*19* mutant mice compared with WT (McClung et al., 2005). Although the mechanism by which *Clock* modulates *TH* expression is unknown, *Clock* has been suggested to bind E-box sequences on the *TH* gene promoter. Moreover, *Clock*Δ*19* mutant mice have shown an increase in bursting and firing rates of VTA dopamine neurons. Such an effect is probably mediated by the downregulation of a voltage-gated potassium channel (*KcnQ2*), induced by the loss of *Clock* in mutants, thus indicating the key implication of *Clock* in affecting the excitability of DA neurons (McClung et al., 2005).

In the striatum, the rhythmical DA and MAO-A content has been found to be regulated by *Per2*. *Per2*^{Brdm1} mutant mice have been observed to display a reduction in *MAO-A* expression in the striatum and a consequent increase in extracellular DA levels, thus suggesting that *Per2* may promote *MAO-A* transcription (Hampp et al., 2008). As a feedback loop, DA has been found to regulate the rhythm of *Per2* expression *via* activation of D2 receptors. Indeed, rats treated with selective D2 antagonists (*i.e.*, raclopide) showed a significant decrease in the rhythmical amplitude of *Per2* transcription in the striatum, which, conversely, was not observed upon treatment with D1 antagonists. In turn, the reduction of *Per2* levels, induced by the administration of 6-hydroxydopamine (6-OHDA), was restored by using D2 agonists, such as quinpirole, whereas the use of D1 agonists had no effect (Hood et al., 2010).

Taken together, these results suggest that fluctuation in extracellular DA levels may be involved in the maintenance of the rhythmical amplitude of *Per2* transcription in the dorsal striatum *via* D2 receptors. Such modulation has been thought to involve the ERK-MAPK intracellular pathway, which is regulated by DA signaling, and leads to the activation of the cAMP-CREB pathway that results in the augmented transcription of *Per2* gene (Hood et al., 2010). Moreover, Imbesi and coworkers, investigating the implication of DA receptors in the regulation of neuronal clock genes expression in cultured mouse striatal neurons, found that treatment with D1 receptor agonists led to an increase in *Per1, Bmal1, Clock, and Npas2* mRNA levels. On the other hand, treatments with D2 and D3 receptor agonists, such as quinpirole, repressed the transcription of *Per1* and *Clock* genes, whereas *Npas2* and *Bmal1* mRNA expression was not affected (Imbesi et al., 2009). Additionally, in mouse ventral striatum, a 24-h variation in the expression of dopamine D3 receptor has been reported. Interestingly, *Rora* and *Rev-erbα* have been found to modulate these oscillations, by possibly binding the D3 receptor promoter. In particular, *Rora* has been found to upregulate D3 receptor transcription, whereas *Rev-erbα* has been reported to periodically inhibit its expression (Ikeda et al., 2013). Moreover, in the *nucleus accumbens* (NAc), D3 receptors have been found to be regulated also by glial *Per2* (Martini et al., 2021). Indeed, mice with a deletion of *Per2* in glial cells showed an increase in D3 receptor mRNA levels compared to control animals (Martini et al., 2021). In particular, *Per2* has been suggested to interact with several nuclear receptors, such as *Rev-erbα* and, to a lesser extent, with *Rora* (Schmutz et al., 2010), both interacting with the D3 receptor's promoter and consequently modulating D3 receptor expression (Ikeda et al., 2013). Together, these studies highlight the putative links between the dopaminergic system and the striatal clockwork.

The Serotonergic System

Serotonin (5-HT) is an important neurotransmitter involved in the coordination and synchronization of the circadian system and melatonin synthesis. The serotonergic system and the master pacemaker are interconnected with each other through several projections, which are probably at the root of their reciprocal regulation. SCN projects indirectly to the median *raphe nucleus* (MRN) and the dorsal *raphe nucleus* (DRN) *via* the dorsomedial hypothalamic nucleus (DMH). In turn, the *raphe nuclei* project directly back to the SCN from the MRN, whereas indirectly *via* the intergeniculate leaflet (IGL) from the DRN (Azmitia and Segal, 1978; Hay-Schmidt et al., 2003; Deurveilher and Semba, 2005).

Clock genes have been found to regulate the expression of genes implicated in the serotonergic pathway in a circadian manner. The *Tph2* gene, encoding for the tryptophan hydroxylase, has been found to exhibit a rhythmical expression in the midbrain of rats, with the highest peak arising 2 h before the light-dark transition, thus resulting in a circadian secretion of 5-HT (Malek et al., 2005). However, *Tph2* mRNA rhythm seems to be indirectly mediated by the SCN through

daily glucocorticoid variation. Indeed, Malek et al. (2007) demonstrated that, in rodent MRN and DRN, the loss of corticosterone daily fluctuations, induced by adrenalectomy, abolished the rhythmical expression of *Thp2* mRNA completely. In contrast, the *Thp2* daily expression pattern was fully restored after the readjustment of plasma corticosterone levels. Nevertheless, the precise mechanisms involved in the circadian regulation of *Thp2* transcription by glucocorticoids are unknown (Malek et al., 2007). Furthermore, both serotonin transporter SERT expression and activity in mouse *raphe nuclei* have been reported to significantly change in a time-dependent manner, displaying higher levels during the dark phase (Ushijima et al., 2012). Likewise, studies on hamsters showed that 5-hydroxyindole-acetic acid (5-HIAA), the principal 5-HT metabolite, is mainly released during the dark phase (Glass et al., 1992), thus suggesting that the release of 5-HT is greater during the active phase and demonstrating that both its synthesis and release follow a circadian rhythmical pattern.

At the same time, the capability of 5-HT, not only to be controlled by the biological clock but in turn to influence circadian functions has been proven by Nakamaru-Ogiso et al. (2012) demonstrating that 5-HT deficiency in rats, induced by an acute tryptophan depletion, led to the disruption of circadian sleep-wake rhythm and disintegrated fragmental patterns. 5-HT plays an important role also in the regulation of photic entrainment of the SCN and it is able to modulate light-induced phase shifts in locomotor activity (Mistlberger et al., 2000; Cuesta et al., 2008). Indeed, 5-HT works as an inhibitor of the retinal output to the central clock, performing both a presynaptic action through 5-HT1B receptors on retinal afferent terminals, as well as a postsynaptic action through 5-HT7 receptors on SCN neurons (Smith et al., 2001). The activation of 5-HT1B receptors has also been associated with the suppression of the inhibitory effect of light on pineal melatonin production (Rea and Pickard, 2000) and with significant light-induced phase shifts, which led to a variation of SCN gene expression. The serotonergic stimulation, obtained through the treatment of the rodent model *Arvicanthis ansorgei* [a diurnal model used for the study of circadian rhythms (Hubbard et al., 2015)] with a 5-HT agonist and selective 5-HT reuptake inhibitors (SSRIs, such as fluoxetine), resulted in behavioral phase-advances and in an increase of light-induced phase-delays and advances (Cuesta et al., 2008). At the molecular level, such light-induced phase shifts, anticipated by serotoninergic activation, have been found to be correlated with changes in clock gene expression in the SCN. Notably, at CT12, *Per2*, and *Rev-erbα* mRNA levels were higher compared to those obtained after a light pulse alone, thus suggesting that they may play a role in the enhancement of light-induced phase-delays. Whereas, due to increased expression of *Per1*, *Rev-erbα*, and *Rev-erbβ* at CT0, these clock genes seemed to be implicated in the reinforcement of light-induced phase advances. On the contrary, *Rorβ* transcription was found to be reduced at CT0 (Cuesta et al., 2008).

Further evidence of the strong interconnection between circadian and serotonergic networks is related to the influence that many serotonergic drugs have on the circadian system. For example, as described before, SSRIs deeply impact the response of the circadian system to environmental light and have been seen to phase advance the firing rate of SCN neurons in rats' brain slice cultures (Sprouse et al., 2006).

The Noradrenergic System

Noradrenaline (NA) is a neurotransmitter mainly synthesized in the *locus coeruleus* (LC), and it is implicated in the modulation of alertness, arousal, cognition, executive functions, and mammalian circadian rhythmicity (Palm et al., 2021). The release of NA from the LC is a very dynamic process fundamental for the correct alternation between the rapid eye movement (REM) phase and the non-rapid eye movement (NREM) phase of sleep. Recent studies have revealed that the activity of LC in releasing NA is higher during wakefulness and NREM sleep, whereas it is lower during REM sleep, thus suggesting the key role of LC in sleep architecture and functions (Osorio-Forero et al., 2022). Moreover, in the LC of rats, the expression of MAO-A and MAO-B is under circadian control due to their rhythmical oscillations that peaks at nighttime, probably thanks to the presence of E-box sequences on their gene promoters (Chevillard et al., 1981).

Animal studies demonstrated that alterations of clock genes expression in the SCN, which also impact clock mRNA levels in the peripheral tissues, are associated with noradrenaline pathways. Notably, NA is able to modulate the physiological expression of *Per1*, *Per2*, and *Bmal1* in mouse livers (Terazono et al., 2003). Administration of adrenaline, both *in vitro* and *in vivo*, increased m*Per1* expression in mouse liver in a concentration-dependent manner. In SCN-lesioned arrhythmic mice, a loss in the liver daily expression of m*Per1*, m*Per2*, and m*Bmal1* and of NA content was further observed, and restored by adrenaline injections. Moreover, in human dermal fibroblasts, the exposure to NA reduced the expression of *Bmal1* at ZT12 and *Per1* at ZT20 after incubation with NA compared to controls. Meanwhile, the expression of *Per3* at CT4 was increased after the incubation with NA compared to cultures without NA treatments (Palm et al., 2021). In addition, in mice, administration of NA for 6 days highly induced *Per1* mRNA transcription in the cerebral cortex during the light phase (Burioka et al., 2008). Together, these findings demonstrate the adrenergic role in regulating clock gene expression and in conveying central clock information to peripheral organs by NA release, probably through the involvement of cAMP-PKA and MAPK-CREB pathways (Terazono et al., 2003; Burioka et al., 2008; Palm et al., 2021).

The Glutamatergic System

Glutamate (Glu) is the primary excitatory neurotransmitter in the mammalian nervous system and it is essential for the maintenance of higher brain functions such as cognition, learning, and memory. Furthermore, it is implicated in brain cellular metabolism and in the regulation of sleep-wake states (Danbolt, 2001; Jones, 2017). Interestingly, astrocytes are primarily responsible for the rhythmic oscillation of extracellular Glu levels, which, in turn, are necessary for molecular timekeeping in the SCN. In order to regulate the balance between Glu uptake and release, astrocytes are

responsible for the uptake of the majority of extracellular Glu through glutamate transporters on the surface of the astrocytic peri-synaptic processes, such as the excitatory amino acid transporters 1 and 2 (EAAT1 and EAAT2; Lehre and Danbolt, 1998). After being re-uptaken, Glu in astrocytes can be metabolized to glutamine by glutamine synthetase and used by neurons as a precursor for the synthesis of Glu or GABA (Waniewski and Martin, 1986). Otherwise, Glu can be oxidatively metabolized to α-ketoglutarate, which is involved in ATP production (Farinelli and Nicklas, 1992). On the other hand, Glu release from astrocytes is mediated by metabotropic glutamate receptors (mGluRs), which, once activated, induce an increase in the astrocytic $[Ca^{2+}]_i$, thus triggering Glu release from astrocytes (Hamilton and Attwell, 2010). The astroglial-released Glu activates extra-synaptic N-methyl-D-aspartate (NMDA) receptors on adjacent excitatory neurons, thus synchronizing excitatory neuronal firing (Fellin et al., 2004; **Figure 2**). Accordingly, the glutamatergic connections to the SCN are mediated by pre-synaptic NMDA/NR2C receptors expressed in the dorsal SCN, which, in turn, once activated by extracellular Glu, increase the GABAergic tone. Indeed, Brancaccio et al. demonstrated that inhibition of NR2C subunits of the NMDA receptors, obtained by treating mouse SCN slices with an NR2C-selective antagonist (*i.e.*, DPQ-1105), led to an alteration of molecular and electrical circadian oscillations in the SCN. Notably, NR2C inhibition abolished circadian oscillations of intracellular Ca^{2+}, induced nighttime depolarization of SCN dorsal neurons, reduced the amplitude, and lengthened the period of *Per2* oscillations (Brancaccio et al., 2017). Such evidence highlights that the astrocytic-Glu/NMDA-NR2C/SCN axis may represent a novel pathway required for the synchronization of SCN neurons. Moreover, in *ex vivo* studies, astrocytes of mouse SCN were found to be active and release higher Glu levels during the circadian nighttime (Brancaccio et al., 2017). Accordingly, another study demonstrated that glutamate concentration is under circadian control, and in rat brain it peaks during the dark phase of the day, mainly in the striatum and *nucleus accumbens* (Castañeda et al., 2004).

A circadian variation has also been seen in the expression of some receptors and transporters involved in the glutamate pathway. For example, Elmenhorst et al. (2016) in an *in vivo* PET experiment on rat brains, found approximately a 10% increase in the availability of metabotropic glutamate receptor mGluR5 during the light phase in different brain regions, such as the cortex, amygdala, *caudate putamen*, and *nucleus accumbens*. Meanwhile, in rodents, the glutamate transporter EAAT3, involved in Glu uptake, has been found to follow a circadian expression within the SCN, showing a peak around the dark-light transition (Cagampang et al., 1996). Brancaccio et al. (2017) demonstrated that EAAT3 inhibition, obtained by treating mouse SCN slices with a selective antagonist, led to an increase in the extracellular Glu levels, and a reduction in amplitude and robustness of *Per2* gene oscillations, resulting in an alteration of the neuronal timekeeping. Similarly, excitatory amino acid transporter 1 (EAAT1) mRNA and protein levels in the SCN, and consequently the glutamate uptake, have been found to follow a diurnal rhythm and to be strongly modulated by clock genes expression. Spanagel and coworkers found that *Per2*^{Brdm1} mutant mice showed a reduction in the SCN expression of EAAT1 compared to wild-type mice, thus resulting in a reduced glutamate uptake by astrocytes and in a hyper-glutamatergic state (Spanagel et al., 2005). Likewise, studies on cortical astrocyte cultures from *Npas2* and *Clock* mutant mice revealed a significant reduction in glutamate uptake compared to wild-type mice due to a decrease in EAAT1 mRNA levels caused by mutations (Beaulé et al., 2009). These results suggest that both Glu release and uptake are orchestrated in a circadian manner, however, the molecular mechanisms by which the clock genes modulate the total Glu uptake are unknown.

The GABAergic System

γ-aminobutyric acid (GABA) is synthesized from Glu and it is the principal inhibitory neurotransmitter in the brain. The timing of GABA synthesis, release, and uptake seems to have a crucial role in the orchestration of SCN rhythm. Notably, the glutamic acid decarboxylase (GAD, the enzyme responsible for GABA synthesis), especially the isoform GAD65, has been reported to show a circadian oscillation. In rat SCN slices, autoradiography revealed higher levels of GAD65 mRNA in the light period rather than in the dark period, with a peak of expression during the transition from dark to light (Huhman et al., 1996). Furthermore, Maejima and coworkers demonstrated the importance of the GABAergic system for the performance of circadian behavior at the correct time of the day through the regulation of SCN neuronal activity. They found that in the SCN of Avp-Vgat$^{-/-}$ mice (mutation resulting in a decrease of GABA release from the vesicular GABA transporter (Vgat) in arginine vasopressin-producing (AVP) neurons), the frequency of GABA-A receptor-mediated postsynaptic currents (mGPSCs) was strongly reduced during daytime compared to control mice. Besides, in the SCN of Avp-Vgat$^{-/-}$ mice, a delay in the peak phase of *Per2:Luc* oscillations has been observed, thus leading to a lengthened activity time of circadian behavioral rhythms. Thus, these results suggest the key role of the GABAergic transmission from AVP neurons in directing the correct timekeeping of SCN outputs from molecular clocks to behavior (Maejima et al., 2021).

Further evidence for GABA involvement in the induction of a rhythmic expression of the core clock genes in neurons, through the activation of GABA-A receptors, comes from Barca-Mayo et al. (2017). In *in vitro* cortical neurons of GABA-treated mice, they found that GABA was able to entrain rhythmic oscillations of *Bmal1*, *Cry1*, and *Per2* expression, and that the inhibition of GABA-A receptor signaling suppressed such rhythms. In *Bmal1cKO* mice (inducible knockout mouse model of *Bmal1* in astrocytes), extracellular GABA levels have been found to be altered, resulting in an over-inhibition of the signaling pathways involved in cognitive functions and in a delay of the active phase. The impairment of GABA levels has been related to the deletion of astrocytic *Bmal1* that decreased the expression of GABA transporters *Gat1* and *Gat3* in the SCN and in astrocytes, in turn reducing extracellular GABA clearance (Barca-Mayo et al., 2017). Furthermore, also the glial deletion of *Per2* gene in mice (G*Per2* mouse model) has been found to alter *Gats* mRNA levels (Martini et al., 2021). Notably, the expression of

Gat1 significantly decreased in the hypothalamus of G*Per2* mice, whereas that of *Gat2* has been reported to increase in the NAc of this mouse model compared to controls (Martini et al., 2021). Together, these findings suggest that astrocytic *Bmal1* and glial *Per2* may regulate the extracellular GABA concentration through the modulation of *Gats* mRNA levels.

Moreover, GABA is also important in the regulation of retinal clock genes fluctuations, since, in cultured m*Per2*^{Luc} retinal explants, it decreased and suppressed the rhythmic amplitude of *Per2* oscillations in a dose-dependent manner, possibly through the activation of GABA-A and GABA-C receptors (Ruan et al., 2008). Only after treating m*Per2*^{Luc} retinal explants with a GABA-A or GABA-C receptor agonist, the amplitude of *Per2:Luc* signals significantly decreased, whereas no effects have been observed with GABA-B receptor agonists (Ruan et al., 2008). Moreover, GABA was able to increase *Per1* and *Bmal1*, but not *Per2* and *Clock* mRNA levels, thus indicating its ability to suppress *Per2* levels acting at the posttranscriptional level, by stimulating casein kinase, which is able to phosphorylate *Per2* for its ubiquitin-mediated proteasomal degradation (Ruan et al., 2008).

THE ROLE OF GLIA IN THE GENERATION OF CIRCADIAN RHYTHMICITY

The existence of an endogenous neuronal circadian timekeeper with the capacity to orchestrate and coordinate physiological and behavioral processes with the external environment is now well established. However, studies on circadian timekeeping are moving beyond the neuronal cell population, since the capability of encoding rhythmical information is not only restricted to neurons but also extends to glial cells. Indeed, as discussed above, the devolution of the control of the glutamatergic and, consequently, of the GABAergic tone to astrocytes, since they are the primarily responsible for the rhythmic oscillation of extracellular Glu levels, suggests that such glial cells synergistically communicate with neurons to establish the 24 h daily rhythm (**Figure 2**). Hence, since astrocytes and microglia are integral parts of the timepiece, the correct functioning of the glial clock system is fundamental for the maintenance of a healthy brain. Recent studies indicate that misalignments in the expression of glial clock genes contribute to the development of different pathological outcomes. Particularly, astrocytic *Clock*, *Per1*, and *Per2* have been found to be involved in the modulation of ATP release (Marpegan et al., 2011) and, subsequently, in the regulation of energy metabolism and glial activity. Therefore, mutations of these clock genes may result in metabolic diseases. Moreover, microglial *Bmal1* has been proven to be an important molecular player in the inflammatory response and in different pathological processes, such as neurological diseases and sleep disorders. Notably, mouse microglial *Bmal1* deficiency has been found to decrease the expression of pro-inflammatory cytokines (*i.e.*, IL-1β, IL-6, and TNFα) and increase that of anti-inflammatory cytokines (*i.e.*, IL-10; Wang et al., 2020), probably owing to the presence of E-boxes sequences on cytokine gene promoters. Likewise, the deletion of mouse astrocytic *Bmal1* leads to the impairment of cognitive functions, majorly affecting the declarative memory (Barca-Mayo et al., 2017), as well as to an imbalance of the GABAergic system (Barca-Mayo et al., 2017), resulting in the development of neurological and sleep disorders. In this regard, another core glial clock component was revealed to play an important role in the regulation of mood-related behaviors, such as anxiety and depression (Martini et al., 2021). G*Per2* mice, in fact, showed significantly less immobility in the forced swim test, thus displaying reduced despair, one of the main manifestations of depression (Martini et al., 2021). Besides, they spent more time in the open field (an anxiety-provoking space) of the elevated O-maze, indicating a reduced anxiety-like behavior in mice lacking *Per2* in glial cells (Martini et al., 2021). Nevertheless, glial *Per2* KO had no influence on circadian parameters since G*Per2* mice did not display any differences in the wheel-running activity and in body temperature fluctuations compared to control animals, thus indicating that the deletion of *Per2* in glial cells did not affect free-running rhythms in mice (Martini et al., 2021). An interesting observation is that, contrary to glial *Per2* KO animals, total *Per2* KO mice exhibited a shortening of the free running period (Martini et al., 2021). Therefore, these data suggest the importance of glial *Per2* in the regulation of mood behaviors through a process which, given the normal maintenance of circadian parameters, is not associated with the circadian clock machinery, but is probably related to the action of glial *Per2* on the glutamatergic, GABAergic, and dopaminergic signaling pathways (Martini et al., 2021).

Collectively, these findings suggest that an abnormal circadian system in glial cells may degenerate into metabolic diseases, immune system dysfunctions, and psychiatric illnesses. Therefore, deepening the knowledge of the role of the glial population in the generation of rhythm may be important for the discovery of new pathways and interactors involved in the development of these pathological disorders. In the following section, we will summarize recent findings reporting the existence of an autonomous rhythmical pattern in glia cells, demonstrating that astrocytes and microglia are not passive participants in the orchestration of rhythm, but play a key role in the regulation of circadian rhythms and in the maintenance of timekeeping within the brain (Hayashi et al., 2013; Fonken et al., 2015; Barca-Mayo et al., 2017; Brancaccio et al., 2017, 2019; Nakazato et al., 2017; Sominsky et al., 2021).

Astrocytes-Neurons Interaction in the Circadian Rhythmicity

Considerable evidence supports the primary involvement of astrocytes in the generation of rhythm, affirming their capacity to influence the molecular clock machinery of the central circadian pacemaker (Barca-Mayo et al., 2017; Brancaccio et al., 2017, 2019). Astrocytes express clock genes and can act as autonomous circadian oscillators (Ewer et al., 1992; Prolo et al., 2005). Ewer et al. (1992) first demonstrated the existence of a circadian clock in glia, by reporting the presence of the core clock component *period* in the astrocytes in *Drosophila melanogaster*. Also, primary cultures of cortical astrocytes derived from *Per2::luciferase* knock-in mice and *Per1::luciferase* transgenic rats were found to express circadian rhythms in the activity of these

two clock genes, with a longer average period in the activity of *Per1::luc* than *Per2::luc* (Prolo et al., 2005). Furthermore, beyond Glu, also some gliotransmitters, such as adenosine triphosphate (ATP), a neuronal transmitter involved in synaptic communication between astrocytes and neurons, are released following a circadian pattern (Womac et al., 2009; Marpegan et al., 2011). In particular, similarly to that observed in SCN cell cultures, extracellular ATP release and accumulation followed a daily rhythm in primary cultures of rat cortical astrocytes, thus suggesting that ATP might represent an important output of the mammalian molecular clock (Womac et al., 2009). Indeed, extracellular ATP levels have been found to strictly depend on clock genes expression. In this context, mouse astrocytes carrying mutations on *Clock*, *Per1*, and *Per2* genes showed a constitutively blunted ATP fluctuation during the day compared to wild-type cultures (Marpegan et al., 2011). Moreover, astrocytes have been suggested to be active during the circadian night, in contrast to neurons, whose peak of activity has been registered during the circadian day. These findings are based on data reporting that, in mouse SCN astrocytes, Glu release peaked during the nighttime in phase with astrocyte $[Ca^{2+}]_i$ levels, that were anti-phasic to those of neuronal $[Ca^{2+}]_i$ (Brancaccio et al., 2017). Overall, these results underline the ability of the astrocyte clock to impose its own rhythm autonomously, thus indicating that astrocytes are actively involved in the maintenance and control of molecular timekeeping within the brain.

However, such rhythmicity of astroglia is partly entrained and sustained by the SCN master clock (Prolo et al., 2005). In co-cultures of mouse cortical astrocytes with adult SCN explants, the amplitude of *Per1* rhythmicity has been observed to be significantly greater than that of primary astrocytes alone (Prolo et al., 2005), thus suggesting the existence of a crosstalk between the master neuronal clock in the SCN and the glial clock. In particular, in addition to SCN neurons, also astrocytes are able to encode circadian information and have been observed to strongly influence the central circadian pathway and the master clock machinery (Brancaccio et al., 2017, 2019; Tso et al., 2017). Notably, the increased release of Glu by astrocytes during the night has been found to be accomplished by a decrease in *Per2* expression rhythms in the SCN, thus denoting the active role played by astrocytes in promoting correct molecular timekeeping in the SCN *via* the glutamatergic signaling (Brancaccio et al., 2017). Furthermore, Brancaccio et al. (2019) using SCN slices of *Cry1/2*-null mice, demonstrated that the expression of *Cry1* alone in astrocytes was sufficient to initiate self-sustained circadian rhythms of *Per2* in the SCN, thus restoring the central molecular clock that was previously repressed, though with a longer time extent than neuronal *Cry1*. The crosstalk between SCN and astrocytes has also been suggested by data on astrocytes affecting the circadian pattern of behavior in mice. Although astrocytes are not directly connected to motor centers, the rhythmicity of locomotor activity, completely lost in *Cry1/2*-null mice, was re-established after the *Cry1* transfection of SCN astrocytes (Brancaccio et al., 2019), thus speculating that the astrocytic TTFL indirectly drives new circadian behaviors by hiring and restoring the neuronal TTFL in the SCN, probably by recruiting the E-box-based TTFL of neurons through the driving of neuronal $[Ca^{2+}]_i$ oscillations (Brancaccio et al., 2019).

In addition, *Bmal1* has also been reported to follow a rhythmical pattern and to strictly impact the circadian communications between astrocytes and neurons (Barca-Mayo et al., 2017; Tso et al., 2017). *Bmal1* deletion in astrocytes has been found to lead to a lengthening of *Per2* and locomotor circadian periodicity (Tso et al., 2017). Moreover, when maintained in constant darkness, a delay and reduction in the active period have been observed in *Bmal1* KO mice, as well as an impairment in cognitive functions mainly affecting the declarative memory (Barca-Mayo et al., 2017). Indeed, *Bmal1* KO mice were subjected to the novel object recognition (NOR) test, where they were exposed to two identical objects for 10 min, and they were subsequently tested by changing one of the familiar objects with a new one after 1 h and 24 h, with the aim to assess short-term and long-term memory respectively (Barca-Mayo et al., 2017). As a result, *Bmal1* KO animals displayed a significant reduction in the discrimination index after both 1 and 24 h, thus demonstrating both short-term and long-term memory being compromised (Barca-Mayo et al., 2017). Notably, oscillations of *Cry1*, *Bmal1*, and *Per2* expression were significantly impaired in the cortex and hippocampus of astrocyte *Bmal1* KO mice, thus demonstrating the existence of a strong intercellular communication and interplay between astrocytes and neurons that influence the circadian time-keeping within the brain and is fundamental for the maintenance of a healthy brain (Barca-Mayo et al., 2017).

Further demonstration of the ability of astrocytes to encode circadian information, and thus to influence the neuronal clock machinery, was provided by the finding that, in co-cultures of mouse synchronous astrocytes with asynchronous primary cortical neurons, the former was able to re-establish the rhythmical expression of *Bmal1*, *Cry1*, and *Per2* in the arrhythmic cortical neurons (Barca-Mayo et al., 2017). In contrast, astrocytes with *Bmal1* deletion failed to induce rhythmicity in the clock genes expression of asynchronous cortical neurons, thus demonstrating the pivotal role of an active astrocyte clock for adequately affecting the neuronal clockwork (Barca-Mayo et al., 2017). Accordingly, the deletion of astrocytic *Bmal1* has been found to impact the neuronal clock through GABA signaling, which acts as a mediator between neuron and astrocyte communication. In co-cultures of astrocytes with asynchronous cortical neurons, the inhibition of the GABA-A receptors prevented the astrocytic induction of a sustained rhythm in neurons, suggesting that the GABAergic pathway is required for the transmission of rhythm from astroglia to neurons (Barca-Mayo et al., 2017). Indeed, in astrocytes with *Bmal1* KO, the expression of GABA transporters *Gat1* and *Gat3* significantly decreased in the cortex and in the SCN compared to WT astrocytes, thus impairing the extracellular levels of GABA, providing the explanation for the reason behind the failure of the arrhythmic astrocytes to synchronize the clock of asynchronous cortical neurons (Barca-Mayo et al., 2017). All these data suggest that the loss of daily rhythm in astrocytes due to the deletion of astrocytic *Bmal1* is sufficient to lengthen and impair circadian rhythms in neurons and in behavior, both *in vitro* and *in vivo*,

demonstrating that astrocytes may actively contribute to the generation of SCN neuronal output rhythm and to internal clock synchronization.

Microglia: The Rhythmicity Around Immune and Inflammatory Response

Circadian clock genes are rhythmically expressed in microglia in several brain areas, such as the hippocampus and the cortex (Hayashi et al., 2013; Fonken et al., 2015; Nakazato et al., 2017). In hippocampal microglia isolated from adult rats, *Per1* and *Per2* expression was found to reach its peak in the middle of the light phase, *Rev-erb* at the end of the light phase, whereas the higher level of *Bmal1* expression was observed at the onset of the light period and in the middle of the dark phase (Fonken et al., 2015). Furthermore, also murine cortical microglia showed a fluctuant expression of *Per1, Per2*, *Rev-erbα*, and *Npas2*, thus supporting the idea of the existence of an autonomous clock machinery in microglia (Nakazato et al., 2011; Hayashi et al., 2013; Nakazato et al., 2017). The presence of the core clock proteins in microglia may also be responsible for the rhythmicity of a variety of microglial functions, such as immune and inflammatory response, by tuning the rhythmic fluctuations in basal inflammatory genes expression, such as cytokines and chemokines (Saijo and Glass, 2011). In rat hippocampal microglia, the expression of interleukin-1β (IL-1β), interleukin-6 (IL6), interleukin 1R1 (IL1R1), and tumor necrosis factor α (TNFα) was strictly affected by the time of the day, and, similarly to clock genes, they were strongly expressed during the light phase (Fonken et al., 2015). In addition, *Bmal1* has been found to be a critical player in the immunological activity of microglial cells, possibly due to the presence of E-box sequences in gene promoters of several cytokines (Nakazato et al., 2017; Wang et al., 2020). In particular, microglial *Bmal1* was found to be a key mediator for the regulation of the expression of IL6 (Nakazato et al., 2017). Accordingly, *Bmal1* deficiency has been found to decrease the expression of pro-inflammatory cytokines (*i.e.*, IL-1β, IL-6, and TNFα) and increase that of anti-inflammatory cytokines (*i.e.*, IL-10) in mouse microglia (Wang et al., 2020). These data support the involvement of the microglial clock system in the regulation of inflammatory responses. Another microglia-associated function with diurnal rhythmicity is the regulation of synaptic strength *via* the circadian secretion of cathepsin S (CatS). CatS is a microglia-specific lysosomal cysteine protease rhythmically secreted during the dark phase, fundamental for the maintenance of neuronal circuitry (Hayashi et al., 2013). Hayashi and coworkers found that CatS expression followed a circadian pattern driven by the intrinsic microglial molecular clock (Hayashi et al., 2013). Accordingly, in WT mouse cortical microglia, CatS transcripts showed a peak at CT14, whereas, in the cortical microglia of *Clock*Δ*19* mutant mice, no diurnal fluctuation of CatS expression was observed, thus suggesting that its transcription was activated and mediated by the binding of *Clock:Bmal1* heterodimer to the E-boxes sequences on the CatS gene promoter (Hayashi et al., 2013). All these data demonstrate the existence of a microglial clock involved in the regulation of microglia-mediated functions, including the neuroimmune roles and the control of the synaptic strength.

Beyond increasing knowledge regarding the presence of an intrinsic clock in microglial cells, data from literature report that, in turn, the microglial clock system may also influence the neuronal clock machinery and rhythms among the CNS. Indeed, ablation of microglia resulted in the disruption of the central circadian system both at molecular and physiological levels (Sominsky et al., 2021). Notably, using Cx3cr1-Dtr rats, a rat model in which microglia is depleted, aberrations in clock gene expression were observed (Sominsky et al., 2021). In the SCN, *Per1* mRNA levels were increased and a reduction in *Bmal1* protein was revealed, whereas, in the hippocampus, the microglial depletion led to a suppression of *Bmal1* expression and to an increase of *Per1* and *Per2* mRNA levels (Sominsky et al., 2021). Moreover, ablation of microglial cells from the CNS led to a disruption of body temperature rhythms, energy metabolism, and diurnal activity profiles. To such effect, Cx3cr1-Dtr rats showed a significant reduction in total energy expenditure during their active phase and also in their diurnal rhythms compared to WT (Sominsky et al., 2021). Accordingly, Sominsky et al. (2021) also observed a total loss of diurnal activity rhythms and a changing in temperature rhythms, with a pattern completely inverse to that of energy expenditure and activity changes. Considered together, these findings suggest that microglia may play a key role in diurnal rhythm generation since its ablation leads to the concomitant disruption of diurnal profiles and to the dysregulation of the expression of certain clock genes in different brain domains. In contrast, Barahona and collaborators showed that, in the cortex, ablation of microglia did not affect the rhythmical pattern of clock genes expression, since in Cx3cr1-Dtr rats clock genes all maintained their diurnal rhythmical expression (Barahona et al., 2022). Due to these conflicting data, further studies on this glia population are required to elucidate its role in the generation of rhythms throughout the brain.

A MATTER OF TIME: WHY UNDERSTANDING THE FUNCTIONING OF THE BIOLOGICAL CLOCK IN THE CNS IS CRUCIAL?

Circadian rhythms are dictated by highly specialized cells of specific brain areas that orchestrate a complex network of coupled self-sustained clocks both in the brain and in peripheral organs. Remarkably, neurons are not the only CNS cell population to orchestrate the rhythm, but also astrocytes and microglia have been reported to harbor an intrinsic autonomous clock and to actively participate in the maintenance of timekeeping within the brain. Moreover, since neurotransmitters play a key role in the diffusion of circadian information among CNS cells and impact the core clock machinery, they have emerged as fine-tuners of daily rhythmicity. Indeed, the bidirectional interplay between neurotransmitters and the circadian clockwork is fundamental to maintain the accuracy and precision in daily timekeeping among different brain areas. In

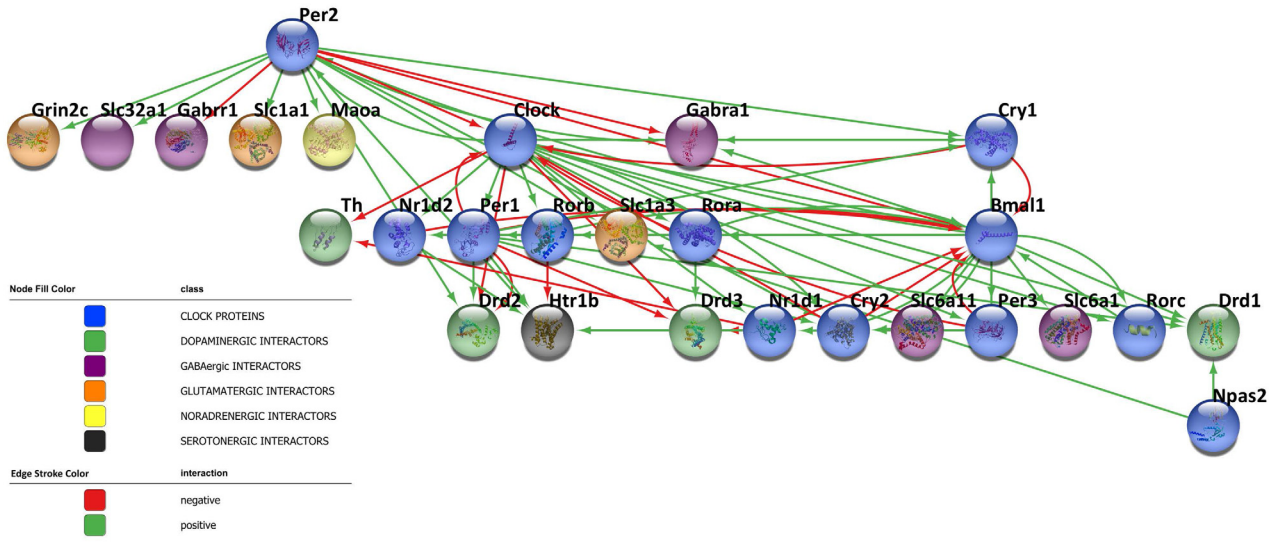

FIGURE 3 | Bidirectional crosstalk between clock proteins and neurotransmitter players. The network contains 27 nodes and the edges represent the crosstalk between the clock proteins and neurotransmitter players depicted by the literature (positive regulation: green line, negative regulation: red line). The different biological processes investigated are shown in the network according to the color legend. The network has been visualized using Cytoscape 3.9.1 (Shannon et al., 2003).

this regard, the network reported in **Figure 3** shows the complex interactions taking place between clock proteins and several neurotransmitter players, as depicted by the literature discussed above, with the aim of illustrating this intricate bidirectional crosstalk (**Figure 3**). However, much is still unknown about the deeper molecular interconnections involved in the orchestration of the temporal variable among CNS cells. Therefore, expanding our knowledge about this complex network appears fundamental to better understand the functioning of the biological clockwork, which represents an extremely dynamic process across the lifespan. Indeed, rhythmic activities have been observed to significantly change during the pace of aging, also contributing to the acceleration of the process. Furthermore, due to the sexually dimorphic nature of some neurotransmitters systems [*e.g.*, the NA system (Joshi and Chandler, 2020), the DA system (Rial et al., 2018), and the 5HT system (Näslund et al., 2013)], the connection between chemical transmission and expression and functions of clock genes in the CNS might account for sex-dependent variability in the circadian timing system. In this regard, seasonality, as well as most of the sex and gender-related-mechanisms, is known to affect the efficiency of learning, memory, and mood control processes (Bailey and Silver, 2014; Urban et al., 2021). Although so far poorly investigated, the interplay linking sex-neurotransmitters-clock genes deserves of course attention, since if disrupted or malfunctioning, might subserve the development of central disorders including those that so far preferentially attracted the interest of the researchers as discussed below.

Noteworthy, although future longitudinal studies are necessary to corroborate such preliminary evidence, the circadian system seems to play a key role in the pathogenesis of psychiatric diseases and neurodegenerative disorders. In particular, circadian rhythms disruption has been described not only as an early warning sign of neurodegenerative diseases but also as a potential risk factor. Evidence from literature suggests the existence of a strict correlation between several neurodegenerative diseases, specifically Alzheimer's disease (AD) and Parkinson's disease (PD), and circadian rhythms destruction (CRD; Videnovic et al., 2014). Accordingly, AD and PD share common features and symptoms ascribable to an abnormal and disrupted circadian pattern (Videnovic et al., 2014). For example, patients with neurodegenerative diseases show frequent disorders in the sleep/wake cycle, with sleep fragmentation and an increase in activity levels in the nighttime, and a prevalence of sleepiness during daytime (Merlino et al., 2010; Breen et al., 2014). Notably, it has been confirmed that an alteration of the molecular clockwork leads to an increase in the oxidative injury of the brain, thus promoting neuronal damage, cell death, and neurodegeneration. Interestingly, several studies on mice found that both global and brain-specific deletion of *Bmal1* induced higher neuronal oxidative damage, synaptic degeneration, severe astrogliosis, impaired neuronal network functional connectivity, and impaired learning and memory, compared to age-matched wild type controls, resulting in premature aging, reduced lifespan, and pathogenesis of neurodegeneration (Musiek et al., 2013). Furthermore, the majority of neurodegenerative disorders are associated with the accumulation of intra- and extra-cellular aggregates (*i.e.*, amyloid-β, phosphorylated tau protein, α-sinuclein), whose clearance is partly controlled by the glymphatic flow. Recent studies on mouse models have found that the glymphatic flow follows a rhythmical circadian pattern with an important upregulation during sleep, thus facilitating the removal of metabolic products accumulated during wakefulness (Hablitz et al., 2020). Remarkably, in mouse models of neurodegenerative disorders (such as APP/PS1 mice, a model of AD), where

circadian rhythms are disturbed, a reduced brain clearance has been reported, due to the presence of disrupted flow patterns of the glymphatic system, thus resulting in a continuous and augmented accumulation of aggregates that, in turn, may promote cell death and degeneration of brain structures (Peng et al., 2016; Rasmussen et al., 2018). In conclusion, expanding our knowledge about the molecular regulation of circadian rhythmicity in CNS cells within different brain areas represents a crucial challenge, with a potential impact on the biological comprehension of the onset of neurodegenerative processes.

AUTHOR CONTRIBUTIONS

FF and CL: conceived the idea. FF, EB, AP, and CL: wrote the manuscript. EP: network analysis. FF, EB, AP, EP, CS, SG, and CL: critical discussion. All authors contributed to the article and approved the submitted version.

FUNDING

Research has been supported by the University of Pavia (grant from PRIN 2020SCBBN2_005 to CL).

REFERENCES

Abrahamson, E. E., and Moore, R. Y. (2001). Suprachiasmatic nucleus in the mouse: retinal innervation, intrinsic organization and efferent projections. *Brain Res.* 916, 172–191. doi: 10.1016/s0006-8993(01)02890-6

Albers, H. E., Walton, J. C., Gamble, K. L., McNeill, J. K., 4th, and Hummer, D. L. (2017). The dynamics of GABA signaling: revelations from the circadian pacemaker in the suprachiasmatic nucleus. *Front. Neuroendocrinol.* 44, 35–82. doi: 10.1016/j.yfrne.2016.11.003

Azmitia, E. C., and Segal, M. (1978). An autoradiographic analysis of the differential ascending projections of the dorsal and median raphe nuclei in the rat. *J. Comp. Neurol.* 179, 641–667. doi: 10.1002/cne.901790311

Bailey, M., and Silver, R. (2014). Sex differences in circadian timing systems: implications for disease. *Front. Neuroendocrinol.* 35, 111–139. doi: 10.1016/j.yfrne.2013.11.003

Barahona, R. A., Morabito, S., Swarup, V., and Green, K. N. (2022). Cortical diurnal rhythms remain intact with microglial depletion. *Sci. Rep.* 12:114. doi: 10.1038/s41598-021-04079-w

Barca-Mayo, O., Pons-Espinal, M., Follert, P., Armirotti, A., Berdondini, L., and De Pietri Tonelli, D. (2017). Astrocyte deletion of Bmal1 alters daily locomotor activity and cognitive functions via GABA signalling. *Nat. Commun.* 8:14336. doi: 10.1038/ncomms14336

Beaulé, C., Swanstrom, A., Leone, M. J., and Herzog, E. D. (2009). Circadian modulation of gene expression, but not glutamate uptake, in mouse and rat cortical astrocytes. *PLoS One* 4:e7476. doi: 10.1371/journal.pone.0007476

Borgland, S. L., Taha, S. A., Sarti, F., Fields, H. L., and Bonci, A. (2006). Orexin A in the VTA is critical for the induction of synaptic plasticity and behavioral sensitization to cocaine. *Neuron* 49, 589–601. doi: 10.1016/j.neuron.2006.01.016

Bourdy, R., and Barrot, M. (2012). A new control center for dopaminergic systems: pulling the VTA by the tail. *Trends Neurosci.* 35, 681–690. doi: 10.1016/j.tins.2012.06.007

Brancaccio, M., Edwards, M. D., Patton, A. P., Smyllie, N. J., Chesham, J. E., Maywood, E. S., et al. (2019). Cell-autonomous clock of astrocytes drives circadian behavior in mammals. *Science* 363, 187–192. doi: 10.1126/science.aat4104

Brancaccio, M., Maywood, E. S., Chesham, J. E., Loudon, A. S. I., and Hastings, M. H. (2013). A Gq-Ca^{2+} axis controls circuit-level encoding of circadian time in the suprachiasmatic nucleus. *Neuron* 78, 714–728. doi: 10.1016/j.neuron.2013.03.011

Brancaccio, M., Patton, A. P., Chesham, J. E., Maywood, E. S., and Hastings, M. H. (2017). Astrocytes control circadian timekeeping in the suprachiasmatic nucleus via glutamatergic signaling. *Neuron* 93, 1420–1435.e5. doi: 10.1016/j.neuron.2017.02.030

Breen, D. P., Vuono, R., Nawarathna, U., Fisher, K., Shneerson, J. M., Reddy, A. B., et al. (2014). Sleep and circadian rhythm regulation in early Parkinson disease. *JAMA Neurol.* 71, 589–595. doi: 10.1001/jamaneurol.2014.65

Brenna, A., and Albrecht, U. (2020). Phosphorylation and circadian molecular timing. *Front. Physiol.* 11:612510. doi: 10.3389/fphys.2020.612510

Brenna, A., Ripperger, J. A., Saro, G., Glauser, D. A., Yang, Z., and Albrecht, U. (2021). PER2 mediates CREB-dependent light induction of the clock gene Per1. *Sci. Rep.* 11:21766. doi: 10.1038/s41598-021-01178-6

Burioka, N., Koyanagi, S., Endo, M., Takata, M., Fukuoka, Y., Miyata, M., et al. (2008). Clock gene dysfunction in patients with obstructive sleep apnoea syndrome. *Eur. Respir. J.* 32, 105–112. doi: 10.1183/09031936.00138207

Cagampang, F. R., Rattray, M., Powell, J. F., Chong, N. W., Campbell, I. C., and Coen, C. W. (1996). Circadian variation of EAAC1 glutamate transporter messenger RNA in the rat suprachiasmatic nuclei. *Brain Res. Mol. Brain Res.* 35, 190–196. doi: 10.1016/0169-328x(95)00203-5

Castañeda, T. R., de Prado, B. M., Prieto, D., and Mora, F. (2004). Circadian rhythms of dopamine, glutamate and GABA in the striatum and nucleus accumbens of the awake rat: modulation by light. *J. Pineal Res.* 36, 177–185. doi: 10.1046/j.1600-079x.2003.00114.x

Chen, S.-K., Badea, T. C., and Hattar, S. (2011). Photoentrainment and pupillary light reflex are mediated by distinct populations of ipRGCs. *Nature* 476, 92–95. doi: 10.1038/nature10206

Chevillard, C., Barden, N., and Saavedra, J. M. (1981). Twenty-four hour rhythm in monoamine oxidase activity in specific areas of the rat brain stem. *Brain Res.* 223, 205–209. doi: 10.1016/0006-8993(81)90825-8

Chung, S., Lee, E. J., Yun, S., Choe, H. K., Park, S.-B., Son, H. J., et al. (2014). Impact of circadian nuclear receptor REV-ERBα on midbrain dopamine production and mood regulation. *Cell* 157, 858–868. doi: 10.1016/j.cell.2014.03.039

Cox, K. H., and Takahashi, J. S. (2019). Circadian clock genes and the transcriptional architecture of the clock mechanism. *J. Mol. Endocrinol.* 63, R93–R102. doi: 10.1530/JME-19-0153

Cuesta, M., Mendoza, J., Clesse, D., Pévet, P., and Challet, E. (2008). Serotonergic activation potentiates light resetting of the main circadian clock and alters clock gene expression in a diurnal rodent. *Exp. Neurol.* 210, 501–513. doi: 10.1016/j.expneurol.2007.11.026

Danbolt, N. C. (2001). Glutamate uptake. *Prog. Neurobiol.* 65, 1–105. doi: 10.1016/s0301-0082(00)00067-8

Daszuta, A., and Barrit, M. C. (1982). Endogenous serotonin (5-HT) and 5-hydroxyindole acetic acid (5-HIAA) levels in large regions and in discrete brain areas of C57BL and BALBc mice at three times of the day. *Brain Res. Bull.* 8, 477–482. doi: 10.1016/0361-9230(82)90004-1

Descarries, L., and Mechawar, N. (2000). Ultrastructural evidence for diffuse transmission by monoamine and acetylcholine neurons of the central nervous system. *Prog. Brain Res.* 125, 27–47. doi: 10.1016/S0079-6123(00)25005-X

Deurveilher, S., and Semba, K. (2005). Indirect projections from the suprachiasmatic nucleus to major arousal-promoting cell groups in rat: implications for the circadian control of behavioural state. *Neuroscience* 130, 165–183. doi: 10.1016/j.neuroscience.2004.08.030

Dibner, C., Schibler, U., and Albrecht, U. (2010). The mammalian circadian timing system: organization and coordination of central and peripheral clocks. *Annu. Rev. Physiol.* 72, 517–549. doi: 10.1146/annurev-physiol-021909-135821

Doyle, S. E., McIvor, W. E., and Menaker, M. (2002). Circadian rhythmicity in dopamine content of mammalian retina: role of the photoreceptors. *J. Neurochem.* 83, 211–219. doi: 10.1046/j.1471-4159.2002.01149.x

Elmenhorst, D., Mertens, K., Kroll, T., Oskamp, A., Ermert, J., Elmenhorst, E.-M., et al. (2016). Circadian variation of metabotropic glutamate receptor 5 availability in the rat brain. *J. Sleep Res.* 25, 754–761. doi: 10.1111/jsr.12432

Ewer, J., Frisch, B., Hamblen-Coyle, M. J., Rosbash, M., and Hall, J. C. (1992). Expression of the period clock gene within different cell types in the brain of *Drosophila* adults and mosaic analysis of these cells' influence on circadian

behavioral rhythms. *J. Neurosci.* 12, 3321–3349. doi: 10.1523/JNEUROSCI.12-09-03321.1992

Fang, L., Yang, Z., Zhou, J., Tung, J.-Y., Hsiao, C.-D., Wang, L., et al. (2015). Circadian clock gene CRY2 degradation is involved in chemoresistance of colorectal cancer. *Mol. Cancer Ther.* 14, 1476–1487. doi: 10.1158/1535-7163.MCT-15-0030

Farinelli, S. E., and Nicklas, W. J. (1992). Glutamate metabolism in rat cortical astrocyte cultures. *J. Neurochem.* 58, 1905–1915. doi: 10.1111/j.1471-4159.1992.tb10068.x

Fellin, T., Pascual, O., Gobbo, S., Pozzan, T., Haydon, P. G., and Carmignoto, G. (2004). Neuronal synchrony mediated by astrocytic glutamate through activation of extrasynaptic NMDA receptors. *Neuron* 43, 729–743. doi: 10.1016/j.neuron.2004.08.011

Flourakis, M., Kula-Eversole, E., Hutchison, A. L., Han, T. H., Aranda, K., Moose, D. L., et al. (2015). A conserved bicycle model for circadian clock control of membrane excitability. *Cell* 162, 836–848. doi: 10.1016/j.cell.2015.07.036

Fonken, L. K., Frank, M. G., Kitt, M. M., Barrientos, R. M., Watkins, L. R., and Maier, S. F. (2015). Microglia inflammatory responses are controlled by an intrinsic circadian clock. *Brain. Behav. Immun.* 45, 171–179. doi: 10.1016/j.bbi.2014.11.009

Fuxe, K., Borroto-Escuela, D. O., Romero-Fernandez, W., Ciruela, F., Manger, P., Leo, G., et al. (2012). On the role of volume transmission and receptor-receptor interactions in social behaviour: focus on central catecholamine and oxytocin neurons. *Brain Res.* 1476, 119–131. doi: 10.1016/j.brainres.2012.01.062

Gau, D., Lemberger, T., von Gall, C., Kretz, O., Le Minh, N., Gass, P., et al. (2002). Phosphorylation of CREB Ser142 regulates light-induced phase shifts of the circadian clock. *Neuron* 34, 245–253. doi: 10.1016/s0896-6273(02)00656-6

Glass, J. D., Randolph, W. W., Ferreira, S. A., Rea, M. A., Hauser, U. E., Blank, J. L., et al. (1992). Diurnal variation in 5-hydroxyindole-acetic acid output in the suprachiasmatic region of the Siberian hamster assessed by *in vivo* microdialysis: evidence for nocturnal activation of serotonin release. *Neuroendocrinology* 56, 582–590. doi: 10.1159/000126277

Gooley, J. J., Lu, J., Chou, T. C., Scammell, T. E., and Saper, C. B. (2001). Melanopsin in cells of origin of the retinohypothalamic tract. *Nat. Neurosci.* 4:1165. doi: 10.1038/nn768

Hablitz, L. M., Plá, V., Giannetto, M., Vinitsky, H. S., Stæger, F. F., Metcalfe, T., et al. (2020). Circadian control of brain glymphatic and lymphatic fluid flow. *Nat. Commun.* 11:4411. doi: 10.1038/s41467-020-18115-2

Hamilton, N. B., and Attwell, D. (2010). Do astrocytes really exocytose neurotransmitters? *Nat. Rev. Neurosci.* 11, 227–238. doi: 10.1038/nrn2803

Hampp, G., Ripperger, J. A., Houben, T., Schmutz, I., Blex, C., Perreau-Lenz, S., et al. (2008). Regulation of monoamine oxidase A by circadian-clock components implies clock influence on mood. *Curr. Biol.* 18, 678–683. doi: 10.1016/j.cub.2008.04.012

Harvey, J. R. M., Plante, A. E., and Meredith, A. L. (2020). Ion channels controlling circadian rhythms in suprachiasmatic nucleus excitability. *Physiol. Rev.* 100, 1415–1454. doi: 10.1152/physrev.00027.2019

Hastings, M. H., Maywood, E. S., and Brancaccio, M. (2018). Generation of circadian rhythms in the suprachiasmatic nucleus. *Nat. Rev. Neurosci.* 19, 453–469. doi: 10.1038/s41583-018-0026-z

Hastings, M. H., Reddy, A. B., and Maywood, E. S. (2003). A clockwork web: circadian timing in brain and periphery, in health and disease. *Nat. Rev. Neurosci.* 4, 649–661. doi: 10.1038/nrn1177

Hattar, S., Kumar, M., Park, A., Tong, P., Tung, J., Yau, K.-W., et al. (2006). Central projections of melanopsin-expressing retinal ganglion cells in the mouse. *J. Comp. Neurol.* 497, 326–349. doi: 10.1002/cne.20970

Hayashi, Y., Koyanagi, S., Kusunose, N., Okada, R., Wu, Z., Tozaki-Saitoh, H., et al. (2013). The intrinsic microglial molecular clock controls synaptic strength via the circadian expression of cathepsin S. *Sci. Rep.* 3:2744. doi: 10.1038/srep02744

Hay-Schmidt, A., Vrang, N., Larsen, P. J., and Mikkelsen, J. D. (2003). Projections from the raphe nuclei to the suprachiasmatic nucleus of the rat. *J. Chem. Neuroanat.* 25, 293–310. doi: 10.1016/s0891-0618(03)00042-5

Herzog, E. D., Aton, S. J., Numano, R., Sakaki, Y., and Tei, H. (2004). Temporal precision in the mammalian circadian system: a reliable clock from less reliable neurons. *J. Biol. Rhythms* 19, 35–46. doi: 10.1177/0748730403260776

Hirasawa, H., Puopolo, M., and Raviola, E. (2009). Extrasynaptic release of GABA by retinal dopaminergic neurons. *J. Neurophysiol.* 102, 146–158. doi: 10.1152/jn.00130.2009

Hood, S., Cassidy, P., Cossette, M.-P., Weigl, Y., Verwey, M., Robinson, B., et al. (2010). Endogenous dopamine regulates the rhythm of expression of the clock protein PER2 in the rat dorsal striatum via daily activation of D2 dopamine receptors. *J. Neurosci.* 30, 14046–14058. doi: 10.1523/JNEUROSCI.2128-10.2010

Hubbard, J., Ruppert, E., Calvel, L., Robin-Choteau, L., Gropp, C.-M., Allemann, C., et al. (2015). Arvicanthis ansorgei, a novel model for the study of sleep and waking in diurnal rodents. *Sleep* 38, 979–988. doi: 10.5665/sleep.4754

Huhman, K. L., Hennessey, A. C., and Albers, H. E. (1996). Rhythms of glutamic acid decarboxylase mRNA in the suprachiasmatic nucleus. *J. Biol. Rhythms* 11, 311–316. doi: 10.1177/074873049601100404

Ikeda, E., Matsunaga, N., Kakimoto, K., Hamamura, K., Hayashi, A., Koyanagi, S., et al. (2013). Molecular mechanism regulating 24-hour rhythm of dopamine D3 receptor expression in mouse ventral striatum. *Mol. Pharmacol.* 83, 959–967. doi: 10.1124/mol.112.083535

Imbesi, M., Yildiz, S., Dirim Arslan, A., Sharma, R., Manev, H., and Uz, T. (2009). Dopamine receptor-mediated regulation of neuronal "clock" gene expression. *Neuroscience* 158, 537–544. doi: 10.1016/j.neuroscience.2008.10.044

Jones, B. E. (2017). Principal cell types of sleep-wake regulatory circuits. *Curr. Opin. Neurobiol.* 44, 101–109. doi: 10.1016/j.conb.2017.03.018

Joshi, N., and Chandler, D. (2020). Sex and the noradrenergic system. *Handb. Clin. Neurol.* 175, 167–176. doi: 10.1016/B978-0-444-64123-6.00012-6

Koike, N., Yoo, S.-H., Huang, H.-C., Kumar, V., Lee, C., Kim, T.-K., et al. (2012). Transcriptional architecture and chromatin landscape of the core circadian clock in mammals. *Science* 338, 349–354. doi: 10.1126/science.1226339

Korshunov, K. S., Blakemore, L. J., and Trombley, P. Q. (2017). Dopamine: a modulator of circadian rhythms in the central nervous system. *Front. Cell. Neurosci.* 11:91. doi: 10.3389/fncel.2017.00091

Lecca, S., Melis, M., Luchicchi, A., Muntoni, A. L., and Pistis, M. (2012). Inhibitory inputs from rostromedial tegmental neurons regulate spontaneous activity of midbrain dopamine cells and their responses to drugs of abuse. *Neuropsychopharmacology* 37, 1164–1176. doi: 10.1038/npp.2011.302

Lehre, K. P., and Danbolt, N. C. (1998). The number of glutamate transporter subtype molecules at glutamatergic synapses: chemical and stereological quantification in young adult rat brain. *J. Neurosci.* 18, 8751–8757. doi: 10.1523/JNEUROSCI.18-21-08751.1998

Lundkvist, G. B., Kwak, Y., Davis, E. K., Tei, H., and Block, G. D. (2005). A calcium flux is required for circadian rhythm generation in mammalian pacemaker neurons. *J. Neurosci.* 25, 7682–7686. doi: 10.1523/JNEUROSCI.2211-05.2005

Maejima, T., Tsuno, Y., Miyazaki, S., Tsuneoka, Y., Hasegawa, E., Islam, M. T., et al. (2021). GABA from vasopressin neurons regulates the time at which suprachiasmatic nucleus molecular clocks enable circadian behavior. *Proc. Natl. Acad. Sci. U S A* 118:e2010168118. doi: 10.1073/pnas.2010168118

Malek, Z. S., Dardente, H., Pevet, P., and Raison, S. (2005). Tissue-specific expression of tryptophan hydroxylase mRNAs in the rat midbrain: anatomical evidence and daily profiles. *Eur. J. Neurosci.* 22, 895–901. doi: 10.1111/j.1460-9568.2005.04264.x

Malek, Z. S., Sage, D., Pévet, P., and Raison, S. (2007). Daily rhythm of tryptophan hydroxylase-2 messenger ribonucleic acid within raphe neurons is induced by corticoid daily surge and modulated by enhanced locomotor activity. *Endocrinology* 148, 5165–5172. doi: 10.1210/en.2007-0526

Marpegan, L., Swanstrom, A. E., Chung, K., Simon, T., Haydon, P. G., Khan, S. K., et al. (2011). Circadian regulation of ATP release in astrocytes. *J. Neurosci.* 31, 8342–8350. doi: 10.1523/JNEUROSCI.6537-10.2011

Martini, T., Ripperger, J. A., Stalin, J., Kores, A., Stumpe, M., and Albrecht, U. (2021). Deletion of the clock gene Period2 (Per2) in glial cells alters mood-related behavior in mice. *Sci. Rep.* 11:12242. doi: 10.1038/s41598-021-91770-7

McClung, C. A., Sidiropoulou, K., Vitaterna, M., Takahashi, J. S., White, F. J., Cooper, D. C., et al. (2005). Regulation of dopaminergic transmission and cocaine reward by the clock gene. *Proc. Natl. Acad. Sci. U S A* 102, 9377–9381. doi: 10.1073/pnas.0503584102

Mendoza, J., and Challet, E. (2014). Circadian insights into dopamine mechanisms. *Neuroscience* 282, 230–242. doi: 10.1016/j.neuroscience.2014.07.081

Merlino, G., Piani, A., Gigli, G. L., Cancelli, I., Rinaldi, A., Baroselli, A., et al. (2010). Daytime sleepiness is associated with dementia and cognitive decline in older Italian adults: a population-based study. *Sleep Med.* 11, 372–377. doi: 10.1016/j.sleep.2009.07.018

Mistlberger, R. E., Antle, M. C., Glass, J. D., and Miller, J. D. (2000). Behavioral and serotonergic regulation of circadian rhythms. *Biol. Rhythm Res.* 31, 240–283. doi: 10.1076/0929-1016(200007)31:3;1-K;FT240

Morin, L. P. (1999). Serotonin and the regulation of mammalian circadian rhythmicity. *Ann. Med.* 31, 12–33. doi: 10.3109/07853899909019259

Musiek, E. S., Lim, M. M., Yang, G., Bauer, A. Q., Qi, L., Lee, Y., et al. (2013). Circadian clock proteins regulate neuronal redox homeostasis and neurodegeneration. *J. Clin. Invest.* 123, 5389–5400. doi: 10.1172/JCI70317

Nakamaru-Ogiso, E., Miyamoto, H., Hamada, K., Tsukada, K., and Takai, K. (2012). Novel biochemical manipulation of brain serotonin reveals a role of serotonin in the circadian rhythm of sleep-wake cycles. *Eur. J. Neurosci.* 35, 1762–1770. doi: 10.1111/j.1460-9568.2012.08077.x

Nakayama, K. (2002). Diurnal rhythm in extracellular levels of 5-hydroxyindoleacetic acid in the medial prefrontal cortex of freely moving rats: an *in vivo* microdialysis study. *Prog. Neuropsychopharmacol. Biol. Psychiatry* 26, 1383–1388. doi: 10.1016/s0278-5846(02)00304-4

Nakazato, R., Hotta, S., Yamada, D., Kou, M., Nakamura, S., Takahata, Y., et al. (2017). The intrinsic microglial clock system regulates interleukin-6 expression. *Glia* 65, 198–208. doi: 10.1002/glia.23087

Nakazato, R., Takarada, T., Yamamoto, T., Hotta, S., Hinoi, E., Yoneda, Y., et al. (2011). Selective upregulation of Per1 mRNA expression by ATP through activation of P2X7 purinergic receptors expressed in microglial cells. *J. Pharmacol. Sci.* 116, 350–361. doi: 10.1254/jphs.11069fp

Narita, M., Nagumo, Y., Hashimoto, S., Narita, M., Khotib, J., Miyatake, M., et al. (2006). Direct involvement of orexinergic systems in the activation of the mesolimbic dopamine pathway and related behaviors induced by morphine. *J. Neurosci.* 26, 398–405. doi: 10.1523/JNEUROSCI.2761-05.2006

Näslund, J., Studer, E., Nilsson, K., Westberg, L., and Eriksson, E. (2013). Serotonin depletion counteracts sex differences in anxiety-related behaviour in rat. *Psychopharmacology (Berl).* 230, 29–35. doi: 10.1007/s00213-013-3133-6

O'Neill, J. S., Maywood, E. S., Chesham, J. E., Takahashi, J. S., and Hastings, M. H. (2008). cAMP-dependent signaling as a core component of the mammalian circadian pacemaker. *Science* 320, 949–953. doi: 10.1126/science.1152506

Olivero, G., Vergassola, M., Cisani, F., Roggeri, A., and Pittaluga, A. (2020). Presynaptic release-regulating metabotropic glutamate receptors: an update. *Curr. Neuropharmacol.* 18, 655–672. doi: 10.2174/1570159X17666191127112339

Osorio-Forero, A., Cherrad, N., Banterle, L., Fernandez, L. M. J., and Lüthi, A. (2022). When the locus coeruleus speaks up in sleep: recent insights, emerging perspectives. *Int. J. Mol. Sci.* 23:5028. doi: 10.3390/ijms23095028

Palm, D., Uzoni, A., Simon, F., Tucha, O., Thome, J., Faltraco, F., et al. (2021). Norepinephrine influences the circadian clock in human dermal fibroblasts from study participants with a diagnosis of attention-deficit hyperactivity disorder. *J. Neural Transm.* 128, 1147–1157. doi: 10.1007/s00702-021-02376-2

Panda, S., Antoch, M. P., Miller, B. H., Su, A. I., Schook, A. B., Straume, M., et al. (2002). Coordinated transcription of key pathways in the mouse by the circadian clock. *Cell* 109, 307–320. doi: 10.1016/s0092-8674(02)00722-5

Parra-Damas, A., Rubió-Ferrarons, L., Shen, J., and Saura, C. A. (2017). CRTC1 mediates preferential transcription at neuronal activity-regulated CRE/TATA promoters. *Sci. Rep.* 7:18004. doi: 10.1038/s41598-017-18215-y

Peng, W., Achariyar, T. M., Li, B., Liao, Y., Mestre, H., Hitomi, E., et al. (2016). Suppression of glymphatic fluid transport in a mouse model of Alzheimer's disease. *Neurobiol. Dis.* 93, 215–225. doi: 10.1016/j.nbd.2016.05.015

Pickard, G. E., Smith, B. N., Belenky, M., Rea, M. A., Dudek, F. E., Sollars, P. J., et al. (1999). 5-HT1B receptor-mediated presynaptic inhibition of retinal input to the suprachiasmatic nucleus. *J. Neurosci.* 19, 4034–4045. doi: 10.1523/JNEUROSCI.19-10-04034.1999

Preitner, N., Damiola, F., Lopez-Molina, L., Zakany, J., Duboule, D., Albrecht, U., et al. (2002). The orphan nuclear receptor REV-ERBα controls circadian transcription within the positive limb of the mammalian circadian oscillator. *Cell* 110, 251–260. doi: 10.1016/s0092-8674(02)00825-5

Prigge, C. L., Yeh, P.-T., Liou, N.-F., Lee, C.-C., You, S.-F., Liu, L.-L., et al. (2016). M1 ipRGCs influence visual function through retrograde signaling in the retina. *J. Neurosci.* 36, 7184–7197. doi: 10.1523/JNEUROSCI.3500-15.2016

Prolo, L. M., Takahashi, J. S., and Herzog, E. D. (2005). Circadian rhythm generation and entrainment in astrocytes. *J. Neurosci.* 25, 404–408. doi: 10.1523/JNEUROSCI.4133-04.2005

Ralph, M. R., Foster, R. G., Davis, F. C., and Menaker, M. (1990). Transplanted suprachiasmatic nucleus determines circadian period. *Science* 247, 975–978. doi: 10.1126/science.2305266

Rasmussen, M. K., Mestre, H., and Nedergaard, M. (2018). The glymphatic pathway in neurological disorders. *Lancet Neurol.* 17, 1016–1024. doi: 10.1016/S1474-4422(18)30318-1

Rea, M. A., and Pickard, G. E. (2000). A 5-HT(1B) receptor agonist inhibits light-induced suppression of pineal melatonin production. *Brain Res.* 858, 424–428. doi: 10.1016/s0006-8993(99)02462-2

Rial, R. V., Canellas, F., Gamundí, A., Akaârir, M., and Nicolau, M. C. (2018). Pleasure: the missing link in the regulation of sleep. *Neurosci. Biobehav. Rev.* 88, 141–154. doi: 10.1016/j.neubiorev.2018.03.012

Romei, C., Bonifacino, T., Milanese, M., Usai, C., and Raiteri, L. (2016). Colocalization of neurotransmitter transporters on the plasma membrane of the same nerve terminal may reflect cotransmission. *Brain Res. Bull.* 127, 100–110. doi: 10.1016/j.brainresbull.2016.08.013

Ruan, G.-X., Allen, G. C., Yamazaki, S., and McMahon, D. G. (2008). An autonomous circadian clock in the inner mouse retina regulated by dopamine and GABA. *PLoS Biol.* 6:e249. doi: 10.1371/journal.pbio.0060249

Saijo, K., and Glass, C. K. (2011). Microglial cell origin and phenotypes in health and disease. *Nat. Rev. Immunol.* 11, 775–787. doi: 10.1038/nri3086

Schmutz, I., Ripperger, J. A., Baeriswyl-Aebischer, S., and Albrecht, U. (2010). The mammalian clock component PERIOD2 coordinates circadian output by interaction with nuclear receptors. *Genes Dev.* 24, 345–357. doi: 10.1101/gad.564110

Schwab, C., DeMaggio, A. J., Ghoshal, N., Binder, L. I., Kuret, J., McGeer, P. L., et al. (2000). Casein kinase 1 delta is associated with pathological accumulation of tau in several neurodegenerative diseases. *Neurobiol. Aging* 21, 503–510. doi: 10.1016/s0197-4580(00)00110-x

Selim, M., Glass, J. D., Hauser, U. E., and Rea, M. A. (1993). Serotonergic inhibition of light-induced fos protein expression and extracellular glutamate in the suprachiasmatic nuclei. *Brain Res.* 621, 181–188. doi: 10.1016/0006-8993(93)90105-v

Shannon, P., Markiel, A., Ozier, O., Baliga, N. S., Wang, J. T., Ramage, D., et al. (2003). Cytoscape: a software environment for integrated models of biomolecular interaction networks. *Genome Res.* 13, 2498–2504. doi: 10.1101/gr.1239303

Shirogane, T., Jin, J., Ang, X. L., and Harper, J. W. (2005). SCFbeta-TRCP controls clock-dependent transcription via casein kinase 1-dependent degradation of the mammalian period-1 (Per1) protein. *J. Biol. Chem.* 280, 26863–26872. doi: 10.1074/jbc.M502862200

Sleipness, E. P., Sorg, B. A., and Jansen, H. T. (2007). Diurnal differences in dopamine transporter and tyrosine hydroxylase levels in rat brain: dependence on the suprachiasmatic nucleus. *Brain Res.* 1129, 34–42. doi: 10.1016/j.brainres.2006.10.063

Smith, B. N., Sollars, P. J., Dudek, F. E., and Pickard, G. E. (2001). Serotonergic modulation of retinal input to the mouse suprachiasmatic nucleus mediated by 5-HT1B and 5-HT7 receptors. *J. Biol. Rhythms* 16, 25–38. doi: 10.1177/074873040101600104

Sominsky, L., Dangel, T., Malik, S., De Luca, S. N., Singewald, N., Spencer, S. J., et al. (2021). Microglial ablation in rats disrupts the circadian system. *FASEB J.* 35:e21195. doi: 10.1096/fj.202001555RR

Spanagel, R., Pendyala, G., Abarca, C., Zghoul, T., Sanchis-Segura, C., Magnone, M. C., et al. (2005). The clock gene Per2 influences the glutamatergic system and modulates alcohol consumption. *Nat. Med.* 11, 35–42. doi: 10.1038/nm1163

Sprouse, J., Braselton, J., and Reynolds, L. (2006). Fluoxetine modulates the circadian biological clock via phase advances of suprachiasmatic nucleus neuronal firing. *Biol. Psychiatry* 60, 896–899. doi: 10.1016/j.biopsych.2006.03.003

Stephan, F. K., and Zucker, I. (1972). Circadian rhythms in drinking behavior and locomotor activity of rats are eliminated by hypothalamic

lesions. *Proc. Natl. Acad. Sci. U S A* 69, 1583–1586. doi: 10.1073/pnas.69.6.1583

Terazono, H., Mutoh, T., Yamaguchi, S., Kobayashi, M., Akiyama, M., Udo, R., et al. (2003). Adrenergic regulation of clock gene expression in mouse liver. *Proc. Natl. Acad. Sci. U S A* 100, 6795–6800. doi: 10.1073/pnas.0936797100

Travnickova-Bendova, Z., Cermakian, N., Reppert, S. M., and Sassone-Corsi, P. (2002). Bimodal regulation of mPeriod promoters by CREB-dependent signaling and CLOCK/BMAL1 activity. *Proc. Natl. Acad. Sci. U S A* 99, 7728–7733. doi: 10.1073/pnas.102075599

Tso, C. F., Simon, T., Greenlaw, A. C., Puri, T., Mieda, M., Herzog, E. D., et al. (2017). Astrocytes regulate daily rhythms in the suprachiasmatic nucleus and behavior. *Curr. Biol.* 27, 1055–1061. doi: 10.1016/j.cub.2017.02.037

Urban, M. W., Lo, C., Bodinayake, K. K., Brunswick, C. A., Murakami, S., Heimann, A. C., et al. (2021). The circadian clock gene Per1 modulates context fear memory formation within the retrosplenial cortex in a sex-specific manner. *Neurobiol. Learn. Mem.* 185:107535. doi: 10.1016/j.nlm.2021.107535

Ushijima, K., Koyanagi, S., Sato, Y., Ogata, T., Matsunaga, N., Fujimura, A., et al. (2012). Role of activating transcription factor-4 in 24-hour rhythm of serotonin transporter expression in the mouse midbrain. *Mol. Pharmacol.* 82, 264–270. doi: 10.1124/mol.112.079079

Videnovic, A., Lazar, A. S., Barker, R. A., and Overeem, S. (2014). "The clocks that time us"--circadian rhythms in neurodegenerative disorders. *Nat. Rev. Neurol.* 10, 683–693. doi: 10.1038/nrneurol.2014.206

Vizi, E. S., Kiss, J. P., and Lendvai, B. (2004). Nonsynaptic communication in the central nervous system. *Neurochem. Int.* 45, 443–451. doi: 10.1016/j.neuint.2003.11.016

Wang, X.-L., Wolff, S. E. C., Korpel, N., Milanova, I., Sandu, C., Rensen, P. C. N., et al. (2020). Deficiency of the circadian clock gene bmal1 reduces microglial immunometabolism. *Front. Immunol.* 11:586399. doi: 10.3389/fimmu.2020.586399

Waniewski, R. A., and Martin, D. L. (1986). Exogenous glutamate is metabolized to glutamine and exported by rat primary astrocyte cultures. *J. Neurochem.* 47, 304–313. doi: 10.1111/j.1471-4159.1986.tb02863.x

Webb, I. C., Baltazar, R. M., Wang, X., Pitchers, K. K., Coolen, L. M., Lehman, M. N., et al. (2009). Diurnal variations in natural and drug reward, mesolimbic tyrosine hydroxylase and clock gene expression in the male rat. *J. Biol. Rhythms* 24, 465–476. doi: 10.1177/0748730409346657

Witkovsky, P. (2004). Dopamine and retinal function. *Doc. Ophthalmol.* 108, 17–40. doi: 10.1023/b:doop.0000019487.88486.0a

Womac, A. D., Burkeen, J. F., Neuendorff, N., Earnest, D. J., and Zoran, M. J. (2009). Circadian rhythms of extracellular ATP accumulation in suprachiasmatic nucleus cells and cultured astrocytes. *Eur. J. Neurosci.* 30, 869–876. doi: 10.1111/j.1460-9568.2009.06874.x

Wong, C. C. P., and Schumann, G. (2012). Integration of the circadian and stress systems: influence of neuropeptides and implications for alcohol consumption. *J. Neural Transm.* 119, 1111–1120. doi: 10.1007/s00702-012-0829-4

Xu, Y., Padiath, Q. S., Shapiro, R. E., Jones, C. R., Wu, S. C., Saigoh, N., et al. (2005). Functional consequences of a CKIdelta mutation causing familial advanced sleep phase syndrome. *Nature* 434, 640–644. doi: 10.1038/nature03453

Yoon, S. O., and Chikaraishi, D. M. (1994). Isolation of two E-box binding factors that interact with the rat tyrosine hydroxylase enhancer. *J. Biol. Chem.* 269, 18453–18462.

Yujnovsky, I., Hirayama, J., Doi, M., Borrelli, E., and Sassone-Corsi, P. (2006). Signaling mediated by the dopamine D2 receptor potentiates circadian regulation by CLOCK:BMAL1. *Proc. Natl. Acad. Sci. U S A* 103, 6386–6391. doi: 10.1073/pnas.0510691103

Conflict of Interest: The authors declare that the research was conducted in the absence of any commercial or financial relationships that could be construed as a potential conflict of interest.

Publisher's Note: All claims expressed in this article are solely those of the authors and do not necessarily represent those of their affiliated organizations, or those of the publisher, the editors and the reviewers. Any product that may be evaluated in this article, or claim that may be made by its manufacturer, is not guaranteed or endorsed by the publisher.

frontiers | Frontiers in Molecular Neuroscience

TYPE Review
PUBLISHED 02 August 2022
DOI 10.3389/fnmol.2022.954541

OPEN ACCESS

EDITED BY
Jun Yan,
The University of Queensland, Australia

REVIEWED BY
Efthimios M. C. Skoulakis,
Alexander Fleming Biomedical Sciences Research Center, Greece
Gemma Navarro,
University of Barcelona, Spain

*CORRESPONDENCE
Barbara Kaltschmidt
barbara.kaltschmidt@uni-bielefeld.de

SPECIALTY SECTION
This article was submitted to Molecular Signalling and Pathways, a section of the journal Frontiers in Molecular Neuroscience

RECEIVED 27 May 2022
ACCEPTED 11 July 2022
PUBLISHED 02 August 2022

CITATION
Kaltschmidt B, Helweg LP, Greiner JFW and Kaltschmidt C (2022) NF-κB in neurodegenerative diseases: Recent evidence from human genetics. *Front. Mol. Neurosci.* 15:954541. doi: 10.3389/fnmol.2022.954541

NF-κB in neurodegenerative diseases: Recent evidence from human genetics

Barbara Kaltschmidt[1,2,3]*, Laureen P. Helweg[2,3], Johannes F. W. Greiner[2,3] and Christian Kaltschmidt[2,3]

[1]Department of Molecular Neurobiology, Bielefeld University, Bielefeld, Germany, [2]Forschungsverbund BioMedizin Bielefeld, Ostwestfalen-Lippe (OWL) (FBMB E.V.), Bielefeld, Germany, [3]Department of Cell Biology, Biological Faculty, University of Bielefeld, Bielefeld, Germany

The transcription factor NF-κB is commonly known to drive inflammation and cancer progression, but is also a crucial regulator of a broad range of cellular processes within the mammalian nervous system. In the present review, we provide an overview on the role of NF-κB in the nervous system particularly including its constitutive activity within cortical and hippocampal regions, neuroprotection as well as learning and memory. Our discussion further emphasizes the increasing role of human genetics in neurodegenerative disorders, namely, germline mutations leading to defects in NF-κB-signaling. In particular, we propose that loss of function mutations upstream of NF-κB such as ADAM17, SHARPIN, HOIL, or OTULIN affect NF-κB-activity in Alzheimer's disease (AD) patients, in turn driving anatomical defects such as shrinkage of entorhinal cortex and the limbic system in early AD. Similarly, E3 type ubiquitin ligase PARKIN is positively involved in NF-κB signaling. PARKIN loss of function mutations are most frequently observed in Parkinson's disease patients. In contrast to AD, relying on germline mutations of week alleles and a disease development over decades, somatic mutations affecting NF-κB activation are commonly observed in cells derived from glioblastoma multiforme (GBM), the most common malignant primary brain tumor. Here, our present review particularly sheds light on the mutual exclusion of either the deletion of NFKBIA or amplification of epidermal growth factor receptor (EGFR) in GBM, both resulting in constitutive NF-κB-activity driving tumorigenesis. We also discuss emerging roles of long non-coding RNAs such as HOTAIR in suppressing phosphorylation of IκBα in the context of GBM. In summary, the recent progress in the genetic analysis of patients, particularly those suffering from AD, harbors the potential to open up new vistas for research and therapy based on TNFα/NF-κB pathway and neuroprotection.

KEYWORDS

NF-κB—nuclear factor kappa B, nervous system, Alzheimer's disease, Parkinson's disease, glioblastoma multiforme (GBM), SHARPIN, PARKIN, HOTAIR

Introduction: What is NF-κB?

The transcription factor nuclear factor kappa light chain enhancer of activated B cells (NF-κB) is a key regulator of inflammation and cancer progression and vitally drives a broad range of cellular processes within the mammalian nervous system (Kaltschmidt and Kaltschmidt, 2009). In the present review, we will particularly shed light on this crucial role of NF-κB in the nervous system as well as in neuroprotection and associated diseases like Alzheimer's disease (AD), Parkinson's disease (PD), and glioblastoma multiforme (GBM). On the molecular level, the NF-κB family comprises five DNA-binding members REL (c-REL), RELA (p65), and RELB (RELB) as well as NFKB1 (p50) and NFKB2 (p52), with the latest lacking transactivation domains (Ghosh et al., 1995). NF-κB-signaling can be distinguished into the canonical, non-canonical and atypical pathway (**Figure 1**). Canonical and non-canonical NF-κB-signaling share a common regulatory element, the inhibitor of κB (IκBα) kinase (IKK). In non-canonical NF-κB-signaling, ligand binding to receptors like CD40 activates IKK1 *via* NF-κB-inducible kinase (NIK). Phosphorylation of IKK1 results in processing of p100 to p52 and subsequent nuclear translocation of p52/RELB (Kaltschmidt et al., 2018; **Figure 1**). Canonical NF-κB-signaling is mediated by phosphorylation of the NEMO/IKK1/IKK2-complex for instance upon binding of ligands to TNF receptor 1 (TNFR1) (**Figure 1**). Phosphorylated IKKs in turn phosphorylate IκBα, which keeps p65/p50 in an inactive cytoplasmic state (Zhang et al., 2017). IKK-dependent phosphorylation of IκBα results in its proteasomal degradation and enables nuclear translocation of p65/p50 and expression of target genes (**Figure 1**). In atypical NF-κB-signaling, exposure of cells to UV light leads to NF-κB activation *via* p38 MAP Kinase (MAPK) activation, in turn resulting in casein kinase 2 (CK2)-mediated phosphorylation and degradation of IκB. In contrast to canonical and non-canonical activation of NF-κB, CK2-dependent atypical phosphorylation of IκB is c-terminal (e.g., at Ser293) and independent to IKK, which phosphorylates IκB at n-terminal phosphorylation sites (such as Ser32 or Ser36) (McElhinny et al., 1996; Sayed et al., 2000; Kato et al., 2003; reviewed in Lin et al., 2010; **Figure 1**). Next to TNFα (Furukawa and Mattson, 1998; Kaltschmidt et al., 1999; **Figure 1**), NF-κB can be also activated by the neurotransmitter glutamate (Guerrini et al., 1995; Kaltschmidt et al., 1995) and its agonists like kainate (Kaltschmidt et al., 1995) and N-methyl-D-aspartate (NMDA) (Meffert et al., 2003) in the nervous system as discussed below.

Overview on the role of NF-κB in the nervous system

When we started in 1992 to work on NF-κB in the nervous system not much was known on that topic. Our own review (Kaltschmidt B. et al., 1993) on this topic suggested an involvement of NF-κB based on the production of reactive oxygen intermediates in various neurological diseases, such as multiple sclerosis (MS), Alzheimer's disease (AD), Parkinson's disease (PD), and others. Today, a Pubmed search with MeSH entries "nervous system disease" and "NF-kappa B" reveals 4,750 results (May 18, 2022), starting in 1993 with two of our own papers.

Synaptosomes

Our starting investigation was a biochemical study with fractionation of rodent brains in so called synaptosomes. Synaptosomes are prepared by shear stress with a Potter type tissue homogenizer followed by gradient fractionation from different brain regions (Whittaker et al., 1964). Why we used synaptosomes? This biochemical preparation provides the opportunity to fractionate the complex brain in simple subcellular compartments. In addition, synaptosomes are a way to enrich NF-κB from total brain lysates. Synaptosomes can be analyzed by standard DNA-binding techniques such as EMSA to identify transcription factors such as NF-κB.

Synaptosomes are composed of pre-synaptic elements stabilized by post-synaptic density elements. Within synapses derived from olfactory bulb, white and gray matter, cerebellum and brain stem we could detect inducible NF-κB activity, with highest activity in gray matter. DNA binding of NF-κB could be inhibited by recombinant IκBα (Kaltschmidt C. et al., 1993), previously called MAD-3. Later on, synaptic localization of NF-κB could be reproduced by several other groups using synaptosomes (e.g., Meberg et al., 1996; Suzuki et al., 1997; Meffert et al., 2003; Schmeisser et al., 2012). In this line, it was reported that RELA could exist in two pools, a soluble one in synaptosomes and a membrane bound in fractions containing post-synaptic density proteins. While the active RELA-pool in the synaptoplasm is initially activated during early memory consolidation, its subsequent translocation into the membranes of the synaptosomes seems important for consolidation of long-term memory in mice (Salles et al., 2015). Furthermore, localization in post-synaptic spines and regulation of synapse growth was shown by Meffert et al. (2003) (Boersma et al., 2011; Dresselhaus et al., 2018). The function of transcription factors in synaptosomes could be within "a dialogue between synapses and genes" as published by Kandel (2001). In this hypothesis a feedback of activated synapses back to the nucleus (so called retrograde transport, see below) can initiate changes in gene transcription. These might direct synaptic enhancement and regrowing of novel synaptic contacts. For this task inducible transcription factors are well suited. Collectively these gathered evidence suggest that NF-κB is a synaptic protein in different brain region such as cerebellum, cortex and hippocampus, olfactory bulb, and brain stem.

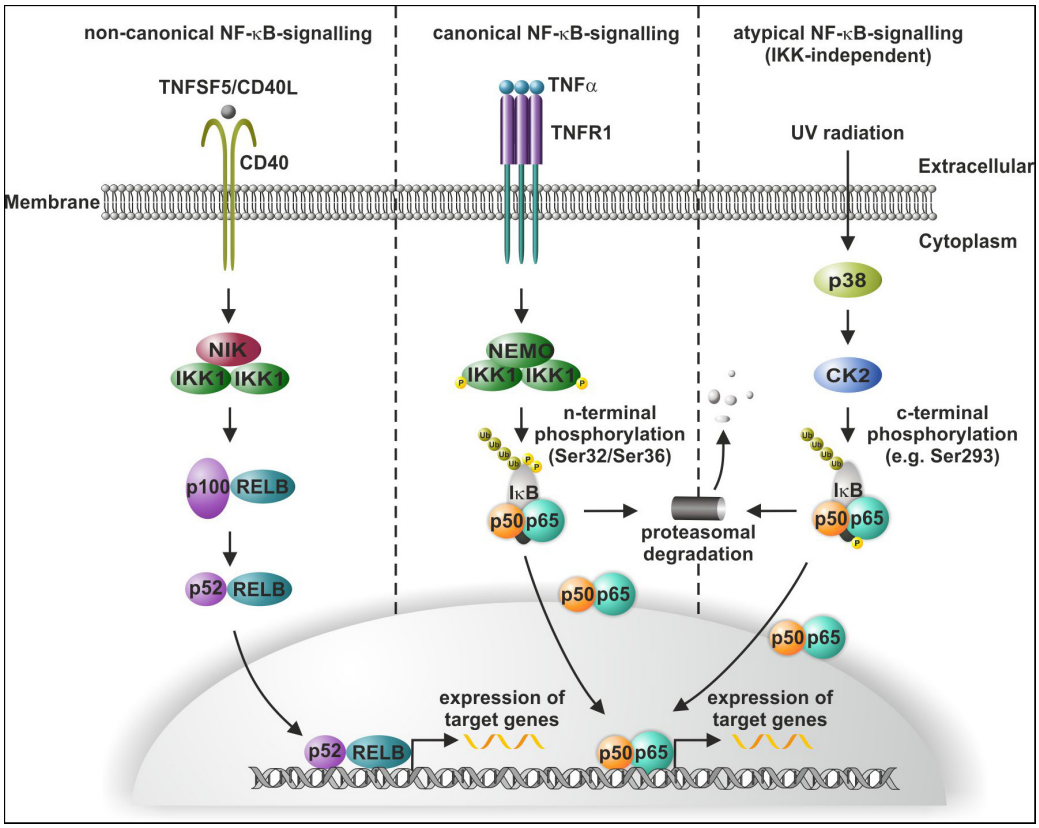

FIGURE 1
Non-canonical, canonical, and atypical NF-κB-signaling. Non-canonical signaling includes CD40-mediated activation of NF-κB-inducible kinase (NIK), which activates (IκBα) kinase (IKK) and leads to the processing of the p100/RELB and translocation of p52/RELB **(left panel)**. In canonical NF-κB-signaling, TNFα-mediated activation of the IKK complex leads to phosphorylation of IκBα and allows the p50/p65 dimer to translocate to the nucleus **(mid panel)**. UV light induces atypical activation of NF-κB-signaling through p38-MAPK activation and consequent IκBα phosphorylation independent to IKK, which again releases the p50/p65 dimer **(right panel)**. Modified from Kaltschmidt et al. (2021).

Retrograde transport in neurons

We could show that NF-κB could be retrogradely transported from the pre-synaptic site to the nucleus in hippocampal neurons (Wellmann et al., 2001). Retrograde transport could be studied by injection of radioactively labeled proteins in animals, like it was shown for transport of nerve growth factor (NGF) in sensory neurons (Stoeckel et al., 1975). Furthermore transport of green fluorescent protein (GFP) fusion proteins could be analyzed by life microscopy (Wellmann et al., 2001), which could be combined with the analysis of transport in photobleached regions (Meffert et al., 2003). Finally transport of single fusion proteins could be studied with blinking probes (Widera et al., 2016). Later on, we could extend this observation with super resolution microscopy (Mikenberg et al., 2007; Widera et al., 2016). In this line, it is important to introduce TNFα, which also can be retrogradely transported in inflammatory lesions of peripheral nerves (Shubayev and Myers, 2001). Accordingly, we demonstrated Hsc70 as a novel interactor of NF-κB potentially involved in retrograde transport in rodent brain (Klenke et al., 2013), while deoxyspergualin, a specific inhibitor of Hsc70, inhibited nuclear import of NF-κB. We have previously shown that NF-κB was activated in microglia of experimental allergic encephalomyelitis (EAE) rats (Kaltschmidt et al., 1994a). In this line, effective treatment of EAE with deoxyspergualin could be shown in two models of acute and chronic relapsing EAE (Schorlemmer and Seiler, 1991). Taken together these data provide evidence for a retrograde transport of NF-κB from activated synapses to the nucleus, one component of the transport complex is Hsc70, which could be inhibited by deoxyspergualin.

Constitutive NF-κB activity in neurons

We discovered constitutive activity (always activated NF-κB in the nucleus) within cortical and hippocampal regions of rodent brains (Kaltschmidt et al., 1994b). Further analysis of NF-κB activity with reporter gene assays could reproduce

this constitutive activity within the neurons of the cortical or the hippocampal region (Schmidt-Ullrich et al., 1996; Bhakar et al., 2002). In particular, Barker and coworkers showed that efficient blocking of endogenous NF-κB activity by recombinant adenovirus led to death of cortical neurons, whereas induction of NF-κB activity resulted in neuroprotection (Bhakar et al., 2002). Evidence for constitutive activity demonstrates that NF-κB is a sensor for neuronal activity of glutamatergic neurons. Anesthesia of cultured neurons with, e.g., NMDA receptor antagonists inhibits constitutive NF-κB activity.

Inducible NF-κB in neurons

Activation of NF-κB in neurons is possible by the neurotransmitter glutamate (Guerrini et al., 1995; Kaltschmidt et al., 1995) and agonists such as kainate (Kaltschmidt et al., 1995) and NMDA (Meffert et al., 2003), as well as by pro-inflammatory cytokines as TNFα (Furukawa and Mattson, 1998; Kaltschmidt et al., 1999; **Figure 1**). Taken together evidence indicated a major role of NF-κB in glutamatergic signaling as well as pro-inflammatory TNF mediated signaling.

Animal models for studying NF-κB in the nervous system

In the beginning of the 21st century, several new transgenic mouse models with specific repression or activation of NF-κB in the nervous system were generated, allowing studies of behavior and learning. Mollie Meffert and coworkers discovered that p65-deficient mice have no synaptic NF-κB. These mice when crossed to TNFR1-deficient mice could survive from TNF-mediated hepatic failure and had a learning defect of spatial learning in a radial arm maze (Meffert et al., 2003). We discovered that expression of transdominant negative IκBα in glutamatergic neurons affected spatial memory formation and repressed expression of the novel NF-κB target gene protein kinase A (catalytic subunit α) (Kaltschmidt et al., 2006). Warner Greene and coworkers discovered that neuronal expression of super-repressor IκB in GABA-ergic interneurons led to enhanced spatial learning and memory (O'Mahony et al., 2006). Later on, it was shown that NF-κB-repression by transdominant negative IKK2 led to impaired learning and memory. The authors further identified insulin-like growth factor 2 (IGF2) as a novel IKK/NF-κB target gene. In this line, IGF2 was able to restore synapse density and promoted spine maturation in IKK/NF-κB signaling-deficient neurons within 24 h (Schmeisser et al., 2012). In contrast, expression of a constitutively active allele of IKK2 in forebrain neurons led to degeneration of microglia and astrocytes as well as spatial learning defects (Maqbool et al., 2013). Therefore evidence indicates NF-κB involvement in learning and memory and additionally in brain regeneration *in vivo*.

Germline mutations affecting NF-κB activation in the context of Alzheimer's disease

Alzheimer's disease (AD) is a devastating neurodegenerative disease and was discovered by Alois Alzheimer in Munich when analyzing brain sections of his patient Auguste Deter, who died in a lunatic asylum in Frankfurt. Alois Alzheimer immediately discovered the presence of "miliary foci" (senile plaques) and very strange changes in neurofibrils, which clump into tangles that eventually replace dead neurons (Alzheimer, 1907). Later on, he extended this observation toward examples of neurofibril tangles and plaques (Alzheimer, 1911). Then, Konrad Beyreuther and coworkers purified plaque proteins and determined the amyloid plaque core protein sequence (Masters et al., 1985). Furthermore, the amyloid A4 beta precursor protein was cloned by the group of Müller-Hill (Kang et al., 1987). Notably, many AD-relevant genes such as BIN1, IκBα, APP, BASE1, COX-2, MnSOD, CuZnSOD, TNFR1, and others are target genes of NF-κB (Snow and Albensi, 2016; **Figure 2**).

However, a recent genetic study using genome wide association of 111,326 clinically diagnosed AD cases and 677,663 controls challenges this one and only hypothesis of the A beta concept and provides additional evidence for AD-linked genes with higher significance. Notably, BIN1 (bridging integrator 1) alleles (p-value: $6 \times 10\hat{}-118$) were most significantly associated to AD, whereas APP (precursors of A beta) had a significance of correlation of only $1 \times 10\hat{}-12$ (Bellenguez et al., 2022). Most interestingly, BIN1 knockout in breast cancers was linked to increased nuclear NF-κB (Ghaneie et al., 2006), suggesting a dual role as inhibitor of NF-κB and as a target gene (Mao et al., 1999; **Figure 2**). BIN1 encodes several isoforms of a nucleocytoplasmic adaptor protein, initially described with tumor suppressor functions. BIN1 may be involved in the regulation of MYC activity and the control of cell proliferation (Sakamuro et al., 1996). Three isoforms of BIN1 were detected in neurons and astrocytes (isoforms 1, 2, and 3) and four isoforms in microglia (isoforms 6, 9, 10, and 12) of human brain (Taga et al., 2020) showing a strong association of BIN1 isoforms expressed by neurons/astrocytes and tangles that might contribute to cognitive decline in AD. Its role as a tumor suppressor gene suggests a function of wt BIN1 allele as an inhibitor of NF-κB activation (Elliott et al., 2000). Additionally, BIN1 transcript levels were increased in AD brains and BIN1 mediates AD risk by modulating Tau pathology (Chapuis et al., 2013). In particular, Chapuis et al. (2013) identified a novel 3 bp insertion allele upstream of BIN1, which is directly linked to increased

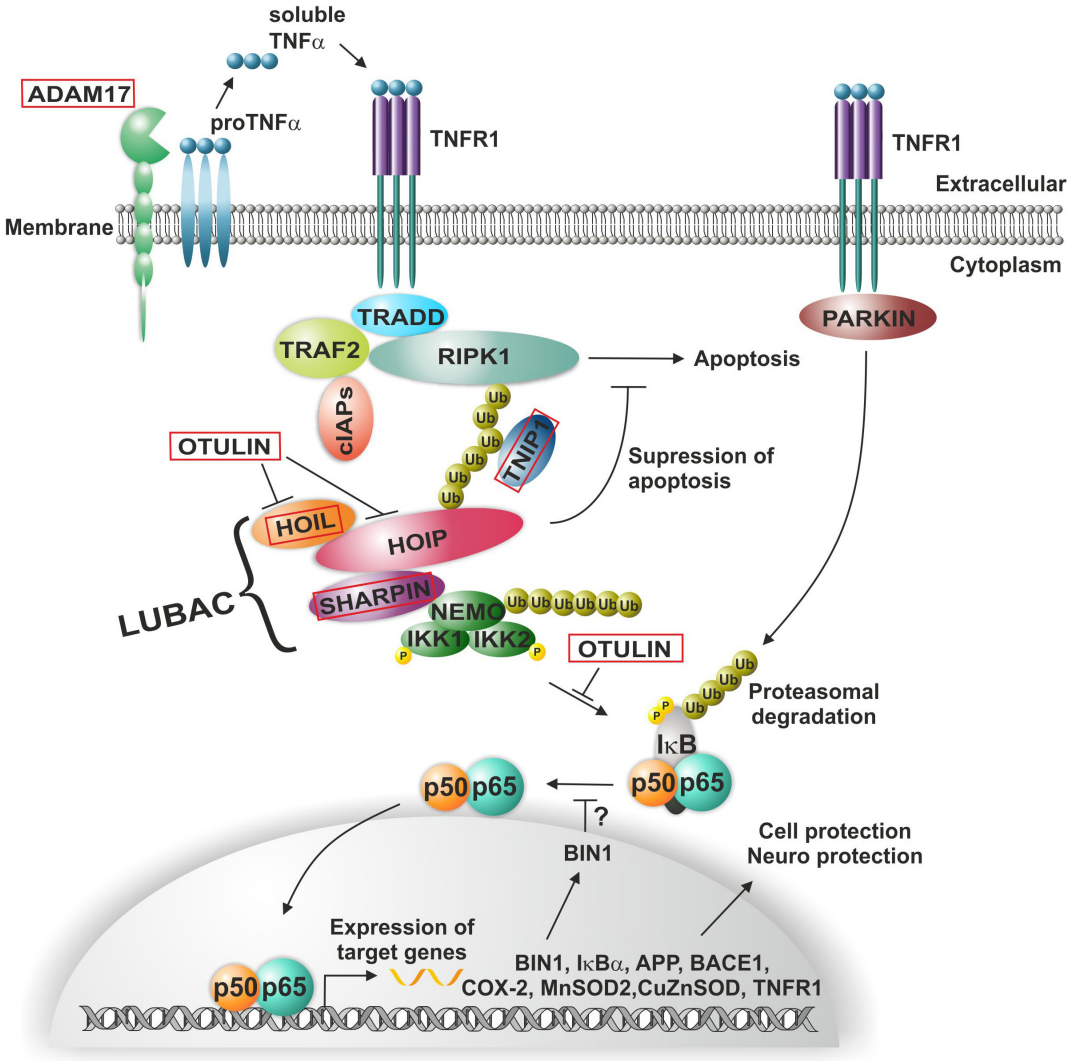

FIGURE 2
NF-κB-signaling in Alzheimer's and Parkinson's disease. ADAM17-induced soluble TNFα mediates the activation of the TNF receptor complex, where poly-ubiquitination leads to the recruitment of the LUBAC complex. Linear ubiquitination of NEMO mediates the activation and phosphorylation of the (IκBα) kinase (IKK) complex and consequent activation of NF-κB p50/p65, in turn driving expression of a range of AD-relevant genes such as BIN1, IκBα, APP, BASE1, COX-2, MnSOD, CuZnSOD, or TNFR1. In PD, activation of NF-κB is mediated by PARKIN in a TNFR1-dependent manner.

BIN1 expression and risk for developing AD. In addition, this novel insertion was associated with Tau accumulation but not with amyloid loads in AD brains. On mechanistic level, knockdown of the BIN1 ortholog Amph suppressed Tau-toxicity in an amyloid-independent manner in *Drosophila*. Coimmunoprecipitation studies further substantiated a direct interaction between Tau and BIN1 in human cells and mouse brains. Although the particular pathogenic mechanism linking BIN1 and Tau in AD progression remains unclear, BIN1 may modulate Tau aggregation/oligomer formation in earlier disease stages (Chapuis et al., 2013). In human induced neurons, BIN1-knockout reduced early endosome signaling and overexpression of the AD-relevant isoform of BIN1 (isoform 1) increased the size of early endosomes and led to neurodegeneration (Lambert et al., 2022). The TNFα pathway with linear ubiquitination was also included in the new genetically associated processes within AD patients (Bellenguez et al., 2022). Interestingly, ADAM17, an extracellular protease leading to soluble TNFα, the TNF receptor interactor TNIP1, and components of the linear ubiquitination machinery linear ubiquitination chain assembly complex (LUBAC): HOIL, SHARPIN, and the negative regulator OTULIN are all affected by mutations in AD patients (**Figure 2**, red boxes). In this context, it might be interesting to note that Mattson and coworkers discovered a neuroprotective effect of TNFα (Cheng et al., 1994). Furthermore, they discovered that TNFα

protected against A beta/glutamate toxicity (Barger et al., 1995; Albensi and Mattson, 2000). Activated NF-κB might direct the expression of antioxidant enzymes such as MnSOD and Calcium-binding proteins such as calbindin. Calcium buffering and reduction of reactive oxygen intermediates by antioxidant enzymes can actively protect against glutamate and Ab mediated induction of apoptosis (see for further discussion: Neuroprotective signal transduction edt. M.P. Mattson Springer Science Press 1998). We could reproduce this observation in cerebellar granule cells and additionally could show that treatment with a low dose of A beta (100 nM) activates p65 specifically and fortifies neurons against a neurotoxic high dose of A beta (Kaltschmidt et al., 1999). In addition also TNFα activated NF-κB at a very sharp peak of 2 ng/ml leading to neuroprotection whereas higher doses of TNF had adversive effects. Furthermore, we could demonstrate that activated NF-κB was restricted to cells in the close vicinity of early plaques in AD patient brains (Kaltschmidt et al., 1997; Ferrer et al., 1998). Interestingly, the overall NF-κB immunoreactivity was quite low in AD brains in comparison to age-matched controls. Recent genetic evidence of potential loss-of-function mutants involved in NF-κB signaling of AD patients might provide a genetic reason for this early correlation (Bellenguez et al., 2022). In this line, human SHARPIN mutants were shown to have less capability of NF-κB activation (Park et al., 2021). Furthermore, SHARPIN mutants (Park et al., 2021) of the LUBAC complex are highly significantly correlated with a reduction in the thickness of the entorhinal cortex, one of the earliest signs of AD (Kobro-Flatmoen et al., 2021; **Figures 3A,B**). Soheili-Nezhad et al. (2020) identified a SHARPIN mutant in AD associated with degeneration of the limbic system and its interconnecting white-matter. Since SHARPIN is a post-synaptic density protein and other components of the TNFα pathway (see also **Figure 2**) are also localized in neurons, we conclude that some mutations present in AD led to a reduced TNFα/NF-κB-driven neuroprotection. Accordingly, a transgenic mouse model with NF-κB ablation in basal forebrain neurons led to a severe degeneration of the dentate gyrus

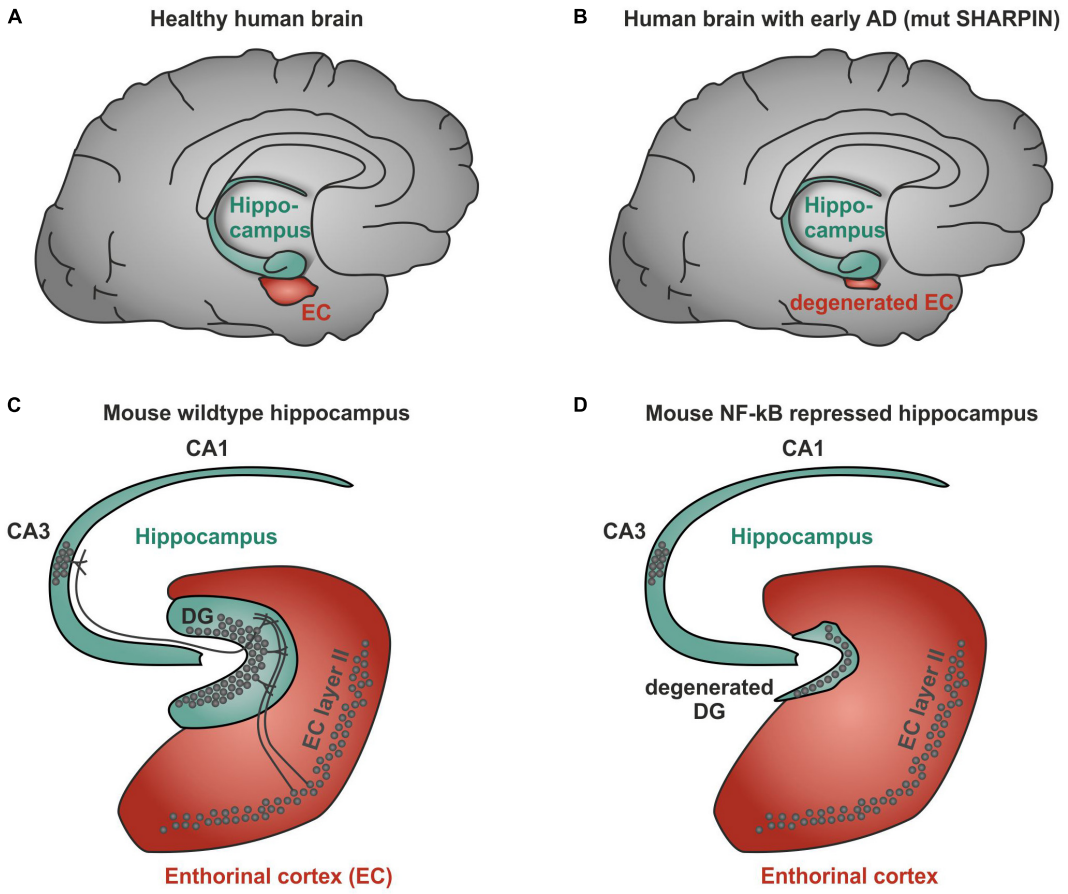

FIGURE 3
NF-κB-mediated degeneration of human and mouse brain. **(A)** Scheme of healthy human brain showing a normal sized entorhinal cortex. **(B)** Human SHARPIN mutated Alzheimer's disease (AD) brain showing a degenerated entorhinal cortex. **(C)** Scheme of healthy NF-κB wildtype mouse brain with normal dentate gyrus. **(D)** NF-κB repression in mice brains leads to a degenerated dentate gyrus.

(**Figures 3C,D**), which could be rescued on the cellular level by reactivation of NF-κB (Imielski et al., 2012). In addition, behavioral deficits were completely repaired. In summary, our discussion emphasizes a potential neuroprotective, regenerative role of NF-κB in neurons of AD. Based on the evidences reported above, we suggest a testable hypothesis where loss of function mutations upstream of NF-κB such as ADAM17, SHARPIN, HOIL, or OTULIN (**Figure 2**) lead to defects in NF-κB signaling including retrograde transport of the signaling endosome and neuroprotection. Finally, these defects might account for the anatomical defects seen in the entorhinal cortex (early AD, **Figure 3**) followed up by the limbic system and finally shrinkage of the cortex (late AD). We hypothesize based on the evidence presented above that the development of the disease is observed over decades of continuous cognitive decline because the defects in AD patients all rely on weak alleles in contrast to knockouts in somatic cells as in GBM (see below). In summary these genetic data demonstrate the involvement of TNF mediated NF-κB activation in neurons of AD patients. Especially loss of function mutations of the NF-κB activator Sharpin alone or together with additional mutations suggest a loss of neuroprotection enhancing the development of AD.

Germline mutations affecting NF-κB activation in the context of Parkinson's disease

Parkinson's disease is another important neurodegenerative disease affecting more than approximately 1% of individuals older than 60 years. It is suggested that oxidative stress induces apoptosis of dopaminergic neurons in the substantia nigra, resulting in neurodegenerative disorders observed in patients diagnosed with PD. PD was first described by James Parkinson in 1817 (Parkinson, 2002), as a disease separated from other neurological disorders and characterized by typical involuntary tremulous motions of body parts, even when not in action. Much later Arvid Carlson discovered the presence of dopamine in the brain (Carlsson et al., 1958). He used a fluorimetric method in combination with ion exchange chromatography. Furthermore he discovered that reserpine isolated from the plant Rauwolfia led to a Parkinson like phenotype in rabbits. Reserpine lead to complete depletion of dopamine which could be restored by injection of L-Dopa. This discovery was rewarded in 2000 with the Nobel Price. The biochemical discovery of replenishing dopamine by L-Dopa was translated to a clinical L-Dopa therapy for PD patients (Ehringer and Hornykiewicz, 1960). Neuropathological analysis revealed neuronal lesions in regions of the motor system rich in dopamine such as the substantia nigra but also within the limbic system and the brain stem. The cellular basis of dopamine release are dopaminergic neurons which release dopamine to other neurons without any direct synaptic contacts (volume transmission) and are relatively few (about 4,00,000) in the human brain (reviewed in Schultz, 2007). Lewy (1912) discovered a hallmark of PD pathology the so called Lewy bodies as neuronal eosinophilic cytoplasmic inclusion bodies in brain stems of PD patients. Neurons dying during the progression of PD are characterized by the presence of Lewy bodies in their perikarya and Lewy neurites in their neuronal processes. Lewy bodies can be immunostained with antibodies raised against α-synuclein. This type of immunostaining reveals many kinds of Lewy bodies ranging from dot- or thread-like forms to very large types (Braak and Braak, 2000). Similar to AD in PD changes in the neuronal cytoskeleton develop but in only a few susceptible types of nerve cells. α-synuclein is a small protein involved in synaptic dopamine release and a major component which is aggregated in a prion-like fashion in Lewy bodies (Steiner et al., 2018). Braak et al. (2003a) developed a new staging system for PD severity using anti-alpha synuclein histochemistry. Based on these data, they proposed a new hypothesis on the pathology of PD: alpha synuclein pathology typical for PD might spread from gut to brain presumable along the vagus nerve (Braak et al., 2003b). Later on indeed gut brain transmission of pathology with concomitant loss of dopaminergic neurons could be observed in mice after injection of prion-like alpha synuclein fibrils into gut muscles (Kim et al., 2019). While exogenous alpha synuclein could lead to mitochondrial disfunction, overexpression of parkin could rescue the mitochondrial disfunction (Wilkaniec et al., 2021).

A long established genetic linkage is the loss of function of Parkin E3 ubiquitin ligase (Panicker et al., 2021). In this line, recent *in vitro* analysis showed that overexpression of PARKIN strongly enhances TNFα-mediated NF-κB activation in HEK-293 cells, suggesting an involvement of this E3 ubiquitin ligase in TNFα-mediated NF-κB signaling by stabilizing LUBAC (Meschede et al., 2020; **Figure 2**).

Furthermore reactive oxygen-mediated neurodegeneration was shown to regulate mRNA expression and survival in neurons derived from neural crest derived stem cells in a sex-specific manner (Ruiz-Perera et al., 2018). In particular we observed that female neurons are more susceptible to oxidative stress-mediated cell death. However, activation of NF-κB (RELA) by TNFα let to significant neuroprotection against oxidative stress-induced cell death in both sexes. While female neurons upregulated the NF-κB target genes SOD2 and IGF2 to induce neuroprotection, male neurons showed elevated expression of the neuroprotective NF-κB target gene PKA cat alpha (Ruiz-Perera et al., 2018). But when cRel, a crucial regulator of neuronal development from neural crest is inhibited, neural crest derived stem cells shift their fate from the neuronal to the oligodendrocytic lineage (Ruiz-Perera et al., 2020; reviewed in Greiner et al., 2019). We therefore conclude that NF-κB seems to be a key player in neuroprotection of both sexes, although the protective gene expression program beneath is sexually dimorphic.

Somatic mutations affecting NF-κB activation in the context of glioblastoma multiforme

Glioblastoma multiforme (GBM) is the most common malignant primary brain and CNS tumor with a very poor prognosis. GBM rapidly developing *de novo* are classified as primary GBM, while GBM developing from low-grade astrocytoma are classified as secondary GBM and show IDH1 mutations (Ohgaki and Kleihues, 2013). NF-κB signaling has been shown to play a central role in glioblastoma growth (reviewed in Smith et al., 2008). Consistently, mesenchymal differentiation mediated by NF-κB has been shown to promote radiation resistance in GBM (Bhat et al., 2013) and inhibition of NF-κB attenuates mesenchymal characteristics and cell proliferation (Wang et al., 2018). Several studies revealed constitutive activation of NF-κB in GBM cells, which promoted invasiveness, angiogenesis and stem cell features such as self-renewal (Raychaudhuri et al., 2007; Xie et al., 2010; Rinkenbaugh et al., 2016; reviewed in Kaltschmidt et al., 2022). Accordingly, we previously reported the GO term "NF-κB binding" to be enriched in a global transcriptome analysis of three primary glioblastoma stem cell populations (Witte et al., 2021).

The oncogenic long non-coding RNA (lncRNA) HOTAIR induces altered histone H3 lysine 27 methylation and thus has been shown to promote the enrichment of the TNFα/NF-κB signaling protein complex, the IκB kinase complex, and the IKK1-IKK2 complex in glioma cells (Wang et al., 2021). Additionally, HOTAIR suppresses the expression of the NF-κB upstream inhibitor UBXN1 *via* histone modification, leading to enhanced IκBα phosphorylation and consequent NF-κB activation, which in turn induces the expression of PD-L1 and enhances T cell killing resistance and immune escape (Chernorudskiy and Gainullin, 2013; Wang et al., 2021; **Figure 4**). In addition to enhanced phosphorylation, a heterozygous deletion of NFKBIA (IκBα) has been reported by Bredel and coworkers in 28% of GBM and 22% of cancer stem-like cells. Analyzing 790 human GBMs revealed a mutual

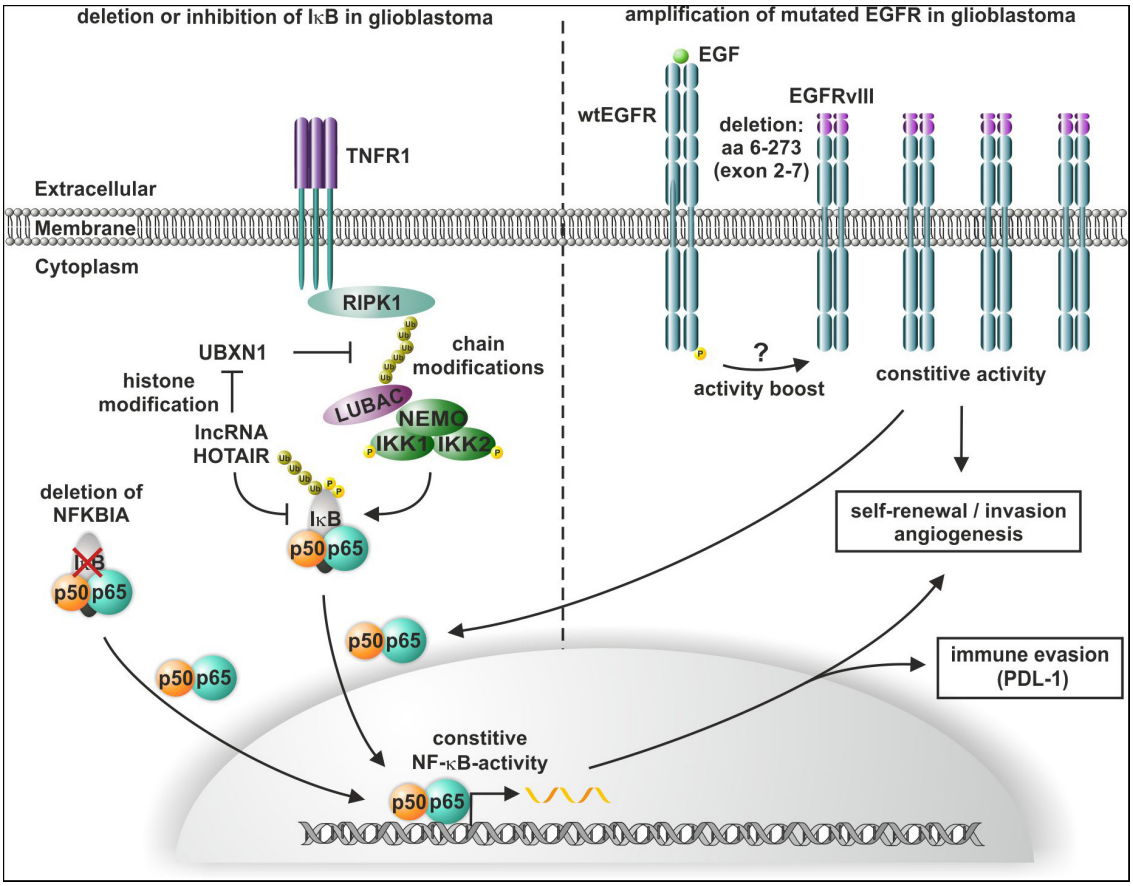

FIGURE 4
Constitutive activation of NF-κB in glioblastoma multiforme (GBM). Heterozygous deletion of NFKBIA or HOTAIR-mediated phosphorylation of IκB leads to the constitutive activation of NF-κB, which in turn induces self-renewal, angiogenesis, and immune escape. NF-κB is also activated by constitutive activity of mutated EGFRvIII, which also confers self-renewal and invasion in GBM.

exclusion of either NFKBIA deletion or EGFR amplification with similar clinical outcomes (Bredel et al., 2011; **Figure 4**). Of note, viral-mediated expression of NFKBIA in established GBM cell lines with NFKBIA deletions or EGFR amplification reduced cell viability, but it did not affect NFKBIA/EGFR wildtype GBM cells. EGFR mutations and consequent overexpression are frequent in GBM, with a majority of GBM containing the constitutively active mutant EGFR, which shows a genetic deletion of exon 2–7 and is named EGFRvIII (Heimberger et al., 2005; **Figure 4**). Other EGFR mutations in GBM include a N-terminal deletion (EGFRvI), deletion of exons 14–15 (EGFRvII), deletion of exons 25–27 (EGFRvIV), and deletion of exons 25–28 (EGFRvV) (An et al., 2018). EGFRvIII overexpression in GBM patients with EGFR amplification was significantly correlated to poor overall survival (Shinojima et al., 2003). On cellular level, several studies linked expression of EGFRvIII in GBM with tumor invasion as well as angiogenesis and inhibition of EGFRvIII inhibited these processes (Zheng et al., 2014; Camorani et al., 2015; Eskilsson et al., 2016; reviewed in Keller and Schmidt, 2017; **Figure 4**). In EGFRvIII overexpressing glioma cells, angiogenesis and tumor growth were promoted by EGFRvIII-mediated activation of NF-κB (Bonavia et al., 2012). EGFRvIII is also linked to self-renewal of GBM cells and connected to GBM stem-like cell populations (Emlet et al., 2014; Kim et al., 2021). Consistently, EGFRvIII and EGFR are downregulated upon differentiation of GBM neurospheres as well as inhibited EGFR signaling induced differentiation with decreased tumorigenic and stem-like cell potential (Stockhausen et al., 2014).

Perspectives and impact

In summary, therapy development for neurological diseases might be successful for PD with stem cell therapy (Piao et al., 2021), perhaps with a combined approach where growth promoting factors are used to enhance the performance of midbrain dopaminergic neuron grafts (Bjorklund and Parmar, 2021). However, more than 50 years of AD research failed to deliver new therapeutic approaches (Yiannopoulou et al., 2019). Despite the complexity of AD, a recent progress in the genetic analysis of AD patients reviewed here might open up new vistas for research and therapy based on TNFα/NF-κB pathway and neuroprotection. We conclude that TNFα-mediated NF-κB activation essential for neuroprotection is hampered by germ line mutations in many AD patients. This evidence provides a testable hypothesis for reduced NF-κB activation in neurons of AD patients. Mutations may act alone as shown for Sharpin in combinations.

Author contributions

BK and CK: conceptualization and funding acquisition. BK, LH, JG, and CK: writing–original draft preparation and writing–review and editing. LH and JG: visualization. All authors read and agreed to the published version of the manuscript.

Funding

This research was funded by the University of Bielefeld. LH was funded by an internal grant of the Bethel Foundation, Bielefeld, Germany. We acknowledged support for the publication costs by the Deutsche Forschungsgemeinschaft and the Open Access Publication Fund of Bielefeld University.

Conflict of interest

The authors declare that the research was conducted in the absence of any commercial or financial relationships that could be construed as a potential conflict of interest.

Publisher's note

All claims expressed in this article are solely those of the authors and do not necessarily represent those of their affiliated organizations, or those of the publisher, the editors and the reviewers. Any product that may be evaluated in this article, or claim that may be made by its manufacturer, is not guaranteed or endorsed by the publisher.

References

Albensi, B. C., and Mattson, M. P. (2000). Evidence for the involvement of TNF and NF-kappaB in hippocampal synaptic plasticity. *Synapse* 35, 151–159. doi: 10.1002/(SICI)1098-2396(200002)35:2<151::AID-SYN8<3.0.CO;2-P

Alzheimer, A. (1907). Über eine eigenartige Erkrankung der Hirnrinde. *Allgemeine Z. Psychatrie Psychisch Gerichtliche Medizin* 64, 146–148.

Alzheimer, A. (1911). über eigenartige Krankheitsfälle des späteren Alters. *Z. Die Gesamte Neurologie Psychiatrie* 4:356. doi: 10.1007/BF02866241

An, Z., Aksoy, O., Zheng, T., Fan, Q. W., and Weiss, W. A. (2018). Epidermal growth factor receptor and EGFRvIII in glioblastoma: signaling pathways and targeted therapies. *Oncogene* 37, 1561–1575. doi: 10.1038/s41388-017-0045-7

Barger, S. W., Horster, D., Furukawa, K., Goodman, Y., Krieglstein, J., and Mattson, M. P. (1995). Tumor necrosis factors alpha and beta protect neurons against amyloid beta-peptide toxicity: evidence for involvement of a kappa B-binding factor and attenuation of peroxide and Ca^{2+} accumulation. *Proc. Natl. Acad. Sci. U.S.A.* 92, 9328–9332. doi: 10.1073/pnas.92.20.9328

Bellenguez, C., Kucukali, F., Jansen, I. E., Kleineidam, L., Moreno-Grau, S., Amin, N., et al. (2022). New insights into the genetic etiology of Alzheimer's disease and related dementias. *Nat. Genet.* 54, 412–436. doi: 10.1038/s41588-022-01024-z

Bhakar, A. L., Tannis, L. L., Zeindler, C., Russo, M. P., Jobin, C., Park, D. S., et al. (2002). Constitutive nuclear factor-kappa B activity is required for central neuron survival. *J. Neurosci.* 22, 8466–8475.

Bhat, K. P. L., Balasubramaniyan, V., Vaillant, B., Ezhilarasan, R., Hummelink, K., Hollingsworth, F., et al. (2013). Mesenchymal differentiation mediated by NF-kappaB promotes radiation resistance in glioblastoma. *Cancer Cell* 24, 331–346. doi: 10.1016/j.ccr.2013.08.001

Bjorklund, A., and Parmar, M. (2021). Dopamine cell therapy: from cell replacement to circuitry repair. *J. Parkinsons Dis.* 11, S159–S165. doi: 10.3233/JPD-212609

Boersma, M. C., Dresselhaus, E. C., De Biase, L. M., Mihalas, A. B., Bergles, D. E., and Meffert, M. K. (2011). A requirement for nuclear factor-kappaB in developmental and plasticity-associated synaptogenesis. *J. Neurosci.* 31, 5414–5425. doi: 10.1523/jneurosci.2456-10.2011

Bonavia, R., Inda, M. M., Vandenberg, S., Cheng, S. Y., Nagane, M., Hadwiger, P., et al. (2012). EGFRvIII promotes glioma angiogenesis and growth through the NF-kappaB, interleukin-8 pathway. *Oncogene* 31, 4054–4066. doi: 10.1038/onc.2011.563

Braak, H., and Braak, E. (2000). Pathoanatomy of Parkinson's disease. *J. Neurol.* 247, II3–II10. doi: 10.1007/PL00007758

Braak, H., Del Tredici, K., Rub, U., de Vos, R. A., Jansen Steur, E. N., and Braak, E. (2003a). Staging of brain pathology related to sporadic Parkinson's disease. *Neurobiol. Aging* 24, 197–211. doi: 10.1016/s0197-4580(02)00065-9

Braak, H., Rüb, U., Gai, W. P., and Del Tredici, K. (2003b). Idiopathic Parkinson's disease: possible routes by which vulnerable neuronal types may be subject to neuroinvasion by an unknown pathogen. *J. Neural Trans.* 110, 517–536. doi: 10.1007/s00702-002-0808-2

Bredel, M., Scholtens, D. M., Yadav, A. K., Alvarez, A. A., Renfrow, J. J., Chandler, J. P., et al. (2011). NFKBIA deletion in glioblastomas. *N. Engl. J. Med.* 364, 627–637. doi: 10.1056/NEJMoa1006312

Camorani, S., Crescenzi, E., Colecchia, D., Carpentieri, A., Amoresano, A., Fedele, M., et al. (2015). Aptamer targeting EGFRvIII mutant hampers its constitutive autophosphorylation and affects migration, invasion and proliferation of glioblastoma cells. *Oncotarget* 6, 37570–37587. doi: 10.18632/oncotarget.6066

Carlsson, A., Lindqvist, M., Magnusson, T., and Waldeck, B. (1958). On the presence of 3-hydroxytyramine in brain. *Science* 127:471. doi: 10.1126/science.127.3296.471

Chapuis, J., Hansmannel, F., Gistelinck, M., Mounier, A., Van Cauwenberghe, C., Kolen, K. V., et al. (2013). Increased expression of BIN1 mediates Alzheimer genetic risk by modulating tau pathology. *Mol. Psychiatry* 18, 1225–1234. doi: 10.1038/mp.2013.1

Cheng, B., Christakos, S., and Mattson, M. P. (1994). Tumor necrosis factors protect neurons against metabolic-excitotoxic insults and promote maintenance of calcium homeostasis. *Neuron* 12, 139–153. doi: 10.1016/0896-6273(94)90159-7

Chernorudskiy, A. L., and Gainullin, M. R. (2013). Ubiquitin system: direct effects join the signaling. *Sci. Signal.* 6:e22. doi: 10.1126/scisignal.2004251

Dresselhaus, E. C., Boersma, M. C. H., and Meffert, M. K. (2018). Targeting of NF-kappaB to dendritic spines is required for synaptic signaling and spine development. *J. Neurosci.* 38, 4093–4103. doi: 10.1523/JNEUROSCI.2663-16.2018

Ehringer, H., and Hornykiewicz, O. (1960). [Distribution of noradrenaline and dopamine (3-hydroxytyramine) in the human brain and their behavior in diseases of the extrapyramidal system]. *Klin. Wochenschr.* 38, 1236–1239. doi: 10.1007/BF01485901

Elliott, K., Ge, K., Du, W., and Prendergast, G. C. (2000). The c-Myc-interacting adaptor protein Bin1 activates a caspase-independent cell death program. *Oncogene* 19, 4669–4684. doi: 10.1038/sj.onc.1203681

Emlet, D. R., Gupta, P., Holgado-Madruga, M., Del Vecchio, C. A., Mitra, S. S., Han, S. Y., et al. (2014). Targeting a glioblastoma cancer stem-cell population defined by EGF receptor variant III. *Cancer Res.* 74, 1238–1249. doi: 10.1158/0008-5472.CAN-13-1407

Eskilsson, E., Rosland, G. V., Talasila, K. M., Knappskog, S., Keunen, O., Sottoriva, A., et al. (2016). EGFRvIII mutations can emerge as late and heterogenous events in glioblastoma development and promote angiogenesis through Src activation. *Neuro Oncol.* 18, 1644–1655. doi: 10.1093/neuonc/now113

Ferrer, I., Marti, E., Lopez, E., and Tortosa, A. (1998). NF-kB immunoreactivity is observed in association with beta A4 diffuse plaques in patients with Alzheimer's disease. *Neuropathol. Appl. Neurobiol.* 24, 271–277. doi: 10.1046/j.1365-2990.1998.00116.x

Furukawa, K., and Mattson, M. P. (1998). The transcription factor NF-kappaB mediates increases in calcium currents and decreases in NMDA- and AMPA/kainate-induced currents induced by tumor necrosis factor-alpha in hippocampal neurons. *J. Neurochem.* 70, 1876–1886. doi: 10.1046/j.1471-4159.1998.70051876.x

Ghaneie, A., Duhadaway, J. B., Zemba-Palko, V., and Prendergast, G. C. (2006). Bin1 expression is lost in breast cancer. *J. Clin. Oncol.* 24(Suppl. 18), 10772–10772. doi: 10.1200/jco.2006.24.18_suppl.10772

Ghosh, G., van Duyne, G., Ghosh, S., and Sigler, P. B. (1995). Structure of NF-kappa B p50 homodimer bound to a kappa B site. *Nature* 373, 303–310. doi: 10.1038/373303a0

Greiner, J. F. W., Merten, M., Kaltschmidt, C., and Kaltschmidt, B. (2019). Sexual dimorphisms in adult human neural, mesoderm-derived, and neural crest-derived stem cells. *FEBS Lett.* 593, 3338–3352. doi: 10.1002/1873-3468.13606

Guerrini, L., Blasi, F., and Denis-Donini, S. (1995). Synaptic activation of NF-kappa B by glutamate in cerebellar granule neurons in vitro. *Proc. Natl. Acad. Sci. U.S.A.* 92, 9077–9081. doi: 10.1073/pnas.92.20.9077

Heimberger, A. B., Suki, D., Yang, D., Shi, W., and Aldape, K. (2005). The natural history of EGFR and EGFRvIII in glioblastoma patients. *J. Transl. Med.* 3:38. doi: 10.1186/1479-5876-3-38

Imielski, Y., Schwamborn, J. C., Luningschror, P., Heimann, P., Holzberg, M., Werner, H., et al. (2012). Regrowing the adult brain: NF-kappaB controls functional circuit formation and tissue homeostasis in the dentate gyrus. *PLoS One* 7:e30838. doi: 10.1371/journal.pone.0030838

Kaltschmidt, B., and Kaltschmidt, C. (2009). NF-kappaB in the nervous system. *Cold Spring Harb. Perspect. Biol.* 1:a001271. doi: 10.1101/cshperspect.a001271

Kaltschmidt, B., Baeuerle, P. A., and Kaltschmidt, C. (1993). Potential involvement of the transcription factor NF-kappa B in neurological disorders. *Mol. Aspects Med.* 14, 171–190. doi: 10.1016/0098-2997(93)90004-w

Kaltschmidt, B., Greiner, J. F. W., Kadhim, H. M., and Kaltschmidt, C. (2018). Subunit-specific role of NF-kappaB in cancer. *Biomedicines* 6:44. doi: 10.3390/biomedicines6020044

Kaltschmidt, B., Ndiaye, D., Korte, M., Pothion, S., Arbibe, L., Prullage, M., et al. (2006). NF-kappaB regulates spatial memory formation and synaptic plasticity through protein kinase A/CREB signaling. *Mol. Cell Biol.* 26, 2936–2946. doi: 10.1128/MCB.26.8.2936-2946.2006

Kaltschmidt, B., Uherek, M., Volk, B., Baeuerle, P. A., and Kaltschmidt, C. (1997). Transcription factor NF-kappaB is activated in primary neurons by amyloid beta peptides and in neurons surrounding early plaques from patients with Alzheimer disease. *Proc. Natl. Acad. Sci. U.S.A.* 94, 2642–2647. doi: 10.1073/pnas.94.6.2642

Kaltschmidt, B., Uherek, M., Wellmann, H., Volk, B., and Kaltschmidt, C. (1999). Inhibition of NF-kappaB potentiates amyloid beta-mediated neuronal apoptosis. *Proc. Natl. Acad. Sci. U.S.A.* 96, 9409–9414. doi: 10.1073/pnas.96.16.9409

Kaltschmidt, B., Witte, K. E., Greiner, J. F. W., Weissinger, F., and Kaltschmidt, C. (2022). Targeting NF-kappaB signaling in cancer stem cells: a narrative review. *Biomedicines* 10:261. doi: 10.3390/biomedicines10020261

Kaltschmidt, C., Greiner, J. F. W., and Kaltschmidt, B. (2021). The Transcription factor NF-kappaB in stem cells and development. *Cells* 10:2042. doi: 10.3390/cells10082042

Kaltschmidt, C., Kaltschmidt, B., and Baeuerle, P. A. (1993). Brain synapses contain inducible forms of the transcription factor NF-kappa B. *Mech. Dev.* 43, 135–147. doi: 10.1016/0925-4773(93)90031-r

Kaltschmidt, C., Kaltschmidt, B., and Baeuerle, P. A. (1995). Stimulation of ionotropic glutamate receptors activates transcription factor NF-kappa B in primary neurons. *Proc. Natl. Acad. Sci. U.S.A.* 92, 9618–9622. doi: 10.1073/pnas.92.21.9618

Kaltschmidt, C., Kaltschmidt, B., Lannes-Vieira, J., Kreutzberg, G. W., Wekerle, H., Baeuerle, P. A., et al. (1994a). Transcription factor NF-kappa B is activated in microglia during experimental autoimmune encephalomyelitis. *J. Neuroimmunol.* 55, 99–106. doi: 10.1016/0165-5728(94)90151-1

Kaltschmidt, C., Kaltschmidt, B., Neumann, H., Wekerle, H., and Baeuerle, P. A. (1994b). Constitutive NF-kappa B activity in neurons. *Mol. Cell Biol.* 14, 3981–3992. doi: 10.1128/mcb.14.6.3981-3992.1994

Kandel, E. R. (2001). The molecular biology of memory storage: a dialogue between genes and synapses. *Science* 294, 1030–1038. doi: 10.1126/science.1067020

Kang, J., Lemaire, H. G., Unterbeck, A., Salbaum, J. M., Masters, C. L., Grzeschik, K. H., et al. (1987). The precursor of Alzheimer's disease amyloid A4 protein resembles a cell-surface receptor. *Nature* 325, 733–736. doi: 10.1038/325733a0

Kato, T. Jr., Delhase, M., Hoffmann, A., and Karin, M. (2003). CK2 is a C-terminal IkappaB kinase responsible for NF-kappaB activation during the UV response. *Mol. Cell* 12, 829–839. doi: 10.1016/s1097-2765(03)00358-7

Keller, S., and Schmidt, M. H. H. (2017). EGFR and EGFRvIII promote angiogenesis and cell invasion in glioblastoma: combination therapies for an effective treatment. *Int. J. Mol. Sci.* 18:1295. doi: 10.3390/ijms18061295

Kim, H. J., Kim, J. Y., Jung, C. W., Lee, Y. S., An, J. Y., Kim, E. H., et al. (2021). ANO1 regulates the maintenance of stemness in glioblastoma stem cells by stabilizing EGFRvIII. *Oncogene* 40, 1490–1502. doi: 10.1038/s41388-020-01612-5

Kim, S., Kwon, S. H., Kam, T. I., Panicker, N., Karuppagounder, S. S., Lee, S., et al. (2019). Transneuronal propagation of pathologic alpha-synuclein from the gut to the brain models Parkinson's disease. *Neuron* 103, 627–641.e7. doi: 10.1016/j.neuron.2019.05.035

Klenke, C., Widera, D., Engelen, T., Muller, J., Noll, T., Niehaus, K., et al. (2013). Hsc70 is a novel interactor of NF-kappaB p65 in living hippocampal neurons. *PLoS One* 8:e65280. doi: 10.1371/journal.pone.0065280

Kobro-Flatmoen, A., Lagartos-Donate, M. J., Aman, Y., Edison, P., Witter, M. P., and Fang, E. F. (2021). Re-emphasizing early Alzheimer's disease pathology starting in select entorhinal neurons, with a special focus on mitophagy. *Ageing Res. Rev.* 67:101307. doi: 10.1016/j.arr.2021.101307

Lambert, E., Saha, O., Soares Landeira, B., Melo de Farias, A. R., Hermant, X., Carrier, A., et al. (2022). The Alzheimer susceptibility gene BIN1 induces isoform-dependent neurotoxicity through early endosome defects. *Acta Neuropathol. Commun.* 10:4. doi: 10.1186/s40478-021-01285-5

Lewy, F. (1912). "Paralysis agitans. I. Pathologische anatomie," in *Handbuch der Neurologie*, ed. M. Lewandowsky (Berlin: Springer).

Lin, Y., Bai, L., Chen, W., and Xu, S. (2010). The NF-kappaB activation pathways, emerging molecular targets for cancer prevention and therapy. *Expert Opin. Ther. Targets* 14, 45–55. doi: 10.1517/14728220903431069

Mao, N. C., Steingrimsson, E., DuHadaway, J., Wasserman, W., Ruiz, J. C., Copeland, N. G., et al. (1999). The murine Bin1 gene functions early in myogenesis and defines a new region of synteny between mouse chromosome 18 and human chromosome 2. *Genomics* 56, 51–58. doi: 10.1006/geno.1998.5709

Maqbool, A., Lattke, M., Wirth, T., and Baumann, B. (2013). Sustained, neuron-specific IKK/NF-kappaB activation generates a selective neuroinflammatory response promoting local neurodegeneration with aging. *Mol. Neurodegener.* 8:40. doi: 10.1186/1750-1326-8-40

Masters, C. L., Simms, G., Weinman, N. A., Multhaup, G., McDonald, B. L., and Beyreuther, K. (1985). Amyloid plaque core protein in Alzheimer disease and down syndrome. *Proc. Natl. Acad. Sci. U.S.A.* 82, 4245–4249. doi: 10.1073/pnas.82.12.4245

McElhinny, J. A., Trushin, S. A., Bren, G. D., Chester, N., and Paya, C. V. (1996). Casein kinase II phosphorylates I kappa B alpha at S-283, S-289, S-293, and T-291 and is required for its degradation. *Mol. Cell Biol.* 16, 899–906. doi: 10.1128/MCB.16.3.899

Meberg, P. J., Kinney, W. R., Valcourt, E. G., and Routtenberg, A. (1996). Gene expression of the transcription factor NF-kappa B in hippocampus: regulation by synaptic activity. *Brain Res. Mol. Brain Res.* 38, 179–190. doi: 10.1016/0169-328x(95)00229-l

Meffert, M. K., Chang, J. M., Wiltgen, B. J., Fanselow, M. S., and Baltimore, D. (2003). NF-kappa B functions in synaptic signaling and behavior. *Nat. Neurosci.* 6, 1072–1078. doi: 10.1038/nn1110

Meschede, J., Sadic, M., Furthmann, N., Miedema, T., Sehr, D. A., Muller-Rischart, A. K., et al. (2020). The parkin-coregulated gene product PACRG promotes TNF signaling by stabilizing LUBAC. *Sci. Signal.* 13:eaav1256. doi: 10.1126/scisignal.aav1256

Mikenberg, I., Widera, D., Kaus, A., Kaltschmidt, B., and Kaltschmidt, C. (2007). Transcription factor NF-kappaB is transported to the nucleus via cytoplasmic dynein/dynactin motor complex in hippocampal neurons. *PLoS One* 2:e589. doi: 10.1371/journal.pone.0000589

Ohgaki, H., and Kleihues, P. (2013). The definition of primary and secondary glioblastoma. *Clin. Cancer Res.* 19, 764–772. doi: 10.1158/1078-0432.Ccr-12-3002

O'Mahony, A., Raber, J., Montano, M., Foehr, E., Han, V., Lu, S. M., et al. (2006). NF-kappaB/Rel regulates inhibitory and excitatory neuronal function and synaptic plasticity. *Mol. Cell Biol.* 26, 7283–7298. doi: 10.1128/MCB.00510-06

Panicker, N., Ge, P., Dawson, V. L., and Dawson, T. M. (2021). The cell biology of Parkinson's disease. *J. Cell Biol.* 220:e202012095. doi: 10.1083/jcb.202012095

Park, J. Y., Lee, D., Lee, J. J., Gim, J., Gunasekaran, T. I., Choi, K. Y., et al. (2021). A missense variant in SHARPIN mediates Alzheimer's disease-specific brain damages. *Transl. Psychiatry* 11:590. doi: 10.1038/s41398-021-01680-5

Parkinson, J. (2002). An essay on the shaking palsy. 1817. *J. Neuropsychiatry Clin. Neurosci.* 14, 223–236; discussion 222. doi: 10.1176/jnp.14.2.223

Piao, J., Zabierowski, S., Dubose, B. N., Hill, E. J., Navare, M., Claros, N., et al. (2021). Preclinical efficacy and safety of a human embryonic stem cell-derived midbrain dopamine progenitor product, MSK-DA01. *Cell Stem Cell* 28, 217–229.e7. doi: 10.1016/j.stem.2021.01.004

Raychaudhuri, B., Han, Y., Lu, T., and Vogelbaum, M. A. (2007). Aberrant constitutive activation of nuclear factor kappaB in glioblastoma multiforme drives invasive phenotype. *J. Neurooncol.* 85, 39–47. doi: 10.1007/s11060-007-9390-7

Rinkenbaugh, A. L., Cogswell, P. C., Calamini, B., Dunn, D. E., Persson, A. I., Weiss, W. A., et al. (2016). IKK/NF-kappaB signaling contributes to glioblastoma stem cell maintenance. *Oncotarget* 7, 69173–69187. doi: 10.18632/oncotarget.12507

Ruiz-Perera, L. M., Greiner, J. F. W., Kaltschmidt, C., and Kaltschmidt, B. (2020). A Matter of choice: inhibition of c-Rel shifts neuronal to oligodendroglial fate in human stem cells. *Cells* 9:1037. doi: 10.3390/cells9041037

Ruiz-Perera, L. M., Schneider, L., Windmoller, B. A., Muller, J., Greiner, J. F. W., Kaltschmidt, C., et al. (2018). NF-kappaB p65 directs sex-specific neuroprotection in human neurons. *Sci. Rep.* 8:16012. doi: 10.1038/s41598-018-34394-8

Sakamuro, D., Elliott, K. J., Wechsler-Reya, R., and Prendergast, G. C. (1996). BIN1 is a novel MYC-interacting protein with features of a tumour suppressor. *Nat. Genet.* 14, 69–77.doi: 10.1038/ng0996-69

Salles, A., Boccia, M., Blake, M., Corbi, N., Passananti, C., Baratti, C. M., et al. (2015). Hippocampal dynamics of synaptic NF-kappa B during inhibitory avoidance long-term memory consolidation in mice. *Neuroscience* 291, 70–80. doi: 10.1016/j.neuroscience.2015.01.063

Sayed, M., Kim, S. O., Salh, B. S., Issinger, O. G., and Pelech, S. L. (2000). Stress-induced activation of protein kinase CK2 by direct interaction with p38 mitogen-activated protein kinase. *J. Biol. Chem.* 275, 16569–16573. doi: 10.1074/jbc.M000312200

Schmeisser, M. J., Baumann, B., Johannsen, S., Vindedal, G. F., Jensen, V., Hvalby, O. C., et al. (2012). IkappaB kinase/nuclear factor kappaB-dependent insulin-like growth factor 2 (Igf2) expression regulates synapse formation and spine maturation via Igf2 receptor signaling. *J. Neurosci.* 32, 5688–5703. doi: 10.1523/JNEUROSCI.0111-12.2012

Schmidt-Ullrich, R., Memet, S., Lilienbaum, A., Feuillard, J., Raphael, M., and Israel, A. (1996). NF-kappaB activity in transgenic mice: developmental regulation and tissue specificity. *Development* 122, 2117–2128. doi: 10.1242/dev.122.7.2117

Schorlemmer, H. U., and Seiler, F. R. (1991). 15-Deoxyspergualin (15-DOS) for therapy in an animal model of multiple sclerosis (MS): disease modifying activity on acute and chronic relapsing experimental allergic encephalomyelitis (EAE). *Agents Actions* 34, 156–160. doi: 10.1007/BF01993265

Schultz, W. (2007). Multiple dopamine functions at different time courses. *Annu. Rev. Neurosci.* 30, 259–288. doi: 10.1146/annurev.neuro.28.061604.135722

Shinojima, N., Tada, K., Shiraishi, S., Kamiryo, T., Kochi, M., Nakamura, H., et al. (2003). Prognostic value of epidermal growth factor receptor in patients with glioblastoma multiforme. *Cancer Res.* 63, 6962–6970.

Shubayev, V. I., and Myers, R. R. (2001). Axonal transport of TNF-alpha in painful neuropathy: distribution of ligand tracer and TNF receptors. *J. Neuroimmunol.* 114, 48–56. doi: 10.1016/s0165-5728(00)00453-7

Smith, D., Shimamura, T., Barbera, S., and Bejcek, B. E. (2008). NF-kappaB controls growth of glioblastomas/astrocytomas. *Mol. Cell Biochem.* 307, 141–147. doi: 10.1007/s11010-007-9593-4

Snow, W. M., and Albensi, B. C. (2016). Neuronal gene targets of NF-kappaB and their dysregulation in Alzheimer's disease. *Front. Mol. Neurosci.* 9:118. doi: 10.3389/fnmol.2016.00118

Soheili-Nezhad, S., Jahanshad, N., Guelfi, S., Khosrowabadi, R., Saykin, A. J., Thompson, P. M., et al. (2020). Imaging genomics discovery of a new risk variant for Alzheimer's disease in the postsynaptic SHARPIN gene. *Hum. Brain Mapp.* 41, 3737–3748. doi: 10.1002/hbm.25083

Steiner, J. A., Quansah, E., and Brundin, P. (2018). The concept of alpha-synuclein as a prion-like protein: ten years after. *Cell Tissue Res.* 373, 161–173. doi: 10.1007/s00441-018-2814-1

Stockhausen, M. T., Kristoffersen, K., Stobbe, L., and Poulsen, H. S. (2014). Differentiation of glioblastoma multiforme stem-like cells leads to downregulation of EGFR and EGFRvIII and decreased tumorigenic and stem-like cell potential. *Cancer Biol. Ther.* 15, 216–224. doi: 10.4161/cbt.26736

Stoeckel, K., Schwab, M., and Thoenen, H. (1975). Specificity of retrograde transport of nerve growth factor (NGF) in sensory neurons: a biochemical and morphological study. *Brain Res.* 89, 1–14. doi: 10.1016/0006-8993(75)90129-8

Suzuki, T., Mitake, S., Okumura-Noji, K., Yang, J. P., Fujii, T., and Okamoto, T. (1997). Presence of NF-kappaB-like and IkappaB-like immunoreactivities in postsynaptic densities. *Neuroreport* 8, 2931–2935. doi: 10.1097/00001756-199709080-00025

Taga, M., Petyuk, V. A., White, C., Marsh, G., Ma, Y., Klein, H. U., et al. (2020). BIN1 protein isoforms are differentially expressed in astrocytes, neurons, and microglia: neuronal and astrocyte BIN1 are implicated in tau pathology. *Mol. Neurodegener.* 15:44. doi: 10.1186/s13024-020-00387-3

Wang, H., Li, L., and Yin, L. (2018). Silencing LncRNA LOXL1-AS1 attenuates mesenchymal characteristics of glioblastoma via NF-kappaB pathway. *Biochem. Biophys. Res. Commun.* 500, 518–524. doi: 10.1016/j.bbrc.2018.04.133

Wang, Y., Yi, K., Liu, X., Tan, Y., Jin, W., Li, Y., et al. (2021). HOTAIR up-regulation activates NF-kappaB to induce immunoescape in gliomas. *Front. Immunol.* 12:785463. doi: 10.3389/fimmu.2021.785463

Wellmann, H., Kaltschmidt, B., and Kaltschmidt, C. (2001). Retrograde transport of transcription factor NF-kappa B in living neurons. *J. Biol. Chem.* 276, 11821–11829. doi: 10.1074/jbc.M009253200

Whittaker, V. P., Michaelson, I. A., and Kirkland, R. J. (1964). The separation of synaptic vesicles from nerve-ending particles ('synaptosomes'). *Biochem. J.* 90, 293–303. doi: 10.1042/bj0900293

Widera, D., Klenke, C., Nair, D., Heidbreder, M., Malkusch, S., Sibarita, J. B., et al. (2016). Single-particle tracking uncovers dynamics of glutamate-induced retrograde transport of NF-kappaB p65 in living neurons. *Neurophotonics* 3:041804. doi: 10.1117/1.NPh.3.4.041804

Wilkaniec, A., Lenkiewicz, A. M., Babiec, L., Murawska, E., Jęśko, H. M., Cieślik, M., et al. (2021). Exogenous alpha-synuclein evoked parkin downregulation promotes mitochondrial dysfunction in neuronal cells. Implications for Parkinson's disease pathology. *Front. Aging Neurosci.* 13:591475. doi: 10.3389/fnagi.2021.591475

Witte, K. E., Hertel, O., Windmöller, B. A., Helweg, L. P., Höving, A. L., Knabbe, C., et al. (2021). Nanopore sequencing reveals global transcriptome signatures of mitochondrial and ribosomal gene expressions in various human cancer stem-like cell populations. *Cancers (Basel)* 13:1136. doi: 10.3390/cancers13051136

Xie, T. X., Xia, Z., Zhang, N., Gong, W., and Huang, S. (2010). Constitutive NF-kappaB activity regulates the expression of VEGF and IL-8 and tumor angiogenesis of human glioblastoma. *Oncol. Rep.* 23, 725–732.

Yiannopoulou, K. G., Anastasiou, A. I., Zachariou, V., and Pelidou, S. H. (2019). Reasons for failed trials of disease-modifying treatments for Alzheimer disease and their contribution in recent research. *Biomedicines* 7:97. doi: 10.3390/biomedicines7040097

Zhang, Q., Lenardo, M. J., and Baltimore, D. (2017). 30 years of NF-kappaB: a blossoming of relevance to human pathobiology. *Cell* 168, 37–57. doi: 10.1016/j.cell.2016.12.012

Zheng, Q., Han, L., Dong, Y., Tian, J., Huang, W., Liu, Z., et al. (2014). JAK2/STAT3 targeted therapy suppresses tumor invasion via disruption of the EGFRvIII/JAK2/STAT3 axis and associated focal adhesion in EGFRvIII-expressing glioblastoma. *Neuro Oncol.* 16, 1229–1243. doi: 10.1093/neuonc/nou046

frontiers | Frontiers in Molecular Neuroscience

TYPE Original Research
PUBLISHED 29 September 2022
DOI 10.3389/fnmol.2022.999833

OPEN ACCESS

EDITED BY
Isabel Varela-Nieto,
Spanish National Research Council (CSIC), Spain

REVIEWED BY
Ignacio del Castillo,
Ramón y Cajal University Hospital, Spain
Ekaitz Errasti Murugarren,
University of Barcelona, Spain

*CORRESPONDENCE
Antonio Sarikas
antonio.sarikas@pmu.ac.at
Silvia Dossena
silvia.dossena@pmu.ac.at

†These authors have contributed equally to this work and share senior authorship

SPECIALTY SECTION
This article was submitted to Molecular Signalling and Pathways, a section of the journal Frontiers in Molecular Neuroscience

RECEIVED 21 July 2022
ACCEPTED 13 September 2022
PUBLISHED 29 September 2022

CITATION
Bernardinelli E, Roesch S, Simoni E, Marino A, Rasp G, Astolfi L, Sarikas A and Dossena S (2022) Novel POU3F4 variants identified in patients with inner ear malformations exhibit aberrant cellular distribution and lack of *SLC6A20* transcriptional upregulation. *Front. Mol. Neurosci.* 15:999833. doi: 10.3389/fnmol.2022.999833

Novel POU3F4 variants identified in patients with inner ear malformations exhibit aberrant cellular distribution and lack of *SLC6A20* transcriptional upregulation

Emanuele Bernardinelli[1], Sebastian Roesch[2], Edi Simoni[3], Angela Marino[4], Gerd Rasp[2], Laura Astolfi[3,5], Antonio Sarikas[1*†] and Silvia Dossena[1*†]

[1]Institute of Pharmacology and Toxicology, Paracelsus Medical University, Salzburg, Austria, [2]Department of Otorhinolaryngology, Head and Neck Surgery, Paracelsus Medical University, Salzburg, Austria, [3]Bioacoustic Research Laboratory, Department of Neuroscience, Biomedical Campus Pietro d'Abano, University of Padua, Padua, Italy, [4]Department of Chemical, Biological, Pharmaceutical, and Environmental Sciences, University of Messina, Messina, Italy, [5]Interdepartmental Research Center of International Auditory Processing Project in Venice (I-APPROVE), Department of Neurosciences, University of Padova, Santi Giovanni e Paolo Hospital, ULSS3, Venice, Italy

Hearing loss (HL) is the most common sensory defect and affects 450 million people worldwide in a disabling form. Pathogenic sequence alterations in the *POU3F4* gene, which encodes a transcription factor, are causative of the most common type of X-linked deafness (X-linked deafness type 3, DFN3, DFNX2). POU3F4-related deafness is characterized by a typical inner ear malformation, namely an incomplete partition of the cochlea type 3 (IP3), with or without an enlargement of the vestibular aqueduct (EVA). The pathomechanism underlying POU3F4-related deafness and the corresponding transcriptional targets are largely uncharacterized. Two male patients belonging to a Caucasian cohort with HL and EVA who presented with an IP3 were submitted to genetic analysis. Two novel sequence variants in *POU3F4* were identified by Sanger sequencing. In cell-based assays, the corresponding protein variants (p.S74Afs*8 and p.C327*) showed an aberrant expression and subcellular distribution and lack of transcriptional activity. These two protein variants failed to upregulate the transcript levels of the amino acid transporter gene *SLC6A20*, which was identified as a novel transcriptional target of POU3F4 by RNA sequencing and RT-qPCR. Accordingly, *POU3F4* silencing by siRNA resulted in downregulation of *SLC6A20* in mouse embryonic fibroblasts. Moreover, we showed for the first time that SLC6A20 is expressed in the

mouse cochlea, and co-localized with POU3F4 in the spiral ligament. The findings presented here point to a novel role of amino acid transporters in the inner ear and pave the way for mechanistic studies of POU3F4-related HL.

KEYWORDS

POU3F4, DFNX2, DFN3, incomplete partition 3, hearing loss, enlarged vestibular aqueduct, *SLC6A20*

Introduction

Congenital hearing loss (HL) is estimated to affect 1 in 1,000 newborns, is the most common sensory defect and affects 450 million people worldwide in a disabling form (Sheffield and Smith, 2019). In developed countries, 60–80% of the reported cases of HL are estimated to result from genetic defects (Shearer et al., 2017), which mostly lie in autosomal genes and in about 1–5% of the cases in genes on the X chromosome (Del Castillo et al., 2022). Among the four types of X-linked HL (DFN2, DFN3, DFN4, and DFN6), X-linked deafness type 2 (DFNX2, also known as DFN3, OMIM #304400) accounts for about 50% of X-linked deafness cases and is associated with pathogenic sequence alterations in the *POU3F4* gene (*BRAIN-4*, *BRN4*, OMIM *300039) (Phippard et al., 1999), which codes for a highly conserved protein belonging to the POU family of transcription factors.

Hereditary HL is often associated with inner ear malformations, which are detectable in about 20% of the patients affected by sensorineural HL (SNHL) (Sennaroglu and Bajin, 2017). The observed abnormalities range from an enlargement of the vestibular aqueduct (EVA) to an incomplete partition of the cochlea (IP) or a complete labyrinthine aplasia, where cochlea and vestibule are completely absent. The most commonly detected abnormality is an EVA, with or without cochlear malformations. EVA can be associated with defects in multiple genes, the most frequently involved being *SLC26A4*, which codes for the anion exchanger pendrin (OMIM *605646). Other genes that have been found mutated in patients with EVA code for the pendrin transcription factor FOXI1 (OMIM *601093), the potassium channel KCNJ10 (OMIM *602208), the gap junction protein connexin-26 (OMIM *121011), and the transcription factor POU3F4 (Roesch et al., 2021).

Pathogenic sequence alterations in *POU3F4* result in a mixed type of HL (conductive and sensorineural), often progressive, associated with characteristic bone abnormalities (de Kok et al., 1995). In this context, a computed tomography (CT) scan of the temporal bone typically reveals a dilation of the internal acoustic canal (IAC) and a malformation of the cochlea, defined as an incomplete partition of type 3 (IP3), with or without an EVA. IP3 is characterized by the absence of the bony modiolus and the septum at the base of the cochlea, while the *interscalar septum* is still partially present. Also, often observed in DFN3 patients are an abnormal calcification and fixation of the stapes and a gusher of cerebrospinal fluid upon opening of the labyrinth during cochlear implant surgery (Sennaroglu and Bajin, 2018).

The transcription factor POU3F4 belongs to the POU superfamily of transcription factors, which are characterized by two DNA binding domains, the POU-specific domain and the POU-homeodomain, both determining the specificity of the binding to target genes (Lee et al., 2009; Malik et al., 2018). Despite a limited knowledge regarding the actual transcriptional targets of POU3F4, its role in the development of the hearing apparatus is well established. During embryonic development of the inner ear, POU3F4 is mainly expressed in the otic mesenchyme surrounding the otic vesicle (Phippard et al., 1999) and plays a role in the development of the otic neural tube and the bony tissue surrounding the auditory-vestibular system, possibly by regulating the expression of ephrin type-A receptor 4 (*EphA4*) and Ephrin-B2 (*Efnb2*) (Coate et al., 2012; Raft et al., 2014). Alterations in the spiral ganglion axon fasciculation and synapse formation observed in *Pou3f4*$^{y/-}$ hemizygous male mice were associated to a lack of EphA4 expression, while the ossification defects of the stapes and other temporal bone structures were linked to a defective regulation of the Ephrin-B2 gene.

In neonatal wild type mice, the highest expression of *Pou3f4* in the inner ear was found in the spiral ligament and remarkable pathological changes were observed in the spiral ligament fibrocytes in *Pou3f4*-deficient mice (Minowa et al., 1999). Spiral ligament fibrocyte adhesion is essential for cochlear K^+ recycling and maintenance of the endocochlear potential and hence the hearing function. Lack of POU3F4 expression in the development of the mouse inner ear leads to a defective adhesion of the fibrocytes in the spiral ligament and consequent degeneration of Cx26/Cx30 gap junction plaques in the inner sulcus (Kidokoro et al., 2014), thus explaining the loss of the endocochlear potential and deafness in *Pou3f4*-deficient mice. Outside of the hearing organ, POU3F4 is mainly expressed in brain (Wu et al., 2021), kidney and pancreas (Naranjo et al., 2010; Tantin, 2013), but its functional role in these organs has not been completely established.

TABLE 1 Summary of the clinical finding of the two index patients.

Patient ID	Ethnicity	Sex	Age (year of birth)	EVA, side	IP3, side	Side affected by HL	Degree of HL	CSF gusher during CI surgery
#569	Caucasian	M	33 (1989)	Bilateral	Bilateral	Both	Severe	Yes, both sides
#667	Caucasian	M	19 (2003)	Left	Bilateral	Both	Right, profound Left, severe	Yes, right side

CI, cochlear implant; CSF, cerebrospinal fluid; EVA, enlarged vestibular aqueduct; HL, hearing loss; IP3, incomplete partition of the cochlea type 3.

The present study was guided by the genetic appraisal of two male patients with mixed HL and IP3 belonging to our Austrian cohort of patients diagnosed with EVA (Roesch et al., 2018). Two novel *POU3F4* sequence variants leading to aberrant protein products were identified in these patients. The two pathogenic POU3F4 protein variants failed to upregulate *SLC6A20*, which was identified as a novel transcriptional target of POU3F4.

Materials and methods

Patient recruitment

Two male subjects diagnosed with HL associated with inner ear malformations (EVA and IP3, **Table 1**) were enrolled in the study. The research was prospectively reviewed and approved by a duly constituted ethics committee (415-E/2092/6-2017, 9 May 2017) and has therefore been performed in accordance with the principles embodied in the 1964 Declaration of Helsinki and its later amendments.[1] Written informed consent was obtained from the subjects or their legal representatives prior to blood sampling and genetic testing. For both patients, imaging studies of the inner ear by computed tomography (CT) of the temporal bones were performed. EVA was defined as an enlargement of the vestibular aqueduct >1.5 mm midway between the endolymphatic sac and the vestibule and fitted the definition criteria for EVA (Valvassori and Clemis, 1978; Vijayasekaran et al., 2007) in both patients. An IP3 was identified as a cochlea of normal size lacking the bony modiolus and the septum at the base of the cochlea, while the *interscalar septum* was partially present (Sennaroglu and Bajin, 2018). Characterization of HL was based on side-specific pure-tone audiometric testing, as well as the patient's history. Related to the time of speech development, the onset of HL was defined as congenital, prelingual, perilingual or postlingual. Clinical course of HL with possible hearing drops was obtained through audiometric tests and patient's history. Surgical reports were screened for intraoperative gusher phenomenon, defined as a visible efflux of cerebro-spinal fluid (CSF) after cochleostomy, during cochlear implant surgery.

Genomic DNA analysis

Patient whole blood was collected via venipuncture in plastic tubes with potassium-ethylenediaminetetraacetic (EDTA) acid as the anticoagulant. Total genomic DNA (gDNA) was purified from ∼350 μl blood with the EZ1® DSP DNA Blood kit (QIAGEN, Hilden, Germany) using the EZ1 Advanced XL platform (QIAGEN) according to the manufacturer's instructions. Quantification was performed with the QIAxpert (QIAGEN) spectrophotometer. Only samples with an absorbance 260/280 between 1.7 and 1.9 were used for downstream analysis. The coding exons and no less than 50 nucleotides of the intro-exon boundaries of *POU3F4*, *GJB2*, *FOXI1* and *KCNJ10* were amplified by end-point polymerase chain reaction (PCR) with the primers indicated in **Supplementary Table 1**. For *POU3F4*, 50 μl PCR reaction contained 1X JumpStart REDAccuTaq Long and Accurate (JS RAT LA) DNA Polymerase buffer (Sigma-Aldrich, St. Louis, MO, USA), 0.3 mM dNTPs (Thermo Fisher Scientific, Waltham, MA, USA), 5% dimethyl sulfoxide (Sigma-Aldrich), 0.4 μM forward and reverse primers, 1.5 units JS RAT LA DNA Polymerase (Sigma-Aldrich) and 100 ng gDNA template. For the other genes, the PCR reaction was similar, with minor modifications. For *SLC26A4*, primers and procedure were formerly described (Roesch et al., 2018). Five μl of each PCR product was run on a 1% agarose gel for size verification, the remnant was purified with the QIAquick PCR purification kit (QIAGEN) and Sanger sequenced in the forward and reverse orientations (Microsynth AG, Switzerland) with the primers indicated in **Supplementary Table 1**. The resulting sequences were compared against the NCBI *Homo sapiens POU3F4* (OMIM ID: *300039, GenBank ID: NG_009936.2), *GJB2* (OMIM ID: *121011, GenBank ID: NG_008358.1), *SLC26A4* (OMIM ID: *605646, GenBank ID: NG_008489.1), *FOXI1* (OMIM ID: *601093, GenBank ID: NG_012068.2), and *KCNJ10* (OMIM ID: *602208, GenBank ID: NG_016411.1) genomic reference sequence assembly. The presence of the two

1 Available online: https://www.wma.net/policies-post/wma-declaration-of-helsinki-ethical-principles-for-medical-research-involving-human-subjects/.

large genomic deletions del(GJB6-D13S1830) and del(GJB6-D13S1854) was verified by multiplex PCR according to the method described in detail by del Castillo (del Castillo et al., 2005).

Plasmid constructs

A pFLAG-CMV^{TM}-4 vector (Sigma-Aldrich), containing the coding sequence (CDS) of wild type or mutated human *POU3F4* cloned from human genomic DNA, was used for subcellular localization analysis by immunocytochemistry and confocal microscopy. Following transfection of cells with this construct, proteins are produced with a N-terminal FLAG epitope (DYKDDDDK). Alternatively, the pEYFP-C1 vector (Clontech, Mountain View, CA, USA) was used for these experiments. In this case, POU3F4 is produced with the enhanced yellow fluorescent protein (EYFP) fused to its N-terminus.

For dual luciferase assay experiments, the *POU3F4* CDS was sub-cloned into a pIRES2-EGFP vector (Clontech). With this construct, an untagged protein product was co-expressed with the transfection marker enhanced green fluorescent protein (EGFP) as two individual proteins. pGL4.11 POU3F4prom–475 + 25 reporter construct for the assay was produced by sub-cloning a fragment of *POU3F4* own promoter (Lee et al., 2009) upstream of the coding sequence of firefly luciferase in a pGL4.11 vector. The pRL-CMV vector, coding for renilla luciferase, was used for the normalization of firefly luciferase signal.

Sequence alterations in the CDS of *POU3F4* were obtained using the QuikChange® Site-directed mutagenesis kit (Stratagene, San Diego, CA, USA). The sequence of all plasmid inserts was verified by Sanger sequencing (Microsynth AG, Balgach, Switzerland).

Cell culture and transfection

HEK293Phoenix (DiCiommo et al., 2004) and HeLa (CCL-2, American Type Culture Collection, ATCC, Manassas, VA, USA) cells were cultured in Dulbecco Modified Eagle's Medium (DMEM) supplemented with 2 mM L-glutamine, 1 mM sodium pyruvate, streptomycin-penicillin and 10% fetal bovine serum (FBS). Mouse embryonic fibroblasts (MEFs, CRL-2991, ATCC) were cultured in high glucose DMEM supplemented with 2 mM L-glutamine, 1 mM sodium pyruvate, streptomycin-penicillin and 10% FBS. Cell cultures were kept in a humidified incubator at 37°C and 5% CO_2.

Transient transfection of HEK293Phoenix and HeLa cells was performed either with the calcium-phosphate co-precipitation method or with Metafectene PRO (Biontex, Munich, Germany) respectively, as previously described (De Moraes et al., 2016).

For *POU3F4* silencing experiments, MEFs were transfected with Metafectene SI + (Biontex) according to the manufacturer's instructions.

Dual luciferase assay

For the dual luciferase assay, HEK293Phoenix cells were seeded in twenty-four-well plates and transiently transfected on the following day with 250, 250, and 20 ng of wild type or mutated pIRES2-EGFP POU3F4 or empty pIRES2-EGFP, pGL4.11 POU3F4prom-472 + 25, and pRL-CMV vectors, respectively. Twenty-four hours later, media containing the transfection mix was replaced with fresh media. Forty-eight hours after transfection, the cells were prepared for the assay using the Dual Luciferase® Assay System (Promega, Madison, Wisconsin, USA). Media was removed and cells were washed once with phosphate buffered saline (PBS, 136.89 mM NaCl, 2.69 mM KCl, 3.21 mM Na_2HPO_4, pH 7.4). Passive lysis buffer (200 µl) was added to each well and cells were incubated at room temperature (RT) for 15 min with shaking, followed by 15 min at -20°C and 15 min at room temperature with shaking. Twenty µl lysate were transferred in the wells of a white ninety-six-well plate for the assay. Fifty µl of luciferase assay reagent (LAR) II were added to each well and luminescence from the Firefly luciferase was detected for 10 s. Fifty µl of STOP & Glo reagent were then added to simultaneously quench the Firefly luciferase signal and activate the Renilla luciferase signal. The Renilla luciferase luminescence was also detected for 10 seconds. Addition of the LARII and STOP & Glo buffers, as well as detection of the luminescence was performed using the VICTOR^{TM} X3 2030 multi-label reader (Perkin Elmer, Waltham, MA, USA).

Subcellular localization analysis with fluorescent fusion proteins

HeLa cells were seeded into 6-well plates, grown overnight, transfected with 1.5 µg of plasmid DNA, transferred on glass slides for microscopy twenty-four hours post-transfection, fixed in 4% paraformaldehyde and imaged forty-eight hours post-transfection. Subcellular localization of POU3F4 variants was determined by co-localization between wild type or mutant POU3F4 with EYFP fused to the N-terminus and 4',6-Diamidino-2-Phenylindole (DAPI), as a marker of the nuclear compartment. Co-localization was detected and quantified as previously described (De Moraes et al., 2016). Shortly, imaging was performed by sequential acquisition with a Leica TCS SP5II AOBS confocal microscope (Leica Microsystems, Wetzlar, Germany) equipped with an HCX PL APO 63x/1.20 Lambda blue water immersion objective and controlled by the LAS AF SP5 software (Leica Microsystems). EYFP was excited with the 514 nm line of the Argon laser and emission was detected

in the 525–600 nm range; DAPI was excited at 405 nm with a diode laser and emission was detected in the 420–485 nm range. Co-localization was quantified and expressed as the Pearson's correlation coefficient (Adler and Parmryd, 2010), overlap coefficient and co-localization rate.

RNA sequencing

HEK293Phoenix cells were transiently transfected with pIRES2-EGFP POU3F4 wild type, POU3F4 p.C327* or the empty pIRES2-EGFP vector as a control. Forty-eight hours after transfection, total RNA was extracted with the RNeasy Micro Kit (QIAGEN) according to the manufacturer's instruction and quantified. Samples were submitted for RNAseq analysis to the Bioinformatics Core Facility, Centre for Molecular Medicine, CEITEC Masaryk University, Brno, Czech Republic. Raw reads were quality checked, pre-processed and mapped to the reference genome with gene annotation (genome version: Ensembl GRCh38) with multiple tools (FastQC, MultiQC STAR, Samtools). Mapped reads were counted and summarized to genes, whereby only uniquely mapped and uniquely assigned reads were counted. The following checks were performed to estimate the overall sample quality: rRNA content estimate (fastqflscreen), read duplication rate (dupRadar, Picard tools), sequenced (targeted) regions (RSeQC, Picard tools), 5'/3' coverage bias (Picard tools), expressed gene biotypes (featureCounts) and library strandedness (RSeQC). Differential genes expression was calculated (edgeR, DESeq2) by comparing all conditions against each other. Gene expression analysis was then manually refined by selecting the significantly upregulated genes.

Western blot

HEK293Phoenix cells for Western blot were transfected with pIRES2-EGFP POU3F4 wild type, POU3F4 p.C327* or the empty pIRES2-EGFP vector. Total protein extraction was performed by denaturing lysis of cells twenty-four hours after transfection. Protein extracts (20 μg) were electrophoresed with constant voltage (120 V) on 12% SDS-PAGE gels. Proteins were transferred overnight onto polyvinylidene fluoride (PVDF) membranes with constant amperage (0.25 mA). The membranes were blocked for 1 h at room temperature in 5% non-fat dry milk in Tris-buffered saline containing 0.01% Tween 20 (TBST). Membranes were incubated overnight at 4°C with the primary antibody (rabbit anti-POU3F4, 711871, Thermo Scientific) diluted in 5% non-fat dry milk in TBST, washed 3 times in TBST and incubated for 1 h at room temperature with the secondary antibody in TBST containing 5% non-fat dry milk. Immunocomplexes were visualized using the ODYSSEY infrared imaging system (LICOR, Lincoln, NE, USA). The membrane was then stripped with a buffer containing 25 mM Glycine, 2% SDS, pH 2 and blotted again with anti-glyceraldehyde-3-phosphate dehydrogenase (GAPDH) antibodies (goat anti-GAPDH, A00191, GenScript, Piscataway, NJ, USA) following the same procedure described above. The anti-rabbit (926-32211, 1:20000 dilution) and the anti-goat (926-32214, 1:20000 dilution) IRD-800-CW secondary antibodies were from LICOR.

RNA extraction and real time PCR analysis

Total RNA from transfected cells was extracted with RNeasy Micro Kit (QIAGEN) according to the manufacturer's instructions and quantified with the QIAxpert (QIAGEN) spectrophotometer.

Total RNA from mouse kidney, small intestine, and lung were from commercial sources (Clontech and AMS Biotechnology Ltd., Abingdon, United Kingdom).

Total RNA extraction from mouse cochlea was performed as following: cochleae were explanted from 2-month-old euthanized wild type C57BL/6J mice and preserved in RNA-Protect solution (QIAGEN) until total RNA extraction was performed. For RNA extraction, RNA-Protect was removed and lysis of the whole cochlea was performed with the Tissue Lyser instrument (QIAGEN) in a QIAzol solution (QIAGEN). Debris were removed by centrifugation and phases were separated by centrifugation after the addition of chloroform. The upper phase was then transferred to a RNeasy MinElute spin column for further purification steps following the protocol provided by the manufacturer (QIAGEN). RNA was quantified with the QIAxpert (QIAGEN) spectrophotometer.

Retrotranscription of the RNA extracted either from cells or from tissues was performed with the QuantiTect Reverse Transcription Kit (QIAGEN) with 1 μg RNA per reaction, according to the manufacturer's instructions. Real Time PCR (RT-qPCR) was performed on the Rotor-Gene Q instrument (QIAGEN) using the GoTaq^{TM} qPCR Master Mix (Promega). Primers were designed for the specific amplification of *POU3F4* or *SLC6A20* transcripts (**Supplementary Table 2**). The indicated housekeeping genes were used for normalization of mRNA abundance. Relative mRNA levels were calculated using the comparative threshold cycle method (ΔΔ CT).

Immunohistochemistry and immunocytochemistry

Cochlea sections for immunohistochemistry were prepared by fixing mice (CBA/J, 12-week-old) whole cochleae in Shandon Glyo-Fixx (Thermo Scientific) overnight at 4°C. Temporal bones were decalcified with Surgipath Decalcifier I (Leica Biosystems) for 20 h at 4°C followed by Surgipath Decalcifier II for 3 h at room temperature. Decalcified cochleae were included

in paraffin with an automatic processor and manual embedding system (SLEE medical GmbH, Nieder-Olm, Germany). Paraffin embedded samples were sectioned with a thickness of 5 μm with a semiautomatic microtome (Thermo Scientific). After paraffin removal and rehydration of the sections, antigen retrieval was performed in sodium citrate buffer (pH 6) for 10 min at 95°C. Endogenous peroxidases were inactivated with a 1% hydrogen peroxide solution and tissue sections were blocked in normal goat serum for 45 min at room temperature before incubation with primary antibodies (rabbit polyclonal anti-POU3F4, P100907_T100, Aviva System Biology, diluted 1:200, or rabbit polyclonal anti-SLC6A20, PA5-104153, Invitrogen, diluted 1:200). Incubation with primary antibodies was performed at 4°C for 16 h. Immunocomplexes were detected with the ABC-kit system (Vector Laboratories) and DAB chromogen (Dako, Agilent, Santa Clara, CA, USA). Nuclei were stained with hematoxylin staining (Leica Biosystems). Slices were finally dehydrated and mounted with Surgipath Micromount (Leica Biosystems) before imaging with an optical microscope ECLIPSE 50i (Nikon Europe, Amstelveen, Netherlands). Images were acquired with the Nis Elements D 3.2 software (Nikon).

Immunocytochemistry was performed as previously described (Meyer et al., 2004; Dossena et al., 2006) with minor modifications. Shortly, HeLa cells were transfected with N-terminally flagged wild type POU3F4, POU3F4 p.S74Afs*8 or POU3F4 p.C327* for 48 h, fixed in Hank's Balanced Salt Solution (HBSS) containing 4% paraformaldehyde for 30 min, permeabilized with HBSS containing 0.2% Triton X-100 for 15 min, blocked with 3% bovine serum albumin (BSA) in HBSS for 1 h at room temperature and incubated overnight at 4°C with a mouse monoclonal anti-FLAG antibody (Sigma-Aldrich) diluted to 20 μg/ml in HBSS containing 0.1% BSA. Next, cells were incubated for 1 h at room temperature with an Alexa Fluor® 488-conjugated goat anti-mouse antibody (Invitrogen Life Technologies, Carlsbad, CA, USA), counterstained with DAPI, mounted in MOWIOL® 4-88 (Sigma-Aldrich) and imaged as described above for the co-localization of the fluorescent signal with the cell nucleus by confocal microscopy.

Statistical analysis

All data are expressed as arithmetic means ± SEM and analyzed with GraphPad Prism software (version 5.00 for MacOSX, GraphPad Software, San Diego, CA, USA). Significant differences between data sets were verified by one-way Analysis of Variance (ANOVA) with Bonferroni's post-test or by unpaired Student's t-test, as appropriate. A p value <0.05 was considered as statistically significant; (n) corresponds to the number of independent measurements.

Results

Clinical features of index patients

Two patients diagnosed with profound to severe bilateral mixed HL at the ENT department of the State hospital in Salzburg (Austria) were submitted to genetic analysis in order to determine the cause of the observed hearing defect.

The first patient (patient ID #569) is a 33-year-old Caucasian male diagnosed with a bilateral severe mixed HL characterized by a progressive loss of hearing from the age of 6. The CT scan of the temporal bone revealed a bilateral EVA and a bilateral IP3 (**Figures 1A,B**). During cochlear implant surgery, a CSF gusher was observed. Both parents have normal hearing.

The second patient (patient ID #667) is a 19-year-old Caucasian male with profound mixed HL in the right ear and severe mixed HL in the left ear, associated with dizziness. From the CT scan, an IP3 was observed on both sides, while the EVA was present on the left side only (**Figures 1C,D**) that, interestingly, is the side diagnosed with the less severe degree of HL. A CSF gusher was observed during surgery also with this patient. In addition to the HL, patient #667 was diagnosed externally with cognitive deficits. Both parents and the brother have normal hearing. Clinical findings concerning the two patients presented here are summarized in **Table 1**. The clinical features displayed by the two patients corresponded to the typical hallmarks associated with genetic defects in *POU3F4*, that are an IP3, EVA, intraoperative CSF gusher, HL often associated with mental deficits and/or vestibular dysfunction (Wang et al., 2021).

Index patient #569 received cochlear implants on both sides, patient #667 on one side, with conventional hearing aid on the other side. All electrodes could be correctly positioned within the cochlea, however, patient #569 needed revision 17 years after primary surgery due to facial nerve stimulation through the implant. Hearing rehabilitation with the cochlear implant in both patients resulted in pure-tone audiometry curve threshold at around 20 dB HL on the implanted side, with 100% numbers and 15% monosyllabics recognition at 65 dB SPL for Freiburger speech audiometry in silence.

Identification of novel *POU3F4* variants

The finding of an IP3 in the two index patients prompted us to analyze *POU3F4*. Due to the presence of an EVA in both patients, all known EVA-related genes were included in the analysis. Genomic DNA was extracted from peripheral blood of index patients and regions of interest were amplified for Sanger sequencing. Two novel sequence variants in the *POU3F4* gene were identified in these patients (**Table 2**). The variant identified in patient #569 is a deletion of an alanine at position g.5284, c.220, resulting in a frameshift and a premature truncation of the

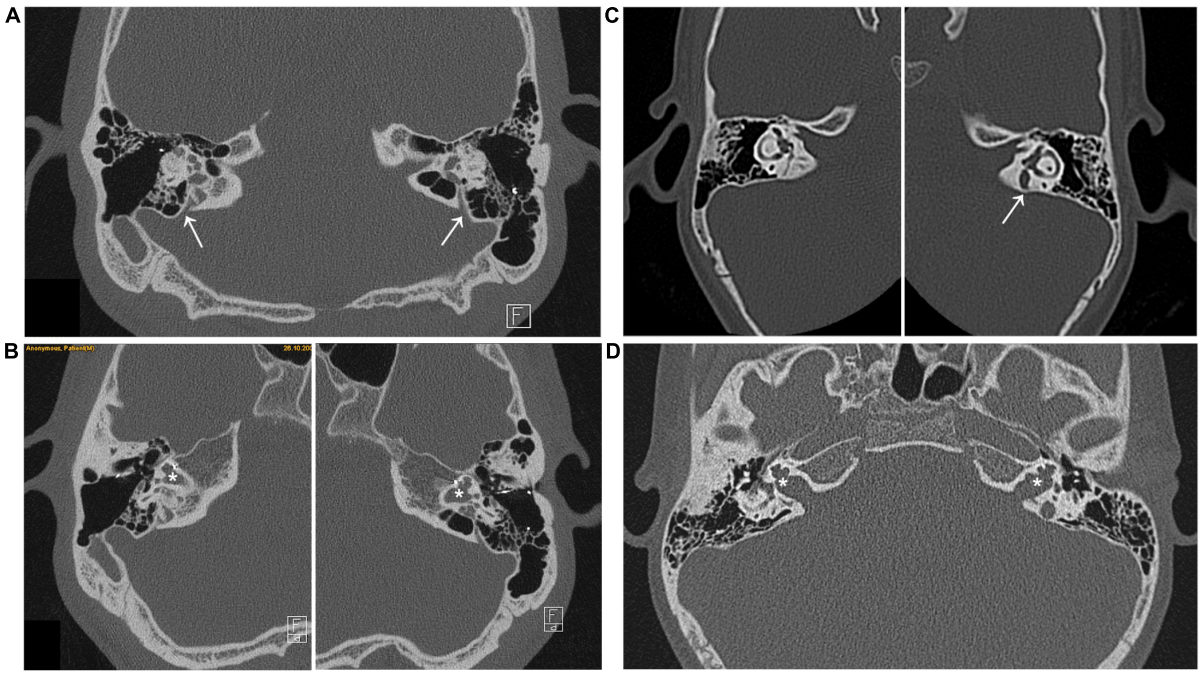

FIGURE 1
Axial CT scan of the index patients showing both sides. **(A,B)** Patient #569, arrows in panel **(A)** indicate the bilateral enlargement of the vestibular aqueduct (EVA), * in panel **(B)** indicate the bilateral incomplete partition of the cochleae with missing modiolus (IP3), a typical hallmark of POU3F4-related deafness. **(C,D)** Patient #667, arrow in panel **(C)** indicates the EVA on the left side, while on the right side the vestibular aqueduct appears normal; * in panel **(D)** indicate the bilateral IP3.

TABLE 2 Summary of *POU3F4* variants identified in the two index patients.

Patient ID	Sex	*POU3F4* (gDNA)		*POU3F4* (cDNA)		POU3F4 (protein)	
#569	M	g.5284delA	–	c.220delA	–	p.S74Afs*8	–
#667	M	g.6045T > A	–	c.979T > A	–	p.C327*	–

Results from the Sanger sequencing were compared to the following NCBI reference sequences: genomic DNA (RefSeq NG_009936.2), mRNA (RefSeq NM_000307.1) and protein product (RefSeq NP_00298.3). *Denotes the STOP codon.

protein at p.82 (g.5284delA, c.220delA, p.S74Afs*8). The variant identified in patient #667 is a conversion of a thymine to an adenine at position g.6045, c.979, resulting in a premature stop codon at position p.327 (g.6045T > A, c.979T > A, p.C327*). Familial pedigrees are shown in Figures 2A,B. The mother of patient #569 is a heterozygote carrier of the mutation identified in the index patient. The genetic status of the mother of patient #667 is unknown. The two sequence variants identified in *POU3F4* are novel, and represent the first report of *POU3F4* mutations in the Austrian population. Electropherograms from the Sanger sequencing and a graphical representation of the protein products resulting from the mutated genes are shown in Figures 2C–E, respectively. Supplementary Table 3 shows the additional genetic findings of index patients #569 and #667. No pathogenic sequence variants were found in the known EVA-related genes *SLC26A4*, *FOXI1*, *KCNJ10* and *GJB2/GJB6*.

Subcellular localization of wild type and mutant POU3F4

The two POU3F4 protein variants identified in the two index patients were reproduced in cell-based assays as fusion proteins with a N-terminal FLAG tag and their expression and subcellular localization was investigated (Supplementary Figure 1 and Figure 3). Imaging was performed in transiently transfected HeLa cells processed for immunocytochemistry with an anti-FLAG antibody. While wild type POU3F4 and POU3F4 variant p.C327* were found to be expressed in the cell nucleus, variant p.S74Afs*8 could not be detected (Supplementary Figure 1), most likely as a result of prompt degradation of this small protein fragment. Although variant p.C327* was exclusively localized in the nucleus, it accumulated in condensed bright spots. Accordingly, co-localization with DAPI gave a Pearson's correlation coefficient of 0.82 ± 0.02,

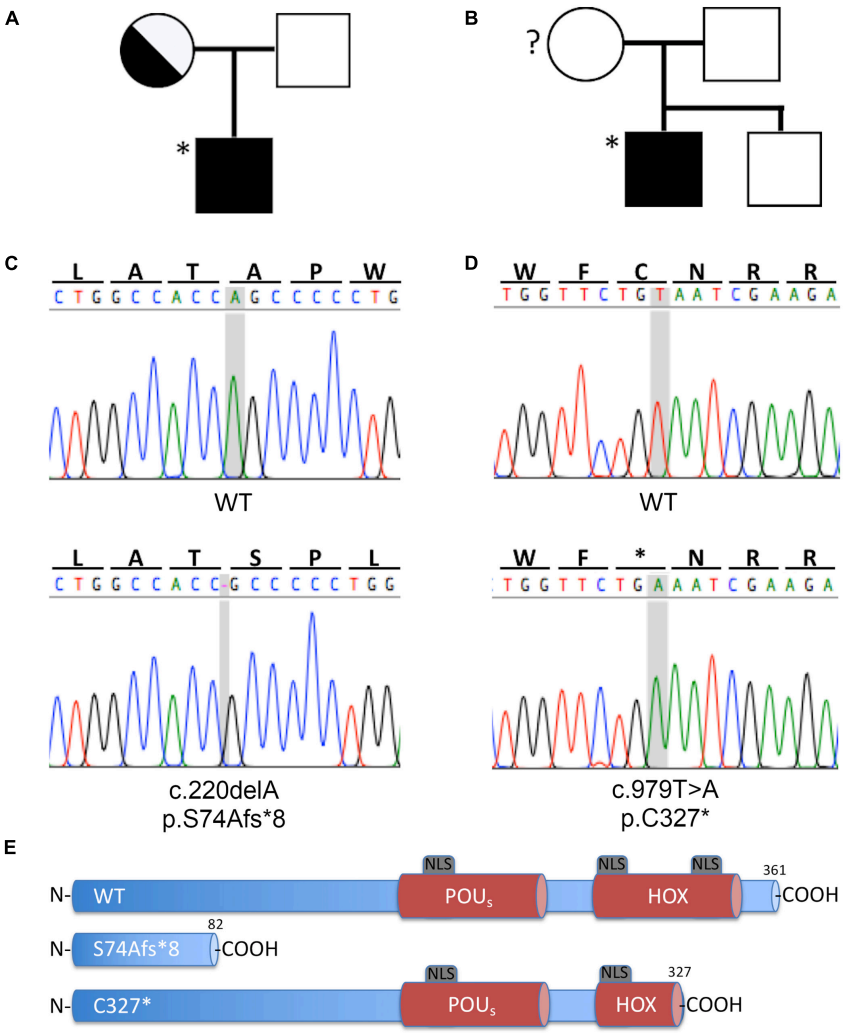

FIGURE 2
Novel *POU3F4* variants identified in two patients of the Austrian cohort with HL and EVA. **(A,B)** Family pedigree of patients #569 and #667, respectively. The index patients are indicated with an asterisk (*). The genotype of the mother of patient #667 is unknown. **(C,D)** Electropherograms from Sanger sequencing of the gDNA of patients #569 and #667, respectively; the position involved in the sequence variation is shaded in gray. **(E)** Graphic representation of the protein products, compared to the wild type protein; both nucleotide sequence alterations lead to a premature protein truncation. HOX, Homeobox DNA binding domain; NLS, nuclear localization sequence; POU_S, POU specific DNA binding domain. Protein structure based on information from Lee et al. (2009).

n = 3, for the wild type protein and 0.48 ± 0.02, n = 4, for p.C327*, thus denoting the dissimilar distribution pattern of the two proteins (Figure 3).

The exclusive nuclear localization of wild type POU3F4 was confirmed following expression of the fusion protein EYFP-POU3F4 in HeLa cells (Supplementary Figure 2). In contrast, protein variant p.S74Afs*8 showed a localization pattern distributed in the whole cell body, probably as a result of a stabilization of the protein fragment by fusion to EYFP. Concerning POU3F4 variant p.C327*, the localization in condensed bright nuclear spots was confirmed. As the protein truncation takes place within the DNA binding homeodomain near the C-terminus (Figure 2E), this variant retains two out of three predicted nuclear localization sequences (NLS) (Lee et al., 2009), which is probably sufficient to direct the protein to the nucleus. The altered expression pattern of the two variants is consistent with a possible pathogenic role.

Analysis of the transcriptional activity of wild type and mutant POU3F4 on a synthetic construct

HEK293Phoenix cells were co-transfected with a plasmid vector carrying the CDS of wild type or mutant *POU3F4*, a plasmid vector carrying the CDS of the firefly luciferase driven

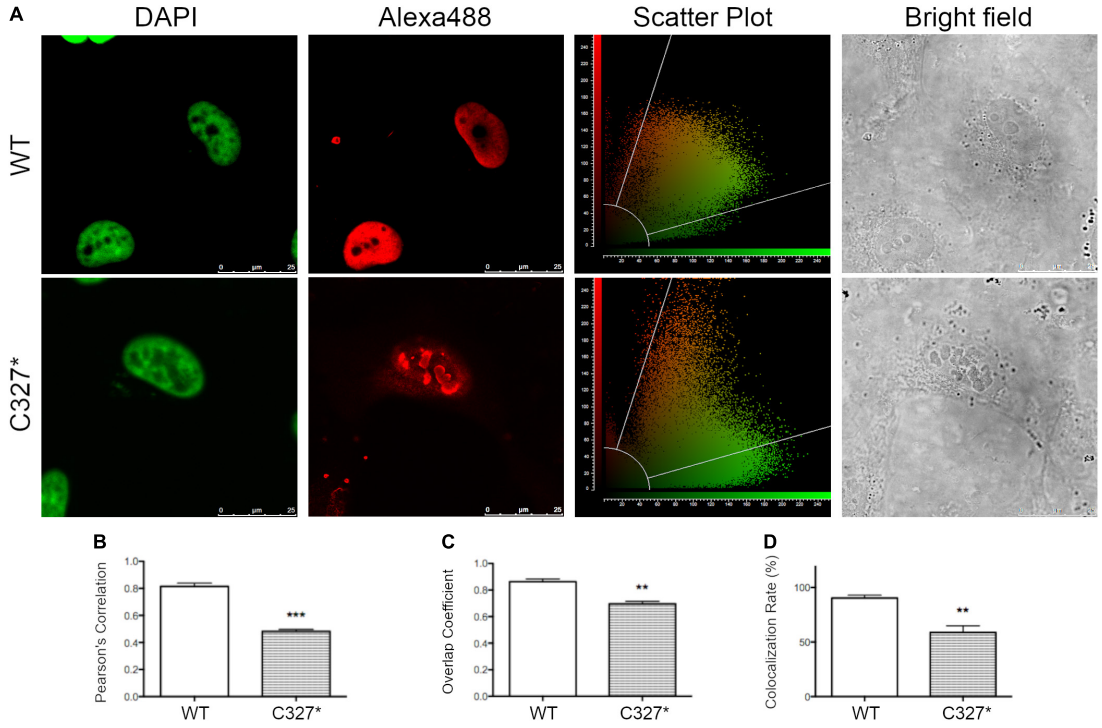

FIGURE 3
The novel POU3F4 p.C327* protein variant identified in the Austrian cohort shows an altered nuclear localization. **(A)** Confocal imaging of the subcellular localization of wild type POU3F4 and POU3F4 variant p.C327*. Co-localization of the nuclear marker DAPI and POU3F4 with a N-terminal FLAG tag imaged 42 h after transfection in HeLa cells is shown. The corresponding scatter plots graphically display the presence or absence of colocalization of the two signals. **(B–D)** Quantification of the co-localization by Pearson's correlation coefficient, overlap coefficient and colocalization rate, respectively. ***$p < 0.001$, **$p < 0.01$ compared to wild type, unpaired, two-tailed Student's *t*-test.

by a portion of *POU3F4* promoter (-472 bp to + 25 bp, where + 1 denotes the A of the starting codon ATG), and a vector carrying the CDS of the renilla luciferase driven by a CMV promoter, as a normalizer. The portion of *POU3F4* promoter employed here was shown to efficiently drive the transcription of reference genes by POU3F4 in Malik et al. (1996) and more recently confirmed in Lee et al. (2009).

Wild type POU3F4 could efficiently drive the transcription of the reporter gene, showing a 26-fold increase in the firefly luciferase signal in comparison to the control (**Figure 4**). POU3F4 p.C327* led to a slight increase in the transcription of the reporter gene over the basal level that was, however, not statistically significant (+7.5-fold, $p > 0.05$). POU3F4 p.S74fs*8 showed no significant increase in the transcription of the reporter gene and was indistinguishable from the control.

Transcriptome analysis in cells overexpressing wild type or mutant POU3F4

HEK293Phoenix cells were transiently transfected with plasmid vectors carrying the CDS of wild type POU3F4, POU3F4 variant p.C327*, or an empty vector (negative control). Total RNA extracted from the transfected cells was submitted to RNA sequencing (RNAseq). The expression profile of cells transfected with wild type POU3F4 was compared to the negative control (**Figures 5A,B**) and to cells transfected with POU3F4 p.C327* (**Figures 5C,D**). As expected, *POU3F4* transcript was found significantly upregulated in wild type and mutant POU3F4-transfected cells compared to control cells, as a result of a successful transfection with similar efficiency for both plasmid vectors (**Figures 5B,D**). Expression of wild type POU3F4 and POU3F4 p.C327* was also confirmed by Western blot (**Figure 5E**). Among the transcripts differentially expressed in wild type POU3F4-transfected cells compared to control, a highly significant upregulation (log2-fold change = 3.488, false discovery rate-adjusted *p*-value = 0.001281) was detected for the amino acid transporter solute carrier family 6 (proline imino transporter), member 20 (*SLC6A20*, SIT1, XTRP3). Further transcripts that were significantly upregulated also include those of the caspase recruitment domain-containing protein *CARD6* (log2-fold change = 2.31, adj. *p*-value = 0.002), the aminopeptidase *ANPEP* (log2-fold change = 3.07, adj. *p*-value = 0.0046), the transcription activator *ETV4* (log2-fold change = 3.37, adj. *p*-value = 0.0029), and the DNA binding

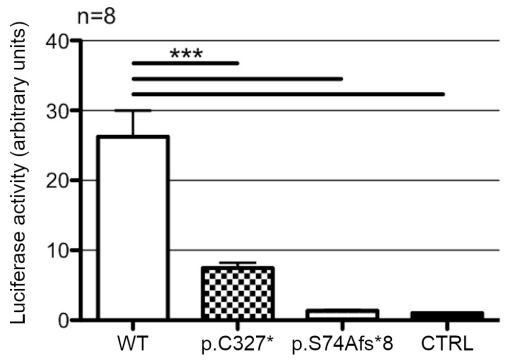

FIGURE 4
Transcriptional activity of wild type POU3F4 and its protein variants. Luciferase activities in HEK293Phoenix cells co-transfected with the reporter construct containing a section of *POU3F4* promoter region (from −472 to +25 bp) and constructs coding for POU3F4 in its wild type form or reproducing the variants identified in the patients. Wild type POU3F4 could efficiently drive the transcription of the reporter gene, while the mutant POU3F4 proteins could not. *n* represents the number of independent transfections. ***$p < 0.001$ compared to wild type, one-way ANOVA with Bonferroni's post-test.

protein *ETV5* (log2-fold change = 2.88, adj. *p*-value = 3.87*10-9), among others (**Figures 5A,B** and **Supplementary Table 4**). Importantly, these transcripts were not upregulated in cells overexpressing the truncated form of POU3F4 (**Figures 5C,D** and **Supplementary Table 4**). *SLC6A20* was chosen for further investigations because of the highest fold-change upregulation resulting from the RNAseq analysis.

The results of the RNAseq were validated by RT-qPCR in HEK293Phoenix cells transiently overexpressing the POU3F4 variants (wild type, pS74Afs*8, or p.C327*), compared to a negative control (cells transfected with an empty vector). The transcript of *SLC6A20* was upregulated in cells overexpressing wild type POU3F4 (log2-fold change = 6.43 ± 0.15, $p < 0.001$, **Figure 6A**). The upregulation of *SLC6A20* was not observed in cells overexpressing any of the two protein variants (no statistically significant differences compared to the negative control were observed, **Figure 6A**). In order to further confirm the functional interaction between Pou3f4 and the candidate target, the expression of *Slc6a20* has been evaluated in cells transfected with a combination of siRNAs designed to silence *Pou3f4* (**Supplementary Table 5**). MEFs have been chosen as they contain detectable basal levels of both transcripts and represent a cell type similar to the fibrocytes of the spiral ligament of the cochlea where POU3F4 is physiologically expressed. The transfection with the selected combination of siRNAs against *Pou3f4* led to a significant reduction in the expression of the target transcript, if compared to control cells transfected with a scrambled siRNA (**Figure 6B**, *Pou3f4* silencing: 69%, $p < 0.01$). In correspondence with the decreased expression of *Pou3f4*, a significant decrease in the expression of the transcript of the putative target gene *Slc6a20* was observed when compared to the negative control (**Figure 6C**, *Slc6a20* expression reduction: 70%, $p < 0.01$).

SLC6A20 is expressed in the mouse cochlea

So far, no evidence was available regarding the expression of SLC6A20 in the inner ear. We determined the expression of *Pou3f4* and *Slc6a20* in the whole cochlea of C57BL/6J mice by RT-qPCR. *Pou3f4* transcript was highly expressed in the cochlea, while it was detectable at very low levels in other mouse tissues such as the lung, liver and small intestine (**Figure 7A**), in agreement with previous findings (Minowa et al., 1999; Uetsuka et al., 2015). *Slc6a20* transcript was highly expressed in the kidney and small intestine as already reported (Takanaga et al., 2005), almost undetectable in lung but, most importantly, clearly detectable in mouse cochlea (**Figure 7B**). These results show that both *Pou3f4* and *Slc6a20* transcripts are expressed in the mouse cochlea.

To confirm the co-expression of POU3F4 and SLC6A20 proteins in the cochlea, immunostaining on slices from the cochlea of wild type mice was performed. Immunohistochemistry with an anti-SLC6A20 antibody showed a protein expression that appeared to be specific when compared to sections stained with the secondary antibody only. SLC6A20 was found in distinct cochlear structures, with prominent expression in the spiral ligament (**Figures 7C–E**). A staining with anti-POU3F4 antibodies confirmed the expression of this transcription factor in the same area of the spiral ligament, as well as in other structures of the cochlea including the *stria vascularis*, as reported in the literature (Minowa et al., 1999; Uetsuka et al., 2015; **Figures 7F–H**). As mentioned above, a negative control staining with the secondary antibody only was performed (**Figures 7I–K**), and gave no signal. These data strongly suggest that POU3F4 and SLC6A20 are co-expressed in the spiral ligament.

Discussion

Typical hallmark of POU3F4-related HL is the presence of an incomplete partition of the cochlea, defined as IP3, which is observed in combination with an EVA in about 50% of cases (Roesch et al., 2021). Two patients from our EVA cohort displayed these typical features and were submitted to DNA analysis for the determination of the genetic defect responsible for the observed phenotype. A defect in the coding sequence of *POU3F4* was identified by Sanger sequencing in both patients, confirming the correlation between IP3 and EVA with *POU3F4* pathogenic sequence alterations.

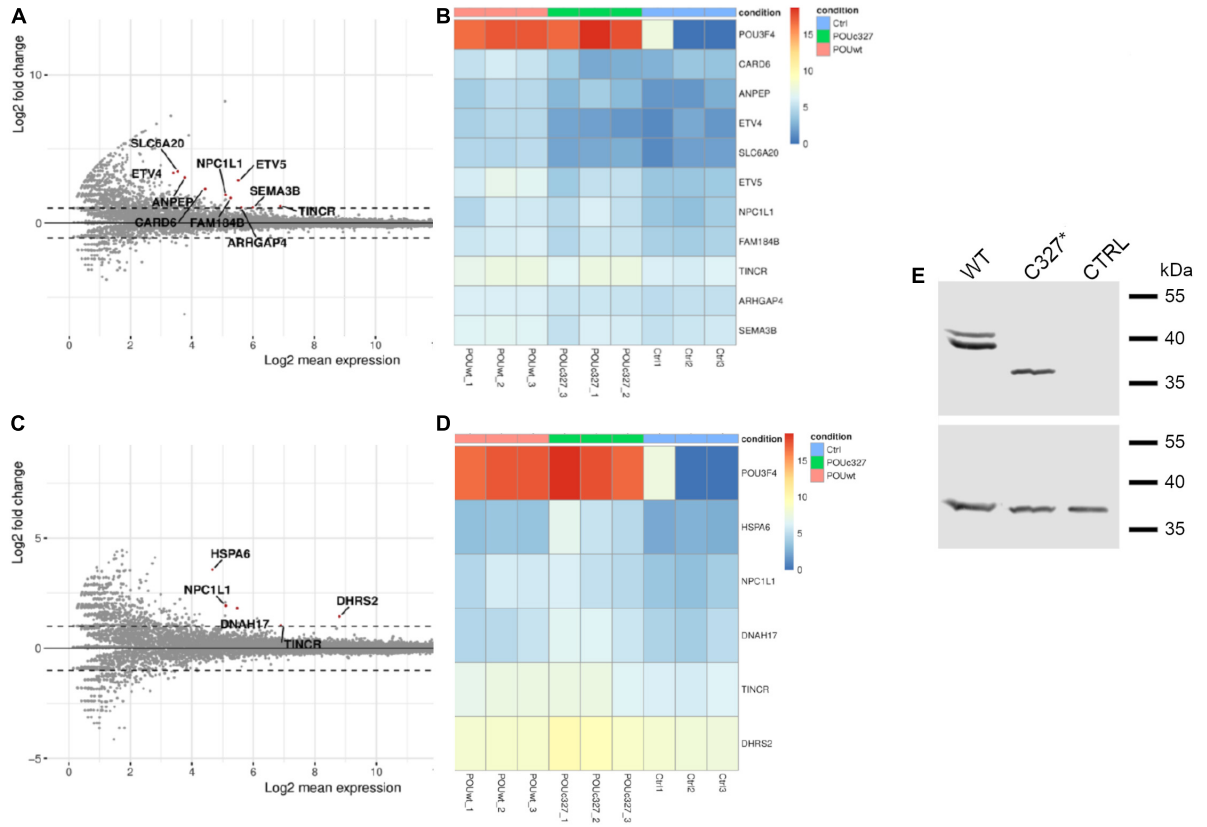

FIGURE 5

Transcriptome analysis (RNAseq) of total RNA extracted from POU3F4-overexpressing HEK293Phoenix cells. The RNAseq analysis was performed on RNA extracted from three independent subcultures of HEK293Phoenix cells transiently transfected with wild type POU3F4, POU3F4 p.C327*, or a control vector encoding solely for the transfection marker EGFP. Volcano plots showing differentially regulated transcripts in wild type POU3F4-transfected cells **(A)** and POU3F4 p.C327*-transfected cells **(C)** compared to control cells are shown. Each dot in the plot represents a transcript identified in the analysis. Above the line indicated with a "0" are the transcripts that were upregulated in transfected cells versus the control cells, below the 0 are the downregulated transcripts. Red dots represent transcripts showing a statistically significant upregulation. Heatmap of the top differentially expressed transcripts (DESeq2 results with independent filtering, adj. p-value <0.05, logFC $\geq \pm 1$) in wild type POU3F4-transfected cells **(B)** and POU3F4 p.C327*-transfected cells **(D)** compared to control. **(E)** Top panel: western blot on total protein extracts from cells overexpressing wild type POU3F4 or POU3F4 p.C327*; control cells were transfected with an empty vector. Bottom panel, the signal of the housekeeping protein GAPDH served as the loading control.

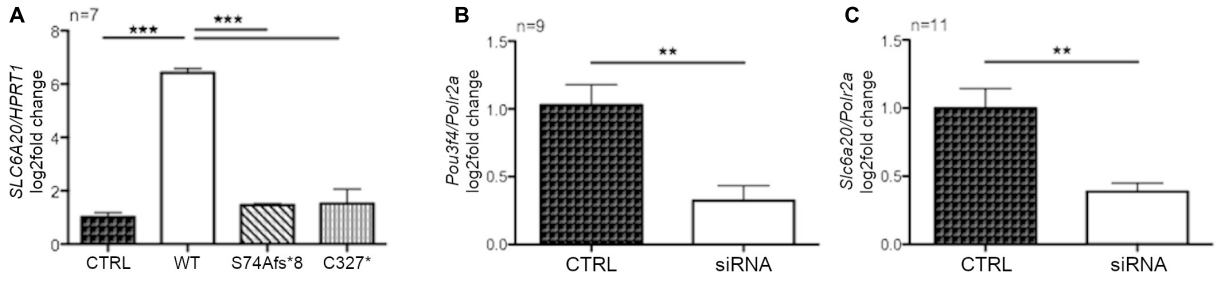

FIGURE 6

POU3F4 regulates the transcription of *SLC6A20*. **(A)** HEK293Phoenix cells were transiently transfected with plasmid vectors coding for wild type POU3F4 or the indicated POU3F4 variants. Cells transfected with an empty vector served as negative control. Total RNA was reverse-transcribed and subjected to RT-qPCR. The levels of the *SLC6A20* transcript were normalized to those of the housekeeping transcript *HPRT1*. The *SLC6A20* transcript was upregulated in HEK293Phoenix cells overexpressing wild type POU3F4, but not in cells overexpressing the POU3F4 variants. ***$p < 0.001$, one-way ANOVA with Bonferroni's post-test. **(B,C)** RT-qPCR on mRNA extracted from MEFs transfected with a combination of siRNAs designed to silence *Pou3f4* or with a scrambled control siRNA (control, CTRL). Expression levels of *Pou3f4* and *Slc6a20* were normalized to those of the housekeeping transcript *Polr2a*. Silencing of *Pou3f4* led to reduced *Slc6a20* expression. n represents the number of biological replicates. **$p < 0.01$, two-tailed, unpaired Student's t-test.

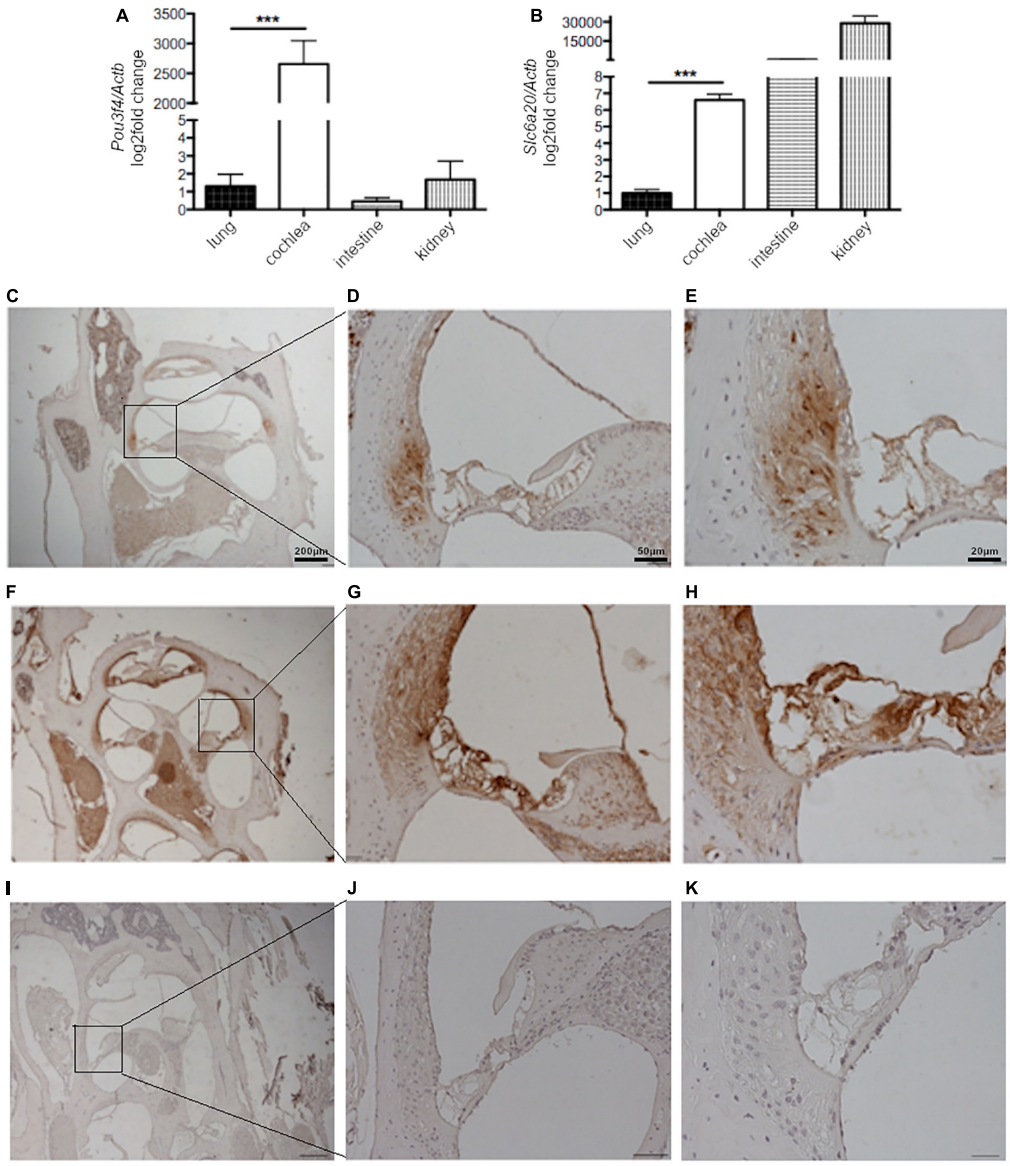

FIGURE 7
Slc6a20 and *Pou3f4* transcripts and proteins are co-expressed in the mouse cochlea. RT-qPCR on mRNA extracted from whole mouse cochlea, lung, intestine, and kidney and expression of **(A)** *Pou3f4* and **(B)** *Slc6a20* transcripts relative to the housekeeping transcript *Actb*. $n = 5$ represents the number of biological replicates. ***$p < 0.001$, two-tailed, unpaired Student's *t*-test. Immunostaining of tissue slices from mouse cochlea with **(C–E)** an anti-SLC6A20 primary antibody, **(F–H)** an anti-POU3F4 primary antibody, and **(I–K)** only the secondary antibody as the negative control. SLC6A20 was clearly localized in the spiral ligament. POU3F4 was more widely distributed in different structures of the cochlea, including the spiral ligament.

When present, EVA in *POU3F4* patients often differs from that classically described in DFNB4/Pendred syndrome. Rather than conical, vestibular aqueducts in *POU3F4* patients are large and symmetrical and become cystic or enlarged from the middle parts to the ends near the vestibule but not at the operculum (Roesch et al., 2021). We observed this EVA variant in index patient #667 (Figure 1C), while EVA in patient #569 appeared rather similar to that described in the context of DFNB4/Pendred syndrome (Figure 1A).

Both gene variants identified in this study (c.220delA and c.979T > A, Figure 2) were novel, and therefore no related functional information was available. In order to determine or exclude the pathogenicity of these gene variants, analysis of the subcellular localization and transcriptional activity of the corresponding protein products was performed.

Both gene variants are predicted to result in a premature stop codon and a truncation of the protein product. The short variant (p.S74Afs*8) lacks both DNA binding domains and

the three predicted NLSs; the longer variant (p.C327*) results from the generation of a stop codon in the middle portion of the second DNA binding domain and therefore the resulting protein product still includes the first DNA binding domain and two of the three predicted NLSs (**Figure 2E**). We observed a defective expression and subcellular localization of both variants when compared to the wild type protein. As expected for a transcription factor, the wild type POU3F4 protein localized exclusively in the nuclear compartment. In contrast, the two variants showed a disturbed subcellular localization, with the longer variant (p.C327*) localizing in the nucleus but, other than the wild type protein, accumulating in bright spots possibly corresponding to the nucleoli (**Figure 3**). The two NLSs that are still present in this protein variant were obviously sufficient for the nuclear targeting. However, the premature truncation of the polypeptide could have unmasked hydrophobic regions, thus causing incorrect folding of the aberrant protein product and leading to its aggregation and condensation in the nucleus. As expected, the shorter variant (p.S74Afs*8), missing a large portion of the polypeptide, could not be detected, probably as a result of prompt degradation (**Supplementary Figure 1**).

An aberrant cellular distribution of two POU3F4 variants similarly leading to truncated protein products was formerly described. These variants were identified in a Jewish family originating from Bulgaria (p.Ile285Argfs*43) and in a N-ethyl-N-nitrosourea (ENU)-induced mutant mouse (p.Cys300*). Both protein variants were largely mislocalized to the cytoplasm in cell-based assays, with a smaller portion remaining in the nucleus and an overall substantial reduction of protein abundance (Parzefall et al., 2013). As protein variant p.C327* was expressed exclusively in the nucleus in our assays (**Figure 3**), it is likely that amino acids 300-327 are essential for nuclear targeting, while downstream C-terminal regions might be important for proper protein folding.

The defective expression and subcellular localization of the protein variants identified in our patients was reflected in their altered transcriptional activity. Both protein variants showed a severe impairment in the transcription efficiency when compared to the wild type, with the longer variant displaying a slightly higher activity than the short variant, though not statistically significant (**Figure 4**). The longer variant, although localized within the nucleus, failed to efficiently drive the transcription of the reporter gene. These results indicate that the C-terminal portion of the HOX domain is essential for the transcriptional activity of POU3F4. These functional and molecular aspects, together with the typical inner ear malformations and the absence of pathogenic sequence alterations in other known EVA-related genes (**Supplementary Table 3**) strongly support the pathogenicity of protein variants p.S74Afs*8 and p.C327*, unequivocally identifying *POU3F4* defects as the genetic determinant for the hearing deficit observed in the two index patients.

Genotype-phenotype correlation in these two patients based on our functional data is not straightforward. Even assuming that variant p.C327* might retain some residual activity compared to p.S74Afs*8, it has to be noted that this variant was identified in the patient with the more severe clinical phenotype in terms of severe to profound hearing loss, which was associated with vestibular dysfunction and cognitive impairment. However, it also has to be noted that this patient presented with unilateral EVA, while the patient harboring the p.S74Afs*8 variant had bilateral EVA. Whether residual or loss of transcriptional activity of POU3F4 variants can be linked to unilateral or bilateral EVA, respectively, requires further investigation.

The molecular mechanism of POU3F4-related HL is largely unknown and its transcriptional targets are only partially characterized. Only few studies could reveal functional targets of POU3F4 in the hearing organ. Coate and colleagues showed that the expression of the receptor tyrosine kinase EphA4 is decreased in *Pou3f4* knockout mice and that POU3F4 binds *EphA4* regulatory elements (Coate et al., 2012), which is important for spiral ganglion axon fasciculation. The same group showed that POU3F4 and the Eph receptor transmembrane ligand Ephrin-B2 exhibit a common spatio-temporal expression pattern during organogenesis (Raft et al., 2014). Although these studies provided evidence for a role of POU3F4 in the development of the spiral ganglion and bony structures of the middle ear, the link with the cochlear malformations typical of POU3F4-related deafness remained unexplained, pointing to the possible existence of additional cochlear targets. Our RNAseq analysis delivered several additional novel putative transcriptional targets of POU3F4 (**Figure 5** and **Supplementary Table 4**) as well as targets that are differentially upregulated by wild type and p.C327* POU3F4 (**Supplementary Table 4**). *CARD6*, *ANPEP*, *ETV4*, *SLC6A20*, *ETV5*, F*AM184B*, *ARHGAP4*, and *SEMA3B* are found significantly upregulated by wild type POU3F4 compared to control (**Figures 5A,B**) and not by POU3F4 p.C327* compared to control (**Figures 5C,D**), leading to speculate that loss or reduction of expression of one or more of these targets might be pathogenic. Of these, *CARD6*, *ETV4*, *SLC6A20*, and *ETV5* are found differentially expressed when comparing POU3F4 p.C327* to the wild type (**Supplementary Table 4**), and might represent the strongest candidates to be linked to the disease phenotype.

Analysis of the targets upregulated by POU3F4 p.C327* compared to control cells (**Figures 5C,D** and **Supplementary Table 4**) revealed an overall loss of function of POU3F4 p.C327* compared to the wild type, including loss of transcriptional activity on all above mentioned targets. However, a limited number of targets still resulted upregulated by POU3F4 p.C327*. Of these targets, some (*NPC1L1* and *TINCR*) were also upregulated by the wild type to a similar, limited extent - the log2 fold change is <2 in both cases. Therefore, the

significance of these findings is currently unclear. Genes that were found significantly upregulated by POU3F4 p.C327* and not by the wild type are *HSPA6*, *DNAH17*, and *DHRS2*. Heat Shock Protein Family A Member 6 (*HSPA6*; OMIM *140555) is a stress-induced heat-shock gene encoding a basic 70-kD protein. Dynein, Axonemal, Heavy Chain 17 (*DNAH17*; OMIM *610063) is a microtubule-associated motor protein expressed in adult testis of which mutations cause spermatogenic failure. *DHRS2* (OMIM *615194) encodes a member of the short-chain dehydrogenases/reductases that reduces proliferation, migration and invasion of cancer cells and well as the production of reactive oxygen species in cancer. With the exception of *DNAH17*, of which the significance is currently unclear in this context, the other two genes might have been upregulated following cellular stress and increased oxidative stress as a consequence of the overexpression of a misfolded protein.

Among the targets significantly upregulated following wild type POU3F4 overexpression, the amino acid transporter SLC6A20 was selected for further investigations. The upregulation of this specific target could be confirmed by RT-qPCR (**Figure 6A**). Interestingly, neither of the two POU3F4 variants identified resulted in upregulation of the *SLC6A20* transcript, further supporting their pathogenicity. Accordingly, silencing of the endogenous *Pou3f4* transcript in a cell model reminiscent of the native cells expressing POU3F4 within the inner ear led to reduced expression of *Slc6a20* (**Figures 6B,C**).

Function and expression of SLC6A20 (OMIM *605616), formerly called Sodium/Imino-acid Transporter 1 (SIT1), have been first characterized by Takanaga et al., who found that this transporter leads to proline uptake in a Na^+– and voltage-dependent, Cl^--stimulated, pH-independent manner and is expressed on the apical membrane of epithelial cells in various portions of the intestine as well as the kidney proximal tubule (Takanaga et al., 2005). According to this seminal study, *SLC6A20* gene variants have been later found to contribute to forms of autosomal dominant hyperglycinuria (phenotype MIM number 138500) as well as digenic iminoglycinuria (phenotype MIM number 242600) (Broer et al., 2008). Iminoglycinuria is a rare autosomal recessive disorder characterized by increased urinary excretion of proline, hydroxyproline, and glycine that has been described in association with mental retardation and sensorineural hearing loss in some cases (Goyer et al., 1968; Swarna et al., 2004). Furthermore, SLC6A20 has been shown to be involved in the transport of other amino acids beside proline, namely hydroxyproline, N-methylaminoisobutyric acid, and betaine (Kowalczuk et al., 2005; Takanaga et al., 2005). It is therefore conceivable that a defective imino acid transport resulting from reduction of expression SLC6A20 in the inner ear as a consequence of POU3F4 loss of function might lead to sensorineural hearing loss, similarly to what was observed in the context of *SLC6A20* pathogenic gene variations.

In addition to pathogenic gene variations, also a reduction of expression of *SLC6A20* in the kidney might in principle lead to iminoglycinuria. However, this defect might be compensated by redundancy of imino acid transporters in the kidney (Verrey et al., 2009).

No evidence of SLC6A20 expression in the inner ear was available so far. In the present study we could show the presence of *Slc6a20* transcript in the mouse cochlea and confirm the expression of *Pou3f4* (**Figures 7A,B**), as already reported in the literature (Minowa et al., 1999). Moreover, we showed here for the first time a spatial co-expression of SLC6A20 and POU3F4 proteins in the same regions of the mouse cochlea and specifically in the area of the spiral ligament (**Figures 7C–H**). Spatial co-expression is a necessary prerequisite for any functional interaction between the two genes/gene products and therefore represents a crucial finding guiding further investigations in the pathophysiological role of POU3F4 and SLC6A20 in the inner ear.

The role of solute transporters and channels is crucial for the function of the auditory system. Ion channels and transporters ensure the maintenance of the endolymph ion composition and pH, which are essential for the transmission of the auditory signal and preservation of the inner ear structures (Lang et al., 2007). Potassium channels permit the recycling of potassium ions from the endolymph and through the organ of Corti, transducing the mechanical sound signal into an electric signal and leading to the release of neurotransmitter and action potentials generation in the efferent auditory nerve terminations (Mittal et al., 2017). Pendrin-mediated Cl^-/HCO_3^- exchange contributes to the osmotic balance and pH regulation of the endolymphatic fluid (Choi et al., 2011). Transporters for organic solutes are also active in the cochlea, contribute to the homeostasis of this organ and allows for the exchange of compounds between the cochlea and the vasculature (Uetsuka et al., 2015). Here we show that the proline imino transporter SLC6A20 seems to be exclusively expressed in a discrete region of the mouse cochlea within the spiral ligament, corresponding to the type II fibrocytes (**Figures 7D,E**). Cochlear fibrocytes form a connective tissue syncytium within the spiral ligament that, together with the *stria vascularis*, plays a fundamental role in the cochlear potassium recycling and maintenance of the endocochlear potential. Five distinct types of fibrocytes can be identified based on their anatomical position within the spiral ligament and their structural characteristics, including the density of cytoplasm, content of organelles, and the extension of the plasma membrane folding. Type II fibrocytes are connected to type I fibrocytes via the connexin network and express a battery of ion channels and transporters, including particularly elevated levels of the Na^+/K^+ ATPase, the inwardly rectifying K^+ channel Kir5.1, the Na^+-K^+-$2Cl^-$ cotransporter-1 (NKCC1) and the glutamate-aspartate transporter SLC1A3/GLAST (Furness et al., 2009; Furness, 2019). These and our findings identify fibrocytes,

and specifically type II fibrocytes, as fundamental players of the amino acids homeostasis within the cochlea, beside K^+ recycling.

Another amino acid transporter, SLC7A8, was previously detected in key structures of the inner ear including the spiral ligament, mostly in type I fibrocytes (Espino Guarch et al., 2018). Espino Guarch and colleagues have shown a correlation between hypofunctional variants of SLC7A8 and age-related HL associated to morphological defects in the spiral ligament and *stria vascularis* in a mouse model (Espino Guarch et al., 2018). The defects observed included a reduction in the number of fibrocytes in the spiral ligament and loss of gap junction expression. Interestingly, these alterations are reminiscent of those observed in *Pou3f4* knockout mice (Kidokoro et al., 2014). These findings and the findings presented here point to the relevance of amino acid homeostasis for the auditory function. Further investigations are necessary in order to define how a possible lack or reduction of SLC6A20 expression could lead to inner ear malformations and HL in POU3F4-related deafness.

Data availability statement

The datasets presented in this study can be found in online repositories. The names of the repository/repositories and accession number(s) can be found below: www.ncbi.nlm.nih.gov, GSE211647.

Ethics statement

The studies involving human participants were reviewed and approved by the Ethics Committee of the County of Salzburg, Austria. The patients/participants provided their written informed consent to participate in this study. Ethical review and approval was not required for the animal study because no animal treatment was performed. Animal sacrifice for tissue harvesting with no animal treatment does not require approval of an animal protocol according to local regulations.

Author contributions

EB, AS, and SD conceived the study. EB, SR, LA, and SD designed the experiments. SR and GR contributed the clinical images and data. EB and ES performed the experiments and analyzed the data. EB wrote the original draft. SD edited the manuscript. AS and SD contributed equally to this work and share senior authorship. All authors participated in the interpretation of results, reviewed and approved the final version of the manuscript.

Funding

EB was supported in part by the Paracelsus Medical University Research Fund, grant number PMU-FFF E-17/25/128-BER.

Acknowledgments

The authors would sincerely like to thank Selma Soyal-Patsch for her advice on the promoter assays and acknowledge the expert secretarial assistance of Elisabeth Mooslechner.

Conflict of interest

The authors declare that the research was conducted in the absence of any commercial or financial relationships that could be construed as a potential conflict of interest.

Publisher's note

Supplementary material

The Supplementary Material for this article can be found online at: https://www.frontiersin.org/articles/10.3389/fnmol.2022.999833/full#supplementary-material

References

Adler, J., and Parmryd, I. (2010). Quantifying colocalization by correlation: The pearson correlation coefficient is superior to the mander's overlap coefficient. *Cytometry A* 77, 733–742. doi: 10.1002/cyto.a.20896

Broer, S., Bailey, C. G., Kowalczuk, S., Ng, C., Vanslambrouck, J. M., Rodgers, H., et al. (2008). Iminoglycinuria and hyperglycinuria are discrete human phenotypes resulting from complex mutations in proline and glycine transporters. *J. Clin. Invest.* 118, 3881–3892. doi: 10.1172/JCI36625

Choi, B. Y., Kim, H.-M., Ito, T., Lee, K.-Y., Li, X., Monahan, K., et al. (2011). Mouse model of enlarged vestibular aqueducts defines temporal requirement of Slc26a4 expression for hearing acquisition. *J. Clin. Invest.* 121, 4516–4525.

Coate, T. M., Raft, S., Zhao, X., Ryan, A. K., Crenshaw, E. B. III, and Kelley, M. W. (2012). Otic mesenchyme cells regulate spiral ganglion axon fasciculation through a Pou3f4/EphA4 signaling pathway. *Neuron* 73, 49–63. doi: 10.1016/j.neuron.2011.10.029

de Kok, Y. J., van der Maarel, S. M., Bitner-Glindzicz, M., Huber, I., Monaco, A. P., Malcolm, S., et al. (1995). Association between X-linked mixed deafness and mutations in the POU domain gene POU3F4. *Science* 267, 685–688. doi: 10.1126/science.7839145

De Moraes, V. C., Bernardinelli, E., Zocal, N., Fernandez, J. A., Nofziger, C., Castilho, A. M., et al. (2016). Reduction of cellular expression levels is a common feature of functionally affected pendrin (SLC26A4) protein variants. *Mol. Med.* 22, 41–53. doi: 10.2119/molmed.2015.00226

del Castillo, F. J., Rodriguez-Ballesteros, M., Alvarez, A., Hutchin, T., Leonardi, E., de Oliveira, C. A., et al. (2005). A novel deletion involving the connexin-30 gene, del(GJB6-d13s1854), found in trans with mutations in the GJB2 gene (connexin-26) in subjects with DFNB1 non-syndromic hearing impairment. *J. Med. Genet.* 42, 588–594. doi: 10.1136/jmg.2004.028324

Del Castillo, I., Morin, M., Dominguez-Ruiz, M., and Moreno-Pelayo, M. A. (2022). Genetic etiology of non-syndromic hearing loss in Europe. *Hum. Genet.* 141, 683–696. doi: 10.1007/s00439-021-02425-6

DiCiommo, D. P., Duckett, A., Burcescu, I., Bremner, R., and Gallie, B. L. (2004). Retinoblastoma protein purification and transduction of retina and retinoblastoma cells using improved alphavirus vectors. *Invest. Ophthalmol. Vis. Sci.* 45, 3320–3329. doi: 10.1167/iovs.04-0140

Dossena, S., Vezzoli, V., Cerutti, N., Bazzini, C., Tosco, M., Sironi, C., et al. (2006). Functional characterization of wild-type and a mutated form of SLC26A4 identified in a patient with pendred syndrome. *Cell. Physiol. Biochem.* 17, 245–256. doi: 10.1159/000094137

Espino Guarch, M., Font-Llitjos, M., Murillo-Cuesta, S., Errasti-Murugarren, E., Celaya, A. M., Girotto, G., et al. (2018). Mutations in L-type amino acid transporter-2 support SLC7A8 as a novel gene involved in age-related hearing loss. *eLife* 7:e31511. doi: 10.7554/eLife.31511

Furness, D. N. (2019). Forgotten fibrocytes: A neglected, supporting cell type of the cochlea with the potential to be an alternative therapeutic target in hearing loss. *Front. Cell. Neurosci.* 13:532. doi: 10.3389/fncel.2019.00532

Furness, D. N., Lawton, D. M., Mahendrasingam, S., Hodierne, L., and Jagger, D. J. (2009). Quantitative analysis of the expression of the glutamate-aspartate transporter and identification of functional glutamate uptake reveal a role for cochlear fibrocytes in glutamate homeostasis. *Neuroscience* 162, 1307–1321. doi: 10.1016/j.neuroscience.2009.05.036

Goyer, R. A., Reynolds, J. Jr., Burke, J., and Burkholder, P. (1968). Hereditary renal disease with neurosensory hearing loss, prolinuria and ichthyosis. *Am. J. Med. Sci.* 256, 166–179. doi: 10.1097/00000441-196809000-00005

Kidokoro, Y., Karasawa, K., Minowa, O., Sugitani, Y., Noda, T., Ikeda, K., et al. (2014). Deficiency of transcription factor Brn4 disrupts cochlear gap junction plaques in a model of DFN3 non-syndromic deafness. *PLoS One* 9:e108216. doi: 10.1371/journal.pone.0108216

Kowalczuk, S., Broer, A., Munzinger, M., Tietze, N., Klingel, K., and Broer, S. (2005). Molecular cloning of the mouse IMINO system: An Na+- and Cl–dependent proline transporter. *Biochem. J.* 386, 417–422. doi: 10.1042/BJ20050100

Lang, F., Vallon, V., Knipper, M., and Wangemann, P. (2007). Functional significance of channels and transporters expressed in the inner ear and kidney. *Am. J. Physiol. Cell Physiol.* 293, C1187–C1208. doi: 10.1152/ajpcell.00024.2007

Lee, H. K., Song, M. H., Kang, M., Lee, J. T., Kong, K. A., Choi, S. J., et al. (2009). Clinical and molecular characterizations of novel POU3F4 mutations reveal that DFN3 is due to null function of POU3F4 protein. *Physiol. Genomics* 39, 195–201. doi: 10.1152/physiolgenomics.00100.2009

Malik, K. F., Kim, J., Hartman, A. L., Kim, P., and Young, W. S. III (1996). Binding preferences of the POU domain protein brain-4: Implications for autoregulation. *Brain Res. Mol. Brain Res.* 38, 209–221. doi: 10.1016/0169-328x(95)00308-f

Malik, V., Zimmer, D., and Jauch, R. (2018). Diversity among POU transcription factors in chromatin recognition and cell fate reprogramming. *Cell. Mol. Life Sci.* 75, 1587–1612. doi: 10.1007/s00018-018-2748-5

Meyer, G., Rodighiero, S., Guizzardi, F., Bazzini, C., Botta, G., Bertocchi, C., et al. (2004). Volume-regulated Cl- channels in human pleural mesothelioma cells. *FEBS Lett.* 559, 45–50. doi: 10.1016/S0014-5793(04)00020-1

Minowa, O., Ikeda, K., Sugitani, Y., Oshima, T., Nakai, S., Katori, Y., et al. (1999). Altered cochlear fibrocytes in a mouse model of DFN3 nonsyndromic deafness. *Science* 285, 1408–1411. doi: 10.1126/science.285.5432.1408

Mittal, R., Aranke, M., Debs, L. H., Nguyen, D., Patel, A. P., Grati, M., et al. (2017). Indispensable role of ion channels and transporters in the auditory system. *J. Cell. Physiol.* 232, 743–758. doi: 10.1002/jcp.25631

Naranjo, S., Voesenek, K., de la Calle-Mustienes, E., Robert-Moreno, A., Kokotas, H., Grigoriadou, M., et al. (2010). Multiple enhancers located in a 1-Mb region upstream of POU3F4 promote expression during inner ear development and may be required for hearing. *Hum. Genet.* 128, 411–419. doi: 10.1007/s00439-010-0864-x

Parzefall, T., Shivatzki, S., Lenz, D. R., Rathkolb, B., Ushakov, K., Karfunkel, D., et al. (2013). Cytoplasmic mislocalization of POU3F4 due to novel mutations leads to deafness in humans and mice. *Hum. Mutat.* 34, 1102–1110. doi: 10.1002/humu.22339

Phippard, D., Lu, L., Lee, D., Saunders, J. C., and Crenshaw, E. B. III (1999). Targeted mutagenesis of the POU-domain gene Brn4/Pou3f4 causes developmental defects in the inner ear. *J. Neurosci.* 19, 5980–5989. doi: 10.1523/JNEUROSCI.19-14-05980.1999

Raft, S., Coate, T. M., Kelley, M. W., Crenshaw, E. B. III, and Wu, D. K. (2014). Pou3f4-mediated regulation of ephrin-b2 controls temporal bone development in the mouse. *PLoS One* 9:e109043. doi: 10.1371/journal.pone.0109043

Roesch, S., Bernardinelli, E., Nofziger, C., Toth, M., Patsch, W., Rasp, G., et al. (2018). Functional testing of SLC26A4 variants-clinical and molecular analysis of a cohort with enlarged vestibular aqueduct from Austria. *Int. J. Mol. Sci.* 19:209. doi: 10.3390/ijms19010209

Roesch, S., Rasp, G., Sarikas, A., and Dossena, S. (2021). Genetic determinants of non-syndromic enlarged vestibular aqueduct: A review. *Audiol. Res.* 11, 423–442. doi: 10.3390/audiolres11030040

Sennaroglu, L., and Bajin, M. D. (2017). Classification and current management of inner ear malformations. *Balkan Med. J.* 34, 397–411. doi: 10.4274/balkanmedj.2017.0367

Sennaroglu, L., and Bajin, M. D. (2018). Incomplete partition type III: A rare and difficult cochlear implant surgical indication. *Auris Nasus Larynx* 45, 26–32. doi: 10.1016/j.anl.2017.02.006

Shearer, A. E., Hildebrand, M. S., and Smith, R. J. H. (2017). "Hereditary hearing loss and deafness overview," in *GeneReviews((R))*, eds M. P. Adam, H. H. Ardinger, R. A. Pagon, S. E. Wallace, L. J. H. Bean, K. Stephens, et al. (Seattle, WA: University of Washington).

Sheffield, A. M., and Smith, R. J. H. (2019). The epidemiology of deafness. *Cold Spring Harb. Perspect. Med.* 9:a033258. doi: 10.1101/cshperspect.a033258

Swarna, M., Jyothy, A., Usha Rani, P., and Reddy, P. P. (2004). Amino acid disorders in mental retardation: A two-decade study from Andhra Pradesh. *Biochem. Genet.* 42, 85–98. doi: 10.1023/b:bigi.0000020464.05335.79

Takanaga, H., Mackenzie, B., Suzuki, Y., and Hediger, M. A. (2005). Identification of mammalian proline transporter SIT1 (SLC6A20) with characteristics of classical system imino. *J. Biol. Chem.* 280, 8974–8984. doi: 10.1074/jbc.M413027200

Tantin, D. (2013). Oct transcription factors in development and stem cells: Insights and mechanisms. *Development* 140, 2857–2866. doi: 10.1242/dev.095927

Uetsuka, S., Ogata, G., Nagamori, S., Isozumi, N., Nin, F., Yoshida, T., et al. (2015). Molecular architecture of the stria vascularis membrane transport system, which is essential for physiological functions of the mammalian cochlea. *Eur. J. Neurosci.* 42, 1984–2002. doi: 10.1111/ejn.12973

Valvassori, G. E., and Clemis, J. D. (1978). The large vestibular aqueduct syndrome. *Laryngoscope* 88, 723–728. doi: 10.1002/lary.1978.88.5.723

Verrey, F., Singer, D., Ramadan, T., Vuille-dit-Bille, R. N., Mariotta, L., and Camargo, S. M. (2009). Kidney amino acid transport. *Pflugers Arch.* 458, 53–60. doi: 10.1007/s00424-009-0638-2

Vijayasekaran, S., Halsted, M. J., Boston, M., Meinzen-Derr, J., Bardo, D. M., Greinwald, J., et al. (2007). When is the vestibular aqueduct enlarged? A statistical analysis of the normative distribution of vestibular aqueduct size. *AJNR Am. J. Neuroradiol.* 28, 1133–1138. doi: 10.3174/ajnr.A0495

Wang, A., Shearer, A. E., Zhou, G. W., Kenna, M., Poe, D., Licameli, G. R., et al. (2021). Peripheral vestibular dysfunction is a common occurrence in children with non-syndromic and syndromic genetic hearing loss. *Front. Neurol.* 12:714543. doi: 10.3389/fneur.2021.714543

Wu, Y., Zhang, X., Wang, J., Jin, G., and Zhang, X. (2021). Research progress of the transcription factor Brn4 (Review). *Mol. Med. Rep.* 23:179. doi: 10.3892/mmr.2020.11818

frontiers | Frontiers in Molecular Neuroscience

TYPE Original Research
PUBLISHED 24 October 2022
DOI 10.3389/fnmol.2022.988993

OPEN ACCESS

EDITED BY
Yuchio Yanagawa,
Gunma University, Japan

REVIEWED BY
Cláudio Gouveia Roque,
Columbia University, United States
Laurence Goutebroze,
Institut National de la Santé et de la Recherche Médicale (INSERM), France

*CORRESPONDENCE
Jens Schuster
jens.schuster@igp.uu.se
Niklas Dahl
niklas.dahl@igp.uu.se

†PRESENT ADDRESS
Jan Hoeber,
Hoffmann-La Roche, Baden, Switzerland

Ambrin Fatima,
Department of Biological and Biomedical Sciences, Aga Khan University, Karachi, Pakistan

Caroline Gallant,
10x Genomics, Stockholm, Sweden

‡These authors have contributed equally to this work

SPECIALTY SECTION
This article was submitted to Brain Disease Mechanisms, a section of the journal Frontiers in Molecular Neuroscience

RECEIVED 07 July 2022
ACCEPTED 20 September 2022
PUBLISHED 24 October 2022

CITATION
Schuster J, Klar J, Khalfallah A, Laan L, Hoeber J, Fatima A, Sequeira VM, Jin Z, Korol SV, Huss M, Nordgren A, Anderlid BM, Gallant C, Birnir B and Dahl N (2022) ZEB2 haploinsufficient Mowat-Wilson syndrome induced pluripotent stem cells show disrupted GABAergic transcriptional regulation and function.
Front. Mol. Neurosci. 15:988993.
doi: 10.3389/fnmol.2022.988993

ZEB2 haploinsufficient Mowat-Wilson syndrome induced pluripotent stem cells show disrupted GABAergic transcriptional regulation and function

Jens Schuster[1]*, Joakim Klar[1], Ayda Khalfallah[1‡], Loora Laan[1‡], Jan Hoeber[1†], Ambrin Fatima[1†], Velin Marita Sequeira[1], Zhe Jin[2], Sergiy V. Korol[2], Mikael Huss[3], Ann Nordgren[4,5], Britt Marie Anderlid[4,5], Caroline Gallant[1†], Bryndis Birnir[2] and Niklas Dahl[1]*

[1]Department of Immunology, Genetics and Pathology, Uppsala University and Science for Life Laboratory, Uppsala, Sweden, [2]Department of Medical Cell Biology, Uppsala University, Uppsala, Sweden, [3]Wallenberg Long-Term Bioinformatics Support, Science for Life Laboratory, Department of Biochemistry and Biophysics, Stockholm University, Stockholm, Sweden, [4]Department of Molecular Medicine and Surgery, Center for Molecular Medicine, Karolinska Institutet, Stockholm, Sweden, [5]Department of Clinical Genetics, Karolinska University Hospital, Stockholm, Sweden

Mowat-Wilson syndrome (MWS) is a severe neurodevelopmental disorder caused by heterozygous variants in the gene encoding transcription factor *ZEB2*. Affected individuals present with structural brain abnormalities, speech delay and epilepsy. In mice, conditional loss of Zeb2 causes hippocampal degeneration, altered migration and differentiation of GABAergic interneurons, a heterogeneous population of mainly inhibitory neurons of importance for maintaining normal excitability. To get insights into GABAergic development and function in MWS we investigated ZEB2 haploinsufficient induced pluripotent stem cells (iPSC) of MWS subjects together with iPSC of healthy donors. Analysis of RNA-sequencing data at two time points of GABAergic development revealed an attenuated interneuronal identity in MWS subject derived iPSC with enrichment of differentially expressed genes required for transcriptional regulation, cell fate transition and forebrain patterning. The ZEB2 haploinsufficient neural stem cells (NSCs) showed downregulation of genes required for ventral telencephalon specification, such as FOXG1, accompanied by an impaired migratory capacity. Further differentiation into GABAergic interneuronal cells uncovered upregulation of transcription factors promoting pallial and excitatory neurons whereas cortical markers were downregulated. The differentially expressed genes formed a neural protein-protein network with extensive connections to well-established epilepsy genes. Analysis of electrophysiological properties in ZEB2 haploinsufficient GABAergic cells revealed overt perturbations manifested as impaired firing of repeated action potentials. Our iPSC model of ZEB2

haploinsufficient GABAergic development thus uncovers a dysregulated gene network leading to immature interneurons with mixed identity and altered electrophysiological properties, suggesting mechanisms contributing to the neuropathogenesis and seizures in MWS.

KEYWORDS

ZEB2, Mowat-Wilson syndrome, FOXG1, epilepsy, neurodevelopmental disease, GABAergic interneurons, transcriptional network, electrophysiology

Introduction

Mowat-Wilson syndrome (MWS) is a rare disease characterized by intellectual disability (ID), speech impairment, epilepsy and Hirschsprung disease (Mowat et al., 1998; Adam et al., 2006; Garavelli and Mainardi, 2007; Ivanovski et al., 2018). Mowat-Wilson syndrome is usually caused by heterozygous *de novo* variants in the *ZEB2* gene encoding the zink-finger E-box binding homeobox (ZEB) 2 transcription factor (Zweier et al., 2002). Epilepsy is one predominant feature in MWS and 80–90% of cases present with either focal, absence or generalized seizures (Garavelli et al., 2017; Ivanovski et al., 2018). Brain imaging of affected individuals has detected structural changes in a majority of cases, predominantly localized to the ventricular temporal horn and hippocampus (Garavelli et al., 2017).

The transcription factor (TF) ZEB2 is a key regulator throughout nervous system development and it is expressed in the neural tube, neural crest cells, hippocampus and the cerebral cortex (Chng et al., 2010; McKinsey et al., 2013; Brinkmann and Quintes, 2017). Mice deficient of Zeb2 (*Zeb2*−/−) die at embryonic day (E) E9.5 with failed closure of the neural tube (Van de Putte et al., 2003) whereas heterozygous mice (*Zeb2*−/+) survive with a reduced number of cortical interneurons and without seizures (Takagi et al., 2015). Conditional neural loss of Zeb2 leads to reduced size of the hippocampus (Miquelajauregui et al., 2007) and immature cortical identity of GABAergic interneurons (van den Berghe et al., 2013) accompanied by increased amounts of GABAergic neurons in the striatum, suggesting a defective migration (McKinsey et al., 2013). While these previous animal studies have brought essential information on the role of Zeb2 for development of GABAergic interneurons, the effects of ZEB2 haploinsufficiency on human GABAergic development and function in MWS remain unclear.

GABAergic interneurons comprise a heterogeneous and mainly inhibitory cell population that is subclassified by transcriptomic signatures (Huang and Paul, 2019). The diversity of interneurons enables a variety of inhibitory control mechanisms on cerebral microcircuits (Hensch, 2005; Haider et al., 2006) to balance network activity as well as to prevent runaway excitation of the neocortex and hippocampus (Kepecs and Fishell, 2014; Paz and Huguenard, 2015; Gouwens et al., 2020). Accordingly, deficient GABAergic activity has been implicated in the etiology of hyperexcitability and seizures (Galanopoulou, 2010; Khoshkhoo et al., 2017; Wang Y. et al., 2017; Pfisterer et al., 2020).

Herein, we used ZEB2 haploinsufficient subject derived induced pluripotent stem cell (iPSC) to model the transcriptional profile and function of GABAergic interneurons in MWS. Our model uncovered a network of co-expressed and differentially expressed genes (DEGs) accompanied by deficient migration in NSCs and altered electrophysiological properties of GABAergic neurons, providing insights into the neuropathogenesis and mechanisms underlying seizures in MWS.

Materials and methods

Subjects

Two full siblings (MW1 and MW2) with typical clinical features of MWS were included in the study. Patient MW1 is a boy delivered in Iraq after a normal pregnancy and he is the first child of healthy non-related parents. After moving to Sweden, the boy was diagnosed with neurodevelopmental delay, facial dysmorphisms, microcephaly, sensorineural hearing loss, hypospadias, retentio testis, aortic stenosis and Mb Hirschsprung. He had his first generalized seizure at age 5 years and walked independently at age 6 years. At age 15 years, he presented with facial features characteristic for MWS, moderate intellectual disability and he has been seizure free since the age of 12 years.

Patient MW2 is a girl delivered in Sweden at full term with generalized growth retardation (birth weight −3SD, body length −2SD, and head circumference −2SD). Corpus callosum agenesis was identified by ultrasound during pregnancy and confirmed after birth. Postnatal investigation revealed patent ductus arteriosus and pulmonary stenosis that resolved spontaneously. Growth retardation remained at 2 years of age (weight −1.5 SD, body length −2SD, head circumference −4SD) and she developed facial characteristics of MWS.

She walked independently at age 2.5 years and had onset of febrile convulsions at the same age. Epilepsy developed later with partial and generalized seizures. The girl has myopia, strabismus, severe intellectual disability, no speech and sleep disorder.

The combined clinical findings made MWS the most likely diagnosis in both siblings. This was confirmed by targeted genetic investigation of the *ZEB2* gene that revealed a heterozygous nonsense variant c.1027C>T (p.Arg343*) in both siblings (**Figure 1A**). The variant, located in exon 8, was previously reported in 10 independent cases with MWS in the ClinVar (VCV000189281.15) database and it is absent from the normal population (gnomAD v2.1.1 database). The variant was therefore classified as Pathogenic (PVS1, PS4, PM2, PP4) according to the criteria from American College of Medical Genetics and Genomics (ACMG) (Richards et al., 2015). The variant was not detected in peripheral blood leukocytes of the healthy parents suggesting parental gonadal mosaicism.

Induced pluripotent stem cells culture and neuronal differentiation

Induced pluripotent stem cell lines were previously established from fibroblasts of the two siblings (MW1, MW2) and two healthy donors (Ctl2, male and Ctl8, female, respectively) (Sobol et al., 2015; Schuster et al., 2019b). The four iPSC lines were matched for passage number (P25-P35), cultured in feeder free Essential-8^{TM} medium (ThermoFisher Scientific, Waltham, MA, United States) on either Matrigel^{TM}, Vitronectin^{TM} (Stem Cell Technologies, Vancouver, Canada) or LN521 (BioLamina, Sundbyberg, Sweden) coated cell culture dishes and passaged as clumps with gentle cell dissociation reagent (GCDR; Stem Cell Technologies, Vancouver, Canada) or as single cells with TrypLExpress (ThermoFisher Scientific, Waltham, MA, United States) (Schuster et al., 2019b). Neurocortical differentiation of iPSCs was carried out as described using Dual-SMAD inhibition that promotes conversion into neural stem cells (NSC) for 10 days followed by directed differentiation into GABAergic cortical lineages for 55 days, i.e., totally 65 days (**Figure 1B**; Schuster et al., 2019a).

Cell cycle and proliferation assay

The four iPSC lines were submitted to Dual Smad inhibition as described above and cultured to 70–80% confluence at d10 (i.e., iPSC-NSC). All samples were run in triplicates.

Proliferation assay

At day 10, iPSC-NSC were incubated with 10 μM EdU for 2 h and subsequently processed using a Click-it® EdU Flow Cytometry Assay kit (ThermoFisher Scientific, Waltham, MA, United States) following recommended protocols. A total of 100,000 events was recorded for all samples on a Fortessa flow cytometer (BD Biosciences, NJ, United States) and subsequently analyzed using FlowJo 10.8.1. A sample of unlabeled cells was used to define the cut-off gate for EdU+ cells. The gate was applied to assess the number of actively dividing cells (i.e., EdU labeled cells) in labeled samples, where all events inside the gate were counted as EdU+.

Cell cycle analysis

Alternatively, iPSC-NSC at d10 were harvested with TryplExpress, fixed and resuspended in FxCycle^{TM} PI/RNase staining solution (ThermoFisher Scientific, Waltham, MA, United States) to stain DNA. A total of 100,000 events was recorded as above and DNA content was plotted using FlowJo 10.8.1. Univariate cell cycle modeling was performed in FlowJo using the Dean-Jett-Fox model as described to derive percentages of cells in G1, S and G2 phase, respectively.

Electrophysiological recordings

Whole-cell patch-clamp recordings were performed at room temperature (20–22°C) on differentiated GABAergic cells from day 65 showing a mature neuronal morphology, i.e., large and complex cell body with three or more neurites. Action potentials were evoked (eAPs) in response to step current injections in both Ctl-iPSC GABA and MW-iPSC GABA cells at a holding potential of −60 mV. An Axopatch 200B amplifier with the signal filtering filtered at 2 kHz, digitizing on-line at 10 kHz using an analog-to-digital converter and pClamp 10.2 software (Molecular Devices, USA) were used as described. Current steps were applied in 10 pA increments, each for 500 ms duration. Data were analyzed with pCLAMP software v10.5 and GraphPad PRISM (La Jolla, CA, USA).

RNA isolation, quantitative real-time RT/PCR, and RNA sequencing

RNA from iPSC and neural cell populations was isolated using a miRNeasy micro kit (Qiagen, Hilden, Germany) and 1 μg of total RNA was reverse transcribed into cDNA using High Capacity cDNA transcription kit (ThermoFisher Scientific, Waltham, MA, United States). Expression of marker genes was compared to the two housekeeping genes *GAPDH* and *ACTB*. FastStart Universal SYBR Green Master mix (Roche, Basel, Switzerland) was used for qPCR with relevant primers. For all analyses, we used samples from three independent differentiation cultures and each sample was analyzed in triplicate. Expression Data (2ˆ-dCT(vsAVERAGE (*GAPDH/ACTB*))) was plotted with the standard error of the mean (SEM) and fold change was presented as 2ˆ-ddCT with SEM (*ACTB*: F-CAGGAGGAGCAATGATCTTGATCT,

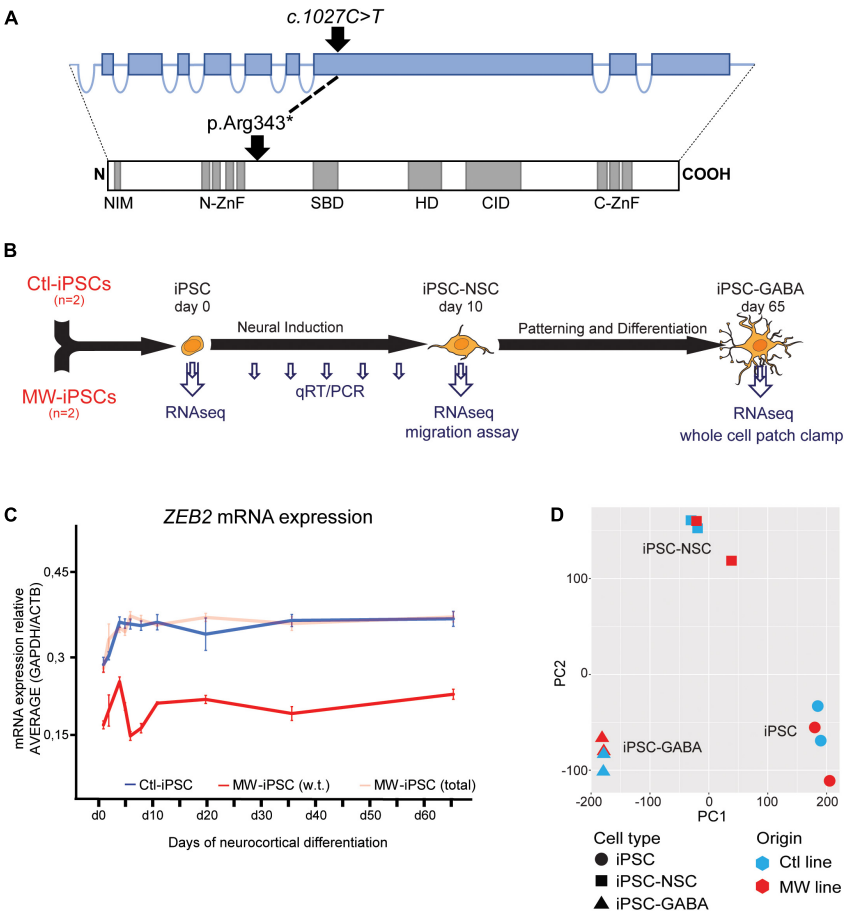

FIGURE 1
(A) Schematic illustration of the *ZEB2* gene structure with relative sizes of coding exons (top, blue boxes) and the corresponding ZEB2 protein architecture (bottom). The positions of the *ZEB2* gene variant and the resulting predicted stop-codon are shown with relation to functional protein domains (gray boxes). NIM, NuRD interacting motif; N-ZnF, N-terminal zink-finger clusters; SBD, Smad-binding domain; HD, Homeodomain-like domain; CID, CtBP-interacting domain; C-ZnF, C-terminal zink-finger clusters (modified from Birkhoff et al., 2021). **(B)** Schematic presentation of the iPSC differentiation procedure and time points of analysis using different methodologies. Induced pluripotent stem cells (iPSC) from two healthy donors (Ctl-iPSCs) and two MWS patients (MW-iPSCs) were harvested for qRT-PCR at d 0, 3, 4, 5, 7, 10, 19, 35, and 65 (small arrows) and for RNA-sequencing at days 0, 10 and 65 (large arrows). Migratory capacity was assessed on confluent iPSC-NSCs at d 10 and electrophysiological activity was investigated on iPSC-GABA after d 65. **(C)** *ZEB2* expression levels quantified by qRT-PCR during neurocortical differentiation of iPSC relative to expression of the housekeeping genes *ACTB* and *GAPDH*. MW-iPSC lines (n = 2), with a heterozygous c.1027C>T stop-variant (p.Arg343*) in exon 8, show reduced w.t. *ZEB2* mRNA levels (red line) when compared to that in Ctl-iPSC lines (n = 2; blue line) indicating haploinsufficiency. The total *ZEB2* mRNA levels in MW-iPSC lines are shown with a shaded red line. Data are presented as mean ± SEM (3 replicates per line). **(D)** Principal component analysis (PCA) of transcriptome data of iPSC, NSC and GABAergic cells derived from MWS patients (MW; n = 2) and healthy donors (Ctl; n = 2), respectively. The samples cluster according to differentiation time points and not according to *ZEB2* genotype.

R-TCATGAAGTGTGACGTGGACATC; *GAPDH*: F-GAAGGTGAAGGTCGGAGTC, R-GAAGATGGTGATGGGATTTC; *ZEB2*: F-CGTTTCTCCCATTCTGGTTC, R-TGTGCGAACTGTAGGAACCA—located in exon 6 and exon 8, respectively, of *ZEB2* mRNA; *FOXG1*: F-CCCTCCCATTTCTGTACGTTT, R-CTGGCGGCTCTTAGAGAT; *VGLUT3*: F-GTCTAAGTGTGGGTCTCTTGTCA, R-TAGCCACCCCTTTGGTATGC; *BCAN*: F-CTCACGCTCGCGCAGTCT, R-TGTCTCCTTCCAGAACATCTGC; *LEF1*: F-AGAGCGAATGTCGTTGCTGA, R-GGCAGCTGTCATTCTTGGAC; *NEUROG2*: F-TGTTAGTGCTGCTCGGATCG, R-GTCTTCTTGATGCGCTGCAC; *NEUROD6*: F-CAGGAGACGATGCGACACTC, R-TGCTTCTGGTCCTCGCATTC; *BARH2L*: For-AGACCAAACTCGACAAGCGG, R-ATTGAGCTGGTGGTCGGAAA; *EBF2*: F-CGGAGATGGATTCGGTCAGG, R-TGAGTGCCGTTGTTGGTCTT; *EOMES*: F-GGGATCTTGCGGAGGACTGG, R-TGTAGTGGGCAGTGGGATTG; HMGA2: F-GGCAGCAAAAACAAGAGTCCC, R-ACTGCTGCTGAGGTAGAAATCG; *ITGB5*: F-GGAGAACCAGAGCGTGTACC, R-AGCAGTTACAGTTGTCCCCG; *LRRK2*: F-CCTGTTGTGGAAGTGTGGGAT, R-TTCAGTATTTTTCCGGTTGTAGCC; *NEUROD1*: F-GAATTCGCCCACGCAGGA, R-ATCAGCCCACTCTCGCTGTA; *SEMA5A*: F-T

CCACCTTCCCCGTGC, R-AGCCCAAGTCTCACACACCA; *POLR2A*: F-CACCGGCCTAGAGTTGTATGCGGAA, R-AAA CTTCCGCATACAACTCTAGGCC; *LHX6*: F-TCATAAAAAG CACACGCCGC, R-TATCGGCTTTGAGGTGGACG).

Paired-end RNA-sequencing libraries were prepared from 1 μg of total RNA using TruSeq stranded total RNA library preparation kit with RiboZero Gold treatment (Illumina, CA, United States) according to manufacturer's protocols. Sequencing was performed on a HiSeq2500 (Illumina, CA, United States) with v4 sequencing chemistry on a total of 3 lanes at the SNP&SEQ Technology Platform, Science for Life Laboratory, Uppsala, Sweden.

PCR, Sanger sequencing and quantification of *ZEB2* expression

We generated cDNA from iPSC and neural cell populations (see above) at specific time points of neurocortical differentiation for amplification of part of the *ZEB2* transcript containing the c.1027C>T variant with PCR primers (*ZEB2*: F-CGTTTCTCCCATTCTGGTTC, R-CCC GTGTGTAGCCATAAGAA). The PCR products were purified using a PCR clean up kit (MN) and Sanger sequenced (Eurofins Genomics, Ebersberg, Germany). The resulting DNA sequence chromatograms were analyzed using the QSVanalyzer software to estimate the relative abundance of wild type (w.t.) versus the variant allele (Carr et al., 2009).

Immunofluorescent staining

Staining was performed on cells fixed with ice-cold 4% paraformaldehyde and subsequently permeabilized in blocking solution (1× phosphate-buffered saline pH 7.4, 1% bovine serum albumin, 0.1% Triton X-100). Primary antibodies against FOXG1 (1:100; abcam, Cambridge, United Kingdom), NESTIN (1:300; R&D systems, MN, United States), MAP2 (1:5,000; abcam, Cambridge, United Kingdom), GABA (1:1,000; Sigma, MO, United States), GAD1 (1:100, Millipore, MA, United States) and SST (1:100, Millipore, MA, United States) were used for immunostaining and quantification. Primary antibodies were allowed to bind overnight separately or in appropriate combinations at 4°C. After washing three times in 1×TBS, 0.05% Tween, the secondary antibodies donkey anti-goat IgG AlexaFluor 633, donkey anti-rabbit IgG AlexaFluor 568 or donkey anti-mouse IgG AlexaFluor 488 (1:1,000; ThermoFisher Scientific, Waltham, MA, United States) were applied alone or in appropriate combinations for 1.5 h at room temperature in the dark. Visualization was performed on a Zeiss 510 confocal microscope (Carl Zeiss Microscopy, Jena, Germany) using Zen 2009 imaging software.

Wound healing scratch assay

At day 10 of neurocortical differentiation, MW-iPSC NCSs and Ctl-iPSC NSCs were re-seeded to obtain 100% confluence the following day. A pipette tip was used to scratch the culture introducing an artificial wound followed by bright field pictures taken at identical positions of the respective slide after 0, 15, and 20h. Closure of the open wound area was quantified using TScratch software (Geback et al., 2009). To circumvent data bias due to differences in the generation of wounds, the assay was repeated three times per iPSC cell line. Additionally, the TScratch analysis was performed as a time series experiment following closure of the wound area over time relative to the open area at start (open area at 20 h vs. open area at 0 h).

Bioinformatic and statistical analysis

Bulk RNA sequencing reads were aligned to the ENSEMBL human reference genome (Homo_sapiens.GRCh37.75) and gene counts were generated using the STAR read aligner (Dobin et al., 2013). Number of expressed transcripts in each cell line was defined as all transcripts with more than one detected count (count > 1). Analysis of the count data to identify differentially expressed transcripts was performed using the DESeq2 package (design = ~ condition) with 2 degrees of freedom (df = ncol(model.matrix(design(dds), colData(dds)))) (Love et al., 2014).

Gene ontology (GO) enrichment analysis using the PANTHER classification system[1] was employed to analyze enrichment of DEGs in GO terms (Mi et al., 2013). Generation of networks was performed using Cytoscape and a STRING protein query with a confidence cut-off = 0.5 (Doncheva et al., 2019). Visualization and data presentation of gene enrichment was performed utilizing the cneplot software contained in the enrichplot R package[2].

To evaluate our cell model of cortical GABAergic interneuronal development, we compared our data with single cell RNA-seq data from the developing human cortex (Nowakowski et al., 2017). Data was downloaded using UCSC cell browser[3] and analyzed using Seurat 3 (Stuart et al., 2019). We performed an unbiased clustering using principal component analysis (PCA), followed by FindNeighbors (20 dimensions), FindClusters (resolution = 1.2), and UMAP dimensionality reduction visualization. We used subset data in Seurat 3 of clusters corresponding to interneurons, excitatory neurons and the neural precursors (**Figure 4**).

1 geneontology.org

2 https://www.bioconductor.org/packages/release/bioc/html/enrichplot.html

3 cells.ucsc.edu

Analysis of putative ZEB2 binding sites was performed using available Chip-Seq ENCODE data (ChIP-seq on eGFP-ZEB2 tagged human HEK293 cells: Accession ENCSR417VWF and for eGFP-ZEB2 tagged human K562 cells: Accession ENCSR322CFO). We lifted Chip-seq peaks (optimal IDR peaks i.e., high-confidence peaks for HEK293: Accession ENCFF232GGZ and for K562: Accession ENCFF129WGK) within 10 kb of our DEGs to identify putative ZEB2 binding sites.

Results

Differentiation of MW-iPSC and Ctl-iPSC generates GABAergic cells with gene expression profiles of forebrain

To get mechanistic insights into GABAergic development in MWS we used iPSC from the two siblings with a heterozygous and pathogenic *ZEB2* variant c.1027C>T (p.Arg343*; **Figure 1A**). Our differentiation protocol yielded a 90% enrichment of cells that stained positive for GABA and the key glutamate-to-GABA-synthesizing enzyme glutamate decarboxylase (GAD1) in both MW-GABA and Ctl-GABA cells (**Supplementary Figure 1A**; Schuster et al., 2019a). Approximately 30% of neuronal cells stained positive for somatostatin (SST), a marker for a large subpopulation of inhibitory interneurons, in all lines (Lim and Marin, 2018). There were no significant differences in growth, morphology or staining of the GABAergic markers when comparing MW-iPSC and Ctl-iPSC derived neural lines (**Supplementary Figures 1A,B**).

The *ZEB2* variant predicts a truncated protein lacking essential functional domains such as the Smad-binding domain, the Homeodomain-like domain, the consensus interaction sequences for CtBP-1/2 co-repressors and the C-terminal zink-finger cluster (**Figure 1A**; Epifanova et al., 2018; Birkhoff et al., 2021). The iPSC derived from the two MWS subjects (MW1-iPSC and MW2-iPSC) were induced for neural differentiation together with iPSC from two healthy donors (Ctl2-iPSC and Ctl8-iPSC) during 10 d to obtain neural stem cells (NSCs) followed by differentiation into GABAergic forebrain lineages for additional 55 days (**Figure 1B**; Chambers et al., 2009; Schuster et al., 2019a). To investigate ZEB2 haploinsufficiency in the MW-iPSCs we analyzed *ZEB2* mRNA levels at different time-points along neural induction and neurocortical differentiation until day 65 (**Figure 1B**). The total *ZEB2* expression increased upon neural induction in all lines from day 0–3 and remained stable from day 10 until day 65 at similar levels in both MW-iPSC and Ctl-iPSC. However, sequence analysis of *ZEB2* RNA across the c.1027C>T variant revealed that the variant was present in approximately 50% of transcripts in the MWS subject derived iPSC lines at all time points (**Figure 1C**). Consequently, the w.t. *ZEB2* levels in the two MW-iPSC lines were approximately halved when compared to Ctl-iPSC throughout differentiation supporting haploinsufficiency for w.t. ZEB2 (**Figure 1C**).

We then performed RNA-sequencing (RNAseq) and assessed the gene expression profiles of MW-iPSC and Ctl-iPSC at day 0 (undifferentiated iPSCs), in NSCs at d10 (iPSC-NSC), and after differentiation into postmitotic GABAergic interneurons (iPSC-GABA) at day 65 (**Figure 1B**). We obtained on average 34.7 million reads (ranging from 24.4×10^6 to 42.7×10^6 reads) from the four lines at all time points. The average numbers of expressed transcripts (>1 count) were 26,180 at day 10 and 28,140 at day 65, respectively. Normalized data were used to calculate the Euclidean distance between samples and all samples clustered according to differentiation time points (**Supplementary Figure 1C**). In addition, principal component analysis (PCA) confirmed that the overall differences in transcriptomes were related to the differentiation time-points and not to the *ZEB2* genotype suggesting similar overall cell compositions in MW-iPSC and Ctl-iPSC (**Figure 1D**; Schuster et al., 2019a). Furthermore, analysis at the three time-points revealed changes in expression (log2(counts)) of neural genes related to the differentiation for each iPSC line (**Supplementary Figure 2A**). The transcriptomic profiles of each of the four lines at day 65 were further validated by comparing the 5,000 most highly expressed transcripts with expression profiles across different brain regions obtained from the Human Gene Atlas and the Allen Brain Atlas (Sunkin et al., 2013; Miller et al., 2014). All four lines showed the closest similarities with transcriptomes of "Prefrontal Cortex" and "Fetal Brain" (Human Gene Atlas; EnrichR combined score > 50), "Dentate gyrus" and "Superficial dorsofrontal area" (Allen Brain Atlas; EnrichR combined score > 50) in neonates (Schuster et al., 2019a).

Differentially expressed genes in MW-iPSC derived GABAergic neurons are enriched in gene ontology terms for cell fate, forebrain development and transcriptional regulation

We next performed a GO analysis using differentially expressed genes (DEGs) in the MW-iPSC vs. Ctl-iPSC lines. The comparison of RNAseq data between the non-induced MW-iPSC and Ctl-iPSC lines revealed similar patterns. However, in NSC we identified 12 DEGs (adjusted p-value < 0.05; **Supplementary Table 1A**) and in GABAergic interneurons the number of DEGs was 93 (adjusted p-value < 0.05; **Supplementary Table 1B**; **Figure 2A**). The RNAseq data was validated by qRT-PCR analysis of 16 DEGs

confirming up-regulation (n = 8) or downregulation (n = 8), respectively (**Supplementary Figures 2B,C**). Expression of two interneuronal markers (*SST* and *GAD1)* at day 65 revealed down-regulation in MW-GABA compared to Ctl-GABA cells from our RNAseq analysis (Log2fold changes −1,5 and −1,1, respectively; **Supplementary Tables 1B,C**). However, the qRT-PCR analysis of both genes did not reach significant differences between the sample groups.

To identify enriched GO terms for biological processes we then analyzed the DEGs in a GO enrichment analysis. The analysis revealed no significant enrichment for DEGs in NSCs at d10. However, when applying the 93 DEGs at d65 we identified the top specific term "Dentate gyrus development" [GO:0021542; 5 DEGs (5%); **Figure 2B**; **Supplementary Tables 2A,B**] among the most enriched categories. The term is placed in a hierarchy under "Forebrain development" [GO:0030900; 20 DEGs (21%)]. Among the top terms we also identified "Cell fate commitment" [GO:0045165; 14 DEGs (15%)] and "Endodermal cell differentiation" [GO:0035987; 24 DEGs (26%); **Figure 2B**; **Supplementary Tables 2A,B**]. Notably, nine DEGs were represented in more than one of the enriched terms for biological processes and four of these DEGs (*GDF7*, *DMRTA2, NEUROD1*, and *EOMES*) formed an interconnected network comprising 23 DEGs (**Figure 3A**). We observed that 15 out of the 23 DEGs are TFs (**Table 1**) and we therefore analyzed the set of 93 DEGs d65 for enrichment in GO terms for molecular function. The analysis revealed the top terms "DNA-binding transcription factor activity, RNA polymerase II-specific" (GO:0000981; 22 DEGs), placed in a hierarchy under the term "Transcription regulator activity" (GO:0140110; 25 DEGs), and the similar term "RNA polymerase II regulatory region sequence-specific DNA binding" (GO:0000977; 23 DEGs; **Supplementary Tables 2C,D**; **Figure 2C**). The entire set of DEGs at day 10 and 65 (n = 105) comprised altogether 28 TFs and transcriptional regulators (27%; **Supplementary Tables 1A,B**).

To further validate interactions among the 93 DEGS at day 65, we then used the Search Tool for the Retrieval of Interacting Genes (STRING). The analysis revealed a protein-protein network that comprised 55 proteins encoded by the DEGs (**Figure 3B**). Moreover, we sought to get mechanistic insights into a possible role of ZEB2 on the regulation of individual DEGs among the top significantly enriched terms. We therefore searched for ZEB2 binding sites among our DEGs using available CHIPseq data (ENCODE) derived from HEK293 and K562 cells. Among the 12 DEGs in NSCs, ZEB2 binding was reported in 10 (83%; **Supplementary Table 1A**; see examples in **Supplementary Figure 2D**) and in 65 among the 93 DEGs in GABAergic cells (70%; **Supplementary Table 1B**). This observation suggests a direct involvement of ZEB2 in the regulation of a large proportion of DEGs identified in our model system.

Taken together, analysis of the gene expression changes in MW-iPSC GABA interneurons revealed enrichment of genes in an interconnected gene regulatory network for biological processes such as cell fate decision, neural patterning and specification.

Transcriptional changes in ZEB2 haploinsufficient GABAergic cells uncover a disrupted identity and dysregulations linked to epilepsy genes

Beyond the DEGs belonging to the top enriched terms, we identified several additional and dysregulated genes important for interneuronal development when comparing MW-iPSC with Ctl-iPSC derived NSCs and GABAergic neurons, respectively. For example, MW-subject derived NSCs showed downregulation of the transcriptional regulators *KMT2D* and *FOXG1,* essential for neuronal lineage commitment (Wang et al., 2016) and neocortical organization (Cargnin et al., 2018). Furthermore, we observed upregulation of the genes encoding the TFs NEUROG2, NEUROD4 and NHLH1 (NSCL1) that promote glutamatergic development while suppressing genes for microglia identity (Roybon et al., 2010; Kim, 2012; Guillemot and Hassan, 2017; Dennis et al., 2019; Aslanpour et al., 2020; Liu et al., 2021; Tutukova et al., 2021). The combined transcriptional changes predict a disrupted GABAergic identity in MW-iPSC and we therefore sought to simulate the lineage trajectory of GABAergic development in our models. To this end we selected two DEGs d65 from our RNAseq data encoding the down-regulated GABAergic marker GAD1 and the upregulated excitatory marker NEUROD6 (**Figure 2A** and **Supplementary Table 1**). We then inferred the expression levels of the two DEGs on pseudo-time trajectories based on gene expression data available from single cells along human cortical development (Nowakowski et al., 2017). In Ctl-iPSC GABA cells the expression levels of both genes displayed trajectories in agreement with that of cortical interneurons originating from early neural progenitors and radial glia, confirming that our protocol generates cortical GABAergic interneurons. In contrast, the expression levels of *NEUROD6* and *GAD1* in MW-iPSC GABA cells simulated a differentiation trajectory directed toward excitatory neurons (**Figure 4** and **Supplementary Table 1B**).

Moreover, given the association between altered GABAergic function and seizures, we then sought to investigate possible interactions of all DEGs with genes associated with epilepsy. We therefore compiled a list of 208 unique genes associated with genetic epilepsy, neurodevelopment and epilepsy syndromes from two recent studies (**Supplementary Table 3**; Wang J. et al., 2017; Jang et al., 2019). Subsequently, we re-analyzed the

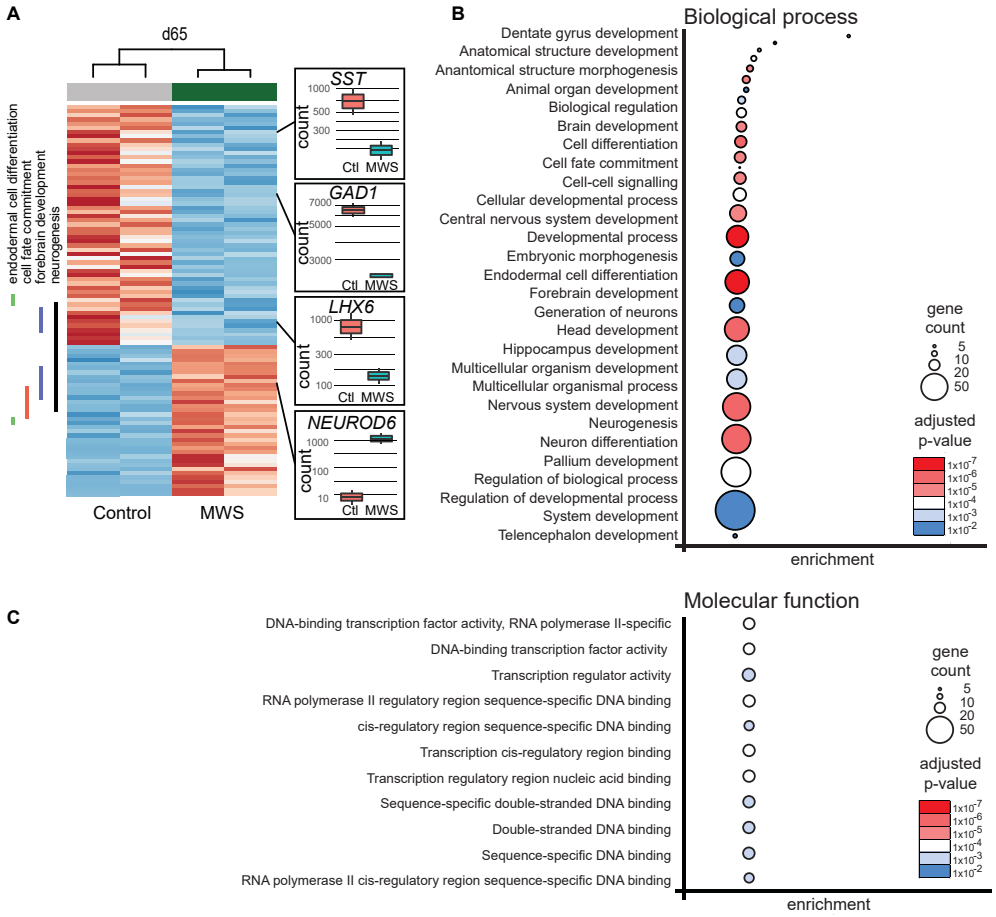

FIGURE 2
(A) Hierarchial clustering (z-scores) of 93 differentially expressed genes in two Ctl-iPSC GABA and two MW-iPSC GABA lines at d65 of differentiation from RNAseq. The expression (normalized counts) of selected genes (*SST*, *GAD1*, *LHX6*, *NEUROD6*) of importance for interneuronal development is highlighted as bar and whisker plots in Ctl-iPSC GABA (n = 2) and MW-iPSC GABA (n = 2). **(B,C)** GO enrichment analysis of 93 DEGs at d65 in MW-iPSC GABA cells showing the top 28 list of biological processes **(B)** and top 11 molecular functions **(C)**. Categories are listed according to adjusted p-values and number of DEGs in each category (gene count; **Supplementary Tables 2A,C**).

105 DEGs together with ZEB2 and the 208 curated epilepsy-associated genes for possible protein-protein interactions using STRING (in total 314 distinct genes; **Supplementary Table 3**; Wang J. et al., 2017; Jang et al., 2019). The analysis disclosed a multiplex network that extended our protein-protein network with 282 of the queried 314 epilepsy-associated genes (89.8%; **Supplementary Figure 3**; **Supplementary Table 3**).

Neural progenitors derived from MWS-patient iPSC exhibit migration defects

In mice, the conditional loss of Zeb2 causes failure of interneuronal precursor cells to migrate tangentially into the cortex (McKinsey et al., 2013; van den Berghe et al., 2013; He et al., 2018). These prior reports, together with the observed downregulation of *LHX6*, a marker for interneuronal migration and laminar positioning (Liodis et al., 2007), in our ZEB2 haploinsufficient GABAergic cells prompted us to investigate the migratory capacity of our iPSC derived NSCs. To test this, we established confluent MW-iPSCs and Ctl-iPSCs derived NSC cultures and performed a wound healing scratch assay for 20 h. Analysis of both Ctl-iPSC NSC cultures revealed that the open area became almost closed after 15 h and completely closed after 20 h post scratching. In contrast, the two MW-iPSC NSC cultures were only partially closed after 20 h (**Figures 5A,B**; p-value = 0.031). To exclude a possible effect of different proliferative capacity on the results we then performed a proliferation assay on MW-iPSC NSC and Ctl-iPSC NSCs. There were no detectable differences in proliferative capacity between the two groups (**Figure 5C**). These findings suggest an impaired migratory capacity in MW-iPSC NSCs.

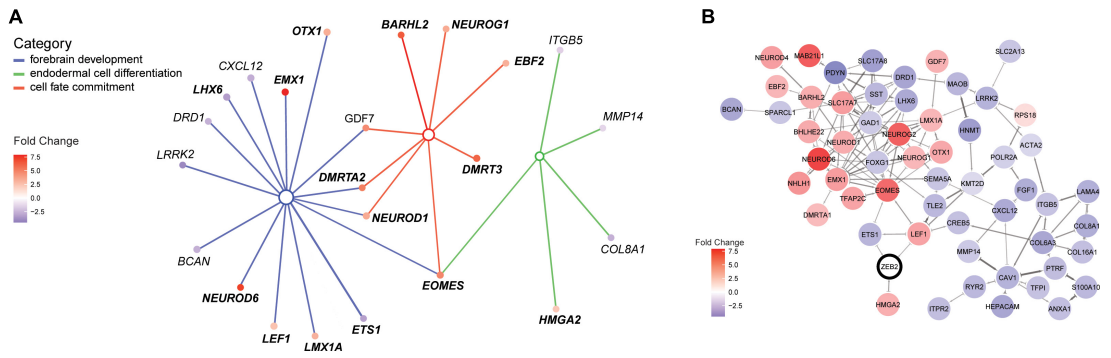

FIGURE 3

ZEB2 haploinsufficiency triggers differential expression of factors in a neural regulatory network. **(A)** Illustration of the interconnected network of DEGs belonging to enriched terms for the biological processes "Forebrain development" [GO:0030900; parent term to dentate gyrus development (GO:0021542); blue lines], "Endodermal cell differentiation" (GO:0035987; green lines) and "Cell fate commitment" (GO:0045165; red lines). The interconnected network was constructed using cnetplot. Interacting DEGs (filled circles) are colored according to gene expression (fold change [log2]). **(B)** STRING network with confidence edges illustrating documented protein interactions between ZEB2 (circled) and 55 out of 105 DEGs detected in our MW-iPSC derived neural cells at d10 and d65. DEGs (filled circles) are color-coded according to gene expression, as in panel **(A)**. The Network was generated using a STRING protein query [run in Cytoscape (Doncheva et al., 2019)] with a confidence cut-off = 0.5. ZEB2 is indicated with a bold outline.

MW-iPSC derived GABAergic interneurons show impaired firing of action potentials

Given the preponderance of seizures in MWS together with the distorted molecular identity of our ZEB2 haploinsufficient GABAergic cells, we sought to investigate if our model was associated with changes in electrophysiological properties. We therefore assessed the electrophysiology of the ZEB2 haploinsufficient GABAergic cells using whole-cell patch clamp analysis. Upon stimulation, the Ctl-iPSC GABA cells required a stimulus of 20 pA or more to fire evoked action potentials (eAPs) whereas the MW-iPSC GABA cells were able to fire one or rarely two eAP at a depolarizing current stimulus of 10 pA (**Figures 5D–E**). Furthermore, the majority of MW-iPSC GABA cells discharged only one single eAP during the depolarizing current injection, irrespective of the injected activation stimulus. In contrast, the Ctl-iPSC GABA cells showed repetitive eAP spikes that increased in number with the strength of current injection until reaching a maximum number of spikes (**Figures 5D,E**). In Ctl-iPSC GABA cells the maximal number of eAPs was 6 at a stimulus of 50 pA with an average amplitude of APs of 84 ± 10 mV, comparable to that of the single eAP in MW-iPSCs (82 ± 11 mV; **Figure 5F**). In addition, while the first eAP amplitude in MW-iPSC and Ctl-iPSC GABA cells showed no significant differences, the delay time for the cells to react to the injected stimulus (i.e., peak latency) was significantly reduced in MW-iPSC GABA cells (**Figure 5F**). Altogether, the electrophysiological analysis shows that MW-iPSC GABA cells respond to lower stimuli when compared to Ctl-iPSC GABA cells but fail to generate subsequent APs, usually required for signal transfer and intercellular activation. The electrophysiological analysis thus indicates impaired biophysical properties of ZEB2 haploinsufficient MW-iPSC GABA cells.

Discussion

The present study was motivated by questions on specific abnormalities in elements, pathways and functions for the development of MWS-subject derived GABAergic cells, a key cell type for the regulation of microcircuitries and ictal activity, to gain insights into mechanisms behind the neuropathology in MWS. We therefore generated NPCs and GABAergic cells derived from iPSCs of two MWS subjects with haploinsufficiency for the w.t. ZEB2 protein and from two healthy donors. Following neural patterning of iPSCs, the differentiation protocol yielded GABAergic interneurons with 90% efficiency in all four lines of which 30% expressed the interneuronal marker SST. The expression of markers NPY, PV, and VIP (Lim et al., 2018) were very low to neglectable, suggesting similarities of our model to that of interneuronal development from hESC (Close et al., 2017). Moreover, our GABAergic cells recapitulated transcriptional programs of neonatal brain regions that coincide with structural changes observed in cases with MWS (Garavelli et al., 2017). Together, this suggest that our model system provides a context to study molecular and functional perturbations of GABAergic interneurons relevant for MWS.

We focused our molecular analysis on protein coding sequences obtained from deep RNAseq at two time-points of GABAergic differentiation, thereby increasing the possibilities to capture temporal gene expression changes associated with

TABLE 1 Differentially expressed genes (DEGs) identified in MW-iPSC NSC and MW-iPSC GABA that belong to the top enriched GO terms for biological processes and molecular functions.

Gene symbol	Gene name	log2 Fold change[a]	p-adj[b]	GO term			
				FD[c]	CFC[c]	ECD[c]	TF[d]
iPSC-NSC (d10)							
FOXG1	Forkhead box protein G1	−1.2	0.0099178	X	X		X
SEMA5A	Semaphorin-5A	−1.2	0.0045	X			
iPSC-GABA (d65)							
BARHL2	BarH-like 2 homeobox protein	1.7	0.0085956		X		X
BCAN	Brevican core protein	−1.8	0.0007659	X			
COL8A1	Collagen alpha-1(VIII) chain	−1.7	0.0042997			X	
CXCL12	Stromal cell-derived factor 1	−1.7	0.0033663	X			
DMRT3	Doublesex- and mab-3-related transcription factor 3	2.3	$1.58E-05$		X		X
DMRTA2	Doublesex- and mab-3-related transcription factor A2	2.3	$2.23E-05$	X	X		X
DRD1	D(1A) dopamine receptor	−1.9	0.0017525	X			
EBF2	Transcription factor COE2	1.5	0.0397296		X		X
EMX1	Homeobox protein EMX1	2.0	0.0004469	X			X
EOMES	Eomesodermin homolog	3.2	$7.41E-14$	X	X	X	X
ETS1	Protein C-ets-1	−1.5	0.0397296	X			X
GDF7	Growth/differentiation factor 7	1.6	0.020917	X	X		
HMGA2	High mobility group protein HMGI-C	1.7	0.0008172			X	X
ITGB5	Integrin beta-5	−1.2	0.0247298			X	
LEF1	Lymphoid enhancer-binding factor 1	1.9	$1.15E-05$	X			X
LHX6	LIM/homeobox protein Lhx6	−1.8	0.0010726	X			X
LMX1A	LIM homeobox transcription factor 1-alpha	1.5	0.0452728	X			X
LRRK2	Leucine-rich repeat serine/threonine-protein kinase 2	−1.6	0.0284824	X			
MMP14	Matrix metalloproteinase-14	−1.1	0.0409523			X	
NEUROD1	Neurogenic differentiation factor 1	−1.1	0.0409523	X	X		X
NEUROD6	Neurogenic differentiation factor 6	4.0	$1.06E-21$	X			X
NEUROG1	Neurogenin-1	1.5	0.0385899		X		X
OTX1	Homeobox protein OTX1	1.8	0.0035067	X			X

[a]relative to expression in Ctl-iPSC GABA.
[b]adjusted p-value after Bonferroni correction.
[c]X indicates gene is contained in the GO terms biological process: FD, forebrain developent; CFC, cell fate committment; ECD, endodermal cell differentiation.
[d]X indicates gene is contained in the GO terms molecular function: TF, transcription regulator activity.

ZEB2 haploinsufficiency. Because of the limited number of biological replicates available (df = 2) in our study we did not expect to detect subtle gene expression differences between the two groups. We therefore used DESeq2 to identify the most pronounced changes in MWS subject derived iPSC (Schurch et al., 2016). The analysis highlights a set of co-dysregulated genes in MW-iPSC GABA cells that are markedly enriched in transcriptional regulation and in interconnected biological processes. The gene expression pattern in the ZEB2 haploinsufficient neural model revealed an attenuated and immature identity of ZEB2 haploinsufficient GABAergic cells, with features of excitatory, glutamatergic and midbrain neuronal cells. For example, in MW-iPSC NSC we observed downregulation of the pan-telencephalic marker *FOXG1* acting as a suppressor of *NEUROG2* expression (Yang et al., 2017; Cargnin et al., 2018). Consequently, we observed increased expression of *NEUROG2,* as well as of *NEUROG1* that inhibits neocorticogenesis, and their downstream targets *NEUROD1*, *NEUROD4* and *NEUROD6* (Schuurmans et al., 2004; Tutukova et al., 2021). The TF NEUROG2 suppresses the microglia program and compromises GABAergic subtype specification (Roybon et al., 2010; Matsuda et al., 2019) while promoting the differentiation of cortical deep layer glutamatergic neurons together with NEUROD1, NEUROD4, and NEUROD6 (Gascon et al., 2017; Han et al., 2018). Since *FOXG1* was identified as a ZEB2 target gene from available ChiP seq data, our ZEB2 haploinsufficient model thus suggests a dysregulation of the transcriptional axis for GABAergic development involving the TFs ZEB2-FOXG1-NEUROG-NEUROD. In addition, MW-GABA cells showed a marked increase in expression of the TF genes *EMX1*, *EOMES/TPR2*, *LMX1* and *LEF1* promoting organization of excitatory progenitor cells in the pallium

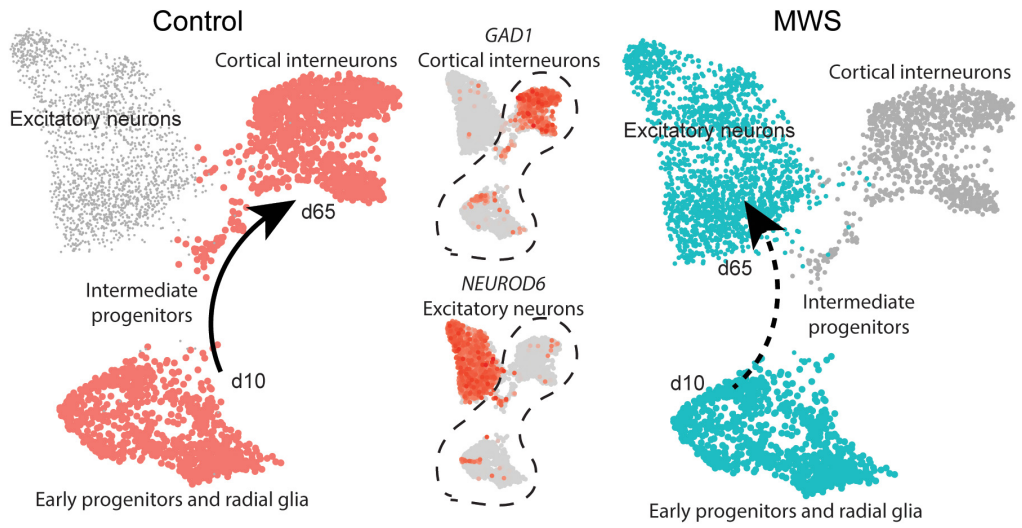

FIGURE 4
MW-iPSC with ZEB2 haploinsufficiency exhibit an aberrant interneuronal differentiation trajectory. The expression levels of *GAD1* and *NEUROD6* in Ctl-iPSC GABA (n = 2) and MW-iPSC GABA from RNAseq were inferred on pseudo-time trajectories of human cortex development. The expression of both genes in Ctl-iPSC GABA (left) are consistent with expression following the expected trajectory of cortical interneurons (Control, cell types highlighted in red). In MW-iPSC derived neural cells (MWS), the *GAD1* and *NEUROD6* expression suggests an early trajectory reminiscent of that for excitatory neuronal subtypes (dashed arrow).

(Kobeissy et al., 2016; Armenteros et al., 2018; Hevner, 2019; Lv et al., 2019; Nouri et al., 2020). In the mouse model depleted of Zeb2 in the medial ganglionic eminence (MGE) from E9, the Zeb2 induced repression of Nkx2-1 is lost leading to cortical interneurons transformed toward a striatal interneuronal subtype characterized by TACR1, NPY, nNOS, and SST expression (McKinsey et al., 2013). Our RNA-seq data from ZEB2 haploinsufficient GABAergic cells d65 showed only a tendency for downregulation of *NKX2-1* together with the striatal markers *TACR1, NPY, NRP1*, and *NOS1*. The reason for the different expression pattern of some striatal markers in our system when compared to the mouse model is unclear but a possible explanation for the incomplete repression of NKX2-1 is the remaining expression of *ZEB2* from the w.t. allele. Another contributing reason could be the differentiation protocol and the 2D culture system used in our study that strongly promotes neocortical lineages.

In mice, the conditional depletion of neural Zeb2 results in a partially stalled migration of cortical Lhx6 positive interneurons (McKinsey et al., 2013) and a misrouting into the ventral and caudal part of telencephalon (van den Berghe et al., 2013). The DNA binding protein LHX6 promotes SST expression, tangential migration, specification and laminar positioning of GABAergic interneurons (Liodis et al., 2007; Miyoshi and Fishell, 2011; Kessaris et al., 2014; Kim et al., 2021). In line with neural Zeb2 deficiency in mice, we observed a reduced expression of *LHX6* in MW-iPSC GABA cells and a marked migration deficiency in MW-iPSC NSCs uncovered by our wound healing assay. These findings support a perturbed GABAergic development and a disrupted program for interneuronal migration in our ZEB2 haploinsufficient model that are relevant for the developmental brain abnormalities observed in MWS subjects.

GABAergic interneurons are critical to maintain the balance between neuronal excitation and inhibition for proper cortical functions. Consistent with this role, malfunction of inhibitory interneurons has been associated with different types of epilepsy. Our multilayer STRING analysis of known epilepsy associated genes together with the 105 DEGs identified in our study uncovered extensive connections, suggesting downstream effects of ZEB2 haploinsufficient GABAergic development on pathways and factors interfering with ictal activity. This is supported by the electrophysiological properties in our MWS model of GABAergic interneurons. Action potentials were considerably fewer and did not respond to increased current injections in MW-iPSC GABA when compared to Ctl-iPSC GABA cells, possibly because of a concomitant reduced peak latency and impaired ability to re-polarize in response to stimuli. Our observations from whole cell patch-clamp analysis of ZEB2 haploinsufficient GABAergic inhibitory interneurons thus indicate a hypoexcitable cell phenotype with impaired responses to stimuli that may contribute to seizures observed in the majority of cases with MWS.

Among its versatile functions, ZEB2 plays a critical role for neuroectoderm formation, ectodermal-to-mesenchymal

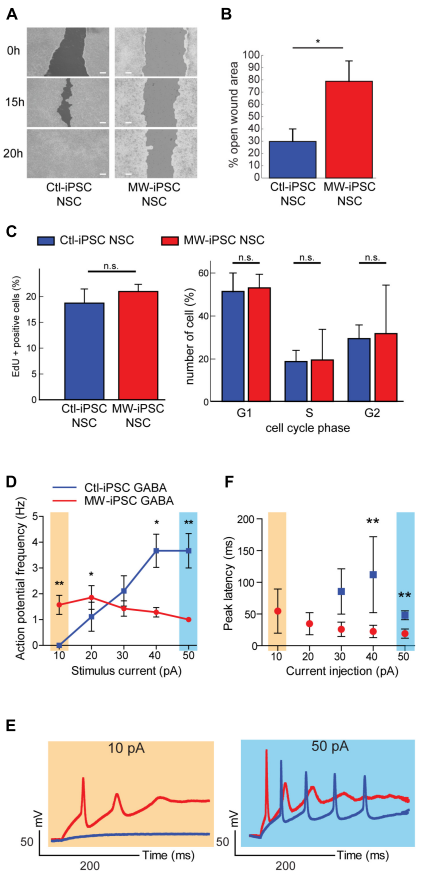

FIGURE 5
MW-iPSC derived neural cells with ZEB2 haploinsufficiency show impaired migration and altered electrophysiology. **(A,B)** Assessment of cell motility of iPSC-NSCs at day 10 using a wound healing scratch assay shows impaired motility in MW-iPSC NSCs. **(A)** Confluent cultures of MW-iPSC NSCs and Ctl-iPSC NSCs at day 10 were scratched and imaged at identical positions after 0 h, 15 h and 20 h. Representative pictures are shown. Size bar 200 μm. **(B)** Quantification of open wound area in MW-iPSC NSCs and Ctl-iPSC NSCs using TScratch software. The remaining open area was quantified at 15 h vs. 0 h (3 replicates per iPSC line) and significantly larger in MW-iPSC NSCs when compared to Ctl-iPSC NSCs (*$p < 0.05$). **(C)** Assessment of Proliferation of iPSC-NSC at day 10 using EdU proliferation assay and cell cycle analysis show similar proliferation activity of patient and control iPSC derived cells (n.s., not significant; $n = 4$ replicates per cell line). **(D–F)** MW-iPSC GABA cells show aberrant firing of action potentials and shorter peak latency time in response to step current injections. **(D)** The maximal frequency of evoked action potentials (eAPs) was markedly reduced in MW-iPSC GABA cells (red line) as compared to control cells (blue line; eAPs (Hz) plotted versus the stimulus current (pA) used). **(E)** Responses to 10 pA (yellow) (left panel) and 50 pA (blue) (right panel) current injections lasting 500 ms in representative MW-iPSC GABA and Ctl-iPSC GABA cells at a holding potential of −60 mV. At a depolarizing current stimulus of 10 pA the MW-iPSC GABA cells were able to fire single eAPs while Ctl-iPSC GABA cells remained silent. At a depolarizing current stimulus of 50 pA, MW-iPSC GABA cells fired still only single eAPs while Ctl-iPSC GABA cells fired multiple consecutive eAPs. **(F)** The peak latency (delay time; ms) of iPSC-GABA cells in response to the injected stimulus (pA) was significantly reduced in MW-iPSC GABA cells at current injections >30 pA. **$p < 0.005$, *$p < 0.05$.

transition (EMT) and crest cell induction (Epifanova et al., 2018). Accordingly, our ZEB2 haploinsufficient model exhibited altered expression of several factors regulating EMT. For example, upregulation was observed for the TF TFAP2C that maintains pluripotency and promotes mesoderm-to-epithelial transition (MET) by repressing neuroectodermal differentiation (Pastor et al., 2018) as well as of the gene encoding KLHL14, that inhibits EMT (Di Lollo et al., 2020), and HMGA2, promoting EMT (Thuault et al., 2008; Kou et al., 2018). This was accompanied by a downregulation of the ZEB2 target gene ETS1 (Theveneau et al., 2007; Wang et al., 2015; Yalim-Camci et al., 2019), maintaining EMT, together with genes for the extracellular matrix proteins MMP14, ITGB5 and COL8A1 that promote delamination of neural crest cells and EMT induction. These data bring further support for a disturbed cell fate switch during GABAergic development that complies with prior data showing dysregulation of EMT and crest cell induction after ZEB2 downregulation (Van de Putte et al., 2007; Chng et al., 2010), as well as the crest cell derived features associated with MWS (Ivanovski et al., 2018).

Our study of ZEB2 haploinsuffient neural cells focused on GABAergic development because of the key regulatory roles on neural circuitries and for preventing harmful ictal activity, a feature observed in the majority of MWS cases. However, ZEB2 is widely expressed in the developing central and peripheral nervous system. Prior studies have shown *Zeb2* expression in, e.g., oligodendrocytes, Bergmann glia cells and brainstem neurons (Nishizaki et al., 2014). Therefore, a perturbed development of a range of brain cell types are likely in MWS in addition to the effects of ZEB2 haploinsufficiency shown and predicted in our study. More complex models of neural differentiation with ZEB2 haploinsufficiency using, e.g., 3D organoids, build up by a mixture of cell types, followed by single cell transcriptome analysis may add important findings to our study.

Taken together, analysis of our ZEB2 haploinsufficient iPSC model of GABAergic development uncover transcriptional changes consistent with a disrupted cell fate switch and an immature and attenuated identity of inhibitory interneurons. This is associated with impaired migratory capacity in neural progenitor cells and hypoexcitable GABAergic interneurons. The combined findings thus suggest perturbed development and function of GABAergic cells in MWS with implications for the formation of different brain structures and for balancing neuronal circuitries.

Conclusion

We show that an iPSC model of GABAergic development in a ZEB2 haploinsufficient iPSC model

of MWS exhibits dysregulations of specific genes along interneuronal differentiation. The dysregulated genes form an interconnected network enriched for transcriptional regulation, cell fate decision and forebrain formation, with extensive connections to genes implicated in epilepsy. Furthermore, our MWS model of GABAergic development exhibits a gene expression profile mixed with that of midbrain and glutamatergic development, leading to an immature and attenuated GABAergic identity. The transcriptional changes in ZEB2 haploinsufficient neural cells are associated with impaired migration of NSCs and altered electrophysiological properties of GABAergic interneurons that correlate with clinical features observed in MWS. The comprehensive data from our study provide a framework for further studies of neuronal development in MWS with the long-term goal to interfere with brain development and seizures in affected individuals.

Data availability statement

The data presented in this study are deposited in the SciLifeLab data repository, accession number 20472144 (doi: 10.17044/scilifelab.20472144.v1).

Ethics statement

Written informed consent was obtained from the minor(s)' legal guardian/next of kin for the publication of any potentially identifiable images or data included in this article.

Author contributions

JS: conceptualization, methodology, formal analysis, investigation, writing—original draft and review and editing, visualization, and project administration. JK: methodology, software, data curation, writing—review and editing, and visualization. AK, LL, ZJ, and SVK: methodology, formal analysis, and investigation. JH: methodology, validation, and investigation. AF and VS: methodology and investigation. MH: software, validation, data curation, and visualization. AN and BMA: resources. CG: validation, formal analysis, and funding acquisition. BB: software, formal analysis, supervision, and funding acquisition. ND: conceptualization, formal analysis, and writing—review and editing, visualization, supervision, project administration, and funding acquisition. All authors contributed to the article and approved the submitted version.

Funding

This work was supported by the Swedish Research Council 2020-01947 and Hjärnfonden (FO2019-0210 and FO2020-0171), Borgström Foundation (AK), AstraZeneca, Uppsala University Hospital, Uppsala University and Science for Life Laboratory. LL was funded by grants from the Sävstaholm Society. MH was financially supported by the Knut and Alice Wallenberg Foundation as part of the National Bioinformatics Infrastructure Sweden at SciLifeLab. Computations were performed on resources provided by SNIC through Uppsala Multidisciplinary Center for Advanced Computational Science (UPPMAX), transcriptomes were generated at the SNP&SEQ platform and imaging was performed at the BioVis Platform, Science for Life Laboratory, Uppsala University. The funders played no role in study design, data collection and interpretation or decision to publish.

Acknowledgments

We thank the study participants and their parents for cooperation.

Conflict of interest

The authors declare that the research was conducted in the absence of any commercial or financial relationships that could be construed as a potential conflict of interest.

Publisher's note

Supplementary material

The Supplementary Material for this article can be found online at: https://www.frontiersin.org/articles/10.3389/fnmol.2022.988993/full#supplementary-material

References

Adam, M. P., Schelley, S., Gallagher, R., Brady, A. N., Barr, K., Blumberg, B., et al. (2006). Clinical features and management issues in Mowat-Wilson syndrome. *Am. J. Med. Genet. A* 140, 2730–2741. doi: 10.1002/ajmg.a.31530

Armenteros, T., Andreu, Z., Hortiguela, R., Lie, D. C., and Mira, H. (2018). BMP and WNT signalling cooperate through LEF1 in the neuronal specification of adult hippocampal neural stem and progenitor cells. *Sci. Rep.* 8:9241. doi: 10.1038/s41598-018-27581-0

Aslanpour, S., Han, S., Schuurmans, C., and Kurrasch, D. M. (2020). Neurog2 acts as a classical proneural gene in the ventromedial hypothalamus and is required for the early phase of neurogenesis. *J. Neurosci.* 40, 3549–3563. doi: 10.1523/JNEUROSCI.2610-19.2020

Birkhoff, J. C., Huylebroeck, D., and Conidi, A. (2021). ZEB2, the Mowat-Wilson syndrome transcription factor: Confirmations, novel functions, and continuing surprises. *Genes (Basel)* 12:1037. doi: 10.3390/genes12071037

Brinkmann, B. G., and Quintes, S. (2017). Zeb2: Inhibiting the inhibitors in Schwann cells. *Neurogenesis (Austin)* 4:e1271495. doi: 10.1080/23262133.2016.1271495

Cargnin, F., Kwon, J. S., Katzman, S., Chen, B., Lee, J. W., and Lee, S. K. (2018). FOXG1 orchestrates neocortical organization and cortico-cortical connections. *Neuron* 100, 1083.e–1096.e. doi: 10.1016/j.neuron.2018.10.016

Carr, I. M., Robinson, J. I., Dimitriou, R., Markham, A. F., Morgan, A. W., and Bonthron, D. T. (2009). Inferring relative proportions of DNA variants from sequencing electropherograms. *Bioinformatics* 25, 3244–3250. doi: 10.1093/bioinformatics/btp583

Chambers, S. M., Fasano, C. A., Papapetrou, E. P., Tomishima, M., Sadelain, M., and Studer, L. (2009). Highly efficient neural conversion of human ES and iPS cells by dual inhibition of SMAD signaling. *Nat. Biotechnol.* 27, 275–280. doi: 10.1038/nbt.1529

Chng, Z., Teo, A., Pedersen, R. A., and Vallier, L. (2010). SIP1 mediates cell-fate decisions between neuroectoderm and mesendoderm in human pluripotent stem cells. *Cell Stem Cell* 6, 59–70. doi: 10.1016/j.stem.2009.11.015

Close, J. L., Yao, Z., Levi, B. P., Miller, J. A., Bakken, T. E., Menon, V., et al. (2017). Single-cell profiling of an *in vitro* model of human interneuron development reveals temporal dynamics of cell type production and maturation. *Neuron* 93, 1035.e–1048.e. doi: 10.1016/j.neuron.2017.02.014

Dennis, D. J., Han, S., and Schuurmans, C. (2019). bHLH transcription factors in neural development, disease, and reprogramming. *Brain Res.* 1705, 48–65. doi: 10.1016/j.brainres.2018.03.013

Di Lollo, V., Canciello, A., Orsini, M., Bernabo, N., Ancora, M., Di Federico, M., et al. (2020). Transcriptomic and computational analysis identified LPA metabolism, KLHL14 and KCNE3 as novel regulators of epithelial-mesenchymal transition. *Sci. Rep.* 10:4180. doi: 10.1038/s41598-020-61017-y

Dobin, A., Davis, C. A., Schlesinger, F., Drenkow, J., Zaleski, C., Jha, S., et al. (2013). STAR: Ultrafast universal RNA-seq aligner. *Bioinformatics* 29, 15–21. doi: 10.1093/bioinformatics/bts635

Doncheva, N. T., Morris, J. H., Gorodkin, J., and Jensen, L. J. (2019). Cytoscape stringapp: Network analysis and visualization of proteomics data. *J. Proteome Res.* 18, 623–632. doi: 10.1021/acs.jproteome.8b00702

Epifanova, E., Babaev, A., Newman, A. G., and Tarabykin, V. (2018). Role of Zeb2/Sip1 in neuronal development. *Brain Res.* 1705, 24–31. doi: 10.1016/j.brainres.2018.09.034

Galanopoulou, A. S. (2010). Mutations affecting GABAergic signaling in seizures and epilepsy. *Pflugers Arch.* 460, 505–523. doi: 10.1007/s00424-010-0816-2

Garavelli, L., and Mainardi, P. C. (2007). Mowat-Wilson syndrome. *Orphanet J. Rare Dis.* 2:42. doi: 10.1186/1750-1172-2-42

Garavelli, L., Ivanovski, I., Caraffi, S. G., Santodirocco, D., Pollazzon, M., Cordelli, D. M., et al. (2017). Neuroimaging findings in Mowat-Wilson syndrome: A study of 54 patients. *Genet. Med.* 19, 691–700. doi: 10.1038/gim.2016.176

Gascon, S., Ortega, F., and Gotz, M. (2017). Transient CREB-mediated transcription is key in direct neuronal reprogramming. *Neurogenesis (Austin)* 4:e1285383. doi: 10.1080/23262133.2017.1285383

Geback, T., Schulz, M. M., Koumoutsakos, P., and Detmar, M. (2009). TScratch: A novel and simple software tool for automated analysis of monolayer wound healing assays. *Biotechniques* 46, 265–274. doi: 10.2144/000113083

Gouwens, N. W., Sorensen, S. A., Baftizadeh, F., Budzillo, A., Lee, B. R., Jarsky, T., et al. (2020). Integrated morphoelectric and transcriptomic classification of cortical GABAergic cells. *Cell* 183, 935.e–953.e. doi: 10.1016/j.cell.2020.09.057

Guillemot, F., and Hassan, B. A. (2017). Beyond proneural: Emerging functions and regulations of proneural proteins. *Curr. Opin. Neurobiol.* 42, 93–101. doi: 10.1016/j.conb.2016.11.011

Haider, B., Duque, A., Hasenstaub, A. R., and McCormick, D. A. (2006). Neocortical network activity in vivo is generated through a dynamic balance of excitation and inhibition. *J. Neurosci.* 26, 4535–4545. doi: 10.1523/JNEUROSCI.5297-05.2006

Han, S., Dennis, D. J., Balakrishnan, A., Dixit, R., Britz, O., Zinyk, D., et al. (2018). A non-canonical role for the proneural gene Neurog1 as a negative regulator of neocortical neurogenesis. *Development* 145:dev157719. doi: 10.1242/dev.157719

He, L., Yu, K., Lu, F., Wang, J., Wu, L. N., Zhao, C., et al. (2018). Transcriptional regulator ZEB2 is essential for Bergmann glia development. *J. Neurosci.* 38, 1575–1587. doi: 10.1523/JNEUROSCI.2674-17.2018

Hensch, T. K. (2005). Critical period plasticity in local cortical circuits. *Nat. Rev. Neurosci.* 6, 877–888. doi: 10.1038/nrn1787

Hevner, R. F. (2019). Intermediate progenitors and Tbr2 in cortical development. *J. Anat.* 235, 616–625. doi: 10.1111/joa.12939

Huang, Z. J., and Paul, A. (2019). The diversity of GABAergic neurons and neural communication elements. *Nat. Rev. Neurosci.* 20, 563–572. doi: 10.1038/s41583-019-0195-4

Ivanovski, I., Djuric, O., Caraffi, S. G., Santodirocco, D., Pollazzon, M., Rosato, S., et al. (2018). Phenotype and genotype of 87 patients with Mowat-Wilson syndrome and recommendations for care. *Genet. Med.* 20, 965–975. doi: 10.1038/gim.2017.221

Jang, S. S., Kim, S. Y., Kim, H., Hwang, H., Chae, J. H., Kim, K. J., et al. (2019). Diagnostic yield of epilepsy panel testing in patients with seizure onset within the first year of life. *Front. Neurol.* 10:988. doi: 10.3389/fneur.2019.00988

Kepecs, A., and Fishell, G. (2014). Interneuron cell types are fit to function. *Nature* 505, 318–326. doi: 10.1038/nature12983

Kessaris, N., Magno, L., Rubin, A. N., and Oliveira, M. G. (2014). Genetic programs controlling cortical interneuron fate. *Curr. Opin. Neurobiol.* 26, 79–87. doi: 10.1016/j.conb.2013.12.012

Khoshkhoo, S., Vogt, D., and Sohal, V. S. (2017). Dynamic, cell-type-specific roles for GABAergic interneurons in a mouse model of optogenetically inducible seizures. *Neuron* 93, 291–298. doi: 10.1016/j.neuron.2016.11.043

Kim, D. W., Liu, K., Wang, Z. Q., Zhang, Y. S., Bathini, A., Brown, M. P., et al. (2021). Gene regulatory networks controlling differentiation, survival, and diversification of hypothalamic Lhx6-expressing GABAergic neurons. *Commun. Biol.* 4:95. doi: 10.1038/s42003-020-01616-7

Kim, W. Y. (2012). NeuroD1 is an upstream regulator of NSCL1. *Biochem. Biophys. Res. Commun.* 419, 27–31. doi: 10.1016/j.bbrc.2012.01.100

Kobeissy, F. H., Hansen, K., Neumann, M., Fu, S., Jin, K., and Liu, J. (2016). Deciphering the role of Emx1 in neurogenesis: A neuroproteomics approach. *Front. Mol. Neurosci.* 9:98. doi: 10.3389/fnmol.2016.00098

Kou, B., Liu, W., Tang, X., and Kou, Q. (2018). HMGA2 facilitates epithelial-mesenchymal transition in renal cell carcinoma by regulating the TGF-beta/Smad2 signaling pathway. *Oncol. Rep.* 39, 101–108. doi: 10.3892/or.2017.6091

Lim, L., and Marin, O. (2018). More than one way to induce a neuron. *Nature* 557, 316–317. doi: 10.1038/d41586-018-04978-5

Lim, L., Mi, D., Llorca, A., and Marin, O. (2018). Development and functional diversification of cortical interneurons. *Neuron* 100, 294–313. doi: 10.1016/j.neuron.2018.10.009

Liodis, P., Denaxa, M., Grigoriou, M., Akufo-Addo, C., Yanagawa, Y., and Pachnis, V. (2007). Lhx6 activity is required for the normal migration and specification of cortical interneuron subtypes. *J. Neurosci.* 27, 3078–3089. doi: 10.1523/JNEUROSCI.3055-06.2007

Liu, F., Zhang, Y., Chen, F., Yuan, J., Li, S., Han, S., et al. (2021). Neurog2 directly converts astrocytes into functional neurons in midbrain and spinal cord. *Cell Death Dis.* 12:225. doi: 10.1038/s41419-021-03498-x

Love, M. I., Huber, W., and Anders, S. (2014). Moderated estimation of fold change and dispersion for RNA-seq data with DESeq2. *Genome Biol.* 15:550. doi: 10.1186/s13059-014-0550-8

Lv, X., Ren, S. Q., Zhang, X. J., Shen, Z., Ghosh, T., Xianyu, A., et al. (2019). TBR2 coordinates neurogenesis expansion and precise microcircuit organization *via* Protocadherin 19 in the mammalian cortex. *Nat. Commun.* 10:3946. doi: 10.1038/s41467-019-11854-x

Matsuda, T., Irie, T., Katsurabayashi, S., Hayashi, Y., Nagai, T., Hamazaki, N., et al. (2019). Pioneer factor NeuroD1 rearranges transcriptional and epigenetic profiles to execute microglia-neuron conversion. *Neuron* 101, 472.e–485.e. doi: 10.1016/j.neuron.2018.12.010

McKinsey, G. L., Lindtner, S., Trzcinski, B., Visel, A., Pennacchio, L. A., Huylebroeck, D., et al. (2013). Dlx1&2-dependent expression of Zfhx1b (Sip1, Zeb2) regulates the fate switch between cortical and striatal interneurons. *Neuron* 77, 83–98. doi: 10.1016/j.neuron.2012.11.035

Mi, H., Muruganujan, A., Casagrande, J. T., and Thomas, P. D. (2013). Large-scale gene function analysis with the PANTHER classification system. *Nat. Protoc.* 8, 1551–1566. doi: 10.1038/nprot.2013.092

Miller, J. A., Ding, S. L., Sunkin, S. M., Smith, K. A., Ng, L., Szafer, A., et al. (2014). Transcriptional landscape of the prenatal human brain. *Nature* 508, 199–206. doi: 10.1038/nature13185

Miquelajauregui, A., Van de Putte, T., Polyakov, A., Nityanandam, A., Boppana, S., Seuntjens, E., et al. (2007). Smad-interacting protein-1 (Zfhx1b) acts upstream of Wnt signaling in the mouse hippocampus and controls its formation. *Proc. Natl. Acad. Sci. U.S.A.* 104, 12919–12924. doi: 10.1073/pnas.0609863104

Miyoshi, G., and Fishell, G. (2011). GABAergic interneuron lineages selectively sort into specific cortical layers during early postnatal development. *Cereb. Cortex* 21, 845–852. doi: 10.1093/cercor/bhq155

Mowat, D. R., Croaker, G. D., Cass, D. T., Kerr, B. A., Chaitow, J., Ades, L. C., et al. (1998). Hirschsprung disease, microcephaly, mental retardation, and characteristic facial features: Delineation of a new syndrome and identification of a locus at chromosome 2q22-q23. *J. Med. Genet.* 35, 617–623. doi: 10.1136/jmg.35.8.617

Nishizaki, Y., Takagi, T., Matsui, F., and Higashi, Y. (2014). SIP1 expression patterns in brain investigated by generating a SIP1-EGFP reporter knock-in mouse. *Genesis* 52, 56–67. doi: 10.1002/dvg.22726

Nouri, P., Gotz, S., Rauser, B., Irmler, M., Peng, C., Trumbach, D., et al. (2020). Dose-dependent and subset-specific regulation of midbrain dopaminergic neuron differentiation by LEF1-mediated WNT1/b-catenin signaling. *Front. Cell Dev. Biol.* 8:587778. doi: 10.3389/fcell.2020.587778

Nowakowski, T. J., Bhaduri, A., Pollen, A. A., Alvarado, B., Mostajo-Radji, M. A., Di Lullo, E., et al. (2017). Spatiotemporal gene expression trajectories reveal developmental hierarchies of the human cortex. *Science* 358, 1318–1323. doi: 10.1126/science.aap8809

Pastor, W. A., Liu, W., Chen, D., Ho, J., Kim, R., Hunt, T. J., et al. (2018). TFAP2C regulates transcription in human naive pluripotency by opening enhancers. *Nat. Cell Biol.* 20, 553–564. doi: 10.1038/s41556-018-0089-0

Paz, J. T., and Huguenard, J. R. (2015). Microcircuits and their interactions in epilepsy: Is the focus out of focus? *Nat. Neurosci.* 18, 351–359. doi: 10.1038/nn.3950

Pfisterer, U., Petukhov, V., Demharter, S., Meichsner, J., Thompson, J. J., Batiuk, M. Y., et al. (2020). Identification of epilepsy-associated neuronal subtypes and gene expression underlying epileptogenesis. *Nat. Commun.* 11:5038. doi: 10.1038/s41467-020-18752-7

Richards, S., Aziz, N., Bale, S., Bick, D., Das, S., Gastier-Foster, J., et al. (2015). Standards and guidelines for the interpretation of sequence variants: A joint consensus recommendation of the American college of medical genetics and genomics and the association for molecular pathology. *Genet. Med.* 17, 405–424. doi: 10.1038/gim.2015.30

Roybon, L., Mastracci, T. L., Ribeiro, D., Sussel, L., Brundin, P., and Li, J. Y. (2010). GABAergic differentiation induced by Mash1 is compromised by the bHLH proteins Neurogenin2, NeuroD1, and NeuroD2. *Cereb. Cortex* 20, 1234–1244. doi: 10.1093/cercor/bhp187

Schurch, N. J., Schofield, P., Gierlinski, M., Cole, C., Sherstnev, A., Singh, V., et al. (2016). How many biological replicates are needed in an RNA-seq experiment and which differential expression tool should you use? *RNA* 22, 839–851. doi: 10.1261/rna.053959.115

Schuster, J., Laan, L., Klar, J., Jin, Z., Huss, M., Korol, S., et al. (2019a). Transcriptomes of Dravet syndrome iPSC derived GABAergic cells reveal dysregulated pathways for chromatin remodeling and neurodevelopment. *Neurobiol. Dis.* 132:104583. doi: 10.1016/j.nbd.2019.104583

Schuster, J., Sobol, M., Fatima, A., Khalfallah, A., Laan, L., Anderlid, B. M., et al. (2019b). Mowat-Wilson syndrome: Generation of two human iPS cell lines (UUIGPi004A and UUIGPi005A) from siblings with a truncating ZEB2 gene variant. *Stem Cell Res.* 39:101518. doi: 10.1016/j.scr.2019.101518

Schuurmans, C., Armant, O., Nieto, M., Stenman, J. M., Britz, O., Klenin, N., et al. (2004). Sequential phases of cortical specification involve neurogenin-dependent and -independent pathways. *EMBO J.* 23, 2892–2902. doi: 10.1038/sj.emboj.7600278

Sobol, M., Raykova, D., Cavelier, L., Khalfallah, A., Schuster, J., and Dahl, N. (2015). Methods of reprogramming to induced pluripotent stem cell associated with chromosomal integrity and delineation of a chromosome 5q candidate Region for growth advantage. *Stem Cells Dev.* 24, 2032–2040. doi: 10.1089/scd.2015.0061

Stuart, T., Butler, A., Hoffman, P., Hafemeister, C., Papalexi, E., Mauck, W. M. III, et al. (2019). Comprehensive integration of single-cell data. *Cell* 177, 1888.e–1902.e. doi: 10.1016/j.cell.2019.05.031

Sunkin, S. M., Ng, L., Lau, C., Dolbeare, T., Gilbert, T. L., Thompson, C. L., et al. (2013). Allen brain atlas: An integrated spatio-temporal portal for exploring the central nervous system. *Nucleic Acids Res.* 41, D996–D1008. doi: 10.1093/nar/gks1042

Takagi, T., Nishizaki, Y., Matsui, F., Wakamatsu, N., and Higashi, Y. (2015). De novo inbred heterozygous Zeb2/Sip1 mutant mice uniquely generated by germ-line conditional knockout exhibit craniofacial, callosal and behavioral defects associated with Mowat-Wilson syndrome. *Hum. Mol. Genet.* 24, 6390–6402. doi: 10.1093/hmg/ddv350

Theveneau, E., Duband, J. L., and Altabef, M. (2007). Ets-1 confers cranial features on neural crest delamination. *PLoS One* 2:e1142. doi: 10.1371/journal.pone.0001142

Thuault, S., Tan, E. J., Peinado, H., Cano, A., Heldin, C. H., and Moustakas, A. (2008). HMGA2 and Smads co-regulate SNAIL1 expression during induction of epithelial-to-mesenchymal transition. *J. Biol. Chem.* 283, 33437–33446. doi: 10.1074/jbc.M802016200

Tutukova, S., Tarabykin, V., and Hernandez-Miranda, L. R. (2021). The role of neurod genes in brain development, function, and disease. *Front. Mol. Neurosci.* 14:662774. doi: 10.3389/fnmol.2021.662774

Van de Putte, T., Francis, A., Nelles, L., van Grunsven, L. A., and Huylebroeck, D. (2007). Neural crest-specific removal of Zfhx1b in mouse leads to a wide range of neurocristopathies reminiscent of Mowat-Wilson syndrome. *Hum. Mol. Genet.* 16, 1423–1436. doi: 10.1093/hmg/ddm093

Van de Putte, T., Maruhashi, M., Francis, A., Nelles, L., Kondoh, H., Huylebroeck, D., et al. (2003). Mice lacking ZFHX1B, the gene that codes for Smad-interacting protein-1, reveal a role for multiple neural crest cell defects in the etiology of Hirschsprung disease-mental retardation syndrome. *Am. J. Hum. Genet.* 72, 465–470. doi: 10.1086/346092

van den Berghe, V., Stappers, E., Vandesande, B., Dimidschstein, J., Kroes, R., Francis, A., et al. (2013). Directed migration of cortical interneurons depends on the cell-autonomous action of Sip1. *Neuron* 77, 70–82. doi: 10.1016/j.neuron.2012.11.009

Wang, C., Kam, R. K., Shi, W., Xia, Y., Chen, X., Cao, Y., et al. (2015). The proto-oncogene transcription factor Ets1 regulates neural crest development through histone deacetylase 1 to mediate output of bone morphogenetic protein signaling. *J. Biol. Chem.* 290, 21925–21938. doi: 10.1074/jbc.M115.644864

Wang, C., Lee, J. E., Lai, B., Macfarlan, T. S., Xu, S., Zhuang, L., et al. (2016). Enhancer priming by H3K4 methyltransferase MLL4 controls cell fate transition. *Proc. Natl. Acad. Sci. U.S.A.* 113, 11871–11876. doi: 10.1073/pnas.1606857113

Wang, J., Lin, Z. J., Liu, L., Xu, H. Q., Shi, Y. W., Yi, Y. H., et al. (2017). Epilepsy-associated genes. *Seizure* 44, 11–20. doi: 10.1016/j.seizure.2016.11.030

Wang, Y., Xu, C., Xu, Z., Ji, C., Liang, J., Wang, Y., et al. (2017). Depolarized GABAergic signaling in subicular microcircuits mediates generalized seizure in temporal lobe epilepsy. *Neuron* 95, 92.e–105.e. doi: 10.1016/j.neuron.2017.06.004

Yalim-Camci, I., Balcik-Ercin, P., Cetin, M., Odabas, G., Tokay, N., Sayan, A. E., et al. (2019). ETS1 is coexpressed with ZEB2 and mediates ZEB2-induced epithelial-mesenchymal transition in human tumors. *Mol. Carcinog.* 58, 1068–1081. doi: 10.1002/mc.22994

Yang, Y., Shen, W., Ni, Y., Su, Y., Yang, Z., and Zhao, C. (2017). Impaired interneuron development after foxg1 disruption. *Cereb. Cortex* 27, 793–808. doi: 10.1093/cercor/bhv297

Zweier, C., Albrecht, B., Mitulla, B., Behrens, R., Beese, M., Gillessen-Kaesbach, G., et al. (2002). "Mowat-Wilson" syndrome with and without hirschsprung disease is a distinct, recognizable multiple congenital anomalies-mental retardation syndrome caused by mutations in the zinc finger homeo box 1B gene. *Am. J. Med. Genet.* 108, 177–181. doi: 10.1002/ajmg.10226

frontiers | Frontiers in Molecular Neuroscience

TYPE Review
PUBLISHED 29 November 2022
DOI 10.3389/fnmol.2022.1072475

OPEN ACCESS

EDITED BY
Estela Maris Muñoz,
CONICET Dr. Mario H. Burgos Institute of Histology and Embryology (IHEM), Argentina

REVIEWED BY
Flavio S. J. De Souza,
CONICET – Institute of Physiology, Molecular Biology and Neurosciences (IFIBYNE), Argentina
Mitsuhiro Hashimoto,
Fukushima Medical University, Japan

*CORRESPONDENCE
Luis R. Hernandez-Miranda
luis.hernandez-miranda@charite.de

SPECIALTY SECTION
This article was submitted to Neuroplasticity and Development, a section of the journal Frontiers in Molecular Neuroscience

RECEIVED 17 October 2022
ACCEPTED 14 November 2022
PUBLISHED 29 November 2022

CITATION
Xia Y, Cui K, Alonso A, Lowenstein ED and Hernandez-Miranda LR (2022) Transcription factors regulating the specification of brainstem respiratory neurons.
Front. Mol. Neurosci. 15:1072475.
doi: 10.3389/fnmol.2022.1072475

Transcription factors regulating the specification of brainstem respiratory neurons

Yiling Xia[1], Ke Cui[1], Antonia Alonso[2,3], Elijah D. Lowenstein[4] and Luis R. Hernandez-Miranda[1]*

[1]The Brainstem Group, Institute for Cell Biology and Neurobiology, Charité Universitätsmedizin Berlin, Corporate Member of Freie Universität Berlin and Humboldt-Universität zu Berlin, Berlin, Germany, [2]Functional Genoarchitecture and Neurobiology Groups, Biomedical Research Institute of Murcia (IMIB-Arrixaca), Murcia, Spain, [3]Department of Human Anatomy and Psychobiology, Faculty of Medicine, University of Murcia, Murcia, Spain, [4]Developmental Biology/Signal Transduction, Max Delbrück Center for Molecular Medicine, Berlin, Germany

Breathing (or respiration) is an unconscious and complex motor behavior which neuronal drive emerges from the brainstem. In simplistic terms, respiratory motor activity comprises two phases, inspiration (uptake of oxygen, O_2) and expiration (release of carbon dioxide, CO_2). Breathing is not rigid, but instead highly adaptable to external and internal physiological demands of the organism. The neurons that generate, monitor, and adjust breathing patterns locate to two major brainstem structures, the pons and medulla oblongata. Extensive research over the last three decades has begun to identify the developmental origins of most brainstem neurons that control different aspects of breathing. This research has also elucidated the transcriptional control that secures the specification of brainstem respiratory neurons. In this review, we aim to summarize our current knowledge on the transcriptional regulation that operates during the specification of respiratory neurons, and we will highlight the cell lineages that contribute to the central respiratory circuit. Lastly, we will discuss on genetic disturbances altering transcription factor regulation and their impact in hypoventilation disorders in humans.

KEYWORDS

transcription factors, brainstem development, progenitor domains, neuronal specification, respiratory neurons

Introduction

In vertebrates, the developing brainstem generates an enormous diversity of neuron types that control bodily homeostasis and process multiple modalities of sensory information (Nieuwenhuys, 2011; Puelles et al., 2013; Venkatraman et al., 2017). These neurons vary not only in their morphological, chemical, and electrophysiological properties, but also in their connectivity patterns that allow them to form elaborate

circuits, such as those required to generate, monitor, and adjust breathing to meet various external and internal physiological demands. How this neuronal diversity emerges during development and how it contributes to functional circuits has been intensively investigated by many generations of neuroscientists, as well as by cellular, molecular, and developmental biologists.

The work of these brainstem enthusiasts has already revealed that neuronal diversity in this brain region depends on the temporal and spatial patterning of local neural progenitors (Gray, 2008, 2013; Alexander et al., 2009; Hernandez-Miranda et al., 2017a; van der Heijden and Zoghbi, 2020; Isik and Hernandez-Miranda, 2022). This patterning is first achieved by early diffusible cues that impose an anterior-posterior identity, and subsequently by other morphogens that provide a distinctive dorsal-ventral molecular signature to progenitor cells. This means that distinct progenitor cells can be distinguished primarily based on their differential expression of numerous transcription factors that commit them to generate specific neuron types. Most transcription factors normally expressed in progenitor cells are later silenced in their progeny, which allows for the postmitotic maturation of the differentiated neurons. At the same time, each neuron type can also be characterized by the expression of particular sets of transcription factors that form part of their cell physiology and identity.

In this review, we aim to summarize our current knowledge on the transcriptional programs that allow for the speciation of brainstem respiratory neurons. We will first present a general overview of the anterior-posterior and dorsal-ventral patterning of the developing brainstem as an entry point to understand its neuronal diversity. Next, we will focus on the specification of three large groups of neurons that play key roles in respiration: (i) the pontine groups, (ii) the dorsal medullary respiratory column, and (iii) the ventral medullary respiratory column. These neurons locate to the pons and the medulla oblongata where they perform a variety of functions, such as respiratory rhythm generation, respiratory modulation, and tissue gas monitoring. Lastly, we will discuss some genetic disturbances that affect breathing and respiratory neuron specification.

Anterior to posterior patterning of the developing brainstem

Brainstem development is an evolutionary conserved process that begins with the specification of the mesencephalon (midbrain) and rhombencephalon (hindbrain) by the isthmic organizer. This organizer is located at the midbrain-hindbrain border and produces diffusible morphogens (particularly Wnt1 and Fgf8 ligands) that act directly on the neighboring nervous tissue to impose midbrain and hindbrain cell fates (Zervas et al., 2004; Dworkin et al., 2012; Gibbs et al., 2017; Gutzman et al., 2018; Hidalgo-Sanchez et al., 2022). Various transcription factors are differentially expressed anterior and posterior to the isthmic organizer, such as the antagonistic homeodomain factors *Otx2* (anterior) and *Gbx2* (posterior), whose expression defines the rostral and caudal regions of the developing central nervous system (**Figure 1A**; Millet et al., 1996, 1999; Broccoli et al., 1999; Hidalgo-Sanchez et al., 1999; Joyner et al., 2000; Katahira et al., 2000; Di Giovannantonio et al., 2014). Alterations in the expression of *Otx2* and *Gbx2* are catastrophic for early brainstem development. For instance, the ablation of *Otx2* and its closely related family member *Otx1* results in the loss of midbrain tissue, which becomes re-specified into more rostral hindbrain-like regions, such as the cerebellum (Acampora et al., 1997; Suda et al., 1997; Meyers et al., 1998). Similarly, the misexpression of *Gbx2* disrupts the correct positioning of the isthmic organizer and the development of rostral hindbrain (Acampora et al., 1997; Wassarman et al., 1997; Millet et al., 1999; Puelles et al., 2003; Waters and Lewandoski, 2006).

The regulation of both *Otx2* and *Gbx2* largely depends on a complex molecular network that centers on the instructive signals of Fgf8 (**Figure 1B**; Crossley et al., 1996; Meyers et al., 1998; Martinez et al., 1999; Matsunaga et al., 2002; Chi et al., 2003; Prakash et al., 2006). About embryonic (E) 7.5 in mice, *Fgf8* expression is activated by the diffusible ligand Fgf4 (from the notochord) that directly induces the presumptive midbrain tissue to express the transcription factor *En1*, which in turns activates *Fgf8* expression in the isthmic organizer (Shamim et al., 1999). Two *Fgf8* isoforms appear to differentially act on the specification of the midbrain and rostral hindbrain. *Fgf8a* safeguards midbrain identities, while *Fgf8b* directs rostral hindbrain development. It is important to note that the expression of both isoforms is indispensable for the development of the midbrain and the hindbrain (Lee et al., 1997; Liu et al., 1999, 2003; Sato et al., 2001; Guo and Li, 2007). Notably, the duration of *Fgf8* expression in the isthmic organizer is crucial, as available evidence shows that its sustained expression is required to restrict *Otx2* rostral to the isthmic organizer, while simultaneously maintaining *Gbx2* caudal to it (Liu et al., 1999; Martinez et al., 1999; Sato and Joyner, 2009). In addition to controlling the expression patterns of *Otx2* and *Gbx2*, Fgf8 induces the expression of the homeodomain transcription factor *Lmx1b*, which primary function is to stabilize *Wnt1* expression in the isthmic organizer. In this regard, several studies show that the concomitant ablation of *Lmx1b* and its family member *Lmx1a* severely alters the specification of the hindbrain, which adopts a "spinal cord-like" fate in *Lmx1a* and *Lmx1b* double mutant mice (Mishima et al., 2009; Su et al., 2014; Glover et al., 2018; Chizhikov et al., 2021). Thus, the establishment of the midbrain–hindbrain border, a prerequisite for brainstem development, relies on a complex molecular network of various transcription factors and signaling cascades (briefly summarized in **Figure 1B**).

Soon after the establishment of the isthmic organizer, the hindbrain undergoes a series of morphological changes that

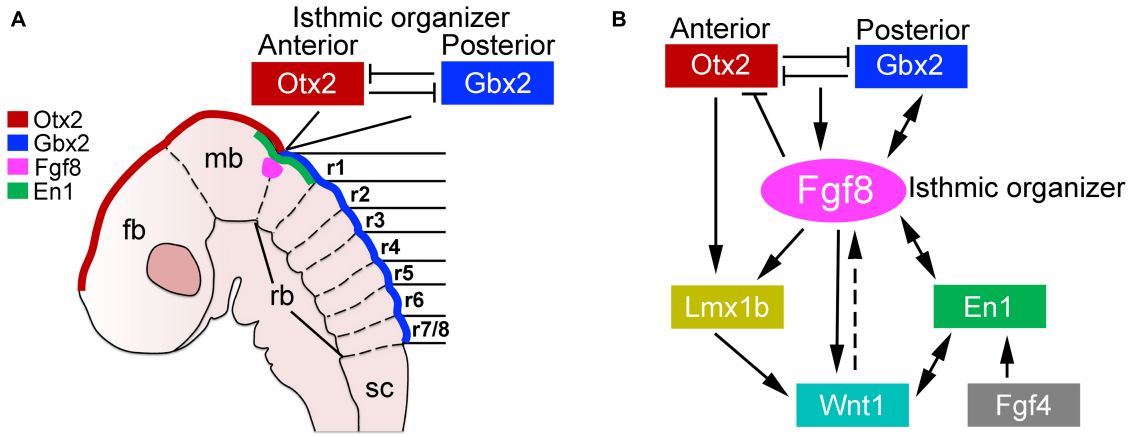

FIGURE 1
Development of the midbrain-hindbrain border. **(A)** Schema illustrating the molecular and anatomical establishment of the anterior and posterior brain regions by the expression of *Otx2* and *Gbx2*, respectively, in a developing mouse embryo (between E8-E8.5). The forebrain (fb), midbrain (mb), rhomboencephalon (rb), and spinal cord (sc) are indicated. The transient morphological segments of the rhombencephalon (rhombomeres, r) are also illustrated. **(B)** Molecular networks acting in the midbrain–hindbrain border for the establishment of the isthmic organizer (see the text). This figure is adapted from our previous publication Lowenstein et al. (2022) that was published under the terms of the Creative Commons Attribution License, which permits unrestricted use and redistribution, provided that the original author and source are credited (https://creativecommons.org/licenses/by/4.0/).

transiently divide it into seven or eight smaller segments called rhombomeres, from which the cerebellum, pons and medulla oblongata emerge (Bally-Cuif and Wassef, 1995; Lumsden and Krumlauf, 1996). In mice, these segments are recognizable at E8.5, whereas in humans they appear by E29 (**Figure 1A**; Lumsden and Krumlauf, 1996). Each of these rhombomeres develops a specific set of cellular and molecular features that distinguishes them from the adjacent nervous tissue. Although still unclear, recent anatomical studies indicate that some of rhombomeres might be further regionalized according to the expression of some patterning genes (Tomas-Roca et al., 2016; Watson et al., 2017, 2019; Hirsch et al., 2021). An interesting trait in the "rhombomerization" of the hindbrain is the differential expression of the Hox superfamily of transcription factors, whose expression creates molecular codes that coincides with the morphological borders of each rhombomere (**Figure 2**; Fienberg et al., 1987; Fraser et al., 1990; Krumlauf et al., 1993; Alexander et al., 2009). One should note that these transcriptional codes are not limited to the hindbrain, as some members of the Hox family are differentially expressed in the developing spinal cord, from which the characteristic cervical, thoracic, lumbar, sacral and coccygeal levels emerge (Alexander et al., 2009). In addition to Hox genes, several other transcription factors show rhombomeric specific expression patterns during early hindbrain development, such as *Pax2* in rhombomere 1, *Meis2* in rhombomeres 2 and 3, *Egr2* (formely known as *Krox20*) in rhombomeres 3 and 5, and *MafB* (previously called *Kreisler*) in rhombomeres 5 and 6 (**Figure 2**; Seitanidou et al., 1997; Rowitch et al., 1999; Bouchard et al., 2000, 2005; Voiculescu et al., 2001; Choe et al., 2002; Manzanares et al., 2002; Giudicelli et al., 2003; Aragon et al., 2005; Stedman et al., 2009). The timely expression of hox genes, as well as the above mentioned transcription factors, is essential for the correct development of each rhombomere and significantly depends on active derivatives of vitamin A, such as retinoic acid (Gavalas and Krumlauf, 2000). Indeed, dietary deficiencies in vitamin A produce gross disturbances in hindbrain "rhombomerization" that can lead to the complete absence of caudal rhombomeres, as manifested by the loss of specific genes and neuron types normally produced in these regions (Gavalas and Krumlauf, 2000; Glover et al., 2006; Kam et al., 2012; Addison et al., 2018). Thus, early brainstem development relies on the function of diffusible ligands (i.e., Fgf8 and retinoids) that determine its anterior-posterior identity.

Dorsal to ventral patterning of the developing brainstem

Once the brainstem acquires its anterior-posterior identity, a second series of diffusible cues further pattern the identity of progenitor cells along its dorsal-ventral axis. During this patterning, the ventralizing Sonic hedgehog (produced by the floor plate), as well as the dorsalizing bone morphogenetic proteins and Wnt ligands (secreted by the roof plate) create concentration gradients that differentially signal onto brainstem progenitor cells (Roelink et al., 1995; Liem et al., 1997; Lee et al., 1998, 2000; Muroyama et al., 2002; Ulloa and Marti, 2010; Hernandez-Miranda et al., 2017a). These gradients create a great

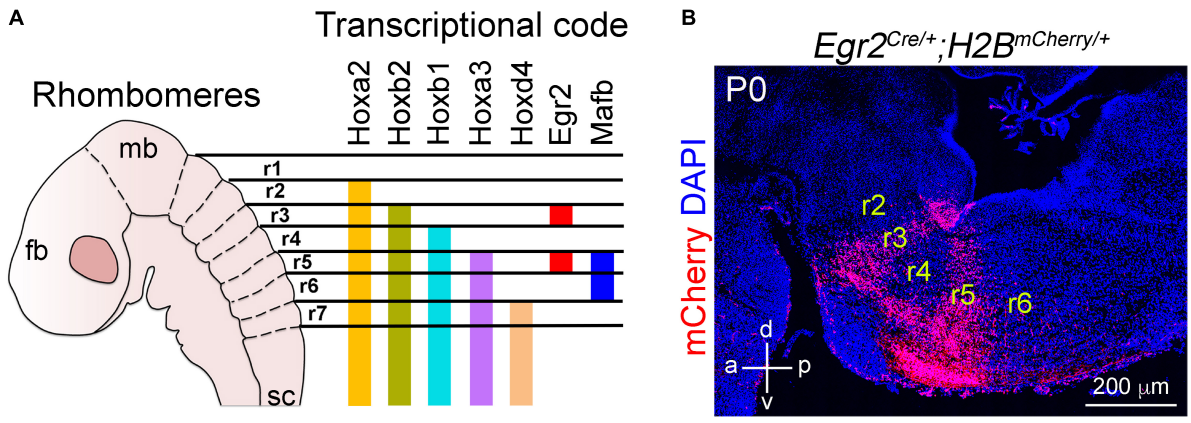

FIGURE 2
Anterior to posterior patterning of the developing brainstem. **(A)** Schema illustrating the segmentation of the brainstem into rhombomeres (r) and selected transcription factors differentially express within these rhombomeres. For more details on Hox gene expression in the developing hindbrain please see Alexander et al. (2009). **(B)** A sagittal section of the mouse brainstem stained with antibodies against mCherry and counterstained with DAPI. The section is taken from $Egr2^{Cre/+};H2B^{mCherry/+}$ mice at birth (P0). In these mice, only r3 and r5 neural derivatives express the nuclear mCherry protein after Cre mediated recombination. This figure is adapted from our previous publication Isik and Hernandez-Miranda (2022) in Handbook of Clinical Neurology, Chapter 5, entitled Early development of the breathing network, published by Elsevier Books. The license number 5392080585902 between Hernandez-Miranda, Charite Universitätsmedizin Berlin and Elsevier allows us to reuse it in a journal/magazine.

diversity of molecularly distinct progenitor domains that vary depending on their spatial distance from the signaling source (**Figure 3** and **Table 1**).

Depending on the rhombomere, six to eight progenitor domains can be distinguished in the dorsal (also known as the alar plate) aspect of the developing hindbrain, while four to five progenitor domains can be identified in its ventral (or basal) plate (**Figure 3**). Outstandingly, there exist great resemblance between the developing hindbrain and the spinal cord, in terms of progenitor domains that locate to their dorsal-ventral axis, which share similar gene expression patterns, illustrating common developmental programs that occur between these two nervous system regions (Gray, 2008, 2013; Di Bonito and Studer, 2017; Hernandez-Miranda et al., 2017a; van der Heijden and Zoghbi, 2020; Diek et al., 2022). In the dorsal-most part of the alar plate, the combinatorial expression of the basic Helix-loop-Helix (bHLH) transcription factor *Olig3* with other bHLH genes distinguishes four progenitor domains that give rise to dorsal (d) class A neurons: dA1, dA2, dA3, and dA4 (**Figure 3** and **Tables 1**, **2** for a list of genes expressed in these progenitors and postmitotic neurons) (Muller et al., 2005; Zechner et al., 2007; Liu et al., 2008; Storm et al., 2009). Ventral to class A progenitors, the alar plate contains four more progenitor domains that collectively generate class B neurons that express and depend on the homeodomain factor *Lbx1* for their proper specification (Gross et al., 2002; Muller et al., 2002; Cheng et al., 2005; Sieber et al., 2007; Pagliardini et al., 2008). The combinatorial expression of *Lbx1* with additional homeodomain transcription factors demarcates class B neurons into four types: dB1, dB2, dB3, and dB4 (**Figure 3** and **Tables 1**, **2**). Like in the alar plate, progenitor cells of the basal plate exhibit specific molecular codes of transcription factor expression that impose distinctive identities to at least five major neuron types: ventral (V) 0, V1, and V2 interneurons as well as somatic motor and vicero/branchio motor neurons (**Figure 3** and **Tables 1**, **2**; Gray, 2008, 2013; Alaynick et al., 2011; Di Bonito and Studer, 2017; van der Heijden and Zoghbi, 2020).

Thus, complex networks of signaling cues pattern the developing brainstem along its anterior-posterior and dorsal-ventral axes to form a molecular grid of longitudinally and transversely distinct progenitor domains, each displaying a particular molecular code of transcription factor expression that singles out the specification of particular neuron types. In the following sections we will discuss the current knowledge of the transcriptional codes that safeguard the specification of pontine and medullary neurons that form the central respiratory circuits in the hindbrain, which collectively generate, monitor and modulate breathing (**Figure 4**).

Development of the anterior respiratory groups

These respiratory groups locate to the pons and include two major structures: (i) the dorso-lateral parabrachial complex and its associated Kölliker-Fuse nucleus (for simplicity here shortened to parabrachial/Kölliker-Fuse complex) that surrounds the cerebellar peduncle, and (ii) the intertrigeminal (also known as the peritrigeminal) region that surrounds the trigeminal motor nucleus. The parabrachial/Kölliker-Fuse

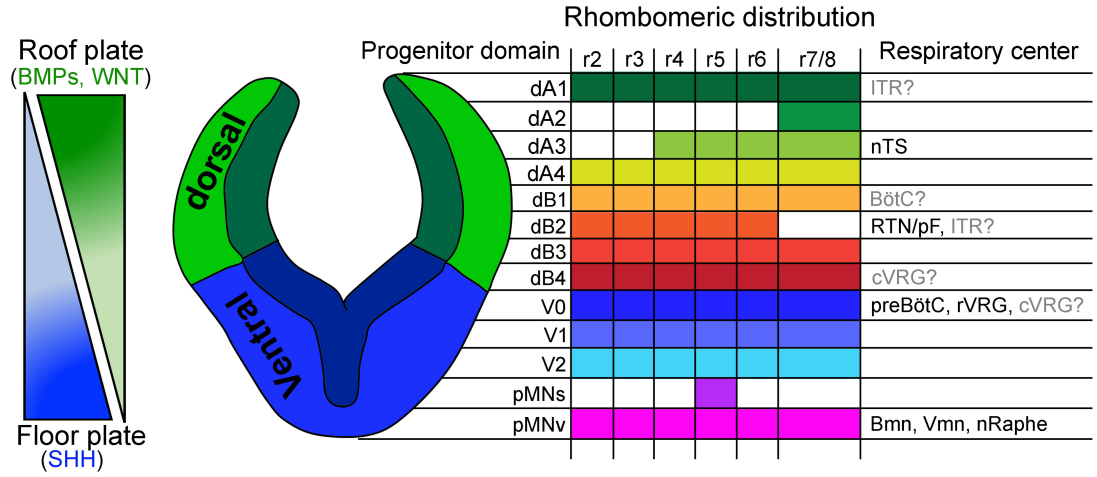

FIGURE 3
Dorsal to ventral patterning of the developing brainstem. Left, schema illustrating concentration gradients formed by the diffusion of bone morphogenic proteins (BMPs)/WNTs and Sonic hedgehog (SHH) morphogens produced by the roof and floor plate, respectively. Right, schema illustrating a transverse section of the developing hindbrain and the patterning of 13 progenitor domains along its dorsal-ventral axis. These progenitors emerge from the differential action of BMP/WNT/SHH concentration gradients. The rhombomeric distribution of each progenitor domain and contribution to brainstem respiratory centers are indicated. Of note, the origin of the intertrigeminal region (ITR), Bötzinger complex (BötC) and caudal ventral respiratory group (cVRG) has not been conclusively determined (see text). nTS, nucleus tractus solitarius; RTN/pF, retrotrapezoid/parafacial nucleus; preBötC, preBötzinger complex; rVRG, rostral ventral respiratory group; Bmm, branchial motor neurons; Vmn, visceral motor neurons; nRaphe, Raphe nuclei. This figure is adapted from our previous publication Isik and Hernandez-Miranda (2022) in Handbook of Clinical Neurology, Chapter 5, entitled Early development of the breathing network, published by Elsevier Books. The license number 5392080585902 between Hernandez-Miranda, Charite Universitätsmedizin Berlin and Elsevier allows us the reuse of it in a journal/magazine.

TABLE 1 Transcription factors expressed in progenitor domains of the developing hindbrain.

Early progenitor domains	bHLH transcription factors	Homeodomain transcription factors
dA1	Olig3, Atoh1	Pax3, Msx1
dA2	Olig3, Ngn1, Ngn2	Pax3, Pax7^{low}, Msx1
dA3	Olig3, Ascl1, Ngn2	Pax3, Pax6, Pax7, Gsx2
dA4	Olig3, Ascl1, Ngn2, Ptf1a	
dB1	Ascl1, Ngn2, Ptf1a	Pax3, Pax6, Pax7, Gsx1/2
dB2		Phox2b
dB3	Ascl1	Pax3, Pax6, Pax7, Gsx1/2, Dbx2
dB4	Ngn1, Ngn2	Pax3, Pax6, Pax7, Dbx2
V0	Ngn1, Ngn2	Dbx1, Dbx2, Pax6, Pax7
V1	Ngn1, Ngn2	Dbx2, Pax6, Nkx6.2
V2	Ngn1, Ngn2	Dbx2, Pax6, Nkx6.1, Nkx6.2
MNs	Olig2	Pax6
MNv	Ascl1	Phox2b (early), Nkx2.2, Nkx2.9

complex is key in the transition phase between inspiration and expiration. It is classically considered the major component of the pontine pneumotaxic center that controls the amount of air inspired in each breath by providing an off-switch for inspiration (Chamberlin and Saper, 1994; Alheid et al., 2004; Song et al., 2006). The function of the intertrigeminal region is yet to be defined, although available evidence suggests that this region might be an anti-apneic breathing center (Radulovacki et al., 2003, 2004a,b; Stoiljkovic et al., 2009; van der Heijden and Zoghbi, 2018).

Using conditional mutagenesis and lineage-tracing experiments, the group of Huda Y. Zoghbi has studied the development of these pontine groups to great effect. These studies show that both the parabrachial/Kölliker-Fuse complex and intertrigeminal region depend on the bHLH transcription factor *Atoh1* (formerly called *Math1*) for their development, as ablation of *Atoh1* results in the absence of these pontine groups

TABLE 2 Transcription factors expressed in neuronal cell types emerging from the developing hindbrain.

Early born neuron types	Transcription factors
dA1	Pou4f1, Barh1, Lhx2, Lhx9, Evx1
dA2	Pou4f1, Lhx1, Lhx5, Foxp2
dA3	Tlx3, Phox2b, Lmx1b
dA4	Foxd3, Foxp2
dB1	Lbx1, Pax2, Lhx1, Lhx5
dB2	Lbx1, Phox2b, Atoh1
dB3	Lbx1, Tlx3, Lmx1b, Prrxl1,
dB4	Lbx1, Pax2, Lhx1, Lhx5, Wt1, bHLHb5, Dmrt3
V0	Evx1, Pax2, Lhx1/5
V1	En1, Pax2, Lhx1/5
V2	Chx10, Sox14, Sox21
PMNs	Isl1/2
PMNv	Phox2b, Isl1/2 (visceral motor neurons) Gata2, Gata3, Lmx1b and Pet1 (Raphe neurons)

in mice (Wang et al., 2005; Rose et al., 2009a,b). Recently, Van der Heijden and Zoghbi traced the rhombomeric origin of the parabrachial/Kölliker-Fuse complex to rhombomere 1, whereas they identified the intertrigeminal region to derive from rhombomere 2 (van der Heijden and Zoghbi, 2018). One should recall that rhombomere 1 development depends on the correct expression of *En1*, whereas *Hoxa2* is the most rostral Hox gene expressed in the developing hindbrain and delimits the border between rhombomeres 1 and 2 (**Figures 1**, **2**). The importance of neurons derived from *En1*-expressing cells to respiration has not been specifically investigated, but an early report showed that *En1* null mutant mice die at birth and present with severe malformations of the cerebellum, midbrain and the parabrachial/Kölliker-Fuse complex (Wurst and Bally-Cuif, 2001). Chatonnet et al. (2007) first explored the function of *Hoxa2*-expressing neurons in respiration in the 2000s, whose work unveiled marked respiratory phenotypes and neonatal death in *Hoxa2* null mutant mice. However, the loss of numerous brainstem structures in these mutant mice precluded the identification of the particular respiratory neurons lost by the constitutive ablations of *En1* or *Hoxa2*.

In the more recent van der Heijden and Zoghbi study, the ablation of *Atoh1* from En1-expressing cells, using $En1^{Cre/+};Atoh1^{LacZ/Flox}$ mice, leads to the absence of a recognizable parabrachial/Kölliker-Fuse complex (van der Heijden and Zoghbi, 2018). Physiologically, the absence of this respiratory group does not affect basal respiratory parameters, although spontaneous apneas and frequent sighing behavior is observed in $En1^{Cre/+};Atoh1^{LacZ/Flox}$ mice. Notably, the specific elimination of the parabrachial/Kölliker-Fuse complex impairs respiratory chemoreflexes to hypoxia (low oxygen) and hypercarbia (high carbon dioxide). Despite the fact the parabrachial/Kölliker-Fuse complex does not sense changes in blood gases by itself, it is known to form reciprocal connections with the nucleus tractus solitarius, a center known to mediate respiratory chemoreflexes (Alheid et al., 2004, 2011; Hernandez-Miranda et al., 2017b). Thus, the loss of communication between the nucleus tractus solitarius and the parabrachial/Kölliker-Fuse complex might account for the impaired chemoreflexes observed in $En1^{Cre/+};Atoh1^{LacZ/Flox}$ mutants. In addition, van der Heijden and Zoghbi restricted the ablation of *Atoh1* to rhombomere 2 by using a transgenic mouse line that specifically expresses Cre in rhombomere 2 derived cells ($Hoxa2^{:CreTG};Atoh1^{LacZ/Flox}$ mice). In doing so, these scientists anatomically demonstrated the aberrant migration and defective location of intertrigeminal neurons in their conditional mutants. Physiologically, these animals show sigh-induced spontaneous apneas and smaller respiratory tidal volumes that led to a mild hypoventilation phenotype, but otherwise they are fully capable to respond to hypoxic and hypercarbic chemoreflexes. Thus, the anterior-posterior origin of the parabrachial/Kölliker-Fuse complex and intertrigeminal region has been assigned to rhombomeres 1 and 2, respectively.

During development, *Atoh1* is transiently expressed (E10.5-E13.5) in progenitor cells of the dA1 domain that encompasses rhombomere 1 (also known as the rostral or upper rhombic lip) and rhombomeres 2–7/8 (known as the caudal or lower rhombic lip) (**Figure 3** and **Table 1**; Ben-Arie et al., 1997; Helms and Johnson, 1998; Bermingham et al., 2001; Storm et al., 2009; Lowenstein et al., 2021). Therefore, the study of van der Heijden and Zoghbi (2018) indicates that the upper rhombic lip is the bona fide origin of the parabrachial/Kölliker-Fuse complex. The progenitor domain that generates the intertrigeminal region remains to be conclusively identified. Given that intertrigeminal neurons express the homeodomain factors *Lbx1* and *Phox2b*, in addition to *Atoh1*, the source of intertrigeminal neurons could be: the dA1 (Atoh1 +) or the dB2 (Phox2b +) progenitor domain in rhombomere 2 (Wang et al., 2005; Dubreuil et al., 2009; Rose et al., 2009a,b; Hernandez-Miranda and Birchmeier, 2015; Ruffault et al., 2015; Hernandez-Miranda et al., 2017a, 2018). Hence, either dA1-derived neurons activate *Phox2b* and *Lbx1* expression or dB2-derived (Phox2b+/Lbx1+) neurons switch on the expression of *Atoh1*. Current evidence suggests that the latter option is the correct, as retrotrapezoid neurons, a subpopulation of dB2 neurons produced in rhombomere 3 or 5, originates from Phox2b + (dB2) progenitors whose progeny subsequently express *Lbx1* and *Atoh1* (Dubreuil et al., 2009; Huang et al., 2012; Hernandez-Miranda et al., 2018).

Development of the dorsal medullary respiratory column

This respiratory column contains neurons known to be critical for the regulation of inspiratory activity. Most neurons forming this respiratory column reside within the

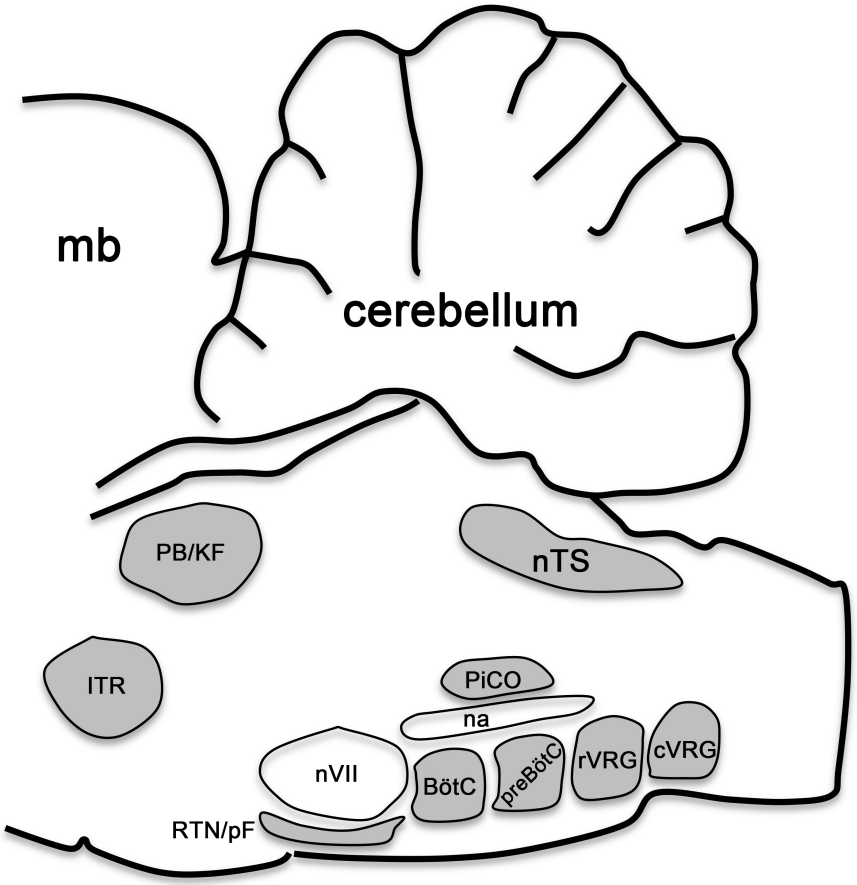

FIGURE 4
Brainstem respiratory groups. Scheme representing the sagittal view of a mouse brainstem. This scheme illustrates the location of respiratory neurons belonging to the intertrigeminal region (ITR), parabrachial/Kölliker-Fuse complex (PB/KF), nucleus tractus solitarius (nTS), retrotrapezoid/parafacial nucleus (RTN/pF), Bötzinger complex (BötC), preBötzinger complex (preBötC), postInspiratory COmplex (PiCO), rostral and caudal ventral respiratory groups (rVRG and cVRG). The cerebellum, midbrain (mb), as well as the facial (nVII) motor nucleus and the nucleus ambiguus (na) are illustrated for anatomical orientation. This figure is adapted from our previous publication Isik and Hernandez-Miranda (2022) in Handbook of Clinical Neurology, Chapter 5, entitled Early development of the breathing network, published by Elsevier Books. The license number 5392080585902 between Hernandez-Miranda, Charite Universitätsmedizin Berlin and Elsevier allows us the reuse of it in a journal/magazine.

nucleus tractus solitarius (nTS, bilaterally located in the dorsal medulla oblongata), although a few neurons belonging to this column can be found in the reticular formation adjacent to the nTS. The nTS extends from the caudal level of the facial motor nucleus (at the border between rhombomeres 6/7) to the cervical spinal cord. It represents the primary entry site of peripheral viscerosensory information into the central nervous system (**Figure 5A**; Machado et al., 1997; Travagli, 2007; Grill and Hayes, 2009). This nucleus contains second order sensory neurons that further process and relay this information to other brain regions in the brainstem (i.e., parabrachial/Kölliker-Fuse complex), forebrain and spinal cord (Aicher et al., 1995, 1996; Alheid et al., 2011). The intermediate (at the level of the area postrema) and caudal regions of the nTS receive cardiovascular and respiratory viscerosensory afferents, while the rostral to intermediate nTS primarily receives digestive information from the vagal and glossopharyngeal nerves (Kumada et al., 1990; Vangiersbergen et al., 1992; Zoccal et al., 2014; Kawai, 2018). With respect to respiration, the intermediate nTS receives afferent information from slowly adapting pulmonary stretch receptors, whereas the caudal nTS receives afferent information from the peripheral chemoreceptors (that is the carotid bodies) and from rapidly adapting pulmonary stretch receptors (Mifflin et al., 1988; Mifflin, 1992, 1993; Machado et al., 1997; Kubin et al., 2006; Chang et al., 2015; Zhao et al., 2022). Furthermore, the nTS harbors several groups of premotor neurons that can control, for instance, the laryngeal and expiratory motor activity used in breathing-associated behaviors, such as in vocalization (Hernandez-Miranda et al., 2017b).

Histological studies traced the origin of excitatory nTS neurons to the dA3 progenitor domain (located between

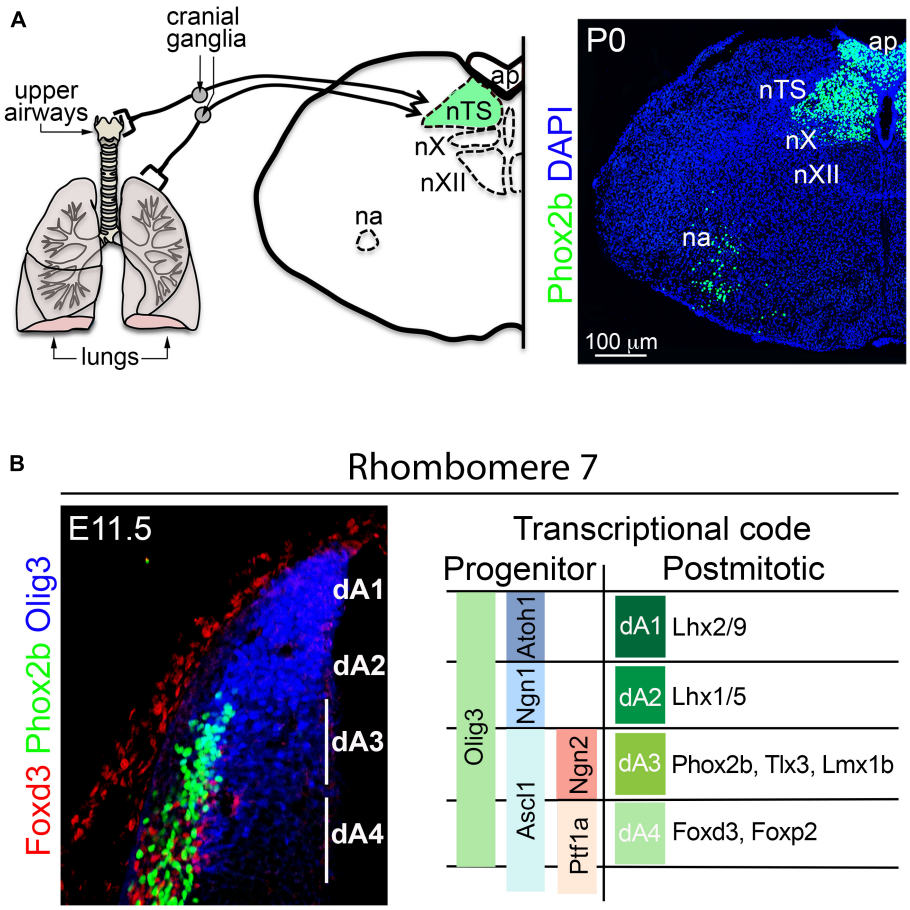

FIGURE 5
Development of the nucleus tractus solitarius. **(A)** Left, schema illustrating the relay of sensory information from the upper and lower airways to the nucleus tractus solitarius (nTS) by cranial (vagal) ganglion neurons. The nucleus ambiguus (na), area postrema (ap), nucleus vagus (nX), and the nucleus hypoglossus (nXII) are displayed as landmarks. Right, transverse section of the brainstem stained with antibodies against Phox2b and counterstained with DAPI. Phox2b expression can be observed in nTS, ap, nX and na neurons. **(B)** Left, transverse section of the dorsal rhombomere 7 stained with antibodies against Olig3, Phox2b and Foxd3 at E11.5 in mice. The expression of Olig3 encompasses the progenitor domains dA1-dA4. Phox2b and Foxd3 are differentially express in neurons emerging from dA3 and dA4, respectively. Right, schema illustrating the differential expression of transcription factors in dA progenitor cells and neurons of the dorsal rhombomere 7. This figure is adapted from our previous publication Isik and Hernandez-Miranda (2022) in Handbook of Clinical Neurology, Chapter 5, entitled Early development of the breathing network, published by Elsevier Books. The license number 5392080585902 between Hernandez-Miranda, Charite Universitätsmedizin Berlin and Elsevier allows us to reuse it in a journal/magazine. The primary data used in this figure was published in Hernandez-Miranda et al. (2017b) under the terms of the Creative Commons Attribution License, which permits unrestricted use and redistribution, provided that the original author and source are credited (https://creativecommons.org/licenses/by/4.0/).

rhombomeres 4 and 7/8; **Figure 3**). This progenitor domain shares molecular traits with a progenitor domain in the spinal cord called dI3 (Muller et al., 2005; Storm et al., 2009; Hernandez-Miranda et al., 2017a). Indeed, neuronal derivatives from these progenitor domains are excitatory and seem to only vary in the expression of the transcription factors *Phox2b* (in dA3 neurons) and *Isl1* (in dI3 neurons), but otherwise they co-express the transcription factors *Pou4f1*, *Tlx3*, *Prrxl1*, and *Lmx1b* (**Figures 3**, **5B**; Chen et al., 2001; Qian et al., 2001, 2002; Cheng et al., 2004; Muller et al., 2005; Liu et al., 2008; D'Autreaux et al., 2011). For over a quarter century the group of Christo Goridis and Jean-François Brunet has characterized the critical roles of *Phox2a* and *Phox2b* in visceral nervous system development. These homeobox transcription factors are necessary for the development of central and peripheral noradrenergic neurons, parasympathetic and sympathetic ganglia, branchial, and visceral motor neurons, as well as primary and secondary viscerosensory neurons (Morin et al., 1997; Pattyn et al., 1997, 1999, 2000a,b, 2006; Fode et al., 1998; Dauger et al., 2003; D'Autreaux et al., 2011; Espinosa-Medina et al., 2016). *Phox2b* is critical for the specification of excitatory nTS neurons, and its mutation precludes the formation of this brainstem center in mice (Pattyn et al., 1999; Dauger et al., 2003;

Hernandez-Miranda et al., 2017b). In addition, most excitatory nTS neurons co-express the transcription factor *Tlx3* (previously known as *Rnx*) that seems to stabilize and maintain the expression of *Phox2b* in nTS neurons (Qian et al., 2001; Dauger et al., 2003; Storm et al., 2009; Hernandez-Miranda et al., 2017b).

In the developing hindbrain, the precise identity of dA3 progenitor cells is determined by the co-expression of the bHLH transcription factors *Olig3*, *Ascl1* and *Ngn2* (**Figure 5B**; Pattyn et al., 2006; Liu et al., 2008; Storm et al., 2009; Hernandez-Miranda et al., 2017a). In addition to excitatory nTS neurons, dA3 progenitors also generate other excitatory neurons that include: area postrema neurons (associated with vomiting reflexes) and caudal (nor)adrenergic neurons (the baroreflex-associated A1 and A2 groups) (Qian et al., 2001; Dauger et al., 2003; Pattyn et al., 2006; Storm et al., 2009; Zhang et al., 2021). Progenitors in the dA3 domain generate these neuron types in a temporal order in which (nor)adrenergic neurons are generated first, followed by excitatory nTS neurons and lastly area postrema neurons (Hernandez-Miranda et al., 2017b). Although most nTS neurons are excitatory, a substantial amount of inhibitory neurons also reside within this nucleus. Inhibitory nTS neurons depend on *Lbx1* and appear to derive from the dB1 or dB2 progenitor domains (Hernandez-Miranda et al., 2018). The rhombomeric origin of the nTS has not been directly investigated, incidental evidence, however, suggests that it primarily originates from rhombomeres 7 & 8, as the ablation of the transcription factor *MafB,* which severely affects the development of rhombomeres 5 and 6, does not significantly interfere with nTS development (Blanchi et al., 2003).

Development of the ventral medullary respiratory column

Several anatomical and physiological distinct groups of respiratory-related neurons have been identified in the ventral medulla oblongata, which form the ventral medullary respiratory column, these groups include: (a) the retrotrapezoid/parafacial nucleus, (b) the Bötzinger complex, (c) the preBötzinger complex, (d) the PiCo complex (dorsal to the Bötzinger and preBötzinger complexes), (e) the rostral ventral and caudal respiratory groups, as well as (f) the raphe obscurus (**Figure 4**). Neurons within these groups can either project onto respiratory premotor neurons or themselves act as premotor neurons to regulate the motoric behavior associated with breathing. Interestingly, three of these groups exhibit intrinsic rhythmic activity during prenatal development: (i) the parafacial nucleus, (ii) the preBötzinger complex and (iii) a newly identified PostInspiratory COmplex (PiCo), and are believed to be central for the generation of the respiratory rhythm (Smith et al., 1991; Onimaru and Homma, 2003; Anderson et al., 2016; Del Negro et al., 2018; Ramirez and Baertsch, 2018). Except for the recently identified PiCo complex, the development of all other ventral respiratory groups has been studied.

Development of the retrotrapezoid/parafacial nucleus

The retrotrapezoid and parafacial nuclei are two small groups of excitatory neurons that are located ventro-laterally to the facial motor nucleus. Whether these groups are genuinely distinct remains to be conclusively determined. However, recent evidence seems to suggest that they are indeed physiologically distinct neuronal populations (Huckstepp et al., 2015, 2016, 2018; Korsak et al., 2018; Zoccal et al., 2018). From an anatomical point of view, retrotrapezoid neurons locate ventrally to the facial motor nucleus and are long known to contain central respiratory chemoreceptor neurons; that is, acid-activated neurons that maintain constant levels of arterial PCO_2 (**Figures 6A,B,F**). For more details on the physiology of retrotrapezoid neurons and other central respiratory chemoreceptor neurons, we refer to the excellent work of Nattie and Li (2012), Guyenet and Bayliss (2015, 2022), Guyenet et al. (2019) and Lopez-Barneo (2022). On the other hand, neurons of the parafacial nucleus are located lateral to the facial motor nucleus. They are thought to control active expiration, a particular type of expiration that is produced when high metabolic demands induce an increase in respiration (Fortin and Thoby-Brisson, 2009; Thoby-Brisson et al., 2009; Bayliss et al., 2015; Huckstepp et al., 2015, 2018; Korsak et al., 2018; Pisanski and Pagliardini, 2019).

In 2009, Dubreuil et al. (2009) identified that virtually all retrotrapezoid and parafacial neurons originate from *Egr2*-expressing cells (that is from rhombomeres 3 and/or 5; see **Figure 2**). Furthermore, they identified their distinctive molecular signature, namely their co-expression of *Phox2b*, *Lbx1,* and *Atoh1* (**Figure 6B**). Ablation of each of these genes leads to the anatomical absence (*Phox2b* and *Lbx1* mutant mice) or aberrant location (*Atoh1* mutants) of retrotrapezoid and parafacial neurons, as well as to the loss of the hypercarbic reflex (the natural acceleration of breathing in response to increasing PCO_2 levels) and neonatal death (Wang et al., 2005; Pagliardini et al., 2008; Dubreuil et al., 2009; Rose et al., 2009a,b; Hernandez-Miranda et al., 2018). The dB2 progenitor domain generates retrotrapezoid and parafacial neurons and is exclusively located between rhombomeres 2 and 6 (**Figures 3**, **6C**). dB2 progenitor cells express *Phox2b* and their postmitotic progeny co-express *Lbx1* in addition to *Phox2b* (**Figure 6C**). A small number of dB2 (Lbx1 + /Phox2b +) neurons migrate ventrally toward the facial motor nucleus and activate the expression of *Atoh1* during their migration (**Figures 6D,E**). The expression of *Atoh1* seems to be essential for the migration and maturation of retrotrapezoid and parafacial nucleus neurons

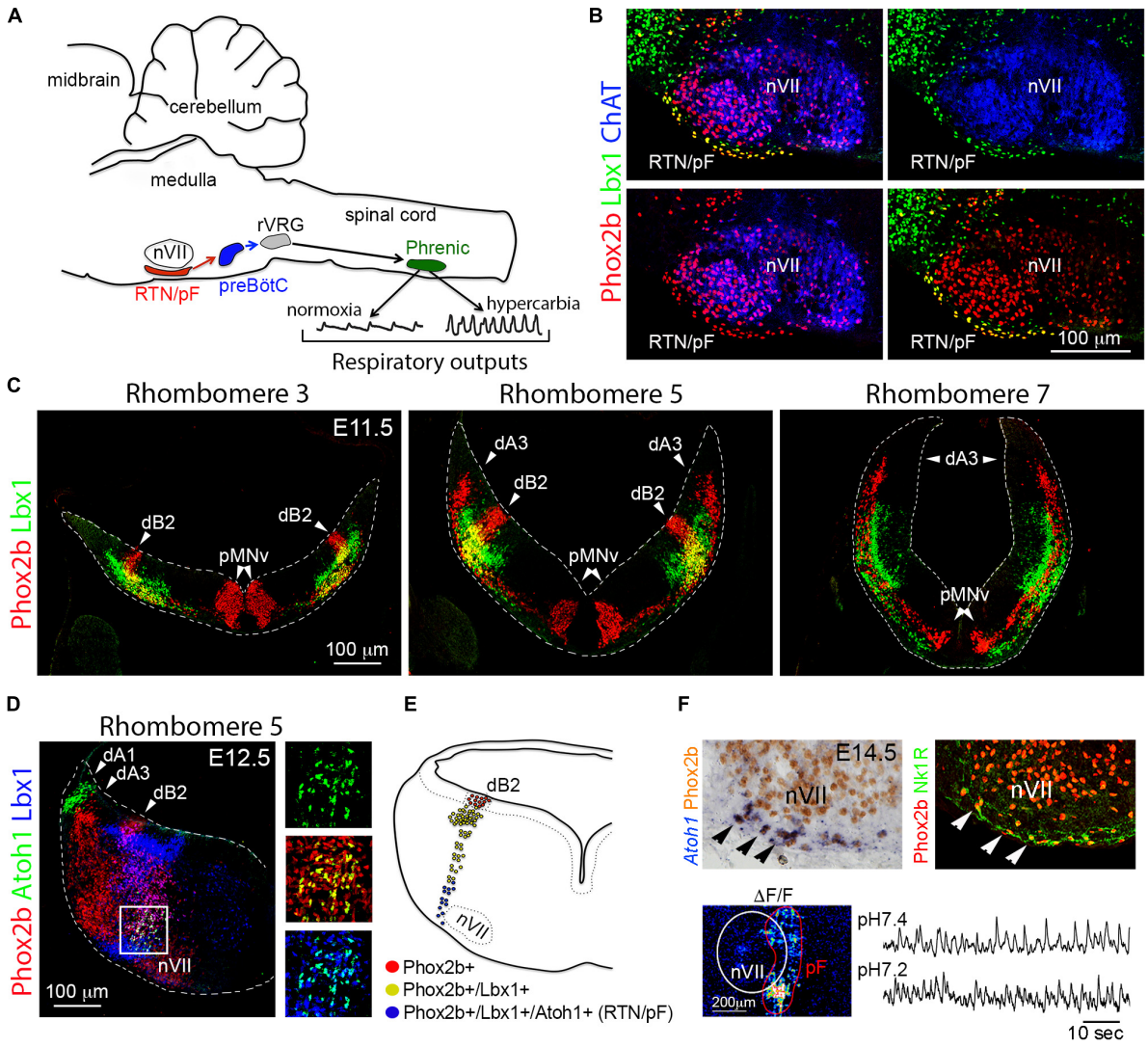

FIGURE 6
Development of the retrotrapezoid/parafacial nucleus. **(A)** Schema representing the location and function of retrotrapezoid/parafacial nucleus (RTN/pF) in mice. Under normal levels of oxygen (normoxia), the activity of the preBötzinger complex (preBötC) controls the firing rate of neurons in the phrenic motor nucleus (Phrenic) by sending signals *via* premotor neurons located in the rostral ventral respiratory group (rVRG). Phrenic motor neurons control diaphragm activity. Under hypercarbia (high levels of PCO_2) RTN/pF neurons increase their firing rate: this adjusts the activity of preBötzinger complex and eventually the firing rate of the phrenic motor neurons, which in turn increases respiration **(B)** Histological characterization of RTN/pF in newborn mice (P0). RTN/pF neurons co-express Phox2b and Lbx1 but not choline-acetyltransferase (ChAT), which distinguishes them from facial motor neurons (nVII) that express Phox2b and ChAT but not Lbx1. **(C)** Histological characterization of dB2 neurons across the indicated rhombomeres (r). dB2 neurons co-express Phox2b and Lbx1 at E11.5 in mice. This molecular signature distinguishes them from the dorsal (dA3 neurons) and ventral (pMNv) cells that express Phox2b but not Lbx1. Note that dB2 neurons emerge from r2 to r6, whereas dA3 neurons originate in r4 to r7/8 and pMNv cells can be found from r2-r7/8 (see text). **(D)** Transverse section of a E12.5 mouse embryo stained with antibodies against Phox2b, Atoh1, and Lbx1. Note that a subset of dB2 neurons (magenta cells) activate the expression of Atoh1 as they reach the facial (nVII) motor nucleus (boxed area). The boxed area is illustrated at the right with different combinations of the fluorescent signals. **(E)** Schema depicting the development of RTN/pF neurons. Phox2b + dB2 progenitor cells differentiate an initiate the expression of Lbx1 in neurons. A subset of Phox2b + /Lbx1 + (dB2) neurons ventrally migrates and activates the expression of Atoh1 as they reach the facial (nVII) motor nucleus. It is the co-expression of Phox2b + /Lbx1 + /Atoh1 + what defines the molecular signature of RTN/pF neurons. **(F)** Upper panels, by E14.5 in mice, RTN/pF neurons (arrowheads) settle underneath the facial motor (nVII) nucleus and express additional marker, such as neurokinin 1 receptor (Nk1R). Lower panels, ventral hindbrain view of a E14.5 wholemount brainstem preparation centered on the facial (nVII) motor nucleus showing Ca2 + green-1AM fluorescence changes (ΔF/F) of parifacial nucleus (pF) activity in physiological (7.4) and low (7.2) pH. This figure is adapted from our previous publication Isik and Hernandez-Miranda (2022) in Handbook of Clinical Neurology, Chapter 5, entitled Early development of the breathing network, published by Elsevier Books. The license number 5392080585902 between Hernandez-Miranda, Charite Universitätsmedizin Berlin and Elsevier allows us to reuse it in a journal/magazine. The primary data used in this figure was published in Hernandez-Miranda and Birchmeier (2015) and Hernandez-Miranda et al. (2018) under the terms of the Creative Commons Attribution License, which permits unrestricted use and redistribution, provided that the original author and source are credited (https://creativecommons.org/licenses/by/4.0/).

(Huang et al., 2012; Ruffault et al., 2015; Hernandez-Miranda et al., 2018). As retrotrapezoid and parafacial neurons mature throughout postnatal life, and for reasons yet to be identified, these neurons silence *Lbx1* and *Atoh1*, but retain *Phox2b*. Several studies show that interfering with the specification of retrotrapezoid and parafacial neurons does not compromise neonatal or postnatal survival in mice. However, the loss of these neurons leads to a range of hypoventilation behaviors and the loss of the hypercarbic reflex in neonatal mice (Ramanantsoa et al., 2011; Huang et al., 2012; Ruffault et al., 2015; Hernandez-Miranda et al., 2018). Notably, transgenic mice lacking retrotrapezoid and parafacial neurons are able to recover some of the ventilatory responses to hypercarbia in adult life (Ramanantsoa et al., 2011; Huang et al., 2012; Ruffault et al., 2015; Hernandez-Miranda et al., 2018). How these animals gain the ability to respond to hypercarbia in adulthood is currently unknown, but this indicates that other chemoreceptor cells, either in the central or peripheral nervous system, can compensate for the loss of retrotrapezoid and parafacial neurons in the adult life.

Development of the Bötzinger complex

The major inhibitory component of the ventral respiratory column is the Bötzinger complex that uses GABA and glycine as its primary neurotransmitters (Shao and Feldman, 1997; Schreihofer et al., 1999; Song et al., 2001). Classic studies showed that the electrophysiological and pharmacological activation of Bötzinger neurons strongly inhibits inspiration and that Bötzinger neurons display decrementing postinspiratory or augmenting firing patterns during expiration (Bongianni et al., 1988; Gang and Lei, 1996). These neurons mutually interact with the preBötzinger complex to regulate the respiratory rhythm (Bryant et al., 1993; Tian et al., 1998; Ezure et al., 2003a,b,c). The Bötzinger complex innervates all other brainstem respiratory neurons and projects to spinal premotor and motor phrenic neurons (Otake et al., 1988; Jiang and Lipski, 1990; Douse and Duffin, 1992; Tian et al., 1998; Smith et al., 2007).

The precise rhombomeric origin and progenitor domain from which the Bötzinger complex develops has not yet been fully investigated. However, circumstantial evidence might indicate that this respiratory group develops from the *Lbx1*-lineage. Indeed, a lineage tracing study by Pagliardini et al. (2008) revealed that virtually all GABAergic and glycinergic neurons found in the anatomical region where the Bötzinger complex resides have a history of *Lbx1* expression, ablation of which results in the absence of GABAergic and glycinergic neurons in this area (Pagliardini et al., 2008). Mature "Bötzinger" neurons lose the expression of *Lbx1* but can be recognized by the expression of *Pax2*, *GABA* and other glycinergic markers (Pagliardini et al., 2008). As abovementioned, *Lbx1* is key for the specification of four distinct neuron types, two of which express *Pax2* and are GABAergic and glycinergic in nature: dB1 and dB4 neurons (**Figure 3** and **Table 2**). In *Lbx1* null mutant mice, *Pax2* expression seems to be uniquely lost from the dB1 domain (that extends from rhombomeres 2–7/8), which might suggest this region as the possible source of Bötzinger neurons (Pagliardini et al., 2008). However, more research is necessary to clearly define the developmental origin of the Bötzinger complex.

Development of the preBötzinger complex

In the early 1990's, the work of Jeffrey C. Smith and Jack L. Feldman identified the preBötzinger complex as essential for generating the respiratory rhythm in mammals (**Figures 7A,B**; Smith et al., 1991). Later studies uncover some molecular markers such as the neurokinin 1 receptor and somatostatin to be expressed by preBötzinger neurons (Smith et al., 1991, 2007; Gray et al., 1999, 2001). How the preBötzinger complex generates the respiratory rhythm is currently the subject of intense investigation and outside the scope of this review, but we recommend the reader the excellent reviews by the groups of Anderson and Ramirez (2017), Ramirez and Baertsch (2018), Rubin and Smith (2019), Ramirez et al. (2022) and Smith (2022).

In 2010, two independent groups defined the V0 progenitor domain (in the basal plate) as the source of the preBötzinger complex (Bouvier et al., 2010; Gray et al., 2010). V0 progenitor cells share molecular traits with the p0 progenitor domain in the ventral spinal cord and are characterized by the expression of Dbx1 and Dbx2, the former is, however, unique for V0 and p0 progenitor cells (**Figure 7C** and **Table 1**; Pierani et al., 1999, 2001). Both Bouvier et al. (2010) and Gray et al. (2010) used $Dbx1^{LacZ}$ mice, which express the reporter protein beta-galactosidase under the control of the *Dbx1* promoter, to lineage trace the preBötzinger complex and demonstrated that all the excitatory and rhythmically active neurons in this region derived from the V0 progenitor domain. Neurons emanating from this domain express the transcription factor *Evx1*, which distinguishes them from the surrounding dB4 and V1 neurons that express *Lbx1* and *En1*, respectively (**Figure 7C** and **Table 2**; Pierani et al., 1999, 2001). Interestingly, V0 neuronal derivatives destined to populate the preBötzinger complex are correctly generated and reach the preBötzinger complex area in *Dbx1* null mutant ($Dbx1^{LacZ/LacZ}$) mice, but these cells do not exhibit intrinsic rhythmicity and fail to adopt their mature molecular identity, as determined by the lack of neurokinin 1 receptor or somatostatin expression in these cells (Bouvier et al., 2010).

Expression of the transcription factor *Pax7* molecularly distinguishes two V0 progenitor subdomains: V0 dorsal ($V0_D$; Pax7 +) and V0 ventral ($V0_V$; Pax7-) (**Figure 7C**). In Bouvier et al. (2010) the authors walked an extra mile and ablated *Dbx1* from the $V0_D$ domain, using $Pax7^{Cre};Dbx1^{LacZ/Flox}$ mice, to elucidate which of these two subdomains generate

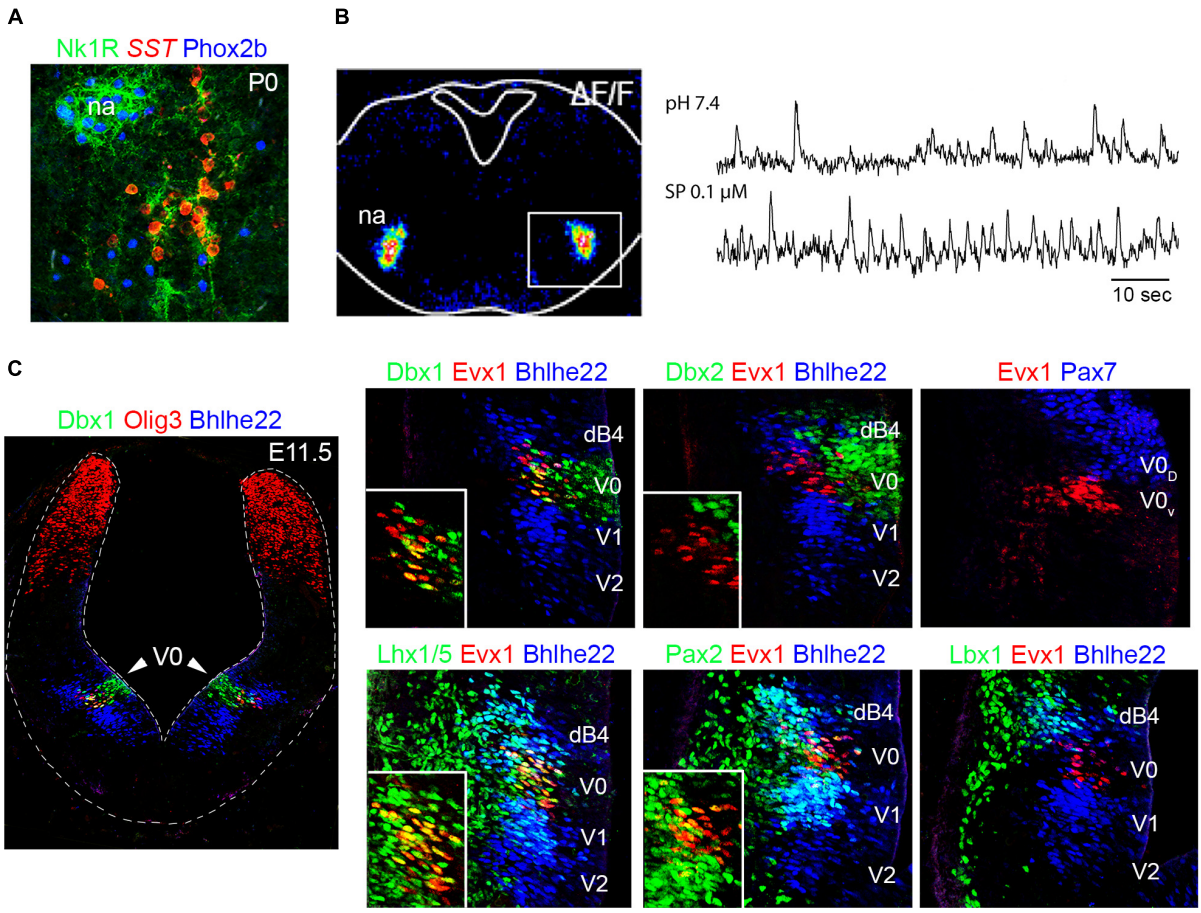

FIGURE 7
Development of the preBötzinger complex. **(A)** The neurons of the preBötzinger complex locate ventral to the nucleus ambiguus (na) and can be distinguished by the co-expression of somatotatin (SST) and neurokinin 1 receptor (Nk1R) in mice at birth (P0). Please note that preBötzinger neurons co-express SST and Nk1R but not Phox2b, while motor neurons of the nucleus ambiguus co-express Nk1R and Phox2b but not SST. **(B)** Left, transverse section of a mouse hindbrain at E14.5 showing Ca2 + green-1AM fluorescence changes (ΔF/F) of preBötzinger complex (boxed area) intrinsic activity. Right, traces illustrating bursts of preBötzinger complex activity in physiological pH or after substance p (SP) treatment, which accelerates their firing. **(C)** Left, transverse section of a E11.5 mouse brainstem at rhombomere 7. The section was stained with antibodies against Dbx1 (green) Olig3 (red) and Bhlhe22 (blue). Note that the V0 progenitor domain can be distinguished by the expression of Dbx1. Right, histological characterization of the V0 progenitor domain and the neurons that emerge from it, using antibodies against Dbx1, Dbx2, Evx1, Pax7, Lhx1/5, Pax2 and Lbx1. Note the Dbx1 + (V0) progenitor domain generates Evx1 + neurons that co-express in addition Lhx1/5 and Pax2 but not Lbx1 (see also **Tables 1**, **2** and text for more details). The expression of Bhlhe22 allows the distinction of the dB4 and V1/V2 domains that sandwich the V0 progenitor domain. A fraction of Dbx1-derived neurons will differentiate into the preBötzinger complex (see text). Insets in the main photographs illustrate the co-expression of Evx1 + cells with the indicated markers. This figure is adapted from our previous publication Isik and Hernandez-Miranda (2022) in Handbook of Clinical Neurology, Chapter 5, entitled Early development of the breathing network, published by Elsevier Books. The license number 5392080585902 between Hernandez-Miranda, Charite Universitätsmedizin Berlin and Elsevier allows us to reuse it in a journal/magazine. The primary data used in this figure was published in Hernandez-Miranda et al. (2017b) under the terms of the Creative Commons Attribution License, which permits unrestricted use and redistribution, provided that the original author and source are credited (https://creativecommons.org/licenses/by/4.0/).

the preBötzinger complex. This elegant experiment found an anatomically, molecularly and physiologically intact preBötzinger complex, demonstrating that this respiratory center emerges from the $V0_V$ subdomain. More recent studies have exploited this developmental knowledge to selectively activate, silence, or ablate Dbx1-derived preBötzinger neurons, resulting in respiratory changes that enhance, depress, or halt breathing in adult mice, respectively (Wang et al., 2014; Vann et al., 2016, 2018).

Even though the anterior-posterior origin of the preBötzinger complex has not yet been identified, an early study indicates that it emerges from the most posterior rhombomeres and partly from rhombomere 6 (*MafB* +). In this context, a study by Blanchi et al. (2003) showed that *MafB* null mutant mice rarely breathe at birth and display limited phrenic nerve activity (Blanchi et al., 2003). Histologically, *MafB* null mutants have a significant, but not complete, loss of preBötzinger neurons (Blanchi et al., 2003). Since *Egr2* null

mutant mice display breathing rhythmicity and can survive for about a day after birth (Chatonnet et al., 2007), it is likely that V0 progenitors in rhombomere 6 generate a fraction of preBötzinger neurons that is complemented by V0 progenitors in rhombomeres 7/8.

Development of the rostral and caudal ventral respiratory groups

The preBötzinger complex controls breathing by activating premotor neurons that in turn regulate multiple brainstem (e.g., hypoglossal or vagal) and spinal cord (phrenic) motor neurons. Caudal to the preBötzinger complex, two sets of respiratory premotor neurons are associated with inspiratory and expiatory motor activity: the rostral (rVRG) and caudal (cVRG) ventral respiratory groups, respectively (Smith et al., 2013). A recent study from the group of Gilles Fortin identified that excitatory rVRG neurons have a history of *Dbx1* expression and, as such, to originate from the V0 progenitor domain (Wu et al., 2017). Even though both preBötzinger neurons and rVRG neurons express *Slc17a6* (vGlut2) and *Pax2*, only the former expresses neurokinin 1 receptor and somatostatin (Bouvier et al., 2010; Gray et al., 2010; Wu et al., 2017). These molecular differences could be explained by their distinct rhombomeric origins and/or by their generation in distinct V0 progenitor subdomains. The development of cVRG neurons has not been yet addressed, but some Dbx1-derivaties neurons can be observed caudal to the rVRG, suggesting that cVRG neurons are also generated from the V0 progenitor domain (Gray, 2013; Wu et al., 2017). An alternative source of cVRG neurons could be the dB4 domain, whose derivatives co-express *Lbx1* and *Wt1* (**Table 2**). Indeed, a recent study reported the presence of GABAergic (*Wt1* +) neurons in the cVRG region (Schnerwitzki et al., 2020).

Development of respiratory serotonergic neurons

The monoamine neurotransmitter serotonin has long been implicated in the control of respiration. Brain serotonin is produced by nine distinct groups of cells (called raphe nuclei), all of which are in the brainstem. Among the distinct raphe nuclei, several lines of research indicate that the midline located raphe obscurus in the medulla oblongata is an important component of the central respiratory chemoreceptor circuit (Jacobs et al., 2002). First, the *en masse* inhibition of serotonergic neurons (Ray et al., 2011), or the targeted inhibition of raphe obscurus neurons (Brust et al., 2014), significantly impairs the chemoreflex to hypercarbia in mice. Second, the optogenetic activation of these raphe neurons accelerates respiration in conscious and anesthetized rodents (Depuy et al., 2011). Lastly, mice genetically engineered to lack raphe neurons display dulled chemoreflexes to hypercarbia (Hodges et al., 2008, 2009; Buchanan and Richerson, 2010).

The ventral-most progenitor domain (termed as pMN; **Figure 3**) in the developing hindbrain initially generates motor neurons, and later all brainstem serotonergic neurons. Due to its proximity to the floor plate, the pMN domain is under the direct influence of Sonic Hedgehog signaling (Marti et al., 1995; Chiang et al., 1996). Molecularly, this progenitor domain is subdivided into a dorsal subdomain (pMNs; expressing the transcription factors *Pax6* and *Olig2*) and a ventral subdomain (pMNv; expressing the transcription factors *Nkx2.2*, *Nkx2.9,* and *Phox2b*) (**Figure 3** and **Table 1**). Detailed histological and genetic analyses showed that the pMNs subdomain generates somatic motor neurons (i.e., hypoglossal motor neurons), whereas the pMNv subdomain generates branchial (e.g., facial motor neurons) and visceral (i.e., nucleus ambiguous) motor neurons (Briscoe et al., 1999; Pattyn et al., 2003). Pioneer studies by Briscoe and colleagues showed that pMNv progenitors first generate branchio/viscero motor neurons before E11.5 in mice, and then serotonergic neurons (Briscoe et al., 1999; Pattyn et al., 2003). One should note that except for rhombomere 4, the pMNv progenitor domain in all other rhombomeres contributes to raphe neurons. pMNv progenitor cells of rhombomere 4 are known to generate a large group of branchial (facial) motor neurons and to have an unusual prolonged expression of *Phox2b* between E9.5 to E12.5, which seems to be attributable to its incapacity to generate serotonergic neurons (Pattyn et al., 2003). Indeed, the silencing of *Phox2b* expression seems to be a molecular switch in the transition of pMNv progenitor cells from first generating branchio/visceromotor neurons to later generating serotonergic neurons in the other rhombomeres (Briscoe et al., 1999; Pattyn et al., 2003, 2004). In support of this, analysis of *Nkx2.2* null mutant mice revealed an unusual extended expression of *Phox2b* within the pMNv domain, which leads to the overproduction of branchio/visceromotor neurons and the absence of serotonergic neurons (Briscoe et al., 1999; Pattyn et al., 2003, 2004). Conversely, the ablation of *Phox2b* results in the early generation of raphe neurons at the expense of branchio/visceromotor cells (Pattyn et al., 2004).

The bHLH transcription factor Ascl1 is critical for development of peripheral (i.e., enteric nervous system) and central (raphe) serotonergic cells (Blaugrund et al., 1996; Pattyn et al., 2004). In the pMNv domain, *Ascl1* is co-expressed with *Phox2b* during the genesis of branchio/visceromotor neurons and is retained by these progenitors throughout the specification of raphe cells (Pattyn et al., 2004). Mutation of *Ascl1* does not affect *Phox2b* expression nor the development of branchio/visceromotor cells, but severely interferes with the specification of raphe neurons, which are completely absent in *Ascl1* null mutant mice (Pattyn et al., 2004). The maturation of raphe neurons is regulated by several other transcription factors, such as *Gata2*, *Gata3*, *Lmx1b* and *Pet1*, of which the null mutation of *Lmx1b* or *Pet1* results in the total loss or a severe

decrease (> 70%) of raphe cells, respectively (Cheng et al., 2003; Ding et al., 2003; Hendricks et al., 2003; Dosumu-Johnson et al., 2018; Okaty et al., 2020).

Cell lineages contributing to respiratory and non-respiratory neurons

From a developmental point of view, most brainstem respiratory neurons emerge from a few molecularly defined cell-lineages and progenitor domains: (i) an *Atoh1*-lineage that contributes to the development of the parabrachial/Kölliker-Fuse complex (dA1, in rhombomere 1) and the intertrigeminal region (either dA1 or dB2, in rhombomere 2); (ii) an *Olig3/Phox2b/Tlx3*-lineage (dA3, in rhombomere 7/8) that generates the dorsal medullary respiratory column (nTS); iii) a *Phox2b/Lbx1/Atoh1*-lineage (dB2, in rhombomere 3 and/or 5) that generates the retrotrapezoid/parafacial nuclei; (iv) an *Lbx1*-lineage (presumably dB1, unknown rhombomeric origin) that produces the Bötzinger complex; v) a *Dbx1*-lineage (V0) that gives rise to the preBötzinger complex (in rhombomeres 6-7/8) and the rVRG (and possibly the cVRG, in rhombomere 7/8) groups of premotor neurons; as well as (vi) an *Nkx2.2/Ascl1/Lmx1b*-lineage that produces raphe serotonergic neurons (pMNv, across rhombomeres).

One should not forget, however, that each of these progenitor domains produce a much greater diversity of neuron types than just respiratory neurons. A good example of this is the dA1 (Atoh1 +) domain in rhombomere 1 (upper rhombic lip). This domain generates: in addition to the parabrachial/Kölliker-Fuse complex, all excitatory deep cerebellar neurons, all cerebellar granule cell progenitors, as well as all cerebellar and cochlear unipolar brush cells (Englund et al., 2006; Fink et al., 2006; Ray and Dymecki, 2009; Hernandez-Miranda et al., 2017a; van der Heijden and Zoghbi, 2018, 2020; Elliott et al., 2021; Lowenstein et al., 2021, 2022; Fritzsch et al., 2022). How these progenitors generate such a vast array of neuron types is currently being investigated and appears to depend on the temporal expression of transcription factors that act as selector genes. In this context, the co-expression of *Atoh1* with *Olig3* is critical for deep cerebellar neuron development, whereas the co-expression of *Atoh1* with *Neurod1* is essential for granule cell progenitor specification and cerebellar and cochlear unipolar brush cell development (Ben-Arie et al., 1997; Chizhikov and Millen, 2003; Gazit et al., 2004; Pan et al., 2009; Machold et al., 2011; Lowenstein et al., 2021). The selector gene for the specification of parabrachial/Kölliker-Fuse complex is presently unknown.

It might not be surprising that across rhombomeres, each progenitor domain generates different neuron types. Nonetheless, an interesting trait of these spatially segregated progenitor domains is that their shared expression of transcription factors might instruct their progeny to synaptically connect and form functional circuits. For instance, both Atoh1 + /Olig3 + (dA1) progenitors in rhombomere 7 or the pdI1 progenitors in the spinal cord (equivalent to dA1) produce second relay neurons that project to the cerebellum and synapse onto granule cells and deep cerebellar neurons that derive from rhombomere 1 dA1 (Atoh1 + /Olig3 +) progenitors (Muller et al., 2005; Liu et al., 2008; Storm et al., 2009; Hernandez-Miranda et al., 2017a; Lowenstein et al., 2021, 2022). Another example of this molecular logic could be the inferior olive-Purkinje cell circuit. Indeed, inferior olive cells that derive from Olig3 + /Ptf1a + (dA4 in rhombomere 7) progenitors send axons that synapse onto Purkinje cells that emerge from Olig3 + /Ptf1a + progenitors in the cerebellar ventricular zone in rhombomere 1 (Liu et al., 2008; Storm et al., 2009; Hernandez-Miranda et al., 2017a; Lowenstein et al., 2021, 2022). To which extent these shared transcriptional codes allow for the interconnection of the distinct neurons that form the brainstem respiratory circuit is presently unknown. However, emerging evidence shows similar developmental strategies, i.e., preBötzinger complex neurons that connect with the rVRG are both derivatives of the V0 domain (Bouvier et al., 2010; Gray et al., 2010; Wu et al., 2017). An even more conspicuous case is the *Phox2b*-lineage that generates virtually all neurons that form the central and peripheral visceral nervous system (Morin et al., 1997; Pattyn et al., 1997, 1999, 2000a,b, 2003, 2004, 2006; Fode et al., 1998; Dauger et al., 2003; D'Autreaux et al., 2011; Espinosa-Medina et al., 2016; Isik and Hernandez-Miranda, 2022). The question of how these developmental strategies emerged during evolution remains to be explored.

Conclusion

The enormous knowledge gained during the last three decades of brainstem development research now allows us to further dissect the function of respiratory neurons with unprecedented detail. Several experimental and theoretical approaches have recently taken advantage of the developmental trajectories of respiratory neurons to explore the complex character of the respiratory rhythm generator or to elucidate different components of the central chemoreceptor circuit (Depuy et al., 2011; Ray et al., 2011; Brust et al., 2014; Wang et al., 2014; Vann et al., 2016, 2018).

Many aspects of how respiratory neuron diversity emerges during development remain to be elucidated. The identification of how the brainstem generates respiratory neurons is critical to understand this complex behavior and essential for the development of new therapeutic approaches for the management of respiratory diseases. In this context, recent studies on the genetic disturbances causing congenital respiratory syndromes are currently steering our views into both the development and function of respiratory neurons. A clear example is the study of congenital central hypoventilation syndrome (CCHS, also known as Ondine's curse; OMIM

209880). Although rare (1 in 200,000 live births), this disorder is life threatening and characterized by slow, apneic and shallow breathing (hypoventilation) while awake and respiratory arrest during sleep (Weese-Mayer et al., 2008, 2017; Sivan et al., 2019; Ceccherini et al., 2022). Frequently, CCHS patients also present with blunted responses to hypercabia and have abnormal levels of PCO_2. Early genetic studies identified *de novo* mutations in *PHOX2B* as the most prevalent cause of CCHS (Amiel et al., 2003). Two types of *PHOX2B* mutations that cause CCHS have been identified: (i) polyalanine repeat expansions, and (ii) non-polyalanine repeat expansions that are more prevalent in severe cases of CCHS (Amiel et al., 2003; Zhou et al., 2021). CCHS patients with *PHOX2B* mutations frequently manifest Hirschsprung's disease, revealing that genetic disturbances on *PHOX2B* can simultaneously alter the development of both the central and peripheral nervous systems (Weese-Mayer et al., 2008, 2017; Sivan et al., 2019; Ceccherini et al., 2022). *PHOX2B* is a central factor in the development and function of the visceral nervous system, whose mutation results in midterm fetal lethality (Dauger et al., 2003). Interestingly, the insertion of a frequent poly-alanine *PHOX2B* mutation (called $PHOX2B^{+7ala}$) into the murine genome has shown that this aberrant expansion only affects a subset of *Phox2b* functions, as only one Phox2b-dependent neuron type (the retrotrapezoid nucleus) does not develop correctly in $Phox2b^{+7ala}$ mutant mice (Dubreuil et al., 2008). More recently, the characterization of a CCHS disease-causing frameshift mutation in *LBX1* has further revealed that this respiratory disorder originates from the misspecification of dB2 neurons in mice, and that this is caused by a lack of cooperativity between *PHOX2B* and *LBX1* (Hernandez-Miranda et al., 2018).

For many years, the size and location of the brainstem was a major impediment to comprehend its physiology. With the advent of new technologies such as single-cell transcriptomics, monosynaptic viral tracing as well as opto- and chemo- genetic tools, several of the long-lasting obstacles associated with the identification and modulation of specific breathing behaviors are now amenable for scientific exploration. There is no doubt that the years to come will foster and propel our understanding of this elementary and humble animal behavior in ways that we can only now imagine.

Author contributions

YX, KC, AA, EL, and LH-M reviewed the literature. LH-M wrote the original draft and edited it with the input from all authors. All authors contributed to the article and approved the submitted final version.

Funding

Work in the Hernandez-Miranda's laboratory is supported by the Fritz-Thyssen-Stiftung (grant no. 10.20.1.004MN) and Deutsche Forschungsgemeinschaft (grant no. 450241946), both granted to LH-M.

Conflict of interest

The authors declare that the research was conducted in the absence of any commercial or financial relationships that could be construed as a potential conflict of interest.

Publisher's note

References

Acampora, D., Avantaggiato, V., Tuorto, F., and Simeone, A. (1997). Genetic control of brain morphogenesis through Otx gene dosage requirement. *Development* 124, 3639–3650. doi: 10.1242/dev.124.18.3639

Addison, M., Xu, Q., Cayuso, J., and Wilkinson, D. G. (2018). Cell identity switching regulated by retinoic acid signaling maintains homogeneous segments in the hindbrain. *Dev. Cell* 45, 606–620.e3.. doi: 10.1016/j.devcel.2018.04.003

Aicher, S. A., Kurucz, O. S., Reis, D. J., and Milner, T. A. (1995). Nucleus tractus solitarius efferent terminals synapse on neurons in the caudal ventrolateral medulla that project to the rostral ventrolateral medulla. *Brain Res.* 693, 51–63. doi: 10.1016/0006-8993(95)00660-I

Aicher, S. A., Saravay, R. H., Cravo, S., Jeske, I., Morrison, S. F., Reis, D. J., et al. (1996). Monosynaptic projections from the nucleus tractus solitarii to C1 adrenergic neurons in the rostral ventrolateral medulla: comparison with input from the caudal ventrolateral medulla. *J. Comp. Neurol.* 373, 62–75. doi: 10.1002/(SICI)1096-9861(19960909)373:1<62::AID-CNE6>3.0.CO;2-B

Alaynick, W. A., Jessell, T. M., and Pfaff, S. L. (2011). SnapShot: spinal cord development. *Cell* 146, 178–178.e1. doi: 10.1016/j.cell.2011.06.038

Alexander, T., Nolte, C., and Krumlauf, R. (2009). Hox genes and segmentation of the hindbrain and axial skeleton. *Annu. Rev. Cell Dev. Biol.* 25, 431–456. doi: 10.1146/annurev.cellbio.042308.113423

Alheid, G. F., Jiao, W., and Mccrimmon, D. R. (2011). Caudal nuclei of the rat nucleus of the solitary tract differentially innervate respiratory compartments within the ventrolateral medulla. *Neuroscience* 190, 207–227. doi: 10.1016/j.neuroscience.2011.06.005

Alheid, G. F., Milsom, W. K., and Mccrimmon, D. R. (2004). Pontine influences on breathing: an overview. *Respir. Physiol. Neurobiol.* 143, 105–114. doi: 10.1016/j.resp.2004.06.016

Amiel, J., Laudier, B., Attie-Bitach, T., Trang, H., De Pontual, L., Gener, B., et al. (2003). Polyalanine expansion and frameshift mutations of the paired-like homeobox gene Phox2B in congenital central hypoventilation syndrome. *Nat. Genet.* 33, 459–461. doi: 10.1038/ng1130

Anderson, T. M., Garcia, A. J. IIIrd, Baertsch, N. A., Pollak, J., Bloom, J. C., Wei, A. D., et al. (2016). A novel excitatory network for the control of breathing. *Nature* 536, 76–80. doi: 10.1038/nature18944

Anderson, T. M., and Ramirez, J. M. (2017). Respiratory rhythm generation: triple oscillator hypothesis. *F1000Research* 6:139. doi: 10.12688/f1000research.10193.1

Aragon, F., Vazquez-Echeverria, C., Ulloa, E., Reber, M., Cereghini, S., Alsina, B., et al. (2005). vHnf1 regulates specification of caudal rhombomere identity in the chick hindbrain. *Dev. Dyn.* 234, 567–576. doi: 10.1002/dvdy.20528

Bally-Cuif, L., and Wassef, M. (1995). Determination events in the nervous system of the vertebrate embryo. *Curr. Opin. Genet. Dev.* 5, 450–458. doi: 10.1016/0959-437X(95)90048-L

Bayliss, D. A., Barhanin, J., Gestreau, C., and Guyenet, P. G. (2015). The role of pH-sensitive task channels in central respiratory chemoreception. *Pflugers Archiv-Eur. J. Physiol.* 467, 917–929. doi: 10.1007/s00424-014-1633-9

Ben-Arie, N., Bellen, H. J., Armstrong, D. L., Mccall, A. E., Gordadze, P. R., Guo, Q. X., et al. (1997). Math1 is essential for genesis of cerebellar granule neurons. *Nature* 390, 169–172. doi: 10.1038/36579

Bermingham, N. A., Hassan, B. A., Wang, V. Y., Fernandez, M., Banfi, S., Bellen, H. J., et al. (2001). Proprioceptor pathway development is dependent on Math1. *Neuron* 30, 411–422. doi: 10.1016/S0896-6273(01)00305-1

Blanchi, B., Kelly, L. M., Viemari, J. C., Lafon, I., Burnet, H., Bevengut, M., et al. (2003). MafB deficiency causes defective respiratory rhythmogenesis and fatal central apnea at birth. *Nat. Neurosci.* 6, 1091–1099. doi: 10.1038/nn1129

Blaugrund, E., Pham, T. D., Tennyson, V. M., Lo, L., Sommer, L., Anderson, D. J., et al. (1996). Distinct subpopulations of enteric neuronal progenitors defined by time of development, sympathoadrenal lineage markers and Mash-1-dependence. *Development* 122, 309–320. doi: 10.1242/dev.122.1.309

Bongianni, F., Fontana, G., and Pantaleo, T. (1988). Effects of electrical and chemical-stimulation of the botzinger complex on respiratory activity in the cat. *Brain Res.* 445, 254–261. doi: 10.1016/0006-8993(88)91187-0

Bouchard, M., Grote, D., Craven, S. E., Sun, Q., Steinlein, P., and Busslinger, M. (2005). Identification of Pax2-regulated genes by expression profiling of the mid-hindbrain organizer region. *Development* 132, 2633–2643. doi: 10.1242/dev.01833

Bouchard, M., Pfeffer, P., and Busslinger, M. (2000). Functional equivalence of the transcription factors Pax2 and Pax5 in mouse development. *Development* 127, 3703–3713. doi: 10.1242/dev.127.17.3703

Bouvier, J., Thoby-Brisson, M., Renier, N., Dubreuil, V., Ericson, J., Champagnat, J., et al. (2010). Hindbrain interneurons and axon guidance signaling critical for breathing. *Nat. Neurosci.* 13, 1066–1074. doi: 10.1038/nn.2622

Briscoe, J., Sussel, L., Serup, P., Hartigan-O'connor, D., Jessell, T. M., Rubenstein, J. L. R., et al. (1999). Homeobox gene Nkx2.2 and specification of neuronal identity by graded Sonic hedgehog signalling. *Nature* 398, 622–627. doi: 10.1038/19315

Broccoli, V., Boncinelli, E., and Wurst, W. (1999). The caudal limit of Otx2 expression positions the isthmic organizer. *Nature* 401, 164–168. doi: 10.1038/43670

Brust, R. D., Corcoran, A. E., Richerson, G. B., Nattie, E., and Dymecki, S. M. (2014). Functional and developmental identification of a molecular subtype of brain serotonergic neuron specialized to regulate breathing dynamics. *Cell Rep.* 9, 2152–2165. doi: 10.1016/j.celrep.2014.11.027

Bryant, T. H., Yoshida, S., Decastro, D., and Lipski, J. (1993). Expiratory neurons of the botzinger complex in the rat - a morphological-study following intracellular labeling with biocytin. *J. Comp. Neurol.* 335, 267–282. doi: 10.1002/cne.903350210

Buchanan, G. F., and Richerson, G. B. (2010). Central serotonin neurons are required for arousal to Co2. *Proc. Natl. Acad. Sci. U. S. A.* 107, 16354–16359. doi: 10.1073/pnas.1004587107

Ceccherini, I., Kurek, K. C., and Weese-Mayer, D. E. (2022). Developmental disorders affecting the respiratory system: Cchs and Rohhad. *Handb. Clin. Neurol.* 189, 53–91. doi: 10.1016/B978-0-323-91532-8.00005-7

Chamberlin, N. L., and Saper, C. B. (1994). Topographic organization of respiratory responses to glutamate microstimulation of the parabrachial nucleus in the rat. *J. Neurosci.* 14, 6500–6510. doi: 10.1523/JNEUROSCI.14-11-06500.1994

Chang, R. B., Strochlic, D. E., Williams, E. K., Umans, B. D., and Liberles, S. D. (2015). Vagal sensory neuron subtypes that differentially control breathing. *Cell* 161, 622–633. doi: 10.1016/j.cell.2015.03.022

Chatonnet, F., Wrobel, L. J., Mezieres, V., Pasqualetti, M., Ducret, S., Taillebourg, E., et al. (2007). Distinct roles of Hoxa2 and Krox20 in the development of rhythmic neural networks controlling inspiratory depth, respiratory frequency, and jaw opening. *Neural Dev.* 2:19. doi: 10.1186/1749-8104-2-19

Chen, Z. F., Rebelo, S., White, F., Malmberg, A. B., Baba, H., Lima, D., et al. (2001). The paired homeodomain protein Drg11 is required for the projection of cutaneous sensory afferent fibers to the dorsal spinal cord. *Neuron* 31, 59–73. doi: 10.1016/S0896-6273(01)00341-5

Cheng, L., Arata, A., Mizuguchi, R., Qian, Y., Karunaratne, A., Gray, P. A., et al. (2004). Tlx3 and Tlx1 are post-mitotic selector genes determining glutamatergic over Gabaergic cell fates. *Nat. Neurosci.* 7, 510–517. doi: 10.1038/nn1221

Cheng, L., Samad, O. A., Xu, Y., Mizuguchi, R., Luo, P., Shirasawa, S., et al. (2005). Lbx1 and Tlx3 are opposing switches in determining Gabaergic versus glutamatergic transmitter phenotypes. *Nat. Neurosci.* 8, 1510–1515. doi: 10.1038/nn1569

Cheng, L. P., Chen, C. L., Luo, P., Tan, M., Qiu, M. S., Johnson, R., et al. (2003). Lmx1b, Pet-1, and Nkx2.2 coordinately specify serotonergic neurotransmitter phenotype. *J. Neurosci.* 23, 9961–9967. doi: 10.1523/JNEUROSCI.23-31-09961.2003

Chi, C. L., Martinez, S., Wurst, W., and Martin, G. R. (2003). The isthmic organizer signal Fgf8 is required for cell survival in the prospective midbrain and cerebellum. *Development* 130, 2633–2644. doi: 10.1242/dev.00487

Chiang, C., Ying, L. T. T., Lee, E., Young, K. E., Corden, J. L., Westphal, H., et al. (1996). Cyclopia and defective axial patterning in mice lacking Sonic hedgehog gene function. *Nature* 383, 407–413. doi: 10.1038/383407a0

Chizhikov, V., and Millen, K. J. (2003). Development and malformations of the cerebellum in mice. *Mol. Genet. Metab.* 80, 54–65. doi: 10.1016/j.ymgme.2003.08.019

Chizhikov, V. V., Iskusnykh, I. Y., Fattakhov, N., and Fritzsch, B. (2021). Lmx1a and Lmx1b are redundantly required for the development of multiple components of the mammalian auditory system. *Neuroscience* 452, 247–264. doi: 10.1016/j.neuroscience.2020.11.013

Choe, S. K., Vlachakis, N., and Sagerstrom, C. G. (2002). Meis family proteins are required for hindbrain development in the zebrafish. *Development* 129, 585–595. doi: 10.1242/dev.129.3.585

Crossley, P. H., Minowada, G., Macarthur, C. A., and Martin, G. R. (1996). Roles for Fgf8 in the induction, initiation, and maintenance of chick limb development. *Cell* 84, 127–136. doi: 10.1016/S0092-8674(00)80999-X

Dauger, S., Pattyn, A., Lofaso, F., Gaultier, C., Goridis, C., Gallego, J., et al. (2003). Phox2b controls the development of peripheral chemoreceptors and afferent visceral pathways. *Development* 130, 6635–6642. doi: 10.1242/dev.00866

D'Autreaux, F., Coppola, E., Hirsch, M. R., Birchmeier, C., and Brunet, J. F. (2011). Homeoprotein Phox2b commands a somatic-to-visceral switch in cranial sensory pathways. *Proc. Natl. Acad. Sci. U S A.* 108, 20018–20023. doi: 10.1073/pnas.1110416108

Del Negro, C. A., Funk, G. D., and Feldman, J. L. (2018). Breathing matters. *Nat. Rev. Neurosci.* 19, 351–367. doi: 10.1038/s41583-018-0003-6

Depuy, S. D., Kanbar, R., Coates, M. B., Stornetta, R. L., and Guyenet, P. G. (2011). Control of breathing by raphe obscurus serotonergic neurons in mice. *J. Neurosci.* 31, 1981–1990. doi: 10.1523/JNEUROSCI.4639-10.2011

Di Bonito, M., and Studer, M. (2017). Cellular and molecular underpinnings of neuronal assembly in the central auditory system during mouse development. *Front. Neural Circuits* 11:18. doi: 10.3389/fncir.2017.00018

Di Giovannantonio, L. G., Di Salvio, M., Omodei, D., Prakash, N., Wurst, W., Pierani, A., et al. (2014). Otx2 cell-autonomously determines dorsal mesencephalon versus cerebellum fate independently of isthmic organizing activity. *Development* 141, 377–388. doi: 10.1242/dev.102954

Diek, D., Smidt, M. P., and Mesman, S. (2022). Molecular organization and patterning of the medulla oblongata in health and disease. *Int. J. Mol. Sci.* 23:9260. doi: 10.3390/ijms23169260

Ding, Y. Q., Marklund, U., Yuan, W. L., Yin, J., Wegman, L., Ericson, J., et al. (2003). Lmx1b is essential for the development of serotonergic neurons. *Nat. Neurosci.* 6, 933–938. doi: 10.1038/nn1104

Dosumu-Johnson, R. T., Cocoran, A. E., Chang, Y., Nattie, E., and Dymecki, S. M. (2018). Acute perturbation of Pet1-neuron activity in neonatal mice impairs cardiorespiratory homeostatic recovery. *eLife* 7:e37857. doi: 10.7554/eLife.37857.022

Douse, M. A., and Duffin, J. (1992). Projections to botzinger expiratory neurons by dorsal and ventral respiratory group neurons. *Neuroreport* 3, 393–396. doi: 10.1097/00001756-199205000-00004

Dubreuil, V., Ramanantsoa, N., Trochet, D., Vaubourg, V., Amiel, J., Gallego, J., et al. (2008). A human mutation in Phox2b causes lack of Co2 chemosensitivity, fatal central apnea, and specific loss of parafacial neurons. *Proc. Natl. Acad. Sci. U S A.* 105, 1067–1072. doi: 10.1073/pnas.0709115105

Dubreuil, V., Thoby-Brisson, M., Rallu, M., Persson, K., Pattyn, A., Birchmeier, C., et al. (2009). Defective respiratory rhythmogenesis and loss of central chemosensitivity in Phox2b mutants targeting retrotrapezoid nucleus neurons. *J. Neurosci.* 29, 14836–14846. doi: 10.1523/JNEUROSCI.2623-09.2009

Dworkin, S., Darido, C., Georgy, S. R., Wilanowski, T., Srivastava, S., Ellett, F., et al. (2012). Midbrain-hindbrain boundary patterning and morphogenesis are regulated by diverse grainy head-like 2-dependent pathways. *Development* 139, 525–536. doi: 10.1242/dev.066522

Elliott, K. L., Pavlinkova, G., Chizhikov, V. V., Yamoah, E. N., and Fritzsch, B. (2021). Neurog1, Neurod1, and Atoh1 are essential for spiral ganglia, cochlear nuclei, and cochlear hair cell development. *Fac. Rev.* 10:47. doi: 10.12703/r/10-47

Englund, C., Kowalczyk, T., Daza, R. A., Dagan, A., Lau, C., Rose, M. F., et al. (2006). Unipolar brush cells of the cerebellum are produced in the rhombic lip and migrate through developing white matter. *J. Neurosci.* 26, 9184–9195. doi: 10.1523/JNEUROSCI.1610-06.2006

Espinosa-Medina, I., Saha, O., Boismoreau, F., Chettouh, Z., Rossi, F., Richardson, W. D., et al. (2016). The sacral autonomic outflow is sympathetic. *Science* 354, 893–897. doi: 10.1126/science.aah5454

Ezure, K., Tanaka, I., and Kondo, M. (2003a). Glycine is used as a transmitter by decrementing expiratory neurons of the ventrolateral medulla in the rat. *J. Neurosci.* 23, 8941–8948. doi: 10.1523/JNEUROSCI.23-26-08941.2003

Ezure, K., Tanaka, I., and Saito, Y. (2003b). Activity of brainstem respiratory neurones just before the expiration-inspiration transition in the rat. *J. Physiology-London* 547, 629–640. doi: 10.1113/jphysiol.2002.032805

Ezure, K., Tanaka, I., and Saito, Y. (2003c). Brainstem and spinal projections of augmenting expiratory neurons in the rat. *Neurosci. Res.* 45, 41–51. doi: 10.1016/S0168-0102(02)00197-9

Fienberg, A. A., Utset, M. F., Bogarad, L. D., Hart, C. P., Awgulewitsch, A., Ferguson-Smith, A., et al. (1987). Homeo box genes in murine development. *Curr. Top. Dev. Biol.* 23, 233–256. doi: 10.1016/S0070-2153(08)60627-4

Fink, A. J., Englund, C., Daza, R. A., Pham, D., Lau, C., Nivison, M., et al. (2006). Development of the deep cerebellar nuclei: transcription factors and cell migration from the rhombic lip. *J. Neurosci.* 26, 3066–3076. doi: 10.1523/JNEUROSCI.5203-05.2006

Fode, C., Gradwohl, G., Morin, X., Dierich, A., Lemeur, M., Goridis, C., et al. (1998). The bhlh protein Neurogenin 2 is a determination factor for epibranchial placode-derived sensory neurons. *Neuron* 20, 483–494. doi: 10.1016/S0896-6273(00)80989-7

Fortin, G., and Thoby-Brisson, M. (2009). Embryonic emergence of the respiratory rhythm generator. *Respiratory Physiol. Neurobiol.* 168, 86–91. doi: 10.1016/j.resp.2009.06.013

Fraser, S., Keynes, R., and Lumsden, A. (1990). Segmentation in the chick embryo hindbrain is defined by cell lineage restrictions. *Nature* 344, 431–435. doi: 10.1038/344431a0

Fritzsch, B., Elliott, K. L., and Yamoah, E. N. (2022). Neurosensory development of the four brainstem-projecting sensory systems and their integration in the telencephalon. *Front. Neural Circuits* 16:913480. doi: 10.3389/fncir.2022.913480

Gang, S., and Lei, L. (1996). Reappraisal of the inspiratory effect of Botzinger complex on phrenic nerve discharge. *Respiration Physiol.* 105, 17–21. doi: 10.1016/0034-5687(96)00022-9

Gavalas, A., and Krumlauf, R. (2000). Retinoid signalling and hindbrain patterning. *Curr. Opin. Genet. Dev.* 10, 380–386. doi: 10.1016/S0959-437X(00)00100-3

Gazit, R., Krizhanovsky, V., and Ben-Arie, N. (2004). Math1 controls cerebellar granule cell differentiation by regulating multiple components of the Notch signaling pathway. *Development* 131, 903–913. doi: 10.1242/dev.00982

Gibbs, H. C., Chang-Gonzalez, A., Hwang, W., Yeh, A. T., and Lekven, A. C. (2017). Midbrain-Hindbrain boundary morphogenesis: at the intersection of Wnt and Fgf signaling. *Front. Neuroanat.* 11:64. doi: 10.3389/fnana.2017.00064

Giudicelli, F., Gilardi-Hebenstreit, P., Mechta-Grigoriou, F., Poquet, C., and Charnay, P. (2003). Novel activities of Mafb underlie its dual role in hindbrain segmentation and regional specification. *Dev. Biol.* 253, 150–162. doi: 10.1006/dbio.2002.0864

Glover, J. C., Elliott, K. L., Erives, A., Chizhikov, V. V., and Fritzsch, B. (2018). Wilhelm His' lasting insights into hindbrain and cranial ganglia development and evolution. *Dev. Biol.* 444, S14–S24. doi: 10.1016/j.ydbio.2018.02.001

Glover, J. C., Renaud, J. S., and Rijli, F. M. (2006). Retinoic acid and hindbrain patterning. *J. Neurobiol.* 66, 705–725. doi: 10.1002/neu.20272

Gray, P. A. (2008). Transcription factors and the genetic organization of brain stem respiratory neurons. *J. Appl. Physiol.* 104, 1513–1521. doi: 10.1152/japplphysiol.01383.2007

Gray, P. A. (2013). Transcription factors define the neuroanatomical organization of the medullary reticular formation. *Front. Neuroanat.* 7:7. doi: 10.3389/fnana.2013.00007

Gray, P. A., Hayes, J. A., Ling, G. Y., Llona, I., Tupal, S., Picardo, M. C. D., et al. (2010). Developmental origin of prebotzinger complex respiratory neurons. *J. Neurosci.* 30, 14883–14895. doi: 10.1523/JNEUROSCI.4031-10.2010

Gray, P. A., Janczewski, W. A., Mellen, N., Mccrimmon, D. R., and Feldman, J. L. (2001). Normal breathing requires preBotzinger complex neurokinin-1 receptor-expressing neurons. *Nat. Neurosci.* 4, 927–930. doi: 10.1038/nn0901-927

Gray, P. A., Rekling, J. C., Bocchiaro, C. M., and Feldman, J. L. (1999). Modulation of respiratory frequency by peptidergic input to rhythmogenic neurons in the PreBotzinger complex. *Science* 286, 1566–1568. doi: 10.1126/science.286.5444.1566

Grill, H. J., and Hayes, M. R. (2009). The nucleus tractus solitarius: a portal for visceral afferent signal processing, energy status assessment and integration of their combined effects on food intake. *Int. J. Obesity* 33, S11–S15. doi: 10.1038/ijo.2009.10

Gross, M. K., Dottori, M., and Goulding, M. (2002). Lbx1 specifies somatosensory association interneurons in the dorsal spinal cord. *Neuron* 34, 535–549. doi: 10.1016/S0896-6273(02)00690-6

Guo, Q. X., and Li, J. Y. H. (2007). Distinct functions of the major Fgf8 spliceform, Fgf8b, before and during mouse gastrulation. *Development* 134, 2251–2260. doi: 10.1242/dev.004929

Gutzman, J. H., Graeden, E., Brachmann, I., Yamazoe, S., Chen, J. K., and Sive, H. (2018). Basal constriction during midbrain-hindbrain boundary morphogenesis is mediated by Wnt5b and focal adhesion kinase. *Biol. Open* 7:bio034520. doi: 10.1242/bio.034520

Guyenet, P. G., and Bayliss, D. A. (2015). Neural control of breathing and Co2 homeostasis. *Neuron* 87, 946–961. doi: 10.1016/j.neuron.2015.08.001

Guyenet, P. G., and Bayliss, D. A. (2022). Central respiratory chemoreception. *Handb. Clin. Neurol.* 188, 37–72. doi: 10.1016/B978-0-323-91534-2.00007-2

Guyenet, P. G., Stornetta, R. L., Souza, G., Abbott, S. B. G., Shi, Y., and Bayliss, D. A. (2019). The retrotrapezoid nucleus: central chemoreceptor and regulator of breathing automaticity. *Trends Neurosci.* 42, 807–824. doi: 10.1016/j.tins.2019.09.002

Helms, A. W., and Johnson, J. E. (1998). Progenitors of dorsal commissural interneurons are defined by Math1 expression. *Development* 125, 919–928. doi: 10.1242/dev.125.5.919

Hendricks, T. J., Fyodorov, D. V., Wegman, L. J., Lelutiu, N. B., Pehek, E. A., Yamamoto, B., et al. (2003). Pet-1 Ets gene plays a critical role in 5-Ht neuron development and is required for normal anxiety-like and aggressive behavior. *Neuron* 37, 233–247. doi: 10.1016/S0896-6273(02)01167-4

Hernandez-Miranda, L. R., and Birchmeier, C. (2015). Co(2) in the spotlight. *eLife* 4:e08086. doi: 10.7554/eLife.08086

Hernandez-Miranda, L. R., Ibrahim, D. M., Ruffault, P. L., Larrosa, M., Balueva, K., Muller, T., et al. (2018). Mutation in Lbx1/Lbx1 precludes transcription factor cooperativity and causes congenital hypoventilation in humans and mice. *Proc. Natl. Acad. Sci. U S A.* 115, 13021–13026. doi: 10.1073/pnas.1813520115

Hernandez-Miranda, L. R., Muller, T., and Birchmeier, C. (2017a). The dorsal spinal cord and hindbrain: from developmental mechanisms to functional circuits. *Dev. Biol.* 432, 34–42. doi: 10.1016/j.ydbio.2016.10.008

Hernandez-Miranda, L. R., Ruffault, P. L., Bouvier, J. C., Murray, A. J., Morin-Surun, M. P., Zampieri, N., et al. (2017b). Genetic identification of a hindbrain nucleus essential for innate vocalization. *Proc. Natl. Acad. Sci. U S A.* 114, 8095–8100. doi: 10.1073/pnas.1702893114

Hidalgo-Sanchez, M., Andreu-Cervera, A., Villa-Carballar, S., and Echevarria, D. (2022). An update on the molecular mechanism of the vertebrate isthmic organizer development in the context of the neuromeric model. *Front. Neuroanatomy* 16:826976. doi: 10.3389/fnana.2022.826976

Hidalgo-Sanchez, M., Simeone, A., and Alvarado-Mallart, R. M. (1999). Fgf8 and Gbx2 induction concomitant with Otx2 repression is correlated with midbrain-hindbrain fate of caudal prosencephalon. *Development* 126, 3191–3203. doi: 10.1242/dev.126.14.3191

Hirsch, D., Kohl, A., Wang, Y., and Sela-Donenfeld, D. (2021). Axonal projection patterns of the dorsal interneuron populations in the embryonic hindbrain. *Front. Neuroanat.* 15:793161. doi: 10.3389/fnana.2021.793161

Hodges, M. R., Tattersall, G. J., Harris, M. B., Mcevoy, S. D., Richerson, D. N., Deneris, E. S., et al. (2008). Defects in breathing and thermoregulation in mice with near-complete absence of central serotonin neurons. *J. Neurosci.* 28, 2495–2505. doi: 10.1523/JNEUROSCI.4729-07.2008

Hodges, M. R., Wehner, M., Aungst, J., Smith, J. C., and Richerson, G. B. (2009). Transgenic mice lacking serotonin neurons have severe apnea and high mortality during development. *J. Neurosci.* 29, 10341–10349. doi: 10.1523/JNEUROSCI.1963-09.2009

Huang, W. H., Tupal, S., Huang, T. W., Ward, C. S., Neul, J. L., Klisch, T. J., et al. (2012). Atoh1 governs the migration of postmitotic neurons that shape respiratory effectiveness at birth and chemoresponsiveness in adulthood. *Neuron* 75, 799–809. doi: 10.1016/j.neuron.2012.06.027

Huckstepp, R. T. R., Cardoza, K. P., Henderson, L. E., and Feldman, J. L. (2015). Role of parafacial nuclei in control of breathing in adult rats. *J. Neurosci.* 35, 1052–1067. doi: 10.1523/JNEUROSCI.2953-14.2015

Huckstepp, R. T. R., Cardoza, K. P., Henderson, L. E., and Feldman, J. L. (2018). Distinct parafacial regions in control of breathing in adult rats. *PLoS One* 13:e0201485. doi: 10.1371/journal.pone.0201485

Huckstepp, R. T. R., Henderson, L. E., Cardoza, K. P., and Feldman, J. L. (2016). Interactions between respiratory oscillators in adult rats. *eLife* 5:e14203. doi: 10.7554/eLife.14203.013

Isik, E. G., and Hernandez-Miranda, L. R. (2022). Early development of the breathing network. *Handb. Clin. Neurol.* 188, 125–149. doi: 10.1016/B978-0-323-91534-2.00002-3

Jacobs, B. L., Martin-Cora, F. J., and Fornal, C. A. (2002). Activity of medullary serotonergic neurons in freely moving animals. *Brain Res. Rev.* 40, 45–52. doi: 10.1016/S0165-0173(02)00187-X

Jiang, C., and Lipski, J. (1990). Extensive monosynaptic inhibition of ventral respiratory group neurons by augmenting neurons in the botzinger complex in the cat. *Exp. Brain Res.* 81, 639–648. doi: 10.1007/BF02423514

Joyner, A. L., Liu, A., and Millet, S. (2000). Otx2, Gbx2 and Fgf8 interact to position and maintain a mid-hindbrain organizer. *Curr. Opin. Cell Biol.* 12, 736–741. doi: 10.1016/S0955-0674(00)00161-7

Kam, R. K., Deng, Y., Chen, Y., and Zhao, H. (2012). Retinoic acid synthesis and functions in early embryonic development. *Cell Biosci.* 2:11. doi: 10.1186/2045-3701-2-11

Katahira, T., Sato, T., Sugiyama, S., Okafuji, T., Araki, I., Funahashi, J., et al. (2000). Interaction between Otx2 and Gbx2 defines the organizing center for the optic tectum. *Mechan. Dev.* 91, 43–52. doi: 10.1016/S0925-4773(99)00262-2

Kawai, Y. (2018). Differential ascending projections from the male rat caudal nucleus of the tractus solitarius: an interface between local microcircuits and global macrocircuits. *Front. Neuroanatomy* 12:63. doi: 10.3389/fnana.2018.00063

Korsak, A., Sheikhbahaei, S., Machhada, A., Gourine, A. V., and Huckstepp, R. T. R. (2018). The role of parafacial neurons in the control of breathing during exercise. *Sci. Rep.* 8:400. doi: 10.1038/s41598-017-17412-z

Krumlauf, R., Marshall, H., Studer, M., Nonchev, S., Sham, M. H., and Lumsden, A. (1993). Hox homeobox genes and regionalisation of the nervous system. *J. Neurobiol.* 24, 1328–1340. doi: 10.1002/neu.480241006

Kubin, L., Alheid, G. F., Zuperku, E. J., and Mccrimmon, D. R. (2006). Central pathways of pulmonary and lower airway vagal afferents. *J. Appl. Physiol.* 101, 618–627. doi: 10.1152/japplphysiol.00252.2006

Kumada, M., Terui, N., and Kuwaki, T. (1990). Arterial baroreceptor reflex: its central and peripheral neural mechanisms. *Prog. Neurobiol.* 35, 331–361. doi: 10.1016/0301-0082(90)90036-G

Lee, K. J., Dietrich, P., and Jessell, T. M. (2000). Genetic ablation reveals that the roof plate is essential for dorsal interneuron specification. *Nature* 403, 734–740. doi: 10.1038/35001507

Lee, K. J., Mendelsohn, M., and Jessell, T. M. (1998). Neuronal patterning by Bmps: a requirement for Gdf7 in the generation of a discrete class of commissural interneurons in the mouse spinal cord. *Genes Dev.* 12, 3394–3407. doi: 10.1101/gad.12.21.3394

Lee, S. M. K., Danielian, P. S., Fritzsch, B., and Mcmahon, A. P. (1997). Evidence that Fgf8 signalling from the midbrain-hindbrain junction regulates growth and polarity in the developing midbrain. *Development* 124, 959–969. doi: 10.1242/dev.124.5.959

Liem, K. F. Jr., Tremml, G., and Jessell, T. M. (1997). A role for the roof plate and its resident Tgfbeta-related proteins in neuronal patterning in the dorsal spinal cord. *Cell* 91, 127–138. doi: 10.1016/S0092-8674(01)80015-5

Liu, A., Losos, K., and Joyner, A. (1999). Fgf8 can activate Gbx2 and transform regions of the rostral mouse brain into a hindbrain fate. *Dev. Biol.* 210, 227–227. doi: 10.1242/dev.126.21.4827

Liu, A. M., Li, J. Y. H., Bromleigh, C., Lao, Z. M., Niswander, L. A., and Joyner, A. L. (2003). Fgf17b and Fgf18 have different midbrain regulatory properties from Fgf8b or activated Fgf receptors. *Development* 130, 6175–6185. doi: 10.1242/dev.00845

Liu, Z., Li, H., Hu, X., Yu, L., Liu, H., Han, R., et al. (2008). Control of precerebellar neuron development by Olig3 bhlh transcription factor. *J. Neurosci.* 28, 10124–10133. doi: 10.1523/JNEUROSCI.3769-08.2008

Lopez-Barneo, J. (2022). Neurobiology of the carotid body. *Handb. Clin. Neurol.* 188, 73–102. doi: 10.1016/B978-0-323-91534-2.00010-2

Lowenstein, E. D., Cui, K., and Hernandez-Miranda, L. R. (2022). Regulation of early cerebellar development. *FEBS J.* Online ahead of print. doi: 10.1111/febs.16426

Lowenstein, E. D., Rusanova, A., Stelzer, J., Hernaiz-Llorens, M., Schroer, A. E., Epifanova, E., et al. (2021). Olig3 regulates early cerebellar development. *eLife* 10:e64684. doi: 10.7554/eLife.64684.sa2

Lumsden, A., and Krumlauf, R. (1996). Patterning the vertebrate neuraxis. *Science* 274, 1109–1115. doi: 10.1126/science.274.5290.1109

Machado, B. H., Mauad, H., Chianca, D. A., Haibara, A. S., and Colombari, E. (1997). Autonomic processing of the cardiovascular reflexes in the nucleus tractus solitarii. *Braz. J. Med. Biol. Res.* 30, 533–543. doi: 10.1590/S0100-879X1997000400015

Machold, R., Klein, C., and Fishell, G. (2011). Genes expressed in Atoh1 neuronal lineages arising from the r1/isthmus rhombic lip. *Gene Exp. Patterns* 11, 349–359. doi: 10.1016/j.gep.2011.03.007

Manzanares, M., Nardelli, J., Gilardi-Hebenstreit, P., Marshall, H., Giudicelli, F., Martinez-Pastor, M. T., et al. (2002). Krox20 and kreisler co-operate in the transcriptional control of segmental expression of Hoxb3 in the developing hindbrain. *EMBO J.* 21, 365–376. doi: 10.1093/emboj/21.3.365

Marti, E., Bumcrot, D. A., Takada, R., and Mcmahon, A. P. (1995). Requirement of 19k form of sonic hedgehog for induction of distinct ventral cell-types in Cns explants. *Nature* 375, 322–325. doi: 10.1038/375322a0

Martinez, S., Crossley, P. H., Cobos, I., Rubenstein, J. L. R., and Martin, G. R. (1999). Fgf8 induces formation of an ectopic isthmic organizer and isthmocerebellar development via a repressive effect on Otx2 expression. *Development* 126, 1189–1200. doi: 10.1242/dev.126.6.1189

Matsunaga, E., Katahira, T., and Nakamura, H. (2002). Role of Lmx1b and Wnt1 in mesencephalon and metencephalon development. *Development* 129, 5269–5277. doi: 10.1242/dev.129.22.5269

Meyers, E. N., Lewandoski, M., and Martin, G. R. (1998). An Fgf8 mutant allelic series generated by Cre- and Flp-mediated recombination. *Nat. Genet.* 18, 136–141. doi: 10.1038/ng0298-136

Mifflin, S. W. (1992). Arterial chemoreceptor input to nucleus-tractus-solitarius. *Am. J. Physiol.* 263, R368–R375. doi: 10.1152/ajpregu.1992.263.2.R368

Mifflin, S. W. (1993). Absence of respiration modulation of carotid-sinus nerve inputs to nucleus-tractus-solitarius neurons receiving arterial chemoreceptor inputs. *J. Autonomic Nervous System* 42, 191–199. doi: 10.1016/0165-1838(93)90364-Z

Mifflin, S. W., Spyer, K. M., and Withingtonwray, D. J. (1988). Baroreceptor inputs to the nucleus tractus solitarius in the Cat - modulation by the hypothalamus. *J. Physiology-London* 399, 369–387. doi: 10.1113/jphysiol.1988.sp017086

Millet, S., Blochgallego, E., Simeone, A., and Alvaradomallart, R. M. (1996). The caudal limit of Otx2 gene expression as a marker of the midbrain/hindbrain boundary: a study using in situ hybridisation and chick/quail homotopic grafts. *Development* 122, 3785–3797. doi: 10.1242/dev.122.12.3785

Millet, S., Campbell, K., Epstein, D. J., Losos, K., Harris, E., and Joyner, A. L. (1999). A role for Gbx2 in repression of Otx2 and positioning the mid/hindbrain organizer. *Nature* 401, 161–164. doi: 10.1038/43664

Mishima, Y., Lindgren, A. G., Chizhikov, V. V., Johnson, R. L., and Millen, K. J. (2009). Overlapping function of Lmx1a and Lmx1b in anterior hindbrain roof plate formation and cerebellar growth. *J. Neurosci.* 29, 11377–11384. doi: 10.1523/JNEUROSCI.0969-09.2009

Morin, X., Cremer, H., Hirsch, M. R., Kapur, R. P., Goridis, C., and Brunet, J. F. (1997). Defects in sensory and autonomic ganglia and absence of locus coeruleus in mice deficient for the homeobox gene Phox2a. *Neuron* 18, 411–423. doi: 10.1016/S0896-6273(00)81242-8

Muller, T., Anlag, K., Wildner, H., Britsch, S., Treier, M., and Birchmeier, C. (2005). The bhlh factor Olig3 coordinates the specification of dorsal neurons in the spinal cord. *Genes Dev.* 19, 733–743. doi: 10.1101/gad.326105

Muller, T., Brohmann, H., Pierani, A., Heppenstall, P. A., Lewin, G. R., Jessell, T. M., et al. (2002). The homeodomain factor lbx1 distinguishes two major programs of neuronal differentiation in the dorsal spinal cord. *Neuron* 34, 551–562. doi: 10.1016/S0896-6273(02)00689-X

Muroyama, Y., Fujihara, M., Ikeya, M., Kondoh, H., and Takada, S. (2002). Wnt signaling plays an essential role in neuronal specification of the dorsal spinal cord. *Genes Dev.* 16, 548–553. doi: 10.1101/gad.937102

Nattie, E., and Li, A. H. (2012). Central chemoreceptors: locations and functions. *Comprehen. Physiol.* 2, 221–254. doi: 10.1002/cphy.c100083

Nieuwenhuys, R. (2011). The structural, functional, and molecular organization of the brainstem. *Front. Neuroanatomy* 5:33. doi: 10.3389/fnana.2011.00033

Okaty, B. W., Sturrock, N., Escobedo Lozoya, Y., Chang, Y., Senft, R. A., Lyon, K. A., et al. (2020). A single-cell transcriptomic and anatomic atlas of mouse dorsal raphe Pet1 neurons. *eLife* 9:e55523. doi: 10.7554/eLife.55523.sa2

Onimaru, H., and Homma, I. (2003). A novel functional neuron group for respiratory rhythm generation in the ventral medulla. *J. Neurosci.* 23, 1478–1486. doi: 10.1523/JNEUROSCI.23-04-01478.2003

Otake, K., Sasaki, H., Ezure, K., and Manabe, M. (1988). Axonal projections from botzinger expiratory neurons to contralateral ventral and dorsal respiratory groups in the cat. *Exp. Brain Res.* 72, 167–177. doi: 10.1007/BF00248512

Pagliardini, S., Ren, J., Gray, P. A., Vandunk, C., Gross, M., Goulding, M., et al. (2008). Central respiratory rhythmogenesis is abnormal in lbx1- deficient mice. *J. Neurosci.* 28, 11030–11041. doi: 10.1523/JNEUROSCI.1648-08.2008

Pan, N., Jahan, I., Lee, J. E., and Fritzsch, B. (2009). Defects in the cerebella of conditional Neurod1 null mice correlate with effective Tg(Atoh1-cre) recombination and granule cell requirements for Neurod1 for differentiation. *Cell Tissue Res.* 337, 407–428. doi: 10.1007/s00441-009-0826-6

Pattyn, A., Goridis, C., and Brunet, J. F. (2000a). Specification of the central noradrenergic phenotype by the homeobox gene Phox2b. *Mol. Cell. Neurosci.* 15, 235–243. doi: 10.1006/mcne.1999.0826

Pattyn, A., Hirsch, M. R., Goridis, C., and Brunet, J. F. (2000b). Control of hindbrain motor neuron differentiation by the homeobox gene Phox2b. *Development* 127, 1349–1358. doi: 10.1242/dev.127.7.1349

Pattyn, A., Guillermot, F., and Brunet, J. F. (2006). Delays in neuronal differentiation in Mash1/Ascl1 mutants. *Dev. Biol.* 295, 67–75. doi: 10.1016/j.ydbio.2006.03.008

Pattyn, A., Morin, X., Cremer, H., Goridis, C., and Brunet, J. F. (1997). Expression and interactions of the two closely related homeobox genes Phox2a and Phox2b during neurogenesis. *Development* 124, 4065–4075. doi: 10.1242/dev.124.20.4065

Pattyn, A., Morin, X., Cremer, H., Goridis, C., and Brunet, J. F. (1999). The homeobox gene Phox2b is essential for the development of autonomic neural crest derivatives. *Nature* 399, 366–370. doi: 10.1038/20700

Pattyn, A., Simplicio, N., Van Doorninck, J. H., Goridis, C., Guillemot, F., and Brunet, J. F. (2004). Ascl1/Mash1 is required for the development of central serotonergic neurons. *Nat. Neurosci.* 7, 589–595. doi: 10.1038/nn1247

Pattyn, A., Vallstedt, A., Dias, J. M., Samad, O. A., Krumlauf, R., Rijli, F. M., et al. (2003). Coordinated temporal and spatial control of motor neuron and serotonergic neuron generation from a common pool of Cns progenitors. *Genes Dev.* 17, 729–737. doi: 10.1101/gad.255803

Pierani, A., Brenner-Morton, S., Chiang, C., and Jessell, T. M. (1999). A sonic hedgehog-independent, retinoid-activated pathway of neurogenesis in the ventral spinal cord. *Cell* 97, 903–915. doi: 10.1016/S0092-8674(00)80802-8

Pierani, A., Moran-Rivard, L., Sunshine, M. J., Littman, D. R., Goulding, M., and Jessell, T. M. (2001). Control of interneuron fate in the developing spinal cord by the progenitor homeodomain protein Dbx1. *Neuron* 29, 367–384. doi: 10.1016/S0896-6273(01)00212-4

Pisanski, A., and Pagliardini, S. (2019). The parafacial respiratory group and the control of active expiration. *Respiratory Physiol. Neurobiol.* 265, 153–160. doi: 10.1016/j.resp.2018.06.010

Prakash, N., Brodski, C., Naserke, T., Puelles, E., Gogoi, R., Hall, A., et al. (2006). A Wnt1-regulated genetic network controls the identity and fate of midbrain-dopaminergic progenitors in vivo. *Development* 133, 89–98. doi: 10.1242/dev.02181

Puelles, E., Acampora, D., Lacroix, E., Signore, M., Annino, A., Tuorto, F., et al. (2003). Otx dose-dependent integrated control of antero-posterior and dorso-ventral patterning of midbrain. *Nat. Neurosci.* 6, 453–460. doi: 10.1038/nn1037

Puelles, L., Harrison, M., Paxinos, G., and Watson, C. (2013). A developmental ontology for the mammalian brain based on the prosomeric model. *Trends Neurosci.* 36, 570–578. doi: 10.1016/j.tins.2013.06.004

Qian, Y., Fritzsch, B., Shirasawa, S., Chen, C. L., Choi, Y., and Ma, Q. (2001). Formation of brainstem (nor)adrenergic centers and first-order relay visceral sensory neurons is dependent on homeodomain protein Rnx/Tlx3. *Genes Dev.* 15, 2533–2545. doi: 10.1101/gad.921501

Qian, Y., Shirasawa, S., Chen, C. L., Cheng, L., and Ma, Q. (2002). Proper development of relay somatic sensory neurons and D2/D4 interneurons requires homeobox genes Rnx/Tlx-3 and Tlx-1. *Genes Dev.* 16, 1220–1233. doi: 10.1101/gad.982802

Radulovacki, M., Pavlovic, S., and Carley, D. W. (2004a). Pontine intertrigeminal region attenuates sleep apneas in rats. *Sleep* 27, 383–387. doi: 10.1093/sleep/27.3.383

Radulovacki, M., Pavlovic, S., Saponjic, J., and Carley, D. W. (2004b). Modulation of reflex and sleep related apnea by pedunculopontine tegmental and intertrigeminal neurons. *Respir Physiol. Neurobiol.* 143, 293–306. doi: 10.1016/j.resp.2004.02.012

Radulovacki, M., Pavlovic, S., Saponjic, J., and Carley, D. W. (2003). Intertrigeminal region attenuates reflex apnea and stabilizes respiratory pattern in rats. *Brain Res.* 975, 66–72. doi: 10.1016/S0006-8993(03)02587-3

Ramanantsoa, N., Hirsch, M. R., Thoby-Brisson, M., Dubreuil, V., Bouvier, J., Ruffault, P. L., et al. (2011). Breathing without Co2 chemosensitivity in conditional Phox2b mutants. *J. Neurosci.* 31, 12880–12888. doi: 10.1523/JNEUROSCI.1721-11.2011

Ramirez, J. M., and Baertsch, N. (2018). Defining the rhythmogenic elements of mammalian breathing. *Physiology* 33, 302–316. doi: 10.1152/physiol.00025.2018

Ramirez, J. M., Vlemincx, E., Baertsch, N. A., and Severs, L. J. (2022). The sigh and related behaviors. *Handb. Clin. Neurol.* 188, 357–372. doi: 10.1016/B978-0-323-91534-2.00015-1

Ray, R. S., Corcoran, A. E., Brust, R. D., Kim, J. C., Richerson, G. B., Nattie, E., et al. (2011). Impaired respiratory and body temperature control upon acute serotonergic neuron inhibition. *Science* 333, 637–642. doi: 10.1126/science.1205295

Ray, R. S., and Dymecki, S. M. (2009). Rautenlippe redux – toward a unified view of the precerebellar rhombic lip. *Curr. Opin. Cell Biol.* 21, 741–747. doi: 10.1016/j.ceb.2009.10.003

Roelink, H., Porter, J. A., Chiang, C., Tanabe, Y., Chang, D. T., Beachy, P. A., et al. (1995). Floor plate and motor neuron induction by different concentrations of the amino-terminal cleavage product of sonic hedgehog autoproteolysis. *Cell* 81, 445–455. doi: 10.1016/0092-8674(95)90397-6

Rose, M. F., Ahmad, K. A., Thaller, C., and Zoghbi, H. Y. (2009a). Excitatory neurons of the proprioceptive, interoceptive, and arousal hindbrain networks share a developmental requirement for Math1. *Proc. Natl. Acad. Sci. U S A.* 106, 22462–22467. doi: 10.1073/pnas.0911579106

Rose, M. F., Ren, J., Ahmad, K. A., Chao, H. T., Klisch, T. J., Flora, A., et al. (2009b). Math1 is essential for the development of hindbrain neurons critical for perinatal breathing. *Neuron* 64, 341–354. doi: 10.1016/j.neuron.2009.10.023

Rowitch, D. H., Kispert, A., and Mcmahon, A. P. (1999). Pax-2 regulatory sequences that direct transgene expression in the developing neural plate and external granule cell layer of the cerebellum. *Brain Res. Dev. Brain Res.* 117, 99–108. doi: 10.1016/S0165-3806(99)00104-2

Rubin, J. E., and Smith, J. C. (2019). Robustness of respiratory rhythm generation across dynamic regimes. *PLoS Comput. Biol.* 15:e1006860. doi: 10.1371/journal.pcbi.1006860

Ruffault, P. L., D'autreaux, F., Hayes, J. A., Nomaksteinsky, M., Autran, S., Fujiyama, T., et al. (2015). The retrotrapezoid nucleus neurons expressing Atoh1 and Phox2b are essential for the respiratory response to Co(2). *eLife* 4:e07051. doi: 10.7554/eLife.07051.017

Sato, T., Araki, I., and Nakamura, H. (2001). Inductive signal and tissue responsiveness defining the tectum and the cerebellum. *Development* 128, 2461–2469. doi: 10.1242/dev.128.13.2461

Sato, T., and Joyner, A. L. (2009). The duration of Fgf8 isthmic organizer expression is key to patterning different tectal-isthmo-cerebellum structures. *Development* 136, 3617–3626. doi: 10.1242/dev.041210

Schnerwitzki, D., Hayn, C., Perner, B., and Englert, C. (2020). Wt1 positive db4 neurons in the hindbrain are crucial for respiration. *Front. Neurosci.* 14:529487. doi: 10.3389/fnins.2020.529487

Schreihofer, A. M., Stornetta, R. L., and Guyenet, P. G. (1999). Evidence for glycinergic respiratory neurons: botzinger neurons express mrna for glycinergic transporter 2. *J. Comp. Neurol.* 407, 583–597. doi: 10.1002/(SICI)1096-9861(19990517)407:4<583::AID-CNE8>3.0.CO;2-E

Seitanidou, T., Schneider-Maunoury, S., Desmarquet, C., Wilkinson, D. G., and Charnay, P. (1997). Krox-20 is a key regulator of rhombomere-specific gene expression in the developing hindbrain. *Mech. Dev.* 65, 31–42. doi: 10.1016/S0925-4773(97)00051-8

Shamim, H., Mahmood, R., Logan, C., Doherty, P., Lumsden, A., and Mason, I. (1999). Sequential roles for Fgf4, En1 and Fgf8 in specification and regionalisation of the midbrain. *Development* 126, 945–959. doi: 10.1242/dev.126.5.945

Shao, X. M., and Feldman, J. L. (1997). Respiratory rhythm generation and synaptic inhibition of expiratory neurons in pre-Botzinger complex: differential roles of glycinergic and Gabaergic neural transmission. *J. Neurophysiol.* 77, 1853–1860. doi: 10.1152/jn.1997.77.4.1853

Sieber, M. A., Storm, R., Martinez-De-La-Torre, M., Muller, T., Wende, H., Reuter, K., et al. (2007). Lbx1 acts as a selector gene in the fate determination of somatosensory and viscerosensory relay neurons in the hindbrain. *J. Neurosci.* 27, 4902–4909. doi: 10.1523/JNEUROSCI.0717-07.2007

Sivan, Y., Zhou, A., Jennings, L. J., Berry-Kravis, E. M., Yu, M., Zhou, L., et al. (2019). Congenital central hypoventilation syndrome: severe disease caused by co-occurrence of two Phox2B variants inherited separately from asymptomatic family members. *Am. J. Med. Genet. A* 179, 503–506. doi: 10.1002/ajmg.a.61047

Smith, J. C. (2022). Respiratory rhythm and pattern generation: brainstem cellular and circuit mechanisms. *Handb. Clin. Neurol.* 188, 1–35. doi: 10.1016/B978-0-323-91534-2.00004-7

Smith, J. C., Abdala, A. P. L., Borgmann, A., Rybak, I. A., and Paton, J. F. R. (2013). Brainstem respiratory networks: building blocks and microcircuits. *Trends Neurosci.* 36, 152–162. doi: 10.1016/j.tins.2012.11.004

Smith, J. C., Abdala, A. P. L., Koizumi, H., Rybak, I. A., and Paton, J. F. R. (2007). Spatial and functional architecture of the mammalian brain stem respiratory network: a hierarchy of three oscillatory mechanisms. *J. Neurophysiol.* 98, 3370–3387. doi: 10.1152/jn.00985.2007

Smith, J. C., Ellenberger, H. H., Ballanyi, K., Richter, D. W., and Feldman, J. L. (1991). Pre-Botzinger complex: a brainstem region that may generate respiratory rhythm in mammals. *Science* 254, 726–729. doi: 10.1126/science.1683005

Song, G., Li, Q., and Lu, M. (2001). Roles of the Botzinger complex in the formation of respiratory rhythm. *Front. Model. Control Breathing* 499:153–157. doi: 10.1007/978-1-4615-1375-9_24

Song, G., Yu, Y., and Poon, C. S. (2006). Cytoarchitecture of pneumotaxic integration of respiratory and nonrespiratory information in the rat. *J. Neurosci.* 26, 300–310. doi: 10.1523/JNEUROSCI.3029-05.2006

Stedman, A., Lecaudey, V., Havis, E., Anselme, I., Wassef, M., Gilardi-Hebenstreit, P., et al. (2009). A functional interaction between Irx and Meis patterns the anterior hindbrain and activates krox20 expression in rhombomere 3. *Dev. Biol.* 327, 566–577. doi: 10.1016/j.ydbio.2008.12.018

Stoiljkovic, M., Radulovacki, M., and Carley, D. W. (2009). Local antagonism of intertrigeminal region metabotropic glutamate receptors exacerbates apneic responses to intravenous serotonin. *Respir. Physiol. Neurobiol.* 165, 137–142. doi: 10.1016/j.resp.2008.10.019

Storm, R., Cholewa-Waclaw, J., Reuter, K., Brohl, D., Sieber, M., Treier, M., et al. (2009). The bhlh transcription factor Olig3 marks the dorsal neuroepithelium of the hindbrain and is essential for the development of brainstem nuclei. *Development* 136, 295–305. doi: 10.1242/dev.027193

Su, C. Y., Kemp, H. A., and Moens, C. B. (2014). Cerebellar development in the absence of Gbx function in zebrafish. *Dev. Biol.* 386, 181–190. doi: 10.1016/j.ydbio.2013.10.026

Suda, Y., Matsuo, I., and Aizawa, S. (1997). Cooperation between Otx1 and Otx2 genes in developmental patterning of rostral brain. *Mechan. Dev.* 69, 125–141. doi: 10.1016/S0925-4773(97)00161-5

Thoby-Brisson, M., Karlen, M., Wu, N., Charnay, P., Champagnat, J., and Fortin, G. (2009). Genetic identification of an embryonic parafacial oscillator coupling to the preBotzinger complex. *Nat. Neurosci.* 12, 1028–1035. doi: 10.1038/nn.2354

Tian, G. F., Peever, J. H., and Duffin, J. (1998). Botzinger-complex expiratory neurons monosynaptically inhibit phrenic motoneurons in the decerebrate rat. *Exp. Brain Res.* 122, 149–156. doi: 10.1007/s002210050502

Tomas-Roca, L., Corral-San-Miguel, R., Aroca, P., Puelles, L., and Marin, F. (2016). Crypto-rhombomeres of the mouse medulla oblongata, defined by molecular and morphological features. *Brain Struct. Funct.* 221, 815–838. doi: 10.1007/s00429-014-0938-y

Travagli, R. A. (2007). The nucleus tractus solitarius: an integrative centre with 'task-matching' capabilities. *J. Physiology-London* 582, 471–471. doi: 10.1113/jphysiol.2007.137091

Ulloa, F., and Marti, E. (2010). Wnt won the war: antagonistic role of Wnt over Shh controls dorso-ventral patterning of the vertebrate neural tube. *Dev. Dyn.* 239, 69–76. doi: 10.1002/dvdy.22058

van der Heijden, M. E., and Zoghbi, H. Y. (2018). Loss of Atoh1 from neurons regulating hypoxic and hypercapnic chemoresponses causes neonatal respiratory failure in mice. *eLife* 7:e38455. doi: 10.7554/eLife.38455.028

van der Heijden, M. E., and Zoghbi, H. Y. (2020). Development of the brainstem respiratory circuit. *Wiley Interdiscip. Rev. Dev. Biol.* 9:e366. doi: 10.1002/wdev.366

Vangiersbergen, P. L. M., Palkovits, M., and Dejong, W. (1992). Involvement of neurotransmitters in the nucleus-tractus-solitarii in cardiovascular regulation. *Physiol. Rev.* 72, 789–824. doi: 10.1152/physrev.1992.72.3.789

Vann, N. C., Pham, F. D., Dorst, K. E., and Del Negro, C. A. (2018). Dbx1 pre-botzinger complex interneurons comprise the core inspiratory oscillator for breathing in unanesthetized adult mice. *eNEURO* 5:ENEURO.0130-18.2018. doi: 10.1523/ENEURO.0130-18.2018

Vann, N. C., Pham, F. D., Hayes, J. A., Kottick, A., and Del Negro, C. A. (2016). Transient suppression of Dbx1 prebotzinger interneurons disrupts breathing in adult mice. *PLoS One* 11:e0162418. doi: 10.1371/journal.pone.0162418

Venkatraman, A., Edlow, B. L., and Immordino-Yang, M. H. (2017). The brainstem in emotion: a review. *Front. Neuroanatomy* 11:15. doi: 10.3389/fnana.2017.00015

Voiculescu, O., Taillebourg, E., Pujades, C., Kress, C., Buart, S., Charnay, P., et al. (2001). Hindbrain patterning: Krox20 couples segmentation and specification of regional identity. *Development* 128, 4967–4978. doi: 10.1242/dev.128.24.4967

Wang, V. Y., Rose, M. F., and Zoghbi, H. Y. (2005). Math1 expression redefines the rhombic lip derivatives and reveals novel lineages within the brainstem and cerebellum. *Neuron* 48, 31–43. doi: 10.1016/j.neuron.2005.08.024

Wang, X. Y., Hayes, J. A., Revill, A. L., Song, H. B., Kottick, A., Vann, N. C., et al. (2014). Laser ablation of Dbx1 neurons in the pre-Botzinger complex stops inspiratory rhythm and impairs output in neonatal mice. *eLife* 3:e03427. doi: 10.7554/eLife.03427.021

Wassarman, K. M., Lewandoski, M., Campbell, K., Joyner, A. L., Rubenstein, J. L., Martinez, S., et al. (1997). Specification of the anterior hindbrain and establishment of a normal mid/hindbrain organizer is dependent on Gbx2 gene function. *Development* 124, 2923–2934. doi: 10.1242/dev.124.15.2923

Waters, S. T., and Lewandoski, M. (2006). A threshold requirement for Gbx2 levels in hindbrain development. *Development* 133, 1991–2000. doi: 10.1242/dev.02364

Watson, C., Bartholomaeus, C., and Puelles, L. (2019). Time for radical changes in brain stem nomenclature-applying the lessons from developmental gene patterns. *Front. Neuroanat.* 13:10. doi: 10.3389/fnana.2019.00010

Watson, C., Shimogori, T., and Puelles, L. (2017). Mouse Fgf8-Cre-LacZ lineage analysis defines the territory of the postnatal mammalian isthmus. *J. Comp. Neurol.* 525, 2782–2799. doi: 10.1002/cne.24242

Weese-Mayer, D. E., Berry-Kravis, E. M., Ceccherini, I., and Rand, C. M. (2008). Congenital central hypoventilation syndrome (Cchs) and sudden infant death syndrome (Sids): kindred disorders of autonomic regulation. *Respir. Physiol. Neurobiol.* 164, 38–48. doi: 10.1016/j.resp.2008.05.011

Weese-Mayer, D. E., Rand, C. M., Zhou, A., Carroll, M. S., and Hunt, C. E. (2017). Congenital central hypoventilation syndrome: a bedside-to-bench success story for advancing early diagnosis and treatment and improved survival and quality of life. *Pediatr. Res.* 81, 192–201. doi: 10.1038/pr.2016.196

Wu, J., Capelli, P., Bouvier, J., Goulding, M., Arber, S., and Fortin, G. (2017). A V0 core neuronal circuit for inspiration. *Nat. Commun.* 8:544. doi: 10.1038/s41467-017-00589-2

Wurst, W., and Bally-Cuif, L. (2001). Neural plate patterning: upstream and downstream of the isthmic organizer. *Nat. Rev. Neurosci.* 2, 99–108. doi: 10.1038/35053516

Zechner, D., Muller, T., Wende, H., Walther, I., Taketo, M. M., Crenshaw, E. B. III, et al. (2007). Bmp and Wnt/beta-catenin signals control expression of the transcription factor Olig3 and the specification of spinal cord neurons. *Dev. Biol.* 303, 181–190. doi: 10.1016/j.ydbio.2006.10.045

Zervas, M., Millet, S., Ahn, S., and Joyner, A. L. (2004). Cell behaviors and genetic lineages of the mesencephalon and rhombomere 1. *Neuron* 43, 345–357. doi: 10.1016/j.neuron.2004.07.010

Zhang, C., Kaye, J. A., Cai, Z., Wang, Y., Prescott, S. L., and Liberles, S. D. (2021). Area postrema cell types that mediate nausea-associated behaviors. *Neuron* 109, 461–472.e5.. doi: 10.1016/j.neuron.2020.11.010

Zhao, Q., Yu, C. D., Wang, R., Xu, Q. J., Dai Pra, R., Zhang, L., et al. (2022). A multidimensional coding architecture of the vagal interoceptive system. *Nature* 603, 878–884. doi: 10.1038/s41586-022-04515-5

Zhou, A., Rand, C. M., Hockney, S. M., Niewijk, G., Reineke, P., Speare, V., et al. (2021). Paired-like homeobox gene (Phox2B) nonpolyalanine repeat expansion mutations (Nparms): genotype-phenotype correlation in congenital central hypoventilation syndrome (Cchs). *Genet Med.* 23, 1656–1663. doi: 10.1038/s41436-021-01178-x

Zoccal, D. B., Furuya, W. I., Bassi, M., Colombari, D. S. A., and Colombari, E. (2014). The nucleus of the solitary tract and the coordination of respiratory and sympathetic activities. *Front. Physiol.* 5:238. doi: 10.3389/fphys.2014.00238

Zoccal, D. B., Silva, J. N., Barnett, W. H., Lemes, E. V., Falquetto, B., Colombari, E., et al. (2018). Interaction between the retrotrapezoid nucleus and the parafacial respiratory group to regulate active expiration and sympathetic activity in rats. *Am. J. Physiology-Lung Cell. Mol. Physiol.* 315, L891–L909. doi: 10.1152/ajplung.00011.2018

frontiers | Frontiers in Aging Neuroscience

TYPE Original Research
PUBLISHED 06 January 2023
DOI 10.3389/fnagi.2022.1073258

OPEN ACCESS

EDITED BY
Veronica Martinez Cerdeño,
University of California, Davis,
United States

REVIEWED BY
Randi Jenssen Hagerman,
University of California, Davis,
United States
Jacob Raber,
Oregon Health & Science University,
United States

*CORRESPONDENCE
Laia Rodriguez-Revenga
✉ lbodi@clinic.cat
Emily G. Allen
✉ emgrave@emory.edu

†These authors have contributed equally to this work and share senior authorship

SPECIALTY SECTION
This article was submitted to Parkinson's Disease and Aging-related Movement Disorders, a section of the journal Frontiers in Aging Neuroscience

RECEIVED 24 October 2022
ACCEPTED 19 December 2022
PUBLISHED 06 January 2023

CITATION
Elias-Mas A, Potrony M, Bague J, Cutler DJ, Alvarez-Mora MI, Torres T, Barcos T, Puig-Butille JA, Rubio M, Madrigal I, Puig S, Allen EG and Rodriguez-Revenga L (2023) Evaluation of AQP4 functional variants and its association with fragile X-associated tremor/ataxia syndrome.
Front. Aging Neurosci. 14:1073258.
doi: 10.3389/fnagi.2022.1073258

Evaluation of AQP4 functional variants and its association with fragile X-associated tremor/ataxia syndrome

Andrea Elias-Mas[1,2,3], Miriam Potrony[4,5,6], Jaume Bague[5,7], David J. Cutler[8], Maria Isabel Alvarez-Mora[4,5,6], Teresa Torres[5,6], Tamara Barcos[4,5], Joan Anton Puig-Butille[5,6,9], Marta Rubio[2,10], Irene Madrigal[4,5,6], Susana Puig[5,6,7], Emily G. Allen[8*†] and Laia Rodriguez-Revenga[4,5,6*†]

[1]Radiology Department, Hospital Universitari Mútua de Terrassa, Terrassa, Barcelona, Spain, [2]Institute for Research and Innovation Parc Taulí (I3PT), Sabadell, Spain, [3]Genetics Doctorate Program, Universitat de Barcelona (UB), Barcelona, Spain, [4]Biochemistry and Molecular Genetics Department, Hospital Clinic of Barcelona, Barcelona, Spain, [5]Institut d'Investigacions Biomèdiques August Pi i Sunyer (IDIBAPS), Barcelona, Spain, [6]CIBER of Rare Diseases (CIBERER), Instituto de Salud Carlos III, Barcelona, Spain, [7]Dermatology Department, Melanoma Unit, Hospital Clínic de Barcelona, Universitat de Barcelona, Barcelona, Spain, [8]Department of Human Genetics, Emory University School of Medicine, Atlanta, GA, United States, [9]Molecular Biology CORE, Hospital Clinic of Barcelona, Barcelona, Spain, [10]Department of Neurology, Parc Taulí Hospital Universitari, Sabadell, Spain

Introduction: Fragile X-associated tremor/ataxia syndrome (FXTAS, OMIM# 300623) is a late-onset neurodegenerative disorder with reduced penetrance that appears in adult *FMR1* premutation carriers (55–200 CGGs). Clinical symptoms in FXTAS patients usually begin with an action tremor. After that, different findings including ataxia, and more variably, loss of sensation in the distal lower extremities and autonomic dysfunction, may occur, and gradually progress. Cognitive deficits are also observed, and include memory problems and executive function deficits, with a gradual progression to dementia in some individuals. Aquaporin 4 (AQP4) is a commonly distributed water channel in astrocytes of the central nervous system. Changes in AQP4 activity and expression have been implicated in several central nervous system disorders. Previous studies have suggested the associations of *AQP4* single nucleotide polymorphisms (SNPs) with brain-water homeostasis, and neurodegeneration disease. To date, this association has not been studied in FXTAS.

Methods: To investigate the association of *AQP4* SNPs with the risk of presenting FXTAS, a total of seven common *AQP4* SNPs were selected and genotyped in 95 *FMR1* premutation carriers with FXTAS and in 65 *FMR1* premutation carriers without FXTAS.

Results: The frequency of *AQP4*-haplotype was compared between groups, denoting 26 heterozygous individuals and 5 homozygotes as carriers of the

minor allele in the FXTAS group and 25 heterozygous and 2 homozygotes in the no-FXTAS group. Statistical analyses showed no significant associations between *AQP4* SNPs/haplotypes and development of FXTAS.

Discussion: Although *AQP4* has been implicated in a wide range of brain disorders, its involvement in FXTAS remains unclear. The identification of novel genetic markers predisposing to FXTAS or modulating disease progression is critical for future research involving predictors and treatments.

KEYWORDS

FXTAS, *AQP4*, *FMR1* premutation, genetic variation, glymphatic system

Introduction

The brain is a high-energy consuming organ with a high metabolic activity, producing a substantial amount of interstitial waste products. Efficient clearance of the brain's metabolic waste is needed in order to avoid their accumulation, causing several neurological diseases (Kaur et al., 2021). Since there is a lack of conventional lymphoid circulation in the brain, the glymphatic system has been postulated as an alternative clearance for the brain waste product (Iliff et al., 2015), though evidence is still incomplete (Hladky and Barrand, 2022).

In the glymphatic system, cerebrospinal fluid (CSF) flows into the brain parenchyma within the periarterial spaces that surround the penetrating cerebral arteries, also called the perivascular spaces. Facilitated by aquaporin 4 (AQP4), CSF flows from the periarterial space into the brain interstitium and mixes with interstitial fluid, which, along with interstitial solutes, travels into the perivenous spaces, draining the fluid and its contents into the deep veins and into the basal meningeal and cervical lymphatic vessels (Hablitz and Nedergaard, 2021). AQP4 is the most abundant water channel in the brain, and, since it has a role regulating fluid exchange between perivascular spaces and the rest of the glymphatic system, it is considered the most important element in it (Nagelhus and Ottersen, 2013; Papadopoulos and Verkman, 2013; Szczygielski et al., 2021).

Alterations of glymphatic fluid circulation through AQPs variations are now emerging as central elements in the pathophysiology of different brain conditions. In fact, dysfunction of AQP4 have been implicated in the pathogenesis of many degenerative disorders, including Alzheimer's disease (AD), vascular cognitive impairment, idiopathic normal-pressure hydrocephalus, Parkinson's disease dementia, frontotemporal dementia and Creutzfeldt-Jakob disease (Zeppenfeld et al., 2017; Nedergaard and Goldman, 2020; Silva et al., 2021; Wang et al., 2022). Furthermore, evidence indicates that genetic variation in *AQP4* modulates sleep quality and architecture, amyloid-β burden and rate and progression of cognitive decline in AD patients (Burfeind et al., 2017; Rainey-Smith et al., 2018; Ulv Larsen et al., 2020).

Despite the relationship between glymphatic dysfunction and neurodegenerative diseases, dysfunction of glymphatic system has not yet been studied in Fragile X-associated tremor/ataxia syndrome (FXTAS) and its association with *AQP4* genetic variants is unknown. FXTAS is a neurodegenerative disorder linked to *FMR1* gene premutation carriers (55–200 CGG repeats) that is associated with cognitive loss that can evolve into dementia. Intranuclear inclusions and increased β amyloid load has been discovered in brains of patients with FXTAS (Cabal-Herrera et al., 2020; Salcedo-Arellano et al., 2021a). On the basis of these observations, we analyzed *AQP4* functional variants with the aim to investigate whether AQP4 could be a new genetic risk factor for FXTAS.

Materials and methods

Study population

The present study was conducted on genotype data from a total of 160 unrelated *FMR1* premutation carriers (95 presenting FXTAS symptoms and 65 without FXTAS clinical symptoms). Participants were identified through previous fragile X syndrome research projects at Emory University (Atlanta, GA, USA), through recruitment efforts at scientific conferences, and through collaborations with other research groups. All participants were enrolled from families with members known to be affected with fragile X-associated conditions and molecularly diagnosed. **Table 1** summarizes general demographics of the participants. FXTAS subjects were screened for eligibility as described in Kong et al. (2022). Briefly, case subjects were male or female premutation carriers with symptoms of tremor or ataxia before age 65, as reviewed by a neurologist. Control individuals, named as the no-FXTAS group, were male premutation carriers that reached age 68 without significant tremor or ataxia symptoms, as reviewed by a neurologist. The protocols and consent forms were approved by the Institutional Review Board at Emory University, and

written informed consent was obtained from all subjects (IRB00074941).

SNPs of the *AQP4* gene and haplotype analysis

Seven tag single nucleotide polymorphisms (SNPs) across *AQP4* gene (NM_001650) were selected according to their location and known functions, based on earlier reports on their associations with clinical phenotypes (Ulv Larsen et al., 2020). The SNPs were considered for those above 15% in Utah Residents with Northern and Western European Ancestry (CEU) population according to minor allele frequency (MAF: 0.15∼0.26). These SNPs included rs162007 (Chr18:26865883, Upstream, MAF 0.16), rs162008 (Chr18:26865728, 5′UTR, MAF 0.20), rs63514 (Chr18:26863457, intron, MAF 0.17), rs335931 (Chr18:26859108, intron, MAF 0.15), rs335930 (Chr18:26856961, intron, MAF 0.23), rs335929 (Chr18:26855623, 3′UTR, MAF 0.14), rs16942851 (Chr18:26851725, downstream, MAF 0.14). The chromosome positions are based on hg38.

Genotyping of *AQP4* SNPs

Whole genome sequencing was performed on samples using Illumina platforms at Hudson Alpha or Novogene as described in Kong et al. (2022). All samples were mapped using PEMapper and called using PECaller (Johnston et al., 2017). Genomic data have been uploaded to the National Institute of Mental Health (NIMH) Data Archive.[1]

Statistical analysis

To test the population homogeneity of the study subjects, the allele frequencies were tested against Hardy-Weinberg equilibrium (HWE) by the $\chi 2$-test. The plink v1.07 toolset was used to perform SNP association and haplotype[2] (Purcell et al., 2007). The power analysis was performed using the "Quanto" tool.[3] Statistical analyses were performed using commercially available software (SPSS SmartViewer, version 18.0; SPSS, Chicago, IL, USA). *P*-values < 0.05 were considered statistically significant. Association tests were corrected using the Benjamini and Hochberg step-up False Discovery Rate (FDR) for multiple comparisons.

1 https://nda.nih.gov/edit_collection.html?id=2380

2 https://zzz.bwh.harvard.edu/plink

3 https://bio.tools/QUANTO

Results

Genotype data from 95 FXTAS and 65 no-FXTAS individuals were analyzed. Table 1 shows the demographic data of FXTAS and no-FXTAS group. Significant differences were found for the age and the CGG repeat size when comparing both groups ($p < 0.0001$ and $p < 0.0001$, respectively). Age difference can be attributed to a bias in the recruitment of no-FXTAS individuals. In order to make sure that *FMR1* permutations in the no-FXTAS group did not have neurologic symptoms older men were included in this cohort. As for the CGG repeat

TABLE 1 Description of the individuals recruited in this study.

	FXTAS cases (n = 95)	No-FXTAS cases (n = 65)
Males/female [no (%)]	80 (84%)/15 (16%)	65 (100%)/0
Age (mean ± SD, *Y*)*	67.70 ± 10.81	77.01 ± 6.38
Age min, max (*Y*)	27–94	66–98
CGG repeat size (mean ± SD)*	93.15 ± 20.33	75.00 ± 15.14
CGG repeat size min, max	55–150	56–150

*$p < 0.0001$ using Student's *t*-test for comparison of means.

TABLE 2 Genotype frequency for each SNP according to presence of FXTAS.

	Genotype	FXTAS (n = 95)	No-FXTAS (n = 65)
rs162007	GG	64 (67.4%)	37 (56.9%)
	GA	26 (27.3%)	25 (38.5%)
	AA	5 (5.3%)	3 (4.6%)
rs162008	CC	64 (67.4%)	36 (55.4%)
	CT	26 (27.3%)	26 (40%)
	TT	5 (5.3%)	3 (4.6%)
rs63514	CC	63 (66.3%)	37 (56.9%)
	CT	27 (28.4%)	25 (38.5%)
	TT	5 (5.3%)	3 (4.6%)
rs335931	AA	63 (66.3%)	38 (58.5%)
	AG	27 (28.4%)	25 (38.5%)
	GG	5 (5.3%)	2 (3%)
rs335930	AA	57 (60%)	36 (55.4%)
	AC	32 (33.7%)	26 (40%)
	CC	6 (6.3)	3 (4.6%)
rs335929	AA	63 (66.3%)	38 (58.5%)
	AC	27 (28.4%)	24 (36.9%)
	CC	5 (5.3%)	3 (4.6%)
rs16942851	TT	64 (67.4%)	38 (58.5%)
	TG	26 (27.3%)	24 (36.9%)
	GG	5 (5.3%)	3 (4.6%)

TABLE 3 Single nucleotide polymorphism (SNP) allele association analysis.

SNP	FXTAS MAF	No-FXTAS MAF	OR (95% CI)	*P*-value	Adj *P*-value
rs16942851	0.19	0.22	0.81 (0.47–1.41)	0.463	0.628
rs335929	0.19	0.22	0.84 (0.49–1.46)	0.538	0.628
rs335930	0.23	0.24	0.96 (0.57–1.63)	0.887	0.887
rs335931	0.19	0.22	0.84 (0.49–1.46)	0.538	0.628
rs63514	0.19	0.24	0.77 (0.45–1.33)	0.348	0.628
rs162008	0.19	0.25	0.72 (0.42–1.23)	0.224	0.628
rs162007	0.19	0.24	0.75 (0.43–1.28)	0.290	0.628

MAF, minor allele frequency; OR, odd-ratio. Adj *p*-value, adjusted *p*-value using Benjamini and Hochberg step-up false discovery rate, for multiple comparisons.

size, the difference found might account for the CGG-repeat dependence described in clinical and neuropathologic features of FXTAS.

In agreement with HWE, there was no deviation detected in any of the analyzed SNPs ($p > 0.3$). All SNPs studied were in linkage disequilibrium (LD), and the pairwise LD coefficient (r^2) ranged between 0.8 and 1. **Table 2** shows the genotype frequency for each SNP according to the presence of FXTAS symptoms. After correction of *p*-values for multiple comparisons, there was no significant difference in frequencies of any of the analyzed SNPs between FXTAS and no-FXTAS group (**Table 3**). Adjustment for sex did not change these results (data not shown). **Table 4** shows the results of the genotype association analysis between *AQP4* polymorphisms and risk of FXTAS, according to different genetic inheritance models.

Discussion

Fragile X-associated tremor/ataxia syndrome is a late-onset neurodegenerative disorder with reduced penetrance, meaning that not all *FMR1* premutation carriers will develop it (Hagerman et al., 2001). Among *FMR1* premutation carriers older than 50 years, it has been estimated that 40% of men and 16% of women will develop FXTAS symptoms, although there is significant variability in the progression of neurological dysfunction (Coffey et al., 2008; Rodriguez-Revenga et al., 2009). The description and characterization of FXTAS is of great interest, because the prevalence of *FMR1* premutation in the general population is relatively high. It has been estimated that *FMR1* premutation affects ∼1 out of 400 males and 1 out of 200 females (Tassone et al., 2012), leading to symptoms of FXTAS in up to 1 in 3000 men older than 50 years. Even though the *FMR1* premutation is the major risk factor for FXTAS, there are still some unknown genetic, epigenetic or environmental factors that might be affecting gene penetrance. Candidate gene SNP association analysis is a commonly used approach to identify risk alleles and their association with clinical traits. In the present study we selected this method to investigate the role of *AQP4* gene variants in FXTAS susceptibility. We hypothesized that *AQP4* polymorphisms could play a role as risk factors for FXTAS. However, we did not find any significant difference in the distributions of alleles, genotypes, and haplotypes between FXTAS and no-FXTAS individuals, after correction for multiple testing.

A myriad of different studies point out *AQP4* gene as a novel candidate gene for brain plasticity and associated with neuropsychiatric and neurodegenerative disorders. According to the human postmortem brain microarray data from the Allen Brain Atlas resources,[4] *AQP4* is most highly expressed in fronto-limbic and temporal cortical regions. Both neuroanatomical areas are linked to cognitive and executive processes, and its disturbance leads to the neuropsychological changes described in many different movement disorders (Robertson et al., 2016). Although indirectly, genome-wide linkage studies have repeatedly pointed out the role of *AQP4* in the development of brain disorders (Dadgostar et al., 2021). Genetic variations, abnormal distribution and quantitative abnormalities of *AQP4* have also been associated with several neurodegenerative disorders, such as AD, Parkinson's disease and amyotrophic lateral sclerosis (reviewed in Mader and Brimberg, 2019). Recently the rs162008, the most prevalent genetic variant of *AQP4*, has been associated with a ∼15% change in AQP4 expression. In AD, genetic variations in *AQP4* were shown to be associated with changes in sleep pattern and increased β-amyloid (Rainey-Smith et al., 2018), as well as to β-amyloid accumulation and disease stage progression (Burfeind et al., 2017; Chandra et al., 2021). Taking everything into account, it is implied that AQP4 distribution and regulation might have crucial role in neuronal activity and function.

Apart from intention tremor and cerebellar ataxia, core clinical features of FXTAS include executive dysfunction which may progress to dementia in some cases (Hagerman et al.,

4 http://www.brain-map.org

10.3389/fnagi.2022.1073258

TABLE 4 Genotype association using different genetic models.

SNP	Allele	Test	OR (95% CI)	*P*-value	Adj *P*-value
rs16942851	G	ADD	1.22 (0.52–2.83)	0.647	0.978
		DOM	0.68 (0.35–1.31)	0.251	0.365
		REC	1.75 (0.33–9.31)	0.512	0.854
rs335929	C	ADD	1.23 (0.53–2.86)	0.634	0.978
		DOM	0.71 (0.37–1.37)	0.313	0.365
		REC	1.75 (0.33–9.31)	0.512	0.854
rs335930	C	ADD	1.38 (0.60–3.15)	0.449	0.978
		DOM	0.83 (0.43–1.57)	0.561	0.561
		REC	2.12 (0.41–10.87)	0.366	0.854
rs335931	G	ADD	1.23 (0.53–2.86)	0.634	0.978
		DOM	0.71 (0.37–1.37)	0.313	0.365
		REC	1.75 (0.33–9.31)	0.512	0.854
rs63514	T	ADD	0.99 (0.47–2.08)	0.978	0.978
		DOM	0.67 (0.35–1.29)	0.229	0.365
		REC	1.15 (0.26–4.98)	0.854	0.854
rs162008	T	ADD	0.97 (0.46–2.04)	0.932	0.978
		DOM	0.60 (0.31–1.15)	0.125	0.365
		REC	1.15 (0.26–4.98)	0.854	0.854
rs162007	A	ADD	0.98 (0.47–2.06)	0.961	0.978
		DOM	0.64 (0.33–1.23)	0.180	0.365
		REC	1.15 (0.26–4.98)	0.854	0.854

ADD, additive model; DOM, dominant model; REC, recessive model. Adj *p*-value, adjusted *p*-value using Benjamini and Hochberg step-up false discovery rate, for multiple comparisons.

2001; Hall et al., 2016). In addition, several conditions affecting sleep quality have been frequently described among FXATS patients (Hamlin et al., 2011; Summers et al., 2014). FXTAS can coexist with other neurodegenerative disorders, such as Parkinson's disease and AD (Aydin et al., 2020; Salcedo-Arellano et al., 2021b), suggesting a synergistic effect on the progression of disease symptoms. On the basis of these observations and the evidence of the consequences of AQP4 dysfunction in neurological conditions, we analyzed genetic variation of *AQP4* gene among FXTAS patients. We compared frequency of alleles, genotypes, and haplotypes of AQP4 between FXTAs and no-FXTAS cases. Results did not find any association between any of the SNPs analyzed and the risk of developing FXTAS (**Table 4**). Furthermore, no association was detected when comparing frequency distribution of the two major *AQP4*-haplotypes. In fact, the frequency detected did not differ from the one described among CEU population (**Table 5**). Although no relationship between genetic variants in *AQP4* gene and FXTAS was found, no association with changes in the development of the disease has been assessed due to lack of clinical information. Similarly with the AD, *AQP4* SNPs have been associated with some aspects of the clinical course, such as faster cognitive decline, rather than the presence or absence of the disease (Burfeind et al., 2017).

TABLE 5 Major allele and minor allele haplotype (HTMa and HTMi) frequencies of *AQP4* functional SNPs across the CEU (Utah residents with ancestry from Northern and Western Europe) population and the FXTAS and no-FXTAS groups.

	Haplotype frequency CEU	FXTAS (*n* = 190)	No-FXTAS (*n* = 130)
HTMa	0.767	0.76842105	0.73846154
HTMi	0.1966	0.18947368	0.22307692

As previously described (Ulv Larsen et al., 2020), examination of the SNPs revealed two conserved haplotypes: HtMa (haplotype for the major allele) and HtMi (haplotype for the minor allele). Haplotype frequency comparison by means of dominant analysis between FXTAS and no-FXTAS group did not show significant differences ($p > 0.05$). Moreover, both groups showed similar haplotype frequency compared to the CEU population (**Table 5**).

Given the sample size this study had limited power. *Post hoc* power analyses showed that the power to detect the

observed odds ratios for FXTAS cases vs. no-FXTAS ranged from 0.05 to 0.19.

This study has two main limitations that might be explained because of the rarity of the disorder. First the relatively small sample size. Power ranged only from 0.05 to 0.19. Second, the age differences between groups and the fact that those individuals considered as no-FXTAS may develop clinical symptoms later in life, masking differences among groups. Nonetheless, to our knowledge we are reporting for the first time, that the *AQP4* SNPs (rs162007, rs162008, rs63514, rs335931, rs335930, rs335929, and rs16942851) and haplotypes were not associated with susceptibility of FXTAS in Caucasian population. Despite this lack of association, further studies are necessary to fully discard the role of AQP4 and glymphatic system in the pathology of FXTAS. There is a need to describe new evidence into how the glymphatic system functions, and how AQP4 dysfunction might take part into FXTAS disease progression.

Data availability statement

The original contributions presented in this study are included in the article, further inquiries can be directed to the corresponding authors.

Ethics statement

The studies involving human participants were reviewed and approved by the Institutional Review Board at Emory University (IRB00074941). The patients/participants provided their written informed consent to participate in this study.

Author contributions

All authors listed have made a substantial, direct, and intellectual contribution to the work, and approved it for publication.

Funding

This work was supported by the Instituto de Salud Carlos III (ISCIII), (through the projects PI17/01067 and PI21/01085), co-funded by the European Union, and AGAUR from the Autonomous Catalan Government (2017SGR1134). The CIBER de Enfermedades Raras is an initiative of the Instituto de Salud Carlos III.

Conflict of interest

The authors declare that the research was conducted in the absence of any commercial or financial relationships that could be construed as a potential conflict of interest.

Publisher's note

All claims expressed in this article are solely those of the authors and do not necessarily represent those of their affiliated organizations, or those of the publisher, the editors and the reviewers. Any product that may be evaluated in this article, or claim that may be made by its manufacturer, is not guaranteed or endorsed by the publisher.

References

Aydin, E., Schneider, A., Protic, D., Wang, J., Martínez-Cerdeño, V., Tassone, F., et al. (2020). Rapidly progressing neurocognitive disorder in a male with FXTAS and Alzheimer's Disease. *Clin. Interv. Aging* 15, 285–292. doi: 10.2147/CIA.S240314

Burfeind, K., Murchison, C., Westaway, S., Simon, M., Erten-Lyons, D., Kaye, J., et al. (2017). The effects of noncoding aquaporin-4 single-nucleotide polymorphisms on cognition and functional progression of Alzheimer's disease. *Alzheimers Dement (N Y)* 3, 348–359. doi: 10.1016/j.trci.2017.05.001

Cabal-Herrera, A., Tassanakijpanich, N., Salcedo-Arellano, M., and Hagerman, R. (2020). Fragile X-associated tremor/ataxia syndrome (FXTAS): Pathophysiology and clinical implications. *Int. J. Mol. Sci.* 21:4391. doi: 10.3390/ijms21124391

Chandra, A., Farrell, C., Wilson, H., Dervenoulas, G., De Natale, E., and Politis, M. (2021). Alzheimer's Disease Neuroimaging Initiative. Aquaporin-4 polymorphisms predict amyloid burden and clinical outcome in the Alzheimer's disease spectrum. *Neurobiol. Aging* 97, 1–9.

Coffey, S., Cook, K., Tartaglia, N., Tassone, F., Nguyen, D., Pan, R., et al. (2008). Expanded clinical phenotype of women with the FMR1 premutation. *Am. J. Med. Genet. A* 146A, 1009–1016. doi: 10.1002/ajmg.a.32060

Dadgostar, E., Tajiknia, V., Shamsaki, N., Naderi-Taheri, M., Aschner, M., Mirzaei, H., et al. (2021). Aquaporin 4 and brain-related disorders: Insights into its apoptosis roles. *EXCLI J.* 20, 983–994. doi: 10.17179/excli2021-3735

Hablitz, L., and Nedergaard, M. (2021). The glymphatic system: A novel component of fundamental neurobiology. *J. Neurosci.* 41, 7698–7711. doi: 10.1523/JNEUROSCI.0619-21.2021

Hagerman, R., Leehey, M., Heinrichs, W., Tassone, F., Wilson, R., Hills, J., et al. (2001). Intention tremor, parkinsonism, and generalized brain atrophy in male carriers of fragile X. *Neurology* 57, 127–130. doi: 10.1212/wnl.57.1.12

Hall, D., Robertson, E., Shelton, A., Losh, M., Mila, M., Moreno, E., et al. (2016). Update on the clinical, radiographic, and neurobehavioral manifestations in FXTAS and FMR1 premutation carriers. *Cerebellum* 15, 578–586. doi: 10.1007/s12311-016-0799-4

Hamlin, A., Liu, Y., Nguyen, D., Tassone, F., Zhang, L., and Hagerman, R. (2011). Sleep apnea in fragile X premutation carriers with and without FXTAS. *Am. J. Med. Genet. B Neuropsychiatr. Genet.* 156B, 923–928. doi: 10.1002/ajmg.b.31237

Hladky, S., and Barrand, M. (2022). The glymphatic hypothesis: The theory and the evidence. *Fluids Barriers CNS* 19:9. doi: 10.1186/s12987-021-00282-z

Iliff, J., Goldman, S., and Nedergaard, M. (2015). Implications of the discovery of brain lymphatic pathways. *Lancet Neurol.* 14, 977–979. doi: 10.1016/S1474-4422(15)00221-5

Johnston, H., Chopra, P., Wingo, T., Patel, V., Epstein, M., Mulle, J., et al. (2017). PEMapper and PECaller provide a simplified approach to whole-genome sequencing. *Proc. Natl. Acad. Sci. U.S.A.* 114, E1923–E1932. doi: 10.1073/pnas.1618065114

Kaur, J., Fahmy, L., Davoodi-Bojd, E., Zhang, L., Ding, G., Hu, J., et al. (2021). Waste clearance in the brain. *Front. Neuroanat.* 15:665803. doi: 10.3389/fnana.2021.665803

Kong, H., Lim, J., Linsalata, A., Kang, Y., Malik, I., Allen, E., et al. (2022). Identification of PSMB5 as a genetic modifier of fragile X-associated tremor/ataxia syndrome. *Proc. Natl. Acad. Sci. U.S.A.* 119:e2118124119. doi: 10.1073/pnas.2118124119

Mader, S., and Brimberg, L. (2019). Aquaporin-4 water channel in the brain and its implication for health and disease. *Cells* 8:90. doi: 10.3390/cells8020090

Nagelhus, E., and Ottersen, O. (2013). Physiological roles of aquaporin-4 in brain. *Physiol. Rev.* 93, 1543–1562. doi: 10.1152/physrev.00011.2013

Nedergaard, M., and Goldman, S. (2020). Glymphatic failure as a final common pathway to dementia. *Science* 370, 50–56. doi: 10.1126/science.abb8739

Papadopoulos, M., and Verkman, A. (2013). Aquaporin water channels in the nervous system. *Nat. Rev. Neurosci.* 14, 265–277. doi: 10.1038/nrn3468

Purcell, S., Neale, B., Todd-Brown, K., Thomas, L., Ferreira, M., Bender, D., et al. (2007). PLINK: A tool set for whole-genome association and population-based linkage analyses. *Am. J. Hum. Genet.* 81, 559–575. doi: 10.1086/519795

Rainey-Smith, S., Mazzucchelli, G., Villemagne, V., Brown, B., Porter, T., Weinborn, M., et al. (2018). Genetic variation in Aquaporin-4 moderates the relationship between sleep and brain Aβ-amyloid burden. *Transl. Psychiatry* 8:47. doi: 10.1038/s41398-018-0094-x

Robertson, E., Hall, D., McAsey, A., and O'Keefe, J. (2016). Fragile X-associated tremor/ataxia syndrome: Phenotypic comparisons with other movement disorders. *Clin. Neuropsychol.* 30, 849–900. doi: 10.1080/13854046.2016.1202239

Rodriguez-Revenga, L., Madrigal, I., Pagonabarraga, J., Xunclà, M., Badenas, C., Kulisevsky, J., et al. (2009). Penetrance of FMR1 premutation associated pathologies in fragile X syndrome families. *Eur. J. Hum. Genet.* 17, 1359–1362. doi: 10.1038/ejhg.2009.51

Salcedo-Arellano, M., Wang, J., McLennan, Y., Doan, M., Cabal-Herrera, A., Jimenez, S., et al. (2021a). Cerebral microbleeds in fragile X-associated tremor/ataxia syndrome. *Mov. Disord.* 36, 1935–1943. doi: 10.1002/mds.28559

Salcedo-Arellano, M., Sanchez, D., Wang, J., McLennan, Y., Clark, C., Juarez, P., et al. (2021b). Case report: Coexistence of alzheimer-type neuropathology in fragile X-Associated tremor ataxia syndrome. *Front. Neurosci.* 15:720253. doi: 10.3389/fnins.2021.720253

Silva, I., Silva, J., Ferreira, R., and Trigo, D. (2021). Glymphatic system, AQP4, and their implications in Alzheimer's disease. *Neurol. Res. Pract.* 3:5. doi: 10.1186/s42466-021-00102-7

Summers, S., Cogswell, J., Goodrich, J., Mu, Y., Nguyen, D., Brass, S., et al. (2014). Prevalence of restless legs syndrome and sleep quality in carriers of the fragile X premutation. *Clin. Genet.* 86, 181–184. doi: 10.1111/cge.12249

Szczygielski, J., Kopańska, M., Wysocka, A., and Oertel, J. (2021). Cerebral microcirculation, perivascular unit, and glymphatic system: Role of Aquaporin-4 as the gatekeeper for water homeostasis. *Front. Neurol.* 12:767470. doi: 10.3389/fneur.2021.767470

Tassone, F., Iong, K., Tong, T., Lo, J., Gane, L., Berry-Kravis, E., et al. (2012). FMR1 CGG allele size and prevalence ascertained through newborn screening in the United States. *Genome Med.* 4:100. doi: 10.1186/gm401

Ulv Larsen, S., Landolt, H., Berger, W., Nedergaard, M., Knudsen, G., and Holst, S. (2020). Haplotype of the astrocytic water channel AQP4 is associated with slow wave energy regulation in human NREM sleep. *PLoS Biol.* 18:e3000623. doi: 10.1371/journal.pbio.3000623

Wang, Y., Huang, C., Guo, Q., and Chu, H. (2022). Aquaporin-4 and cognitive disorders. *Aging Dis.* 13, 61–72. doi: 10.14336/AD.2021.0731

Zeppenfeld, D., Simon, M., Haswell, J., D'Abreo, D., Murchison, C., Quinn, J., et al. (2017). Association of Perivascular localization of aquaporin-4 With cognition and alzheimer disease in aging brains. *JAMA Neurol.* 74, 91–99. doi: 10.1001/jamaneurol.2016.4370

frontiers | Frontiers in Molecular Neuroscience

TYPE Review
PUBLISHED 09 January 2023
DOI 10.3389/fnmol.2022.1072046

OPEN ACCESS

EDITED BY
Estela Maris Muñoz,
CONICET Dr. Mario H. Burgos Institute of Histology and Embryology (IHEM), Argentina

REVIEWED BY
Laura Maggi,
Sapienza University of Rome, Italy
Stephen C. Noctor,
University of California, Davis, United States

*CORRESPONDENCE
Shashank Kumar Maurya
✉ smaurya1@zoology.du.ac.in;
✉ maurya.shashankkumar@gmail.com

SPECIALTY SECTION
This article was submitted to Neuroplasticity and Development, a section of the journal Frontiers in Molecular Neuroscience

RECEIVED 17 October 2022
ACCEPTED 15 December 2022
PUBLISHED 09 January 2023

CITATION
Maurya SK, Gupta S and Mishra R (2023) Transcriptional and epigenetic regulation of microglia in maintenance of brain homeostasis and neurodegeneration. *Front. Mol. Neurosci.* 15:1072046. doi: 10.3389/fnmol.2022.1072046

Transcriptional and epigenetic regulation of microglia in maintenance of brain homeostasis and neurodegeneration

Shashank Kumar Maurya[1]*, Suchi Gupta[2] and Rajnikant Mishra[3]

[1]Biochemistry and Molecular Biology Laboratory, Department of Zoology, University of Delhi, New Delhi, India, [2]Tech Cell Innovations Private Limited, Centre for Medical Innovation and Entrepreneurship (CMIE), All India Institute of Medical Sciences, New Delhi, India, [3]Biochemistry and Molecular Biology Laboratory, Department of Zoology, Banaras Hindu University, Varanasi, India

The emerging role of microglia in brain homeostasis, neurodegeneration, and neurodevelopmental disorders has attracted considerable interest. In addition, recent developments in microglial functions and associated pathways have shed new light on their fundamental role in the immunological surveillance of the brain. Understanding the interconnections between microglia, neurons, and non-neuronal cells have opened up additional avenues for research in this evolving field. Furthermore, the study of microglia at the transcriptional and epigenetic levels has enhanced our knowledge of these native brain immune cells. Moreover, exploring various facets of microglia biology will facilitate the early detection, treatment, and management of neurological disorders. Consequently, the present review aimed to provide comprehensive insight on microglia biology and its influence on brain development, homeostasis, management of disease, and highlights microglia as potential therapeutic targets in neurodegenerative and neurodevelopmental diseases.

KEYWORDS

microglia, brain homeostasis, transcription factors, epigenetic changes, brain immunity, neurological diseases

1. Introduction

In 1932, del Rio-Hortega coined the term "microglial cell" to define a small group of mesodermally-derived, non-neuronal, phagocytic, non-astrocytic, and migratory cells in the central nervous system (CNS). Microglial cells are distinct from macroglial cells, which include oligodendroglia (del Rio-Hortega, 1932). Microglia contribute toward neurogenesis, synaptogenesis, and maintenance of brain homeostasis (Nayak et al., 2014). Microglial cells also secrete growth factors for restoring neurons and cause phagocytosis of cell debris during neurological diseases (Fu et al., 2014). In response to acute inflammation, microglial cells enhance brain inflammation by releasing nitric oxide (NO), reactive oxygen species

(ROS), and pro-inflammatory cytokines such as TNF-α, and IFN-γ, which promote recruitment of lymphocytes to damage sites from the blood. These lymphocytes take over the function of microglia and maintain brain homeostasis (London et al., 2013; Skaper et al., 2018). While regulating brain homeostasis during healthy and disease conditions, microglia undergo alteration at transcripts and protein levels and show different morphological changes. However, uniform consensus on characterization of microglia morphologies is still under debate (Paolicelli et al., 2022). Since microglia play an active role in the pathophysiology of a number of CNS diseases. Therefore understanding microglial mechanisms of action in regulation of brain physiology is essential for the development of therapeutic modality.

During normal aging, neuroinflammation, and age-related disease, microglia are hypo-motile, chronically express pro-inflammatory signaling molecules and burdened with lysosomal cargo (Olmedillas Del Moral et al., 2019). Microglia bind to the soluble and membrane-bound mediators, regulate the local microenvironment of neurons and astrocytes, neurogenesis, synaptic pruning, support neurite formation, the outgrowth of dopaminergic axons, and laminar structure of the cortex (Andoh and Koyama, 2021; Maurya et al., 2021). Microglia also mediate synaptic transmission, synaptic structures modification or elimination (Akiyoshi et al., 2018). They interact with neurons *via* various signaling molecules including transforming growth factor-β (TGF-β), brain-derived neurotrophic factor (BDNF), and complement proteins including CR3 and C1q (Cornell et al., 2022). Epigenome and genome-wide transcriptome studies have shown that microglia are different from other glial cells and tissue macrophages (Cuadros et al., 2022). A number of microglia specific signature genes have been identified to be involved in diverse functions of microglia. Similarly, multiple key transcription factors such as Spi1, Sall1, Mef2c, and Mafb regulate microglial transcriptomes. Epigenetic modulations in the enhancer repertoire of target genes also shape immune memory in microglia (Butovsky and Weiner, 2018; Yeh and Ikezu, 2019). However, molecular mechanisms and the consequences of restoring microglial functions in neurodegenerative diseases are poorly understood. Further, understanding the various facets of microglia biology will facilitate the early detection, and management of neurological diseases. Therefore, the present review intends to present transcriptional and epigenetic factors mediated regulation of microglia functions in maintenance of brain homeostasis in normal and disease conditions.

2. Origin of microglia

In 1932, del Río Hortega, nervous tissue preparation using silver-carbonate staining showed a small cell body structure with various ramified cell processes. These cells were further described as microglial cells, differentiating them from the astrocytes and oligodendrocytes (macroglia). Till 1990s, scientists discussed heavily regarding ectodermal or mesodermal origin of microglia (Ginhoux et al., 2013). Further, fate mapping experiments showed that microglia have monocytic blood origin (Ginhoux et al., 2010). Mice deficient in Pu.1, a key regulator of hematopoietic development were reported devoid of microglia (Mckercher et al., 1996; Iwasaki et al., 2005; Beers et al., 2006). The Pu.1 and stem cell leukemia/T-cell acute lymphoblastic leukemia 1 (Scl/Tal-1) showed to regulate the development of erythromyeloid progenitors in the yolk sac of the mouse embryo at 8.5 post conception (E8.5; Mcgrath et al., 2015; Perdiguero and Geissmann, 2016). The subset erythromyeloid progenitor's cells matures into $CX3CR1^{+}$ cells and become microglial progenitors in the yolk sac and migrates into the brain between E9.5 and E14.5 (Rigato et al., 2011). Similarly, at around 4.5 to 5.5 gestational weeks, microglia invade the forebrain (Monier et al., 2007; Verney et al., 2010; Menassa and Gomez-Nicola, 2018) and the major entry and circulation starts around 16 weeks (Rezaie and Male, 1999; Rezaie et al., 2005; Verney et al., 2010; Menassa and Gomez-Nicola, 2018). After postnatal development, the microglia are observed to reside in the brain and regulate its population size in normal healthy brain by self-renewal capacity of CNS (Ginhoux et al., 2010; Ginhoux and Guilliams, 2018). Thus, microglia are brain specific immune cells which interact with other brain cells including neurons and regulate various physiological activity in the brain during normal and disease conditions.

3. Microglia and its interaction with brain cells

3.1. Neurons

Although microglia have been known for a long time to play an important role in fostering inflammatory responses in the CNS, it is now evident that these functions, particularly in the healthy brain, are much more diverse. The functional repertoire of microglia also includes biochemical homeostasis maintenance, maturation of developing neuronal circuits, and their reorganization. There is mounting evidence that neurons inform microglia about their status and are therefore involved in regulating microglial activation and motility, whereas microglia also regulate neuronal activities (Umpierre and Wu, 2021). It has been established that microglia can detect neuronal activity, modulate neuronal function, and recognize neuronal damage at an early stage (Ronzano et al., 2021). In addition, numerous studies have shown that microglia interact with neurons at the neuronal soma, a function that is dependent on purinergic signaling and may aid in neuroprotection (Illes et al., 2020; Ronzano et al., 2021). Initial segment of the axon is another site of interaction between microglia and neurons. Here, microglial processes overlap this segment and their responses to neuroinflammation may vary (Baalman et al., 2015; Benusa and Lafrenaye, 2020; Ronzano et al., 2021). The bi-directional communication by various ligands and receptors are essential for

cross-talk between neurons and microglia in maintaining brain homeostasis which gets altered in disease conditions.

3.1.1. The signaling mechanism for microglia–neuron interactions

Microglia express a wide variety of neurotransmitter receptors, including glutamatergic receptors, serotonin receptors, etc., whose stimulation affects essential functions, such as cytokine production, cellular motility, and phagocytosis. The molecules released by microglia activate respective neuronal receptors, enabling microglial control of neurotransmission (Figure 1A). In response to pathological stimuli, neuronal regulatory mechanisms are compromised. These alterations disrupt the specific communication pathways between microglia and neurons, thereby disrupting the neuronal circuits associated with functions. Several molecules and receptors with specific roles in microglia-neuronal interactions have been identified.

Purinergic signaling evolves as a central system in the kinetics of neuron-to-microglia interaction and influences microglial behavior *via* interactions with other systems (Inoue, 2017; Szepesi et al., 2018; Calovi et al., 2019). In pathology, it is known that this signaling is essential for epileptogenesis. Microglia in necrotic regions have an amoeboid shape and respond more rapidly to purinergic stimuli as indicated by experimental seizures and temporal lobe epilepsy patients, indicating an elevated expression of purinergic receptors (Morin-Brureau et al., 2018).

CX3CL1, also known as Fractalkine, is a transmembrane chemokine that is secreted by neurons in the central nervous system (CNS) and signals through its unique receptor, CX3CR1, which is expressed by microglia (Chen et al., 2016). It has been demonstrated that the CX3CL1/CX3CR1 signaling pathway regulates bidirectional interaction between neurons and microglia and maintains neural–immune communication (Paolicelli et al., 2014; Mecca et al., 2018). In particular, mice with Cx3cr1 deletion have been reported to display abnormal pruning of dendritic spine, synapse maturation, altered functional connectivity, and behavioral defects (Paolicelli et al., 2011; Zhan et al., 2014). The loss of CX3CR1 signaling has been linked to neuronal degeneration, as observed in PD and ALS animal models (Pawelec et al., 2020). In ischemic mice brain, silencing of Cx3cr1 using siRNA showed to reduces microglia activation, white matter lesions, and cognitive deficits and attenuate the elevated expression levels of Cx3cr1, p38Mapk, Pkc, Tnf-α, Il-1, and Il-6 (Liu et al., 2015). Further the same group has also reported that exogenous

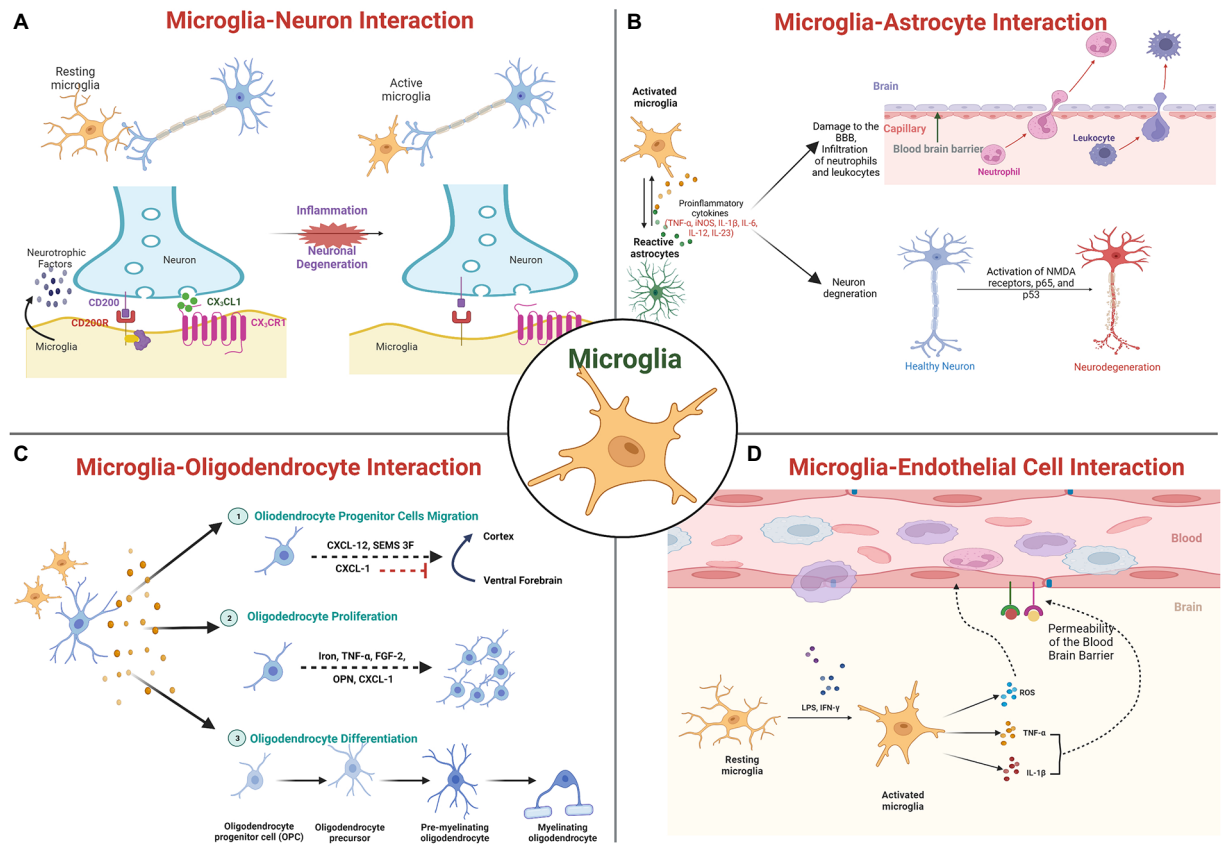

FIGURE 1
Molecular interaction of microglia with brain cells: **(A)** Microglia-Neuronal interactions; **(B)** Microglia-Astrocyte interaction; **(C)** Microglia-Oligodendrocyte interactions; and **(D)** Microglia-Cerebrovascular endothelial cells interactions.

Cxc3l1 administration to BV2 microglial cells treated with oxygen–glucose deprivation (OGD) showed increased expression of cytokines IL-1 and TNF-α, which got attenuated by silencing Cxc3r1 or by inhibiting p38Mapk indicating putative role of CX3CRL1/CX3CR1 axis in pathophysiology of brain ischemia (Liu et al., 2015). Clinical studies demonstrate an association between CX3CR1 polymorphisms and an early progression of ALS symptoms and delayed AD, as well as a shorter survival time. Additionally, CX3CR1 variants have been linked to an increased risk of neurodevelopmental disorders, such as ASD and schizophrenia (Lopez-Lopez et al., 2014; Hanger et al., 2020; Puntambekar et al., 2022).

In addition, complement receptors regulate a variety of microglial functions, including motility, phagocytosis, and cytokine release. These processes are relevant to the refinement of brain circuitry. Neurodegenerative disorders, which are characterized by a massive loss of neurons, an abundance of misfolded proteins, and adverse synaptic changes, alter these functions (Hickman et al., 2018). Intriguingly, both human and rodent neurodegenerative disease models exhibited a massive activation and overexpression of complement factors and receptors. Microglia are reported to express high levels of the complement system receptors C1q, C3, and C5 (CR3 and CR5) under pathological conditions or early in postnatal development (Hong et al., 2016; Petralla et al., 2021). TREM2, an innate immune receptor that is also expressed on the membrane of microglia and is involved in numerous processes, including activation, proliferation, clustering, and survival, is another signaling mechanism. Upon binding with ligands such as LPS, DNA, phospholipids, Trem2 receptor gets activated and inhibit inflammatory response mediated by TLR and promote apoptotic body clearance by enhancing microglial migratory and phagocytic activity (Zheng et al., 2018). Human genetic studies that link mutations in the TREM2 gene to an increased risk of neurodegenerative disorders provide support for the significance of TREM2 in neurodegeneration (Yaghmoor et al., 2014). Likewise, neurodevelopmental disorders exhibit altered TREM2 pathway activity. Autistic patients have been found to have reduced levels of TREM2 (Filipello et al., 2018). Furthermore, the interaction between the neuronal CD200 glycoprotein and the microglial CD200R receptor has also been reported to facilitate neuron–microglia communication, resulting in the formation of the CD200-CD200R complex for the regulation of brain inflammatory pathology (Lyons et al., 2007; Walker and Lue, 2013). Intriguingly, a decrease in expression of microglial CD200R and neuronal CD200 was observed associated with the aging process, indicating abnormal microglial activation may be a cause of susceptibility to neuroinflammation and neurodegenerative diseases (Walker and Lue, 2013). Despite being less conventional, neurotrophins such as BDNF, NGF, etc. are also involved in crosstalk between microglia and neurons, as microglia also secretes such factors and both neurons and microglia express their receptors (Szepesi et al., 2018). Accumulating evidence indicates that the microglial endocannabinoid system functions as a "non-canonical" signaling mechanism in the management of neuron–microglia crosstalk, thereby assisting microglia in regulating brain inflammation (Castillo et al., 2012; Scipioni et al., 2022). CB1Rs are predominantly expressed in neurons, whereas CB2Rs are characteristic of microglia, especially during neuroinflammation (Komorowska-Müller and Schmöle, 2021). In healthy brains, eCB production by microglia was reported consistently low and elevated in diseased brains. eCB signaling in microglia is distinguished by particular degradation pathways (Tanaka et al., 2020). Specifically, inhibiting them reduces neuroinflammation without affecting eCB signaling in neurons.

3.1.2. Exosomes in microglia–neuron interaction

In addition to these signaling mechanisms for microglia-neuronal interaction, accumulating evidence suggests that nano-vesicles known as exosomes with sizes ranging from 40 to 100 nm, secreted by microglia, may serve as important intercellular signaling mediators (Guo et al., 2021). These exosomes exert their effects by transporting specific cargos, such as proteins, microRNAs (miRNAs), and messenger RNAs (mRNAs) for cell to cell communication. It has been demonstrated that microglial exosomes can be transported to and taken up by neurons, which may be beneficial or detrimental to CNS diseases (Liu et al., 2019; Guo et al., 2021). miRNAs, mRNAs, proteins, etc. can be incorporated into multivesicular bodies (MVBs) intracellularly and then secreted by microglial exosomes. MVBs are formed by the inward protrusion of the endocytic membrane, later fuse with plasma membrane to release exosomes. Microglial cells, on the other hand, release microvesicles (MV), which are larger than 200 nm in diameter, through plasma membrane budding (Brites and Fernandes, 2015; Scott, 2017). Exosomes are predominantly enriched with receptors and kinases, indicating their role in cellular signaling. The presence of mitochondrial, centrosomal, and ribosomal proteins on MVs suggests their roles in protein translation. In addition, microglial exosomes are involved in antigen presentation, such as the transfer of antigens, indicating a functional role in immune response and are essential for regulating the brain-immune system interaction (Kalluri and LeBleu, 2020; Guo et al., 2021; Hazrati et al., 2022). Studies have revealed that neurodegenerative disease-related proteins are transported by microglial exosomes. The ability of activated microglia to release exosomes containing misfolded proteins such as α-synuclein, tau, Aβ, and cytokines has been documented (Španić et al., 2019; Aires et al., 2021). Additionally, they contain the insulin-degrading enzyme (IDE), which can degrade the Aβ peptide. Importantly, upon activation, microglial cells exhibit a high degree of plasticity, thereby releasing exosomes affecting the distant brain regions. The activated microglia are suggested to spread misfolded proteins either through membrane leakage or exosomes after migrated cells die, making them an efficient disease transporter (Aires et al., 2021; Guo et al., 2021). The relationship between

microglial exosomes and the pathogenesis and progression of neurodegenerative diseases has garnered considerable attention. However, exosome related molecular mechanisms of microglia functions in pathogenesis and therapeutics of neurodegenerative diseases are still under investigation.

3.2. Non-neuronal cells

As mentioned previously, microglia cells also exert their primary functions toward non-neuronal cells such as astrocytes, oligodendrocytes, vascular cells, etc., and a great deal of research focuses on their dyadic interactions. Recently, crosstalk between microglia and astrocytes has dominated glial research. Emerging evidence indicates that signals derived from microglia and astrocytes are the functional determinants (Figure 1B). Microglia and astrocytes develop bidirectional communication and autocrine feedback for tight reciprocal alteration during CNS insult or injury by releasing diverse signaling molecules (Matejuk and Ransohoff, 2020). Interactions between microglia and astrocytes are fundamental to neuronal functions and dysfunctions (Ricci et al., 2009). Microglia can modulate neuronal activity and receive information from astrocytes since these astrocytes express membrane receptors for all known neurotransmitters (Pascual et al., 2012). Astrocytes reduce microglial activation by upregulating TGF-β and Galectin-1, thereby decreasing antigens presentation-related factors secretion such as pro-inflammatory cytokines, NO, ROS, and TNF-α (Xu et al., 2020). The significance of Galectin-1 secretion has been hypothesized based on the improved clinical outcomes in a mouse model of experimental autoimmune encephalomyelitis (EAE; de Jong et al., 2020). IL-1, which is predominantly produced by microglia, is closely linked to neuronal disorders, increases astrocyte neurotoxicity, and may also contribute to their protective function (Hansen et al., 2018). Microglia express abundant purinergic receptors, and ATP released by astrocytes in response to a local injury activates local microglia (Franke et al., 2012). Astrocyte Ca + ion waves, which are involved in synaptic activity and regulate microcirculation, glutamate production, and release, and ion homeostasis, also spread to microglia (Hung et al., 2010).

Oligodendrocytes are non-neuronal cells that produce myelin for the myelination process, a crucial step in the development of the CNS. Myelin sheath is composed of oligodendrocyte plasma membranes with specific protein composition and multiple layers. Each oligodendrocyte produces multiple myelin internodes that insulate numerous axons in their vicinity, thereby facilitating faster action potential conduction. The evidence of crosstalk between microglia and oligodendrocytes in the repair, genesis, and regulation of myelin-producing cells has also been reported (Peferoen et al., 2014; Figure 1C). Oligodendrocytes have the ability to regulate microglial activity through the production of chemokines, cytokines, and chaperokines. By inhibiting apoptosis of oligodendrocyte precursors and promoting their differentiation, non-activated microglia promote oligodendrocyte survival and increases the number of mature oligodendrocytes (Kalafatakis and Karagogeos, 2021). Activation of the p38 MAPK in microglia mediates growth factor production and is essential for apoptosis of oligodendrocytes in SCI (Yune et al., 2007). Further, the report also suggests microglia activation inhibits oligodendrocyte progenitor cell (OPC) proliferation and induces apoptosis (Yune et al., 2007; Peferoen et al., 2014). Similar observations have been made in MS lesions, indicating a correlation between oligodendrocyte damage and microglial activity in MS. After spinal cord injury, microglia have been observed in close proximity to dying oligodendrocytes and they may promote oligodendrocyte survival (Miller et al., 2007). This proximity after injury suggests a mechanism by which microglia may influence the survival of oligodendrocytes and OPCs, highlighting the dual role that microglia may play in CNS injury.

Furthermore, Cerebrovascular endothelial cells (CVEs) are well known to create physical and functional barriers, separating CNS from peripheral circulation by forming brain microvasculature, and are in permanent bidirectional communication with microglia cells (Figure 1D). Microglia are attracted by a breach in the BBB, and its activation cause increased production of pro-inflammatory mediators such as TNF-α and IL-1b, as well as inducible nitric oxide synthase (iNOS) expression level (Wang et al., 2015; Kang et al., 2020) leading to neuroinflammation and progression of neurodegenerative diseases (Takata et al., 2021). Mice lacking CD200R produce more Tnf-α in response to the gram-negative bacterial endotoxin lipopolysaccharide (LPS; Walker and Lue, 2013). CVEs contain TNF receptors (TNFRs), to which TNF-α binds. After ischemia and in humans with neurodegenerative diseases, brain TNF-α levels rise, and this rise is largely due to activated microglia. Microglia are found in close proximity to vascular endothelial cells (VECs), indicating a possible role in promoting the formation of healthy CNS vascular networks and regulating the process in the adult brain (Zhao et al., 2018). Two angiogenic factors, ephrin-A3 and ephrin-A4, were highly expressed in CVEs treated with microglial culture supernatant, indicating that microglia induce *in vitro* angiogenesis in brain endothelial cells (Li et al., 2014). Similarly, Stat3, which is predominantly expressed by activated microglia and other macrophages 24 to 72 h after cerebral ischemia, is said to promote angiogenesis by regulating the migration and proliferation of CVEs. Inhibiting Stat3 phosphorylation within 72 h of cerebral ischemia decreased lesion size (Hoffmann et al., 2015). CVEs also express MMP-3 (matrix metalloproteinases-3), which plays a crucial role in disruption of blood–spinal cord barrier (BSCB) following spinal cord injury (SCI), contributing to activation of the microglia and enhanced inflammation (Behl et al., 2021).

4. Microglia and their association with learning, memory, and cognition

Synapse remodeling is an ongoing process in the adult brain that alters synaptic connections and is required for encoding memory in the neural circuit (Südhof, 2018). The mechanisms that contribute to remodeling synapses are essential for flexible learning and memory (Benson and Huntley, 2012). Microglia surveillance has been linked to synaptic maturation. Microglia has been reported to actively engulf synaptic material and play an important role in synaptic pruning and hence microglia surveillance has been associated with synaptic maturation. Further, it has been proposed that deficits in microglia function may lead to synaptic abnormalities in some neurodevelopmental disorders (Paolicelli et al., 2011). It has been reported that microglia make activity-dependent contact with synapses in order to regulate synaptic density and connectivity (Andoh and Koyama, 2021). Multiple studies have demonstrated that microglia along with neural ensemble connectivity and memory strength, also regulate memory quality (i.e., the ability to distinguish between similar contexts; Nguyen et al., 2020; Wang et al., 2020). The removal of microglia leads to changes in organization and activity of glutamatergic synapses (Basilico et al., 2022). Microglial autophagy is also shown to regulate synapses and neurobehavior. Deletion of atg7, which is vital for autophagy, from myeloid cell-specific lysozyme M-Cre mice resulted in increased dendritic spines, synaptic markers, altered connectivity between brain regions, social behavioral defects and repetitive behaviors. Further, atg-7 deficient microglia showed impaired synaptosome degradation whereas increase in immature dendritic filopodia in neurons were observed in neurons co-cultured with atg-7 deficient microglia (Kim et al., 2017). Microglial Bdnf is shown to increase phosphorylation of a key mediator of synaptic plasticity in neurons, i.e., tropomyosin-related kinase receptor B and regulate learning and memory *via* BDNF signaling as removal of Bdnf from microglia restates deficits in multiple learning task due to microglia depletion (Parkhurst et al., 2013). CD47-SIRPα interaction and signaling has also been observed to regulate microglia mediated synaptic pruning and cognitive ability in neurodegeneration (Lehrman et al., 2018; Ding et al., 2021). During the initial pathological stage of perioperative neurocognitive disorders (PND), microglia mediated astrocyte activation leads to long-term synaptic inhibition and cognitive deficiencies (Li et al., 2020). The majority of studies have identified that IL-33 signaling *via* microglia is crucial for memory quality. Interleukin-33 (IL-33) is expressed in an experience-dependent manner by adult hippocampal neurons and defines a subset of neurons primed for synaptic plasticity. The loss of microglial IL-33 receptor or neuronal IL-33 results in altered spine plasticity, decreased newborn neuronal integration, and reduced accuracy of distant fear memories. The precision of memory and neuronal IL-33 reported diminished in aged mice, and gain of IL-33 function alleviates age-related declines in spine plasticity (Nguyen et al., 2020). Studies have shown that neuronal IL-33 directs microglia mediated engulfment of the extracellular matrix (ECM) and that its absence results in weakened ECM engulfment and ECM proteins accumulation in contact with synapses (Vainchtein et al., 2018). These findings identify a cellular mechanism by which microglia regulate experience-dependent synaptic remodeling and facilitate memory consolidation. Another study by Wang et al. (2020) reported that the C1q-dependent complement pathway is majorly involved in microglia mediated synapse elimination, and that CD55, a complement pathways inhibitor, disrupt C1q-dependent complement pathway and microglia in memory-storing engram cells in dentate gyrus (Wang et al., 2020). Another interaction is *via* the CD200/CD200R pathway, in which CD200R is expressed by microglia and CD200 is expressed by neurons (Sun et al., 2020). In the presence of amyloid beta, CD200 knockout mice exhibit greater phagocytosis than wild-type mice (Lyons et al., 2007). Apart from playing an important role in pathophysiology of neurodegeneration, the CX3CL1/CX3CR1 axis is also reported to influence synaptic plasticity and cognition. The CX3CL1 has been shown to inhibit hippocampal LTP through adenosine receptor 3 activity (Maggi et al., 2009). CX3CR1 deficiency is observed to show reduced neurogenesis, impaired synaptic plasticity and cognitive functions (Bachstetter et al., 2011; Rogers et al., 2011). The decrease in CX3CL1-CX3CR1 signaling and cognitive deficits has also been noted in Streptozotocin (STZ) induced mice (Kawamura et al., 2020). Thus, microglia protect strong, active synapses essential for learning and memory *via* this pathway. However, understanding the molecular mechanism of microglia function in regulation of learning and memory, neuronal-microglial communications in healthy and different brain pathologies still require further investigation.

5. Key genes and proteins involved in microglial function(s) in brain

During age-related disease, normal aging and neuroinflammation, microglia are observed to be hypo-motile, loaded with lysosomal cargo, and persistently express pro-inflammatory signaling molecules (Spittau, 2017; Pluvinage et al., 2019). Epigenome and genome-wide transcriptome studies have revealed that microglia are different from other glial cells and tissue macrophages. Further, it was identified that CX3C chemokine receptor 1 (Cx3cr1), Triggering receptor expressed on myeloid cells 2 (Trem2), Spalt like transcription factor 1 (Sall1), Transmembrane protein 119 (Tmem119), Sialic-acid-binding immunoglobulin-like lectin-h (Siglec-H), Olfactomedin-like 3 (Olfml3) and P2 purinergic receptor (P2ry12) specifically expressed in microglia (Chiu et al., 2013; Galatro et al., 2017) are involved in the regulation of its physiology and could act as a possible drug target in neurodegenerative diseases. In activated microglia, ionized binding protein1 (Iba1) contributes in actin-bundling and regulates

membrane ruffling, cell migration, and phagocytosis (Ohsawa et al., 2004). The Iba1 has been reported as a more suitable marker than plasma membrane and trans-membrane-specific markers for structural analysis of microglia (Korzhevskii and Kirik, 2016). The Cx3cr1 plays an important role in microglia-neurons communication (Bolós et al., 2018). Trem2 has proven essential for maintaining microglial metabolic fitness during stress and sustaining the microglial response in pathological conditions (Ulland et al., 2017). Spalt like transcription factor 1 (Sall1), regulates microglia identity and functions (Buttgereit et al., 2016) and P2ry12 serves as chemotactic receptors, guiding the microglial cell processes movement near to local sites of CNS injury (Lou et al., 2016). The Tmem119, a protein of unknown function, serves as a marker of microglia (Bennett et al., 2016). However, Siglec-H allows histological identification of microglia and microglia-specific gene manipulation in the nervous system (Konishi et al., 2017). The Olfml3, a secreted glycoprotein proves critical in the development and functional organization of the CNS, hematopoietic system, and a new target gene of Tgf-β1/Smad2 whose expression is restricted to the microglia in the brain (Neidert et al., 2018).

Additional 30 genes (*ADAM28, ACY3, ALOX5AP, ADORA3, C1QB, CD33, C3, CIITA, CD84, CSF2RA, CPED1, FCER1G, DHRS9, FYB, HPGDS, GPR34, LAPTM5, IGSF6, P2RY13, LY86, SASH3, RASAL3, SPN, SELPLG, SUSD3, SUCNR1, TBXAS1, TLR7, SYK,* and *TREM2*) have been reported to express strongly in various healthy human brain regions (Bonham et al., 2019). However, they are vulnerable in Alzheimer's disease (AD) *via* cell-type expression profiling tool (CellMapper; Bonham et al., 2019) and are also related to gene networks of both aging and neurodegenerative diseases (Mukherjee et al., 2019). In pre-clinical stages of AD, an increase in pro-inflammatory DAM protein expression was associated with neurofibrillary tangle and tau pathology (Rangaraju et al., 2018). Various reports have suggested the involvement of the complement production and signaling (C1, C1q, C3, CR1, Factor B, Factor D, and Properdin), NLRP3 inflammasome activation (VRAC, NLRP3 P2X7,), and TREM2/DAP12 signaling (TREM2, PLCγ2, SHIP-1, and Apolipoprotein E) in the regulation of microglial survival and proliferation, actin cytoskeleton polarization, cytoskeleton organization, stimulating microglial phagocytosis, cytokine production, immune responses, and could be potential therapeutic targets in modulating microglial functions for AD (Konishi and Kiyama, 2018; Mecca et al., 2018). The molecular mechanisms and the significance of restoring microglial functions to age-related brain dysfunction are still elusive. Further, an understanding of disease-associated microglia (DAM) heterogeneity, its key regulators, and emerging "microgliome" are also required to differentiate transcriptionally distinct and neurodegeneration-specific microglial profiles for drug discovery and clinical research (Sousa et al., 2017). Thus, the discovery and identification of specific microglia signature genes and similarly preserved networks in animal models will provide mechanistic insights into microglia function(s) in neurodegenerative diseases.

6. Transcriptional regulation of microglial genes in normal and disease conditions

6.1. Regulation of microglial genes in healthy brain

PU.1 is the most abundant ETS-domain transcription factor encoded by the *Spi1* (murine) or *SPI1* (human) gene. It activates gene expression during immune cell development by binding to a purine-rich sequence (PU box). The PU.1 is reported to continuously express from erythromyeloid progenitors (EMPs) to adulthood microglia (Butovsky and Weiner, 2018). The transcription factors PU.1 and IRF8 are known to largely regulate microglia development and functional maintenance. PU.1 deficient mice lack parenchymal microglia whereas induction of PU.1 expression in human cortical organoids leads to generation of microglia like cells (Beers et al., 2006; Cakir et al., 2022). Silencing of PU.1 shown to suppress genes response for antigen presentation, pro-inflammatory response, reduces microglia number and their ramification and phagocytosis activity (Smith et al., 2013; Huang et al., 2017; Rustenhoven et al., 2018). Chromatin Immunoprecipitation followed by sequencing reveals PU.1 binds to a number of microglia sensome genes and proposed that aberrant regulation of PU.1 target genes may lead to neurodegenerative diseases by changing microglial transcriptional network (Satoh et al., 2014).

Various studies have reported the importance of PU.1 in regulating microglia function and homeostasis (Nayak et al., 2014). However, additional research is needed to understand how various transcription factors are associated with maintaining the microglial identity and functions in the homeostatic brain.

6.2. Regulation of microglial genes in brain pathology

In the transgenic mouse models of AD, increased expression of markers associated with microglial activation such as CLEC7A, and Galectin-3, and decreased expression of homeostatic markers including P2RY12 suggest a switch in a specific population of microglia associated with an amyloid plaque from homeostatic to reactive state (Butovsky and Weiner, 2018; García-Revilla et al., 2022). Further, dystrophic neurites in normal aging and neurodegenerative diseases lead to a phenotype switch from homeostatic to neurodegenerative microglia (MGnD) by stimulating the TREM2-APOE pathway (Pimenova et al., 2017). APOE and TGFβ are reported to be the major upstream regulators of MGnD microglia. APOE upregulation induces gene expression of transcription factors *Bhlhe40, Tfec, Atf,* and inflammatory miR-155, leading to the inflammatory response and decreasing microglial homeostatic transcriptional factors including *Spi1, Mef2a, Mafb, Smad3* (Krasemann et al., 2017). In the SOD1 mouse

model of ALS, it has been observed that targeting miR-155 restores abnormal microglia and attenuates disease (Butovsky et al., 2015). In a PS19 mice model of neurodegenerative tauopathy and AD, microglia-specific transcription factors *Irf8, Spi1,* and *Runx1* are observed to be significantly upregulated, whereas complement C3aR deletion, the complement factor C3 complement receptor that mediates neuroimmune crosstalk, decreases *Irf8, Spi1,* and *Runx1* expression and rescues tau pathology and attenuates neuroinflammation, synaptic deficits, and the deleterious effect (Lian et al., 2015; Hong et al., 2016; Litvinchuk et al., 2018).

Aging showed to have an influence on microglia. The expression of pro-inflammatory genes in adult microglia increases with maturation and aging indicating reduced plasticity and a reactive state in the adult stage. In aging mice, transcripts of the microglial sensome required for sensing endogenous ligands, such as *Gpr34, Fcrl1, P2ry12, Trem2,* and *Dap12*, were downregulated, whereas genes involved in microbe recognition and host defense system, such as *Cd74, Tlr2, Ltf, Cxcl16,* and *Clec7a* were upregulated (Boche and Gordon, 2022). The age-dependent transcriptional module including *SPI, IRF8, RUXN1,* and *TAL1* is reported to regulate microglial markers (Wehrspaun et al., 2015). Additional analysis suggested a significant correlation between TLRs for communication with pathogen-associated molecular patterns, microglia surface receptors (P2RY12, CX3CR1, and TREM2), and aging, highlighting the age-dependent change in microglial plasticity (Kierdorf and Prinz, 2013; Wehrspaun et al., 2015). Recent research by Olah et al. suggests that the APOE2 haplotype protects human microglia from the increased expression of an aging gene set. In aged microglia, their findings revealed upregulation of *CD33, INPP5D, MS4A4A, SORL1,* and *TREM2*, but no change in PU.1. The discrepancy may be explained by the fact that the average age of the postmortem tissue donors was 95 years older than in previous studies and that their cohort consisted primarily of females (Olah et al., 2018).

NF-kB activation in microglia has also been shown to be associated with the development of a classic M1 pro-inflammatory phenotype (Orihuela et al., 2016). The nuclear accumulation of p50/RelA dimer is associated with early phase of inflammatory response by activating transcription of proinflammatory cytokines such as iNOS, Tnf-α, IL-1β, IL-6, and proteolytic enzymes in microglia (Kaminska et al., 2016). The production of mature p50 and p52 are processed by proteasome cleavage of NF-κB precursors (Harhaj and Dixit, 2012; Collins et al., 2016). The activation of IRF and NF-κB transcription factor pathways are important initial steps involved in immune activation.

In cultured microglial cells, signaling through the prostaglandin-E2 (PGE2) EP4 receptor modulates genes enriched in targets of IRF1, IRF7, and NF-κB transcription and attenuated levels of Aβ-induced inflammatory factors and potentiated Aβ phagocytosis (Kaminska et al., 2016). In microglia treated with LPS, IRF7 expression was observed to increase, and IRF7 knockdown was found to decrease phosphorylation of STAT1 and expression of LPS-induced genes (Zhao et al., 2017). Similarly, IRF8 deficient microglia observed to have reduced microglial marker IBA1 expression, less elaborated processes, decreased phagocytic capacity and showed less proliferative potential in mixed glial culture (Horiuchi et al., 2012). Overexpression of IRF8 is reported to promote expression of inflammatory genes whereas its deficiency prevents expression of these genes in microglia culture from the spinal cord. In peripheral nerve injury, IRF8 showed elevated expression level and implicated in regulating microglial migration (Masuda et al., 2012, 2014).

7. Microglia and their involvement in neuroinflammation

Growing evidence implicates microglia as key regulators of neuroinflammation, shedding light on their role in pathological processes. Studies highlight the various activation mechanisms of brain microglial cells. One such mechanism is classical activation, in which microglia secrete pro-inflammatory factors such as Interleukin-1 (IL-1), Interleukin-6 (IL-6), and TNF-α in response to an insult, in addition to an increase in the production of NO and ROS. These factors damage the surrounding neuronal cells (London et al., 2013). Microglia cells of M1 phenotype are the first line of defense because they can eliminate invading pathogens, such as bacteria and viruses, by recognizing pathogen-associated molecular patterns (PAMPs; Orihuela et al., 2016). PAMPs activate Toll-like receptors (TLRs) on microglia, specifically TLR4 to induce the production of proinflammatory cytokines (Fiebich et al., 2018). Impacts of TLR4 have been observed in neurodegenerative diseases such as AD and PD, and chronic neuroinflammation after stroke and spinal cord injury (Pascual et al., 2021). Microglia also adopts an alternative activation pathway known as the M2 phenotype triggered by Interleukin-4 (IL-4) or Interleukin-13 (IL-13), resulting in the secretion of anti-inflammatory cytokines such as Interleukin-10 (IL-10; Orihuela et al., 2016; Amo-Aparicio et al., 2021). The phenotypic changes of microglia cells from a pro-inflammatory to an anti-inflammatory state ensures the clearance of debris and deposition of extracellular matrix for tissue repair (Arcuri et al., 2017). Otherwise, the production of proinflammatory cytokines, NO, and ROS would be elevated. This can result in progressive cell death and damage to the tissues. However, this coordination between the two phenotypes of microglia is altered during chronic activation of microglia and thus causes inflammation in neurodegenerative diseases (Figure 2A).

Furthermore, transcriptome studies have demonstrated that activation of microglia is variable, suggesting that M1 (Ramified cells) and M2 (amoeboid cells) signify a range of activation patterns instead of just a separate cell subtypes (Correale, 2014). The M1/M2 model alone is reported to lack accuracy to explain microglia activation and its heterogeneity *in vivo* (Colonna and Butovsky, 2017). The report also suggests microglia heterogeneity in pineal gland (Muñoz, 2022). Consequently, there is no standard morphological classification, which makes it difficult to relate data from various independent studies and avoids impartial

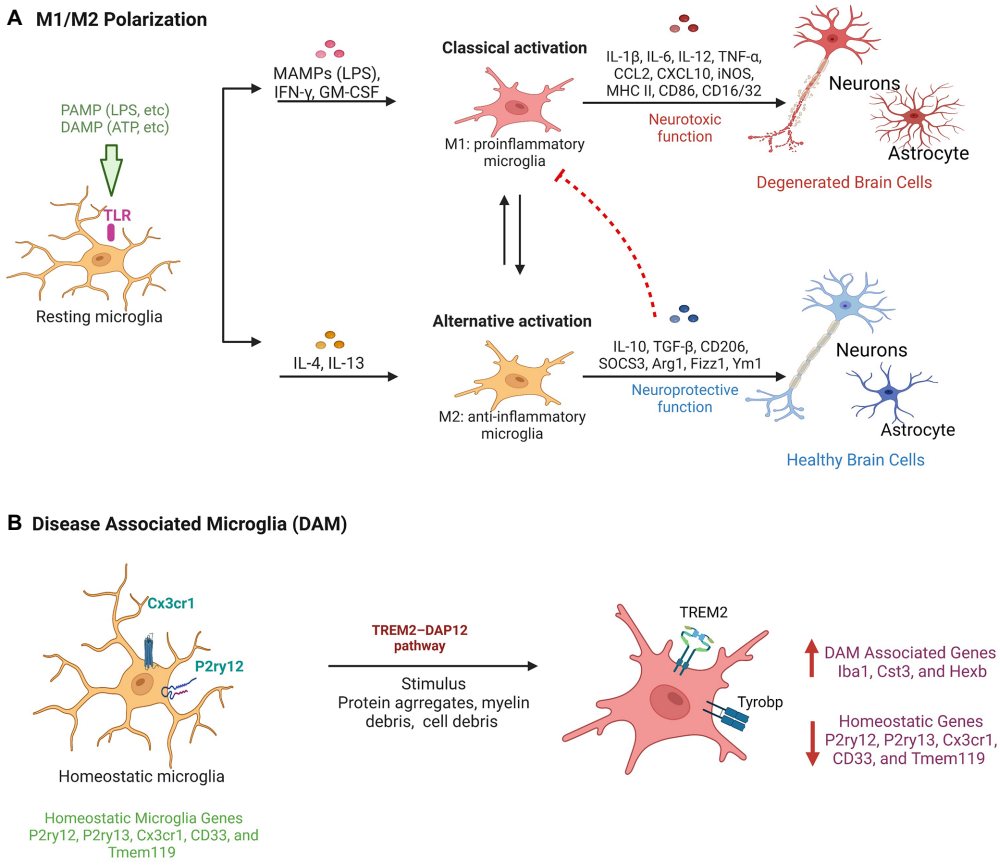

FIGURE 2
Microglial activation pathways in neuroprotection and neurodegeneration. **(A)** Classical Pathway: PAMPs/DAMPs activate TLRs such as TLR-4 on resting microglia and result in a phenotypic transition to M1 type microglia and secrete pro-inflammatory factors having neurotoxic functions. Alternative pathway: Factors such as IL-4 and IL-13 modulates the transition of microglia to M2 phenotype and provide neuro-protective function by secreting anti-inflammatory cytokines. **(B)** Diagrammatic representation showing molecular changes in homeostatic microglia leads to their conversion in disease associated microglia phenotype during neurodegeneration.

quantification of pathological status and therapeutic effects (Paolicelli et al., 2022). Further, in neurodegenerative conditions such as AD, ALS, aging a comprehensive single-cell RNA analysis of CNS immune cells identified disease-associated microglia (DAM), a subpopulation of microglia with a distinct transcriptional and functional signature. DAM is associated with the expression of neurodegenerative disease-related genes (Figure 2B). DAM are immune cells that express typical microglial markers such as Cst3, Iba1, and Hexb, concurrently with the downregulation of "homeostatic" microglial genes, such as Cx3cr1, Tmem119, P2ry12, P2ry13, and CD33 (Butovsky et al., 2014). DAM also exhibits upregulation of genes involved in lipid metabolism, phagocytic and lysosomal, pathways such as Apoe, Ctsd, Lpl, Tyrobp, and Trem2, which are known AD risk factors. DAM can be activated by a variety of stimuli, including myelin debris, protein aggregates, and cell debris, *via* the TREM2–DAP12 pathway, and can contribute to the apoptotic cells clearance, inflammatory cytokines, and myelin debris (Deczkowska et al., 2018). Therefore, the discovery of DAM in different neurodegenerative diseases paved the way for the development of a therapy targeting the universal and intrinsic mechanism for combating neuronal death that is shared by multiple neurodegenerative diseases. However, to make effective use of their therapeutic potential, it will be necessary to conduct extensive research to better comprehend the microglia phenotype, disease specific microglia characterization in CNS pathology.

7.1. Microglia and Alzheimer's disease

Alzheimer's disease (AD) is the most prevalent neurological disorder, characterized by progressive cognitive decline and memory loss in most patients. It affects approximately 1 in 9 people aged 65 and over (10.7%). Alzheimer's dementia prevalence increases with age: 5% of those aged 65 to 74, 13.1% of those aged 75 to 84, and 33.2% of those aged 85 and older have Alzheimer's dementia (2022 Alzheimer's disease facts and figures, 2022). Mostly during the early stages of AD, beta-amyloid (Aβ) protein secreted from neurons misfolds and forms senile plaques in the extracellular space of neuronal cells that leads to the formation of

neurofibrillary tangles that is an aggregate of hyperphosphorylated Tau protein (Murphy and LeVine 3rd, 2010). An association between an immune/microglial gene network and AD neuropathology has also been reported (Zhang et al., 2013). In this condition, activation of microglia plays dual role as acute microglial activation reduces Aβ accumulation by increasing phagocytosis or clearance (Wang et al., 2015). In contrast, chronic microglial activation contributes to neurotoxicity and synaptic loss (Lull and Block, 2010), *via* the activation of multiple proinflammatory cascades (Figure 3A). Remarkably, multiple studies on AD patients and mouse models have demonstrated that activated microglia, immunoglobulins, and complement components are closely associated with Aβ deposits in the brain. It has been demonstrated *in-vitro* that Aβ1-42 activates microglia *via* CD36 and the TLR2–TLR6 heterodimer, which then expresses copious amounts of proinflammatory factors such as IL-1, TNF-α, MIP-1, and MCP-1 (Mizuno, 2012). In addition, Aβ protein stimulated conditioned media from microglia leads to increased iNOS levels and nitrotyrosine immunoreactivity (Combs et al., 2001). Further, NO synthesis inhibition using L-NMMA can ameliorate spatial memory impairment in AD (Ren et al., 2022). Furthermore, elevated levels of chemokines and proinflammatory cytokines in cerebrospinal fluid (CSF) confirm the pathological role of microglia in AD patients (Wang et al., 2015). Apart from neuroinflammation, inflammation and systemic infections have also been associated with an increased risk of developing AD. Further, microglial activation is also responsible for the hyperphosphorylation of tau and the formation of fibrillary cells through the CX3CR1 pathway. Chemokine receptor CX3CR1 is predominantly expressed on microglia and maintains the quiescent state of microglia by binding to its ligand, fractalkine (CX3CL1), which is expressed in both soluble and membrane-bound forms in neurons. Tau competes with CX3CL1 for interaction with its receptor, CX3CR1, in the AD brain, where fractalkine expression is reduced. Particularly, deletion of CX3CR1 in microglia increases IL-1 secretion and tau fibrillary tangle formation (Pawelec et al., 2020). Microglia depletion has been reported to inhibit tau proliferation, indicating that microglia actively contribute to tau pathology during AD pathogenesis (Asai et al., 2015). In

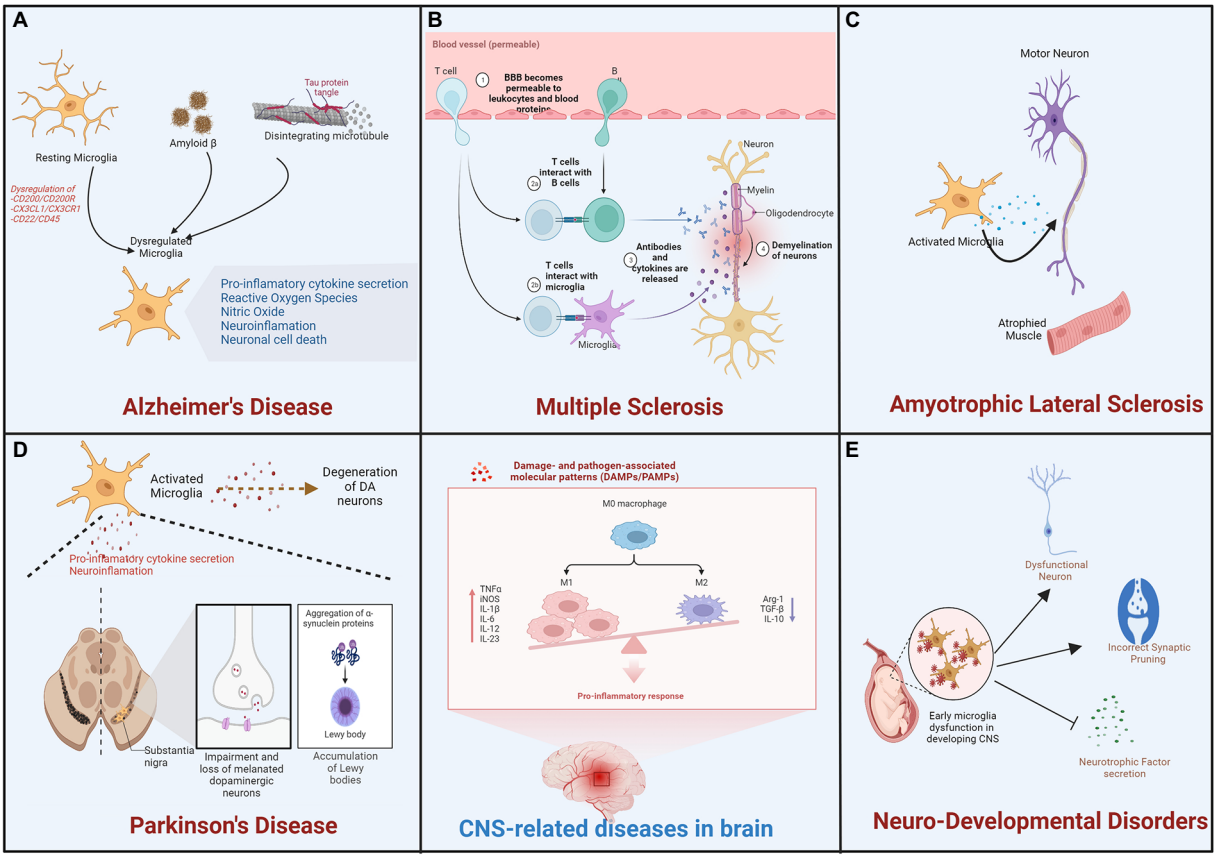

FIGURE 3
Microglial activation is involved in the progression of neurodevelopmental and degenerative diseases. During pathological processes, alternation in microglial function and activation process is involved in neurodegenerative diseases such as **(A)** Alzheimer's disease (AD), **(B)** Multiple Sclerosis (MS), **(C)** Amyotrophic Lateral Sclerosis (ALS), and **(D)** Parkinson's Disease (PD) as well as **(E)** neurodevelopmental diseases.

addition, microglia express pattern recognition receptors (PRRs), an innate immune cell receptor that responds to molecular patterns associated with danger or pathogens (DAMPs or PAMPs), i.e., exogenous pathogenic molecules. Additionally, PRRs bind to diverse Aβ species with varying affinities. Recent research has demonstrated that, in the human AD cortex under definite conditions, Aβ species of high-molecular-weight break down into small oligomeric Aβ species which are neurotoxic in nature, and *in vivo* administration of this species to mice activates microglia. The activated microglia get identified by elevated levels of CD68 and diminished ramification. *In vitro* study suggests that Aβ by binding to PRRs, such as receptors for advanced glycation products (RAGE), toll-like receptors (TLRs), and scavenger receptors activates microglia (Wilkinson and El Khoury, 2012). Importantly, proinflammatory molecules such as TNF-α and IL-1, and other inflammatory intermediates increased production leads to compromised microglial phagocytosis upon PAMP or DAMP binding to PRRs. It appears that the expression profile of cytokines from microglia influences the phagocytotic index of microglia. Further, greater Aβ load and phagocytic index was also observed in microglia that produced IL-1 and IL-1R (Sarlus and Heneka, 2017). Interestingly, genome-wide association studies (GWAS) have reported 38 genetic loci found strongly associated with the risk of late-onset Alzheimer's disease (LOAD). Many of them are related to neuroinflammation and are observed to be microglial cells specific such as ε4 isoform of the ApoE, Trem2, Cr1, Cd33, or Abca7, etc. (Neuner et al., 2020; Wightman et al., 2021). This provides additional support for the hypothesis that microglia reactions are likely a cause as well as a consequence of AD. To explore these functions and the association of microglial genes with disease states, however, in-depth research is necessary.

7.2. Microglia and multiple sclerosis

Multiple sclerosis (MS) affects approximately 2.8 million people worldwide, according to the most comprehensive global study to date. Since 2013, the Atlas of Multiple Sclerosis reveals that the number of people living with MS has increased in every region. The report indicates that 85% of people are initially diagnosed with relapsing–remitting MS, which is characterized by periods of relapse and remission, while 12% are initially diagnosed with progressive MS (Goldenberg, 2012; Klineova and Lublin, 2018). The MS is a chronic inflammatory and neurodegenerative disease of the central nervous system (CNS) that affects the white and gray matter characterized as focal lesions of inflammation, axonal loss, gliosis, and demyelination (Lassmann, 2018). It is regarded as a multifaceted, heterogeneous disease with varying patterns and mechanisms of tissue injury that are frequently difficult to treat. The course of disease for the remaining 3% is unknown at the time of initial diagnosis. In the early stages of multiple sclerosis, brain biopsies revealed subcortical and cortical demyelination and the presence of phagocytic cells (Popescu et al., 2013). As measured by the expression of the microglia-specific marker TMEM119, which is absent in macrophages, this pool of phagocytic cells in MS lesions consists of approximately 40% microglia cells (Wang et al., 2019).

Activated microglia were observed in animal models of MS, and experimental autoimmune encephalomyelitis (EAE). They were critical to the inflammation of CNS, demyelination and remyelination processes of multiple sclerosis (Robinson et al., 2014). Remyelination is the process of myelin regeneration that occurs concurrently with or after demyelination and it is characterized by the appearance of myelin around the axon (Chari, 2007). Clearance of debris and proliferation of oligodendrocytes are essential remyelination processes, followed by recruitment and proliferation of OPCs, which differentiate into mature myelinating oligodendrocytes (Bradl and Lassmann, 2010). Through the expression of anti-inflammatory molecules, phagocytosis of debris, and tissue repair, microglia promote remyelination. Microglia secrete factors such as TNF-α, IGF-1, and FGF-2 that promote oligodendrocyte proliferation (Kalafatakis and Karagogeos, 2021). IL-4 injection increased oligodendrocyte proliferation in the spinal cord of EAE mice, suggesting the potential involvement of microglia/macrophages in remyelination (Luo et al., 2017). In another similar study, oligodendrocyte differentiation in cerebellar slices was improved *in-vitro* by culture in M2 microglia-conditioned medium and decreased *in-vivo* after M2 microglia depletion; blocking of activin A secreted by M2 microglia inhibited oligodendrocyte differentiation during remyelination (Kalafatakis and Karagogeos, 2021). During the early phase of multiple sclerosis, however, remyelination is impaired because M2 microglia cells (neuroprotective) acquire a different phenotype (neurotoxic microglia) and secrete proinflammatory molecules that can damage the myelin sheath and contribute to oligodendrocyte loss (Luo et al., 2017; Kalafatakis and Karagogeos, 2021). Crosstalk between these activated neurotoxic microglia and other immune cells leads to the activation of T cells during demyelination and remyelination in multiple sclerosis (Matejuk et al., 2021; Figure 3B).

7.3. Microglia and amyotrophic lateral sclerosis

A degenerative disorder affecting motor neurons (MNs) of the cerebral cortex, brainstem, and spinal cord, amyotrophic lateral sclerosis is also known as Lou Gehrig's disease in the United States. It also results in the death of upper and lower motor neurons, which control voluntary muscle contractions. This causes symptoms including muscle stiffness and twitching, limb weakness due to a gradual reduction in muscle size, and difficulty swallowing or speaking (Zarei et al., 2015).

In addition, up to 50 % of patients develop frontotemporal dementia (FTD), which is characterized by progressive degeneration of the frontal and temporal lobes, behavioral and personality changes, and a decline in language and executive function (Ferrari et al., 2011). In the late stages of the disease, the weakened diaphragm and intercostal muscles typically result in respiratory failure and death. PET analysis of a small cohort of amyotrophic lateral sclerosis (ALS) patients has demonstrated the activation of microglia in ALS patients. This study revealed diffuse microglial activation in both motor and extra-motor regions of the brain (Muzio et al., 2021). In addition, studies on human postmortem tissues and mouse models of ALS have revealed an increase in activated microglia in regions of the brain with neuronal loss (Figure 3C). In addition to the altered state of microglia observed in ALS, evidence also suggests that the disease is associated with microglial degeneration (Brites and Vaz, 2014). In transgenic mutant SOD1G93A, with aggregated SOD1 also known as mice model of ALS leads to degeneration of mononuclear phagocytes including microglia and infiltrating monocytes in brain (Brites and Vaz, 2014; Liu and Wang, 2017). In postmortem ALS spinal cord tissue, upregulation of microglial receptors including toll-like receptors TLR2 and TLR4 and co-receptor CD14 has also been reported (Liu and Wang, 2017). NF-kB is a master regulator of inflammatory responses and has been associated with microglial involvement in ALS models (Frakes et al., 2014). Neurotoxic NADPH oxidase has been associated with ALS. A correlation exists between decreased NOX2 activity and increased survival in ALS patients (Marrali et al., 2014).

7.4. Microglia and Parkinson's disease

Parkinson's disease (PD) is the second most prevalent form of neurodegeneration. It manifests clinically as motor symptoms such as tremor, slow movement, rigidity, imbalance, walking etc., and a wide range of non-motor complications like dementia, mental health disorders, cognitive impairment, pain, sleep disorders, and other sensory disturbances (DeMaagd and Philip, 2015). Motor impairments, including involuntary movements (dyskinesias) and painful involuntary muscle contractions (dystonias), causing difficulty in mobility, speech, and various other aspects of life (Sveinbjornsdottir, 2016). These motor symptoms are caused by the degeneration of DA (dopaminergic) neurons located in the pars compacta of the substantia nigra (SN) in a progressive manner. The striatum is innervated by DA neurons, and their degeneration is associated with a substantial reduction in DA striatal content (Zhai et al., 2018). Loss of DA neurons is frequently associated with the formation of Lewy bodies (LB), which are aggregates of misfolded α-synuclein in the SN, but also in other brain regions (Power et al., 2017). Sustained α-synuclein burden leads to aberrant microglial activation, and targeting microglial activation states by suppressing their deleterious pro-inflammatory neurotoxicity has been proposed as a therapeutic approach for PD treatment. Similarly, increased levels of pro-inflammatory cytokines IL-1β, TNF-α and iNOS mRNA, degeneration of nigral dopaminergic neurons has been reported in Parkin deficient mice (Frank-Cannon et al., 2008; Tran et al., 2011). Aberrant microglial activation and increased astrogliosis has also been observed in aged parkin-null mice (Rodriguez-Navarro et al., 2007). Thus, loss of Parkin is also reported to influence activated microglia survival and cause chronic neuroinflammation (Dionísio et al., 2019).

Remarkably, in the postmortem PD patients SN, neuronal cell death was observed along with significant microglial activation in the affected brain region. These activated microglia reported to produce a variety of inflammatory mediators, such as NOS2, IL-6, COX2, TNF-α, and ROS, result in the long-term and continuous loss of DA neurons (Marogianni et al., 2020). In the SN of living PD patients, positron emission tomography (PET) analysis consistently detects activated microglia and significant death of dopamine (DA) neurons. In addition, reactive microglia are observed in brain regions other than SN, indicating that microglia play a global role in the development of PD (Belloli et al., 2020). PET imaging has confirmed potent activation of microglia in a 6-hydroxydopamine (6-OHDA)-induced PD model, and depletion of TNF-α by pharmacological neutralization or by a dominant-negative mutant should reduce the loss of dopaminergic neurons and improve behavioral performance (More and Choi, 2016). In another PD model established with 1-methyl-4-phenyl-1,2,3,6 tetrahydropyridine (MPTP), microglial activation in the SN has also been confirmed by a dramatic morphological change (Meredith and Rademacher, 2011). Significantly, deletion of TLR-4 in microglia inhibits their activation, thereby promoting the survival of DA neurons (Cui et al., 2020). Further, it was hypothesized that neurotoxic reactive species produced by microglia, such as superoxide and nitric oxide, induce cellular stress and contribute to neuronal loss in PD (Drechsel and Patel, 2008). In addition, the cerebrospinal fluid of PD patients was found to be toxic to DA neurons *in vitro* due to the high concentration of cytokines and autoantibodies against quinone proteins altered by DA oxidation (Whitton, 2007). Reports also suggest neuroprotective role of microglia in PD by initiating neuron–glia crosstalk, regulating microRNA, releasing anti-inflammatory cytokines such as IL-4, Arg1, Tgf-beta, activating multiple receptors and suppressing the expression of neurotoxic genes by modifying histone tails (Le et al., 2016). However, continuous stimulus from endogenous factors such as α-synuclein aggregates contribute to elevated inflammation in the brain and succeed the protective effects of microglia and thus drive the chronic and progressive neurodegeneration observed in PD (Le et al., 2016; Bido et al., 2021). These findings strongly suggest that inflammation mediated by microglia plays a pathogenic role in PD (Figure 3D).

7.5. Microglia and neurodevelopmental disease

Microglia are believed to play a crucial role in neurogenesis, the transformation of precursor cells into neurons. During normal neurodevelopment, microglia induce apoptosis and phagocytosis in a number of newborn neurons; however, in the adult brain, this process is restricted to neurogenic niches. In addition, *in-vivo* analysis of prenatal brain studies reveals that microglia phagocytose neural progenitor cells, which may contribute to neurodevelopmental disorders such as ID (intellectual disability), ADHD (attention-deficit/hyperactivity disorder), ASD (autism spectrum disorder), CD (communication disorders), SLD (specific learning disorder), and MDs (motor disorders), which affect 2–4 percent of the world's population (Figure 3E). Due to the difficulty in studying embryonic systems, most studies examining the role of microglia in neurogenesis employ *in vitro* or adult neurogenesis methodologies. Vargas et al., 2005 were the first to demonstrate an inflammatory phenotype in the postmortem brains of individuals with ASD. Neuropathological examination of the cerebral and cerebellar cortices of individuals with autism spectrum disorder revealed increased microglial activation, characterized by elevated expression of MHC class II (Needleman and McAllister, 2012). In addition, increased expression of pro-and anti-inflammatory factors, including CCL2, IL-6, and TGF-β, was observed in the brain and cerebrospinal fluid (CSF). In the post-mortem brain of ASD, expression level analysis of pro-inflammatory cytokines in tissue and CSF suggest altered immune response and their link with region specific brain inflammation (Goines and Ashwood, 2013). Similarly, GWAS analysis of ASD brains showed genes related to activated microglia, immune and inflammatory functions suggesting astrocyte and microglial immune dysregulation (Davoli-Ferreira et al., 2021). Along with it, alteration in microglia morphology, spatial distribution and density was also reported in ASD brain. In addition to having a higher density in the cerebral and cerebellar cortices of ASD patients, microglia exhibit enlarged cell bodies, processes thickening and retraction. ASD-associated microglia also extend filopodia from their processes (Morgan et al., 2010; Davoli-Ferreira et al., 2021). Similar studies have demonstrated the role of microglial cells in inducing the loss of cortical gray matter in schizophrenia patients by pruning synapses, phagocytosing stressed neurons, and inhibiting the release of neurotrophic factors such as BDNF (Mallya and Deutch, 2018). In a systematic review by Trépanier et al., 2016 multiple studies reported an increase in the expression of microglial markers in the postmortem brains of schizophrenia patients as compared to control subjects. In addition, a meta-analysis conducted by van Kesteren et al., 2017 revealed an increase in the number of microglia in specific brain regions, such as the temporal cortex, in the postmortem brains of schizophrenia patients compared to those of control subjects. Nevertheless, there have been numerous contradictory studies regarding microglial cell activation and neurodevelopmental disease (NDD). To better comprehend the role of microglial cells and associated factors, patients must be subjected to a comprehensive analysis and screening.

8. Possible transcriptional target in microglia for regulating brain homeostasis in neurodegenerative diseases

For an extended period of time, the difficulty of microglia-specific conditional gene targeting has hindered the thorough understanding of microglia residing in the CNS and their functions. However, recent developments have produced a variety of strategies to combat non-specificity. Multiple signature genes have been proposed as being essential for microglia function. It has been discovered that the transcriptional regulator Sall1 is highly expressed in adult microglia. Sall1 controls a unique transcriptional signature permitting microglia function and fate in the regulation of homeostasis in the adult CNS. Deletion of Sall1 in microglia leads to dysregulated neurogenesis and microglia activation which further affects cognitive and behavioral function and impairs memory formation. It has been proposed that Sall1 could act as the master transcriptional regulator of housekeeping functions and the non-reactive state of microglia, which are essential for CNS homeostasis. In addition, Sall1CreER mice were reported to target microglia without targeting other MPS members (Buttgereit et al., 2016). Microglia's development, proliferation, migration, differentiation, and survival are governed by the CSF1R, a key signaling node. CSF1R signaling was required for adult microglial survival. In the 5Xfad mouse model of AD, the CSF1R inhibitors (PLX3397 and PLX5622) deplete microglia and prevent plaque formation in brain parenchyma (Spangenberg et al., 2019; Green et al., 2020). Another CSF1R inhibitor, JNJ-40346527 (JNJ-527), inhibits microglial proliferation and reduces tau-induced neurodegeneration (Mancuso et al., 2019). Signaling of TGF-R has been linked to the formation and maintenance of microglia. Further, microglia-specific deletion of TGF-R led to a discovery that TGF-R signaling is involved in maintaining the homeostatic phenotype of adult microglia but not their survival (Zöller et al., 2018).

Modulating mitochondrial function and reactive oxygen species (ROS) levels, PGC-1α has also been implicated in the pathogenesis of numerous neurological disorders (Panes et al., 2022). Reduced PGC-1 expression was preceded by decreased expression of mitochondrial antioxidants and uncoupling proteins (UCPs) in multiple sclerosis patients,

resulting in neuronal loss and neurodegeneration (Witte et al., 2013). Furthermore, PGC-1 α reported to upregulate mitochondrial antioxidants SOD2 and GPx1, reduces ROS generation, and attenuated MPTP-induced neurodegenerative processes in a PD model (Piccinin et al., 2021). PGC-1α significantly suppresses oxidative damage and the production of proinflammatory mediators in primary human astrocytes (Nijland et al., 2014). In the microglia of an animal model of acute ischemic stroke (AIS) and stroke patients, the altered expression of PGC-1α was reported. Overexpression of microglial PGC-1α has been suggested to inhibit neuroinflammatory responses. PGC-1α may also stimulate mitophagy and autophagy *via* unc-51-like kinase 1 (ULK1), which inhibits hyperactivation of the NLRP3 inflammasome, thereby reducing neuroinflammation and neurological deficits (Han et al., 2021). The neuroprotective effects of PGC-1α were eliminated when autophagy and mitophagy were inhibited pharmacologically and genetically. Consequently, targeting microglial PGC-1α may be advantageous for the treatment of AIS. Microglial activation suppression is one of the well-established anti-inflammatory effects of fasting and the ketogenic diet. The activation of GPR109A by beta-hydroxybutyrate inhibits NF-kB signaling and the production of pro-inflammatory cytokines in microglia and promotes neuroprotective phenotype in microglia (Fu et al., 2015). Magnolol (MA) reduced chronic unpredictable mild stress (CUMS)-induced depressive-like behavior by inhibiting M1 microglia polarization and promoting M2 microglia polarization through Nrf2/HO-1/NLRPP signaling. Transfection of Nrf2 siRNA confirmed the role of Nrf2 in the modulation of microglia polarization by MA. In addition, the enhanced effect of MA on Nrf2 was a result of the inhibition of Nrf2 ubiquitination (Li et al., 2018; Tao et al., 2021).

Hypoxia causes oxidative stress and induction of both phosphorylation and S-glutathionylation of transcription factor STAT1 which leads to its aberrant activation in M1 microglia. Report also showed reduced hypoxia-M1 microglia phenotype upon STAT1 silencing suggesting the strong link between hypoxia-STAT1 and STAT1-microglia activation (Butturini et al., 2019). Another transcription factor STAT3, also known to regulate inflammatory gene expression and microglial activity in response to various CNS insults. Aberrant activation of STAT3 after cerebral ischemia leads to neuroinflammatory processes and promotes transcription and expression of genes involved in proinflammatory mediators including inflammatory enzymes. Following ischemic injury, STAT3 overactivation in microglia causes microglia activation and inflammatory responses in the dentate gyrus (DG) and brain cortex region (Chen et al., 2017). Similarly, STAT6 deficiency has been shown to exacerbate local inflammation, enlarges brain tissue loss, clearance of dead/dying neurons and worsens long-term functional deficits. Early after stroke, STAT6 is reported to mediate effective efferocytosis and anti-inflammatory responses of microglia and STAT6/Arg1 signaling is proposed to be a viable therapeutic target to regulate microglia functions and promote long-term favorable outcomes during brain injury (Cai et al., 2019).

TFEB (Transcription factor EB) functions as the master regulator of lysosomal function. The deacetylation of TFEB intensifies its contribution to microglial degradation of fAβ and reduces amyloid plaques in brain slices from APP/PS1 mice (Bao et al., 2016). Pyruvate kinase M2 (PKM2), an essential glycolytic rate-limiting enzyme, interacts directly with the pro-inflammatory transcription factor ATF2 (activating transcription factor 2) to link pyroptosis and glycolysis in microglia, which may represent crucial crosstalk between neuroinflammation and metabolic reprogramming and in the CNS. Treatment of brain and muscle ARNT-like 1 (Bmal1) deficient mice treated with MPTP reported significant reductions in numbers of dopaminergic neurons (DANs) in the substantia nigra pars compacta (SNpc), tyrosine hydroxylase protein level in the striatum, dopamine (DA), and 3,4-dihydroxyphenylacetic acid content, respectively indicating that Bmal1 may play a crucial role in the survival of DANs and in maintaining the normal function signaling pathway in the brain by regulating microglia-mediated neuroinflammation. Disruption of the basic helix–loop–helix (bHLH) transcription factor lymphoblastoid leukemia-derived sequence 1 (Lyl-1) basic helix–loop–helix domain induces an increase in the emergence of primitive macrophage progenitors followed by a defect in their differentiation. These defects are linked to a disruption in the expression of gene sets associated with neurodevelopment. The microglia number was also found to decrease in the developing brain under Lyl-1 deficiency (Wang et al., 2021).

MEF2a (Myocyte enhancer factor 2a), that is exclusively expressed in adult microglia, is essential for maintaining the microglial phenotype and establishing the epigenetic landscape. MEF2a motif analysis revealed an increased proportion of adult microglia gene promoters associated with regulatory regions (Yeh and Ikezu, 2019). Similarly, MEF2c (Myocyte enhancer factor 2c) is diminished in aged mice due to increased expression of type-1 interferon (IFN-1) in 5x FAD mouse model representing early microglial changes in AD related pathology (Xue et al., 2021). TNF-α, a proinflammatory cytokine associated with aging, induces IBA1 intensity in immunohistochemistry study in MEF2c-deficient mice (Deczkowska et al., 2017). Following LPS stimulation *in vitro*, microglia lacking MEF2c secreted more proinflammatory cytokines and displayed less social preference (Deczkowska et al., 2017). Hematopoietic precursors express a high level of Runt-related transcription factor 1 (RUNX1). The enrichment of the RUNX1 binding motif in the enhancer landscapes of adult microglia suggests a possible role in the maintenance of the adult microglial

phenotype (Lopez-Atalaya et al., 2018). V-maf musculoaponeurotic fibrosarcoma oncogene homolog B (MAFB) reported to be specifically expressed in adult microglia. During aging, MAFB expression is observed to increase significantly. Further, it is known to play a key role in the maturation and differentiation of adult microglia, and is proposed to regulate microglia response under stressful or pathological conditions. MAFB regulates expression of immune and viral genes and promotes anti-inflammatory phenotypes. In the presence of GM-CSF, MAFB-deficient microglia exhibit increased self-renewal and decreased P2ry12 and Ccl2 expression (Koshida et al., 2015). Hhex is reported to negatively regulate microglia inflammation-related genes, and TLR2/4 activation decreases Hhex, thereby promoting TLR4-mediated neuroinflammation (Sakate et al., 2022).

9. Epigenetic factors and their key role in the regulation of microglia function in normal and disease conditions

In microglia, lineage-determining transcription factors including PU.1 and SALL1 form complexes with gene enhancers and become co-activators to regulate the transcription of targeted genes. The tightly regulated acetylation of histone H4 on the promoter and intron-1 region of the PU.1 locus was reported essential for allowing the interaction between RNA polymerase II and locus (Laribee and Klemsz, 2005). Further, it was observed that histone deacetylase (HDAC) activity is essential for association of RNA polymerase II with PU.1 promoter (Laribee and Klemsz, 2005). Further, altering catalytic activity of HDACs by treatment of valproic acid and vorinostat are shown to regulate microglial transcriptomes *via* PU.1 suppression (Dragunow et al., 2006; Rustenhoven et al., 2018). Another epigenetic regulator, Runx1t1 (Runt-related transcription factor 1; translocated to, 1) also interacts with HDACs, epigenetically regulates Cdk4 and LAT controls the proliferation and nitric oxide production of microglia (Baby et al., 2014). Inhibiting HDAC1 and HDAC2 has been shown to suppress inflammatory response of chronically activated microglia, thus proposed as a therapeutic approach toward management of neuroinflammation (Durham et al., 2017). In mice, ablation of Hdac1 and Hdac2 leads to impaired microglia development during the prenatal stage whereas they did not have any effect on microglia survival during homeostasis in the adult stage. Deletion of Hdac1 and Hdac2 from microglia of AD mice model lead to enhanced phagocytosis, decreased amyloid deposition and improved cognitive impairment (Datta et al., 2018). Further, the presence of active histone H3 at the lysine 4 (H3K4) region, in both wild-type and MGnD microglia indicates that disease-associated regions primed in MGnD can also be primed in homeostatic microglia. Histone methylation occurring on the amino (N) terminal tail of the core histone H3 (H3K27me3) is known to be associated with the downregulation of nearby genes *via* the formation of heterochromatin regions and thus regulates the efficient clearance of apoptotic cells and debris by microglial cells (Petralla et al., 2021). It was observed that epigenetic modification of H3K27me3 leads to suppression of clearance-related genes and this affects the region-dependent phagocytic activity of microglia (Ayata et al., 2018).

In *Mecp2* null mice, microglia activation and loss have been observed with disease progression (Cronk et al., 2015). In Rett Syndrome, Mecp2 deficiency is reported to cause microglial activation and dysfunction (Kahanovitch et al., 2019). Mecp2 regulates glutamate synthesis and mitochondria function in microglia by acting as a transcriptional repressor of the major glutamate transporter, SNAT1 (Jin et al., 2015). Mecp2 depletion causes an increase in histone acetylation at enhancer regions of Fkbp5, a canonical glucocorticoid target gene, and recruitment of nuclear receptor co-repressor 2 (NCOR2) and HDAC3 complex leading to dysregulation of genes involved in glucocorticoid signaling, hypoxia response and inflammatory responses, suggesting Mecp2 is critical for maintaining immune cell function including microglia (Yeh and Ikezu, 2019).

Reports also indicate factors that can lead to epigenetic modification in microglia are peripheral immune stimulation and cerebral beta-amyloidosis. The activation of HIF-1a and mTOR pathways in response to cerebral beta amyloidosis cause transcriptional and functional alterations linked with increased immune response genes and inflammation in MGnD. In LPS-treated amyloid-β precursor protein (APP) transgenic mice, H3K4me1 increased levels in putative enhancers reported related to phagocytic function (Wendeln et al., 2018). Therefore, more precise epigenetic studies are necessary for the genetic targeting of specific HDACs in microglia. Apart from histone modifications, microRNAs (miRNAs) are also involved in regulating the CNS epigenetic landscape. miRNAs are small non-coding RNA molecules, known to regulate gene expression. In brain, mRNA and miRNA microarray assays analysis identified miR-155 and miR-124 as regulator of development of microglial cells, microglia activation pathways and microglia quiescence in the CNS (Ponomarev et al., 2011; Cardoso et al., 2012).

10. Conclusion and future prospective

Microglia are brain specific immune cells, interacts with neurons, astrocytes, oligodendrocytes and play an important role in maintenance of brain homeostasis *via* performing

regular immunological surveillance, regulating neuroinflammation, maintaining synaptic plasticity, cognition etc. To better understand the role of microglia in brain homeostasis, further research is required to decipher the gene-specific functions of microglia and their interconnections with other brain cells. Further, microglia physiology is also critical for progression of neurodegenerative diseases. Despite the many advancements made in recent years, there are still many unanswered questions. Exciting new pharmacological agents that target not only the deleterious functions of microglia, but also mechanisms that promote endogenous repair, are likely to become available in the near future. Overall, future studies will facilitate clinical advancement and investigation of the role of microglia in a variety of nervous system functions.

Author contributions

SM designed the study. SM and SG did a literature survey, wrote the part of the manuscript, and compiled the manuscript. RM reviewed and edited the manuscript. All authors contributed to the article and approved the submitted version.

Funding

SM acknowledges financial support from the Institute of Eminence, University of Delhi (IOE/2021/12/FRP) and University of Delhi, Delhi-110007.

Conflict of interest

SG was employed by Tech Cell Innovations Private Limited.

The remaining authors declare that the research was conducted in the absence of any commercial or financial relationships that could be construed as a potential conflict of interest.

Publisher's note

References

2022 Alzheimer's disease facts and figures (2022). Alzheimer's disease facts and figures. *Alzheimers Dement.* 18, 700–789. doi: 10.1002/alz.12638

Aires, I. D., Ribeiro-Rodrigues, T., Boia, R., Ferreira-Rodrigues, M., Girão, H., Ambrósio, A. F., et al. (2021). Microglial extracellular vesicles as vehicles for neurodegeneration spreading. *Biomol. Ther.* 11:770. doi: 10.3390/biom11060770

Akiyoshi, R., Wake, H., Kato, D., Horiuchi, H., Ono, R., Ikegami, A., et al. (2018). Microglia enhance synapse activity to promote local network synchronization. *eNeuro* 5:2018. doi: 10.1523/ENEURO.0088-18.2018

Amo-Aparicio, J., Garcia-Garcia, J., Francos-Quijorna, I., Urpi, A., Esteve-Codina, A., Gut, M., et al. (2021). Interleukin-4 and interleukin-13 induce different metabolic profiles in microglia and macrophages that relate with divergent outcomes after spinal cord injury. *Theranostics* 11, 9805–9820. doi: 10.7150/thno.65203

Andoh, M., and Koyama, R. (2021). Microglia regulate synaptic development and plasticity. *Dev. Neurobiol.* 81, 568–590. doi: 10.1002/dneu.22814

Arcuri, C., Mecca, C., Bianchi, R., Giambanco, I., and Donato, R. (2017). The pathophysiological role of microglia in dynamic surveillance, phagocytosis and structural remodeling of the developing CNS. *Front. Mol. Neurosci.* 10:191. doi: 10.3389/fnmol.2017.00191

Asai, H., Ikezu, S., Tsunoda, S., Medalla, M., Luebke, J., Haydar, T., et al. (2015). Depletion of microglia and inhibition of exosome synthesis halt tau propagation. *Nat. Neurosci.* 18, 1584–1593. doi: 10.1038/nn.4132

Ayata, P., Badimon, A., Strasburger, H. J., Duff, M. K., Montgomery, S. E., Loh, Y. E., et al. (2018). Epigenetic regulation of brain region-specific microglia clearance activity. *Nat. Neurosci.* 21, 1049–1060. doi: 10.1038/s41593-018-0192-3

Baalman, K., Marin, M. A., Ho, T. S., Godoy, M., Cherian, L., Robertson, C., et al. (2015). Axon initial segment-associated microglia. *J. Neurosci. Off. J. Soc. Neurosci.* 35, 2283–2292. doi: 10.1523/JNEUROSCI.3751-14.2015

Baby, N., Li, Y., Ling, E. A., Lu, J., and Dheen, S. T. (2014). Runx1t1 (runt-related transcription factor 1; translocated to, 1) epigenetically regulates the proliferation and nitric oxide production of microglia. *PLoS One* 9:e89326. doi: 10.1371/journal.pone.0089326

Bachstetter, A. D., Morganti, J. M., Jernberg, J., Schlunk, A., Mitchell, S. H., Brewster, K. W., et al. (2011). Fractalkine and CX 3 CR1 regulate hippocampal neurogenesis in adult and aged rats. *Neurobiol. Aging* 32, 2030–2044. doi: 10.1016/j.neurobiolaging.2009.11.022

Bao, J., Zheng, L., Zhang, Q., Li, X., Zhang, X., Li, Z., et al. (2016). Deacetylation of TFEB promotes fibrillar Aβ degradation by upregulating lysosomal biogenesis in microglia. *Protein Cell* 7, 417–433. doi: 10.1007/s13238-016-0269-2

Basilico, B., Ferrucci, L., Ratano, P., Golia, M. T., Grimaldi, A., Rosito, M., et al. (2022). Microglia control glutamatergic synapses in the adult mouse hippocampus. *Glia* 70, 173–195. doi: 10.1002/glia.24101

Beers, D. R., Henkel, J. S., Xiao, Q., Zhao, W., Wang, J., Yen, A. A., et al. (2006). Wild-type microglia extend survival in PU.1 knockout mice with familial amyotrophic lateral sclerosis. *Proc. Natl. Acad. Sci. U. S. A.* 103, 16021–16026. doi: 10.1073/pnas.0607423103

Behl, T., Kaur, G., Sehgal, A., Bhardwaj, S., Singh, S., Buhas, C., et al. (2021). Multifaceted role of matrix metalloproteinases in neurodegenerative diseases: pathophysiological and therapeutic perspectives. *Int. J. Mol. Sci.* 22:1413. doi: 10.3390/ijms22031413

Belloli, S., Morari, M., Murtaj, V., Valtorta, S., Moresco, R. M., and Gilardi, M. C. (2020). Translation imaging in Parkinson's disease: focus on Neuroinflammation. *Front. Aging Neurosci.* 12:152. doi: 10.3389/fnagi.2020.00152

Bennett, M. L., Bennett, F. C., Liddelow, S. A., Ajami, B., Zamanian, J. L., Fernhoff, N. B., et al. (2016). New tools for studying microglia in the mouse and human CNS. *Proc. Natl. Acad. Sci. U. S. A.* 113, E1738–E1746. doi: 10.1073/pnas.1525528113

Benson, D. L., and Huntley, G. W. (2012). Building and remodeling synapses. *Hippocampus* 22, 954–968. doi: 10.1002/hipo.20872

Benusa, S. D., and Lafrenaye, A. D. (2020). Microglial process convergence on axonal segments in health and disease. *Neuroimmunol. Neuroinflamm.* 2020, 23–39. doi: 10.20517/2347-8659.2019.28

Bido, S., Muggeo, S., Massimino, L., Marzi, M. J., Giannelli, S. G., Melacini, E., et al. (2021). Microglia-specific overexpression of α-synuclein leads to severe dopaminergic neurodegeneration by phagocytic exhaustion and oxidative toxicity. *Nat. Commun.* 12:6237. doi: 10.1038/s41467-021-26519-x

Boche, D., and Gordon, M. N. (2022). Diversity of transcriptomic microglial phenotypes in aging and Alzheimer's disease. *Alzheimers Dement.* 18, 360–376. doi: 10.1002/alz.12389

Bolós, M., Perea, J. R., Terreros-Roncal, J., Pallas-Bazarra, N., Jurado-Arjona, J., Ávila, J., et al. (2018). Absence of microglial CX3CR1 impairs the synaptic integration of adult-born hippocampal granule neurons. *Brain Behav. Immun.* 68, 76–89. doi: 10.1016/j.bbi.2017.10.002

Bonham, L. W., Sirkis, D. W., and Yokoyama, J. S. (2019). The transcriptional landscape of microglial genes in aging and neurodegenerative disease. *Front. Immunol.* 10:1170. doi: 10.3389/fimmu.2019.01170

Bradl, M., and Lassmann, H. (2010). Oligodendrocytes: biology and pathology. *Acta Neuropathol.* 119, 37–53. doi: 10.1007/s00401-009-0601-5

Brites, D., and Fernandes, A. (2015). Neuroinflammation and depression: microglia activation, extracellular microvesicles and microRNA dysregulation. *Front. Cell. Neurosci.* 9:476. doi: 10.3389/fncel.2015.00476

Brites, D., and Vaz, A. R. (2014). Microglia centered pathogenesis in ALS: insights in cell interconnectivity. *Front. Cell. Neurosci.* 8:117. doi: 10.3389/fncel.2014.00117

Butovsky, O., Jedrychowski, M. P., Cialic, R., Krasemann, S., Murugaiyan, G., Fanek, Z., et al. (2015). Targeting miR-155 restores abnormal microglia and attenuates disease in SOD1 mice. *Ann. Neurol.* 77, 75–99. doi: 10.1002/ana.24304

Butovsky, O., Jedrychowski, M. P., Moore, C. S., Cialic, R., Lanser, A. J., Gabriely, G., et al. (2014). Identification of a unique TGF-β-dependent molecular and functional signature in microglia. *Nat. Neurosci.* 17, 131–143. doi: 10.1038/nn.3599

Butovsky, O., and Weiner, H. L. (2018). Microglial signatures and their role in health and disease. *Nat. Rev. Neurosci.* 19, 622–635. doi: 10.1038/s41583-018-0057-5

Buttgereit, A., Lelios, I., Yu, X., Vrohlings, M., Krakoski, N. R., Gautier, E. L., et al. (2016). Sall1 is a transcriptional regulator defining microglia identity and function. *Nat. Immunol.* 17, 1397–1406. doi: 10.1038/ni.3585

Butturini, E., Boriero, D., Carcereri de Prati, A., and Mariotto, S. (2019). STAT1 drives M1 microglia activation and neuroinflammation under hypoxia. *Arch. Biochem. Biophys.* 669, 22–30. doi: 10.1016/j.abb.2019.05.011

Cai, W., Dai, X., Chen, J., Zhao, J., Xu, M., Zhang, L., et al. (2019). STAT6/Arg1 promotes microglia/macrophage efferocytosis and inflammation resolution in stroke mice. *JCI Insight* 4:e131355. doi: 10.1172/jci.insight.131355

Cakir, B., Tanaka, Y., Kiral, F. R., Xiang, Y., Dagliyan, O., Wang, J., et al. (2022). Expression of the transcription factor PU.1 induces the generation of microglia-like cells in human cortical organoids. *Nat. Commun.* 13:430. doi: 10.1038/s41467-022-28043-y

Calovi, S., Mut-Arbona, P., and Sperlágh, B. (2019). Microglia and the purinergic signaling system. *Neuroscience* 405, 137–147. doi: 10.1016/j.neuroscience.2018.12.021

Cardoso, A. L., Guedes, J. R., Pereira de Almeida, L., and Pedroso de Lima, M. C. (2012). miR-155 modulates microglia-mediated immune response by down-regulating SOCS-1 and promoting cytokine and nitric oxide production. *Immunology* 135, 73–88. doi: 10.1111/j.1365-2567.2011.03514.x

Castillo, P. E., Younts, T. J., Chávez, A. E., and Hashimotodani, Y. (2012). Endocannabinoid signaling and synaptic function. *Neuron* 76, 70–81. doi: 10.1016/j.neuron.2012.09.020

Chari, D. M. (2007). Remyelination in multiple sclerosis. *Int. Rev. Neurobiol.* 79, 589–620. doi: 10.1016/S0074-7742(07)79026-8

Chen, S., Dong, Z., Cheng, M., Zhao, Y., Wang, M., Sai, N., et al. (2017). Homocysteine exaggerates microglia activation and neuroinflammation through microglia localized STAT3 overactivation following ischemic stroke. *J. Neuroinflammation* 14:187. doi: 10.1186/s12974-017-0963-x

Chen, P., Zhao, W., Guo, Y., Xu, J., and Yin, M. (2016). CX3CL1/CX3CR1 in Alzheimer's disease: a target for neuroprotection. *Biomed. Res. Int.* 2016:8090918. doi: 10.1155/2016/8090918

Chiu, I. M., Morimoto, E. T., Goodarzi, H., Liao, J. T., O'Keeffe, S., Phatnani, H. P., et al. (2013). A neurodegeneration-specific gene-expression signature of acutely isolated microglia from an amyotrophic lateral sclerosis mouse model. *Cell Rep.* 4, 385–401. doi: 10.1016/j.celrep.2013.06.018

Collins, P. E., Mitxitorena, I., and Carmody, R. J. (2016). The ubiquitination of NF-κB subunits in the control of transcription. *Cells* 5:23. doi: 10.3390/cells5020023

Colonna, M., and Butovsky, O. (2017). Microglia function in the central nervous system during health and neurodegeneration. *Annu. Rev. Immunol.* 35, 441–468. doi: 10.1146/annurev-immunol-051116-052358

Combs, C. K., Karlo, J. C., Kao, S. C., and Landreth, G. E. (2001). Beta-Amyloid stimulation of microglia and monocytes results in TNFalpha-dependent expression of inducible nitric oxide synthase and neuronal apoptosis. *Journal of Neuroscience* 21, 1179–1188. doi: 10.1523/JNEUROSCI.21-04-01179.2001

Cornell, J., Salinas, S., Huang, H. Y., and Zhou, M. (2022). Microglia regulation of synaptic plasticity and learning and memory. *Neural Regen. Res.* 17, 705–716. doi: 10.4103/1673-5374.322423

Correale, J. (2014). The role of microglial activation in disease progression. *Mult. Scler.* 20, 1288–1295. doi: 10.1177/1352458514533230

Cronk, J. C., Derecki, N. C., Ji, E., Xu, Y., Lampano, A. E., Smirnov, I., et al. (2015). Methyl-CpG binding protein 2 regulates microglia and macrophage gene expression in response to inflammatory stimuli. *Immunity* 42, 679–691. doi: 10.1016/j.immuni.2015.03.013

Cuadros, M. A., Sepulveda, M. R., Martin-Oliva, D., Marín-Teva, J. L., and Neubrand, V. E. (2022). Microglia and microglia-like cells: similar but different. *Front. Cell. Neurosci.* 16:816439. doi: 10.3389/fncel.2022.816439

Cui, W., Sun, C., Ma, Y., Wang, S., Wang, X., and Zhang, Y. (2020). Inhibition of TLR4 induces M2 microglial polarization and provides neuroprotection via the NLRP3 Inflammasome in Alzheimer's disease. *Front. Neurosci.* 14:444. doi: 10.3389/fnins.2020.00444

Datta, M., Staszewski, O., Raschi, E., Frosch, M., Hagemeyer, N., Tay, T. L., et al. (2018). Histone deacetylases 1 and 2 regulate microglia function during development, homeostasis, and neurodegeneration in a context-dependent manner. *Immunity* 48, 514–529.e6. doi: 10.1016/j.immuni.2018.02.016

Davoli-Ferreira, M., Thomson, C. A., and McCoy, K. D. (2021). Microbiota and microglia interactions in ASD. *Front. Immunol.* 12:676255. doi: 10.3389/fimmu.2021.676255

de Jong, C. G. H. M., Gabius, H. J., and Baron, W. (2020). The emerging role of galectins in (re)myelination and its potential for developing new approaches to treat multiple sclerosis. *Cell. Mol. Life Sci.* 77, 1289–1317. doi: 10.1007/s00018-019-03327-7

Deczkowska, A., Keren-Shaul, H., Weiner, A., Colonna, M., Schwartz, M., and Amit, I. (2018). Disease-associated microglia: a universal immune sensor of neurodegeneration. *Cell* 173, 1073–1081. doi: 10.1016/j.cell.2018.05.003

Deczkowska, A., Matcovitch-Natan, O., Tsitsou-Kampeli, A., Ben-Hamo, S., Dvir-Szternfeld, R., Spinrad, A., et al. (2017). Mef2C restrains microglial inflammatory response and is lost in brain ageing in an IFN-I-dependent manner. *Nat. Commun.* 8:717. doi: 10.1038/s41467-017-00769-0

del Rio-Hortega, P. (1932). "Microglia" in *Cytology & Cellular Pathology of the nervous system*. ed. W. Penfield (New York, NY: Paul B. Hoeber, Inc.), 483–534.

DeMaagd, G., and Philip, A. (2015). Parkinson's disease and its management: part 1: disease entity, risk factors, pathophysiology, clinical presentation, and diagnosis. *PT* 40, 504–532.

Ding, X., Wang, J., Huang, M., Chen, Z., Liu, J., Zhang, Q., et al. (2021). Loss of microglial SIRPα promotes synaptic pruning in preclinical models of neurodegeneration. *Nat. Commun.* 12:2030. doi: 10.1038/s41467-021-22301-1

Dionísio, P. E. A., Oliveira, S. R., Amaral, J. S. J. D., and Rodrigues, C. M. P. (2019). Loss of microglial Parkin inhibits necroptosis and contributes to Neuroinflammation. *Mol. Neurobiol.* 56, 2990–3004. doi: 10.1007/s12035-018-1264-9

Dragunow, M., Greenwood, J. M., Cameron, R. E., Narayan, P. J., O'Carroll, S. J., Pearson, A. G., et al. (2006). Valproic acid induces caspase 3-mediated apoptosis in microglial cells. *Neuroscience* 140, 1149–1156. doi: 10.1016/j.neuroscience.2006.02.065

Drechsel, D. A., and Patel, M. (2008). Role of reactive oxygen species in the neurotoxicity of environmental agents implicated in Parkinson's disease. *Free Radic. Biol. Med.* 44, 1873–1886. doi: 10.1016/j.freeradbiomed.2008.02.008

Durham, B. S., Grigg, R., and Wood, I. C. (2017). Inhibition of histone deacetylase 1 or 2 reduces induced cytokine expression in microglia through a protein synthesis independent mechanism. *J. Neurochem.* 143, 214–224. doi: 10.1111/jnc.14144

Ferrari, R., Kapogiannis, D., Huey, E. D., and Momeni, P. (2011). FTD and ALS: a tale of two diseases. *Curr. Alzheimer Res.* 8, 273–294. doi: 10.2174/156720511795563700

Fiebich, B. L., Batista, C., Saliba, S. W., Yousif, N. M., and de Oliveira, A. (2018). Role of microglia TLRs in neurodegeneration. *Front. Cell. Neurosci.* 12:329. doi: 10.3389/fncel.2018.00329

Filipello, F., Morini, R., Corradini, I., Zerbi, V., Canzi, A., Michalski, B., et al. (2018). The microglial innate immune receptor TREM2 is required for synapse elimination and Normal brain connectivity. *Immunity* 48, 979–991.e8. doi: 10.1016/j.immuni.2018.04.016

Frank-Cannon, T. C., Tran, T., Ruhn, K. A., Martinez, T. N., Hong, J., Marvin, M., et al. (2008). Parkin deficiency increases vulnerability to inflammation-related nigral degeneration. *Journal of Neuroscience* 28, 10825–10834. doi: 10.1523/JNEUROSCI.3001-08.2008

Frakes, A. E., Ferraiuolo, L., Haidet-Phillips, A. M., Schmelzer, L., Braun, L., Miranda, C. J., et al. (2014). Microglia induce motor neuron death via the classical NF-κB pathway in amyotrophic lateral sclerosis. *Neuron* 81, 1009–1023. doi: 10.1016/j.neuron.2014.01.013

Franke, H., Verkhratsky, A., Burnstock, G., and Illes, P. (2012). Pathophysiology of astroglial purinergic signalling. *Purinergic Signal* 8, 629–657. doi: 10.1007/s11302-012-9300-0

Fu, R., Shen, Q., Xu, P., Luo, J. J., and Tang, Y. (2014). Phagocytosis of microglia in the central nervous system diseases. *Mol. Neurobiol.* 49, 1422–1434. doi: 10.1007/s12035-013-8620-6

Fu, S. P., Wang, J. F., Xue, W. J., Liu, H. M., Liu, B. R., Zeng, Y. L., et al. (2015). Anti-inflammatory effects of BHBA in both in vivo and in vitro Parkinson's disease models are mediated by GPR109A-dependent mechanisms. *J. Neuroinflammation* 12:9. doi: 10.1186/s12974-014-0230-3

Galatro, T. F., Holtman, I. R., Lerario, A. M., Vainchtein, I. D., Brouwer, N., Sola, P. R., et al. (2017). Transcriptomic analysis of purified human cortical microglia reveals age-associated changes. *Nat. Neurosci.* 20, 1162–1171. doi: 10.1038/nn.4597

García-Revilla, J., Boza-Serrano, A., Espinosa-Oliva, A. M., Soto, M. S., Deierborg, T., Ruiz, R., et al. (2022). Galectin-3, a rising star in modulating microglia activation under conditions of neurodegeneration. *Cell Death Dis.* 13:628. doi: 10.1038/s41419-022-05058-3

Ginhoux, F., Greter, M., Leboeuf, M., Nandi, S., See, P., Gokhan, S., et al. (2010). Fate mapping analysis reveals that adult microglia derive from primitive macrophages. *Science* 330, 841–845. doi: 10.1126/science.1194637

Ginhoux, F., and Guilliams, M. (2018). Editorial for cellular immunology special issue on "tissue macrophages". *Cell. Immunol.* 330, 1–4. doi: 10.1016/j.cellimm.2018.07.010

Ginhoux, F., Lim, S., Hoeffel, G., Low, D., and Huber, T. (2013). Origin and differentiation of microglia. *Front. Cell. Neurosci.* 7:45. doi: 10.3389/fncel.2013.00045

Goines, P. E., and Ashwood, P. (2013). Cytokine dysregulation in autism spectrum disorders (ASD): possible role of the environment. *Neurotoxicol. Teratol.* 36, 67–81. doi: 10.1016/j.ntt.2012.07.006

Goldenberg, M. M. (2012). Multiple sclerosis review. *PT* 37, 175–184. PMID: 22605909

Green, K. N., Crapser, J. D., and Hohsfield, L. A. (2020). To kill a microglia: a case for CSF1R inhibitors. *Trends Immunol.* 41, 771–784. doi: 10.1016/j.it.2020.07.001

Guo, M., Hao, Y., Feng, Y., Li, H., Mao, Y., Dong, Q., et al. (2021). Microglial exosomes in neurodegenerative disease. *Front. Mol. Neurosci.* 14:630808. doi: 10.3389/fnmol.2021.630808

Han, B., Jiang, W., Cui, P., Zheng, K., Dang, C., Wang, J., et al. (2021). Microglial PGC-1α protects against ischemic brain injury by suppressing neuroinflammation. *Genome Med.* 13:47. doi: 10.1186/s13073-021-00863-5

Hanger, B., Couch, A., Rajendran, L., Srivastava, D. P., and Vernon, A. C. (2020). Emerging developments in human induced pluripotent stem cell-derived microglia: implications for modelling psychiatric disorders with a neurodevelopmental origin. *Front. Psych.* 11:789. doi: 10.3389/fpsyt.2020.00789

Hansen, D. V., Hanson, J. E., and Sheng, M. (2018). Microglia in Alzheimer's disease. *J. Cell Biol.* 217, 459–472. doi: 10.1083/jcb.201709069

Harhaj, E. W., and Dixit, V. M. (2012). Regulation of NF-κB by deubiquitinases. *Immunol. Rev.* 246, 107–124. doi: 10.1111/j.1600-065X.2012.01100.x

Hazrati, A., Soudi, S., Malekpour, K., Mahmoudi, M., Rahimi, A., Hashemi, S. M., et al. (2022). Immune cells-derived exosomes function as a double-edged sword: role in disease progression and their therapeutic applications. *Biomarker Res.* 10:30. doi: 10.1186/s40364-022-00374-4

Hickman, S., Izzy, S., Sen, P., Morsett, L., and El Khoury, J. (2018). Microglia in neurodegeneration. *Nat. Neurosci.* 21, 1359–1369. doi: 10.1038/s41593-018-0242-x

Hoffmann, C. J., Harms, U., Rex, A., Szulzewsky, F., Wolf, S. A., Grittner, U., et al. (2015). Vascular signal transducer and activator of transcription-3 promotes angiogenesis and neuroplasticity long-term after stroke. *Circulation* 131, 1772–1782. doi: 10.1161/CIRCULATIONAHA.114.013003

Hong, S., Beja-Glasser, V. F., Nfonoyim, B. M., Frouin, A., Li, S., Ramakrishnan, S., et al. (2016). Complement and microglia mediate early synapse loss in Alzheimer mouse models. *Science* 352, 712–716. doi: 10.1126/science.aad8373

Horiuchi, M., Wakayama, K., Itoh, A., Kawai, K., Pleasure, D., Ozato, K., et al. (2012). Interferon regulatory factor 8/interferon consensus sequence binding protein is a critical transcription factor for the physiological phenotype of microglia. *J. Neuroinflammation* 9:227. doi: 10.1186/1742-2094-9-227

Huang, K. L., Marcora, E., Pimenova, A. A., Di Narzo, A. F., Kapoor, M., Jin, S. C., et al. (2017). A common haplotype lowers PU.1 expression in myeloid cells and delays onset of Alzheimer's disease. *Nat. Neurosci.* 20, 1052–1061. doi: 10.1038/nn.4587

Hung, J., Chansard, M., Ousman, S. S., Nguyen, M. D., and Colicos, M. A. (2010). Activation of microglia by neuronal activity: results from a new in vitro paradigm based on neuronal-silicon interfacing technology. *Brain Behav. Immun.* 24, 31–40. doi: 10.1016/j.bbi.2009.06.150

Illes, P., Rubini, P., Ulrich, H., Zhao, Y., and Tang, Y. (2020). Regulation of microglial functions by purinergic mechanisms in the healthy and diseased CNS. *Cells* 9:1108. doi: 10.3390/cells9051108

Inoue, K. (2017). Purinergic signaling in microglia in the pathogenesis of neuropathic pain. Proceedings of the Japan academy. *Proc. Jpn. Acad. Ser. B Phys. Biol. Sci.* 93, 174–182. doi: 10.2183/pjab.93.011

Iwasaki, H., Somoza, C., Shigematsu, H., Duprez, E. A., Iwasaki-Arai, J., Mizuno, S., et al. (2005). Distinctive and indispensable roles of PU.1 in maintenance of hematopoietic stem cells and their differentiation. *Blood* 106, 1590–1600. doi: 10.1182/blood-2005-03-0860

Jin, L. W., Horiuchi, M., Wulff, H., Liu, X. B., Cortopassi, G. A., Erickson, J. D., et al. (2015). Dysregulation of glutamine transporter SNAT1 in Rett syndrome microglia: a mechanism for mitochondrial dysfunction and neurotoxicity. *J. Neurosci. Off. J. Soc. Neurosci.* 35, 2516–2529. doi: 10.1523/JNEUROSCI.2778-14.2015

Kahanovitch, U., Patterson, K. C., Hernandez, R., and Olsen, M. L. (2019). Glial dysfunction in MeCP2 deficiency models: implications for Rett syndrome. *Int. J. Mol. Sci.* 20:3813. doi: 10.3390/ijms20153813

Kalafatakis, I., and Karagogeos, D. (2021). Oligodendrocytes and microglia: key players in myelin development. *Biomol. Ther.* 11:1058. doi: 10.3390/biom11071058

Kalluri, R., and LeBleu, V. S. (2020). The biology, function, and biomedical applications of exosomes. *Science* 367:eaau6977. doi: 10.1126/science.aau6977

Kaminska, B., Mota, M., and Pizzi, M. (2016). Signal transduction and epigenetic mechanisms in the control of microglia activation during neuroinflammation. *Biochim. Biophys. Acta* 1862, 339–351. doi: 10.1016/j.bbadis.2015.10.026

Kang, R., Gamdzyk, M., Lenahan, C., Tang, J., Tan, S., and Zhang, J. H. (2020). The dual role of microglia in blood-brain barrier dysfunction after stroke. *Curr. Neuropharmacol.* 18, 1237–1249. doi: 10.2174/1570159X18666200529150907

Kawamura, N., Katsuura, G., Yamada-Goto, N., Novianti, E., Inui, A., and Asakawa, A. (2020). Reduced brain fractalkine-CX3CR1 signaling is involved in the impaired cognition of streptozotocin-treated mice. *IBRO Rep.* 9, 233–240. doi: 10.1016/j.ibror.2020.09.002

Kierdorf, K., and Prinz, M. (2013). Factors regulating microglia activation. *Front. Cell. Neurosci.* 7:44. doi: 10.3389/fncel.2013.00044

Kim, H. J., Cho, M. H., Shim, W. H., Kim, J. K., Jeon, E. Y., Kim, D. H., et al. (2017). Deficient autophagy in microglia impairs synaptic pruning and causes social behavioral defects. *Mol. Psychiatry* 22, 1576–1584. doi: 10.1038/mp.2016.103

Klineova, S., and Lublin, F. D. (2018). Clinical course of multiple sclerosis. *Cold Spring Harb. Perspect. Med.* 8:a028928. doi: 10.1101/cshperspect.a028928

Komorowska-Müller, J. A., and Schmöle, A. C. (2021). CB2 receptor in microglia: the Guardian of self-control. *Int. J. Mol. Sci.* 22:19. doi: 10.3390/ijms22010019

Konishi, H., and Kiyama, H. (2018). Microglial TREM2/DAP12 signaling: a double-edged sword in neural diseases. *Front. Cell. Neurosci.* 12:206. doi: 10.3389/fncel.2018.00206

Konishi, H., Kobayashi, M., Kunisawa, T., Imai, K., Sayo, A., Malissen, B., et al. (2017). Siglec-H is a microglia-specific marker that discriminates microglia from CNS-associated macrophages and CNS-infiltrating monocytes. *Glia* 65, 1927–1943. doi: 10.1002/glia.23204

Korzhevskii, D. E., and Kirik, O. V. (2016). Brain microglia and microglial markers. *Neurosci. Behav. Physiol.* 46, 284–290. doi: 10.1007/s11055-016-0231-z

Koshida, R., Oishi, H., Hamada, M., and Takahashi, S. (2015). MafB antagonizes phenotypic alteration induced by GM-CSF in microglia. *Biochem. Biophys. Res. Commun.* 463, 109–115. doi: 10.1016/j.bbrc.2015.05.036

Krasemann, S., Madore, C., Cialic, R., Baufeld, C., Calcagno, N., El Fatimy, R., et al. (2017). The TREM2-APOE pathway drives the transcriptional phenotype of dysfunctional microglia in neurodegenerative diseases. *Immunity* 47, 566–581.e9. doi: 10.1016/j.immuni.2017.08.008

Laribee, R. N., and Klemsz, M. J. (2005). Histone H4 HDAC activity is necessary for expression of the PU.1 gene. *Biochim. Biophys. Acta* 1730, 226–234. doi: 10.1016/j.bbaexp.2005.08.003

Lassmann, H. (2018). Multiple sclerosis pathology. *Cold Spring Harb. Perspect. Med.* 8:a028936. doi: 10.1101/cshperspect.a028936

Le, W., Wu, J., and Tang, Y. (2016). Protective microglia and their regulation in Parkinson's disease. *Front. Mol. Neurosci.* 9:89. doi: 10.3389/fnmol.2016.00089

Lehrman, E. K., Wilton, D. K., Litvina, E. Y., Welsh, C. A., Chang, S. T., Frouin, A., et al. (2018). CD47 protects synapses from excess microglia-mediated pruning during development. *Neuron* 100, 120–134.e6. doi: 10.1016/j.neuron.2018.09.017

Li, D., Chen, M., Meng, T., and Fei, J. (2020). Hippocampal microglial activation triggers a neurotoxic-specific astrocyte response and mediates etomidate-induced long-term synaptic inhibition. *J. Neuroinflammation* 17:109. doi: 10.1186/s12974-020-01799-0

Li, C., Chen, T., Zhou, H., Zhang, C., Feng, Y., Tang, F., et al. (2018). Schisantherin a attenuates Neuroinflammation in activated microglia: role of Nrf2 activation through ERK phosphorylation. *Cell. Physiol. Biochem.* 47, 1769–1784. doi: 10.1159/000491059

Li, K. L., Huang, H. Y., Ren, H., and Yang, X. L. (2022). Role of exosomes in the pathogenesis of inflammation in Parkinson's disease. *Neural Regen. Res.* 17, 1898–1906. doi: 10.4103/1673-5374.335143

Li, Y., Liu, D. X., Li, M. Y., Qin, X. X., Fang, W. G., Zhao, W. D., et al. (2014). Ephrin-A3 and ephrin-A4 contribute to microglia-induced angiogenesis in brain endothelial cells. *Anat. Rec.* 297, 1908–1918. doi: 10.1002/ar.22998

Lian, H., Yang, L., Cole, A., Sun, L., Chiang, A. C., Fowler, S. W., et al. (2015). NFκB-activated astroglial release of complement C3 compromises neuronal morphology and function associated with Alzheimer's disease. *Neuron* 85, 101–115. doi: 10.1016/j.neuron.2014.11.018

Litvinchuk, A., Wan, Y. W., Swartzlander, D. B., Chen, F., Cole, A., Propson, N. E., et al. (2018). Complement C3aR inactivation attenuates tau pathology and reverses an immune network deregulated in Tauopathy models and Alzheimer's disease. *Neuron* 100, 1337–1353.e5. doi: 10.1016/j.neuron.2018.10.031

Liu, W., Bai, X., Zhang, A., Huang, J., Xu, S., and Zhang, J. (2019). Role of exosomes in central nervous system diseases. *Front. Mol. Neurosci.* 12:240. doi: 10.3389/fnmol.2019.00240

Liu, J., and Wang, F. (2017). Role of Neuroinflammation in amyotrophic lateral sclerosis: cellular mechanisms and therapeutic implications. *Front. Immunol.* 8:1005. doi: 10.3389/fimmu.2017.01005

Liu, Y., Wu, X. M., Luo, Q. Q., Huang, S., Yang, Q. W., Wang, F. X., et al. (2015). CX3CL1/CX3CR1-mediated microglia activation plays a detrimental role in ischemic mice brain via p38MAPK/PKC pathway. *Journal of Cerebral Blood Flow and Metabolism* 35, 1623–1631. doi: 10.1038/jcbfm.2015.97

London, A., Cohen, M., and Schwartz, M. (2013). Microglia and monocyte-derived macrophages: functionally distinct populations that act in concert in CNS plasticity and repair. *Front. Cell. Neurosci.* 7:34. doi: 10.3389/fncel.2013.00034

Lopez-Atalaya, J. P., Askew, K. E., Sierra, A., and Gomez-Nicola, D. (2018). Development and maintenance of the brain's immune toolkit: microglia and non-parenchymal brain macrophages. *Dev. Neurobiol.* 78, 561–579. doi: 10.1002/dneu.22545

Lopez-Lopez, A., Gamez, J., Syriani, E., Morales, M., Salvado, M., Rodríguez, M. J., et al. (2014). CX3CR1 is a modifying gene of survival and progression in amyotrophic lateral sclerosis. *PLoS One* 9:e96528. doi: 10.1371/journal.pone.0096528

Lou, N., Takano, T., Pei, Y., Xavier, A. L., Goldman, S. A., and Nedergaard, M. (2016). Purinergic receptor P2RY12-dependent microglial closure of the injured blood-brain barrier. *Proc. Natl. Acad. Sci. U. S. A.* 113, 1074–1079. doi: 10.1073/pnas.1520398113

Lull, M. E., and Block, M. L. (2010). Microglial activation and chronic neurodegeneration. *Neurotherapeutics* 7, 354–365. doi: 10.1016/j.nurt.2010.05.014

Luo, C., Jian, C., Liao, Y., Huang, Q., Wu, Y., Liu, X., et al. (2017). The role of microglia in multiple sclerosis. *Neuropsychiatr. Dis. Treat.* 13, 1661–1667. doi: 10.2147/NDT.S140634

Lyons, A., Downer, E. J., Crotty, S., Nolan, Y. M., Mills, K. H., and Lynch, M. A. (2007). CD200 ligand receptor interaction modulates microglial activation in vivo and in vitro: a role for IL-4. *J. Neurosci. Off. J. Soc. Neurosci.* 27, 8309–8313. doi: 10.1523/JNEUROSCI.1781-07.2007

Maggi, L., Trettel, F., Scianni, M., Bertollini, C., Eusebi, F., Fredholm, B. B., et al. (2009). LTP impairment by fractalkine/CX3CL1 in mouse hippocampus is mediated through the activity of adenosine receptor type 3 (A3R). *J. Neuroimmunol.* 215, 36–42. doi: 10.1016/j.jneuroim.2009.07.016

Mallya, A. P., and Deutch, A. Y. (2018). (micro)glia as effectors of cortical volume loss in schizophrenia. *Schizophr. Bull.* 44, 948–957. doi: 10.1093/schbul/sby088

Mancuso, R., Fryatt, G., Cleal, M., Obst, J., Pipi, E., Monzón-Sandoval, J., et al. (2019). CSF1R inhibitor JNJ-40346527 attenuates microglial proliferation and neurodegeneration in P301S mice. *Brain J. Neurol.* 142, 3243–3264. doi: 10.1093/brain/awz241

Marogianni, C., Sokratous, M., Dardiotis, E., Hadjigeorgiou, G. M., Bogdanos, D., and Xiromerisiou, G. (2020). Neurodegeneration and inflammation-an interesting interplay in Parkinson's disease. *Int. J. Mol. Sci.* 21:8421. doi: 10.3390/ijms21228421

Marrali, G., Casale, F., Salamone, P., Fuda, G., Caorsi, C., Amoroso, A., et al. (2014). NADPH oxidase (NOX2) activity is a modifier of survival in ALS. *J. Neurol.* 261, 2178–2183. doi: 10.1007/s00415-014-7470-0

Masuda, T., Nishimoto, N., Tomiyama, D., Matsuda, T., Tozaki-Saitoh, H., Tamura, T., et al. (2014). IRF8 is a transcriptional determinant for microglial motility. *Purinergic Signal* 10, 515–521. doi: 10.1007/s11302-014-9413-8

Masuda, T., Tsuda, M., Yoshinaga, R., Tozaki-Saitoh, H., Ozato, K., Tamura, T., et al. (2012). IRF8 is a critical transcription factor for transforming microglia into a reactive phenotype. *Cell Rep.* 1, 334–340. doi: 10.1016/j.celrep.2012.02.014

Matejuk, A., and Ransohoff, R. M. (2020). Crosstalk between astrocytes and microglia: an overview. *Front. Immunol.* 11:1416. doi: 10.3389/fimmu.2020.01416

Matejuk, A., Vandenbark, A. A., and Offner, H. (2021). Cross-talk of the CNS with immune cells and functions in health and disease. *Front. Neurol.* 12:672455. doi: 10.3389/fneur.2021.672455

Maurya, S. K., Bhattacharya, N., Mishra, S., Bhattacharya, A., Banerjee, P., Senapati, S., et al. (2021). Microglia specific drug targeting using natural products for the regulation of redox imbalance in neurodegeneration. *Front. Pharmacol.* 12:654489. doi: 10.3389/fphar.2021.654489

McGrath, K. E., Frame, J. M., Fegan, K. H., Bowen, J. R., Conway, S. J., Catherman, S. C., et al. (2015). Distinct sources of hematopoietic progenitors emerge before HSCs and provide functional blood cells in the mammalian embryo. *Cell Rep.* 11, 1892–1904. doi: 10.1016/j.celrep.2015.05.036

McKercher, S. R., Torbett, B. E., Anderson, K. L., Henkel, G. W., Vestal, D. J., Baribault, H., et al. (1996). Targeted disruption of the PU.1 gene results in multiple hematopoietic abnormalities. *EMBO J.* 15, 5647–5658. doi: 10.1002/j.1460-2075.1996.tb00949.x

Mecca, C., Giambanco, I., Donato, R., and Arcuri, C. (2018). Microglia and aging: the role of the TREM2-DAP12 and CX3CL1-CX3CR1 axes. *Int. J. Mol. Sci.* 19:318. doi: 10.3390/ijms19010318

Menassa, D. A., and Gomez-Nicola, D. (2018). Microglial dynamics during human brain development. *Front. Immunol.* 9:1014. doi: 10.3389/fimmu.2018.01014

Meredith, G. E., and Rademacher, D. J. (2011). MPTP mouse models of Parkinson's disease: an update. *J. Parkinsons Dis.* 1, 19–33. doi: 10.3233/JPD-2011-11023

Miller, B. A., Crum, J. M., Tovar, C. A., Ferguson, A. R., Bresnahan, J. C., and Beattie, M. S. (2007). Developmental stage of oligodendrocytes determines their response to activated microglia in vitro. *J. Neuroinflammation* 4:28. doi: 10.1186/1742-2094-4-28

Mizuno, T. (2012). The biphasic role of microglia in Alzheimer's disease. *Int. J. Alzheimers Dis.* 2012:737846. doi: 10.1155/2012/737846

Monier, A., Adle-Biassette, H., Delezoide, A. L., Evrard, P., Gressens, P., and Verney, C. (2007). Entry and distribution of microglial cells in human embryonic and fetal cerebral cortex. *J. Neuropathol. Exp. Neurol.* 66, 372–382. doi: 10.1097/nen.0b013e3180517b46

More, S. V., and Choi, D. K. (2016). Emerging preclinical pharmacological targets for Parkinson's disease. *Oncotarget* 7, 29835–29863. doi: 10.18632/oncotarget.8104

Morgan, J. T., Chana, G., Pardo, C. A., Achim, C., Semendeferi, K., Buckwalter, J., et al. (2010). Microglial activation and increased microglial density observed in the dorsolateral prefrontal cortex in autism. *Biol. Psychiatry* 68, 368–376. doi: 10.1016/j.biopsych.2010.05.024

Morin-Brureau, M., Milior, G., Royer, J., Chali, F., Le Duigou, C., Savary, E., et al. (2018). Microglial phenotypes in the human epileptic temporal lobe. *Brain J. Neurol.* 141, 3343–3360. doi: 10.1093/brain/awy276

Mukherjee, S., Klaus, C., Pricop-Jeckstadt, M., Miller, J. A., and Struebing, F. L. (2019). A microglial signature directing human aging and neurodegeneration-related gene networks. *Front. Neurosci.* 13:2. doi: 10.3389/fnins.2019.00002

Muñoz, E. M. (2022). Microglia in circumventricular organs: the pineal gland example. *ASN Neuro* 14:175909142211356. doi: 10.1177/17590914221135697

Murphy, M. P., and LeVine, H. (2010). Alzheimer's disease and the amyloid-beta peptide. *J. Alzheimers Dis.* 19, 311–323. doi: 10.3233/JAD-2010-1221

Muzio, L., Viotti, A., and Martino, G. (2021). Microglia in Neuroinflammation and neurodegeneration: from understanding to therapy. *Front. Neurosci.* 15:742065. doi: 10.3389/fnins.2021.742065

Nayak, D., Roth, T. L., and McGavern, D. B. (2014). Microglia development and function. *Annu. Rev. Immunol.* 32, 367–402. doi: 10.1146/annurev-immunol-032713-120240

Needleman, L. A., and McAllister, A. K. (2012). The major histocompatibility complex and autism spectrum disorder. *Dev. Neurobiol.* 72, 1288–1301. doi: 10.1002/dneu.22046

Neidert, N., von Ehr, A., Zöller, T., and Spittau, B. (2018). Microglia-specific expression of Olfml3 is directly regulated by transforming growth factor β1-induced Smad2 signaling. *Front. Immunol.* 9:1728. doi: 10.3389/fimmu.2018.01728

Neuner, S. M., Tcw, J., and Goate, A. M. (2020). Genetic architecture of Alzheimer's disease. *Neurobiol. Dis.* 143:104976. doi: 10.1016/j.nbd.2020.104976

Nguyen, P. T., Dorman, L. C., Pan, S., Vainchtein, I. D., Han, R. T., Nakao-Inoue, H., et al. (2020). Microglial remodeling of the extracellular matrix promotes synapse plasticity. *Cell* 182, 388–403.e15. doi: 10.1016/j.cell.2020.05.050

Nijland, P. G., Witte, M. E., van het Hof, B., van der Pol, S., Bauer, J., Lassmann, H., et al. (2014). Astroglial PGC-1alpha increases mitochondrial antioxidant capacity and suppresses inflammation: implications for multiple sclerosis. *Acta Neuropathol. Commun.* 2:170. doi: 10.1186/s40478-014-0170-2

Ohsawa, K., Imai, Y., Sasaki, Y., and Kohsaka, S. (2004). Microglia/macrophage-specific protein Iba1 binds to fimbrin and enhances its actin-bundling activity. *J. Neurochem.* 88, 844–856. doi: 10.1046/j.1471-4159.2003.02213.x

Olah, M., Patrick, E., Villani, A. C., Xu, J., White, C. C., Ryan, K. J., et al. (2018). A transcriptomic atlas of aged human microglia. *Nat. Commun.* 9:539. doi: 10.1038/s41467-018-02926-5

Olmedillas Del Moral, M., Asavapanumas, N., Uzcátegui, N. L., and Garaschuk, O. (2019). Healthy brain aging modifies microglial calcium signaling in vivo. *Int. J. Mol. Sci.* 20:589. doi: 10.3390/ijms20030589

Orihuela, R., McPherson, C. A., and Harry, G. J. (2016). Microglial M1/M2 polarization and metabolic states. *Br. J. Pharmacol.* 173, 649–665. doi: 10.1111/bph.13139

Panes, J. D., Wendt, A., Ramirez-Molina, O., Castro, P. A., and Fuentealba, J. (2022). Deciphering the role of PGC-1α in neurological disorders: from mitochondrial dysfunction to synaptic failure. *Neural Regen. Res.* 17, 237–245. doi: 10.4103/1673-5374.317957

Paolicelli, R. C., Bisht, K., and Tremblay, M. È. (2014). Fractalkine regulation of microglial physiology and consequences on the brain and behavior. *Front. Cell. Neurosci.* 8:129. doi: 10.3389/fncel.2014.00129

Paolicelli, R. C., Bolasco, G., Pagani, F., Maggi, L., Scianni, M., Panzanelli, P., et al. (2011). Synaptic pruning by microglia is necessary for normal brain development. *Science* 333, 1456–1458. doi: 10.1126/science.1202529

Paolicelli, R. C., Sierra, A., Stevens, B., Tremblay, M. E., Aguzzi, A., Ajami, B., et al. (2022). Microglia states and nomenclature: A field at its crossroads. *Neuron* 110, 3458–3483. doi: 10.1016/j.neuron.2022.10.020

Parkhurst, C. N., Yang, G., Ninan, I., Savas, J. N., Yates, J. R. 3rd, Lafaille, J. J., et al. (2013). Microglia promote learning-dependent synapse formation through brain-derived neurotrophic factor. *Cell* 155, 1596–1609. doi: 10.1016/j.cell.2013.11.030

Pascual, O., Ben Achour, S., Rostaing, P., Triller, A., and Bessis, A. (2012). Microglia activation triggers astrocyte-mediated modulation of excitatory neurotransmission. *Proc. Natl. Acad. Sci. U. S. A.* 109, E197–E205. doi: 10.1073/pnas.1111098109

Pascual, M., Calvo-Rodriguez, M., Núñez, L., Villalobos, C., Ureña, J., and Guerri, C. (2021). Toll-like receptors in neuroinflammation, neurodegeneration, and alcohol-induced brain damage. *IUBMB Life* 73, 900–915. doi: 10.1002/iub.2510

Pawelec, P., Ziemka-Nalecz, M., Sypecka, J., and Zalewska, T. (2020). The impact of the CX3CL1/CX3CR1 Axis in neurological disorders. *Cells* 9:2277. doi: 10.3390/cells9102277

Peferoen, L., Kipp, M., van der Valk, P., van Noort, J. M., and Amor, S. (2014). Oligodendrocyte-microglia cross-talk in the central nervous system. *Immunology* 141, 302–313. doi: 10.1111/imm.12163

Perdiguero, E. G., and Geissmann, F. (2016). The development and maintenance of resident macrophages. *Nat. Immunol.* 17, 2–8. doi: 10.1038/ni.3341

Petralla, S., De Chirico, F., Miti, A., Tartagni, O., Massenzio, F., Poeta, E., et al. (2021). Epigenetics and communication mechanisms in microglia activation with a view on technological approaches. *Biomol. Ther.* 11:306. doi: 10.3390/biom11020306

Piccinin, E., Sardanelli, A. M., Seibel, P., Moschetta, A., Cocco, T., and Villani, G. (2021). PGC-1s in the spotlight with Parkinson's disease. *Int. J. Mol. Sci.* 22:3487. doi: 10.3390/ijms22073487

Pimenova, A. A., Marcora, E., and Goate, A. M. (2017). A tale of two genes: microglial Apoe and Trem2. *Immunity* 47, 398–400. doi: 10.1016/j.immuni.2017.08.015

Pluvinage, J. V., Haney, M. S., Smith, B., Sun, J., Iram, T., Bonanno, L., et al. (2019). CD22 blockade restores homeostatic microglial phagocytosis in ageing brains. *Nature* 568, 187–192. doi: 10.1038/s41586-019-1088-4

Ponomarev, E. D., Veremeyko, T., Barteneva, N., Krichevsky, A. M., and Weiner, H. L. (2011). MicroRNA-124 promotes microglia quiescence and suppresses EAE by deactivating macrophages via the C/EBP-α-PU.1 pathway. *Nat. Med.* 17, 64–70. doi: 10.1038/nm.2266

Popescu, B. F., Pirko, I., and Lucchinetti, C. F. (2013). Pathology of multiple sclerosis: where do we stand? *Continuum* 19, 901–921. doi: 10.1212/01.CON.0000433291.23091.65

Power, J. H., Barnes, O. L., and Chegini, F. (2017). Lewy bodies and the mechanisms of neuronal cell death in Parkinson's disease and dementia with Lewy bodies. *Brain Pathol.* 27, 3–12. doi: 10.1111/bpa.12344

Puntambekar, S. S., Moutinho, M., Lin, P. B., Jadhav, V., Tumbleson-Brink, D., Balaji, A., et al. (2022). CX3CR1 deficiency aggravates amyloid driven neuronal pathology and cognitive decline in Alzheimer's disease. *Molecular neurodegeneration* 17:47. doi: 10.1186/s13024-022-00545-9

Rangaraju, S., Dammer, E. B., Raza, S. A., Rathakrishnan, P., Xiao, H., Gao, T., et al. (2018). Identification and therapeutic modulation of a pro-inflammatory subset of disease-associated-microglia in Alzheimer's disease. *Mol. Neurodegener.* 13:24. doi: 10.1186/s13024-018-0254-8

Ren, P., Xiao, B., Wang, L. P., Li, Y. S., Jin, H., and Jin, Q. H. (2022). Nitric oxide impairs spatial learning and memory in a rat model of Alzheimer's disease via disturbance of glutamate response in the hippocampal dentate gyrus during spatial learning. *Behav. Brain Res.* 422:113750. doi: 10.1016/j.bbr.2022.113750

Rezaie, P., Dean, A., Male, D., and Ulfig, N. (2005). Microglia in the cerebral wall of the human telencephalon at second trimester. *Cereb. Cortex* 15, 938–949. doi: 10.1093/cercor/bhh194

Rezaie, P., and Male, D. (1999). Colonisation of the developing human brain and spinal cord by microglia: a review. *Microsc. Res. Tech.* 45, 359–382. doi: 10.1002/(SICI)1097-0029(19990615)45:6<359::AID-JEMT4>3.0.CO;2-D

Ricci, G., Volpi, L., Pasquali, L., Petrozzi, L., and Siciliano, G. (2009). Astrocyte-neuron interactions in neurological disorders. *J. Biol. Phys.* 35, 317–336. doi: 10.1007/s10867-009-9157-9

Rigato, C., Buckinx, R., Le-Corronc, H., Rigo, J. M., and Legendre, P. (2011). Pattern of invasion of the embryonic mouse spinal cord by microglial cells at the time of the onset of functional neuronal networks. *Glia* 59, 675–695. doi: 10.1002/glia.21140

Robinson, A. P., Harp, C. T., Noronha, A., and Miller, S. D. (2014). The experimental autoimmune encephalomyelitis (EAE) model of MS: utility for understanding disease pathophysiology and treatment. *Handb. Clin. Neurol.* 122, 173–189. doi: 10.1016/B978-0-444-52001-2.00008-X

Rodríguez-Navarro, J. A., Casarejos, M. J., Menéndez, J., Solano, R. M., Rodal, I., Gómez, A., et al. (2007). Mortality, oxidative stress and tau accumulation during ageing in parkin null mice. *Journal of Neurochemistry* 103, 98–114. doi: 10.1111/j.1471-4159.2007.04762.x

Rogers, J. T., Morganti, J. M., Bachstetter, A. D., Hudson, C. E., Peters, M. M., Grimmig, B. A., et al. (2011). CX3CR1 deficiency leads to impairment of hippocampal cognitive function and synaptic plasticity. *J. Neurosci. Off. J. Soc. Neurosci.* 31, 16241–16250. doi: 10.1523/JNEUROSCI.3667-11.2011

Ronzano, R., Roux, T., Thetiot, M., Aigrot, M. S., Richard, L., Lejeune, F. X., et al. (2021). Microglia-neuron interaction at nodes of Ranvier depends on neuronal activity through potassium release and contributes to remyelination. *Nat. Commun.* 12:5219. doi: 10.1038/s41467-021-25486-7

Rustenhoven, J., Smith, A. M., Smyth, L. C., Jansson, D., Scotter, E. L., Swanson, M., et al. (2018). PU.1 regulates Alzheimer's disease-associated genes in primary human microglia. *Mol. Neurodegener.* 13:44. doi: 10.1186/s13024-018-0277-1

Sakate, R., Nishiyama, M., Fukuda, Y., Kitaoka, S., and Furuyashiki, T. (2022). The transcription factor Hhex regulates inflammation-related genes in microglia. *J. Pharmacol. Sci.* 149, 166–171. doi: 10.1016/j.jphs.2022.04.006

Sarlus, H., and Heneka, M. T. (2017). Microglia in Alzheimer's disease. *J. Clin. Invest.* 127, 3240–3249. doi: 10.1172/JCI90606

Satoh, J., Asahina, N., Kitano, S., and Kino, Y. (2014). A comprehensive profile of ChIP-Seq-based PU.1/Spi1 target genes in microglia. *Gene Regulat. Syst. Biol.* 8, GRSB.S19711–GRSB.S19139. doi: 10.4137/GRSB.S19711

Scipioni, L., Ciaramellano, F., Carnicelli, V., Leuti, A., Lizzi, A. R., De Dominicis, N., et al. (2022). Microglial endocannabinoid Signalling in AD. *Cells* 11:1237. doi: 10.3390/cells11071237

Scott, H. (2017). Extracellular microRNAs as messengers in the central and peripheral nervous system. *Neuronal Signal.* 1:NS20170112. doi: 10.1042/NS20170112

Skaper, S. D., Facci, L., Zusso, M., and Giusti, P. (2018). An inflammation-centric view of neurological disease: beyond the neuron. *Front. Cell. Neurosci.* 12:72. doi: 10.3389/fncel.2018.00072

Smith, A. M., Gibbons, H. M., Oldfield, R. L., Bergin, P. M., Mee, E. W., Faull, R. L., et al. (2013). The transcription factor PU.1 is critical for viability and function of human brain microglia. *Glia* 61, 929–942. doi: 10.1002/glia.22486

Sousa, C., Biber, K., and Michelucci, A. (2017). Cellular and molecular characterization of microglia: a unique immune cell population. *Front. Immunol.* 8:198. doi: 10.3389/fimmu.2017.00198

Spangenberg, E., Severson, P. L., Hohsfield, L. A., Crapser, J., Zhang, J., Burton, E. A., et al. (2019). Sustained microglial depletion with CSF1R inhibitor impairs parenchymal plaque development in an Alzheimer's disease model. *Nat. Commun.* 10:3758. doi: 10.1038/s41467-019-11674-z

Španić, E., Langer Horvat, L., Hof, P. R., and Šimić, G. (2019). Role of microglial cells in Alzheimer's disease tau propagation. *Front. Aging Neurosci.* 11:271. doi: 10.3389/fnagi.2019.00271

Spittau, B. (2017). Aging microglia-phenotypes, functions and implications for age-related neurodegenerative diseases. *Front. Aging Neurosci.* 9:194. doi: 10.3389/fnagi.2017.00194

Südhof, T. C. (2018). Towards an understanding of synapse formation. *Neuron* 100, 276–293. doi: 10.1016/j.neuron.2018.09.040

Sun, H., He, X., Tao, X., Hou, T., Chen, M., He, M., et al. (2020). The CD200/CD200R signaling pathway contributes to spontaneous functional recovery by enhancing synaptic plasticity after stroke. *J. Neuroinflammation* 17:171. doi: 10.1186/s12974-020-01845-x

Sveinbjornsdottir, S. (2016). The clinical symptoms of Parkinson's disease. *J. Neurochem.* 139, 318–324. doi: 10.1111/jnc.13691

Szepesi, Z., Manouchehrian, O., Bachiller, S., and Deierborg, T. (2018). Bidirectional microglia-neuron communication in health and disease. *Front. Cell. Neurosci.* 12:323. doi: 10.3389/fncel.2018.00323

Takata, F., Nakagawa, S., Matsumoto, J., and Dohgu, S. (2021). Blood-brain barrier dysfunction amplifies the development of Neuroinflammation: understanding of cellular events in brain microvascular endothelial cells for prevention and treatment of BBB dysfunction. *Front. Cell. Neurosci.* 15:661838. doi: 10.3389/fncel.2021.661838

Tanaka, M., Sackett, S., and Zhang, Y. (2020). Endocannabinoid modulation of microglial phenotypes in neuropathology. *Front. Neurol.* 11:87. doi: 10.3389/fneur.2020.00087

Tao, W., Hu, Y., Chen, Z., Dai, Y., Hu, Y., and Qi, M. (2021). Magnolol attenuates depressive-like behaviors by polarizing microglia towards the M2 phenotype through the regulation of Nrf2/HO-1/NLRP3 signaling pathway. *Phytomedicine* 91:153692. doi: 10.1016/j.phymed.2021.153692

Tran, T. A., Nguyen, A. D., Chang, J., Goldberg, M. S., Lee, J. K., and Tansey, M. G. (2011). Lipopolysaccharide and tumor necrosis factor regulate Parkin expression via nuclear factor-kappa B. *PLOS ONE* 6:e23660. doi: 10.1371/journal.pone.0023660

Trépanier, M. O., Hopperton, K. E., Mizrahi, R., Mechawar, N., and Bazinet, R. P. (2016). Postmortem evidence of cerebral inflammation in schizophrenia: a systematic review. *Mol. Psychiatry* 21, 1009–1026. doi: 10.1038/mp.2016.90

Ulland, T. K., Song, W. M., Huang, S. C., Ulrich, J. D., Sergushichev, A., Beatty, W. L., et al. (2017). TREM2 maintains microglial metabolic fitness in Alzheimer's disease. *Cell* 170, 649–663.e13. doi: 10.1016/j.cell.2017.07.023

Umpierre, A. D., and Wu, L. J. (2021). How microglia sense and regulate neuronal activity. *Glia* 69, 1637–1653. doi: 10.1002/glia.23961

Vainchtein, I. D., Chin, G., Cho, F. S., Kelley, K. W., Miller, J. G., Chien, E. C., et al. (2018). Astrocyte-derived interleukin-33 promotes microglial synapse engulfment and neural circuit development. *Science* 359, 1269–1273. doi: 10.1126/science.aal3589

van Kesteren, C. F., Gremmels, H., de Witte, L. D., Hol, E. M., Van Gool, A. R., Falkai, P. G., et al. (2017). Immune involvement in the pathogenesis of schizophrenia: a meta-analysis on postmortem brain studies. *Transl. Psychiatry* 7:e1075. doi: 10.1038/tp.2017.4

Vargas, D. L., Nascimbene, C., Krishnan, C., Zimmerman, A. W., and Pardo, C. A. (2005). Neuroglial activation and neuroinflammation in the brain of patients with autism. *Ann. Neurol.* 57, 67–81. doi: 10.1002/ana.20315

Verney, C., Monier, A., Fallet-Bianco, C., and Gressens, P. (2010). Early microglial colonization of the human forebrain and possible involvement in periventricular white-matter injury of preterm infants. *J. Anat.* 217, 436–448. doi: 10.1111/j.1469-7580.2010.01245.x

Walker, D. G., and Lue, L. F. (2013). Understanding the neurobiology of CD200 and the CD200 receptor: a therapeutic target for controlling inflammation in human brains? *Future Neurol.* 8, 321–332. doi: 10.2217/fnl.13.14

Wang, C., Yue, H., Hu, Z., Shen, Y., Ma, J., Li, J., et al. (2020). Microglia mediate forgetting via complement-dependent synaptic elimination. *Science* 367, 688–694. doi: 10.1126/science.aaz2288

Wang, S., Ren, D., Arkoun, B., Kaushik, A. L., Matherat, G., Lécluse, Y., et al. (2021). Lyl-1 regulates primitive macrophages and microglia development. *Commun. Biol.* 4:1382. doi: 10.1038/s42003-021-02886-5

Wang, W. Y., Tan, M. S., Yu, J. T., and Tan, L. (2015). Role of pro-inflammatory cytokines released from microglia in Alzheimer's disease. *Annals Transl. Med.* 3:136. doi: 10.3978/j.issn.2305-5839.2015.03.49

Wang, J., Wang, J., Wang, J., Yang, B., Weng, Q., and He, Q. (2019). Targeting microglia and macrophages: a potential treatment strategy for multiple sclerosis. *Front. Pharmacol.* 10:286. doi: 10.3389/fphar.2019.00286

Wehrspaun, C. C., Haerty, W., and Ponting, C. P. (2015). Microglia recapitulate a hematopoietic master regulator network in the aging human frontal cortex. *Neurobiol. Aging* 36, 2443.e9–2443.e20. doi: 10.1016/j.neurobiolaging.2015.04.008

Wendeln, A. C., Degenhardt, K., Kaurani, L., Gertig, M., Ulas, T., Jain, G., et al. (2018). Innate immune memory in the brain shapes neurological disease hallmarks. *Nature* 556, 332–338. doi: 10.1038/s41586-018-0023-4

Whitton, P. S. (2007). Inflammation as a causative factor in the aetiology of Parkinson's disease. *Br. J. Pharmacol.* 150, 963–976. doi: 10.1038/sj.bjp.0707167

Wightman, D. P., Jansen, I. E., Savage, J. E., Shadrin, A. A., Bahrami, S., Holland, D., et al. (2021). A genome-wide association study with 1,126,563 individuals identifies new risk loci for Alzheimer's disease. *Nat. Genet.* 53, 1276–1282. doi: 10.1038/s41588-021-00921-z

Wilkinson, K., and El Khoury, J. (2012). Microglial scavenger receptors and their roles in the pathogenesis of Alzheimer's disease. *Int. J. Alzheimers Dis.* 2012:489456. doi: 10.1155/2012/489456

Witte, M. E., Nijland, P. G., Drexhage, J. A., Gerritsen, W., Geerts, D., van Het Hof, B., et al. (2013). Reduced expression of PGC-1α partly underlies mitochondrial changes and correlates with neuronal loss in multiple sclerosis cortex. *Acta Neuropathol.* 125, 231–243. doi: 10.1007/s00401-012-1052-y

Xu, S., Lu, J., Shao, A., Zhang, J. H., and Zhang, J. (2020). Glial cells: role of the immune response in ischemic stroke. *Front. Immunol.* 11:294. doi: 10.3389/fimmu.2020.00294

Xue, F., Tian, J., Yu, C., Du, H., and Guo, L. (2021). Type I interferon response-related microglial Mef2c deregulation at the onset of Alzheimer's pathology in 5×FAD mice. *Neurobiol. Dis.* 152:105272. doi: 10.1016/j.nbd.2021.105272

Yaghmoor, F., Noorsaeed, A., Alsaggaf, S., Aljohani, W., Scholtzova, H., Boutajangout, A., et al. (2014). The role of TREM2 in Alzheimer's disease and other neurological disorders. *J. Alzheimers Dis. Parkinson.* 4:160. doi: 10.4172/2161-0460.1000160

Yeh, H., and Ikezu, T. (2019). Transcriptional and epigenetic regulation of microglia in health and disease. *Trends Mol. Med.* 25, 96–111. doi: 10.1016/j.molmed.2018.11.004

Yune, T. Y., Lee, J. Y., Jung, G. Y., Kim, S. J., Jiang, M. H., Kim, Y. C., et al. (2007). Minocycline alleviates death of oligodendrocytes by inhibiting pro-nerve growth factor production in microglia after spinal cord injury. *J. Neurosci. Off. J. Soc. Neurosci.* 27, 7751–7761. doi: 10.1523/JNEUROSCI.1661-07.2007

Zarei, S., Carr, K., Reiley, L., Diaz, K., Guerra, O., Altamirano, P. F., et al. (2015). A comprehensive review of amyotrophic lateral sclerosis. *Surg. Neurol. Int.* 6:171. doi: 10.4103/2152-7806.169561

Zhai, S., Tanimura, A., Graves, S. M., Shen, W., and Surmeier, D. J. (2018). Striatal synapses, circuits, and Parkinson's disease. *Curr. Opin. Neurobiol.* 48, 9–16. doi: 10.1016/j.conb.2017.08.004

Zhan, Y., Paolicelli, R. C., Sforazzini, F., Weinhard, L., Bolasco, G., Pagani, F, et al. (2014). Deficient neuron-microglia signaling results in impaired functional brain connectivity and social behavior. *Nat. Neurosci.* 17, 400–406. doi: 10.1038/nn.3641

Zhang, B., Gaiteri, C., Bodea, L. G., Wang, Z., McElwee, J., Podtelezhnikov, A. A., et al. (2013). Integrated systems approach identifies genetic nodes and networks in late-onset Alzheimer's disease. *Cell* 153, 707–720. doi: 10.1016/j.cell.2013.03.030

Zhao, X., Eyo, U. B., Murugan, M., and Wu, L. J. (2018). Microglial interactions with the neurovascular system in physiology and pathology. *Dev. Neurobiol.* 78, 604–617. doi: 10.1002/dneu.22576

Zhao, S. C., Ma, L. S., Chu, Z. H., Xu, H., Wu, W. Q., and Liu, F. (2017). Regulation of microglial activation in stroke. *Acta Pharmacol. Sin.* 38, 445–458. doi: 10.1038/aps.2016.162

Zheng, H., Cheng, B., Li, Y., Li, X., Chen, X., and Zhang, Y. W. (2018). TREM2 in Alzheimer's disease: microglial survival and energy metabolism. *Front. Aging Neurosci.* 10:395. doi: 10.3389/fnagi.2018.00395

Zöller, T., Schneider, A., Kleimeyer, C., Masuda, T., Potru, P. S., Pfeifer, D., et al. (2018). Silencing of TGFβ signalling in microglia results in impaired homeostasis. *Nat. Commun.* 9:4011. doi: 10.1038/s41467-018-06224-y

frontiers | Frontiers in Molecular Neuroscience

TYPE Mini Review
PUBLISHED 06 February 2023
DOI 10.3389/fnmol.2023.1114015

OPEN ACCESS

EDITED BY
Estela Maris Muñoz,
CONICET Dr. Mario H. Burgos Institute of Histology and Embryology (IHEM), Argentina

REVIEWED BY
Luis R. Hernandez-Miranda,
Charité Universitätsmedizin Berlin, Germany
John Mason,
University of Edinburgh, United Kingdom

*CORRESPONDENCE
Ignacio E. Schor
✉ ieschor@fbmc.fcen.uba.ar

†These authors share first authorship

SPECIALTY SECTION
This article was submitted to Neuroplasticity and Development, a section of the journal Frontiers in Molecular Neuroscience

RECEIVED 02 December 2022
ACCEPTED 16 January 2023
PUBLISHED 06 February 2023

CITATION
Arcuschin CD, Pinkasz M and Schor IE (2023) Mechanisms of robustness in gene regulatory networks involved in neural development. *Front. Mol. Neurosci.* 16:1114015. doi: 10.3389/fnmol.2023.1114015

Mechanisms of robustness in gene regulatory networks involved in neural development

Camila D. Arcuschin[1,2†], Marina Pinkasz[1†] and Ignacio E. Schor[1,2*]

[1]Instituto de Fisiología, Biología Molecular y Neurociencias (IFIBYNE), Universidad de Buenos Aires—Consejo Nacional de Investigaciones Científicas y Técnicas (CONICET), Buenos Aires, Argentina, [2]Departamento de Fisiología, Biología Molecular y Celular, Facultad de Ciencias Exactas y Naturales, Universidad de Buenos Aires, Buenos Aires, Argentina

The functions of living organisms are affected by different kinds of perturbation, both internal and external, which in many cases have functional effects and phenotypic impact. The effects of these perturbations become particularly relevant for multicellular organisms with complex body patterns and cell type heterogeneity, where transcriptional programs controlled by gene regulatory networks determine, for example, the cell fate during embryonic development. Therefore, an essential aspect of development in these organisms is the ability to maintain the functionality of their genetic developmental programs even in the presence of genetic variation, changing environmental conditions and biochemical noise, a property commonly termed robustness. We discuss the implication of different molecular mechanisms of robustness involved in neurodevelopment, which is characterized by the interplay of many developmental programs at a molecular, cellular and systemic level. We specifically focus on processes affecting the function of gene regulatory networks, encompassing transcriptional regulatory elements and post-transcriptional processes such as miRNA-based regulation, but also higher order regulatory organization, such as gene network topology. We also present cases where impairment of robustness mechanisms can be associated with neurodevelopmental disorders, as well as reasons why understanding these mechanisms should represent an important part of the study of gene regulatory networks driving neural development.

KEYWORDS

robustness, neuronal differentiation, transcriptional regulation, development, regulatory elements, gene regulatory networks, genetic variation

Introduction

In the development of multicellular organisms, gene regulatory networks (GRN) that determine cell fate and drive differentiation must be resilient to genetic, environmental or random perturbations, including changing temperature, variable number of embryonic cell progeny, gene expression noise, retrotransposon insertions, epigenetic constraint relaxation, and somatic or germline point mutations. Decades ago, Waddington introduced the idea of canalized development (Waddington, 1942) and from there on the concept of robustness has emerged as a key feature of biological processes that favors a uniform outcome (phenotype) in the presence of variable conditions (Barkai and Shilo, 2007; Félix and Wagner, 2008). The importance of robustness during organisms development and its impact on evolution, as well as several examples across different models has been already extensively reviewed before (see for example Scharloo, 1991; Kirschner and Gerhart, 1998; de Visser et al., 2003; Félix and Wagner, 2008; Payne and Wagner, 2015). Here, we aim to present examples of robustness mechanisms assisting gene expression regulation necessary for neural development.

Assessing robustness of developmental processes

Proper development is crucial for survival of multicellular organisms. Since this process faces perturbations in the form of high rates of genetic variation (Keightley, 2012), environmental changing conditions or even stochastic noise, it is not surprising that developmental robustness mechanisms have appeared across the evolution. But before discussing robustness mechanisms, it is important to clarify how robustness can be identified.

In its simplest conceptual meaning, robustness implies the persistence of a phenotype in the face of perturbation. However, considering the mentioned sources of perturbations to which each individual is exposed, robustness can be associated, as suggested by Félix and Wagner, with the lack of phenotype variability amongst a population (Félix and Wagner, 2008). This association originates in some of the first examples in which developmental robustness has been studied, such as bristle number and *ocelli* with bristles in *Drosophila*, and *vibrissae* number in mice (Scharloo, 1991). However, not all biological traits need to be robust and robustness does not always mean lack of variability at all levels of analysis (Hiesinger and Hassan, 2018). In nature, some phenotypes may seem to lack robustness and show variability between individuals because there is no selective pressure acting on that variable phenotype. But sometimes, some level of variability is actively used to acquire a specific output, as observed for example in the variability of cell-to-cell expression of Dscam1 isoforms which regulates self-avoidance in *Drosophila melanogaster* mushroom bodies (Kise and Schmucker, 2013; Lawrence Zipursky and Grueber, 2013).

Following Waddington's idea of canalization (Waddington, 1942), we normally see robustness of developmental processes buffering minor variations, such as noisy gene expression (Eldar et al., 2002; Arias and Hayward, 2006; Urban and Johnston, 2018) or disruption of single regulatory elements (Kvon et al., 2021), while larger perturbations (such as complete ablation of a gene) could be able to override most robustness mechanisms. In this review we will focus on mechanisms affecting regulation of gene expression and GRN function, although many molecular and cellular features are able to buffer phenotypes against perturbations, including exploratory behavior (Sperry, 1963; Kirschner and Gerhart, 1998; Wit and Hiesinger, 2023), progenity compensation between lineages (Enriquez et al., 2018), chaperones-target interactions (Sato, 2018), or weak linkage of protein interactions in cell signaling (Kirschner and Gerhart, 1998; Hartman et al., 2001).

The nervous system as a developmental model

The majority of adult neural cell diversity is generated in the embryonic and early postnatal stages in mammals, and larval stages in *Drosophila*, from a pool of undifferentiated neural stem and progenitor cells (Mira and Morante, 2020). Neural stem cells are multipotent and generate the main cell types of the nervous system: neurons, oligodendrocytes, and astrocytes. Typically, stem cells initially generate neurons and afterwards glial cells, and this switch from neurogenesis to gliogenesis requires changes in stem cell properties that are dependent on extrinsic and intrinsic factors (Qian et al., 2000; Temple, 2001; Ohtsuka and Kageyama, 2019; Villalba et al., 2021). Many signaling pathways are known to regulate this switch in cell specification (Perrimon et al., 2012; Maury et al., 2015). For example in mammals, signals such as Bone morphogenetic protein 2 (BMP2) and erythropoietin (Epo) induce proneural gene expression (Bertrand et al., 2002). To prevent other cells from differentiating to neurons, Notch signaling downregulates proneural genes (Lowell et al., 2006; Lathia et al., 2008; Sjöqvist and Andersson, 2019; Bocci et al., 2020). These pathways maintain a balance between progenitors entering a neuron differentiation pathway and progenitors remaining undifferentiated and available to produce other types of nervous system cells (Bertrand et al., 2002). In addition to this general neural differentiation program gradients of morphogens, molecules secreted by specific sources that can diffuse through the tissue, determine cell fate along specific axes. For example, in the development of the neural tube, a gradient of Sonic Hedgehog (Shh) control cell types along the ventral-dorsal axis. Interestingly, the Shh gradient is able to create boundaries that define cell type in a very robust manner (Hernandez-Miranda et al., 2017; Sagner and Briscoe, 2017, 2019; Xia et al., 2022). This process uses Shh concentration along time and space as input, and depends on incoherent feedforward (Mangan and Alon, 2003) and feedback loops that connect Shh signaling with the expression of the Olig2, Nkx2.2, and Pax6 transcriptional regulators (Balaskas et al., 2012).

While most neurogenesis in mammals occurs during development or very early in the newborn, there has been an increased interest in the past years in adult neurogenesis (Ernst et al., 2014; Falk and Götz, 2017; Denoth-Lippuner and Jessberger, 2021). New neurons in the adult can contribute to normal pattern separation, cognition and learning (Clelland et al., 2009; Sahay et al., 2011; Nakashiba et al., 2012) and it has been shown a reduction of this process in patients with neurodegenerative disease such as Alzheimer's (Moreno-Jiménez et al., 2019; Tobin et al., 2019). However, the presence of newborn neurons in the human adult hippocampus has been recently disputed (Paredes et al., 2018; Sorrells et al., 2018; Alvarez-Buylla et al., 2022). Although this issue remains controversial, elucidating mechanisms that ensure the robustness in neural development might be relevant also in the adult brain.

In summary, nervous system development in metazoans is a highly complex process influenced by many factors that converge on interconnected gene regulatory networks (GRNs) dictating specific spatio-temporal differentiation patterns of cells. It is therefore expected, as many other developmental processes, to be sensitive to perturbations, both from the cellular environment and the external environment (McGrath et al., 2011), which suggests that some of the key steps in this process might exhibit robustness mechanisms. The idea of robustness in neurodevelopment is supported by genetic evidence, such as that even in the presence of high levels of inter-individual genetic variation (Keightley, 2012), the human neurodevelopmental transcriptome is much more robust across individuals than across time or regions (Silbereis et al., 2016).

Mechanisms of robustness in developmental gene regulatory networks

Over the years, evidence of different mechanisms that give robustness to embryonic development has accumulated (Arias and Hayward, 2006; Barkai and Shilo, 2007; Félix and Wagner, 2008; Rogers and Schier, 2011; Payne and Wagner, 2015), although not so much is known in particular for the development of the nervous system, specially in vertebrates. Nevertheless, we will present some examples affecting gene expression programs involved in development, to illustrate how these mechanisms operate.

Robustness at the level of individual gene expression

Even though development and differentiation are controlled by GRNs consisting of several genes, these networks have hierarchies, implying that reduced expression variability for some specific highly connected genes might be advantageous for the regulatory function of the network as a whole. For example, it has been identified that in many gene regulatory networks there are genes that act as master regulators (Carro et al., 2010; Tutukova et al., 2021), corresponding to regulatory bottlenecks. Therefore, we will present examples of mechanisms that control robustness in the regulation of gene expression, both at the transcriptional and post-transcriptional levels.

The most basic form in which transcription of a certain gene can be robust to, for example, a genetic perturbation is the fact that most individual transcription factors (TFs) are typically able to bind to many different sequences, which are connected to each other in the "genotype space" (Badis et al., 2009; Payne and Wagner, 2014, 2015). This allows TF binding conservation in the presence of binding site variation. In addition, commonly regulated binding sites tend to be spatially clustered in the genome within regulatory elements (Berman et al., 2002), providing a further level of robustness to binding site turnover. While TF redundancy provides robustness on the function of an individual enhancer, the presence of redundant enhancer regions have been also shown to act as a buffer against perturbations (Frankel et al., 2010; Kvon et al., 2021). Genes involved in development are enriched in more than one enhancer whereas housekeeping genes are usually controlled by a single regulatory region (Cannavò et al., 2016; Kvon et al., 2021), and redundant enhancers are depleted in GWAS-or eQTL-associated SNPs compared to single enhancers (Song and Ovcharenko, 2018), suggesting a lower impact of genetic variation in these genomic regions. Several genes with key roles in neuronal development seem to have a regulatory architecture with redundant enhancers. For example, redundant enhancers were identified controlling the expression of Shh in the ventral spinal cord, hindbrain, and telencephalon (Jeong et al., 2006). In zebrafish, six elements were described to regulate Krox20 expression in the hindbrain. Krox20 is a transcription factor important for hindbrain segmentation and patterning and highly conserved in vertebrate evolution. These elements were found to act redundantly at some extent, since while deletion of one element leads to a mild reduction in expression, deletion of two regulatory elements is needed to see a drastic impairment of Krox20 expression (Torbey et al., 2018). In mice, removal of an enhancer region located upstream of the promoter for Pax3, a transcription factor required for normal neural crest development, was insufficient to inhibit neural crest expression of Pax3 and resulted in a viable mouse. This observation led to the identification of a functionally redundant intronic enhancer that might be involved in robustness of Pax3 expression in the developing neural crest (Degenhardt et al., 2010). In addition to the enhancer configuration, the presence of redundancy at the TF level, for example due to gene duplication, can also act as a robustness mechanism in development. One example in the nervous system is the partially redundant role of the Gsx1 and Gsx2 TFs in the control of neuronal vs. glial differentiation of neuronal progenitors in the ventral telencephalon of mice (Chapman et al., 2018).

Post transcriptional mechanisms also contribute to robustness in neural development. Micro RNAs (miRNAs) in particular have been proposed as gene expression buffers in regulatory networks and are usually involved in regulatory feedback and feedforward loops (Tsang et al., 2007; Ebert and Sharp, 2012; Ghosh et al., 2014). One example of a miRNA-based post-transcriptional mechanism of developmental process robustness is the regulation of cyclin D1 expression by miR-20a/b and miR-23a in mouse cortical neurogenesis. Cyclin D1 induces expression of miR-20a/b and represses miR-23a in a feedback regulatory network. When any of these miRNAs are inhibited, the variance and the mean expression of cyclin D1 protein in progenitors increases, reducing neuronal differentiation (Ghosh et al., 2014). In another example, *Drosophila*'s miR-9a reduction and consequent dysregulation of the *senseless* transcription factor make cell phenotype more sensitive to genomic and environmental variation (Cassidy et al., 2013). Interestingly, miR-9a is conserved at the sequence level from flies to humans, suggesting that it may have a similar role in mammalian neurogenesis (Li et al., 2006).

Finally, we want to present two other elements that have lately been proposed as having a role in gene expression robustness: chromatin conformation and the promoter architecture. The organization of the genome in topologically associating domains (TADs) impacts the regulatory landscape of mammalian genomes. TAD boundaries, typically formed in regions containing clusters of CTCF binding sites, are important to instruct interactions between regulatory elements, such as enhancers and promoters, and the TAD organization has been proposed to bring robustness and precision to gene expression in development (Despang et al., 2019; Anania et al., 2022). Promoter-enhancer interactions can be also aided by CTCF-mediated chromatin loops, increasing robustness of enhancer regulation on gene expression. For example, a recent study (Paliou et al., 2019) found that loss of the interaction between the Shh gene promoter and a distal enhancer through the deletion of CTCF binding sites causes a mild decrease of Shh expression and no phenotypic change by itself, but sensitizes Shh expression to partial disruptions of the distal enhancer. Regarding the influence of the gene promoter, evidence from population genomics for both vertebrates and invertebrates

strongly suggests that certain promoter architectures are associated with higher genetic robustness, perhaps buffering levels of gene expression against the effects of genetic variation (Schor et al., 2017; Sigalova et al., 2020; Einarsson et al., 2022). The relevance of these features in the development of the nervous system remains yet to be assessed.

Robustness at higher levels of complexity

While robustness exists for the expression of individual key regulators of a process, some robustness features arise when the GRN and their related signaling pathways are considered (Félix and Wagner, 2008). The topology of developmental regulatory pathways is characterized by the extensive interplay between them, the presence of feedback and feedforward loops and the redundant outputs that bring robustness to perturbations (Arias and Hayward, 2006; Barkai and Shilo, 2009). Morphogen gradients acting in the neural tube development display a great precision not only in their space and time specific extracellular levels but even more in their intracellular expression (Vetter and Iber, 2022). Regulatory loops are in part responsible for these properties, and at the same time seem to account for tolerance to perturbations of morphogen systems (Barkai and Shilo, 2009; Irons et al., 2010; Rogers and Schier, 2011). These loops are evident, for example, when analyzing the canonical Shh response (Figure 1). Shh binds to the receptor Ptc, inhibiting its repressive function over Smo, another membrane protein that subsequently triggers Shh signaling pathways. These pathways result in the activation of Gli transcription factors (TF), which drive chromatin remodeling and transcriptional regulation at different regulatory elements along the ventral-dorsal axis, inducing transcription of specific target genes (Vokes et al., 2008; Oosterveen et al., 2012; Delás et al., 2022). Remarkably, this includes a feedback loop through the upregulation of the PTCH1 gene, which codes for Ptc, resulting in an Shh-induced increase of Ptc levels (Goodrich et al., 1996; Marigo and Tabin, 1996; Sagner and Briscoe, 2017). Since the receptor has the ability also to endocyte and degrade Shh, this system also acts as a negative feedback loop to buffer variations in Shh levels and prevent its diffusion to further regions (Chen and Struhl, 1996; Dessaud et al., 2007; Rogers and Schier, 2011; Ferent et al., 2019). In addition, the response to Shh is mediated by a network of interconnected TFs downstream Gli, including Pax6, Olig2, and Nkx2.2, which plays important roles in the specific transcriptional responses and the adaptation of cells to variable spatio-temporal Shh concentration, while at the same time provides robustness against transient variation of the GRN effectors (Dessaud et al., 2010; Balaskas et al., 2012).

In the previous cases we evaluate robustness at the molecular and cellular level. However, for many complex phenotypes, variability at these levels can be compensated by mechanisms at a higher order. For example, the total number of astrocytes in the fly thorax neuropil is robust to variations in the astrocytes produced by the main precursor lineage, because secondary lineages may compensate for variability through an unknown plastic mechanism (Enriquez et al., 2018). Thus, in many cases it is important to study variability and compensation at different levels of organization (molecular—cellular—cell populations—system) to fully understand robustness of a specific phenotype.

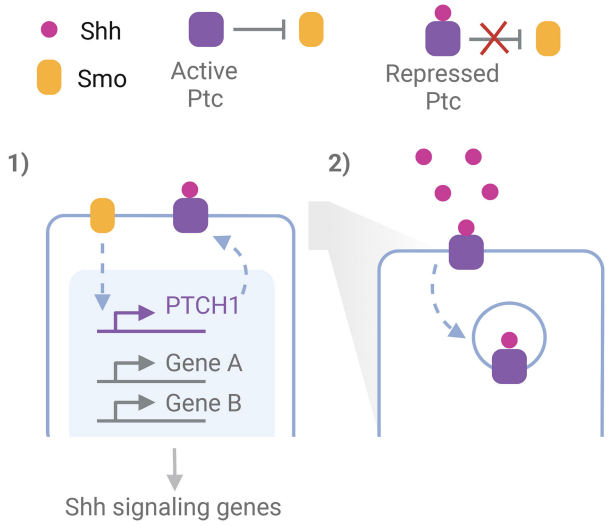

FIGURE 1
Example of network-level robustness for the action of a morphogen in neurodevelopment. Two feed-back loops participate in the robustness mechanism for the cellular responde to Shh in the neural tube: 1. Smo indirectly induces transcription of the PTCH1 gene. This gene codes for the protein Ptc, which represses Smo activity and is inhibited by Shh binding; 2. After Shh binding, Ptc mediates its endocytosis and degradation. Inspired in Sagner and Briscoe (2017) and Ferent et al. (2019). Created with BioRender.com.

Developmental disorders and robustness to genetic variation

During neurodevelopment, disruption of robustness mechanisms at different levels or excessive perturbation levels that overtake them can lead to developmental disorders. For example, regarding miRNA-based feedback mechanisms, haploinsufficiency of the miR-17/92 cluster is found in some cases of Feingold syndrome, a disease that affects development and produces, among other phenotypes, microcephaly. Moreover, an hemizygous deletion of the cluster causes related symptomatology in mice (de Pontual et al., 2011). Even gene redundancy can be insufficient to buffer the effect of some mutations; while the two related tubulin genes TUBB2A and TUBB2B can partially compensate the loss of each other on their role in neuronal development, missense mutation causing gain-of-function phenotypes for one of these genes can trigger aberrant behavior unable to be counteracted by the paralogue, and this can lead to cortical malformations (Bittermann et al., 2019). For heterozygous loss-of-function mutations in X-linked genes, there might be a cross-over between the expression of the mutated allele and a skewness in the X-chromosome inactivation (XCI) process. Rett syndrome, which causes dementia, seizures and microcephaly

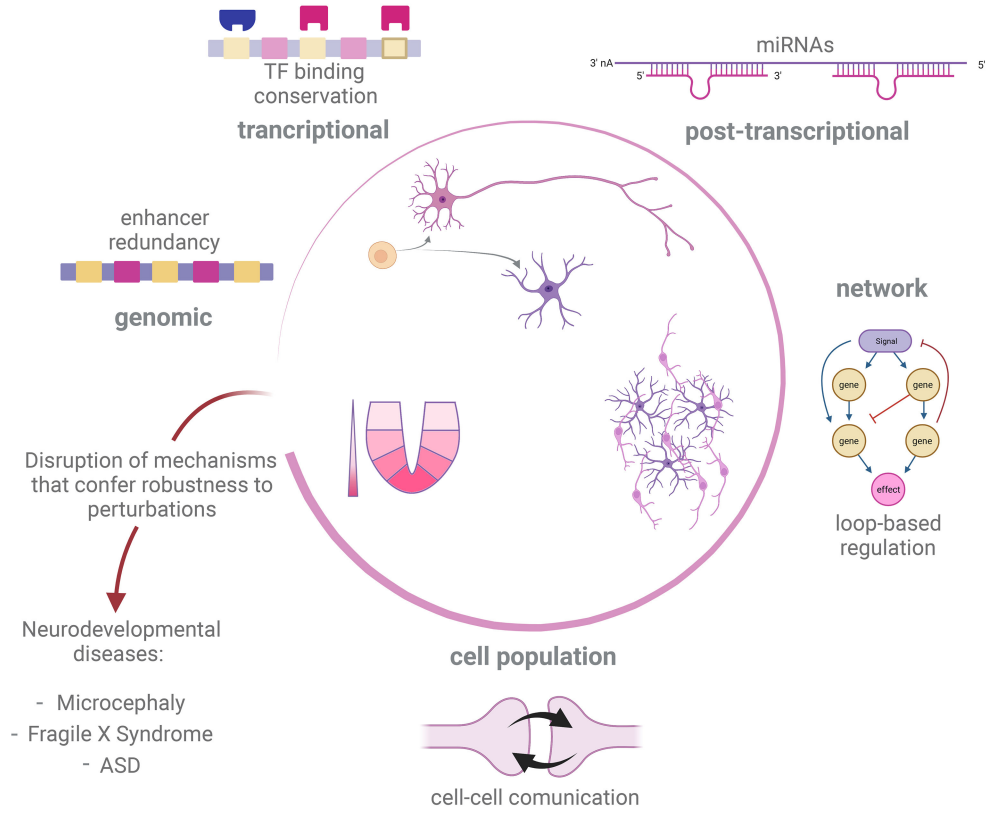

FIGURE 2
Robustness mechanism underlying development of nervous system. Development of the nervous system in different metazoan species is tuned by distinct but overlapping regulatory processes, such as sensing of morphogen gradients, cell-cell communication and GRN governing cell fate decisions. In order to correctly deliver such a complex output, different strategies promote robustness against internal or external perturbations at different levels of regulation. Disruption of robustness mechanisms could impair success of some of these developmental processes and therefore trigger neurodevelopmental disease and abnormal conditions, such as microcephaly, Fragile X Syndrome and ASD. Created with BioRender.com.

among other phenotypes, is associated with mutations in the X-linked gene coding for MeCP2, a transcriptional regulator that binds to 5 hmC in regulatory regions of neurodevelopmental genes (Jang et al., 2017). Typically, since XCI occurs randomly in each cell, heterozygous mutant females are mosaic, and most of them actually show mild or no symptoms. However, there is evidence that in some cases of MeCP2 mutations an unbalanced XCI is seen in favor to the wild-type allele as well as a selective growth advantage of wild-type expressing cells over mutated ones (Dragich et al., 2000; Young and Zoghbi, 2004; Chahrour and Zoghbi, 2007). In other scenarios, disease symptoms will appear after a threshold of perturbation is exceeded, suggesting a limit for effectiveness of robustness mechanisms. For example, the number of CGG repeats expansion on the 5' UTR of the FMR1 gene is clearly related to the probability of having Fragile X Syndrome mental disorder. While normal individuals have between 6 and 40 CGG repeats, and in premutation cases this number can increase between 55 and 199, full-mutation cases that show disease symptoms will show a number of repeats in the range 200–230 (Nolin et al., 1996; Kronquist et al., 2008).

Of particular relevance to human health, common genetic variation is a pervasive source of perturbations for the regulatory systems of biological processes. Common variation can be seen as small-effect perturbations, which by itself are not enough to significantly affect high-order phenotypes. However, they can interact additively or non-additively with other perturbations, for example contributing to a higher chance of having a particular disease. In particular, we use the term cryptic genetic variation to define common variants that are potential disruptors of the normal expression patterns but do normally not affect phenotypes observed in a population due to, for example, epistatic interactions with other variants (Gibson and Dworkin, 2004; Gibson, 2009), allowing them to persist in the population due to lack of sufficient purifying selection. Over the last years there has been a growing interest to elucidate how common variation can shape diseases or developmental disorders using, for instance, genome wide association studies (GWAS). Most variants identified by GWAS studies are in non-coding regions, suggesting that in most cases functional common variation affects gene expression regulation (Edwards et al., 2013). While having small effects on high-level phenotypes, the high number and frequency in the population of these common variants make them an important contributor to human disease. In ASD and other neuropsychiatric disorders, for example, accountability for genetic risk is more likely to reside in common variation (Gaugler et al., 2014; Autism Spectrum Disorder Working Group of the Psychiatric Genomics Consortium and Ripke, 2019), and genes involved in corticogenesis seem to

be enriched in ASD-linked common variation (Parikshak et al., 2015; Autism Spectrum Disorder Working Group of the Psychiatric Genomics Consortium and Ripke, 2019).

Discussion

We have shown possible mechanisms at different levels of organization by which regulation of developmental processes in the nervous system can be robust to genetic and non-genetic perturbations (Figure 2). In many cases, the mechanisms of developmental robustness have been studied in relatively simple model organisms, such as *C. elegans* or *D. melanogaster*, while the study of robustness is still an underdeveloped aspect in the field of vertebrate neurodevelopment, perhaps with the exception of morphogens action (Barkai and Shilo, 2009; Irons et al., 2010; Balaskas et al., 2012; Perrimon et al., 2012; Vetter and Iber, 2022). In the present text we have presented examples of how perturbation of developmental GRNs can give rise to atypical developmental conditions and disease. We therefore believe that a deeper understanding of mechanisms that give robustness to nervous system development is needed to fully understand the genetic aspects of disorders affecting this process.

Regarding how robustness mechanisms originate, it is still an open question whether they can be heritable traits subjected to natural selection, as it is uncertain to what extent the mechanisms contributing to neurodevelopment have arised by evolutionary refinement across history. Some evidences question this idea of developmental refining, at least in human evolution, postulating that hominid brain is particularly vulnerable to perturbations in part because its great expansion in such a short evolutionary time couldn't have allowed the evolution of robust developmental trajectories (McGrath et al., 2011). In this sense, there is a significant need to test neurodevelopmental robustness mechanisms in different mammalian species to address if their role could be ancestral or if robustness of GRN involved in neuronal development has evolved repeatedly through convergence from other pre-existing mechanisms (Conant and Wagner, 2003).

Author contributions

All authors have made a substantial and direct contribution to the work, including writing, reviewing and editing of the manuscript, and approved it for publication.

Funding

IS is a CONICET researcher, while CA and MP are recipients of a fellowship from the CONICET. The group was supported by grants from CONICET (PIP 11220170100714CO), FONCYT (PICT-2017-2538 and PICT-2018-03779), both within the Ministerio de Ciencia y Técnica de Argentina, and the Chan-Zuckerberg Initiative (Grant #221790).

Acknowledgments

We want to thank Pedro Salaberry and Martin Iungman for very useful discussion and insights.

Conflict of interest

The authors declare that the research was conducted in the absence of any commercial or financial relationships that could be construed as a potential conflict of interest.

Publisher's note

References

Alvarez-Buylla, A., Cebrian-Silla, A., Sorrells, S. F., Nascimento, M. A., Paredes, M. F., Garcia-Verdugo, J. M., et al. (2022). Comment on "Impact of neurodegenerative diseases on human adult hippocampal neurogenesis." Science 376, eabn8861. doi: 10.1126/science.abn8861

Anania, C., Acemel, R. D., Jedamzick, J., Bolondi, A., Cova, G., Brieske, N., et al. (2022). *In vivo* dissection of a clustered-CTCF domain boundary reveals developmental principles of regulatory insulation. *Nat. Genet.* 54, 1026–1036. doi: 10.1038/s41588-022-01117-9

Arias, A. M., and Hayward, P. (2006). Filtering transcriptional noise during development: Concepts and mechanisms. *Nat. Rev. Genet.* 7, 34–44. doi: 10.1038/nrg1750

Autism Spectrum Disorder Working Group of the Psychiatric Genomics Consortium, BUPGEN, Major Depressive Disorder Working Group of the Psychiatric Genomics Consortium, 23andMe Research Team, Grove, J., Ripke, S., et al. (2019). Identification of common genetic risk variants for autism spectrum disorder. *Nat. Genet.* 51, 431–444. doi: 10.1038/s41588-019-0344-8

Badis, G., Berger, M. F., Philippakis, A. A., Talukder, S., Gehrke, A. R., Jaeger, S. A., et al. (2009). Diversity and complexity in DNA recognition by transcription factors. *Science* 324, 1720–1723. doi: 10.1126/science.1162327

Balaskas, N., Ribeiro, A., Panovska, J., Dessaud, E., Sasai, N., Page, K. M., et al. (2012). Gene regulatory logic for reading the Sonic Hedgehog signaling gradient in the vertebrate neural tube. *Cell* 148, 273–284. doi: 10.1016/j.cell.2011.10.047

Barkai, N., and Shilo, B.-Z. (2007). Variability and robustness in biomolecular systems. *Mol. Cell* 28, 755–760. doi: 10.1016/j.molcel.2007.11.013

Barkai, N., and Shilo, B.-Z. (2009). Robust generation and decoding of morphogen gradients. *Cold Spring Harb. Perspect. Biol.* 1, a001990. doi: 10.1101/cshperspect.a001990

Berman, B. P., Nibu, Y., Pfeiffer, B. D., Tomancak, P., Celniker, S. E., Levine, M., et al. (2002). Exploiting transcription factor binding site clustering to identify cis-regulatory modules involved in pattern formation in the *Drosophila* genome. *Proc. Natl. Acad. Sci. U. S. A.* 99, 757–762. doi: 10.1073/pnas.231608898

Bertrand, N., Castro, D. S., and Guillemot, F. (2002). Proneural genes and the specification of neural cell types. *Nat. Rev. Neurosci.* 3, 517–530. doi: 10.1038/nrn874

Bittermann, E., Abdelhamed, Z., Liegel, R. P., Menke, C., Timms, A., Beier, D. R., et al. (2019). Differential requirements of tubulin genes in mammalian forebrain development. *PLoS Genet.* 15, e1008243. doi: 10.1371/journal.pgen.1008243

Bocci, F., Onuchic, J. N., and Jolly, M. K. (2020). Understanding the principles of pattern formation driven by notch signaling by integrating experiments and theoretical models. *Front. Physiol.* 11, 929. doi: 10.3389/fphys.2020.00929

Cannavò, E., Khoueiry, P., Garfield, D. A., Geeleher, P., Zichner, T., Gustafson, E. H., et al. (2016). Shadow enhancers are pervasive features of developmental regulatory networks. *Curr. Biol.* 26, 38–51. doi: 10.1016/j.cub.2015.11.034

Carro, M. S., Lim, W. K., Alvarez, M. J., Bollo, R. J., Zhao, X., Snyder, E. Y., et al. (2010). The transcriptional network for mesenchymal transformation of brain tumours. *Nature* 463, 318–325. doi: 10.1038/nature08712

Cassidy, J. J., Jha, A. R., Posadas, D. M., Giri, R., Venken, K. J. T., Ji, J., et al. (2013). miR-9a minimizes the phenotypic impact of genomic diversity by buffering a transcription factor. *Cell* 155, 1556–1567. doi: 10.1016/j.cell.2013.10.057

Chahrour, M., and Zoghbi, H. Y. (2007). The story of Rett syndrome: From clinic to neurobiology. *Neuron* 56, 422–437. doi: 10.1016/j.neuron.2007.10.001

Chapman, H., Riesenberg, A., Ehrman, L. A., Kohli, V., Nardini, D., Nakafuku, M., et al. (2018). Gsx transcription factors control neuronal versus glial specification in ventricular zone progenitors of the mouse lateral ganglionic eminence. *Dev. Biol.* 442, 115–126. doi: 10.1016/j.ydbio.2018.07.005

Chen, Y., and Struhl, G. (1996). Dual roles for patched in sequestering and transducing Hedgehog. *Cell* 87, 553–563. doi: 10.1016/S0092-8674(00)81374-4

Clelland, C. D., Choi, M., Romberg, C., Clemenson, G. D., Fragniere, A., Tyers, P., et al. (2009). A functional role for adult hippocampal neurogenesis in spatial pattern separation. *Science* 325, 210–213. doi: 10.1126/science.1173215

Conant, G. C., and Wagner, A. (2003). Convergent evolution of gene circuits. *Nat. Genet.* 34, 264–266. doi: 10.1038/ng1181

de Pontual, L., Yao, E., Callier, P., Faivre, L., Drouin, V., Cariou, S., et al. (2011). Germline deletion of the miR-17∼92 cluster causes skeletal and growth defects in humans. *Nat. Genet.* 43, 1026–1030. doi: 10.1038/ng.915

de Visser, J. A. G. M., Hermisson, J., Wagner, G. P., Meyers, L. A., Bagheri-Chaichian, H., Blanchard, J. L., et al. (2003). Perspective: Evolution and detection of genetic robustness. *Evolution* 57, 1959–1972. doi: 10.1111/j.0014-3820.2003.tb00377.x

Degenhardt, K. R., Milewski, R. C., Padmanabhan, A., Miller, M., Singh, M. K., Lang, D., et al. (2010). Distinct enhancers at the Pax3 locus can function redundantly to regulate neural tube and neural crest expressions. *Dev. Biol.* 339, 519–527. doi: 10.1016/j.ydbio.2009.12.030

Delás, M. J., Kalaitzis, C. M., Fawzi, T., Demuth, M., Zhang, I., Stuart, H. T., et al. (2022). Developmental cell fate choice in neural tube progenitors employs two distinct cis-regulatory strategies. *Dev. Cell* 2022, S1534580722008164. doi: 10.1101/2022.06.06.494792

Denoth-Lippuner, A., and Jessberger, S. (2021). Formation and integration of new neurons in the adult hippocampus. *Nat. Rev. Neurosci.* 22, 223–236. doi: 10.1038/s41583-021-00433-z

Despang, A., Schöpflin, R., Franke, M., Ali, S., Jerkovi,ć, I., Paliou, C., et al. (2019). Functional dissection of the Sox9–Kcnj2 locus identifies nonessential and instructive roles of TAD architecture. *Nat. Genet.* 51, 1263–1271. doi: 10.1038/s41588-019-0466-z

Dessaud, E., Ribes, V., Balaskas, N., Yang, L. L., Pierani, A., Kicheva, A., et al. (2010). Dynamic assignment and maintenance of positional identity in the ventral neural tube by the morphogen Sonic Hedgehog. *PLoS Biol.* 8, e1000382. doi: 10.1371/journal.pbio.1000382

Dessaud, E., Yang, L. L., Hill, K., Cox, B., Ulloa, F., Ribeiro, A., et al. (2007). Interpretation of the Sonic Hedgehog morphogen gradient by a temporal adaptation mechanism. *Nature* 450, 717–720. doi: 10.1038/nature06347

Dragich, J., Houwink-Manville, I., and Schanen, C. (2000). Rett syndrome: A surprising result of mutation in MECP2. *Hum. Mol. Genet.* 9, 2365–2375. doi: 10.1093/hmg/9.16.2365

Ebert, M. S., and Sharp, P. A. (2012). Roles for MicroRNAs in conferring robustness to biological processes. *Cell* 149, 515–524. doi: 10.1016/j.cell.2012.04.005

Edwards, S. L., Beesley, J., French, J. D., and Dunning, A. M. (2013). Beyond GWASs: Illuminating the dark road from association to function. *Am. J. Hum. Genet.* 93, 779–797. doi: 10.1016/j.ajhg.2013.10.012

Einarsson, H., Salvatore, M., Vaagenso, C., Alcaraz, N., Bornholdt Lange, J., Rennie, S., et al. (2022). Promoter sequence and architecture determine expression variability and confer robustness to genetic variants. *eLife* 11, e80943. doi: 10.7554/eLife.80943.sa2

Eldar, A., Dorfman, R., Weiss, D., et al. (2002). Robustness of the BMP morphogen gradient in Drosophila embryonic patterning. *Nature.* 419, 304–308. doi: 10.1038/nature01061

Enriquez, J., Rio, L. Q., Blazeski, R., Bellemin, S., Godement, P., Mason, C., et al. (2018). Differing strategies despite shared lineages of motor neurons and glia to achieve robust development of an adult neuropil in *Drosophila*. *Neuron* 97, 538–554.e5. doi: 10.1016/j.neuron.2018.01.007

Ernst, A., Alkass, K., Bernard, S., Salehpour, M., Perl, S., Tisdale, J., et al. (2014). Neurogenesis in the striatum of the adult human brain. *Cell* 156, 1072–1083. doi: 10.1016/j.cell.2014.01.044

Falk, S., and Götz, M. (2017). Glial control of neurogenesis. *Curr. Opin. Neurobiol.* 47, 188–195. doi: 10.1016/j.conb.2017.10.025

Félix, M.-A., and Wagner, A. (2008). Robustness and evolution: Concepts, insights and challenges from a developmental model system. *Heredity* 100, 132–140. doi: 10.1038/sj.hdy.6800915

Ferent, J., Giguère, F., Jolicoeur, C., Morin, S., Michaud, J.-F., Makihara, S., et al. (2019). Boc acts *via* numb as a Shh-dependent endocytic platform for Ptch1 internalization and Shh-mediated axon guidance. *Neuron* 102, 1157–1171.e5. doi: 10.1016/j.neuron.2019.04.003

Frankel, N., Davis, G. K., Vargas, D., Wang, S., Payre, F., and Stern, D. L. (2010). Phenotypic robustness conferred by apparently redundant transcriptional enhancers. *Nature* 466, 490–493. doi: 10.1038/nature09158

Gaugler, T., Klei, L., Sanders, S. J., Bodea, C. A., Goldberg, A. P., Lee, A. B., et al. (2014). Most genetic risk for autism resides with common variation. *Nat. Genet.* 46, 881–885. doi: 10.1038/ng.3039

Ghosh, T., Aprea, J., Nardelli, J., Engel, H., Selinger, C., Mombereau, C., et al. (2014). MicroRNAs establish robustness and adaptability of a critical gene network to regulate progenitor fate decisions during cortical neurogenesis. *Cell Rep.* 7, 1779–1788. doi: 10.1016/j.celrep.2014.05.029

Gibson, G. (2009). Decanalization and the origin of complex disease. *Nat. Rev. Genet.* 10, 134–140. doi: 10.1038/nrg2502

Gibson, G., and Dworkin, I. (2004). Uncovering cryptic genetic variation. *Nat. Rev. Genet.* 5, 681–690. doi: 10.1038/nrg1426

Goodrich, L. V., Johnson, R. L., Milenkovic, L., McMahon, J. A., and Scott, M. P. (1996). Conservation of the Hedgehog/patched signaling pathway from flies to mice: Induction of a mouse patched gene by Hedgehog. *Genes Dev.* 10, 301–312. doi: 10.1101/gad.10.3.301

Hartman, J. L., Garvik, B., and Hartwell, L. (2001). Principles for the buffering of genetic variation. *Science* 291, 1001–1004. doi: 10.1126/science.1056072

Hernandez-Miranda, L. R., Müller, T., and Birchmeier, C. (2017). The dorsal spinal cord and hindbrain: From developmental mechanisms to functional circuits. *Dev. Biol.* 432, 34–42. doi: 10.1016/j.ydbio.2016.10.008

Hiesinger, P. R., and Hassan, B. A. (2018). The evolution of variability and robustness in neural development. *Trends Neurosci.* 41, 577–586. doi: 10.1016/j.tins.2018.05.007

Irons, D. J., Wojcinski, A., Glise, B., and Monk, N. A. M. (2010). Robustness of positional specification by the Hedgehog morphogen gradient. *Dev. Biol.* 180–93. doi: 10.1016/j.ydbio.2010.03.022

Jang, H., Shin, W., Lee, J., and Do, J. (2017). CpG and Non-CpG methylation in epigenetic gene regulation and brain function. *Genes* 8, 148. doi: 10.3390/genes8060148

Jeong, Y., El-Jaick, K., Roessler, E., Muenke, M., and Epstein, D. J. (2006). A functional screen for sonic hedgehog regulatory elements across a 1 Mb interval identifies long-range ventral forebrain enhancers. *Development* 133, 761–772. doi: 10.1242/dev.02239

Keightley, P. D. (2012). Rates and fitness consequences of new mutations in humans. *Genetics* 190, 295–304. doi: 10.1534/genetics.111.134668

Kirschner, M., and Gerhart, J. (1998). Evolvability. *Proc. Natl. Acad. Sci. U. S. A.* 95, 8420–8427. doi: 10.1073/pnas.95.15.8420

Kise, Y., and Schmucker, D. (2013). Role of self-avoidance in neuronal wiring. *Curr. Opin. Neurobiol.* 23, 983–989. doi: 10.1016/j.conb.2013.09.011

Kronquist, K. E., Sherman, S. L., and Spector, E. B. (2008). Clinical significance of tri-nucleotide repeats in Fragile X testing: A clarification of American College of Medical Genetics guidelines. *Genet. Med.* 10, 845–847. doi: 10.1097/GIM.0b013e31818c2606

Kvon, E. Z., Waymack, R., Gad, M., and Wunderlich, Z. (2021). Enhancer redundancy in development and disease. *Nat. Rev. Genet.* 22, 324–336. doi: 10.1038/s41576-020-00311-x

Lathia, J. D., Mattson, M. P., and Cheng, A. (2008). Notch: From neural development to neurological disorders. *J. Neurochem.* 107, 1471–1481. doi: 10.1111/j.1471-4159.2008.05715.x

Lawrence Zipursky, S., and Grueber, W. B. (2013). The molecular basis of self-avoidance. *Annu. Rev. Neurosci.* 36, 547–568. doi: 10.1146/annurev-neuro-062111-150414

Li, Y., Wang, F., Lee, J.-A., and Gao, F.-B. (2006). MicroRNA-9a ensures the precise specification of sensory organ precursors in *Drosophila*. *Genes Dev.* 20, 2793–2805. doi: 10.1101/gad.1466306

Lowell, S., Benchoua, A., Heavey, B., and Smith, A. G. (2006). Notch promotes neural lineage entry by pluripotent embryonic stem cells. *PLoS Biol.* 4, e121. doi: 10.1371/journal.pbio.0040121

Mangan, S., and Alon, U. (2003). Structure and function of the feed-forward loop network motif. *Proc. Natl. Acad. Sci. U. S. A.* 100, 11980–11985. doi: 10.1073/pnas.2133841100

Marigo, V., and Tabin, C. J. (1996). Regulation of patched by sonic hedgehog in the developing neural tube. *Proc. Natl. Acad. Sci. U. S. A.* 93, 9346–9351. doi: 10.1073/pnas.93.18.9346

Maury, Y., Côme, J., Piskorowski, R. A., Salah-Mohellibi, N., Chevaleyre, V., Peschanski, M., et al. (2015). Combinatorial analysis of developmental cues efficiently converts human pluripotent stem cells into multiple neuronal subtypes. *Nat. Biotechnol.* 33, 89–96. doi: 10.1038/nbt.3049

McGrath, J. J., Hannan, A. J., and Gibson, G. (2011). Decanalization, brain development and risk of schizophrenia. *Transl. Psychiatry* 1, e14–e14. doi: 10.1038/tp.2011.16

Mira, H., and Morante, J. (2020). Neurogenesis from embryo to adult – Lessons from flies and mice. *Front. Cell Dev. Biol.* 8, 533. doi: 10.3389/fcell.2020.00533

Moreno-Jiménez, E. P., Flor-García, M., Terreros-Roncal, J., Rábano, A., Cafini, F., Pallas-Bazarra, N., et al. (2019). Adult hippocampal neurogenesis is abundant in

neurologically healthy subjects and drops sharply in patients with Alzheimer's disease. *Nat. Med.* 25, 554–560. doi: 10.1038/s41591-019-0375-9

Nakashiba, T., Cushman, J. D., Pelkey, K. A., Renaudineau, S., Buhl, D. L., McHugh, T. J., et al. (2012). Young dentate granule cells mediate pattern separation, whereas old granule cells facilitate pattern completion. *Cell* 149, 188–201. doi: 10.1016/j.cell.2012.01.046

Nolin, S. L., Lewis, F. A., Ye, L. L., Houck, G. E., Glicksman, A. E., Limprasert, P., et al. (1996). Familial transmission of the FMR1 CGG repeat. *Am. J. Hum. Genet.* 59, 1252–1261.

Ohtsuka, T., and Kageyama, R. (2019). Regulation of temporal properties of neural stem cells and transition timing of neurogenesis and gliogenesis during mammalian neocortical development. *Semin. Cell Dev. Biol.* 95, 4–11. doi: 10.1016/j.semcdb.2019.01.007

Oosterveen, T., Kurdija, S., Alekseenko, Z., Uhde, C. W., Bergsland, M., Sandberg, M., et al. (2012). Mechanistic differences in the transcriptional interpretation of local and long-range Shh morphogen signaling. *Dev. Cell* 23, 1006–1019. doi: 10.1016/j.devcel.2012.09.015

Paliou, C., Guckelberger, P., Schöpflin, R., Heinrich, V., Esposito, A., Chiariello, A. M., et al. (2019). Preformed chromatin topology assists transcriptional robustness of *Shh* during limb development. *Proc. Natl. Acad. Sci. U. S. A.* 116, 12390–12399. doi: 10.1073/pnas.1900672116

Paredes, M. F., Sorrells, S. F., Cebrian-Silla, A., Sandoval, K., Qi, D., Kelley, K. W., et al. (2018). Does adult neurogenesis persist in the human hippocampus? *Cell Stem Cell* 23, 780–781. doi: 10.1016/j.stem.2018.11.006

Parikshak, N. N., Gandal, M. J., and Geschwind, D. H. (2015). Systems biology and gene networks in neurodevelopmental and neurodegenerative disorders. *Nat. Rev. Genet.* 16, 441–458. doi: 10.1038/nrg3934

Payne, J. L., and Wagner, A. (2014). The robustness and evolvability of transcription factor binding sites. *Science* 343, 875–877. doi: 10.1126/science.1249046

Payne, J. L., and Wagner, A. (2015). Mechanisms of mutational robustness in transcriptional regulation. *Front. Genet.* 6, 322. doi: 10.3389/fgene.2015.00322

Perrimon, N., Pitsouli, C., and Shilo, B.-Z. (2012). Signaling mechanisms controlling cell fate and embryonic patterning. *Cold Spring Harb. Perspect. Biol.* 4, a005975. doi: 10.1101/cshperspect.a005975

Qian, X., Shen, Q., Goderie, S. K., He, W., Capela, A., Davis, A. A., et al. (2000). Timing of CNS cell generation: A programmed sequence of neuron and glial cell production from isolated murine cortical stem cells. *Neuron* 28, 69–80. doi: 10.1016/S0896-6273(00)00086-6

Rogers, K. W., and Schier, A. F. (2011). Morphogen gradients: From generation to interpretation. *Annu. Rev. Cell Dev. Biol.* 27, 377–407. doi: 10.1146/annurev-cellbio-092910-154148

Sagner, A., and Briscoe, J. (2017). Morphogen interpretation: Concentration, time, competence, and signaling dynamics. *Wiley Interdiscip. Rev. Dev. Biol.* 6, e271. doi: 10.1002/wdev.271

Sagner, A., and Briscoe, J. (2019). Establishing neuronal diversity in the spinal cord: A time and a place. *Development* 146, dev182154. doi: 10.1242/dev.182154

Sahay, A., Scobie, K. N., Hill, A. S., O'Carroll, C. M., Kheirbek, M. A., Burghardt, N. S., et al. (2011). Increasing adult hippocampal neurogenesis is sufficient to improve pattern separation. *Nature* 472, 466–470. doi: 10.1038/nature09817

Sato, A. (2018). Chaperones, canalization, and evolution of animal forms. *Int. J. Mol. Sci.* 19, 3029. doi: 10.3390/ijms19103029

Scharloo, W. (1991). Canalization: Genetic and developmental aspects. *Annu. Rev. Ecol. Syst.* 22, 65–93. doi: 10.1146/annurev.es.22.110191.000433

Schor, I. E., Degner, J. F., Harnett, D., Cannavò, E., Casale, F. P., Shim, H., et al. (2017). Promoter shape varies across populations and affects promoter evolution and expression noise. *Nat. Genet.* 49, 550–558. doi: 10.1038/ng.3791

Sigalova, O. M., Shaeiri, A., Forneris, M., Furlong, E. E., and Zaugg, J. B. (2020). Predictive features of gene expression variation reveal mechanistic link with differential expression. *Mol. Syst. Biol.* 16, e9539. doi: 10.15252/msb.20209539

Silbereis, J. C., Pochareddy, S., Zhu, Y., Li, M., and Sestan, N. (2016). The cellular and molecular landscapes of the developing human central nervous system. *Neuron* 89, 248–268. doi: 10.1016/j.neuron.2015.12.008

Sjöqvist, M., and Andersson, E. R. (2019). Do as I say, Not(ch) as I do: Lateral control of cell fate. *Dev. Biol.* 447, 58–70. doi: 10.1016/j.ydbio.2017.09.032

Song, W., and Ovcharenko, I. (2018). Dichotomy in redundant enhancers points to presence of initiators of gene regulation. *BMC Genom.* 19, 947. doi: 10.1186/s12864-018-5335-0

Sorrells, S. F., Paredes, M. F., Cebrian-Silla, A., Sandoval, K., Qi, D., Kelley, K. W., et al. (2018). Human hippocampal neurogenesis drops sharply in children to undetectable levels in adults. *Nature* 555, 377–381. doi: 10.1038/nature25975

Sperry, R. W. (1963). Chemoaffinity in the orderly growth of nerve fiber patterns and connections. *Proc. Natl. Acad. Sci. U. S. A.* 50, 703–710. doi: 10.1073/pnas.50.4.703

Temple, S. (2001). The development of neural stem cells. *Nature* 414, 112–117. doi: 10.1038/35102174

Tobin, M. K., Musaraca, K., Disouky, A., Shetti, A., Bheri, A., Honer, W. G., et al. (2019). Human hippocampal neurogenesis persists in aged adults and Alzheimer's disease patients. *Cell Stem Cell* 24, 974-982.e3. doi: 10.1016/j.stem.2019.05.003

Torbey, P., Thierion, E., Collombet, S., de Cian, A., Desmarquet-Trin-Dinh, C., Dura, M., et al. (2018). Cooperation, cis-interactions, versatility and evolutionary plasticity of multiple cis-acting elements underlie krox20 hindbrain regulation. *PLoS Genet.* 14, e1007581. doi: 10.1371/journal.pgen.1007581

Tsang, J., Zhu, J., and van Oudenaarden, A. (2007). MicroRNA-mediated feedback and feedforward loops are recurrent network motifs in mammals. *Mol. Cell* 26, 753–767. doi: 10.1016/j.molcel.2007.05.018

Tutukova, S., Tarabykin, V., and Hernandez-Miranda, L. R. (2021). The role of neurod genes in brain development, function, and disease. *Front. Mol. Neurosci.* 14, 662774. doi: 10.3389/fnmol.2021.662774

Urban, E. A., and Johnston, R. J., Jr. (2018). Buffering and amplifying transcriptional noise during cell fate specification. *Front. Genet.* 9, 591. doi: 10.3389/fgene.2018.00591

Vetter, R., and Iber, D. (2022). Precision of morphogen gradients in neural tube development. *Nat. Commun.* 13, 1145. doi: 10.1038/s41467-022-28834-3

Villalba, A., Götz, M., and Borrell, V. (2021). "The regulation of cortical neurogenesis," in *Current Topics in Developmental Biology*. ed G. J. Bashaw (Amsterdam: Elsevier), 1–66. doi: 10.1016/bs.ctdb.2020.10.003

Vokes, S. A., Ji, H., Wong, W. H., and McMahon, A. P. (2008). A genome-scale analysis of the *cis* -regulatory circuitry underlying sonic hedgehog-mediated patterning of the mammalian limb. *Genes Dev.* 22, 2651–2663. doi: 10.1101/gad.1693008

Waddington, C. H. (1942). Canalization of development and the inheritance of acquired characters. *Nature* 150, 563–565. doi: 10.1038/150563a0

Wit, C. B., and Hiesinger, P. R. (2023). Neuronal filopodia: From stochastic dynamics to robustness of brain morphogenesis. *Semin. Cell Dev. Biol.* 133, 10–19. doi: 10.1016/j.semcdb.2022.03.038

Xia, Y., Cui, K., Alonso, A., Lowenstein, E. D., and Hernandez-Miranda, L. R. (2022). Transcription factors regulating the specification of brainstem respiratory neurons. *Front. Mol. Neurosci.* 15, 1072475. doi: 10.3389/fnmol.2022.1072475

Young, J. I., and Zoghbi, H. Y. (2004). X-chromosome inactivation patterns are unbalanced and affect the phenotypic outcome in a mouse model of Rett syndrome. *Am. J. Hum. Genet.* 74, 511–520. doi: 10.1086/382228

frontiers | Frontiers in Molecular Neuroscience

TYPE Original Research
PUBLISHED 03 March 2023
DOI 10.3389/fnmol.2023.1130249

OPEN ACCESS

EDITED BY
Wolfgang Baehr,
The University of Utah, United States

REVIEWED BY
T. Michael Redmond,
National Eye Institute (NIH), United States
Orson Lutz Moritz,
University of British Columbia,
Canada
Monica Akula,
Otopathology Laboratory,
Massachusetts Eye and Ear Infirmary,
Harvard Medical School,
United States

*CORRESPONDENCE
Riccardo Natoli
✉ Riccardo.natoli@anu.edu.au

SPECIALTY SECTION
This article was submitted to
Molecular Signalling and Pathways,
a section of the journal
Frontiers in Molecular Neuroscience

RECEIVED 23 December 2022
ACCEPTED 13 February 2023
PUBLISHED 03 March 2023

CITATION
Aggio-Bruce R, Schumann U, Cioanca AV, Chen FK, McLenachan S, Heath Jeffery RC, Das S and Natoli R (2023) Serum miRNA modulations indicate changes in retinal morphology.
Front. Mol. Neurosci. 16:1130249.
doi: 10.3389/fnmol.2023.1130249

Serum miRNA modulations indicate changes in retinal morphology

Riemke Aggio-Bruce[1,2], Ulrike Schumann[1,3], Adrian V. Cioanca[1], Fred K. Chen[4,5,6,7], Samuel McLenachan[4,5], Rachael C. Heath Jeffery[4,5,7], Shannon Das[1] and Riccardo Natoli[1,2]*

[1]The John Curtin School of Medical Research, The Australian National University, Acton, ACT, Australia, [2]The School of Medicine and Psychology, Acton, ACT, Australia, [3]The Save Sight Institute, Faculty of Medicine and Health, The University of Sydney, Sydney, NSW, Australia, [4]Centre of Ophthalmology and Visual Science, The University of Western Australia, Perth, WA, Australia, [5]Lions Eye Institute, Perth, WA, Australia, [6]Ophthalmology, Department of Surgery, University of Melbourne, East Melbourne, VIC, Australia, [7]Centre for Eye Research Australia, Royal Victorian Eye and Ear Hospital, East Melbourne, VIC, Australia

Background: Age-related macular degeneration (AMD) is the leading cause of vision loss in the developed world and the detection of its onset and progression are based on retinal morphological assessments. MicroRNA (miRNA) have been explored extensively as biomarkers for a range of neurological diseases including AMD, however differences in experimental design and the complexity of human biology have resulted in little overlap between studies. Using preclinical animal models and clinical samples, this study employs a novel approach to determine a serum signature of AMD progression.

Methods: Serum miRNAs were extracted from mice exposed to photo-oxidative damage (PD; 0, 1, 3 and 5days), and clinical samples from patients diagnosed with reticular pseudodrusen or atrophic AMD. The expression of ~800 miRNAs was measured using OpenArray™, and differential abundance from controls was determined using the HTqPCR R package followed by pathway analysis with DAVID. MiRNA expression changes were compared against quantifiable retinal histological indicators. Finally, the overlap of miRNA changes observed in the mouse model and human patient samples was investigated.

Results: Differential miRNA abundance was identified at all PD time-points and in clinical samples. Importantly, these were associated with inflammatory pathways and histological changes in the retina. Further, we were able to align findings in the mouse serum to those of clinical patients.

Conclusion: In conclusion, serum miRNAs are a valid tool as diagnostics for the early detection of retinal degeneration, as they reflect key changes in retinal health. The combination of pre-clinical animal models and human patient samples led to the identification of a preliminary serum miRNA signature for AMD. This study is an important platform for the future development of a diagnostic serum miRNA panel for the early detection of retinal degeneration.

KEYWORDS

age-related macular degeneration, microRNA, diagnostics, serum miRNAs, neurodegeneration

1. Introduction

Age-related macular degeneration (AMD) is the leading cause of irreversible blindness in the elderly population in the western world (Klein et al., 2007; Heath Jeffery et al., 2021). In many cases, the disease is slow progressing and chronic with early stages presenting as relatively asymptomatic (Deloitte Access Economics et al., 2011). Current diagnosis and disease grading is predominantly based on the presentation of small, subretinal lipid deposits called drusen, pigment changes in the central macular region, and self-reported scotomas or 'blind spots' (Fine et al., 2000; Klein et al., 2007; Ardeljan and Chan, 2013). In addition, a newly classified form of drusen, reticular pseudodrusen (RPD), has demonstrated clinical significance as a risk factor of progression to one of two forms of late-stage AMD, atrophic AMD (geographic atrophy (GA)) or neovascular AMD (Boddu et al., 2014; Domalpally et al., 2019). However, retinal imaging is used for clinical stratification and therefore is of little use in understanding molecular complexity of AMD, especially when considering that molecular events likely precede histopathological changes. Thus, we propose a combinatorial approach that utilizes both imaging data and serum biomarkers, which is easily explored in pre-clinical animal models as these limit the variability derived from confounding factors such as co-morbidities. The photo-oxidative damage (PD) mouse model, which exposes the rodent retina to bright light (Natoli et al., 2016), has been used extensively to explore molecular facets common to AMD, including oxidative stress, chemokine response, activation of the complement cascade, and immune cell recruitment (Noell et al., 1966; Chen et al., 2004; White et al., 2007; O'Koren et al., 2016; Song et al., 2017). Thus, the model provides a controlled system, enabling detailed investigation into the nuanced molecular changes and their correlations to retinal disease progression especially regarding retinal inflammatory diseases, such as AMD.

MicroRNAs (miRNA) have been shown to be regulated in response to retinal degenerations (Saxena et al., 2015; Chu-Tan et al., 2018; Fernando et al., 2020; Aggio-Bruce et al., 2021; Chu-Tan et al., 2021). MiRNAs are short non-coding RNAs that repress messenger RNA (mRNA) translation by binding to their 3′ untranslated region (Andreeva and Cooper, 2014). As only a short region of complementarity is required for binding, a single miRNA can regulate a large number of targets, often within the same biological pathway (Bandyra Katarzyna et al., 2012). Consequently, miRNAs control almost all biological processes in health and disease and are highly conserved across species (Lu et al., 2008; McCreight et al., 2017). Because of their regulatory role, the modulation of miRNAs also occurs in disease (Askou et al., 2017; Berber et al., 2017; Romano et al., 2017; Chu-Tan et al., 2018), making them ideal targets to determine disease states. Therefore, miRNAs have been explored as a diagnostic tool in many biological systems (Chen et al., 2008; Gilad et al., 2008; Mitchell et al., 2008; Roy and Sen, 2011; Weiland et al., 2012), including the retina (Ertekin et al., 2014; Grassmann et al., 2014; Szemraj et al., 2015; Ménard et al., 2016; Berber et al., 2017; Ren et al., 2017; Romano et al., 2017; Szemraj et al., 2017; ElShelmani et al., 2020). Additionally, miRNAs are abundant in biofluids including tears, saliva, urine, plasma, and serum, making them easily accessible using minimally invasive methods (Chen et al., 2008; Mitchell et al., 2008; McDonald et al., 2011). Further, serum miRNAs are highly stable due to resistance to ribonuclease digestion, integration with RNA-binding proteins and incorporation into extracellular nanovesicles, including exosomes (Chen et al., 2008; Jung et al., 2010; Arroyo et al., 2011; Sanz-Rubio et al., 2018). This high stability and their role in pathology has accelerated research into miRNAs as prognostic tools for disease such as cancer, cardiovascular disease, and neurodegenerative diseases, including retinal degenerations (Chen et al., 2008; Gilad et al., 2008; Lu et al., 2008; Mitchell et al., 2008; McManus and Ambros, 2011; Lukiw et al., 2012; Grasso et al., 2014).

During the last decade, studies into the use of miRNAs as a biomarker for AMD has identified numerous candidates for disease prediction (Grassmann et al., 2014; Szemraj et al., 2015; Ménard et al., 2016; Berber et al., 2017; Ren et al., 2017; Romano et al., 2017). However, due to differing methodologies in the fractionation and collection of samples [serum, tears and plasma (Berber et al., 2017; Roser et al., 2018; Felekkis and Papaneophytou, 2020)], complexities in histological presentation, and the presence of co-morbidities, there is little consensus between studies (Keller et al., 2017). Additionally, a limitation of these studies has been their primary focus on intermediate to late stages of retinal degeneration (Grassmann et al., 2014; Ren et al., 2017; Romano et al., 2017; Elbay et al., 2019; ElShelmani et al., 2020), with little reported for early disease manifestation. However, the development of a diagnostic panel that can identify changes in circulation that reflect early retinal degenerations is essential for successful therapeutic intervention.

In the current study, global serum miRNA analysis was performed to elucidate potential circulating biomarkers for AMD disease progression. Using the pre-clinical PD model, we identified circulating miRNA changes that correlated to changes in overall retinal miRNA expression and abundance. MiRNAs dysregulated as a consequence of progressive degeneration were further associated with inflammatory and apoptosis pathways. Moreover, samples of patients with RPD or GA demonstrated changes in miRNA abundance which correlated to retinal volume. We found the expression of several serum miRNAs, including miR-26a/b-5p, let-7d-5p, miR-19a-3p and miR-574-3p, to be similarly altered in both clinical and PD samples, demonstrating the suitability of this study in overcoming the limitations of current biomarker development. Taken together, these results demonstrate a serum miRNA signature, important for the early detection of retinal degeneration.

2. Materials and methods

2.1. Animal handling and photo-oxidative damage

All experiments were conducted in accordance with the ARVO Statement for Use of Animals in Ophthalmic and Vision Research. The study was approved by the Australian National University (ANU) Animal Experimentation Ethics Committee (Application ID: 2017/41).

Abbreviations: AMD, age related macular degeneration; ARVO, association for research in vision and ophthalmology; ANU, Australian National University; DR, dim-reared; GA, geographic atrophy; IBA-1, ionized calcium-binding adaptor molecule 1; INL, inner nuclear layer; miRNA, microRNA; ONL, outer nuclear layer; PD, photo-oxidative damage; RPD, reticular pseudodrusen; TUNEL, terminal deoxynucleotidyl transferase dUTP nick end labeling.

C57BL/6J mice (Jackson Laboratories, MA, United States) were raised in dim (5 lux), 12-h cyclic light conditions, and were used as dim-reared (DR) controls for this study. To induce PD, C57BL/6J mice at postnatal day 60 were exposed to 100 K lux natural emission LED light for 1, 3 and 5 days with free access to food and water. Animals were euthanised by administration of CO_2, and eyes and retinas collected and processed for histological and molecular analysis as described previously (Natoli et al., 2016). Whole blood was collected from the left eye into 1.5 ml Eppendorf tubes (Eppendorf, Germany) by a qualified technician, *via* retro-orbital bleeds using non-heparinised capillary tubes. Serum was separated by first clotting whole blood samples at room temperature for 20 min followed by centrifugation at 1000 x g for 10 min at 4°C.

To control for possible circadian rhythm and gender effects, blood was collected at the same time each day and female animals only were used across the experimental groups. Four mice were used for each sample, with four to six samples per experimental group. Prior to starting this study, we obtained advice from the ANU Statistical Consulting Unit. We further considered the ANU's ethical requirements of replace, reduce, refine as well as Mead's resource equation of diminishing returns. Together, these suggested that our animal numbers are sufficient for these experiments. Histology was assessed for each rodent retina and the results averaged within each sample.

2.2. Clinical samples, ethics approval and consent to participate

This work adhered to the tenets of the Declaration of Helsinki and was approved by the University of Western Australia Human Research Ethics Committee (protocol: RA/4/1/7916 and 2021/ET000151). Patients were recruited through the Lions Eye Institute (Perth, Western Australia, Australia). Before commencing the study, written informed consent was obtained from the study participants.

Ten patients clinically diagnosed with the presence of reticular pseudodrusen in one or both eyes (early AMD; age: 76 ± 6 years), and five patients with late-stage AMD (geographic atrophy (GA); age: 74 ± 5 years) were included in this study (Supplementary Table S1). RPD diagnosis was made independently by two clinicians (FKC and RCHJ) and was based on the presence of five or more hyporeflective lesions using near-infrared reflectance imaging, which coincided with a hyperreflective deposit above the retinal pigment epithelium (RPE) using spectral domain-optic coherence tomography (SD-OCT) (Wu et al., 2016) imaging. GA was defined by a well demarcated area of outer retinal layer and RPE loss associated with hypoautofluorescence (Holz et al., 2017). The control group consisted of 10 age-matched (72 ± 2 years) participants with no signs of AMD or other retinal pathologies graded by the same clinicians. Venous blood was collected in sterile, dry vacutainer tubes and serum was separated by centrifugation at 2,000 x g for 15 min at 4°C. Serum was stored at-80°C until further processing.

Retinal images were processed using the Heidelberg Spectralis OCT software (Heidelberg Engineering, Germany). The outer nuclear layer (ONL) thickness was measured for each segment at a 1, 2.22, 3.45 mm diameter circles centered around the macular region. The 1 mm volume was used as an indicator of foveal integrity. As this small central zone is often spared in early stages of degeneration, the 3.45 mm volume was also measured as it encompassed the primary lesion on all patients.

2.3. TUNEL

Retinal cryosections, cut in the parasagittal plane, were prepared and cell death analyzed using a terminal deoxynucleotidyl transferase dUTP nick end labeling (TUNEL) kit (Roche Applied Science, Germany), as described previously (Natoli et al., 2010). For quantification of photoreceptor cell death, TUNEL$^+$ cells in the outer nuclear layer (ONL) were counted along the full length of the retinal section. For each animal, cells were counted in technical duplicate, averaging the counts for each sample group. Significance between the DR control and each PD time point was assessed by one-way ANOVA with Tukey's multiple comparison post-test.

2.4. IBA-1 Immunostaining

Immunohistochemical analysis of retinal cryosections was performed as described previously (Rutar et al., 2015). Immune cells were immunolabeled with primary mouse anti-rabbit IBA-1 (1:1000, Wako, Osaka, Japan) and secondary goat anti-rabbit Alexa 488 (1:500, Thermo Fisher Scientific, MA, United States). Quantification of IBA-1$^+$ cells was performed across the superior and inferior retina. The number of IBA-1$^+$ cells in the outer retina was quantified as the total counts in the ONL and subretinal space. Significance between the DR control and each PD time point was analyzed by one-way ANOVA with Tukey's multiple comparison post-test.

Nuclear layers were visualized by staining cryosections with bisbenzimide solution (1:10,000 of a 10 mg/ml stock; Calbiochem, United States). The ONL thickness was measured at increments of 600 µm across the entire retina, including the optic nerve head.

2.5. Confocal imaging

Fluorescence was visualized and captured using a ZEISS LSM800 with Airyscan Super-resolution confocal microscope (Carl Zeiss Microscopy, Germany). Images were obtained using uniform gain settings with excitation wavelengths of 488 nm (green; IBA-1 staining), 561 nm (red; TUNEL staining) and 358 nm (bisbenzimide), and processed using ZEISS Zen (blue edition) software.

2.6. miRNA extraction and cDNA preparation

Extraction and purification of miRNAs was performed using the miRVana miRNA isolation kit (Thermo Fisher Scientific) following the manufacturer's instructions. An Agilent 2,100 Bioanalyser with an Agilent small RNA kit (Agilent Technologies, United States) was used to test miRNA purity and concentration.

The OpenArray™ reverse transcription reaction and pre-amplification reaction was performed using the 'Optimized protocol with low sample input' (Thermo Fisher Scientific). Reverse transcription and pre-amplification reaction were cycled with a

standard PreAmp thermal cycling protocol with 16 cycles on a Veriti 96-well thermal cycler (Applied Biosystems, CA, United States).

2.7. OpenArray™

The PreAmp product was diluted 1:20 in 0.1X Tris-EDTA buffer (pH 8.0). OpenArray™ 384-well loading plates were prepared according to the manufacturer's instructions (Thermo Fisher Scientific). TaqMan™ OpenArray™ Rodent/Human MicroRNA panels were loaded using the OpenArray™ AccuFill™ loader system. Three samples were run on each Array, running four Arrays simultaneously. Post-run, quality control (QC) images were assessed for sample and plate inconsistencies and run quality. Arrays that did not pass QC were repeated.

2.8. miRNA OpenArray™ data processing

Both human and mouse miRNA OpenArray™ data were processed as follows: Ct data was filtered by first assigning an "undetermined" label to OpenArray™ wells that had amplification score < 1.24, Ct value >30 or were found outside the top/bottom 10% quantile of each group. MiRNAs with "undetermined" expression in more than 20% of the samples were subsequently removed (Supplementary Figure S1A). From a total of 747 miRNA assayed on the mouse array cards and 715 assayed on the human cards, 199 and 248 were retained after filtering, respectively. Remaining Ct values were imported into the HTqPCR R (Dvinge and Bertone, 2009) packages and normalized using rank invariant miRNAs as reference genes (Mar et al., 2009) then transferred to the *limma* (Ritchie et al., 2015) package for statistical modeling (Supplementary Figure S1B). Linear models were built using the lmFit function, then moderated t-statistics were computed using empirical Bayes moderation (eBayes function) and *p*-values and fold changes were extracted with top Table. The need for inclusion of covariates (experimental batch (array), age, sex) into linear regression models was assessed by (Klein et al., 2007) visually examining the association of each covariate with sample clusters identified by principal component analysis (Supplementary Figure S1C; Heath Jeffery et al., 2021) by observing the effect each covariate has on the distribution of p-values (Supplementary Figure S1D). Both the mouse and human data sets required adjustments for experimental batch, and additional corrections for age were necessary for the latter (Supplementary Figure S1C). Chord diagrams were generated using the circlize R package (Gu et al., 2014) and all other plots were generated using ggplot2 in R unless otherwise indicated.

2.9. Network and pathway analysis

The targets of differentially accumulated miRNAs in the 5 day PD samples and the GA patient samples were determined using miRNet (Chang et al., 2020) v2.0 using miRTarBase v8.0 genes as targets. The target list was filtered for interactions validated by HITS/PAR-CLIP and/or reporter assays. The DAVID functional annotation tool (Huang et al., 2009; Sherman et al., 2022) was used to determine the functional annotation clustering using GOTERM_BP/CC/MF_DIRECT, Reactome and Wikipathways. A minimum miRNA/mRNA network was created using miRNet by using differentially expressed miRNAs as seed nodes then the only mRNAs added to the network are those that create links between miRNA seed nodes. This ensures that each mRNA added to the network is targeted by at least two miRNAs.

2.10. Statistical analysis

Where expression was compared between two groups, an unpaired Student's *t*-test was performed and for group comparisons a one-way ANOVA with Tukey's *post hoc* test was used to determine significance. ANOVA analysis was performed using GraphPad Prism V8 (GraphPad Software, La Jolla, CA, United States). Statistical significance was determined by $p < 0.05$. Relationships between miRNA expression changes and histological measures were tested by Spearman's correlation using the rcorr function of the Hmisc R package using a loess fit for non-linear correlations (Harrell and Harrell, 2019) and $p < 0.01$ was used as significance threshold. Results from correlation analyzes were graphed with corrplot (Wei et al., 2017).

3. Results

3.1. Circulating miRNA profiles are altered in response to photo-oxidative damage

Our previous work using the PD model has consistently shown changes in retinal miRNA expression in response to degeneration (Saxena et al., 2015; Chu-Tan et al., 2018; Fernando et al., 2020; Aggio-Bruce et al., 2021; Chu-Tan et al., 2021). In this study we investigated if these changes could also be detected in serum, to investigate the utility of serum miRNAs as a diagnostic for retinal stress, particularly at early stages.

Serum samples were obtained from C57BL/6 J mice at day 0 (DR), 1, 3 and 5 days PD (Figure 1A). A total of five and seven miRNAs were found to be differentially abundant in serum from 1 day PD (Figure 1Bi; Supplementary Table S2A) and 3 days PD (Figure 1Bii; Supplementary Table S2B), respectively. This was markedly increased at 5 days PD with 61 miRNAs differentially abundant (Figure 1Biii; Supplementary Table S2C). Of these, 33 demonstrated a significant increase, with miR-342-3p showing the largest fold increase, while 28 miRNAs exhibited a significant decrease, with miR-20a showing the largest fold change ($p < 0.05$). Further, miRNAs with changing abundance at 1 day did not overlap with those differentially abundant at 3 or 5 days PD (Figure 1C). However, five of the seven miRNAs differentially abundant at 3 days were also differentially abundant at 5 days PD, comprising miR-214-3p, miR-574-3p, miR-434-3p, miR-26a-5p and miR-126a-3p.

Significantly differently abundant serum miRNAs at 5 days PD were submitted to miRNet (Chang et al., 2020) to identify interactions with validated target mRNAs. The target lists were then submitted to DAVID (Huang et al., 2009; Sherman et al., 2022) to identify associations with biological pathways. This revealed a strong association with immune response pathways, VEGF signaling as well as neuronal signaling terms (Figure 1D; Supplementary Table S3).

FIGURE 1
Serum miRNA profiles are altered in response to photo-oxidative damage (PD). **(A)** Schematic showing the experimental workflow. Whole blood was collected from mice at 1, 3 and 5days PD using dim-reared (DR) animals as control (i). Serum was separated and total RNA purified, enriching for small RNAs (ii). miRNA expression was analyzed using mouse OpenArrays (iii) and differential expression analysis performed between each PD group and the DR control (iv). n=4–6 samples. **(B)** Volcano plots showing differentially expressed miRNAs. Five, seven and 61 miRNAs were significantly (p<0.05) differentially expressed between DR and (i) 1day PD, (ii) 3days PD, and (iii) 5days PD, respectively. See also Table S 2. **(C)** Chord diagram showing overlap of differentially expressed miRNAs across all time points. Five miRNAs (miR-126a-3p, miR-26a-5p, miR-434-3p, miR-574-3p and miR-214-3p) were differentially expressed at both 3days and 5days PD. **(D)** Pathway analysis of mRNAs targeted by miRNAs differentially expressed at 5days PD. Targets were identified using miRNet and filtered for those validated by HITS/PAR-CLIP or reporter assays. Pathway analysis of validated targets was performed using DAVID and significantly enriched (p<0.05) pathways are associated with interleukin, and VEGF and neuronal signaling (see also Supplementary Table S3).

This data clearly indicates that detectable changes in serum miRNA composition do occur in early stages of retinal damage and are associated with known important molecular pathways involved in AMD. Further, this data revealed that miRNA dysregulation is progressively exacerbated across the PD paradigm, suggesting an association with the underlying pathology.

3.2. Circulating miRNA expression patterns correlates to histological changes in the retina

To understand whether the progressive serum miRNA changes are indeed indicative of the underlying retinal pathology, we investigated if changes in miRNA abundance could be correlated to specific histological measures, including thinning of the ONL (photoreceptor row count; Figure 2A), apoptosis (TUNEL$^+$ cell count; Figures 2B–F) and recruitment of immune cells into the outer retina (IBA-1$^+$ cell count; Figures 2G–K). The individual fold change per sample of all miRNAs was plotted against these histological measures and Spearman's correlation analysis was performed to identify miRNAs with significant correlation ($p < 0.05$; Supplementary Table S4; Supplementary Figure S2). Due to the large number of significant findings, only correlations with $p < 0.01$ are shown here. Photoreceptor row counts were found to correlate to 22 miRNAs (Figure 2L), with IBA-1$^+$ cell counts correlating to 25 miRNAs (Figure 2M) and TUNEL$^+$ cell counts showing significant correlation to 30 miRNAs (Figure 2N), which included miRNAs with known roles in the retina (shown in individual plots) such as miR-182, miR-182 and miR-26a.

Taken together, we show distinct correlations between serum miRNA changes and changes in retinal morphology, strongly suggesting that miRNAs are reflective of pathology. This highlights the need for further exploration into serum miRNA modulations in relation to the progression of retinal degeneration.

3.3. Circulating miRNAs are differentially accumulated in patients with reticular pseudodrusen and geographic atrophy

Serum samples were obtained from healthy individuals and patients diagnosed with reticular pseudodrusen (RPD) and geographic atrophy (GA) from the Lions Eye Institute (WA, Australia) and analyzed for relative miRNA levels (Figure 3A). We identified a significant difference in the abundance of nine miRNAs between healthy controls and RPD patients, with four upregulated and five downregulated (Figure 3Bi; Supplementary Table S5A; $p < 0.05$). Comparatively, there were a total of 43 miRNAs that were significantly differentially abundant between healthy controls and GA patients (Figure 3Bii; Supplementary Table S5B). Of these, 20 miRNAs were downregulated and 23 were upregulated. Comparison between RPD and GA patients revealed differential abundance of 26 miRNAs, with 11 downregulated and 15 upregulated in GA (Figure 3Biii; Supplementary Table S5C).

Several miRNAs were modulated in multiple groups (Figure 3C). Five miRNAs, miR-584-5p, miR-483-3p, miR-29b-3p, miR-17-5p and miR-155-5p, were modulated in both the healthy-GA and healthy-RPD comparisons, whereas 14 miRNAs were modulated in both the healthy-GA and RPD-GA comparisons. Interestingly, one miRNA, miR-21-5p, was found to be modulated in all three comparisons, with a-0.63 and-1.41 fold change in RPD and GA, respectively (Figure 3C; Supplementary Table S5).

To determine the biological pathways these differentially abundant miRNAs might play a role in, we performed pathway analysis using DAVID. As the number of differentially regulated miRNAs in RPD patients was insufficient for pathway analysis, we focussed on those dysregulated in GA. Significantly modulated serum miRNAs were submitted to miRNet (Chang et al., 2020) to identify interactions with validated target mRNAs before pathway analysis was performed. Enriched processes involved in transcription and protein activity were common to mRNA targets of both upregulated and downregulated miRNAs (Figure 3D; Supplementary Table S6). Pathways involved in infection response, TGF/SMAD signaling, and adaptive immune response were associated with mRNA targets of downregulated miRNAs, while MAPK, VEGF, NTRK and apoptosis signaling were associated with mRNA targets of upregulated miRNAs. Taken together, these findings aligned to those observed in the PD mouse model.

3.4. Modulation of miRNAs across patients correlates to retinal volume

As we were able to correlate changes in serum miRNA abundance to retinal morphology in the PD model, we asked whether serum miRNA changes are also indicative of patient retinal pathology. Representative fundus and optical coherence tomography (OCT) images demonstrated distinct retinal pathology between patients with drusen, RPD and atrophy/thinning of the outer retina (Figures 4A–D; Supplementary Table S7). The volume of the outer nuclear layer (ONL), at circle diameters; 1, 2.22, 3.45 mm centered around the macula, was measured using the Heidelberg spectralis software and correlated to miRNA expression (Supplementary Figure S3). The abundance changes of two miRNAs, miR-331-3p and miR-182-5p, were found to negatively correlate to the 1 mm diameter volume of the ONL (Figure 4E). The changes in abundance of 11 miRNAs correlated to the total volume of the ONL measured (3.45 mm diameter), three of which demonstrated a positive correlation (Figure 4F). This data demonstrates the potential for this type of analysis to be utilized as a strategy for predicting complex disease outcomes from serum miRNA abundance. However, future investigation using a larger sample size is required.

3.5. Modulated serum miRNAs show similarities between 5days PD and patients diagnosed with geographic atrophy

Although human and mouse gene expression profiles are distinct, our data clearly indicates similarities; not unexpected as the PD model recapitulates key aspects of AMD. Therefore, we asked whether using miRNAs that are dysregulated in both PD and human patients could be used to define a miRNA AMD disease signature. Firstly, we compared all miRNAs present in both datasets and identified 105 orthologous miRNAs (Figure 5A). Next, we plotted the differential abundance of all 105 human and mouse miRNAs, which revealed commonly modulated miRNAs (eight) in the 5-day PD and GA samples (Figure 5B). One miRNA, miR-574-3p, was significantly upregulated and seven miRNAs were significantly downregulated in both samples (Figures 5C,D). Minimum network analysis using miRNet revealed interactions with genes involved in transcription, inflammation and apoptosis (Figure 5E; Supplementary Table S6), strongly suggesting that these miRNAs are indicative of retinal pathology.

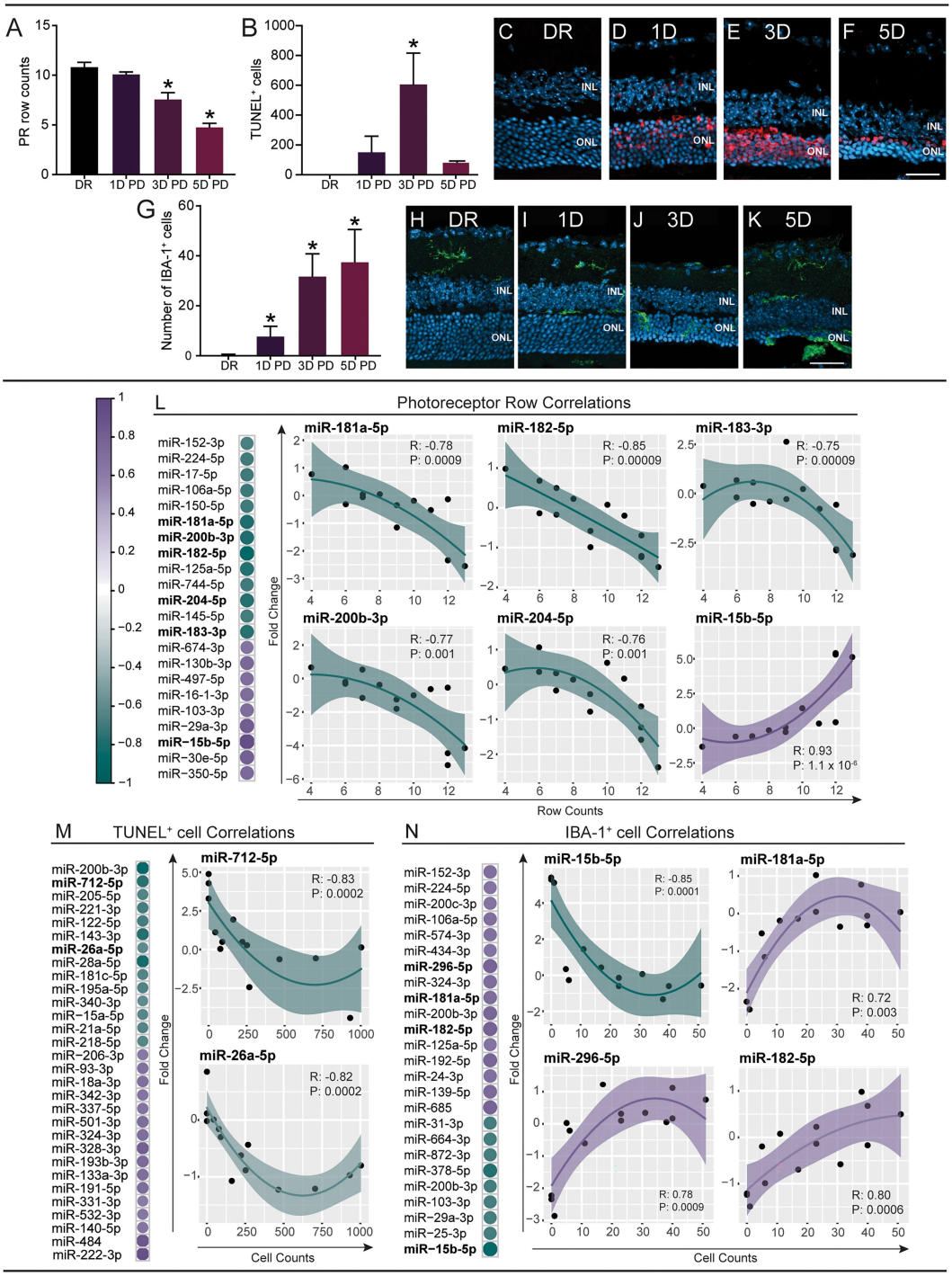

FIGURE 2
Expression changes of circulating miRNAs correlate to pathological changes in the retina. miRNA expression changes (fold change) at each PD time point were compared to photoreceptor row counts (PR rows), TUNEL⁺ cell counts and IBA⁺ cell counts using Spearman's correlation (p<0.01; see Supplementary Table S4). **(A–K)** Immunohistochemical analysis of retinal cryosections. **(A–F)** Apoptotic photoreceptor cells were stained using TUNEL and sections were counterstained with bisbenzimide [representative images **(C–F)**]. There was a decrease in the number of PR rows at the site of damage (500μm from the optic nerve head) across the PD paradigm, which was significant at 3days and 5days PD **(A)**. Photoreceptor cell death increased at 1day PD and was significantly increased at 3days PD, before decreasing at 5days PD **(B)**. **(G–K)** Inflammation (infiltrating microglia/macrophages) was analyzed by immunostaining cryosections using an anti-IBA-1 antibody and counting IBA-1⁺ cells in the ONL [Representative images of the site of damage **(H–K)**]. A significant increase was identified at 1day, 3days and 5days PD **(G)**. Scale bar=500μm. INL=inner nuclear layer, ONL=outer nuclear layer. Error bars indicate SEM. Statistical significance was determined by one-way ANOVA (n=12–16 per group, p<0.05). **(L)** The expression changes of 22 miRNAs were significantly correlated to PR row counts. **(M)** The expression changes of 30 miRNAs were significantly correlated to TUNEL⁺ cell counts. **(N)** 25 miRNAs were significantly correlated to IBA-1⁺ cell count. The relationship between miRNA fold changes and PR, IBA, TUNEL was summarized using a loess fit. The fit clearly show that most relationships are non-linear therefore we used Spearman's rank-based statistic to examine the significance of the correlation. Shaded area shows the 95% confidence interval.

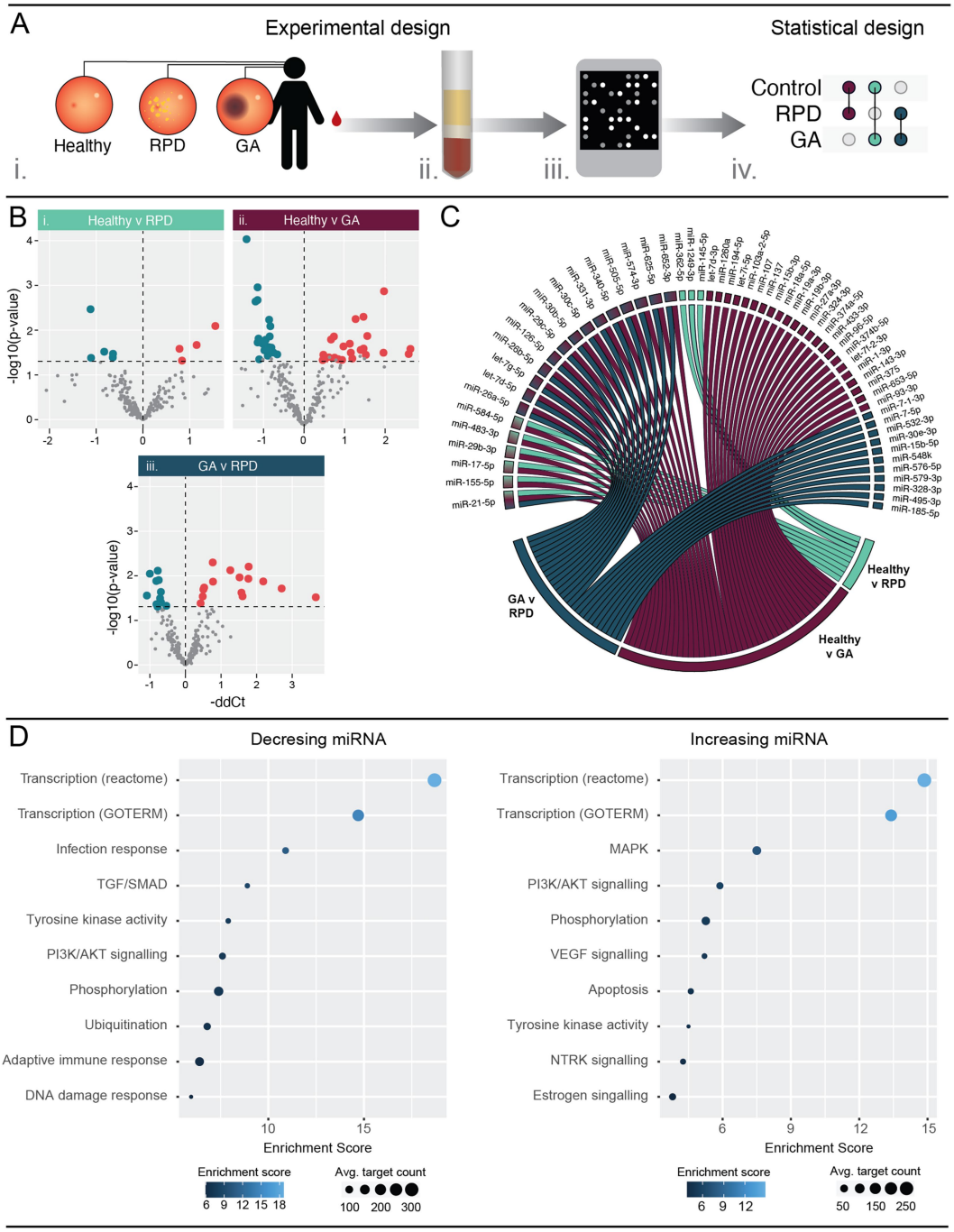

FIGURE 3
Circulating serum miRNA are differently expressed in patients with RPD and GA when compared to healthy controls. **(A)** Schematic showing the experimental workflow. Blood samples were obtained from patients with no retinal pathology (healthy), reticular pseudodrusen (RPD), or atrophic AMD (GA) (i). Serum was separated and RNA purified enriching for small RNAs (ii). miRNA expression was analyzed using human OpenArrays (iii) and differential expression analysis performed between healthy and disease groups (iv) (n=5–10 samples). **(B)** Volcano plots showing differentially regulated miRNAs. Nine and 43 miRNAs were significantly (p<0.05) modulated in RPD and GA patients compared to healthy controls. Additionally, 26 miRNAs showed significant modulation between RPD and GA groups. See also Table S5. **(C)** Chord diagram showing overlap of modulated miRNAs across all groups. A single miRNA, miR-21-5p, was significantly regulated between all three groups. Five miRNAs were differentially regulated in both GA and RPD groups compared to controls, and 14 miRNAs were significantly regulated in GA patients compared to both healthy and RPD groups. **(D)** Pathway analysis of mRNAs targeted by miRNAs significantly modulated in GA patients were identified using miRNet and filtered for those validated by HITS/PAR-CLIP or reporter assays. Pathway analysis of validated targets was performed using DAVID and significantly enriched (p<0.05) pathways are associated with transcription, protein activity and PI3K/AKT signaling. MAPK and apoptosis signaling was uniquely associated with mRNA targets of upregulated miRNAs, whereas infection and adaptive immune response were uniquely associated with mRNA targets of downregulated miRNAs. See also Supplementary Table S6.

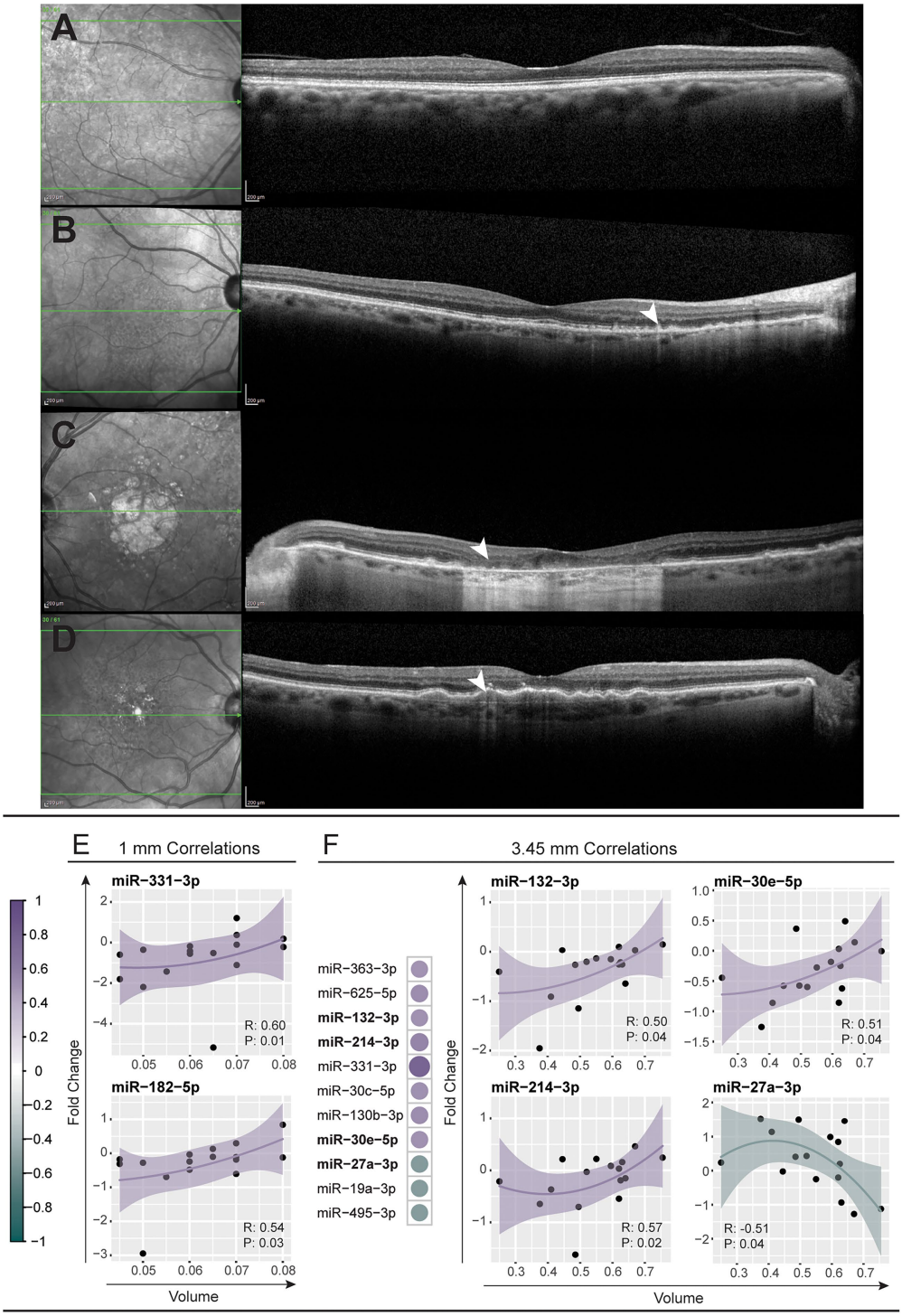

FIGURE 4
Modulation of miRNAs across patients corelates to retinal volume. **(A–D)** Representative near-infrared (left column) and optical coherence tomography (right column) fundus images across the macular region of a healthy control **(A)** and patients with reticular pseudodrusen **(B)**, geographic atrophy secondary to AMD **(C)**, and large confluent drusen with early RPE depigmentation and hypertransmission defect **(D)**. **(E,F)** Modulations in miRNA abundance across all patient samples were correlated (Spearman's correlation, $p<0.05$) against the volume of the central retina within 1mm and 3.45mm diameter circles centered on the macula (see also Supplementary Table S7). **(E)** Two miRNAs, miR-331-3p and miR-182-5p, showed positive correlation to the 1mm volume of patient retinas. **(F)** Eleven miRNAs correlated to the 3.45mm volume with scatter plots shown for the top four most correlated miRNAs. A positive correlation was observed for miR-30e-5p, miR-132-3p and miR-214-3p and a negative correlation for miR-27a-3p. The solid line indicates perfect correlation with the shaded area indicating variance.

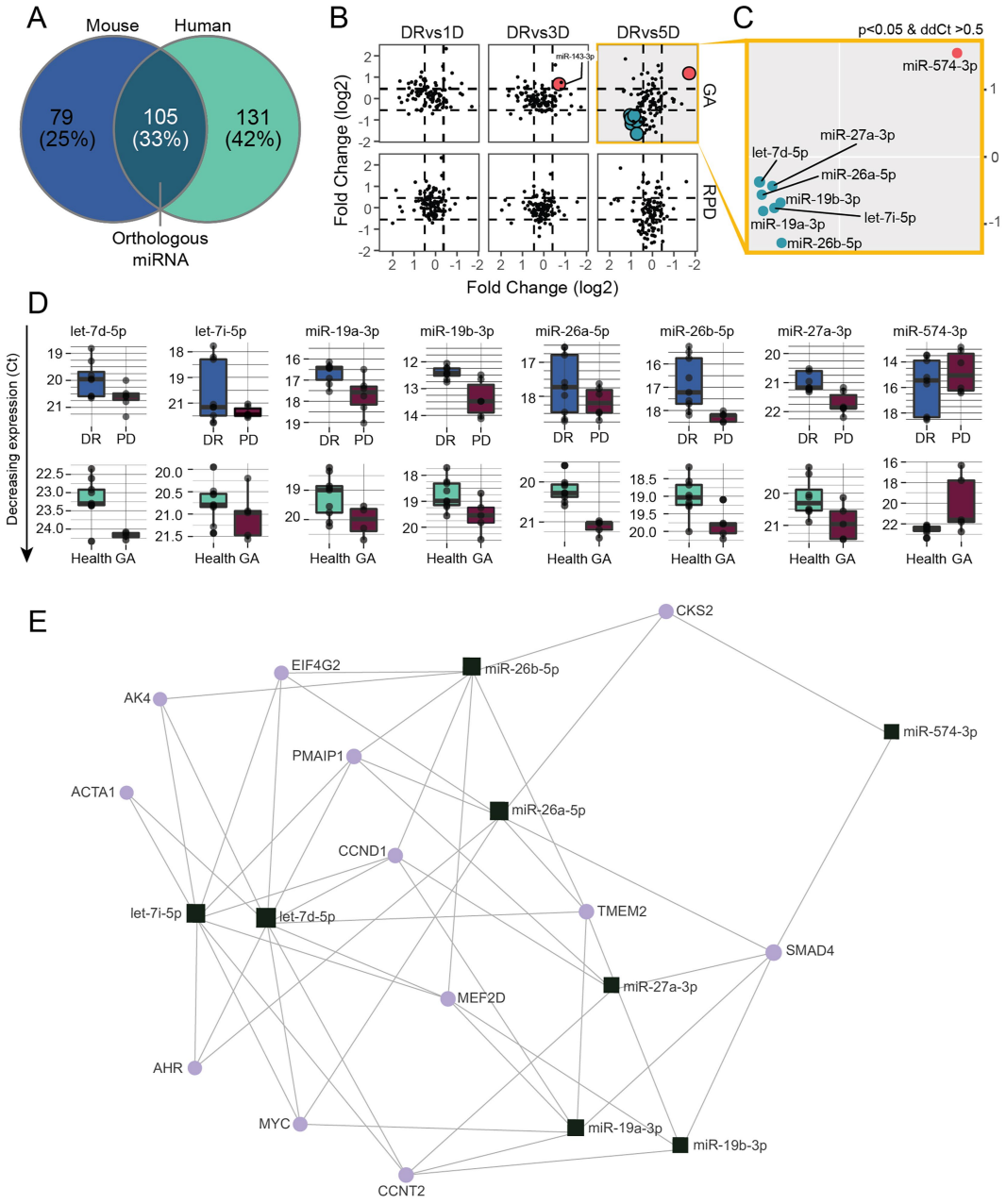

FIGURE 5
Modulated serum miRNAs show similarities between 5days PD and human GA patients. **(A)** Venn diagram showing the overlap of miRNAs detected in mouse and human samples. **(B)** miRNA expression changes (ddCt) at 1, 3 and 5days PD were plotted against miRNA expression changes (ddCt) of RPD and GA patients. **(C)** Eight miRNAs were significantly ($p<0.05$) differentially regulated in both 5days PD and GA samples, with miR-574-3p upregulated and miR-27a-3p, miR-26a-5p, miR-26b-5p, miR-19a-3p, mi-19b-3p let-7d-5p and let-7i-5p downregulated in both groups. **(D)** Box plots showing the expression changes of each miRNA differentially regulated in both groups. **(E)** Minimum miRNA/mRNA network analysis of the eight common differentially regulated miRNAs using miRNet. The plot shows the predicted interactions of each miRNA (square) with several key genes (circles) involved in transcription (CCNT2, SMAD4), inflammation (AK4, AHR) and apoptosis (PMAIP1, MEF2D).

4. Discussion

Due to the central role of miRNAs in the regulation of biological processes, especially inflammation and disease progression (He and Hannon, 2004), circulating miRNA have been identified as an attractive, non-invasive prognostic tool for multiple neurological disorders (Li et al., 2007; Chen et al., 2008; Mitchell et al., 2008; Jung et al., 2010; McDonald et al., 2011; Weiland et al., 2012), including AMD (Grasso et al., 2014). However, candidate miRNA diagnostic markers of AMD have primarily been established based on late stages of disease, with little investigations into early-stage disease markers (Ertekin et al., 2014; Grassmann et al., 2014; Szemraj et al., 2015; Ménard et al., 2016; Berber et al., 2017; Ren et al., 2017; Romano et al., 2017; Szemraj et al., 2017; ElShelmani et al., 2020). Further, to our knowledge, existing studies have not gone beyond simple differential expression profiling to narrow the target panel. This study advances

AMD biomarker research in multiple ways: (1) utilizing a pre-clinical animal model that recapitulates aspects of AMD as well as human patient samples, (2) identification of modulated miRNAs that correlated with retinal pathology, and (3) overlapping pre-clinical and clinical data to refine a preliminary miRNA panel with higher stringency.

Here we demonstrate that circulating miRNAs are modulated in response to photo-oxidative damage-induced photoreceptor degeneration and immune cell migration, even at early-stages. Furthermore, *via* pathway analysis, we showed that potential diagnostic miRNA targets demonstrate an association with neuronal processes and inflammation. Additionally, we show that the modulation of some miRNAs correlated to distinct changes in retinal morphology. We then corroborated these findings using human serum from patients with a diagnosis of RPD or GA. Finally, we identified candidate miRNAs that showed similar modulations between human and rodent samples at late stages. Taken together, this work identified circulating miRNA changes that closely reflect pathogenic processes in the retina, making them ideal candidate biomarkers for early-stage AMD diagnostics.

4.1. Circulating miRNAs are linked to photoreceptor degeneration

The clinical potential of diagnostic biomarkers relies not only on the ability to accurately detect the presence of pathological features, but, more importantly, the identification of disease onset prior to the development of pathologies (drusen deposits and pigmentary changes) through traditionally imaging techniques (fundus imaging) (Klein et al., 1992, 2007; Fine et al., 2000; van Lookeren et al., 2014). The regulation of miRNAs in late-stage AMD has been widely reported (Ertekin et al., 2014; Grassmann et al., 2014; Szemraj et al., 2015; Ménard et al., 2016; Berber et al., 2017; Ren et al., 2017; Romano et al., 2017; Szemraj et al., 2017; ElShelmani et al., 2020) however, with minimal overlap between studies, likely due to compounding factors such as co-morbidities, sample collection, and method of analysis.

Given the limitations of early diagnostic capabilities, we utilized a well-established rodent PD model that recapitulates important facets of AMD (Natoli et al., 2016) to identify differentially modulated miRNA at all stages of disease progression. We showed here that, although early stages of photo-oxidative damage (1-day) do not show substantial histological changes, there are already detectable miRNA changes in the circulation. These miRNAs included miR-128a-3p, miR-200b-3p, miR-410-3p and miR-218-5p, which have shown to be involved in inflammation and oxidative stress processes and to play a role in neurodegenerative disorders including AMD (Wang et al., 2019; Wu et al., 2020; Xiong et al., 2021; Yang et al., 2021; ElShelmani et al., 2021a; Acuña et al., 2022). This suggests that their presence in circulation reflects early changes in retinal homeostasis and we hypothesize that these miRNAs have the potential to be early indicators of disease onset. Importantly, we show that modulation of these four miRNAs was unique to 1 day PD, demonstrating their utility as a signature for early degeneration.

Of further interest was miR-126a-3p, which increased in serum at 3 days and 5 days PD in correlation to changes in photoreceptor rows and IBA-1$^+$ cell counts. MiR-126a-3p has been shown to protect against oxidative stress in the brain (Tan et al., 2021), be associated with protection of photoreceptors in retinitis pigmentosa (Wang and Smith, 2019), and to decrease in the choroid in response to neovascularisation (Desjarlais et al., 2019).

We show that in response to the whole PD time-course, molecular pathways linked to modulated circulating miRNAs are associated with Interleukin signaling, cell migration and TGF/SMAD signaling. This is unsurprising, as PD-induced miRNA modulations in the retina are primarily associated with the inflammatory response and related pathways (Saxena et al., 2015). Further, signaling between the retina and circulation under ongoing stress is essential to mediate the infiltration of monocytes into the retina during degeneration (Perez and Caspi, 2015; Zhou et al., 2017). Of note, in this study we found that a number of modulated miRNAs correlated to IBA-1$^+$ cell counts, such as miR-148a-3p and miR-152-3p, which have been shown to play a role in the inflammatory response in both the retina/choroid (Tsunekawa et al., 2017; Desjarlais et al., 2019) and circulating peripheral blood mononuclear cells (Wang et al., 2020; Zhang J et al., 2020; Tao et al., 2021). Additionally, miR-148a-3p has been shown to promote the classical M1 activation of macrophages, thereby increasing pro-inflammatory properties of the cell (Huang et al., 2017; Zhang P et al., 2020). Conversely, miRNAs miR-103, miR-181a and miR-24, which are also correlated to IBA-1$^+$ cell counts, have been shown to regulate pro-inflammatory factors expressed by microglia (Bian et al., 2020). This regulation has been shown to occur *via* communication by extracellular vesicles (EVs) from neural progenitor cells to microglia. Further, it has been suggested that EVs released from photoreceptors during early stages of retinal degeneration communicate a stress response within the retina (Wooff et al., 2020). Therefore, it is possible that these EVs enter the blood stream from the retina contributing to the modulations in miRNA abundance identified. Further, several studies have shown that EV-based miRNA biomarker development could result in a more specific and stringent panel for disease detection (Cheng et al., 2014; Barile and Vassalli, 2017), highlighting the need of future work to investigate the modulations of serum EV-derived miRNAs in AMD.

Taken together, these findings support the notion that these circulating miRNA are associated with retina-specific degeneration, leading to the identification of prospective diagnostic miRNAs.

4.2. Clinical serum miRNA profiles demonstrate consistencies with mouse data and current literature

Existing clinical studies into miRNAs as biomarkers for AMD, both atrophic and neovascular AMD, have identified miR-27a, miR-34, miR-106b, miR-126, miR-146a, miR-155, miR-361, miR-424-5p, miR-93-3p, and miR-21-5p among many others (Ertekin et al., 2014; Grassmann et al., 2014; Szemraj et al., 2015; Ménard et al., 2016; Ren et al., 2017; Romano et al., 2017). Our investigation of clinical samples revealed miR-93-3p to increase in atrophic AMD patient samples. This increase potentially aligns to current findings by ElShelmani et al. (2020), that identified an increase in miR-93 in the serum of neovascular AMD patients (ElShelmani et al., 2020), however, did not define which arm of miR-93 (−3p or-5p), a drawback common to existing AMD biomarker literature. As each miRNA exhibits unique biological functions, identifying the precise sequence is essential for future functional studies.

To further validate our findings, we correlated the human serum miRNA modulations to a histological measure, ONL volume. We found correlations between the abundance of three miRNA, miR-19a, miR-27a and miR-132-3p, showing a trend direction that aligns to previous findings in AMD patients (Ren et al., 2017; Romano et al., 2017; Elbay et al., 2019; ElShelmani et al., 2020, 2021b). To further refine our panel to be highly stringent, we identified differentially regulated miRNAs common to the PD model and AMD patient samples, which revealed that let-7i-5p, let-7d-5p, miR-19a-3p, miR-19b-3p, miR-26a-5p, miR-26b-5p, miR-27a-3p, and mir-574-3p are similarly modulated. Some of these miRNAs have been identified previously in association with AMD, with miR-26a-5p and miR-27a-3p showing directional changes consistent with the literature (Grassmann et al., 2014; Szemraj et al., 2015) and let-7d-5p and miR-574-3p showing a directional change opposite to that reported in the literature (Ertekin et al., 2014; ElShelmani et al., 2020). Additionally, miR-27a-3p is a mediator of the inflammatory response (Zhang et al., 2018), and its overexpression was associated with increased oxidative stress and retinal damage (Ren et al., 2021), and increasing in aging mouse retinas (Hermenean et al., 2021). Interestingly, here we show that modulation in miR-26a-5p and miR-27a-3p correlated with histological features, specifically $TUNEL^+$ cell count and retinal volume, respectively.

Importantly, we further identified several modulated serum miRNAs that are known to be highly abundant in the human retina, including miR-96, miR-26a/b and miR-143-3p interestingly, these miRNAs have not been previously reported to be differentially regulated in circulation in response to AMD. Of note was miR-96, a member of the miR-182/96/183 miRNA cluster, which is highly expressed in mature photoreceptors and the inner nuclear layer of the retina (Pawlick et al., 2021). Similarly, the mouse serum data revealed a change in miR-181a, which is highly expressed in the retina, particularly photoreceptors (Pawlick et al., 2021). Consistent with these functions, the mouse data demonstrated a correlation of miR-181a, miR-182 and miR-183 to photoreceptor row counts. To our knowledge this cluster has not previously been identified in serum in association with AMD.

Taken together, these findings support our hypothesis that changes in retinal homeostasis can be identified in the circulation, as these miRNAs are likely to originate from the retina. However, in the current study, we identified a number of miRNAs that showed modulations that were different from previous reports. For instance, here miR-21-5p was shown to decrease in both RPD and atrophic AMD patients, whereas miR-21-5p was previously identified to increase in patients with neovascular AMD (Szemraj et al., 2015). Similar to Ren et al. (2017), we identified significant modulations of miR-29b in RPD and GA serum samples, and of miR-27a-3p in GA alone. However, in opposition to Ren et al. (2017), we observed downregulation of both in our data. Moreover, our study showed inconsistency with multiple studies that have reported miR-223, miR-146, and/or miR-155 to be promising biomarkers for retinal degeneration (Ertekin et al., 2014; Szemraj et al., 2015; Romano et al., 2017; ElShelmani et al., 2020). There are several pre-analytical and post-analytical factors that could influence these discrepancies (McDonald et al., 2011). Firstly, our small sample size, sample collection, processing, and quality control could influence the miRNA profile (Blondal et al., 2013; Keller et al., 2017; Lee et al., 2017). The findings reported by Ren et al. (2017) and Ertekin et al. (2014) analyzed whole blood and plasma, respectively, whereas we profiled serum fractions to avoid miRNA contributions from cellular components. Further, we used an OpenArray™ approach, which only targets a subset of known miRNAs and is an amplification-based technique. As such, the normalization strategies are considered to have a significant outcome on results (Faraldi et al., 2019). Here we used a set of normalization controls based on global normalization, one of the most commonly used and recommended normalization tools (Mestdagh et al., 2009). We further used highly stringent thresholds for our amplification data to minimize the chance of a type I error. Additionally, we analyzed the contribution of covariates such as sex and age to miRNA expression and corrected our analysis accordingly, which is rarely reported in the existing literature. Other known AMD risk factors such as diet and smoking and genetic predisposition should be taken into account in future studies. Further, variability due to normalization can be avoided by measuring absolute abundance using sequencing techniques, which would also allow unbiased detection of all miRNAs present. Additionally, sequencing approaches would enable transcriptome-wide analyzes, which could include other small RNA species as well as non-coding RNAs and mRNAs, facilitating the development of a more specific diagnostic panel.

Overall, while we have utilized a number of strategies to identify and validate miRNA targets, there remains a clear need for further optimization and expansion of this body of work to a larger cohort.

4.3. Translation to a clinical setting through targeted analysis strategies mediated by biosensors

While the development of an accurate predictive panel for AMD pathogenesis is still in its infancy, there remains an unmet need for the development of tools that can allow effective, specific and timely detection of miRNAs in a clinical setting. The successful implementation of a biomarker panel to support clinical diagnosis relies on fast and robust detection of molecules of interest. Using sequencing-based methods are costly and require skilled personnel, an impediment to translation into clinical use. Target-specific methods such as electrochemical detection through biosensors present ideal strategies for translation into the clinic. Biosensors do not require special training and can be miniaturized, ideal for point-of-care or at home utilization. Thus, biosensors are excellent choices as companion diagnostics for rapid diagnosis as well as ongoing day-to-day monitoring of therapeutic intervention success. A wide variety of studies have manufactured electrochemical biosensors for miRNA detection (Gillespie et al., 2018), but their direct application in serum samples remains challenging, highlighting the need for further research.

4.4. Conclusion

The manifestation and progression of atrophic AMD in its early stages is relatively asymptomatic, and once vision loss ensues there is no effective treatment available. Therefore, early, minimally invasive detection is essential for the development of novel interventions. However, the nature of late clinical diagnosis and the

presence of co-morbidities creates a challenge in identifying early markers of disease. By utilizing the rodent photo-oxidative damage model we were able to identify miRNA, such as let-7i/g-5p, miR-26a-5p, miR-19a-3p and miR-574-3p, in circulation indicative of early stages of neuronal cell death and subsequent retinal inflammation. We were further able to show similar abundance changes of these miRNAs in human AMD samples, highlighting their potential as indicators of late-stage AMD. Finally, quantification of the key miRNAs presented here in a larger human patient cohort will provide essential validation in the progression of this panel to a clinical setting. This analysis demonstrates a unique methodological approach to elucidate a miRNA diagnostic signature of both early and late AMD.

Data availability statement

The original contributions presented in the study are included in the article/Supplementary material, further inquiries can be directed to the corresponding author.

Ethics statement

The studies involving human participants were reviewed and approved by University of Western Australia Human Research Ethics Committee. The patients/participants provided their written informed consent to participate in this study. The animal study was reviewed and approved by Australian National University Animal Experimentation Ethics Committee.

Author contributions

RA-B conducted PD experiments including sample processing and running the associated OpenArrays™. RA-B, US, and SD performed human sample processing including running on the OpenArrays™. FC, SM, and RH provided the human blood samples and collected and graded the retinal images. RA-B and AC performed the OpenArray™ data analysis. RA-B and US were major contributors to writing the manuscript. RN and FC conceived the study. RN provided funding to conduct the study. All authors have read and approved the final manuscript.

Funding

The authors acknowledge the Discovery Translation Fund (RN, RAG), the ANU Translational Fellowship (RN), the NHMRC Ideas grant (APP1127705; RN), the NSW RNA Future Leader Program (EMC Researcher Grant; US) and the NHMRC Investigator Grant (MRF1142962; FC) for support of this work.

Acknowledgments

The authors would like to acknowledge the Australian Phenomics Facility at the ANU for performing the blood collection required to perform the mouse analysis.

Conflict of interest

The authors declare that the research was conducted in the absence of any commercial or financial relationships that could be construed as a potential conflict of interest.

Publisher's note

Supplementary material

The Supplementary material for this article can be found online at: https://www.frontiersin.org/articles/10.3389/fnmol.2023.1130249/full#supplementary-material

References

Acuña, S. M., Zanatta, J. M., de Almeida, B. C., Floeter-Winter, L. M., and Muxel, S. M. (2022). miR-294 and miR-410 negatively regulate Tnfa, arginine transporter Cat1/2, and Nos2 mRNAs in murine macrophages infected with Leishmania amazonensis. *Noncoding RNA* 8:17. doi: 10.3390/ncrna8010017

Aggio-Bruce, R., Chu-Tan, J. A., Wooff, Y., Cioanca, A. V., Schumann, U., and Natoli, R. (2021). Inhibition of microRNA-155 protects retinal function through attenuation of inflammation in retinal degeneration. *Mol. Neurobiol.* 58, 835–854. doi: 10.1007/s12035-020-02158-z

Andreeva, K., and Cooper, N. G. F. (2014). MicroRNAs in the neural retina. *Int. J. Genomics* 2014:165897, 1–14. doi: 10.1155/2014/165897

Ardeljan, D., and Chan, C.-C. (2013). Aging is not a disease: distinguishing age-related macular degeneration from aging. *Prog. Retin. Eye Res.* 37, 68–89. doi: 10.1016/j.preteyeres.2013.07.003

Arroyo, J. D., Chevillet, J. R., Kroh, E. M., Ruf, I. K., Pritchard, C. C., Gibson, D. F., et al. (2011). Argonaute2 complexes carry a population of circulating microRNAs independent of vesicles in human plasma. *Proc. Natl. Acad. Sci. U. S. A.* 108, 5003–5008. doi: 10.1073/pnas.1019055108

Askou, A. L., Alsing, S., Holmgaard, A., Bek, T., and Corydon, T. J. (2017). Dissecting microRNA dysregulation in age-related macular degeneration: new tragets for eye gene therapy. *Acta Ophthalmol.* 96, 9–23. doi: 10.1111/aos.13407

Bandyra Katarzyna, J., Said, N., Pfeiffer, V., Górna Maria, W., Vogel, J., and Luisi, B. F. (2012). The seed region of a small RNA drives the controlled destruction of the target mRNA by the endoribonuclease RNase E. *Mol. Cell* 47, 943–953. doi: 10.1016/j.molcel.2012.07.015

Barile, L., and Vassalli, G. (2017). Exosomes: therapy delivery tools and biomarkers of diseases. *Pharmacol. Ther.* 174, 63–78. doi: 10.1016/j.pharmthera.2017.02.020

Berber, P., Grassmann, F., Kiel, C., and Weber, B. H. F. (2017). An eye on age-related macular degeneration: the role of MicroRNAs in disease pathology. *Mol. Diagn. Ther.* 21, 31–43. doi: 10.1007/s40291-016-0234-z

Bian, B., Zhao, C., He, X., Gong, Y., Ren, C., Ge, L., et al. (2020). Exosomes derived from neural progenitor cells preserve photoreceptors during retinal degeneration by inactivating microglia. *J. Extracell. Vesicles* 9:1748931. doi: 10.1080/20013078.2020.1748931

Blondal, T., Jensby Nielsen, S., Baker, A., Andreasen, D., Mouritzen, P., Wrang Teilum, M., et al. (2013). Assessing sample and miRNA profile quality in serum and plasma or other biofluids. *Methods* 59, S1–S6. doi: 10.1016/j.ymeth.2012.09.015

Boddu, S., Lee, M. D., Marsiglia, M., Marmor, M., Freund, K. B., and Smith, R. T. (2014). Risk factors associated with reticular pseudodrusen versus large soft drusen. *Am J. Ophthalmol.* 157, 985–93.e2. doi: 10.1016/j.ajo.2014.01.023

Chang, L., Zhou, G., Soufan, O., and Xia, J. (2020). miRNet 2.0: network-based visual analytics for miRNA functional analysis and systems biology. *Nucleic Acids Res.* 48, W244–W251. doi: 10.1093/nar/gkaa467

Chen, X., Ba, Y., Ma, L., Cai, X., Yin, Y., Wang, K., et al. (2008). Characterization of microRNAs in serum: a novel class of biomarkers for diagnosis of cancer and other diseases. *Cell Res.* 18, 997–1006. doi: 10.1038/cr.2008.282

Chen, L., Wu, W., Dentchev, T., Zeng, Y., Wang, J., Tsui, I., et al. (2004). Light damage induced changes in mouse retinal gene expression. *Exp. Eye Res.* 79, 239–247. doi: 10.1016/j.exer.2004.05.002

Cheng, L., Sharples, R. A., Scicluna, B. J., and Hill, A. F. (2014). Exosomes provide a protective and enriched source of miRNA for biomarker profiling compared to intracellular and cell-free blood. *J. Extracell. Vesicles* 3:23743. doi: 10.3402/jev.v3.23743

Chu-Tan, J. A., Cioanca, A. V., Feng, Z.-P., Wooff, Y., Schumann, U., Aggio-Bruce, R., et al. (2021). Functional microRNA targetome undergoes degeneration-induced shift in the retina. *Mol. Neurodegener.* 16:60. doi: 10.1186/s13024-021-00478-9

Chu-Tan, J. A., Rutar, M., Saxena, K., Aggio-Bruce, R., Essex, R. W., Valter, K., et al. (2018). MicroRNA-124 Dysregulation is associated with retinal inflammation and photoreceptor death in the degenerating retinaMicroRNA-124 Dysregulation in the degenerating retina. *Invest. Ophthalmol. Vis. Sci.* 59, 4094–4105. doi: 10.1167/iovs.18-24623

Deloitte Access EconomicsMitchell, P., Heraghty, J., and Cummins, R.. (2011). *Eyes on the Future: A Clear Outlook on Age-related Macular Degeneration*. Sydney NSW: Macular Degeneration Foundation Australia. 144.

Desjarlais, M., Rivera, J. C., Lahaie, I., Cagnone, G., Wirt, M., Omri, S., et al. (2019). MicroRNA expression profile in retina and choroid in oxygen-induced retinopathy model. *PLoS One* 14:e0218282. doi: 10.1371/journal.pone.0218282

Domalpally, A., Agrón, E., Pak, J. W., Keenan, T. D., Ferris, F. L. III, Clemons, T. E., et al. (2019). Prevalence, risk, and genetic Association of Reticular Pseudodrusen in age-related macular degeneration: age-related eye disease study 2 report 21. *Ophthalmology* 126, 1659–1666. doi: 10.1016/j.ophtha.2019.07.022

Dvinge, H., and Bertone, P. (2009). HTqPCR: high-throughput analysis and visualization of quantitative real-time PCR data in R. *Bioinformatics* 25, 3325–3326. doi: 10.1093/bioinformatics/btp578

Elbay, A., Ercan, S. C., Akbaş, F., Bulut, H., and Ozdemir, H. (2019). Three new circulating microRNAs may be associated with wet age-related macular degeneration. *Scand. J. Clin. Lab. Invest.* 79, 388–394. doi: 10.1080/00365513.2019.1637931

ElShelmani, H., Brennan, I., Kelly, D. J., and Keegan, D. (2021b). Differential circulating MicroRNA expression in age-related macular degeneration. *Int. J. Mol. Sci.* 22:12321. doi: 10.3390/ijms222212321

ElShelmani, H., Wride, M. A., Saad, T., Rani, S., Kelly, D. J., and Keegan, D. (2020). Identification of novel serum MicroRNAs in age-related macular degeneration. *Transl. Vis. Sci. Technol.* 9:28. doi: 10.1167/tvst.9.4.28

ElShelmani, H., Wride, M. A., Saad, T., Rani, S., Kelly, D. J., and Keegan, D. (2021a). The role of deregulated MicroRNAs in age-related macular degeneration pathology. *Transl. Vis. Sci. Technol.* 10:12. doi: 10.1167/tvst.10.2.12

Ertekin, S., Yıldırım, O., Dinç, E., Ayaz, L., Fidancı, S. B., and Tamer, L. (2014). Evaluation of circulating miRNAs in wet age-related macular degeneration. *Mol. Vis.* 20, 1057–1066.

Faraldi, M., Gomarasca, M., Sansoni, V., Perego, S., Banfi, G., and Lombardi, G. (2019). Normalization strategies differently affect circulating miRNA profile associated with the training status. *Sci. Rep.* 9:1584. doi: 10.1038/s41598-019-38505-x

Felekkis, K., and Papaneophytou, C. (2020). Challenges in using circulating micro-RNAs as biomarkers for cardiovascular diseases. *Int. J. Mol. Sci.* 21:561. doi: 10.3390/ijms21020561

Fernando, N., Wong, J. H. C., Das, S., Dietrich, C., Aggio-Bruce, R., Cioanca, A. V., et al. (2020). MicroRNA-223 regulates retinal function and inflammation in the healthy and degenerating retina. *Front. Cell Dev. Biol.* 8:516. doi: 10.3389/fcell.2020.00516

Fine, S. L., Berger, J. W., Maguire, M. G., and Ho, A. C. (2000). Age-related macular degeneration. *N. Engl. J. Med.* 342, 483–492. doi: 10.1056/NEJM200002173420707

Gilad, S., Meiri, E., Yogev, Y., Benjamin, S., Lebanony, D., Yerushalmi, N., et al. (2008). Serum MicroRNAs are promising novel biomarkers. *PLoS One* 3:e3148. doi: 10.1371/journal.pone.0003148

Gillespie, P., Ladame, S., and O'Hare, D. (2018). Molecular methods in electrochemical microRNA detection. *Analyst* 144, 114–129. doi: 10.1039/c8an01572d

Grassmann, F., Schoenberger, P. G. A., Brandl, C., Schick, T., Hasler, D., Meister, G., et al. (2014). A circulating MicroRNA profile is associated with late-stage Neovascular age-related macular degeneration. *PLoS One* 9:e107461. doi: 10.1371/journal.pone.0107461

Grasso, M., Piscopo, P., Confaloni, A., and Denti, M. A. (2014). Circulating miRNAs as biomarkers for neurodegenerative disorders. *Molecules* 19, 6891–6910. doi: 10.3390/molecules19056891

Gu, Z., Gu, L., Eils, R., Schlesner, M., and Brors, B. (2014). Circlize implements and enhances circular visualization in R. *Bioinformatics* 30, 2811–2812. doi: 10.1093/bioinformatics/btu393

Harrell, F. E., and Harrell, M. F. E.. (2019). *Package 'Hmisc'*. Vienna, Australia: The R Foundation, 235–236.

He, L., and Hannon, G. J. (2004). MicroRNAs: small RNAs with a big role in gene regulation. *Nat. Rev. Genet.* 5, 522–531. doi: 10.1038/nrg1379

Heath Jeffery, R. C., Mukhtar, S. A., Lopez, D., Preen, D. B., McAllister, I. L., Mackey, D. A., et al. (2021). Incidence of newly registered blindness from age-related macular degeneration in Australia over a 21-year period: 1996-2016. *Asia Pac. J. Ophthalmol.* 10, 442–449. doi: 10.1097/APO.0000000000000415

Hermenean, A., Trotta, M. C., Gharbia, S., Hermenean, A. G., Peteu, V. E., Balta, C., et al. (2021). Changes in retinal structure and ultrastructure in the aged mice correlate with differences in the expression of selected retinal miRNAs. *Front. Pharmacol.* 11:593514. doi: 10.3389/fphar.2020.593514

Holz, F. G., Sadda, S. R., Staurenghi, G., Lindner, M., Bird, A. C., Blodi, B. A., et al. (2017). Imaging protocols in clinical studies in advanced age-related macular degeneration: recommendations from classification of atrophy consensus meetings. *Ophthalmology* 124, 464–478. doi: 10.1016/j.ophtha.2016.12.002

Huang, D. W., Sherman, B. T., and Lempicki, R. A. (2009). Systematic and integrative analysis of large gene lists using DAVID bioinformatics resources. *Nat. Protoc.* 4, 44–57. doi: 10.1038/nprot.2008.211

Huang, F., Zhao, J. L., Wang, L., Gao, C. C., Liang, S. Q., An, D. J., et al. (2017). miR-148a-3p mediates notch signaling to promote the differentiation and M1 activation of macrophages. *Front. Immunol.* 8:1327. doi: 10.3389/fimmu.2017.01327

Jung, M., Schaefer, A., Steiner, I., Kempkensteffen, C., Stephan, C., Erbersdobler, A., et al. (2010). Robust MicroRNA stability in degraded RNA preparations from human tissue and cell samples. *Clin. Chem.* 56, 998–1006. doi: 10.1373/clinchem.2009.141580

Keller, A., Rounge, T., Backes, C., Ludwig, N., Gislefoss, R., Leidinger, P., et al. (2017). Sources to variability in circulating human miRNA signatures. *RNA Biol.* 14, 1791–1798. doi: 10.1080/15476286.2017.1367888

Klein, R., Klein, B. E. K., Knudtson, M. D., Meuer, S. M., Swift, M., and Gangnon, R. E. (2007). Fifteen-year cumulative incidence of age-related macular degeneration: the beaver dam eye study. *Ophthalmology* 114, 253–262. doi: 10.1016/j.ophtha.2006.10.040

Klein, R., Klein, B. E. K., and Linton, K. L. P. (1992). Prevalence of age-related Maculopathy: the beaver dam eye study. *Ophthalmology* 99, 933–943. doi: 10.1016/S0161-6420(92)31871-8

Lee, I., Baxter, D., Lee, M. Y., Scherler, K., and Wang, K. (2017). The importance of standardization on analyzing circulating RNA. *Mol. Diagn. Ther.* 21, 259–268. doi: 10.1007/s40291-016-0251-y

Li, J., Smyth, P., Flavin, R., Cahill, S., Denning, K., Aherne, S., et al. (2007). Comparison of miRNA expression patterns using total RNA extracted from matched samples of formalin-fixed paraffin-embedded (FFPE) cells and snap frozen cells. *BMC Biotechnol.* 7:36. doi: 10.1186/1472-6750-7-36

Lu, M., Zhang, Q., Deng, M., Miao, J., Guo, Y., Gao, W., et al. (2008). An analysis of human microRNA and disease associations. *PLoS One* 3:e3420. doi: 10.1371/journal.pone.0003420

Lukiw, W. J., Surjyadipta, B., Dua, P., and Alexandrov, P. N. (2012). Common micro RNAs (miRNAs) target complement factor H (CFH) regulation in Alzheimer's disease (AD) and in age-related macular degeneration (AMD). *Int J Biochem Mol Biol* 3, 105–116.

Mar, J. C., Kimura, Y., Schroder, K., Irvine, K. M., Hayashizaki, Y., Suzuki, H., et al. (2009). Data-driven normalization strategies for high-throughput quantitative RT-PCR. *BMC Bioinformatics* 10:110. doi: 10.1186/1471-2105-10-110

McCreight, J. C., Schneider, S. E., Wilburn, D. B., and Swanson, W. J. (2017). Evolution of microRNA in primates. *PLoS One* 12:e0176596:e0176596. doi: 10.1371/journal.pone.0176596

McDonald, J. S., Milosevic, D., Reddi, H. V., Grebe, S. K., and Algeciras-Schimnich, A. (2011). Analysis of circulating MicroRNA: Preanalytical and analytical challenges. *Clin. Chem.* 57, 833–840. doi: 10.1373/clinchem.2010.157198

McManus, D. D., and Ambros, V. (2011). Circulating MicroRNAs in cardiovascular disease. *Circulation* 124, 1908–1910. doi: 10.1161/CIRCULATIONAHA.111.062117

Ménard, C., Rezende, F. A., Miloudi, K., Wilson, A., Tétreault, N., Hardy, P., et al. (2016). MicroRNA signatures in vitreous humour and plasma of patients with exudative AMD. *Oncotarget* 7, 19171–19184. doi: 10.18632/oncotarget.8280

Mestdagh, P., Van Vlierberghe, P., De Weer, A., Muth, D., Westermann, F., Speleman, F., et al. (2009). A novel and universal method for microRNA RT-qPCR data normalization. *Genome Biol.* 10:R64. doi: 10.1186/gb-2009-10-6-r64

Mitchell, P. S., Parkin, R. K., Kroh, E. M., Fritz, B. R., Wyman, S. K., Pogosova-Agadjanyan, E. L., et al. (2008). Circulating microRNAs as stable blood-based markers for cancer detection. *Proc. Natl. Acad. Sci.* 105, 10513–10518. doi: 10.1073/pnas.0804549105

Natoli, R., Jiao, H., Barnett, N. L., Fernando, N., Valter, K., Provis, J. M., et al. (2016). A model of progressive photo-oxidative degeneration and inflammation in the pigmented C57BL/6J mouse retina. *Exp. Eye Res.* 147, 114–127. doi: 10.1016/j.exer.2016.04.015

Natoli, R., Zhu, Y., Valter, K., Bisti, S., Eells, J., and Stone, J. (2010). Gene and noncoding RNA regulation underlying photoreceptor protection: microarray study of dietary antioxidant saffron and photobiomodulation in rat retina. *Mol. Vis.* 16, 1801–1822.

Noell, W. K., Walker, V. S., Kang, B. S., and Berman, S. (1966). Retinal damage by light in rats. *Invest. Ophthalmol. Vis. Sci.* 5, 450–473.

O'Koren, E. G., Mathew, R., and Saban, D. R. (2016). Fate mapping reveals that microglia and recruited monocyte-derived macrophages are definitively distinguishable by phenotype in the retina. *Sci. Rep.* 6:6. doi: 10.1038/srep20636

Pawlick, J. S., Zuzic, M., Pasquini, G., Swiersy, A., and Busskamp, V. (2021). MiRNA regulatory functions in photoreceptors. *Front. Cell Dev. Biol.* 8:8. doi: 10.3389/fcell.2020.620249

Perez, V. L., and Caspi, R. R. (2015). Immune mechanisms in inflammatory and degenerative eye disease. *Trends Immunol.* 36, 354–363. doi: 10.1016/j.it.2015.04.003

Ren, C., Hu, W., Wei, Q., Cai, W., Jin, H., Yu, D., et al. (2021). MicroRNA-27a promotes oxidative-induced RPE cell death through targeting FOXO1. *Biomed. Res. Int.* 2021, 1–17. doi: 10.1155/2021/6666506

Ren, C., Liu, Q., Wei, Q., Cai, W., He, M., Du, Y., et al. (2017). Circulating miRNAs as potential biomarkers of age-related macular degeneration. *Cell. Physiol. Biochem.* 41, 1413–1423. doi: 10.1159/000467941

Ritchie, M. E., Phipson, B., Wu, D., Hu, Y., Law, C. W., Shi, W., et al. (2015). Limma powers differential expression analyses for RNA-sequencing and microarray studies. *Nucleic Acids Res.* 43:e47. doi: 10.1093/nar/gkv007

Romano, G. L., Platania, C. B. M., Drago, F., Salomone, S., Ragusa, M., Barbagallo, C., et al. (2017). Retinal and circulating miRNAs in age-related macular degeneration: An *in vivo* animal and human study. *Front. Pharmacol.* 8:168. doi: 10.3389/fphar.2017.00168

Roser, A. E., Caldi Gomes, L., Schünemann, J., Maass, F., and Lingor, P. (2018). Circulating miRNAs as diagnostic biomarkers for Parkinson's disease. *Front. Neurosci.* 12:625. doi: 10.3389/fnins.2018.00625

Roy, S., and Sen, C. K. (2011). MiRNA in innate immune responses: novel players in wound inflammation. *Physiol. Genomics* 43, 557–565. doi: 10.1152/physiolgenomics.00160.2010

Rutar, M., Natoli, R., Chia, R., Valter, K., and Provis, J. M. (2015). Chemokine-mediated inflammation in the degenerating retina is coordinated by Müller cells, activated microglia, and retinal pigment epithelium. *J. Neuroinflammation* 12:8. doi: 10.1186/s12974-014-0224-1

Sanz-Rubio, D., Martin-Burriel, I., Gil, A., Cubero, P., Forner, M., Khalyfa, A., et al. (2018). Stability of circulating exosomal miRNAs in healthy subjects. *Sci. Rep.* 8:10306. doi: 10.1038/s41598-018-28748-5

Saxena, K., Rutar, M., Provis, J. M., and Natoli, R. (2015). Identification of miRNAs in a model of retinal degenerations. *Invest. Ophthalmol. Vis. Sci.* 56:1820. doi: 10.1167/iovs.14-15449

Sherman, B. T., Hao, M., Qiu, J., Jiao, X., Baseler, M. W., Lane, H. C., et al. (2022). DAVID: a web server for functional enrichment analysis and functional annotation of gene lists (2021 update). *Nucleic Acids Res.* 50, W216–W221. doi: 10.1093/nar/gkac194

Song, D., Sulewski, M. E., Wang, C., Song, J., Bhuyan, R., Sterling, J., et al. (2017). Complement C5a receptor knockout has diminished light-induced microglia/macrophage retinal migration. *Mol. Vis.* 23, 210–218.

Szemraj, M., Bielecka-Kowalska, A., Oszajca, K., Krajewska, M., Goś, R., Jurowski, P., et al. (2015). Serum MicroRNAs as potential biomarkers of AMD. *Med. Sci. Monit.* 21, 2734–2742. doi: 10.12659/MSM.893697

Szemraj, M., Oszajca, K., Szemraj, J., and Jurowski, P. (2017). MicroRNA expression analysis in serum of patients with congenital hemochromatosis and age-related macular degeneration (AMD). *Med. Sci. Monit.* 23, 4050–4060. doi: 10.12659/MSM.902366

Tan, Y., Zhou, F., Yang, D., Zhang, X., Zeng, M., and Wan, L. (2021). MicroRNA-126a-5p exerts Neuroprotective effects on ischemic stroke via targeting NADPH oxidase 2. *Neuropsychiatr. Dis. Treat.* 17, 2089–2103. doi: 10.2147/NDT.S293611

Tao, B., Xiang, W., Li, X., He, C., Chen, L., Xia, X., et al. (2021). Regulation of toll-like receptor-mediated inflammatory response by microRNA-152-3p-mediated demethylation of MyD88 in systemic lupus erythematosus. *Inflamm. Res.* 70, 285–296. doi: 10.1007/s00011-020-01433-y

Tsunekawa, T., Kaneko, H., Takayama, K., Hwang, S.-J., Oishi, A., Nagasaka, Y., et al. (2017). Correlation between miR-148 expression in vitreous and severity of Rhegmatogenous retinal detachment. *Biomed. Res. Int.* 2017, 1–8. doi: 10.1155/2017/3427319

van Lookeren, C. M., LeCouter, J., Yaspan, B. L., and Ye, W. (2014). Mechanisms of age-related macular degeneration and therapeutic opportunities. *J. Pathol.* 232, 151–164. doi: 10.1002/path.4266

Wang, Z., Liao, Y., Wang, L., Lin, Y., Ye, Z., Zeng, X., et al. (2020). Small RNA deep sequencing reveals novel miRNAs in peripheral blood mononuclear cells from patients with IgA nephropathy. *Mol. Med. Rep.* 22, 3378–3386. doi: 10.3892/mmr.2020.11405

Wang, J., and Smith, S. B. (2019). "A novel mechanism of sigma 1 receptor Neuroprotection: modulation of miR-214-3p" in *Retinal Degenerative Diseases*. eds. C. B. Rickman, C. Grimm, R. E. Anderson, J. D. Ash, M. M. LaVail and J. G. Hollyfield (Cham: Springer International Publishing)

Wang, Y., Xu, N., Zhao, S., Jiao, T., Fu, W., Yang, L., et al. (2019). miR-410-3p suppresses cytokine release from fibroblast-like Synoviocytes by regulating NF-κB signaling in rheumatoid arthritis. *Inflammation* 42, 331–341. doi: 10.1007/s10753-018-0896-2

Wei, T., Simko, V., Levy, M., Xie, Y., Jin, Y., and Zemla, J. J. S. (2017). Package 'corrplot'. *Statistician* 56:e24.

Weiland, M., Gao, X.-H., Zhou, L., and Mi, Q.-S. (2012). Small RNAs have a large impact. *RNA Biol.* 9, 850–859. doi: 10.4161/rna.20378

White, D. A., Hauswirth, W. W., Kaushal, S., and Lewin, A. S. (2007). Increased sensitivity to light-induced damage in a mouse model of autosomal dominant retinal disease. *Invest. Ophthalmol. Vis. Sci.* 48, 1942–1951. doi: 10.1167/iovs.06-1131

Wooff, Y., Cioanca, A. V., Chu-Tan, J. A., Aggio-Bruce, R., Schumann, U., and Natoli, R. (2020). Small-medium extracellular vesicles and their miRNA cargo in retinal health and degeneration: mediators of homeostasis, and vehicles for targeted gene therapy. *Front. Cell. Neurosci.* 14:160. doi: 10.3389/fncel.2020.00160

Wu, Z., Ayton, L. N., Luu, C. D., Baird, P. N., and Guymer, R. H. (2016). Reticular Pseudodrusen in intermediate age-related macular degeneration: prevalence, detection, clinical, environmental, and genetic associations. *Invest. Ophthalmol. Vis. Sci.* 57, 1310–1316. doi: 10.1167/iovs.15-18682

Wu, L., Zhang, G., Guo, C., Zhao, X., Shen, D., and Yang, N. (2020). MiR-128-3p mediates TNF-α-induced inflammatory responses by regulating Sirt1 expression in bone marrow mesenchymal stem cells. *Biochem. Biophys. Res. Commun.* 521, 98–105. doi: 10.1016/j.bbrc.2019.10.083

Xiong, J., He, X., Xu, Y., Zhang, W., and Fu, F. (2021). MiR-200b is upregulated in plasma-derived exosomes and functions as an oncogene by promoting macrophage M2 polarization in ovarian cancer. *J. Ovarian Res.* 14:74. doi: 10.1186/s13048-021-00826-9

Yang, Y., Zhao, F., Yuan, Z., Wang, C., Chen, K., and Xiao, W. (2021). Inhibition of miR-218-5p reduces myocardial ischemia-reperfusion injury in a Sprague-Dawley rat model by reducing oxidative stress and inflammation through MEF2C/NF-κB pathway. *Int. Immunopharmacol.* 101:108299. doi: 10.1016/j.intimp.2021.108299

Zhang, P., Li, L. Q., Zhang, D., and Shen, Y. (2018). Over-expressed miR-27a-3p inhibits inflammatory response to spinal cord injury by decreasing TLR4. *Eur. Rev. Med. Pharmacol. Sci.* 22, 5416–5423. doi: 10.26355/eurrev_201809_15800

Zhang, P., Lu, B., Zhang, Q., Xu, F., Zhang, R., Wang, C., et al. (2020). LncRNA NEAT1 sponges MiRNA-148a-3p to suppress Choroidal neovascularization and M2 macrophage polarization. *Mol. Immunol.* 127, 212–222. doi: 10.1016/j.molimm.2020.08.008

Zhang, J., Xu, X., Huang, X., Zhu, H., Chen, H., Wang, W., et al. (2020). Analysis of microRNA expression profiles in porcine PBMCs after LPS stimulation. *Innate Immun.* 26, 435–446. doi: 10.1177/1753425920901560

Zhou, Y.-D., Yoshida, S., Peng, Y.-Q., Kobayashi, Y., Zhang, L.-S., and Tang, L.-S. (2017). Diverse roles of macrophages in intraocular neovascular diseases: a review. *Int. J. Ophthalmol.* 10, 1902–1908. doi: 10.18240/ijo.2017.12.18

frontiers | Frontiers in Molecular Neuroscience

TYPE Brief Research Report
PUBLISHED 17 April 2023
DOI 10.3389/fnmol.2023.1126438

OPEN ACCESS

EDITED BY
Estela Maris Muñoz,
CONICET Dr. Mario H. Burgos Institute of Histology and Embryology (IHEM), Argentina

REVIEWED BY
Fernando Garcia-Moreno,
Achucarro Basque Center for Neuroscience, Spain
Ashwin S. Shetty,
Harvard University, United States

*CORRESPONDENCE
Vijay K. Tiwari
✉ v.tiwari@qub.ac.uk;
✉ tiwari@health.sdu.dk

SPECIALTY SECTION
This article was submitted to Neuroplasticity and Development, a section of the journal Frontiers in Molecular Neuroscience

RECEIVED 17 December 2022
ACCEPTED 15 March 2023
PUBLISHED 17 April 2023

CITATION
Singh A and Tiwari VK (2023) Transcriptional networks of transient cell states during human prefrontal cortex development. *Front. Mol. Neurosci.* 16:1126438. doi: 10.3389/fnmol.2023.1126438

Transcriptional networks of transient cell states during human prefrontal cortex development

Aditi Singh[1] and Vijay K. Tiwari[1,2,3,4]*

[1]Wellcome-Wolfson Institute for Experimental Medicine, School of Medicine, Dentistry and Biomedical Science, Queens University, Belfast, United Kingdom, [2]Institute of Molecular Medicine, University of Southern Denmark, Odense C, Denmark, [3]Danish Institute for Advanced Study (DIAS), Odense M, Denmark, [4]Department of Clinical Genetics, Odense University Hospital, Odense C, Denmark

The human brain is divided into various anatomical regions that control and coordinate unique functions. The prefrontal cortex (PFC) is a large brain region that comprises a range of neuronal and non-neuronal cell types, sharing extensive interconnections with subcortical areas, and plays a critical role in cognition and memory. A timely appearance of distinct cell types through embryonic development is crucial for an anatomically perfect and functional brain. Direct tracing of cell fate development in the human brain is not possible, but single-cell transcriptome sequencing (scRNA-seq) datasets provide the opportunity to dissect cellular heterogeneity and its molecular regulators. Here, using scRNA-seq data of human PFC from fetal stages, we elucidate distinct transient cell states during PFC development and their underlying gene regulatory circuitry. We further identified that distinct intermediate cell states consist of specific gene regulatory modules essential to reach terminal fate using discrete developmental paths. Moreover, using *in silico* gene knock-out and over-expression analysis, we validated crucial gene regulatory components during the lineage specification of oligodendrocyte progenitor cells. Our study illustrates unique intermediate states and specific gene interaction networks that warrant further investigation for their functional contribution to typical brain development and discusses how this knowledge can be harvested for therapeutic intervention in challenging neurodevelopmental disorders.

KEYWORDS

cell-fate, cortical development, lineage, transition states, gene perturbation, trajectory

1. Introduction

The human brain consists of billions of cells across diverse anatomical yet functionally interconnected regions (Mu et al., 2019). The cerebral cortex is the largest structure in the human brain and is responsible for perception, cognition, and memory-related functions (Cadwell et al., 2019). In the course of evolution, the human cerebral cortex has expanded markedly by more than three times than other closest higher organisms (Yeo et al., 2011; Eze et al., 2021). Cortical expansion underlies the proliferation and upsurge of cellular heterogeneity in specific cortical layers during distinct periods of gestational development (Kriegstein et al., 2006).

The enormous diversity of brain cell types with precise context comes from a pool of neural stem cells (NSCs; Fan et al., 2018; Yang et al., 2022). This progenitor pool of NSCs is known to have several subtypes that are identified in the developing brain from early to late gestation as the cortex matures (Eze et al., 2021) such that they primarily give rise to neurons in early gestation weeks, but as it transforms later in the second trimester, they majorly generate the glial cell populations of the cortex (Fan et al., 2018; Eze et al., 2021).

Neural stem cells in the cortex undergo state transitions in a highly asynchronous fashion to progress towards a specific lineage. During this process, cells undergo several metastable transient states, and characterizing these states is essential to better understand the key steps of cell fate determination during cortical development and how their disruption may predispose to certain neurodevelopmental disorders (Del-Valle-Anton and Borrell, 2022; Singh et al., 2022). This knowledge can be further harnessed for developing targeted therapy approaches.

The single-cell RNA sequencing (scRNA-seq) approach has enabled the investigation of the dynamics of cellular diversity during brain development at an unprecedented scale (Jeong and Tiwari, 2018; Luecken and Theis, 2019). Studies have begun to use the derived knowledge to advance our understanding of lineage relationships (Mayer et al., 2018; Velmeshev et al., 2021). However, much of what is known about cortical development and its regulatory framework has been examined in non-human model systems. Consequently, we do not yet fully understand the intermediate cell transition states and their regulatory gene networks during human brain development (Fleck et al., 2022). It is possible to use advanced computational approaches to reconstruct the developmental trajectories from single-cell transcriptomics (scRNA-seq) datasets (Fletcher et al., 2018). The construction of the lineage trajectories takes advantage of the fact that developmentally related cells tend to share similar transcriptomic profiles. Consequently, lineage approaches can be used to order cells along differentiation trajectories and to study cell fate decisions (Luecken and Theis, 2019). Recent algorithms that model the dynamics of biological processes use the time-series or even snapshot scRNA-seq data to place the cells in the temporal order of lineage development using their gene expression profiles and also identify the intermediate states which are more plastic in nature and important for fate switches (Maclean, 2022). Hence, using state-of-the-art algorithms of lineage evolution and identifying their high-confidence regulatory genetic drivers is an efficient method for selecting novel candidates contributing toward fate transitions.

In this study, we used publicly available scRNA-seq datasets comprising early to late stages of human PFC development to decipher the distinct transient states during the specification of various cell fates and their underlying gene regulatory circuitry. We further reveal that distinct intermediate cell states can reach the same terminal fate using discrete developmental paths. We identified the differential transcriptomic feature of these cell states and further validated key regulators of these features during oligodendrocyte progenitor cells (OPCs) lineage specification, using *in silico* perturbation analysis. Furthermore, we highlight novel gene interaction networks that warrant further investigation in experimental models for their role in cell fate development, maturation, and overall brain functions.

2. Methods

2.1. Selection and processing of scRNA-seq datasets

There are several single-cell datasets available for the developing human brain with a greater number of cells but none of them covers a range of embryonic days. We attempted to combine the dataset, but owing to several variabilities related to the origin of the lab, sequencing techniques, and platforms, it was better to use a single dataset, and therefore, we selected the data from Zhong et al. (2018). The data gathered involved a smart-seq-based scRNA-seq dataset with 2,309 cells and an average of 2,654 detected genes per cell. Furthermore, it covers a wide range of developmental stages despite a low number of cells having good gene coverage. Notably, we used another dataset from gestation week (GW) 25 with 15,811 cells for human PFC and validated our findings (Bhaduri et al., 2021), which is from the 10X chromium platform with v3 chemistry.

Single-cell data analysis and pre-processing, including data normalization and dimension reduction, were performed using Seurat version '4.3.0' (Hao et al., 2021) in R. First, count matrices of gene expression were imported to Seurat, and following the assessment of QC metrics of datasets, only cells expressing at least 750 genes with expression in at least three cells were taken for further analysis. Here, cells with only a maximum of 10% mitochondrial genes were included. The UMI counts were then normalized for each cell by the total expression, multiplied by 10,000, and log-transformed. Then, the top 2,000 highly variable features were selected, and data scaling was performed before principal component analysis (PCA) on the first significant 20 PCs based on the elbow of standard deviations of PCs. Finally, cell dimensionality reduction was performed through UMAP and cell clusters were annotated into cell types based on markers (Supplementary Table S1) from the source paper in addition to the current updated literature which mostly aligned with the source dataset.

Seurat data was then converted to the python-based format of cell rank (Lange et al., 2022) using SeuratDisk v '0.0.0.9020,' which is an interface for HDF5-Based Single-Cell File Formats. These h5ad files were imported into Scanpy and used for cell rank as well as PAGA in downstream analysis.

2.2. Computation of fate probabilities

Initially, to estimate cell–cell transition possibilities, we used CellRank (Lange et al., 2022) and computed initial and terminal states and the fate probabilities of the cell for reaching the terminal states. We used the CytoTRACE kernel of CellRank to reconstruct the cellular trajectory based on cell similarity analysis (Herring et al., 2022). This kernel bypasses the need to define a root cell for pseudotime calculations and predicted the cellular plasticity states based on transcriptional diversity (Shen et al., 2021). CytoTRACE algorithm further feeds this calculated pseudotime into another kernel to calculate a KNN graph where edges indicate the direction of increasing pseudotime and point into the direction of increasing differentiation state. Furthermore, a transition matrix was constructed based on the pseudotemporal ordering and KNN graph, and it was projected onto a UMAP plot. We used the original force-directed layout to plot cells, colored by cell-type clusters.

2.3. PAGA method for fate connectivities

To relate the clusters of cells that might be developmentally related to one another, we quantified the connectivity of cell clusters using the partitioned approximate graph abstraction (PAGA) method (Wolf et al., 2019). It is based on the Scanpy (Wolf et al., 2018) package and constructs a k-nearest neighbor graph of cells where partitions are a group of connected cells at a certain resolution *via* the Leiden method. We used the clustering resolution of 0.4–0.6,

and the PAGA graph was acquired by combining a node with each partition and linking each node by weighted edges that characterize a statistical measure of connectivity between the nodes or PAGA partitions (Yu et al., 2021). PAGA discarded false edges with low weights and revealed the denoised topology of the global data at the selected resolution. The nodes that did not connect in the PAGA graph are cells that do not have any significant connections at all. The PAGA nodes were then arranged in a desired path as per the observed significance, and cells were ordered in that path to trace gene expression changes along the trajectories. We used differential expression analysis from Scanpy to calculate the highly significant gene in one node in comparison to the rest of the node or PAGA partitions.

2.4. Gene perturbations

We used the iQcell platform (Heydari et al., 2022) v.1.1.0 to investigate the gene regulatory networks. It is a program to understand, simulate, and further analyze workable logical gene regulatory networks from scRNA-seq data, which uses gene expression datasets along with their pseudotime profile to infer gene interactions and their regulatory features. Gene regulatory networks allow the simulation of hypotheses leading developmental programs and also infer the direction of regulation, i.e., positive or negative regulation of gene pairs in a network. In the network, genes were placed in a hierarchy as per their expression densities in pseudotime. iQcell requires a discrete form of input for the mRNA levels as on/off, and we used k-means clustering for the discretization of gene expression levels as default. Before running the simulations, we defined the initial state of the simulation through iQcell, which found the initial cell states, i.e., cell genotype from the discretized expression with early pseudo-time value by averaging the state of each gene over the cells.

3. Results

We began by using a publicly available dataset that covers gestation week (GW) 8–26 to span key developmental stages with good coverage for distinct cell types (Zhong et al., 2018). The cells were clustered into major cortical cell types using the marker set from the literature (Supplementary Table S1) which matched with the source dataset for broad cell-type classification. The developmental stages were separated into early (8–13 GW), mid (16–19 GW), and late (23–26 GW) stages (Figure 1A). These developmental stages were then revalidated for the proportion of major cell types and then investigated for genetic lineage drivers of the cell state transitions in early, mid, and late stages toward a specific fate.

3.1. Distinct lineage transition paths at early, mid, and late gestation times

Biological systems exist in a dynamic state during development with active cell-fate transitions. Computational algorithms can infer the developmental trajectory and predict cell fate by the sequential ordering of cells using their transcriptomic profiles. For such time-based ordering of transcriptomic states in cortical cells, we selected cells that originate within the cortex, while microglia and interneurons, the cell types that have a separate origin and majorly migrate to the cortex, were removed as mentioned previously (Nowakowski et al., 2017; Zhong et al., 2018; Bhaduri et al., 2021).

Then, we used the CellRank method to infer the cell state dynamics in the early, mid, and late stages of gestation. CellRank uses similarity-based trajectory inference with directional information to create probabilistic trajectories in cell fate directions. We identified the probable terminal fates (macrostate) and the calculated probability of each cell to achieve the terminal fates. Subsequently, we created a global map of fate potentials in the form of initial, terminal, and intermediate cell states of the system and assigned each cell the probability of reaching each terminal macrostate (Figure 1B). At early gestation, most of the cells were arranged in vRG (ventricular radial glia) to IP (intermediate progenitor) axis, and few cells could be seen toward immature cortical plate (CP) neurons from IP as well as vRG. Overall, it is clear that most of the cells at early embryonic development are in the center, indicating less committed or plastic states. However, the cells in mid-gestation showed more density on the axis of vRG to mature CP neurons. Interestingly, as we moved to the late gestation stages, we observed the emergence of additional terminal states, i.e., glial population, and interestingly, here the cellular fate probabilities diverged toward the neuronal as well as oligodendrocyte lineage. Moreover, there were many immature cells and/or progenitors from both neuronal and glial lineage which were clustered toward the center.

3.2. Fate connectivities provide multiple lineage transition paths toward a terminal cell fate

We then wanted to identify the lineage-specific genes toward neuronal or glial fates and therefore compared the fate probabilities to uncover lineage-specific gene expression patterns and putative lineage drivers. Given that CellRank provided the terminal states and lineage drivers by automated computation of fate probabilities and does not need manual identification of root cell population within CyTOtrace kernel, we questioned if we could find overlapping lineage drivers in transient states through a topology-preserving map of single cells. Therefore, we used partition-based graph abstraction (PAGA) which constructs a simplified representation of the developmental trajectory using a graph-based approach, through similarities and differences between cells based on their gene expression profiles, and then simplifies the graph into a set of clusters or partitions that correspond to distinct cell types. Thus, we achieved the discrete cell types and continuous cell transitions toward these cell types, where both the continuous and disconnected nature of biological cell types are preserved at multiple resolutions (Figures 1C–E). Here, each node represents a cell type and edges measure the strength of connectivity between nodes or the similarity of cell types.

PAGA explores the complex trajectory structure with multiple branching in a general graph form for all embryonic stages (Figures 1C–E), where we identified the root cells and terminal fates (clusters) by specific markers (Supplementary Figures S1–S4). Namely, the root cell was selected using the expression of marker genes for radial glia (PAX6, SOX2; Supplementary Figures S1–S3) and defined the PAGA path as the transitions toward IP (EOMES; Figure 1C; Supplementary Figures S1–S3), different neuronal cells (NEUROD1,

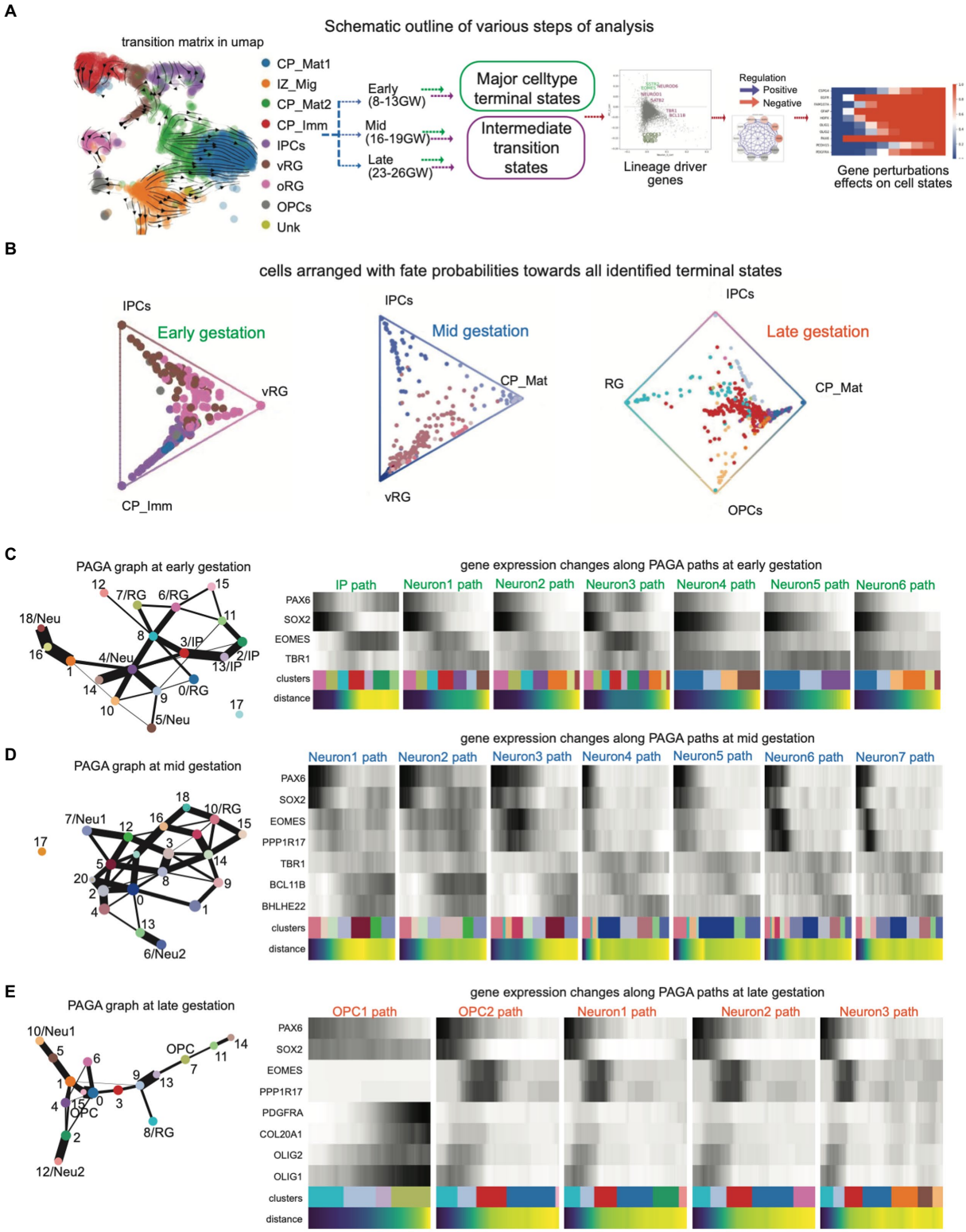

FIGURE 1
(A) Schematic outline of various steps of analysis: The scRNAseq dataset was processed for QC analysis and cluster identification with known cell type markers. Developmental stages were separated into early (8–13 GW), mid- (16–19 GW), and late (23–26 GW) stages and then terminal fates and their intermediate states were analyzed using CellRank and PAGA, resulting in lineage-specific novel genes. Gene regulatory network (GRN) and perturbation analysis were performed using the iQcell platform; **(B)** Summarized fate probabilities toward all terminal states. In this representation, uncommitted progenitors and immature cells can be seen near the center and committed cells are placed near one edge; **(C–E)** PAGA graphs show cell clusters in which only terminal major cell states are named while the rest of the cells are arranged in a graph connected with weighted edges for their nature. The PAGA graphs capture the proximity of progenitors and strong connections within neuronal clusters and then glial clusters; **(C)** PAGA graphs (left) and gene changes along PAGA paths (right) at early embryonic brain development; **(D)** PAGA graphs (left) and gene changes along PAGA paths (right) at mid-stage embryonic brain development; **(E)** PAGA graphs (left) and gene changes along PAGA paths (right) at late-stage embryonic brain development.

BCL11B, and SATB2; Figures 1C,D; Supplementary Figures S1–S3), or OPCs (OLIG1 and PDGFRA; Figure 1E; Supplementary Figure S4). The sequence of transition paths to cell fates is mentioned in Supplementary Table S2. IP and Neuron1 path in early stages, Neuron3 path in mid-stages and OPC1 in late stages show a smooth transition of gene expression profiles. Interestingly, these states contain several transient intermediate cell states, i.e., the PAGA connecting cell clusters which can transition from the root RG cells to the terminal fates, and are of major interest being connected to separate fates with discrete gene expression profiles.

3.3. Transition state-specific gene sets at early, mid, and late gestation times

We next performed a hierarchical clustering of all identified terminal and intermediate cellular states with their variable gene features in the early, mid, and late stages of gestation (Supplementary Figure S5; Figure 2A). As evident in early stages, most cells showed gene expression profile in plastic states in RG and IP states and then transition to the neurons (Supplementary Figure S5A). Furthermore, the later stages showed discrete patterns of cell type (Supplementary Figure S5B; Figure 2C), which is indicative of increased neuronal differentiation. Neurogenesis began early in development and declines during late embryonic development, while gliogenesis was observed in post-mid-embryonic stages and continues in parallel to neuronal maturation and synapse formation till the postnatal stages. We constructed a diffusion pseudotime from PAGA which validates the OPC lineage evolving at a later pseudotime point and hence our choice of root and terminal cell clusters (Figure 2B). Here, we paid special attention to OPCs as there are still critical gaps in understanding lineage drivers of OPC fate switches. We identified top lineage-specific genes for OPC from CellRank and PAGA algorithms and validated top lineage drivers by plotting the distribution of log odds for OPCs versus other cell fates per cell across cell types together on a Seurat clustering global map. Log-odds ratio confirmed the lineage specificity by comparison of OPC markers genes (Figure 2C) and neuronal genes (Figure 2D). The pre-OPC lineage genes (Figure 2E) were also validated by log-odds ratio. In addition, we confirmed their expression in a pseudotime plot for lineage specificity and identified targets of some novel transcription factors using specificity in pseudotime (Supplementary Figure S6). Therefore, these gene are the ideal candidates the ideal candidates for investigating their regulatory effect on OPC lineage commitment and progression.

3.4. Perturbation analysis reveals a role for distinct gene interactions in the lineage trajectory of OPCs

We employed the iQcell platform to construct novel gene regulatory networks (GRN) and subsequently investigated the effects of perturbing gene expression states and their effect on cell fates in late embryonic stage scRNAseq data of PFC. In addition, we validated the similar GRNs and perturbation effects in a larger dataset (>15,000 cells) of late embryonic (GW25) PFC.

The first essential step in iQCELL methodology was to calculate gene correlations which later contribute to GRN identifications but scRNA-seq datasets suffer from false negative reads of mRNA or dropout effect that impacts genes with low copy numbers and consequently the gene correlations. Therefore, iQcell uses the Markov Affinity-based Graph Imputation of Cells (MAGIC) algorithm to correct the data for dropout effects and takes advantage of the higher numbers of genes to infer gene network relations (Van Dijk et al., 2018). MAGIC simply computed the affinities between neighbor cells and applied it to recover the undercounted values of individual gene expression.

After data imputation, we identified the interesting genes for GRN inference in two ways: first, by automated selection plus overlap with PAGA genes and CellRank lineage drivers which mostly aligned with our selection of genes containing OPC lineage genes (Supplementary Figures S6, S7A), and second, by manually curating to keep only transcription factors in top candidates (Figure 3A). In a functional GRN created by iQcell, interactions are not necessarily biophysically direct rather they capture the consequence of regulatory relations.

The iQcell filtered the number of gene interactions through binarization of the gene expression counts clustering into expressed and non-expressed states (Figure 3A; Supplementary Figure S7A) and formed a gene interaction hierarchy. The resulting directional network served as the foundation for inferring executable GRNs (Figure 3B; Supplementary Figure S7B). We then identified the initial cell states of interacting genes for simulating the perturbations (Figure 3C; Supplementary Figure S7C). Initial states were based on interaction networks and regulatory profiles (Figures 3B,C; Supplementary Figures S7B,C), which show ideal OPC profiles for known transcriptional regulators. Moreover, neuronal genes were observed to be blocking the OPC lineage genes and vice versa (Supplementary Figure S7C). Here, the gene interaction networks were assigned the signs (+/−) based on Pearson correlation. Positive means genes are positively regulating each other and negative means one can repress the other. iQcell uses discrete expression levels of genes; therefore, the expression levels of mRNA counts were converted to on/off levels. Although the GRNs here essentially did not show direct modulation, it is interesting to observe how few genes (FIBIN, OLIG2, PMP2, and BCAN) show unidirectional regulation having a single interacting effector gene while other genes in a superior hierarchy such as OLIG1, EGFR, and PCDH15 show more than one effector of the regulation (Supplementary Figure S7C). PAX6 showed autoregulation, which is known to be essential for controlling the balance between neurogenesis and neural stem cell self-renewal (Supplementary Figure S7).

It is further important to consider that these predictive regulatory interactions are based on the temporal gene expression in the lineage, and not all of these predicted genes are transcription factors. Nevertheless, we validated the nature of these interactions in a larger scRNAseq dataset containing 15,811 cells with a total of ~19,000 genes (Supplementary Figure S7D). Here, we could observe some filtering of these interactions and additional negative regulators but there is still retention of interaction patterns between important OPC genes. Then, we focused on our selected TF candidates and their interactions with established OPC lineage regulators in the larger dataset. Expression for these was validated in PAGA-based OPC clusters (Supplementary Figure S8). The resulting TF regulatory networks are quite discrete, where we observed OLIG2 regulating different genes including NKX2-2, which has been implicated in oligodendrocyte differentiation, and it further appears to regulate OLIG1 and SOX10. Furthermore, the negative regulation of NEUROD1 is expected in OPC

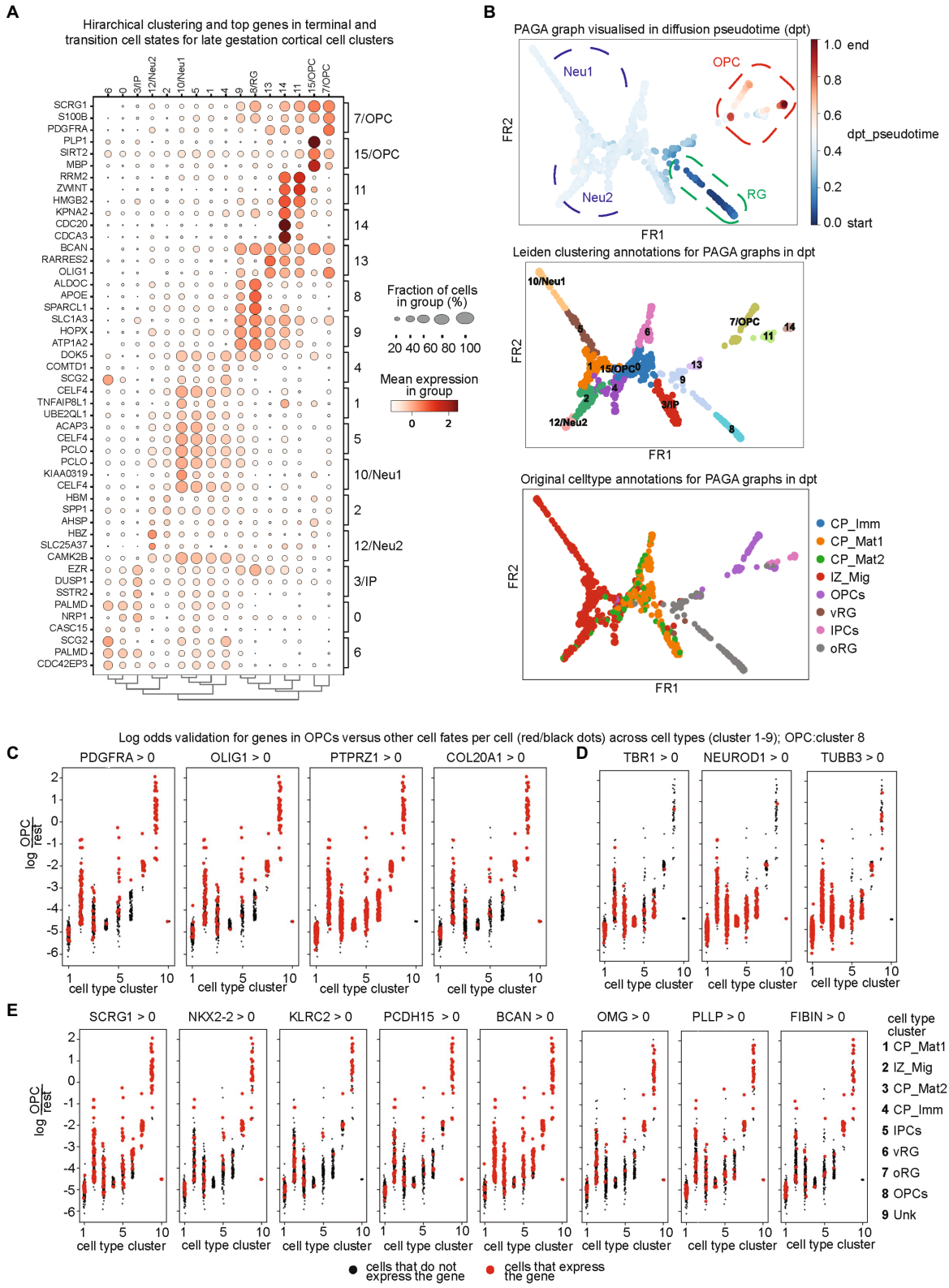

FIGURE 2
(A) Cellular state-specific top gene sets at late gestation time: Hierarchical clustering of identified PAGA clusters and their top genes in terminal and transition cell states for late gestation cortical cells. Fraction of cell numbers is represented in percentage (%), indicated by the circle size and mean expression intensity from low (white color) to high (red); **(B)** Diffusion pseudotime (dpt_pseudotime) plot for PAGA clusters (upper panel), which is then annotated into the PAGA cluster annotations (middle) and then the original cluster annotations from the initial dataset (bottom panel). All annotations show great alignment and confirm the accuracy of diffusion pseudotime. The dpt_pseudotime panel shows the radial glia lineage in dark blue, then neuronal in light blue, and later OPC lineage in red; **(C–E)** Validation of top lineage drivers by plotting the distribution of log odds for OPCs versus other cell fates per cell across cell types. Log-odds ratio confirmed the lineage specificity by comparison of OPC markers genes **(C)**, neuronal genes **(D)**, and the pre-OPC lineage genes.

lineage, but it is interesting to notice the negative regulation of NEUROD1 by SOX8 along with PAX6, where PAX6 appears to be positively regulating SOX8 (Figure 3C). We performed the simulations for normal, gene overexpression (OE) and knockout (KO) conditions and performed the Principal Component Analysis (PCA) to observe any differences (Figure 3D). Based on the role of regulatory genes as observed in GRNs, we simulated the normal OPC profile with the absence of PAX6, SOX8, and NEUROD1 and the presence of the rest of the TFs (Figure 3E, where the blue circle indicates the gene on and gray indicates off and similarly, their state in perturbation type) and performed the sequential perturbations for these TFs to analyze the attractor state that represents the long-term behavior of simulations linked to biological phenotypes.

The principal component analysis of simulated profiles for normal and perturbed conditions shows huge variation in cell states, as well as a developing trajectory in the pseudo time for perturbed KO states (Figure 3D). Gene perturbation effects showed that the overexpression of genes does not largely affect the fate (Figure 3F) or expression state of other genes but knock out does (Figure 3G). The knockout of OLIG2 affected all analyzed gene expression states related to OPC lineage as they are downstream in GRN, while OLIG1 KO caused the absence of SOX10 and PRRX1 as well as NKX2-2, which is upstream to OLIG1. Similarly, NR0B1 KO affected the SIRT2 expression state. We also found that FIBIN, OLIG2, PMP2, BCAN, and SCRG1 have important roles in regulating the lineage but not in deciding the fate as shown in the knockout analysis of all selected genes (Supplementary Figure S7E). These perturbation states provide interesting observations for gene interactions that might affect how OPCs develop into oligodendrocytes and affect their maturation and placement in the brain.

4. Discussion

The cerebral cortex is strikingly enlarged in humans and known to be responsible for our mental abilities such as intelligence, cognition, and perception (Reillo et al., 2011; Yeo et al., 2011). Constituent cortical cell types are generated during embryonic brain development through a series of neurogenic and gliogenic processes (Eze et al., 2021). However, the molecular regulatory sequence of the events underlying these developmental processes is less well understood. Therefore, characterizing the cellular and molecular heterogeneity of the human cortex is essential to understand its functional regulations and understand how its disruption may contribute to the emergence of neurodevelopmental disorders.

Cortical cell types express varying transcription factor combinations at distinct phases of development (Singh et al., 2022). These transcription factors (TFs) are critical to specify correct signals and driving the development of distinct neural cell types in the brain. Here, using single-cell transcriptomic datasets of the developing prefrontal cortex from GW8-26 (Zhong et al., 2018) and late gestation stage (GW25) (Bhaduri et al., 2021), we characterized and validated the molecular regulatory features of cell fate transitions at early, mid, and late stages of embryonic brain development. It is known that cell fate decisions are stochastic and more so at the early embryonic development, and at the later time points, more deterministic fates are made as they arise from more committed precursors and a complex regulatory network of TFs, specific to each state. Nonetheless, this transcriptomic complexity almost certainly exceeded several-fold through several transient transcriptomic cell states that exist during development. Understanding cortical development, hence, necessitates characterizing these transient cell states. It has been proposed that these transient cellular states are more plastic in nature and able to undergo specific changes in core gene regulatory programs and enable the specification or conversion into various cell fates (Goldman and Poss, 2020). This is also relevant to illustrate how cortical stem cells can be directed to specific cell fates for disease modeling or treatment. Hence, we calculated the fate probabilities for each cell using the CellRank algorithm on the scRNAseq dataset and ordered the cells in initial, terminal, and intermediate states, taking into account the gradual and stochastic nature of cellular fate decisions. Single-cell transcriptomics (scRNA-seq) has advanced our knowledge concerning cellular heterogeneity and discrete regulatory networks. scRNA-seq captures a snapshot of sequenced cells at one timepoint, but those individual cells can represent a reasonably wide range of dynamic stages or cell states; therefore, it is more practical to arrange them in the temporal order of cell states to infer the trajectory of cell fate transition and identify the intermediate transient states crucial for cell-type specification (MacLean et al., 2018). Consequently, we analyzed the gene expression dynamics with respect to different fates and identified the most prominent regulators of cell fate decisions. Given the terminal states, we computed the probability of how likely a cell will transition toward any of these terminal states and plotted the computed fate probabilities in the force-directed embedding. To understand the cell transition paths in depth, we used the PAGA program and characterized that neural stem cells can reach a cell fate using distinct intermediate states making them traverse a distinct molecular path that might be regulated through a variety of intrinsic and extrinsic signals. By analyzing the gene expression dynamics along each path, it is clearer to see the gradual dynamics of a cell fate and assess the correct or more feasible path with defined genetic circuitry.

The majority of the neuronal cells develop during embryonic brain development, and there is little evidence and still an undergoing debate that neurons are generated in the adult brain. Most of the proliferating cells in the adult brain have oligodendroglial lineage origin that can still proliferate, differentiate, and mature into oligodendrocytes later in the adult brain (Kuhn et al., 2019). In the late stage of embryonic brain development, a spike in gliogenesis and OPC lineage has been detected in abundance during the second trimester of embryonic brain development. Analysis of transcriptional processes has revealed a distinct period of OPC generation in mouse and human embryonic development. Thus, to analyze human cortex-specific regulation of OPC lineage, we explored the regulatory features of certain pre-OPC lineage genes, that were inferred from lineage analysis and already known in OPCs to likely affect the development and maturation (Huang et al., 2020). We used the iQcell platform (Heydari et al., 2022) to infer the gene regulatory network and analyze the effect of gene manipulations on cellular dynamics. These genes were selected as top overlapping features from CellRank (Lange et al., 2022) and PAGA (Wolf et al., 2019) intermediate states as lineage drivers. iQcell modeled the gene interactions as Boolean logic function and then simulated the effect of gene knockout or overexpression as a result of normalizing their level from pseudo time levels. It was evident that only certain factors have a role in lineage commitment while the rest are important in a hierarchical manner for different functions during the differentiation and maturation of OPCs. Overexpression of these genes does not show huge changes and as expected neuronal perturbations do not affect the glial cells and vice versa. Although, initially, the low cell number and especially low cell number per developmental stage tend to affect the analysis outcomes, still the most prominent features

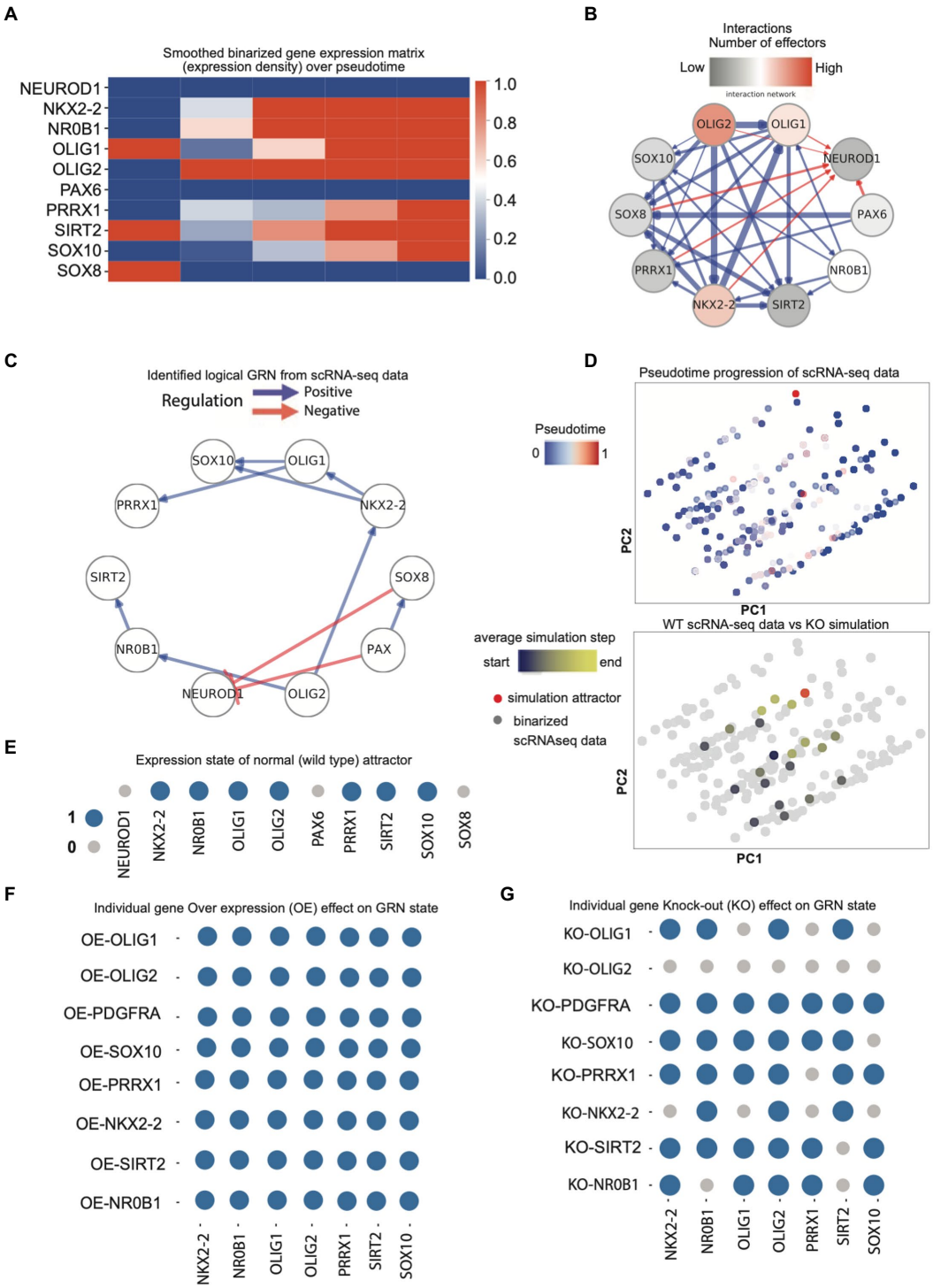

FIGURE 3
(A) Initial smoothed binarized gene expression states for neuronal and OPC genes (expression density). Gene expression values are binarized by clustering, then averaged over a pseudo-time window, and thereafter sorted based on transition points from early to late. Red means high expression and blue means low expression; **(B)** the set of all possible gene–gene interactions, filtered by interaction hierarchy and mutual information. Positive and negative interactions are represented by blue and red edges, respectively. Edge width represents the relative amount of mutual information of the interaction. **(C)** The provisional GRN for OPC lineage genes shows the direction of gene regulation for selected candidates. The GRN is obtained by constraining the possible interactions both to follow the *in vivo* data progression when executed as a logical network and maximize the mutual information between gene pairs. Positive and negative interactions are represented by blue and red edges, respectively. **(D)** Upper panel: The PCA plot of the binarized scRNA-seq data color-coded with the pseudo-time values attributed to each cell. The binarization is performed by clustering the scRNA-seq expressions into expressed or not expressed levels; lower panel: The PCA plot of the simulated developmental trajectories is overlaid on the binarized scRNA-seq. The detected attractor is colored red. The simulated data are color coded by the value of the average simulation step (average distance to the attractor of simulation); **(E)** Expression states of the GRN model steady-state attractor. Genes that are expressed (1) and not expressed (0) are represented with blue and gray circles, respectively; **(F)** Expression states of the model attractors under sequential overexpression (OE) perturbations; **(G)** Expression states of the model attractors under knock-out (KO) perturbations.

are well captured. Furthermore, we ruled out the major concern of low cell numbers and revalidated our observations using a stage-specific higher read and cell number dataset of GW25 with 15,811 cells for OPC lineage GRN identifications and gene perturbation effects.

Along with the characteristic OPC genes, we observed contributions of the novel SOX group TFs toward the OPC lineage, such as SOX8 repressing the neurogenic genes for OPC fate switches and SOX10 being a downstream effector of OLIG1. SOX10 has been widely studied in promoting oligodendrocyte differentiation in humans (García-León et al., 2018) as well as in other species (Takada et al., 2010; Hornig et al., 2013), but the role of SOX8 in OPC cell lineage is not well-defined (Stolt et al., 2005; Wang et al., 2014). OLIG1 and OLIG2 mediated the regulation of certain important TFs such as NR0B1 and PRRX1, and their downstream effectors is an interesting avenue to be explored in OPC maintenance or differentiation to oligodendrocytes. Overall, we established these sequential GRNs in two scRNA-seq datasets and also identified novel TF regulatory networks. We validated that scRNA-seq has the power to identify lineage drivers and that iQcell can filter genes that are not significant in lineage commitment while still having other roles. Therefore, these genes should be investigated for their regulatory roles in future experimental studies.

Data availability statement

Publicly available datasets were analyzed in this study. This data can be found at https://www.ncbi.nlm.nih.gov/, GSE104276 and https://data.nemoarchive.org/biccn/grant/u01_devhu/kriegstein/transcriptome/scell/10x_v2/human/processed/counts/.

Author contributions

AS analyzed data and wrote the manuscript. VT supervised the study and wrote the manuscript. All authors contributed to the article and approved the submitted version.

Funding

This study was supported by the Deutsche Forschungsgemeinschaft TI 799/1-3 and Novo Nordisk Foundation P3110103 grants to VT.

Acknowledgments

We would like to thank the members of the Tiwari lab for their cooperation and critical feedback throughout this study. The support from the Facilities of the Queen's University Belfast and the University of Southern Denmark is gratefully acknowledged.

Conflict of interest

The authors declare that the research was conducted in the absence of any commercial or financial relationships that could be construed as a potential conflict of interest.

Publisher's note

Supplementary material

The Supplementary material for this article can be found online at: https://www.frontiersin.org/articles/10.3389/fnmol.2023.1126438/full#supplementary-material

References

Bhaduri, A., Sandoval-Espinosa, C., Otero-Garcia, M., Oh, I., Yin, R., Eze, U. C., et al. (2021). An atlas of cortical arealization identifies dynamic molecular signatures. *Nature* 598, 200–204. doi: 10.1038/s41586-021-03910-8

Cadwell, C. R., Bhaduri, A., Mostajo-Radji, M. A., Keefe, M. G., and Nowakowski, T. J. (2019). Development and arealization of the cerebral cortex. *Neuron* 103, 980–1004. doi: 10.1016/j.neuron.2019.07.009

Del-Valle-Anton, L., and Borrell, V. (2022). Folding brains: from development to disease modeling. *Physiol. Rev.* 102, 511–550. doi: 10.1152/physrev.00016.2021

Eze, U. C., Bhaduri, A., Haeussler, M., Nowakowski, T. J., and Kriegstein, A. R. (2021). Single-cell atlas of early human brain development highlights heterogeneity of human neuroepithelial cells and early radial glia. *Nat. Neurosci.* 24, 584–594. doi: 10.1038/s41593-020-00794-1

Fan, X., Dong, J., Zhong, S., Wei, Y., Wu, Q., Yan, L., et al. (2018). Spatial transcriptomic survey of human embryonic cerebral cortex by single-cell RNA-seq analysis. *Cell Res.* 28, 730–745. doi: 10.1038/s41422-018-0053-3

Fleck, J. S., Jansen, S. M. J., Wollny, D., Zenk, F., Seimiya, M., Jain, A., et al. (2022). Inferring and perturbing cell fate regulomes in human brain organoids. *Nature*, 1–8. doi: 10.1038/s41586-022-05279-8

Fletcher, R. B., Das, D., and Ngai, J. (2018). Creating lineage trajectory maps via integration of single-cell RNA-sequencing and lineage tracing: integrating transgenic lineage tracing and single-cell RNA-sequencing is a robust approach for mapping developmental lineage trajectories and cell fate changes. *BioEssays* 40:1800056. doi: 10.1002/bies.201800056

García-León, J. A., Kumar, M., Boon, R., Chau, D., One, J., Wolfs, E., et al. (2018). SOX10 single transcription factor-based fast and efficient generation of oligodendrocytes from human pluripotent stem cells. *Stem Cell Rep* 10, 655–672. doi: 10.1016/j.stemcr.2017.12.014

Goldman, J. A., and Poss, K. D. (2020). Gene regulatory programmes of tissue regeneration. *Nat. Rev. Genet.* 21, 511–525. doi: 10.1038/s41576-020-0239-7

Hao, Y., Hao, S., Andersen-Nissen, E., Mauck Iii, W. M., Zheng, S., Butler, A., et al. (2021). Integrated analysis of multimodal single-cell data. *Cells* 184:e29, 3573–3587.e29. doi: 10.1016/j.cell.2021.04.048

Herring, C. A., Simmons, R. K., Freytag, S., Poppe, D., Moffet, J. J., Pflueger, J., et al. (2022). Human prefrontal cortex gene regulatory dynamics from gestation to adulthood at single-cell resolution. *Cells* 185:e28, 4428–4447.e28. doi: 10.1016/j.cell.2022.09.039

Heydari, T. A., Langley, M., Fisher, C. L., Aguilar-Hidalgo, D., Shukla, S., Yachie-Kinoshita, A., et al. (2022). IQCELL: a platform for predicting the effect of gene perturbations on developmental trajectories using single-cell RNA-seq data. *PLoS Comput. Biol.* 18:e1009907. doi: 10.1371/journal.pcbi.1009907

Hornig, J., Fröb, F., Vogl, M. R., Hermans-Borgmeyer, I., Tamm, E. R., and Wegner, M. (2013). The transcription factors Sox10 and Myrf define an essential regulatory network module in differentiating oligodendrocytes. *PLoS Genet.* 9:e1003907. doi: 10.1371/journal.pgen.1003907

Huang, W., Bhaduri, A., Velmeshev, D., Wang, S., Wang, L., Rottkamp, C. A., et al. (2020). Origins and proliferative states of human oligodendrocyte precursor cells. *Cells* 182:e11, 594–608.e11. doi: 10.1016/j.cell.2020.06.027

Jeong, H., and Tiwari, V. K. (2018). Exploring the complexity of cortical development using single-cell transcriptomics. *Front. Neurosci.* 12:31. doi: 10.3389/fnins.2018.00031

Kriegstein, A., Noctor, S., and Martínez-Cerdeño, V. (2006). Patterns of neural stem and progenitor cell division may underlie evolutionary cortical expansion. *Nat. Rev. Neurosci.* 7, 883–890. doi: 10.1038/nrn2008

Kuhn, S., Gritti, L., Crooks, D., and Dombrowski, Y. (2019). Oligodendrocytes in development, myelin generation and beyond. *Cells* 8:1424. doi: 10.3390/cells8111424

Lange, M., Bergen, V., Klein, M., Setty, M., Reuter, B., Bakhti, M., et al. (2022). CellRank for directed single-cell fate mapping. *Nat. Methods* 19, 159–170. doi: 10.1038/s41592-021-01346-6

Luecken, M. D., and Theis, F. J. (2019). Current best practices in single-cell RNA-seq analysis: a tutorial. *Mol. Syst. Biol.* 15:e8746. doi: 10.15252/msb.20188746

Maclean, A. L. (2022). Profiling intermediate cell states in high resolution. *Cell Rep Methods* 2:100204. doi: 10.1016/j.crmeth.2022.100204

Maclean, A. L., Hong, T., and Nie, Q. (2018). Exploring intermediate cell states through the lens of single cells. *Curr Opinion Syst Biol* 9, 32–41. doi: 10.1016/j.coisb.2018.02.009

Mayer, C., Hafemeister, C., Bandler, R. C., Machold, R., Batista Brito, R., Jaglin, X., et al. (2018). Developmental diversification of cortical inhibitory interneurons. *Nature* 555, 457–462. doi: 10.1038/nature25999

Mu, Q., Chen, Y., and Wang, J. (2019). Deciphering brain complexity using single-cell sequencing. *Genomics Proteomics Bioinformatics* 17, 344–366. doi: 10.1016/j.gpb.2018.07.007

Nowakowski, T. J., Bhaduri, A., Pollen, A. A., Alvarado, B., Mostajo-Radji, M. A., Di Lullo, E., et al. (2017). Spatiotemporal gene expression trajectories reveal developmental hierarchies of the human cortex. *Science* 358, 1318–1323. doi: 10.1126/science.aap8809

Reillo, I., De Juan Romero, C., García-Cabezas, M. Á., and Borrell, V. (2011). A role for intermediate radial glia in the tangential expansion of the mammalian cerebral cortex. *Cereb. Cortex* 21, 1674–1694. doi: 10.1093/cercor/bhq238

Shen, S., Sun, Y., Matsumoto, M., Shim, W. J., Sinniah, E., Wilson, S. B., et al. (2021). Integrating single-cell genomics pipelines to discover mechanisms of stem cell differentiation. *Trends Mol. Med.* 27, 1135–1158. doi: 10.1016/j.molmed.2021.09.006

Singh, A., Mahesh, A., Noack, F., Cardoso De Toledo, B., Calegari, F., and Tiwari, V. K. (2022). Tcf12 and NeuroD1 cooperatively drive neuronal migration during cortical development. *Development* 149:dev200250. doi: 10.1242/dev.200250

Stolt, C. C., Schmitt, S., Lommes, P., Sock, E., and Wegner, M. (2005). Impact of transcription factor Sox8 on oligodendrocyte specification in the mouse embryonic spinal cord. *Dev. Biol.* 281, 309–317. doi: 10.1016/j.ydbio.2005.03.010

Takada, N., Kucenas, S., and Appel, B. (2010). Sox10 is necessary for oligodendrocyte survival following axon wrapping. *Glia* 58, 996–1006. doi: 10.1002/glia.20981

Van Dijk, D., Sharma, R., Nainys, J., Yim, K., Kathail, P., Carr, A. J., et al. (2018). Recovering gene interactions from single-cell data using data diffusion. *Cells* 174:e27. doi: 10.1016/j.cell.2018.05.061

Velmeshev, D., Chavali, M., Nowakowski, T. J., Bhade, M., Mayer, S., Goyal, N., et al. (2021). Molecular diversity and lineage commitment of human interneuron progenitors. *BioRxiv* 2021:444045. doi: 10.1101/2021.05.13.444045

Wang, J., Pol, S. U., Haberman, A. K., Wang, C., O'bara, M. A., and Sim, F. J. (2014). Transcription factor induction of human oligodendrocyte progenitor fate and differentiation. *Proc. Natl. Acad. Sci.* 111, E2885–E2894. doi: 10.1073/pnas.1408295111

Wolf, F. A., Angerer, P., and Theis, F. J. (2018). SCANPY: large-scale single-cell gene expression data analysis. *Genome Biol.* 19:15. doi: 10.1186/s13059-017-1382-0

Wolf, F. A., Hamey, F. K., Plass, M., Solana, J., Dahlin, J. S., Göttgens, B., et al. (2019). PAGA: graph abstraction reconciles clustering with trajectory inference through a topology preserving map of single cells. *Genome Biol.* 20, 1–9. doi: 10.1186/s13059-019-1663-x

Yang, L., Li, Z., Liu, G., Li, X., and Yang, Z. (2022). Developmental origins of human cortical oligodendrocytes and astrocytes. *Neurosci. Bull.* 38, 47–68. doi: 10.1007/s12264-021-00759-9

Yeo, B. T., Krienen, F. M., Sepulcre, J., Sabuncu, M. R., Lashkari, D., Hollinshead, M., et al. (2011). The organization of the human cerebral cortex estimated by intrinsic functional connectivity. *J. Neurophysiol.* 106, 1125–1165. doi: 10.1152/jn.00338.2011

Yu, Y., Zeng, Z., Xie, D., Chen, R., Sha, Y., Huang, S., et al. (2021). Interneuron origin and molecular diversity in the human fetal brain. *Nat. Neurosci.* 24, 1745–1756. doi: 10.1038/s41593-021-00940-3

Zhong, S., Zhang, S., Fan, X., Wu, Q., Yan, L., Dong, J., et al. (2018). A single-cell RNA-seq survey of the developmental landscape of the human prefrontal cortex. *Nature* 555, 524–528. doi: 10.1038/nature25980

frontiers | Frontiers in Molecular Neuroscience

TYPE Original Research
PUBLISHED 05 May 2023
DOI 10.3389/fnmol.2023.1139287

OPEN ACCESS

EDITED BY
Estela Maris Muñoz,
CONICET Dr. Mario H. Burgos Institute of Histology and Embryology (IHEM), Argentina

REVIEWED BY
Ariel A. Di Nardo,
Centre National de la Recherche Scientifique (CNRS), France
Alex Shcheglovitov,
The University of Utah, United States
Sui Wang,
Stanford University, United States

*CORRESPONDENCE
Noel J. Buckley
✉ noel.buckley@psych.ox.ac.uk
Shankar Subramaniam
✉ shsubramaniam@ucsd.edu

†These authors have contributed equally to this work

RECEIVED 06 January 2023
ACCEPTED 14 April 2023
PUBLISHED 05 May 2023

CITATION
Gupta S, Polit LD, Fitzgerald M, Rowland HA, Murali D, Buckley NJ and Subramaniam S (2023) Temporal transcriptional control of neural induction in human induced pluripotent stem cells.
Front. Mol. Neurosci. 16:1139287.
doi: 10.3389/fnmol.2023.1139287

Temporal transcriptional control of neural induction in human induced pluripotent stem cells

Shakti Gupta[1†], Lucia Dutan Polit[2†], Michael Fitzgerald[1], Helen A. Rowland[3], Divya Murali[1], Noel J. Buckley[3*] and Shankar Subramaniam[1,4*]

[1]Department of Bioengineering, University of California, San Diego, San Diego, CA, United States, [2]Maurice Wohl Clinical Neuroscience Institute, King's College London, London, United Kingdom, [3]Department of Psychiatry and Kavli Institute for Nanoscience Discovery, University of Oxford, Oxford, United Kingdom, [4]Departments of Computer Science and Engineering, and Cellular and Molecular Medicine, University of California, San Diego, San Diego, CA, United States

Introduction: Neural induction of human induced pluripotent stem cells represents a critical switch in cell state during which pluripotency is lost and commitment to a neural lineage is initiated. Although many of the key transcription factors involved in neural induction are known, we know little of the temporal and causal relationships that are required for this state transition.

Methods: Here, we have carried out a longitudinal analysis of the transcriptome of human iPSCs undergoing neural induction. Using the temporal relationships between the changing profile of key transcription factors and subsequent changes in their target gene expression profiles, we have identified distinct functional modules operative throughout neural induction.

Results: In addition to modules that govern loss of pluripotency and gain of neural ectoderm identity, we discover other modules governing cell cycle and metabolism. Strikingly, some of these functional modules are retained throughout neural induction, even though the gene membership of the module changes. Systems analysis identifies other modules associated with cell fate commitment, genome integrity, stress response and lineage specification. We then focussed on OTX2, one of the most precociously activated transcription factors during neural induction. Our temporal analysis of OTX2 target gene expression identified several OTX2 regulated gene modules representing protein remodelling, RNA splicing and RNA processing. Further CRISPRi inhibition of OTX2 prior to neural induction promotes an accelerated loss of pluripotency and a precocious and aberrant neural induction disrupting some of the previously identified modules.

Discussion: We infer that OTX2 has a diverse role during neural induction and regulates many of the biological processes that are required for loss of pluripotency and gain of neural identity. This dynamical analysis of transcriptional changes provides a unique perspective of the widespread remodelling of the cell machinery that occurs during neural induction of human iPSCs.

KEYWORDS

pluripotency, induced pluripotent stem cell, neural induction, transcription, OTX2

1. Introduction

Human iPSCs serve as excellent cellular models for neural lineage specification. Neuronal development from iPSC offers the potential to discover molecular pathways governing neurological pathologies and provide screens for target and therapeutic discovery. Furthermore, recent studies have demonstrated that iPSC-derived neurons reflect key aspects of clinical

phenotype of the individual from whom the iPSCs were derived in a patient-specific manner (Lagomarsino et al., 2021; Ng et al., 2022), opening the door to using iPSC-derived neurons to discover pathogenic mechanisms and deliver personalized treatment. However, realization of this vision is hampered by the considerable variation that exists in the efficiency with which individual iPSCs generate neurons (Volpato and Webber, 2020). Differentiating iPSCs to neurons is a multi-step process and each step introduces more potential for variation. The first step on this developmental journey is neural induction, the initiating process by which pluripotent iPSCs become committed to a neural fate and transition to multipotent neural precursors (Stern, 2006). Understanding the temporally-relevant molecular mechanisms that drive this transition is critical to driving consistent differentiation toward neurons.

Our current understanding of vertebrate neural induction is based on the 'default model' whereby the neural plate emerges from dorsal ectoderm *via* blockade of BMP/NODAL signaling through release of inhibitors and other inductive and permissive signals originating from the organizer and flanking epidermis (Hemmati-Brivanlou and Melton, 1997). This default model of neural induction has now been shown to be broadly conserved across mammals and has also been demonstrated in human embryonic stem cells (Ozair et al., 2013). Neural induction can be recapitulated in human pluripotent stem cells using dual SMAD inhibition to block BMP/NODAL signaling (Chambers et al., 2009), a process that is sufficient to initiate neural induction and concurrently suppress pluripotency. Several key transcription factors expressed early during neural induction have been identified including some, such as PAX6 and ZNF521, that are necessary and sufficient to drive neural induction in human ESCs (Zhang et al., 2010; Kamiya et al., 2011). Others such as ZEB2 and NR2F2 have a dual function and act to concurrently directly suppress pluripotency factors such as POUF51 and activate pro-neural induction factors such as PAX6 (Ozair et al., 2013). Changes in cell state during development require wholesale remodeling of the cells' regulatory and physical landscape reflected in timely and coordinated regulation of the epigenome, proteome and metabolome. The regulatory factors that orchestrate this transition from pluripotency to a specified lineage act transiently over specific time periods to achieve intermediate end point cell states. For the most part the resultant regulatory networks have been inferred from transcriptome data harvested from the end points of the developmental trajectory and the resulting interaction maps are static and fail to capture the dynamical aspects of the network throughout the developmental transition. However, deciphering the temporal aspects of involvement of specific regulatory factors is now possible from studying the transcription landscape changes during the lineage specification and it is this perspective that motivated the work presented here.

In this study, our goal was primarily to investigate the early-stage cell state regulators during neural induction using a fine-grained transcriptomic analyses. We harvested transcriptome data throughout 8 days of neural induction of human iPSCs, and captured the temporal profile of key transcription factors and their target genes to identify functional modules that are operative during neural induction. Our systems analysis revealed, in addition to canonical modules associated with loss of pluripotency and gain of neural identity, a number of additional modules, including those that regulate cell cycle, metabolism, genome integrity and stress. Two key factors include KEAP and NRF2, genes that regulate cellular response to numerous stressors, including oxidative, metabolic stressors (Baird and Yamamoto, 2020). Strikingly, even though some of these modules are operative throughout neural induction, the gene membership of the modules changes, indicating a degree of redundancy of gene membership in retaining module functionality. In order to validate the power of our analysis, we used CRISPRi to knock down expression of one of the most precociously expressed transcription factors during neural induction, OTX2 (Acampora et al., 2013). We find that loss of OTX2 leads to an accelerated loss of pluripotency and an accelerated and aberrant neural induction and disrupts many of the previously identified modules. Our analysis of the dynamics of transcriptional changes provides a unique perspective of the dynamics of transcriptional modules and widespread remodeling of the cell machinery, illustrating the tight coupling between changes in cell state and lineage and regulation of basic cellular machinery that occurs during neural induction of human iPSCs.

2. Materials and methods

2.1. Neural differentiation from human ESCs and iPSCs

Three human induced pluripotent stem cell (hiPSC) lines (CTR M1 04, CTR_M2_42 and CTR_M3_36s), derived from neurotypic males from ages ranging between 35 to 55 years, were used to generate two time series namely 0–48 h (h) and 0–8 days (d). These iPSC lines were maintained in Essential 8™ medium (Thermo Fisher) without antibiotics at 37°C, 5% CO_2, 5% O_2 on Geltrex™ (Thermo Fisher) coated plates. Differentiation of iPSCs was carried out as previously described (Shi et al., 2012; Lee et al., 2020). Briefly. As iPSCs reached 100% confluence, media was switched from Essential 8™ medium (Thermo Fisher) to neural induction medium. Neural induction medium comprised 50% Neurobasal medium (Thermo), including B-27 (Thermo) and GlutaMAX (Thermo), and 50% DMEM/F12 (Thermo) supplemented with N-2 (Thermo) and GlutaMAX (Thermo). The dual SMAD inhibitors (2i) 100 nM LDN193189 (Sigma Aldrich) and 10 μM SB431542 (Sigma Aldrich) with and without the inclusion of the WNT inhibitor XAV939 were also added for the first 7 days. The medium was changed daily throughout the differentiation. Data generated by all three cell lines and two neural induction protocols showed the similarity based on the principle component analysis (PCA) and changes in key pluripotency and neuroectoderm transcription factors (Supplementary Figure S1). Thus, The CTR M3 36S line was analyzed for the 0–48 h time series containing 8 time points, 0, 2, 4, 8, 18, 24, 30, and 48 h and the CTR M1 04 line was analyzed for 0–8 days time series containing 7 time points, 0, 1, 2, 3, 4, 6, and 8 d. The cell line CTR M2 42 was analyzed at time points 0,1,2,3,4,6 and 8 and was used exclusively for the generation of the PCA.

2.2. RNA isolation, analysis, library preparation, and sequencing

RNA was extracted at time points: day 0 (before the addition of differentiation media) and days 1, 2, 3, 4, 6 and 8 after induction. RNA was harvested and lysed with Trizol reagent (Life technologies, 15,596,026) and isolated by centrifugation with 100% Chloroform, following by 100% isopropanol and lastly by 75% ethanol. The RNA

was purified with Qiaquick PCR purification kit (Quiagen, 28,106) and quantified with the NanoDrop 1,000 Spectrophotometer (Thermo scientific). The quality control was assessed by analyzing the RNA with the Agilent RNA 6000 nano Kit (Agilent technologies, 5,067–1,511) in combination with the Agilent 2,100 Bioanalyzer system.

RNAseq libraries were prepared with the Truseq RNA Kit. Briefly, mRNA was purified from total RNA followed by cDNA synthesis. Subsequently, the cDNA was end-paired, A-tailed and custom indexing adapters were ligated. Samples were size selected and pooled for sequencing. Libraries were multiplexed at 8 samples per lane and sequenced in a Hiseq 2,500 Sequencing System (Ilumina) to a depth of 20–30 million reads per sample.

2.3. OTX2 knockdown

For CRISPRi experiments, iPSCs bearing a dCas9-KRAB construct under control of the inducible tetO promoter and integrated into the AAVS1 locus (Mandegar et al., 2016) were passaged onto Geltrex (Life Tech) coated plates at 10% confluency. iPSCs were then transduced with lentiviral particles carrying OTX2 gRNAs in the MRP253 backbone. A gRNA sequence targeting the dominant OTX2 transcription start site (GGAAAGTCGGCCCAAATCGG) was sourced from Gilbert et al. (2014). Lentiviral particles bearing the gRNAs were used at a ratio of 1:8 for 24 h in the presence of 10 μM ROCk inhibitor (Y27632, Stratech). Lentiviral media was removed and exchanged for standard Essential 8™ medium (ThermoFisher) for 24 h before being cultured with 1.5 μg/ml puromycin for 24 h. Cells were then cultured in standard Essential 8™. RNA was isolated using standard protocols (Gilbert et al., 2014). CRISPRi iPSCs were plated out, and 2 μg/mL doxycycline (Sigma) added 48 h before iPSCs reached confluence (excluding controls). Once confluent, iPSCs were switched to neural induction medium with or without doxycycline. Neural induction medium comprised 50% Neurobasal medium including B27 and 50% DMEM/F12 supplemented with N2 and Glutamax. The dual SMAD inhibitors 1 μM dorsomorphin and 10 μM SB431542 were also added. Cell media was changed daily and cells in neural induction medium were collected at time points of 0, 1, 2 and 7 days following initiation of neural induction. OTX2 expression was monitored using RT-PCR and RNAseq was carried on an Illumina NovaSeq6000 using 150 bp, PE flow cells. We thank the Oxford Genomics Centre at the Wellcome Centre for Human Genetics (funded by Wellcome Trust grant reference 203,141/Z/16/Z) for the generation and initial processing of sequencing data.'

2.4. Real-time polymerase chain reaction (Q-PCR)

The primers were designed with Primer3Plus (v. 0.4.0) software (Supplementary Table S1). Gene sequences were extracted from the NCBI GenBank and the University of California and Santa Cruz (UCSC) genome and bioinformatics browser (Supplementary Table S1). Complementary DNA (cDNA) was synthetized from 1 μg of RNA using M-MLV Reverse Transcriptase enzyme (Promega, M1701) following manufacturer's instructions. Real-time polymerase chain reaction (Q-PCR) assays were conducted by using iQ Sybr Green supermix (Bio-rad, 178,880) according to the provider specifications. Amplifications were performed in a Bio-Rad PTC-200 Peltier thermal cycler detection system. The housekeeping gene GAPDH was used to normalize the genes expression levels between technical replicates. The Pfaffl comparative method of relative quantification was used to quantify gene relative expression of each sample at different time points. The reference sample used to compare the gene expression of all cell lines was randomly designated as the time point 0 of the 3 technical replicates (Supplementary Figure S2). The means between samples were compared by a one-way ANOVA test with Bonferroni correction with 95% confidence interval with Prism package of GraphPad software.

2.5. Immunocytochemistry

Approximately 100,000 cells were plated on each well of Nunclon delta surface 96 well plates (Thermo Fisher148761) and fixed at different time points with 4% paraformaldehyde (PFA) (Thermo Fisher, 28,906) in PBS 1X for 15 min at room temperature. The wells were washed 3 times with 1X PBS and permeabilized and blocked by incubation with 4% normal donkey serum (Sigma Aldrich, D9663) in 1X PBST. The nuclei were stained by incubation with Hoechst 33342 (Thermo Fisher, H3570). Cells were incubated with specific dilutions of mouse monoclonal and rabbit polyclonal primary antibodies together according to the provider specifications (Supplementary Table S2). Validation of the antibodies binding specificity was assessed by replacing primary antibodies with the same dilution of purified mouse IgG (Merck Millipore, CS200621) or rabbit IgG as controls (Thermo Fisher, 02–6,102). Immunoreactivity was analyzed by using Alexa Fluor 594 conjugated donkey anti-mouse IgG (Invitrogen, A-21203) and Alexa Fluor 488 conjugated donkey anti-rabbit IgG (Invitrogen, R37118) both diluted to 1:250 ratio in blocking buffer.

Images were acquired with a 20X objective with the Cell insight CX5 High Content Screen Platform (Thermo Fisher, CX51110). Expression was quantified using the bioapplication Cell Health Profiling from the iDev software package (Thermo Fisher). Hoechst staining was used to assess cell viability. Specific staining intensity, shape and size parameters were established to identify positive and negative labeled cells. A total of 3 wells were analyzed per primary antibody pair with 61 acquired fields per well. The means of the percentages of positive cells at each time point were statistically compared by a two-way ANOVA test with 95% confidence interval with Bonferroni correction with Prism package of GraphPad software.

2.6. RNA-seq data analysis

RNA-seq fastq files were aligned to the Human Reference Genome (version hg38) and FPKM counts (Refgene) were generated using the Omicsoft Aligner (OSA; Hu et al., 2012). Only genes with FPKM counts greater than 1 in any sample were included in further analysis. For the time-series data, a gene was called differentially expressed (DE) based on a fold change (FC) cutoff of 2 (up or down) detected at a minimum of 2 time points with respect to time 0. However, because of the availability of replicates in OTX2 knockdown experiment, DESEQ2 with value of p cutoff of 0.05 and FC cutoff of 1.3 was used for DE gene identification. Enrichment analysis was performed using

Gene set Enrichment Analysis (GSEA) to identify the biological significance (Subramanian et al., 2005). GSEA was used to avoid the limitation due to 1 replicate and high cut off used for DE analysis in time-series data as it uses the information of all the genes in the enrichment process. Gene Ontology (GO) and Reactome, Kyoto Encyclopedia of Genes and Genomes (KEGG) pathways were used to identify overrepresented annotation terms.

2.7. Protein–protein interaction networks

Protein–protein interaction (PPI) analysis was performed using STRING database in Cytoscape.[1] For the PPI analysis, union of all DE genes from all time points were used. For example, DE genes from all the time points in 48 dataset were combined to generate the 48 h PPI network. PPI edge confidence score of 0.9 and 0.7 were used for TF networks and OTX2 targets networks, respectively. Network modules were identified using Glay method in Cytoscape and annotated manually.

2.8. Transcription factor-target analysis

TRANSFAC® data was used initially as the source for Transcription factor (TF)–target gene information. However, curation of TRANSFAC was over-represented by the large number of immune system and disease studies, thus the analysis using TRANSFAC data produced spurious results indicating a major role of JUN, FOS and STATs in neural induction. To overcome this problem, ChIP-seq data on human embryonic stem cells (ESCs) from Tsankov et al. (2015) were used. Bed files were downloaded from GEO [GSE61475]. Peaks in the promoter region, −2000 – 500 base pair from transcription start site, were annotated using TxDb in R. To identify OTX2 targets important for the neural induction, the targets of OTX2 at 0 h were subtracted from the targets of OTX2 at 120 h, resulting in 1623 targets.

3. Results

3.1. Phenotypic changes in early neural induction

In this study, transcriptomic data were harvested throughout 0–48 h and 0–8 days of neural induction of human iPSCs. These datasets were then used to infer the transcriptional regulatory mechanisms operative throughout the early stages of neural induction. Monotonically increasing number of DE genes (Figure 1A) in both time series corroborated the start of the neural induction. In the 0–48 h dataset, upregulation of cell cycle genes was seen (Figure 1B) as evidenced by regulation of cyclins such as CCND1, CCNB1, and CCNE1 and their upstream regulators CDK2, CDK4, and CDK6. The cell cycle master transcriptional regulation factors, E2F1 and FOXM1, genes were also upregulated but did not qualify as DE in our data. E2F1 mainly regulates, G1, S and G1-S phase transition genes such as CDC6, CDK6, RBL1 and CDKN1C. E2F1 but can also directly upregulate FOXM1, which in turn, regulates G2, M, G2-M phase transition genes such as CDC25A, STAG1, MEIS2, and KIF24. Upregulation of E2F1 and FOXM1 can be attributed to the inhibition of TGFB and BMP2 resulting from the use of dual-SMAD inhibition used to initiate neural induction. However, the regulation of cell cycle genes was less prominent in the 0–8 days dataset.

Stem cell differentiation is accompanied by the increase in reactive oxygen species (ROS) and oxidative stress (Hu et al., 2018) and this was supported by the observed increase in NOX4 and NOXA1 in the 0–48 h dataset. Oxidative stress can lead to the stabilization of NRF2 and prevent KEAP1 mediated proteasomal degradation of NRF2 (Lin et al., 2016), which was seen to be upregulated in the 0–48 h dataset. Upregulation of KEAP1 in the 0 -48 h dataset can be attributed to the response to oxidative stress (Baird and Yamamoto, 2020). Upregulation of NRF2 was accompanied by transcriptional regulation of its targets responsible for regulation of distinct aspects of oxidative stress including glutathione metabolism (GCLM, GCLC, SLC7A11, SLC1A5), redox metabolism (TXNRD1, SRXN1), iron metabolism (HMOX1), NADPH production (ME1) and detoxification (NQO1), as seen in 48 h dataset (Figure 1C). Glutathione metabolism also plays a critical role in maintaining genomic integrity, which is essential for neural induction (Chui et al., 2020). Increases in expression of glutamine transporters further lead to increase in mitochondrial oxidative phosphorylation and this increase in oxidative phosphorylation was inferred from the increase in NADH dehydrogenases (NDUFC2, NDUFA5, NDUFA9 and NDUFA12) and ATPases (APT6V1B1, ATP6V1D, ATP6V0D1 and ATP6V0E1). Though glycolysis is a major source of energy required to maintain stem cell functions, early differentiation of human pluripotent stem cells (hiPSC) has been reported to be accompanied by a switch from glycolysis to oxidative phosphorylation (Zhang et al., 2012; Zheng et al., 2016) owing to the increased energy demands. Our data supported the decrease in glycolysis and increase in oxidative phosphorylation within 48 h of initiation of neural induction (Figure 1D). In addition to increases in glutamine uptake and glutathione metabolism, a reciprocal down-regulation of glucose transporter (SLC2A1), glycolysis gate keepers (HK1 and HK2), glycolysis pathway genes (PGK1, PGM1, ENO1 and PKM) and lactic acid utilization genes (LDHA) was also observed. Taken together, these observations showed a dynamic regulation of multiple transcriptional modules during the cell state transition from iPSC through neural induction to neuroectodermal stem cell neural that couple gain of neural identity and loss of pluripotency with changes in key cellular processes including regulation of cell cycle, metabolism and stress response.

To understand the temporal transcriptional regulation of neural induction, knowledge-based lists of pluripotency genes, neural induction transcription factors and neuroectoderm markers were curated (Figure 1E) and analyzed based on protein–protein interactions (PPI, see method section). For PPI analyses, union of DE genes across all time points were taken. 0–48 h and 0–8 days datasets identified 3,893 and 6,071 genes, respectively. PPI analysis of the 0–48 h dataset identified a loss of pluripotency module, as demonstrated by the staged loss of pluripotency markers, ZIC3, NANOG and POU5F1 (Figures 1E,F; Supplementary Figure S4), as early as 8 h after initiation of neural induction, with subsequent loss of LCK and KLF5 from 2d (Figure 1E) accompanied by a reciprocal

1 https://cytoscape.org

10.3389/fnmol.2023.1139287

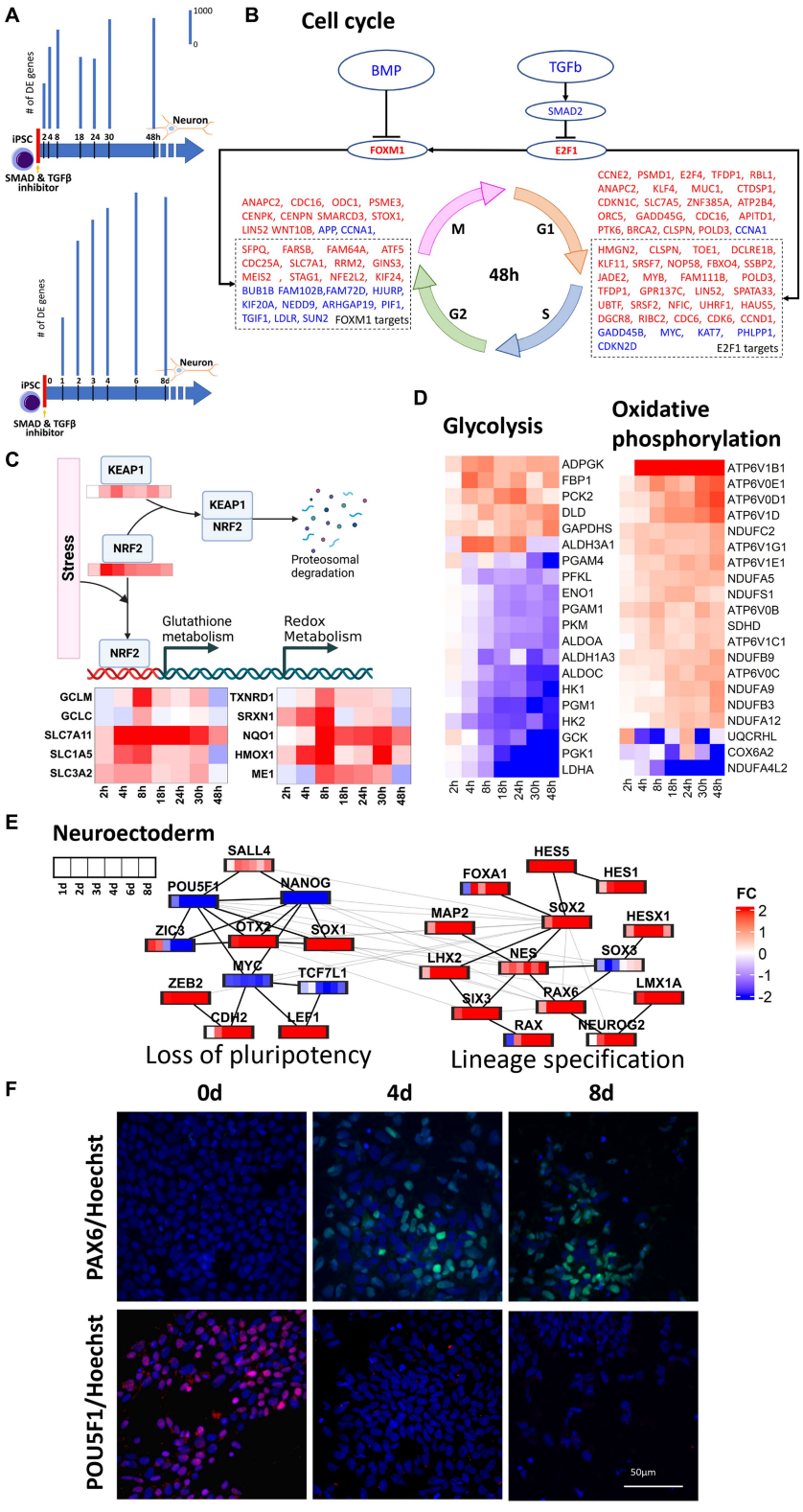

FIGURE 1
Regulation of key cellular pathways during neural induction. For this analysis we used 1 cell line (CTR_M1_04) and 1 replicate/well. **(A)** represents a schematic of the experimental design and bar plots indicate the number of differentially regulated (DE) genes identified from RNA-seq measurements in two time series, 0–48h and 0–8days. Bar plots showing a temporal increase in DE genes. DE genes were computed with respect to their respective expression at d0. **(B)** E2F1 and FOXM1 mediated upregulation of cell cycle in 0–48h. Upregulation and downregulation of the gene was represented as red and blue font color, respectively. **(C)** NRF2 mediated regulation of oxidative metabolism. **(D)** Heatmaps show the decrease in glycolysis and concurrent increase in oxidative phosphorylation in the 0–48h dataset. **(E)** protein–protein interaction analysis of pluripotency and neuroectoderm transcription factors using the 0–8d dataset. **(F)** PAX6 and POU5F1 immunocytochemistry analyses of differentiating neural cells. Expression of the neuroectodermal marker PAX6 (top -green) and the pluripotency marker POU5F1 (bottom -red) at time points iPSC, 0d (left), 4d (middle) and 8d (right). The cells nuclei are stained with Hoechst and is shown in blue. The immunocytochemistry statistical analyses shows that the expression of PAX6 significantly increases after 4d of neural induction, whereas POU5F1 is highly expressed in iPSC and is not detected at time points d4 and d8. Three independent replicates/wells for the cell line CTR_M1_04 were used for the immunocytochemical analysis.

increase in neural stem cell markers NES and SOX1. In the 0–8 days dataset, in addition to loss of pluripotency, a neural lineage specification module was identified, characterized by up-regulation of several key transcription factors known to regulate both transcription and chromatin dynamics during neural induction, including OTX2, SOX2, RAX, LHX2 and SIX3 (Figure 1E). Another key regulator of both pluripotency and neural induction, SOX2 was also identified as a key regulator based on protein interaction analysis, while up-regulation of WNT regulators, LEF1 and ZEB2 (Supplementary Figures S3, S4), and increasing expression of neuroectoderm markers, PAX6, NEUROG2 and LMX1A (Figures 1E,F), underscored the transition of iPSCs toward the neural lineage. The outcome of these PPI analyses thus underscored the tight coupling of lineage specification and regulation of key cellular processes seen in our analysis of DE genes.

3.2. Global interaction network of transcription factors

We further constructed PPI networks using all DE TFs to provide a global view of the dynamic changes in transcriptional regulation throughout neural induction. In 0–48 h dataset (Figure 2A), upregulation of TFs associated with immediate early response and stress response was seen, probably as a consequence of the dual SMADi initiation of neural induction. Moreover, in addition to regulation of stress response, MAF genes also play a role in cortical development (Pai et al., 2020). Further, several nuclear receptor TFs, known to be regulators of stemness were also downregulated during this time period. Cell cycle regulatory TFs (CDC6, LEF1, NKFB1A, RBL1, TFDP1, SMARCA2) were seen to be upregulated, as observed earlier. Though MYC is downregulated, our data show that E2F1 and FOXM1 which drive early phases of cell cycle are upregulated. In addition to these modules, an increase in TFs associated with genome integrity and genome stability (DNMT3A, DNMT3B, BRCA1, BMI1, TP53BP1, RPA2) was observed, congruent with the maintenance of stemness during differentiation (Li et al., 2020) while, a module of pluripotency genes was reciprocally down-regulated.

Many of the functional modules identified in the 0–48 h time series were also evident in the 0–8 days time series, but strikingly the TF membership of the modules was only partially conserved (Figure 2B). Thus, pluripotency maintenance genes, which were downregulated in 0–48 h dataset, were further downregulated in the 0–8 days timepoints. In addition to the decrease in expression of canonical pluripotency factors, POU5F1 and MYC, seen at 0–48 h, downregulation of their target genes CEBPD, MXI1, PRDM14, and CDCA7L was also evident, indicating a consolidated loss of pluripotency. ZIC3, upregulated at 0–48 h and required for maintenance of pluripotency, was downregulated from 3d onwards at the onset of neuroectodermal differentiation (Morrison and Brickman, 2006). In 0–8 days, neural stem cell markers DACH1 and PAX6 were upregulated indicating formation of neuroectodermal stem cells while HSF2, a cortical developmental marker, was also upregulated in 0–8d (Chang et al., 2006) congruent their cortical identity. Concurrent upregulation of TFEB, PAX8, ZEB2, and SNAI2 is consistent with maintenance of a precursor/multipotent state prior further differentiation of these cells toward neuronal and glial lineages (Yuizumi et al., 2021).

3.3. Characterization and validation of OTX2 role in early neural induction

Our studies identified OTX2 as one of the most precociously expressed transcription factors during neural induction (Supplementary Figures S5A,B). OTX2 is known to play a pivotal role during three distinct stages of neurodevelopment, including (i) maintenance of the naiive pluripotent ground state and for transition to the primed pluripotent state (Yang et al., 2014) (ii) coordinate repression of pluripotency and activation of neural induction (Greber et al., 2011; Malchenko et al., 2014) (iii) control of rostral fate specification of telencephalon and mesencephalon (Simeone, 1998; Simeone et al., 2011). Furthermore, OTX2 has been suggested to act as a pioneer factor (Boulay et al., 2017) indicating its potential as a driver of state transition. This convergence of precocious temporal expression and known functionality suggested that manipulation of OTX2 expression would be an appropriate test to validate our model of dynamic transcriptional regulation during neural induction. TRANSFAC® data was initially used as the source for TF-target gene information. However, curation of TRANSFAC was over-represented by the large number of immune system and disease studies such as cancer. Accordingly, we were concerned that analysis using TRANSFAC data could produce spurious results such as indicating a major role of JUN, FOS and STATs in neural induction. To overcome this problem, ChIP-seq data on POU5F1, NANOG and OTX2 derived from human embryonic stem cells (ESCs) from Tsankov et al. (2015) were used to more faithfully recapitulate TF-target gene interactions in human iPSCs. OTX2 chip-seq produced 1,623 targets genes. The intersect of OTX2 targets genes and the combined gene lists of 0–48 h and 0–8d dataset, used for PPI analysis, resulted in 310 and 507 genes. PPI analysis of these 310 and 507 genes emphasized the role of OTX2 in cell cycle specially speckle formation and spliceosome function as evidenced by upregulation of SRSF1, SRSF2, SRSF7, FUS and SF1 in the 48 h dataset and SRSF1, SRSF2, FUS and DHX9 in the 0–8d dataset, indicating a direct role of OTX2 in regulation of the spliceosome machinery. In addition to upregulation of spliceosome, ribosome genes (RRS1, RPF2, and METTL1) were also upregulated in 0–48 h dataset and notch signaling (NOTCH2, SEL1L, and DLL1) was upregulated at 0–8d dataset.

In order to validate the causality implied by our analysis of the dynamic transcriptional landscape during neural induction, we used CRISPRi to knock down (KD) expression of OTX2 (Supplementary Figure S5C), indicated by our analysis above to be involved in regulation of several key cellular processes during neural induction and one of the most precociously expressed transcription factors during neural induction (Acampora et al., 2013). Doxycycline (Dox) was used to induce expression of a dCas9-KRAB construct to inhibit expression of OTX2 for 48 h prior to neural induction. Samples were collected for RNAseq at 0, 1, 2 and 7 days. Control samples (DOX-) were also collected at the same time (Figure 3A). Data were analyzed by calculating fold change in gene expression for OTX KD versus WT at each time point. To analyze the effect of OTX2 KD, the top 50 downregulated genes (Figure 3B) were selected based on ranking of mean of FC of 0–8d dataset minus FC of KD at D7. Enrichment of these 50 genes (Figure 3C) indicated a disruption of neural induction. Known targets of OTX2 such as PAX2 and LHX2 were downregulated in top 50 genes while other neural differentiation genes including LHX5, LMX1A

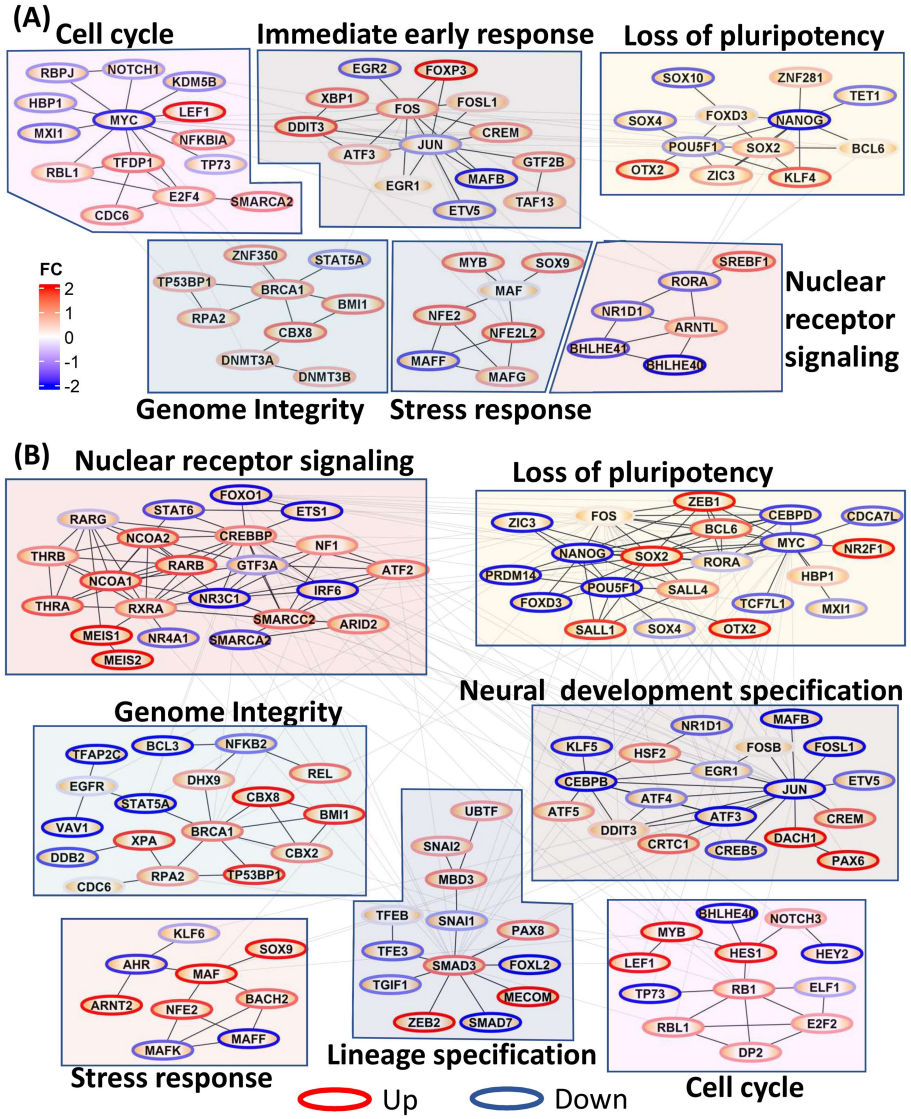

FIGURE 2
Protein–protein interaction (PPI) network of all transcription factors. Network modules were identified using Glay method in Cytoscape and annotated manually. Node borders were colored red and blue based on the average fold change of the TF across all time points. **(A)** PPI network showing the increase in cell cycle, immediate early gene response, stress response, genome integrity, and loss of pluripotency in 0–48h dataset. **(B)** PPI network showing increases in nuclear receptor signaling, genome integrity, stress response, lineage specification, loss of pluripotency and neural development specification in the 0–8d dataset.

and NEUROG2, involved in neuronal patterning, were also downregulated. Forty two cell cycle genes were downregulated in OTX2 KD, while cell cycle inhibitors (RB1, SMAD3 and CDKN1A) were upregulated thus indicating overall suppression of cell cycle. Downregulation of spliceosome genes, SRSF3, SRSF6, SRSF8, and SRSF10 was also observed (Figures 3D–F), thus conforming our hypothesis on the role of OTX2 in regulation of splicing. Furthermore, kinetochore genes, CENPN, CENPE, CENPK, and BUB3, were also downregulated (Figure 3G). This downregulation of spliceosome and kinetochore genes further supports the downregulation of cell cycle. Interestingly, the regulation of notch and cAMP signaling pathway was further enhanced compared to WT (Figure 3E; Supplementary Figure S6). Importantly, the effects of CRISPRi KD of OTX2 corroborate the regulatory modules inferred from our DE gene and PPI analyses.

4. Discussion

During the course of cortical neural induction, iPSCs go through a series of cell states, starting from the pluripotent stem cells and culminating in multipotent neuroectodermal stem cells, which then undergo further maturation before terminal differentiation into cortical neurons. Our results show the transcriptional and regulatory mechanisms that are associated with this transition across time. BMP signaling is required for the maintenance of pluripotency in human stem cells (Osnato et al., 2021) and blockade of BMP signaling using dual SMAD inhibiton has become the standard protocol for inducing neural induction toward early neuroectoderm (Tomishima, 2012). Our study shows precise transcriptional regulatory mechanisms that orchestrate this

induction process in a temporally relevant manner. In parallel we differentiated iPSC using WNT inhibition for 7 days to determine if the molecular events underlaying neuronal differentiation are significantly altered by using an alternative neural induction protocol. The results indicate that WNT inhibition does not significantly alter the gene expression patterns during the initial 8 days of neural induction (Supplementary Figure S1).

We show, as expected, the suppression of canonical stemness TFs, POU5F1, and NANOG beginning as early as day 1, continuing into day 8, while lineage-altering factors ZIC2, SOX2, and KLF4 increased in expression over this time period. Interestingly, during the 48 h time frame, in addition to loss of pluripotency, we saw regulation of immediately early response genes jun-fos signaling, genes that are responsible for maintaining genome integrity during the rapid

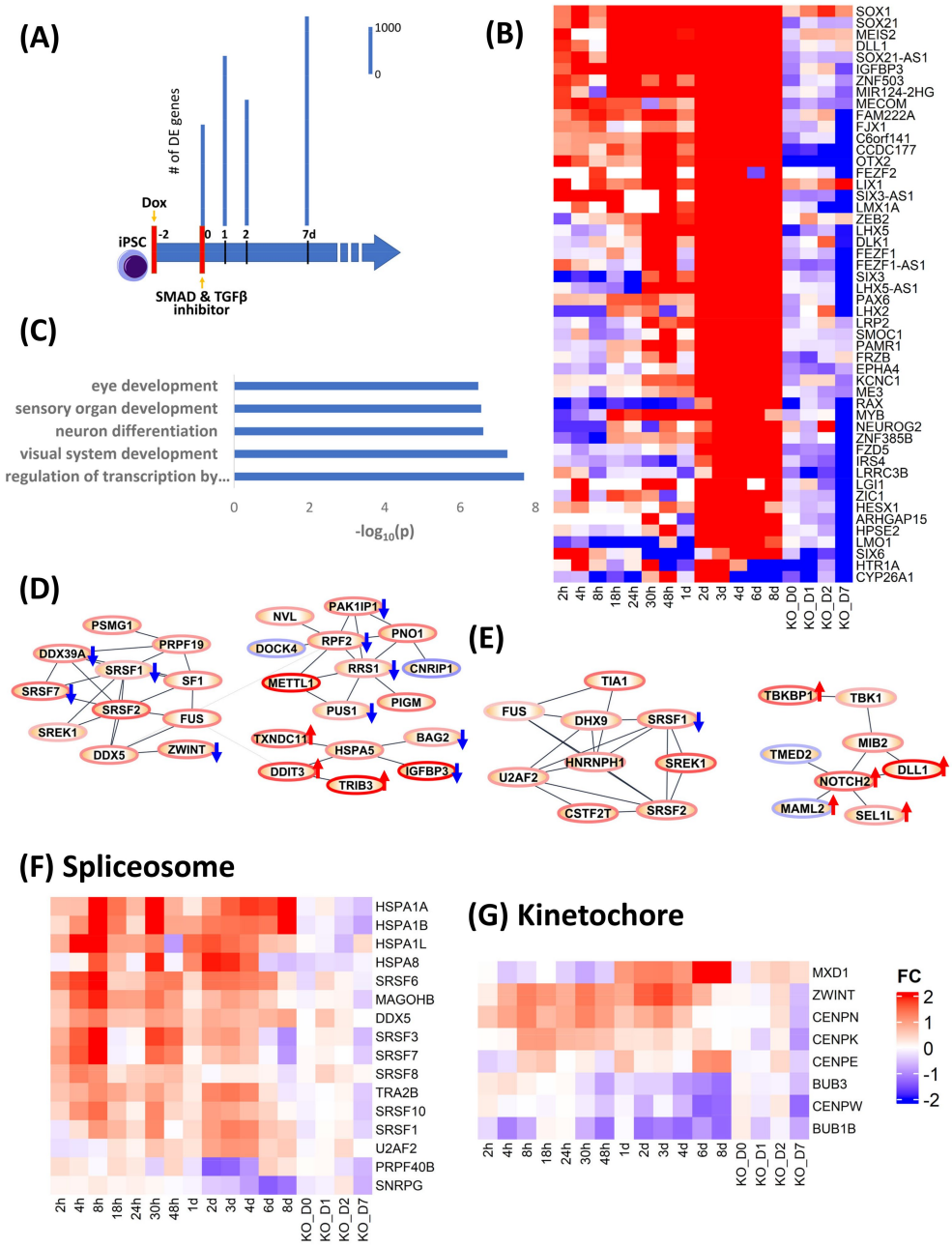

FIGURE 3
Validation of role of OTX2 in neural induction using CRISPRi KD of OTX2. **(A)** schematic of experimental design. Doxycycline (Dox) was used to initiate the KD of OTX2 for 48h prior to neural induction. Bar plots show differentially regulated (DE) genes from RNA-seq measurements in the time points, 0, 1, 2, and 7d. DE genes were computed with respect to same time Dox$^-$ control point. **(B)** Heatmap of the top 50 downregulated genes to show the effect of OTX2 KD. **(C)** Barplot of GO biological processes enrichment of top 50 downregulated genes in OTX2 KD. **(D,E)** PPI network of OTX2 selected targets based on Tsankov et al. (2015) in the 0–48h and 0–8d datasets, respectively. Node border colors, red and blue, show average up- and down-regulation, respectively, of the genes. The effect of OTX2 KD is shown as red (up) and blue (down) arrow on the nodes. **(F,G)** Heatmaps show the downregulation of spliceosome and kinetochore pathway genes.

alterations in chromatin topology and expression of key stress response genes. Loss of pluripotency is strongly coupled to stress response, as evidenced by the induction of KEAP and NRF2 genes, precursors to the pathway that is a principal protective response to oxidative and other stresses (Baird and Yamamoto, 2020). We also found that NRF2 regulates transcription of several stress response genes as seen in our analysis of the 0 – 48 h dataset, with KEAP serving as the sensor. Further KEAP1-NRF2 pathways promote metabolic reprogramming *via* control of central carbon metabolism through the pentose phosphate pathway and glutamine metabolism (Lin et al., 2016; Sayin et al., 2017).

Further, repression of the stemness genes concomitantly led to suppression of pluripotency maintenance genes while activating expression of several zinc finger genes responsible for inducing changes in chromatin topology with concomitant changes in the cell state. Our results also show that in the initial 48 h time frame, several cell cycle processes are robustly activated at each phase of the cell cycle implying the progression from pluripotency. Moreover, we observed repression of several nuclear receptor superfamily genes, establishing the temporal links between pluripotency and the NR superfamily TFs, which are known to be required for both maintenance and suppression of pluripotency (Jeong and Mangelsdorf, 2009; Wagner and Cooney, 2013). While loss of pluripotency is initiated in within 48 h of the induction process, it persists for 8 days while robustly activating the expression of SOX2 and SALL4 genes, which crosstalk with the stemness TFs to coordinate activation of the transcriptional framework that concurrently represses stemness genes while activating early neural induction genes. This tightly coupled repression of pluripotency and activation of neural induction was reflected in the transcription factor complex comprising POU5F1, SOX2, NANOG, MYC, SALL2, SALL4, CTNNB1, OTX2, and LKF4, all of which were regulated during the 8 day neural induction period. This tight transcription factor complex functions to orchestrate the Janus face of the cell fate, namely concurrent loss of pluripotency and the activation of neural induction. Our perturbation using CRISPRi to knock-down OTX2 expression sharply illuminated the functional and temporal complexity of this complex. While broadly the OTX2 knock-down did not alter the cell fate, it did change the kinetics of the induction process, manifested as a delay in the repression of pluripotency and a disruption of neural induction, accompanied by downregulation of several components of spliceosome machinery, and several kinetochore genes, the latter resulting in disruption of the normal kinetics of the cell cycle.

Our results show an interesting interplay among several processes precisely orchestrated in a temporally defined manner during neural induction. The overall transition can be summarized into three distinct stages. First, during the temporal dynamics spanning the entire 8-day period, the cell state changes dynamically manifest as loss of pluripotency and a gain of neural identity. This process is defined by repression of the pluripotency transcription factors, POU5F1 and NANOG, and activation of KLF4, along with regulation of other pluripotency and chromatin state modifiers, OTX2, HDAC1, ZIC3, and ZEB2. The latter two are zinc finger factors known to alter the chromatin topology in the pluripotent state to a lineage state (Kwak et al., 2018). Second, In the first 2 days of neural induction, the key processes that accompany the loss of pluripotency include immediate early response, processes for maintenance of genome integrity, and induction of a metabolic switch from a predominantly glycolytic state to a more oxidative state. The key transcription factors that account for these processes include, JUN, FOS, CREM, NFE2, MYB, NRF2, and KEAP1, the latter of which serves to induce the metabolic switch. Third, in the transition from the early lineage state in the 2 day post neural induction period to d8, the key process is progression to a neuroectodermal state, orchestrated by the canonical neural factors, PAX6, NEUROG2, SOX11, DACH1, ASCL1, and HES5 (Ozair et al., 2013). We illustrate our overall schematic of temporally defined neural induction processes in Figure 4.

The above mechanisms pose interesting questions on the lineage specification in neurological disorders of genetic origin such as familial Alzheimer's disease (FAD) induced by specific mutations in PSEN1, PSEN2 or APP proteins. It has been established that transcription factors NRF2 and REST play a crucial role in defining cell fate outcomes in FAD (Caldwell et al., 2020, 2022). Not surprisingly, the endpoint lineage in these iPSC-derived diseased neurons is dedifferentiation to neuronal precursor states and reduced expression of neuron lineage genes. Our study has implications for understanding neurodevelopmental disorders as well as neurodegeneration. Toward addressing the former, our study recommends targeted perturbations to enhance specific neural induction stages or repress progression to other lineages. In our study on neurodegenerative disorders, we demonstrated that neurons dedifferentiate into distinct precursor-like stages offering potential interventions to reinitiate progression into the neuronal stages (Caldwell et al., 2020, 2022). A longer study exploring this lineage specification to the 50 day point when the neuronal precursors become mature is in progress.

Much of our understanding of the gene regulatory pathways underlying the initial steps of neuronal development is largely based on animal models, particularly in Xenopus and mouse. We summarize here, some of the most salient observations. In Xenopus, Foxd4 is expressed in the neuroectodermal precursors and promotes the expression of Gmnn, Sox11 and Zic2. Foxd4, Gmnn, Zic2 and Sox11 block non-neural induction by inhibiting BMP/WNT pathways and their targets (Klein and Moody, 2015). The default neural induction model suggests that inhibition BMP and TGFβ is sufficient to induce neural differentiation in the competent ectoderm by preventing expression of the epidermal and mesodermal transcription network promoted by BMP and TGFß, respectively (Marchal et al., 2009; Andoniadou and Martinez-Barbera, 2013; Klein and Moody, 2015) SoxB1 family members Sox1, Sox2 and Sox3 are up-regulated downstream of Foxd4, Gmnn and Zic2 and are necessary to maintain self-renewing progenitors and stablish spatial identity of neural cells. Additionally, SoxB1 factors maintain neuroectodermal fate by inhibiting expression of Vent2, a BMP target necessary for epidermis differentiation (Rogers et al., 2009; Lee et al., 2014). Zic1, Zic3, Irx1-3 are up-regulated upstream of early bHLH pro-neural factors and are required to maintain neural progenitors in a proliferative state and for temporarily inhibit neural differentiation genes (Aruga and Mikoshiba, 2011; Moody et al., 2013; Sankar et al., 2016). Subsequently, activation of bHLH family factors is required for transition of neuroectodermal cells to neural progenitors (Kageyama et al., 2005; Dhanesh et al., 2016).

Studies in human iPSCs have enabled identification of important markers and drivers of neural differentiation including PAX6, ZEB2, ZNF521, NESTIN and NR2F2 (Ardhanareeswaran et al., 2017). In humans, PAX6 is sufficient and necessary for neural induction possibly by repressing pluripotency genes such as OCT4, NANOG,

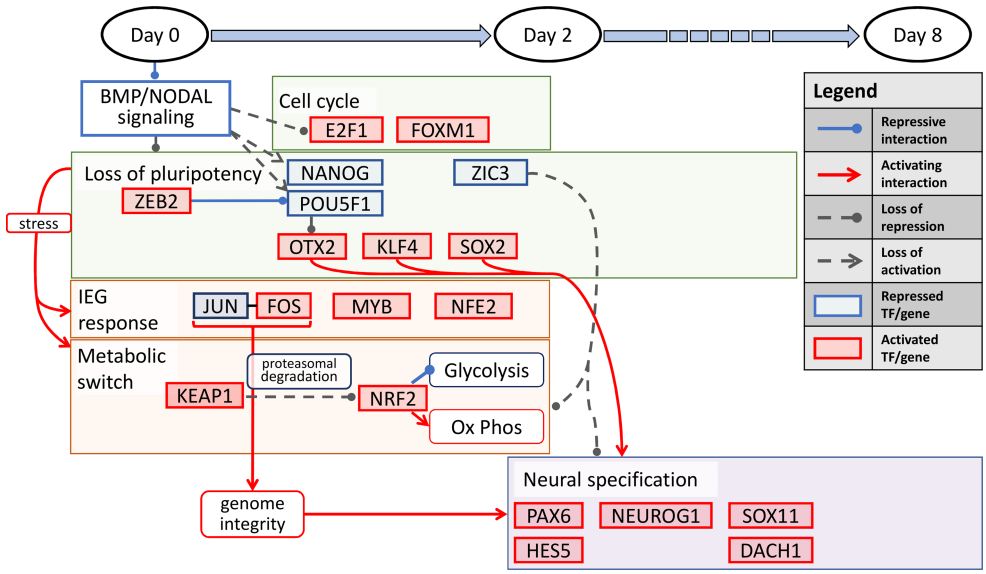

FIGURE 4
A temporally-associated regulatory network for neural induction. Dual SMAD inhibition causes an increase in cell cycle *via* upregulation of E2F1 and FOXM1 accompanied by the loss of pluripotency due to repression of NANOG and POU5F1. The loss of pluripotency in turn leads to neuronal induction *via* OTX2, KLF4 and SOX2. In addition, stress induced IEG response and metabolic switch from glycolysis to OXPHOS further allude to the increase in genome integrity and neuronal specification throughout neural induction.

and MYC. However, OCT4, NANOG and SOX2 knockdown in ESCs induces trophoblastic fate suggesting that inhibition of pluripotency genes is a pre-requisite but not sufficient for neuroectodermal differentiation. It has been proposed that neuroectodermal differentiation is potentiated by PAX6 activation of neuronal progenitor genes including SIX3, LHX2, FGF8, NR2F2, TBR2, and WNT5b (Zhang et al., 2010; Blake and Ziman, 2014). Similarly, it has been suggested that ZEB2 is necessary for neuroectodermal progression and maintenance by antagonizing Activin/Nodal and BMP signaling by direct interaction with SMAD proteins (Conidi et al., 2011; Tang et al., 2015). ESC/iPSC studies have demonstrated that up-regulation of neuroectodermal markers PAX6, SOX1, NCAM, ZIC1, and ZEB2, and loss of pluripotency/self-renewal markers OCT4, NANOG, and KLF4 occurs at day 5–7 after hPSCs induction (Kamiya et al., 2011; van de Leemput et al., 2014; Huang et al., 2016). Subsequently, chromatin modification genes such us TET2, KATB2, and SIRT1 were differentially expressed after 6 and 10 days of neural induction (Huang et al., 2016). These studies, and others, have provided an overview of the molecular factors required for the specific spatiotemporal regulation of neural differentiation. However, the dynamic genetic and regulatory programs underlying the progression from pluripotency state to neural competence remain to be investigated. Here, we provide a unique insight into the initial molecular events that govern the transition of iPSCs to neuroectodermal fate and subsequently contribute to the identification of relevant disease processes. Overall, our study of the dynamics of transcriptional changes during neural induction points to the tight coupling that occurs between transcriptional modules that determine changes in cell state during the transition from pluripotent stem cell to multipotent neural stem cell. This coupling occurs not only at the level of lineage specification but also in parallel regulation of modules that regulate key cellular processes including cell cycle, cellular stress and metabolism. This insight clearly illustrates the importance of taking a dynamic and holistic perspective of cell state transitions to account for the wholesale changes in transcriptional dynamics and cellular rewiring that represents changes in cell state. We anticipate that further studies will dissect further the contribution of other key TFs toward governing the cell state transitions during neural induction.

Data availability statement

The original contributions presented in the study are publicly available. Data is submitted in GEO repository. This data can be found here: https://www.ncbi.nlm.nih.gov/geo/query/acc.cgi?acc=GSE223624 accession ID: GSE223624.

Author contributions

SG: data analysis and drafting of manuscript. LP: data acquisition. MF: data acquisition and analysis. HR: data acquisition and critiquing of manuscript. DM: data analysis. NB: experimental design and interpretation, drafting, and critiquing of manuscript. SS: data analysis and interpretation, drafting, and critiquing of manuscript. All authors contributed to the article and approved the submitted version.

Funding

The authors wish to acknowledge funding support from NIH grants, R01 LM012595 (SS), OT2 OD030544 (SS), R01 HL106579-07 (SS) and the Joan and Irwin Jacobs endowed professorship (SS), SENESCYT PhD scholarship (LP), and Mano Maurya in the Subramaniam laboratory for discussions on analytical methods used.

Conflict of interest

The authors declare that the research was conducted in the absence of any commercial or financial relationships that could be construed as a potential conflict of interest.

Publisher's note

All claims expressed in this article are solely those of the authors and do not necessarily represent those of their affiliated organizations, or those of the publisher, the editors and the reviewers. Any product that may be evaluated in this article, or claim that may be made by its manufacturer, is not guaranteed or endorsed by the publisher.

Supplementary material

The Supplementary material for this article can be found online at: https://www.frontiersin.org/articles/10.3389/fnmol.2023.1139287/full#supplementary-material

References

Acampora, D., Di Giovannantonio, L. G., and Simeone, A. (2013). Otx2 is an intrinsic determinant of the embryonic stem cell state and is required for transition to a stable epiblast stem cell condition. *Development* 140, 43–55. doi: 10.1242/dev.085290

Andoniadou, C. L., and Martinez-Barbera, J. P. (2013). Developmental mechanisms directing early anterior forebrain specification in vertebrates. *Cell. Mol. Life Sci.* 70, 3739–3752. doi: 10.1007/s00018-013-1269-5

Ardhanareeswaran, K., Mariani, J., Coppola, G., Abyzov, A., and Vaccarino, F. M. (2017). Human induced pluripotent stem cells for modelling neurodevelopmental disorders. *Nat. Rev. Neurol.* 13, 265–278. doi: 10.1038/nrneurol.2017.45

Aruga, J., and Mikoshiba, K. (2011). Role of BMP, FGF, calcium signaling, and Zic proteins in vertebrate neuroectodermal differentiation. *Neurochem. Res.* 36, 1286–1292. doi: 10.1007/s11064-011-0422-5

Baird, L., and Yamamoto, M. (2020). The molecular mechanisms regulating the KEAP1-NRF2 pathway. *Mol. Cell. Biol.* 40:e00099-20. doi: 10.1128/MCB.00099-20

Blake, J. A., and Ziman, M. R. (2014). Pax genes: regulators of lineage specification and progenitor cell maintenance. *Development* 141, 737–751. doi: 10.1242/dev.091785

Boulay, G., Awad, M. E., Riggi, N., Archer, T. C., Iyer, S., Boonseng, W. E., et al. (2017). OTX2 activity at distal regulatory elements shapes the chromatin landscape of group 3 Medulloblastoma. *Cancer Discov.* 7, 288–301. doi: 10.1158/2159-8290.CD-16-0844

Caldwell, A. B., Liu, Q., Schroth, G. P., Galasko, D. R., Yuan, S. H., Wagner, S. L., et al. (2020). Dedifferentiation and neuronal repression define familial Alzheimer's disease. *Sci. Adv.* 6:eaba5933. doi: 10.1126/sciadv.aba5933

Caldwell, A. B., Liu, Q., Zhang, C., Schroth, G. P., Galasko, D. R., Rynearson, K. D., et al. (2022). Endotype reversal as a novel strategy for screening drugs targeting familial Alzheimer's disease. *Alzheimers Dement.* 18, 2117–2130. doi: 10.1002/alz.12553

Chambers, S. M., Fasano, C. A., Papapetrou, E. P., Tomishima, M., Sadelain, M., and Studer, L. (2009). Highly efficient neural conversion of human ES and iPS cells by dual inhibition of SMAD signaling. *Nat. Biotechnol.* 27, 275–280. doi: 10.1038/nbt.1529

Chang, Y., Östling, P., Åkerfelt, M., Trouillet, D., Rallu, M., Gitton, Y., et al. (2006). Role of heat-shock factor 2 in cerebral cortex formation and as a regulator of p35 expression. *Genes Dev.* 20, 836–847. doi: 10.1101/gad.366906

Chui, A., Zhang, Q., and Shi, S. H. (2020). Oxidative stress regulates progenitor behavior and cortical neurogenesis. *Development* 147:dev184150. doi: 10.1242/dev.184150

Conidi, A., Cazzola, S., Beets, K., Coddens, K., Collart, C., Cornelis, F., et al. (2011). Few Smad proteins and many Smad-interacting proteins yield multiple functions and action modes in TGFbeta/BMP signaling *in vivo*. *Cytokine Growth Factor Rev.* 22, 287–300. doi: 10.1016/j.cytogfr.2011.11.006

Dhanesh, S. B., Subashini, C., and James, J. (2016). Hes1: the maestro in neurogenesis. *Cell. Mol. Life Sci.* 73, 4019–4042. doi: 10.1007/s00018-016-2277-z

Gilbert, L. A., Horlbeck, M. A., Adamson, B., Villalta, J. E., Chen, Y., Whitehead, E. H., et al. (2014). Genome-scale CRISPR-mediated control of gene repression and activation. *Cells* 159, 647–661. doi: 10.1016/j.cell.2014.09.029

Greber, B., Coulon, P., Zhang, M., Moritz, S., Frank, S., Müller-Molina, A. J., et al. (2011). FGF signalling inhibits neural induction in human embryonic stem cells. *EMBO J.* 30, 4874–4884. doi: 10.1038/emboj.2011.407

Hemmati-Brivanlou, A., and Melton, D. (1997). Vertebrate embryonic cells will become nerve cells unless told otherwise. *Cells* 88, 13–17. doi: 10.1016/S0092-8674(00)81853-X

Hu, J., Ge, H., Newman, M., and Liu, K. (2012). OSA: a fast and accurate alignment tool for RNA-Seq. *Bioinformatics* 28, 1933–1934. doi: 10.1093/bioinformatics/bts294

Hu, Q., Khanna, P., Ee Wong, B. S., Lin Heng, Z. S., Subhramanyam, C. S., Thanga, L. Z., et al. (2018). Oxidative stress promotes exit from the stem cell state and spontaneous neuronal differentiation. *Oncotarget* 9, 4223–4238. doi: 10.18632/oncotarget.23786

Huang, C. T., Tao, Y., Lu, J., Jones, J. R., Fowler, L., Weick, J. P., et al. (2016). Time-course gene expression profiling reveals a novel role of non-canonical WNT signaling during neural induction. *Sci. Rep.* 6:32600. doi: 10.1038/srep32600

Jeong, Y., and Mangelsdorf, D. J. (2009). Nuclear receptor regulation of stemness and stem cell differentiation. *Exp. Mol. Med.* 41, 525–537. doi: 10.3858/emm.2009.41.8.091

Kageyama, R., Ohtsuka, T., Hatakeyama, J., and Ohsawa, R. (2005). Roles of bHLH genes in neural stem cell differentiation. *Exp. Cell Res.* 306, 343–348. doi: 10.1016/j.yexcr.2005.03.015

Kamiya, D., Banno, S., Sasai, N., Ohgushi, M., Inomata, H., Watanabe, K., et al. (2011). Intrinsic transition of embryonic stem-cell differentiation into neural progenitors. *Nature* 470, 503–509. doi: 10.1038/nature09726

Klein, S. L., and Moody, S. A. (2015). Early neural ectodermal genes are activated by Siamois and twin during blastula stages. *Genesis* 53, 308–320. doi: 10.1002/dvg.22854

Kwak, S., Kim, T. W., Kang, B. H., Kim, J. H., Lee, J. S., Lee, H. T., et al. (2018). Zinc finger proteins orchestrate active gene silencing during embryonic stem cell differentiation. *Nucleic Acids Res.* 46, 6592–6607. doi: 10.1093/nar/gky454

Lagomarsino, V. N., Pearse, R. V., Liu, L., Hsieh, Y. C., Fernandez, M. A., et al. (2021). Stem cell-derived neurons reflect features of protein networks, neuropathology, and cognitive outcome of their aged human donors. *Neuron* 109, 3402–3420.e9. doi: 10.1016/j.neuron.2021.08.003

Lee, H. K., Lee, H. S., and Moody, S. A. (2014). Neural transcription factors: from embryos to neural stem cells. *Mol. Cells* 37, 705–712. doi: 10.14348/molcells.2014.0227

Lee, H., Nowosiad, P., Dutan Polit, L. M., Price, J., Srivastava, D. P., and Thuret, S. (2020). Apolipoprotein E expression pattern in human induced pluripotent stem cells during in vitro neural induction. *F1000Res* 9:353. doi: 10.12688/f1000research.23580.1

Li, J., Shang, Y., Wang, L., Zhao, B., Sun, C., Li, J., et al. (2020). Genome integrity and neurogenesis of postnatal hippocampal neural stem/progenitor cells require a unique regulator Filia. *Sci. Adv.* 6. doi: 10.1126/sciadv.aba0682

Lin, T.-Y., Cantley, L. C., and DeNicola, G. M. (2016). "NRF2 rewires cellular metabolism to support the antioxidant response" in *The transcription factor Nrf2*. eds. J. Morales-Gonzalez, A. Morales-Gonzalez and E. Madrigal-Santillan (London: IntechOpen) doi: 10.5772/65141

Malchenko, S., Xie, J., de Fatima Bonaldo, M., Vanin, E. F., Bhattacharyya, B. J., et al. (2014). Onset of rosette formation during spontaneous neural differentiation of hESC and hiPSC colonies. *Gene* 534, 400–407. doi: 10.1016/j.gene.2013.07.101

Mandegar, M. A., Huebsch, N., Frolov, E. B., Shin, E., Truong, A., Olvera, M. P., et al. (2016). CRISPR interference efficiently induces specific and reversible gene silencing in human iPSCs. *Cell Stem Cell* 18, 541–553. doi: 10.1016/j.stem.2016.01.022

Marchal, L., Luxardi, G., Thomé, V., and Kodjabachian, L. (2009). BMP inhibition initiates neural induction via FGF signaling and Zic genes. *Proc. Natl. Acad. Sci. U. S. A.* 106, 17437–17442. doi: 10.1073/pnas.0906352106

Moody, S. A., Klein, S. L., Karpinski, B. A., Maynard, T. M., and Lamantia, A. S. (2013). On becoming neural: what the embryo can tell us about differentiating neural stem cells. *Am. J Stem Cells* 2, 74–94.

Morrison, G. M., and Brickman, J. M. (2006). Conserved roles for Oct4 homologues in maintaining multipotency during early vertebrate development. *Development* 133, 2011–2022. doi: 10.1242/dev.02362

Ng, B., Rowland, H. A., Wei, T., Arunasalam, K., Hayes, E. M., Koychev, I., et al. (2022). Neurons derived from individual early Alzheimer's disease patients reflect their clinical vulnerability. *Brain Commun.* 4:fcac267. doi: 10.1093/braincomms/fcac267

Osnato, A., Brown, S., Krueger, C., Andrews, S., Collier, A. J., Nakanoh, S., et al. (2021). TGFbeta signalling is required to maintain pluripotency of human naive pluripotent stem cells. *elife* 10:10. doi: 10.7554/eLife.67259

Ozair, M. Z., Kintner, C., and Brivanlou, A. H. (2013). Neural induction and early patterning in vertebrates. *Wiley Interdiscip. Rev. Dev. Biol.* 2, 479–498. doi: 10.1002/wdev.90

Pai, E. L., Chen, J., Fazel Darbandi, S., Cho, F. S., Lindtner, S., and Chu, J. S. (2020). Maf and Mafb control mouse pallial interneuron fate and maturation through neuropsychiatric disease gene regulation. *elife*:9. doi: 10.7554/eLife.54903

Rogers, C. D., Moody, S. A., and Casey, E. S. (2009). Neural induction and factors that stabilize a neural fate. *Birth Defects Res. C Embryo Today* 87, 249–262. doi: 10.1002/bdrc.20157

Sankar, S., Yellajoshyula, D., Zhang, B., Teets, B., Rockweiler, N., and Kroll, K. L. (2016). Gene regulatory networks in neural cell fate acquisition from genome-wide chromatin association of geminin and Zic1. *Sci. Rep.* 6:37412. doi: 10.1038/srep37412

Sayin, V. I., LeBoeuf, S. E., Singh, S. X., Davidson, S. M., Biancur, D., Guzelhan, B. S., et al. (2017). Activation of the NRF2 antioxidant program generates an imbalance in central carbon metabolism in cancer. *elife* 6:6. doi: 10.7554/eLife.28083

Shi, Y., Kirwan, P., and Livesey, F. J. (2012). Directed differentiation of human pluripotent stem cells to cerebral cortex neurons and neural networks. *Nat. Protoc.* 7, 1836–1846. doi: 10.1038/nprot.2012.116

Simeone, A. (1998). Otx1 and Otx2 in the development and evolution of the mammalian brain. *EMBO J.* 17, 6790–6798. doi: 10.1093/emboj/17.23.6790

Simeone, A., di Salvio, M., di Giovannantonio, L. G., Acampora, D., Omodei, D., and Tomasetti, C. (2011). The role of otx2 in adult mesencephalic-diencephalic dopaminergic neurons. *Mol. Neurobiol.* 43, 107–113. doi: 10.1007/s12035-010-8148-y

Stern, C. D. (2006). Neural induction: 10 years on since the 'default model'. *Curr. Opin. Cell Biol.* 18, 692–697. doi: 10.1016/j.ceb.2006.09.002

Subramanian, A., Tamayo, P., Mootha, V. K., Mukherjee, S., Ebert, B. L., Gillette, M. A., et al. (2005). Gene set enrichment analysis: a knowledge-based approach for interpreting genome-wide expression profiles. *Proc. Natl. Acad. Sci. U. S. A.* 102, 15545–15550. doi: 10.1073/pnas.0506580102

Tang, K., Peng, G., Qiao, Y., Song, L., and Jing, N. (2015). Intrinsic regulations in neural fate commitment. *Develop. Growth Differ.* 57, 109–120. doi: 10.1111/dgd.12204

Tomishima, M. (2012). "Neural induction – dual SMAD inhibition" in *StemBook*. ed. T. S. C. R. Community (Cambridge (MA): Harvard Stem Cell Institute)

Tsankov, A. M., Gu, H., Akopian, V., Ziller, M. J., Donaghey, J., Amit, I., et al. (2015). Transcription factor binding dynamics during human ES cell differentiation. *Nature* 518, 344–349. doi: 10.1038/nature14233

van de Leemput, J., Boles, N. C., Kiehl, T. R., Corneo, B., Lederman, P., Menon, V., et al. (2014). CORTECON: a temporal transcriptome analysis of in vitro human cerebral cortex development from human embryonic stem cells. *Neuron* 83, 51–68. doi: 10.1016/j.neuron.2014.05.013

Volpato, V., and Webber, C. (2020). Addressing variability in iPSC-derived models of human disease: guidelines to promote reproducibility. *Dis. Model. Mech.* 13. doi: 10.1242/dmm.042317

Wagner, R. T., and Cooney, A. J. (2013). Minireview: the diverse roles of nuclear receptors in the regulation of embryonic stem cell pluripotency. *Mol. Endocrinol.* 27, 864–878. doi: 10.1210/me.2012-1383

Yang, S. H., Kalkan, T., Morissroe, C., Marks, H., Stunnenberg, H., Smith, A., et al. (2014). Otx2 and Oct4 drive early enhancer activation during embryonic stem cell transition from naive pluripotency. *Cell Rep.* 7, 1968–1981. doi: 10.1016/j.celrep.2014.05.037

Yuizumi, N., Harada, Y., Kuniya, T., Sunabori, T., Koike, M., Wakabayashi, M., et al. (2021). Maintenance of neural stem-progenitor cells by the lysosomal biosynthesis regulators TFEB and TFE3 in the embryonic mouse telencephalon. *Stem Cells* 39, 929–944. doi: 10.1002/stem.3359

Zhang, X., Huang, C. T., Chen, J., Pankratz, M. T., Xi, J., Li, J., et al. (2010). Pax6 is a human neuroectoderm cell fate determinant. *Cell Stem Cell* 7, 90–100. doi: 10.1016/j.stem.2010.04.017

Zhang, J., Nuebel, E., Daley, G. Q., Koehler, C. M., and Teitell, M. A. (2012). Metabolic regulation in pluripotent stem cells during reprogramming and self-renewal. *Cell Stem Cell* 11, 589–595. doi: 10.1016/j.stem.2012.10.005

Zheng, X., Boyer, L., Jin, M., Mertens, J., Kim, Y., Ma, L., et al. (2016). Metabolic reprogramming during neuronal differentiation from aerobic glycolysis to neuronal oxidative phosphorylation. *elife* 5:5. doi: 10.7554/eLife.13374

Frontiers in
Molecular Neuroscience

Leading research into the brain's molecular structure, design and function

Part of the most cited neuroscience series, this journal explores and identifies key molecules underlying the structure, design and function of the brain across all levels.

Discover the latest Research Topics

See more →

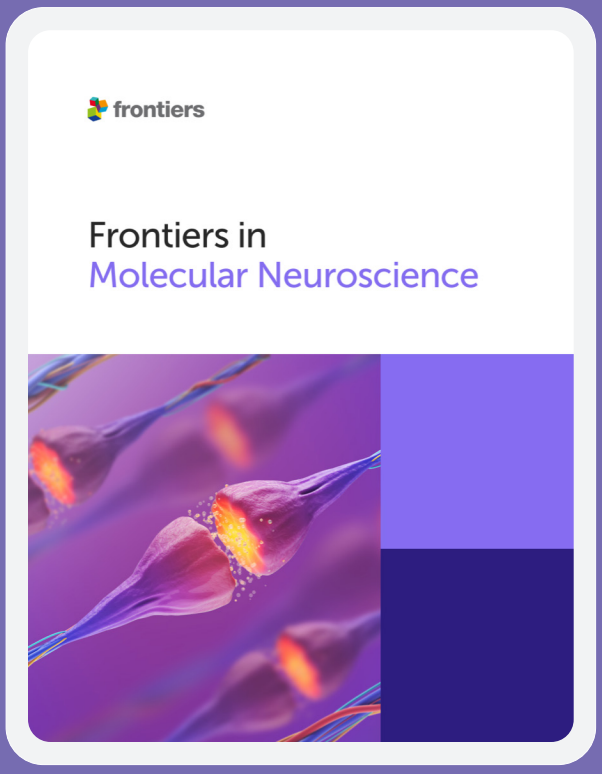

Frontiers

Avenue du Tribunal-Fédéral 34
1005 Lausanne, Switzerland
frontiersin.org

Contact us

+41 (0)21 510 17 00
frontiersin.org/about/contact